DEVELOPMENT OF ONE-POT TECHNIQUES FOR ACCESSING NITROBENZENES, PYRIDINES AND FUSED-AZIRIDINES

Ph.D. Thesis

By

S BANUPRAKASH GOUD

(1901231006)

DEPARTMENT OF CHEMISTRY

INDIAN INSTITUTE OF TECHNOLOGY INDORE

DECEMBER 2024

DEVELOPMENT OF ONE-POT TECHNIQUES FOR ACCESSING NITROBENZENES, PYRIDINES AND FUSED-AZIRIDINES

A THESIS

Submitted in partial fulfillment of the requirements for the award of the degree

of

DOCTOR OF PHILOSOPHY

by

S BANUPRAKASH GOUD

(1901231006)

DEPARTMENT OF CHEMISTRY

INDIAN INSTITUTE OF TECHNOLOGY INDORE

DECEMBER 2024

INDIAN INSTITUTE OF TECHNOLOGY INDORE

I hereby certify that the work which is being presented in the thesis entitled **DEVELOPMENT OF ONE-POT TECHNIQUES FOR ACCESSING NITROBENZENES, PYRIDINES AND FUSED-AZIRIDINES** in the partial fulfillment of the requirements for the award of the degree of **DOCTOR OF PHILOSOPHY** and submitted in the **DEPARTMENT OF CHEMISTRY, Indian Institute of Technology Indore**, is an authentic record of my own work carried out during the time period from **January 2020 to December 2024** under the supervision of **Prof. Sampak Samanta, Department of Chemistry, Indian Institute of Technology Indore.**

The matter presented in this thesis has not been submitted by me for the award of any other degree of this or any other institute.

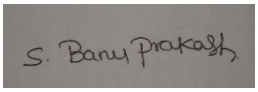

23/06/2025

signature of the student with date
(S BANUPRAKASH GOUD)

This is to certify that the above statement made by the candidate is correct to the best of my/our knowledge.

23/06/2025

Signature of Thesis Supervisor #1 with date

(Prof. SAMPAK SAMANTA)

S BANUPRAKASH GOUD has successfully given his Ph.D. Oral Examination held on **23/June/2025**.

23/06/2025

Signature of Thesis Supervisor #1 with date

(Prof. SAMPAK SAMANTA)

ACKNOWLEDGEMENTS

The research done for my Ph.D. is not solely my endeavor but a collective outcome of the generous contributions of many altruistic individuals. I take the opportunity to recognize them and express my heartfelt admiration.

I wish to convey my profound thanks and respect to Dr. Sampak Samanta, Professor, Department of Chemistry, IIT Indore, for including me in his distinguished group of Synthetic Organic Chemistry. His unwavering direction, support, and assistance throughout the entirety of the thesis process are ineffable. I take pride in having experienced complete autonomy in my research work with him, consistently surrounded by his elegant demeanor.

In addition to my advisor, I express gratitude to my PSPC members, Dr. Abhinav Raghuvanshi, and Prof. Shaikh M. Mobin, for their valuable suggestions and support.

I wish to convey my heartfelt gratitude to Prof. Suhas S. Joshi, the Director of IIT Indore, for his unwavering support in all facets and for offering exceptional infrastructure and amenities at our institution.

I extend my heartfelt gratitude to Prof. Tushar Kanti Mukherjee, Head of the Department of Chemistry, and the other faculty members, including Dr. Selvakumar Sermadurai, Prof. Rajneesh Misra, Prof. Suman Mukhopadhyay, Prof. Apruba K. Das, Prof. Sanjay Kumar Singh, Prof. Biswarup Pathak, Dr. Tridib Kumar Sarma, Prof. Anjan Chakraborty, Dr. Satya S. Bulusu, Prof. Chelvam Venkatesh, Dr. Amrendra Kumar Singh, Dr. Debayan Sarkar, Dr. Dipak Kumar Roy, Dr. Umesh A. Kshirsagar, and Dr. Pravarthana Dhanapal for fostering a encouraging environment within the department.

I wish to express sincere gratitude to my teachers: Mr. Ch. Srikanth, Ms. Mantha, Dr. Venugopal, Dr. Koteshwar rao Ravulapally, Dr. Pochampally Jalapathi, Dr. Gopal Reddy, Dr. Macha Ramesh, Dr. Rajesh Kumar Pogaku, who have imparted knowledge to me throughout my schooling and higher education. Without their endorsement, counsel, and assistance, I would not have achieved such progress.

The completion of the Ph.D. work was contingent upon the support of non-teaching staff members. I wish to extend my sincere gratitude to Mr. Kinny Pandey, Dr. Ravinder, Mr. Nitin, Mr. Ghanshyam Bhavsar, Mr. Atul Singh, from SIC, as well as Mr. Manish Kushwaha, Mr. Rameshwar Dohare, and Mr. P. K. Parthiban from the Chemistry office at IIT Indore.

I express my heartiest gratitude to my phenomenal Friends, Ms. Allepuram Rameshwari, Mr. Gutti Pawan, and Mr. Mudavath Srikanth, Mr. Vadla Balakrishna who have been with me and encouraged during ups and downs of my professional and personal life.

I express my gratitude to both previous and present group members: Dr. Debashis Majee, Dr. Soumitra Guin, Ms. Rajni Lodhi, Mr. Raju Lal Dhakar, Mr. Pundalik Baliram Polawad, Mr. Hritik Prakash, Mr. Kevin Patel, Mr. Hemonta, Mr. Ankur, Mr. Arjun Mr. Shishupal, Mr. Sanjay Kumar for their exceptional collaboration and for fostering a conducive work environment.

Collaborating with numerous pals throughout my Ph.D. has been a great one, since they provided substantial assistance in various facets. I wish to express my gratitude to Dr. Chinthakuntla Mahender, Dr. Salla Nithyanth Kumar, Mr. Shivaji cheepurapalli, Mr. Milan Kumar, Mr. Ashu Singh, Dr. Sarath Kumar, Dr. Reena Kyarikwal, Dr. Rishi Ranjan, Dr. Soumya Kanti De, Mr. Naveen Kumar, Mr. Pawan Pratap, Mr. Praveen Kumar, Mr. Shiva Shankar, Ms. Sneha, Mr. Amardeep Kumar, Mr. Deepak Pandey, Dr. Soumyadeep Patra, Mr. Chinmay K Patel, Mr. Bhabani Shankar, Mr. Delip Pandey, Mr. Rahul Yadav, Mr. Pankaj Kumar, Mr. Vishal, Ms. Bhanu Priya, Dr. Neha, Mr. Sumit Mohapatra, Dr. Mayank Kumar, Dr. Surya Sekar, Ms. Nisha Kumari, Ms. Manvi Rajan, Mr. Ashis, Mr. Prince Kumar Mr. Vadla Balakrishna, Mr. Vijay Goud, Mr. Saidul Sura, Mr. Ravi Pothuraj, Ms. Swetha Sirikonda, Ms. Bharathi Mr. K Shekar, Mr. Shivva Rajesh Kumar, Mr. Keloth Narender, for their generosity, kind support and for providing co-operative environment throughout my Ph.D. work.

I am deeply thankful to my entire family, particularly my lovely parents, Surya Jangaiah Goud, and Surya Nageshwari as well as my lovely brothers Surya Saiteja Goud, and Surya Akhil Goud. I am thrilled to have a supportive and

caring wife, Ms. Surya Sunitha Goud, on this journey. I convey my respect, affection, and thanks to my esteemed uncles Shivaih Goud, and Raghuramulu Goud for their unwavering love and support. Without the unwavering support, care, and affection of all of them, my achievement would have been unattainable.

I would like to express my thanks to University Grants Commission (UGC), New Delhi for my JRF as well as SRF fellowship which fortified me to perform my work comfortably.

Finally, I would like to thank all the others who supported, and encouraged me to make my Ph.D. journey successful.

S BANUPRAKASH GOUD

IIT Indore

Dedicated to

My Father

SURYA JANGAIAH GOUD

TABLE OF CONTENTS

ABSTRACT

The primary objective of this thesis is to establish one-pot synthetic protocols for the efficient synthesis of synthetically and pharmacologically appealing carbocycles and *N*-containing heterocyclic frameworks, such as nitrobenzenes, pyridines, and aziridines, utilizing simple and easily accessible starting materials.

The first chapter commences with a comprehensive introduction detailing the synthesis and application of functionalized nitrobenzene, pyridine, and aziridine scaffolds, including historical context and documented synthetic pathways for the construction of the aforementioned class of carbocyclic and *N*-heterocyclic compounds through diverse synthetic adaptations.

The second chapter addresses an efficient pyrrolidine:4-ClBzOH salt catalyzed a [3+3] cyclization reaction involving *β*-alkyl-substituted nitroalkenes as 1,3-binucleophiles and diverse *β*-aryl/alkyl/alkenyl-substituted acroleins in an open-atmosphere. This tunable organocatalytic process preferentially forms one C-C and one C=C bond, demonstrating a broad substrate scope and yielding various substituted nitroarenes in good to high yields. Moreover, this organocatalytic method is characterized by several advantageous attributes, including the avoidance of toxic metal catalysts, the absence of external oxidants and nitrating agents, complete carbon efficiency, exceptional functional group tolerance, water as the sole by-product, and the circumvention of pre-functionalized arenes, etc. Additionally, a variety of significant heterocycles and carbocycles, including 2-arylcarbazole, 2,6-diphenylindole, 2′-chloro-1,1′:4′,1″ -terphenyl, and 1:1′:4′,1″ terphenyl, were synthesized from nitroarenes using our distinctive methodologies.

The third chapter delineates an efficient $Cu(OAc)_2$/DABCO-mediated one-pot synthesis of highly substituted biologically significant 2-aminonicotinonitriles featuring a valuable phenolic moiety with satisfactory yields. This reaction proceeds between cyclic sulfamidate imines as 1C1N sources and acyclic/cyclic vinyl malononitriles as 4C sources for pyridine synthesis through a vinylogous Mannich cycloaromatization sequence, forming two new C–N bonds under mild conditions. This *de novo* method applies to gram-scale synthesis, highlighting the

method's practicality and accommodating a diverse array of substrates with high functional group tolerance.

The fourth chapter describes an in situ produced photoactive copper(I) complex-catalyzed aziridination reaction involving cyclic N-sulfonyl imines and α-aryl substituted vinyl azides, utilizing blue LEDs irradiation. This innovative SET method offers a benign, sustainable, and pragmatic approach for synthesizing resourceful sulfamidate-fused aziridines, with acceptable chemical yields and outstanding diastereoselectivities. A few pharmacologically appealing benzo[*f*][1,2,3]oxathiazepine dioxides and fused isoxazoline frameworks were successfully achieved through our novel metal-free ring-expansion techniques, demonstrating the synthetic utility of the obtained aziridines.

The last chapter of this thesis tackles the conclusion and future implications of the proficient procedures implemented throughout the research.

LIST OF PUBLICATIONS

A. Publications from thesis work:

1. Goud S B., Majee D., Guin S., Rathor S. S., Patel A. K., Samanta S. (2021), Reversal reactivity of β-alkylnitroalkenes as 1,3-binucleophiles: application to nitroarenes using organocatalysis, *Asian J. Org. Chem.*, 10, 1650–1654 (DOI: 10.1002/ajoc.202100216).
2. Goud S B., Guin S., Prakash M., Samanta S. (2022), $Cu(OAc)_2$/DABCO-mediated domino reaction of vinyl malononitriles with cyclic sulfamidate imines: access to 6-hydroxyaryl-2-aminonicotinonitriles, *Org. Biomol. Chem.*, 20, 352-357 (DOI: 1039/D1OB02095A).
3. Goud S B., Dhakar R. L., Samanta S. (2024), Copper(I)-photocatalyzed diastereoselective aziridination of *N*-sulfonyl imines with vinyl azides: application to benzo[*f*][1,2,3]oxathiazepines dioxides and fused isoxazolines, *Chem. Asian J.*, 19, e202300904 (DOI: 10.1002/asia.202300904).

B. Other publications

1. Lodhi R., Goud S B., Samanta S. (2024), One-pot π-extension approach of iminoindoles-to-α-carbolines as blue-light emitters using the cooperative basic system, *New J. Chem.*, 48, 14163-14169 (DOI: 10.1039/d4nj01868k).
2. Dhakar R. L., Goud S B., Samanta S. (2025), Base-promoted and copper(I)-catalyzed Tandem Cyclization-C(sp^2)-N coupling of vinyl malanonitriles with *Ortho*-nitrochalcones: access to acridones and their fused deerivatives, *J. Org. Chem.*, 90, 3698-3718 (DOI:10.1021/acs.joc.4c03125).

Conferences:

- Poster presentation in **"In-house Chemistry Symposium"** (CHEM 2022) organized by Department of Chemistry, Indian Institute of Technology Indore, 11th March 2022.
- Poster presentation in **"International Conference on Sustainable Chemistry-2023"**organized by Department of Chemistry, Indian Institute of Technology Indore, From 22nd - 23rd February, 2023.

LIST OF ABBREVIATIONS

HCl	Hydrochloric acid
HNO_3	Nitric acid
H_2SO_4	Sulfuric acid
DMF	N, N-Dimethylformamide
$NaNO_2$	Sodium nitrite
$Pd_2(dba)_3$	Tris(dibenzylideneacetone)dipalladium(0)
TDA	4,4′-Thiodianiline
t-BuOH	*tert*-butyl alcohol
i-PrOH	Isopropyl alcohol
([Dsim]NO_3)	1,3-Disulfonicacid imidazolium nitrite
$[Ru(bpy)_3]Cl_2$	Tris(bipyridine)ruthenium(II) chloride
MeCN	Acetonitrile
$Pd(OAc)_2$	Palladium acetate
$AgNO_2$	Silver nitrite
$K_2S_2O_8$	Potassium persulfate
DCE	1,2-Dichloroethane
$Bi(NO_3)_3 \cdot 5H_2O$	Bismuth(III) nitrate pentahydrate
Ac_2O	Acetic anhydride
CH_3NO_2	Nitromethane
KI	Potassium iodide
TBHP	*tert*-butyl hydroperoxide
H_2O_2	Hydrogen peroxide

K_2CO_3	Potassium carbonate
NH_4OAc	Ammonium acetate
EtOH	Ethanol
$NaNH_2$	Sodium amide
AcOH	Acetic acid
CH_2Cl_2	1,2-Dichloroethane
BINAP	(2,2′-bis(diphenylphosphino)-1,1′-binaphthyl)
DABCO	1,4-Diazabicyclo[2.2.2]octane
THF	Tetrahydrofuran
Cs_2CO_3	Cesium carbonate
CuCl	Copper(I) chloride
Bu_3SnCl	Tributyltin chloride
DMA	Dimethylacetamide
DCM	Dichloromethane
HBr	Hydrogen bromide
NH_2OH	Hydroxylamine
Et_3N	Triethylamine
$(NH_4)_2CO_3$	Ammonium carbonate
GO	Graphene Oxide
CuI	Copper(I) iodide
Na_2SO_4	Sodium sulfate
KOH	Potassium hydroxide

TsCl	Tosyl chloride
$HClSO_3$	Chlorosulfuric acid
NaOH	Sodium hydroxide
Na_2CO_3	Sodium carbonate
$NaBH_4$	Sodium borohydride
MeOH	Methanol
DMAP	4-Dimethylaminopyridine
DMF	*N*, *N*-Dimethylformamide
NaH	Sodium hydride
NMM	*N*-Methylmorpholine
NIS	*N*-Iodosuccinimide
NBS	*N*-Bromosuccinimide
K_3PO_4	Potassium phosphate
TfOH	Trifluoromethanesulfonic acid
MS	Molecular sieves
$AgNO_3$	Silver nitrate
TMSCl	Trimethylsilyl chloride
AgTFA	Silver trifluoroacetate
$CHCl_3$	Chloroform
Ph_3P	Triphenylphosphine
KF	Potassium fluoride
B_2pin_2	Bis (pinacolato)diboron
$Cu(OAc)_2$	Copper acetate

$Yb(PFO)_3$	Ytterbium perfluorooctanoate
$FeCl_3$	Ferric Chloride
TFA	Trifluoroacetic acid
DBU	1,8-Diazabicyclo[5.4.0]undec-7-ene
DIPEA	*N*,*N*-Diisopropylethylamine
$Cu(OTf)_2$	Copper triflate
$CuBr_2$	Copper (II) bromide
$Zn(OTf)_2$	Zinc trifluoromethanesulfonate
$Gd(OTf)_3$	Gadolinium triflate
$Nd(OTf)_3$	Neodymium (III) trifluoromethanesulfonate
$In(OTf)_3$	Indium(III) trifluoromethanesulfonate
$ZnCl_2$	Zinc chloride
NH_4Cl	Ammonium chloride
DMSO	Dimethyl sulfoxide
K_2HPO_4	Dipotassium phosphate
$Pd(PPh_3)_4$	Tetrakis(triphenylphosphine)palladium(0)
EtOAc	Ethyl acetate
N_2	Nitrogen gas
O_2	Oxygen gas
H_2	Hydrogen gas
δ	Chemical shift
d	Doublet
q	Quartet

R_f	Retardation factor
s	Singlet
m	Multiplet
t	Triplet
Hz	Hertz
MHz	Megahertz
J	Coupling constant
ppm	Part-per-million
TLC	Thin-layer chromatography
ee	Enantiomeric excess
dr	Diastereomeric ratio
DMSO-d_6	Deuterated dimethyl sulfoxide
$CDCl_3$	Deuterated chloroform
D_2O	Deuterium oxide
ESI-MS	Electronspray ionization mass spectrometry
LC-MS	Liquid chromatography-mass spectrometry
NMR	Nuclear magnetic resonance
SC-XRD	Single Crystal X-ray Diffractometers
TOF-MS	Time of flight mass spectrometry
MW	Microwave
UV	Ultraviolet radiation
Vis	Visible
λ	Wavelength

μ	Micro
π	Pi
α	Alpha
nm	Nanometer
cm	Centimeter
°	Degree
mL	Milliliter
M	Molar
CV	Cyclic voltammetry
Bu_4NPF_6	Tetrabutylammonium hexafluophosphate

LIST OF FIGURES

LIST OF SCHEMES

LIST OF TABLES

Chapter 1

Introduction

1.1 One-pot reaction

Efficient design and invention of new chemical methods are paramount research topics in synthetic organic and medicinal chemistry to create structurally complex molecules. In this context, "one-pot or pot-economic reactions have emerged as one of the pragmatic routes. These reactions enable the creation of structurally and stereochemically complex molecules within a single container, making the process extremely beneficial by considerably reducing chemical waste, saving extra workforce and time, and avoiding hazardous substances. Importantly, this method can perform multiple bond-forming transformations in one go without requiring additional reagents, catalysts, or steps for purification and isolation. One-pot reactions such as domino, cascade, and tandem processes are generally acknowledged for supremacy over traditional techniques, as illustrated in **Figure 1.1.**[1-5]

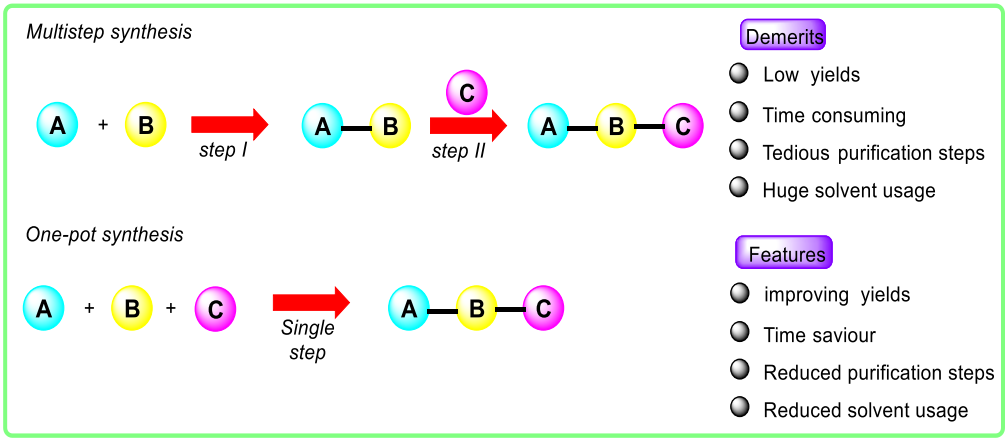

Figure 1.1. A comparative analysis of one-pot and multistep synthesis.

In 1971, Robinson and his colleagues reported for the first time a one-pot procedure for making N-alkyl bicyclic natural alkaloid tropinone involving succinaldehyde, acetone dicarboxylic acid, and methyl amine in an aqueous solution. This one-pot technique affords an unstable tropinonedicarboxylic acid

intermediate, followed by decarboxylation (losing two molecules of CO_2) in acidic conditions under heating conditions to form a novel class of tropinone. It is an essential component in synthesizing anti-colic and spasmolytic drugs, especially those about the tropine alkaloid family **(Scheme 1.1)**[4]

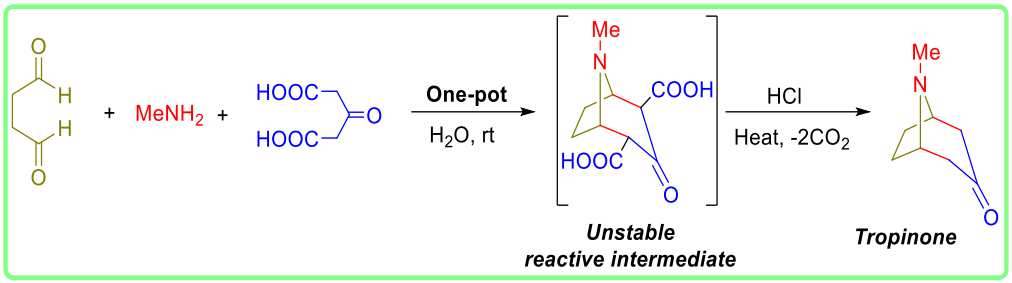

Scheme 1.1. Robinson one-pot condensation reaction method for obtaining tropinone.

Since its debut, synthetic organic chemists have consistently favoured the "one-pot" approach. Nowadays, this creative method is extensively used to produce a wide breadth of natural products, pharmaceutical chemicals, drug scaffolds, and synthetic intermediates. Inspired by the above precedence, our research group has substantially contributed to this field by advancing several one-pot tactics for accessing fascinating classes of carbo- and heterocyclic scaffolds. These include substituted nitroarenes, pyridines and fused aziridines. These substances may exhibit a wide range of therapeutic activities, such as anti-inflammatory, anti-fungal, anti-cancer, anti-HIV, and anti-microbial effects, demonstrating their significance and practicality in medicinal chemistry.

1.2. Background

1.2.1. General structure, historical background, and importance of nitrobenzenes

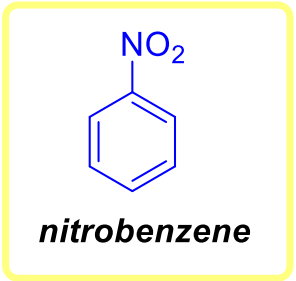

Figure 1.2. The general structure of nitrobenzene.

The nitro group attached to benzene moieties is a distinctive and adaptable functional group in organic, and medicinal chemistry. Eilhardt Mitscherlich, a German chemist, who devised nitrobenzene for the first time in 1834. Its chemical formula is $C_6H_5NO_2$. Moreover, it is a water-insoluble pale-yellow colour with an almond like odor **(Figure 1.2)**. Notably, the nitro group of benzenes could quickly transmute into various functionalities, including amine, azide, amide, hydroxylamine, sulfonamide, azo, etc., and several complex heterocycles. Additionally, many nitrobenzene derivatives exhibit various biological actions and hold substantial promise for use in numerous scientific domains (**Figure 1.3).**[6-14]

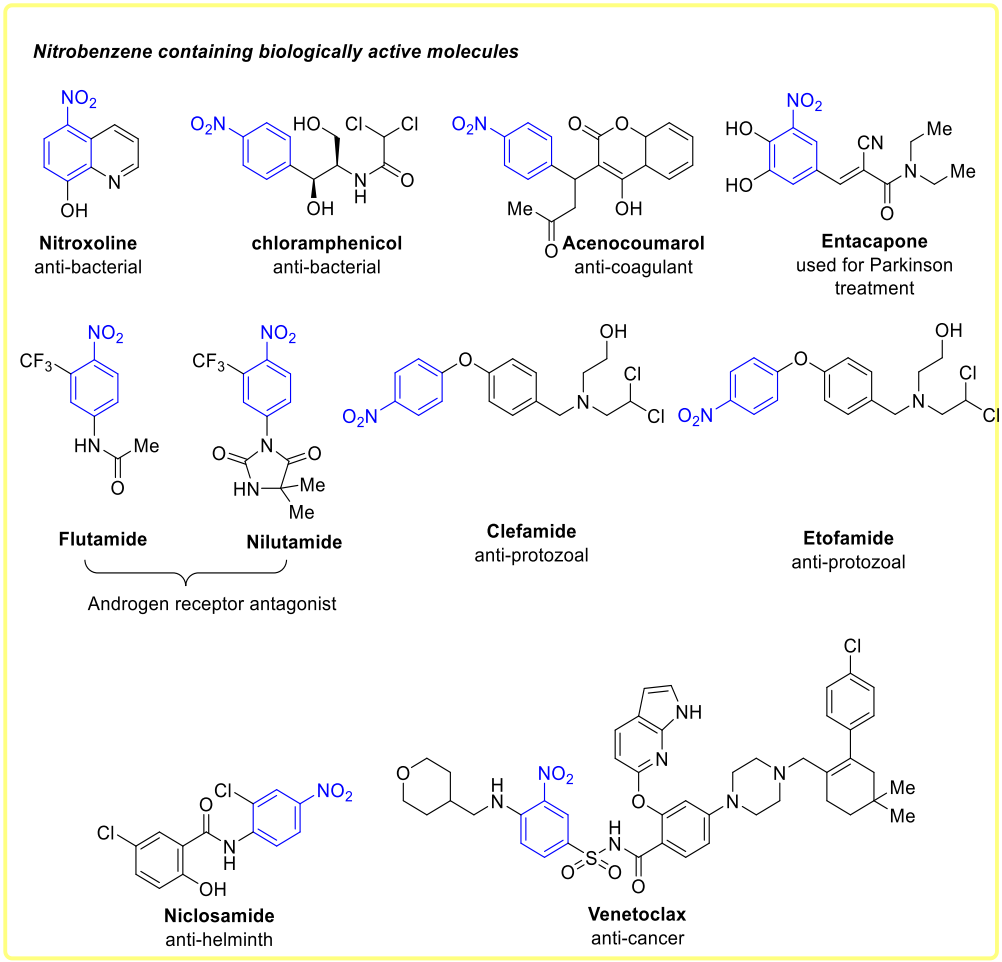

Figure 1.3. A few examples of nitrobenzene containing biologically active molecules.

1.2.2. General structure, historical background, and importance of Pyridines

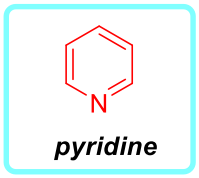

Figure 1.4. The general structure of pyridine.

Pyridine is a six-membered aromatic N-containing heterocyclic molecule with molecular formula C_5H_5N **(Figure 1.4**). This aza-arene ring is structurally like benzene, where a N-atom replaces one methine group. Pyridine is a colorless, alkaline liquid with an unpleasant smell. The first experiment conducted by Anderson in 1849, who investigated the pyrolysis of bones, is associated with the discovery of the pyridine nucleus. Anderson was able to isolate picoline, the first known pyridine. Later, he isolated pyridine in a pure form through fractional oil distillation. However, after decades, the proper chemical structure was reported in 1869 and 1871 by Wilhem Körner and James Dewar, respectively. There are many reasons why the pyridine core is so appealing because it constructs many bioactive natural alkaloids, drug molecules, pharmaceuticals, agrochemicals etc. (**Figure 1.5)**.[15-23]

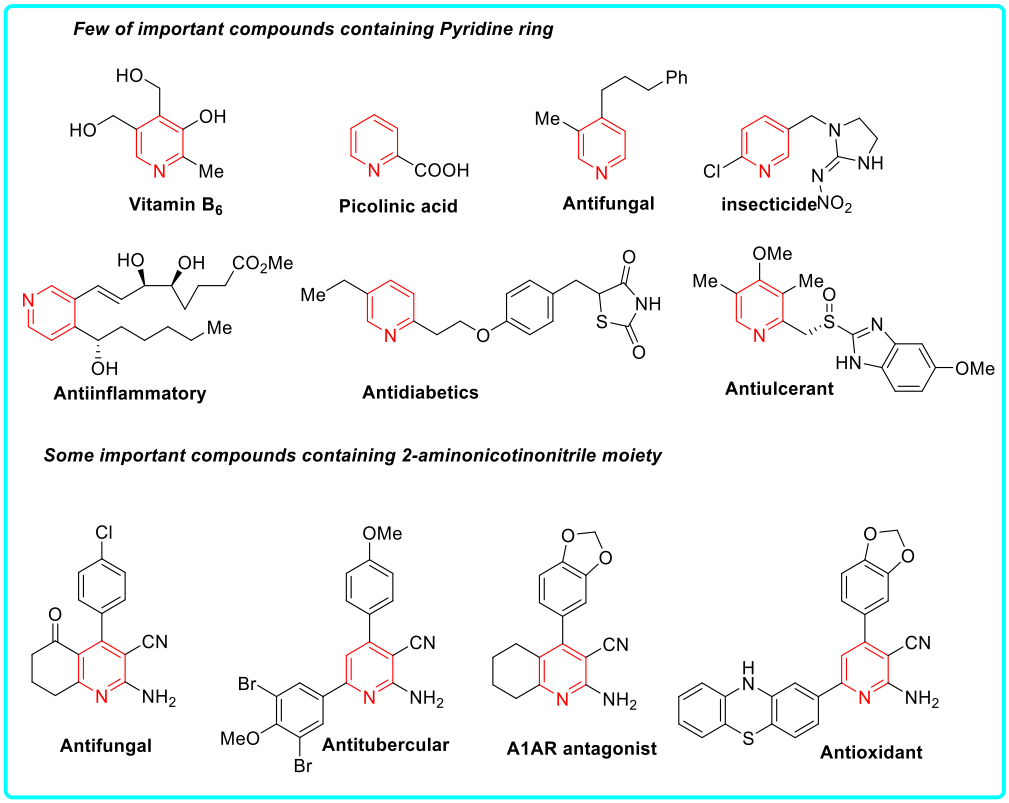

Figure 1.5. Few important molecules, containing pyridine, and 2-amininicotinonitrile as the core.

1.2.3. General structure, historical background, and importance of Aziridines

Figure 1.6. The general structure of aziridine.

The aziridine represents a unique class of three-membered saturated heterocycle that contains one nitrogen atom **(Figure 1.6**). This petite heterocyclic ring is highly reactive due to its intrinsic ring strain, making it a valuable opportunity to serve as multifaceted, highly reactive intermediate. Aziridines could rapidly convert into various value-added N-containing compounds that are useful in drug discovery programs. Furthermore, they are critical structural units ubiquitously presented in many bioactive natural molecules, active pharmaceutical ingredients, and synthetic molecules with great biological

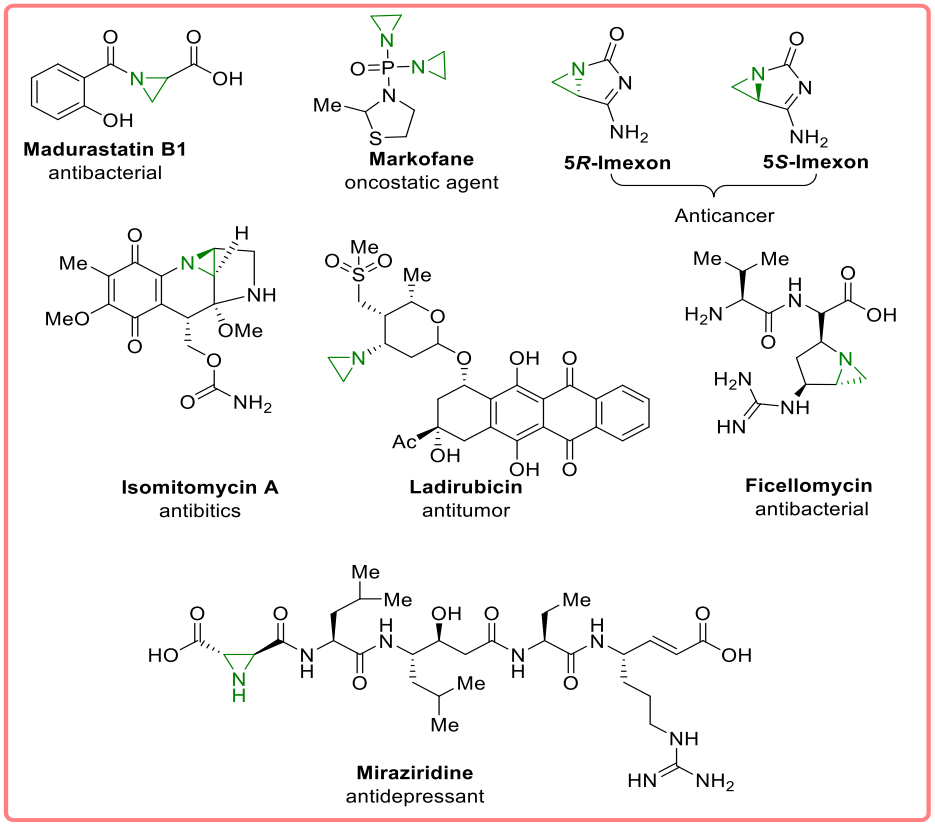

Figure 1.7. Few important molecules contain aziridine as the core.

importance. In 1888, aziridine was first discovered by Siegmund Gabriel **(Figure 1.7).**[24-33]

The following section will cover several methods for obtaining functionalized nitrobenzenes, pyridines, and aziridines.

1.3. Literature study

1.3.1 Synthesis of substituted nitrobenzene frameworks:

It is well known that nitroarenes play a very important role in synthetic organic and medicinal chemistry. Consequently, countless methods have been recorded for the synthesis of nitrobenzenes. This section includes some essential studies on the topic.

1.3.1.1. Traditional synthesis of nitrobenzene

In 1834, Mitscherlich synthesized the first nitrobenzene by reacting fuming nitric acid with benzene derived from coal tar. Later, Mansfield employed a mixed acid (HNO_3:H_2SO_4 =1:1) as a nitrating agent for the nitration of benzene. This mixed acid generates in situ nitronium ion (NO_2^+), which acts as the reactive species for aromatic electrophilic substitution (**Scheme 1.2).**[34-37]

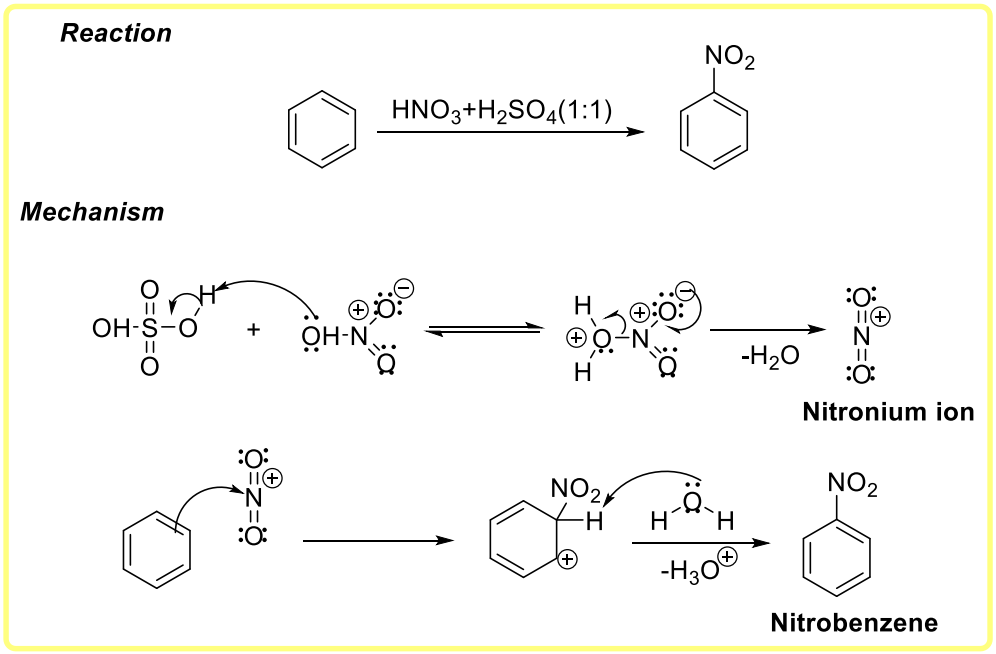

Scheme 1.2. Synthesis of nitrobenzene via electrophilic substitution reaction.

1.3.1.2. Synthesis of nitrobenzenes *via* regiospecific *ipso*-nitration

In 2005, Koizumi *et al.* invented a regiospecific *ipso*-nitration of iodobenzenes. This nitration technique utilizes tetra-*n*-butylammonium nitrite (n-Bu_4NNO_2) as a powerful nitrating agent, combined with catalytic amounts of *N*,*N*'-dimethylethylenediamine, and Cu bronze. This process leads to nitroarenes with satisfactory chemical yields ranging from 23% to 91% **(Scheme 1.3).**[38]

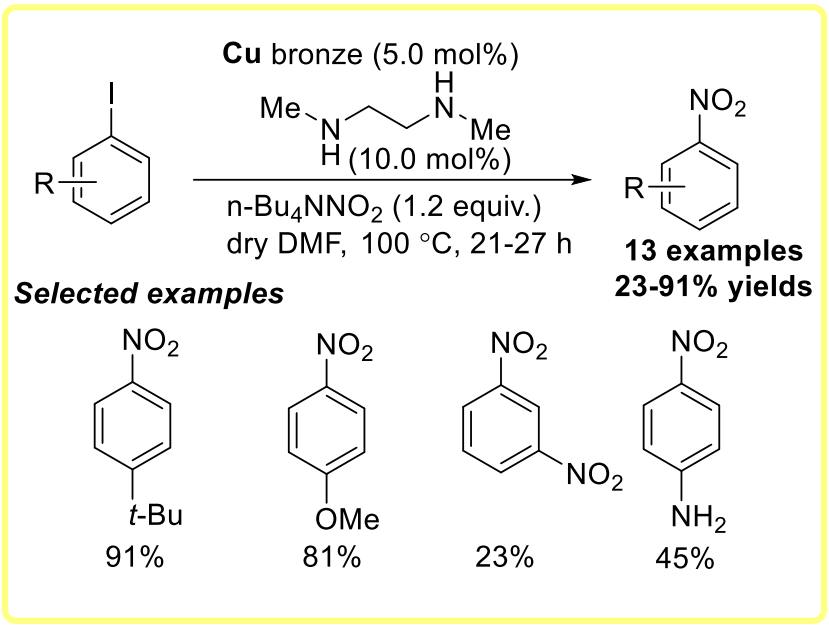

Scheme 1.3. Cu-catalyzed a regiospecific *ipso*-nitration of iodoarenes.

Based on the author's proposed mechanism, Cu(I) species may be oxidative in addition to the carbon–iodo bond to form a Cu(III)-complex (**A**). Then, the iodide ion is replaced with an in situ-generated nitrite ion, forming intermediate **B**, which undergoes reductive elimination to make nitrobenzene and regenerate a Cu(I) complex for the next cycle (**Scheme 1.4**).

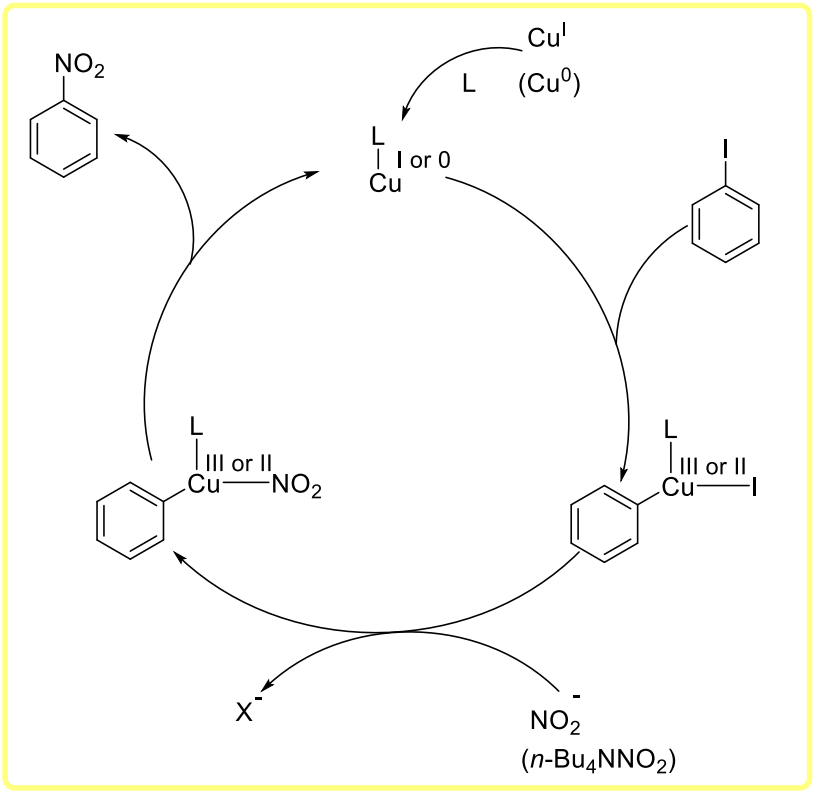

Scheme 1.4. A proposed catalytic cycle for the synthesis of nitrobenzene.

In 2009, Buchwald *et al*. reported a novel Pd(0)-catalyzed *ipso*-nitration of aryl chlorides/triflates using $NaNO_2$ in the presence of catalytic amounts of *t*-BuBrettPhos and TDA at 130 °C in *t*-BuOH, leading to 74-99% yields of nitroarenes. This protocol offers excellent regioselectivity and operates effectively under weakly basic conditions, enabling good compatibility with various functional groups **(Scheme 1.5).**[39]

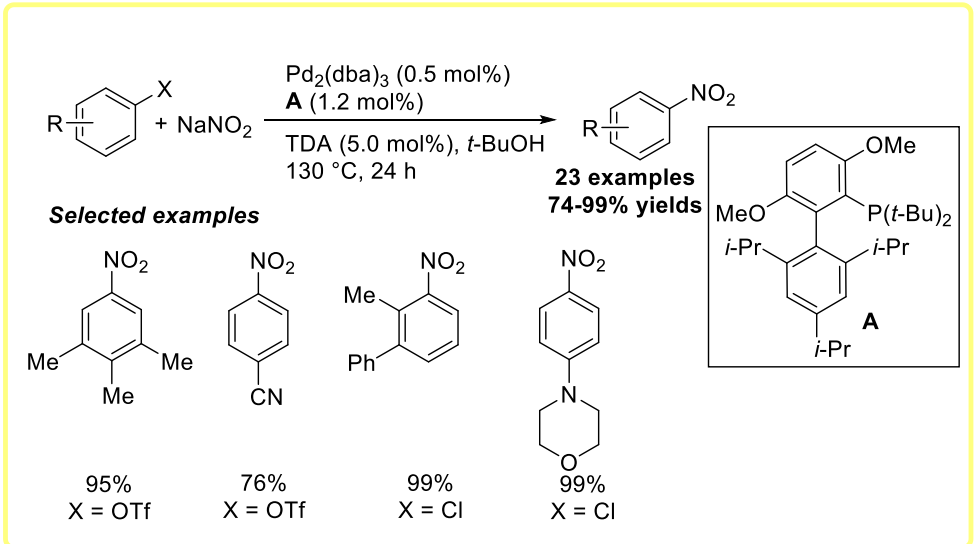

Scheme 1.5. Pd-catalyzed *ipso*-nitration of aryl chlorides/triflates.

In 2018, Zolfigol *et al* employed a robust 1,3-disulfonic acid imidazolium nitrate ([Dsim]NO_3) as a liquid nitrating agent for the *ipso*-nitration of diverse arylboronic acids at room temperature under solvent-free conditions to produce several nitrobenzene derivatives in good to excellent yields (**Scheme 1.6).**[40]

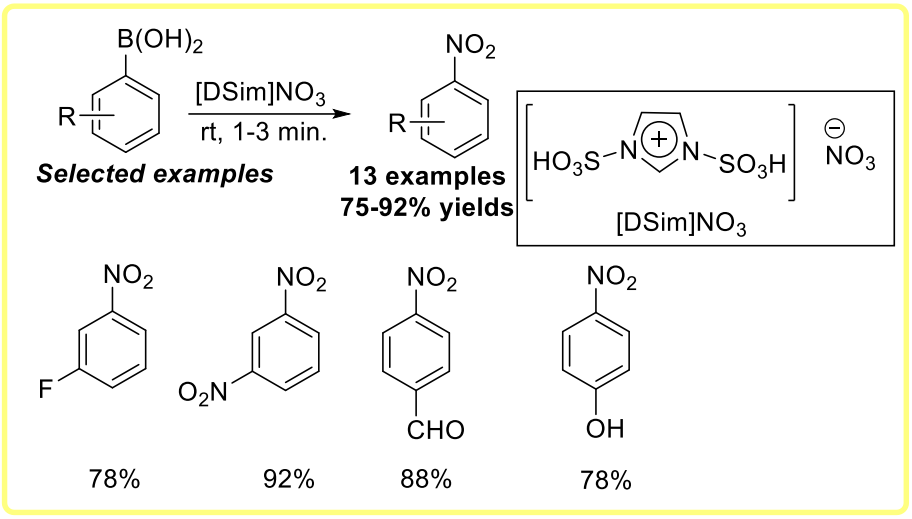

Scheme 1.6. Synthesis of nitroarenes by using 1,3-disulfonic acid imidazolium nitrate ([Dsim]NO_3).

In 2020, Katayev *et al.* accomplished a photoactive Ru(II)-complex-catalyzed regioselective *ipso*-nitration of arylboronic acids using 1-nitropyrrolidine-2,5-dione as a metal-free, recyclable, and bench-stable nitrating reagent irradiated by Blue-LEDs at room temperature, capable making various nitrobenzenes in

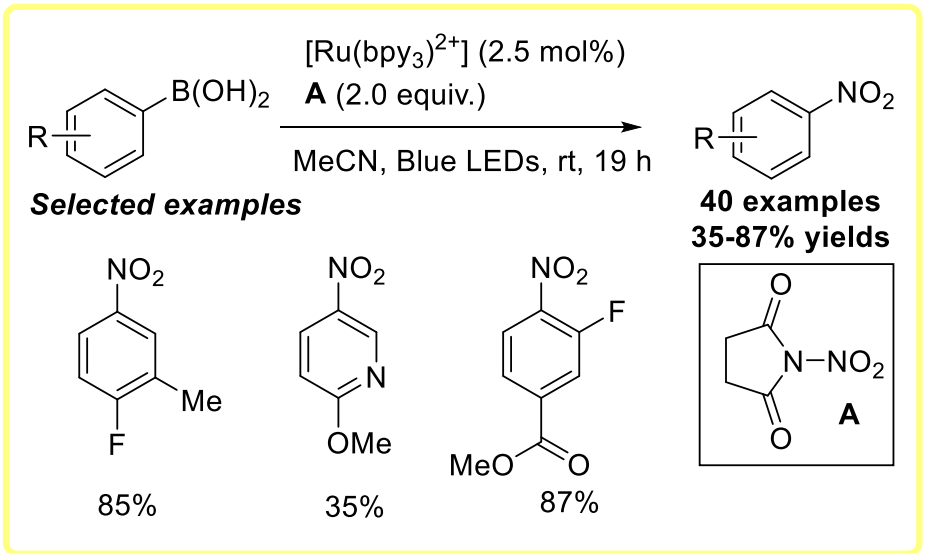

Scheme 1.7. Photocatalytic synthesis of nitrobenzenes.

a variable range of yields (35-87%) in **Scheme 1.7.** Notably, this photocatalytic method was also applied to heteroaryl-substituted boronic acids, which worked nicely under identical conditions.[41]

1.3.1.3. Regiospecific chelation-assisted C(sp^2)-H nitration

In 2010, Xu and colleagues reported a Pd(II)-catalyzed highly regioselective *ortho*-nitration of aryl group of quinoxalines in the presence of $AgNO_2$ and $K_2S_2O_8$ at 130 °C. This mononitration reaction affords good to high yields of the corresponding nitroarene derivatives in **Scheme 1.8.**[42]

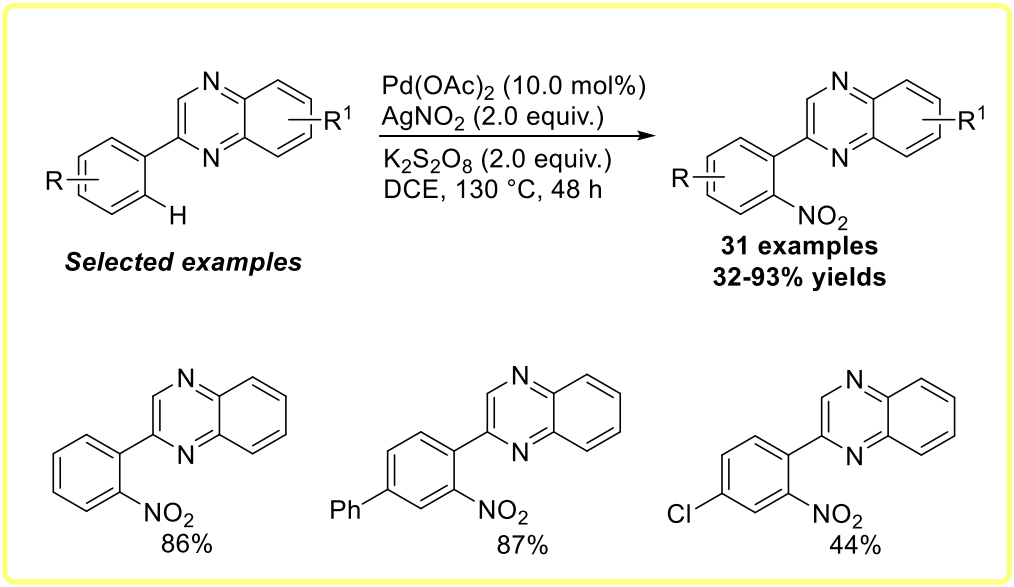

Scheme 1.8. Pd(II)-catalyzed regioselective *ortho*-nitration of 2-arylquinoxaliones.

In 2013, Duan *et al.* demonstrated a simple regioselective *ortho*-nitration of the N-phenyl carboxamides using $Bi(NO_3)_3$ as a nitrating agent in the presence of acetic anhydride. The reaction proceeds at room temperature and allows for the synthesis of *ortho*-nitrated products in good to excellent yields and a variable range of regioselectivities (*ortho/para* = 0.9:1 to 49:1) **(Scheme 1.9).**[43]

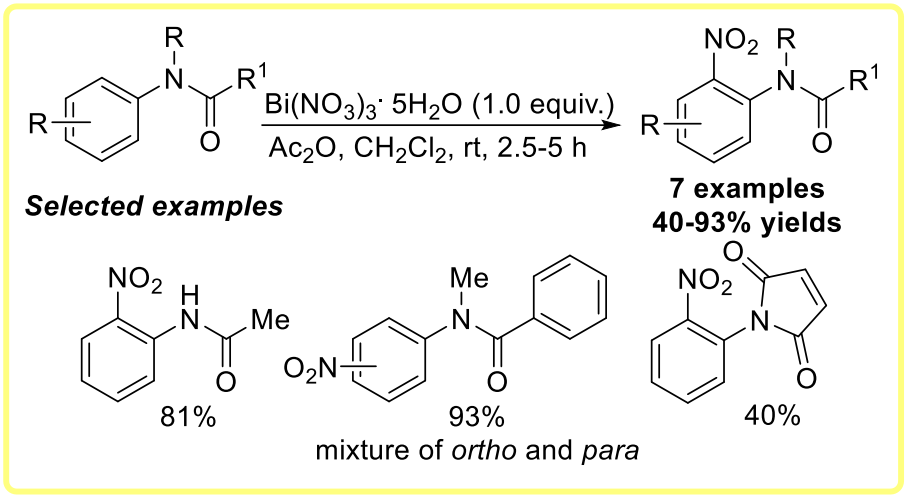

Scheme 1.9. Regioselective *ortho*-nitration of N-aryl carboxamides.

In 2014, Liang *et al.* developed a highly regioselective and straightforward approach for the direct oxidative nitration of aromatic sulfonamides using sodium nitrite as the nitrating reagent in the presence of oxone in MeCN at 50 °C. Moreover, this process is attractive due to its mild conditions, strong compatibility with functional groups, simple operation, and high yields (**Scheme 1.10).**[44]

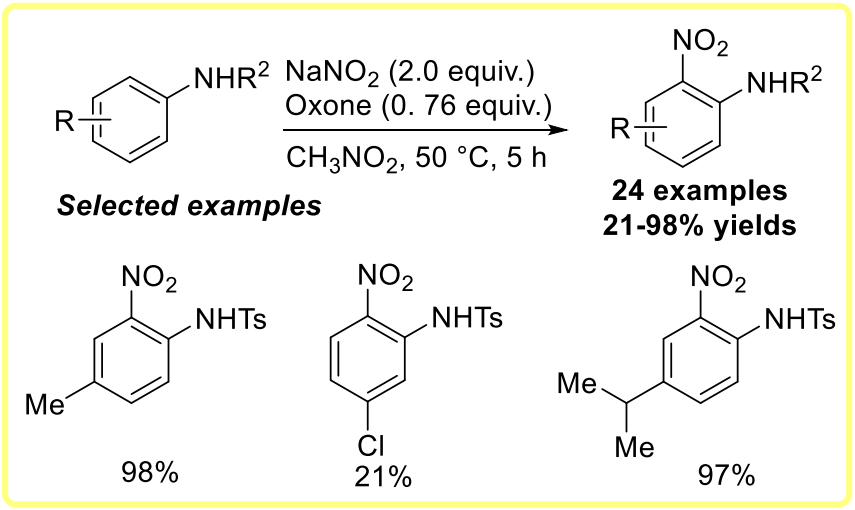

Scheme 1.10. Regioselective nitration of aromatic sulfonamides.

1.3.1.4. Conversion of arylamines to nitroarenes

In 2009, Reddy and co-workers developed an efficient, metal-free oxidative method for the conversion of aromatic primary amines to nitroarenes using

potassium iodide acting as a catalyst and *tert*-butyl hydroperoxide acting as an external oxidant. This catalytic system is applicable to a variety of electron-rich and electron-poor substituted aromatic amines (**Scheme 1.11).**[45]

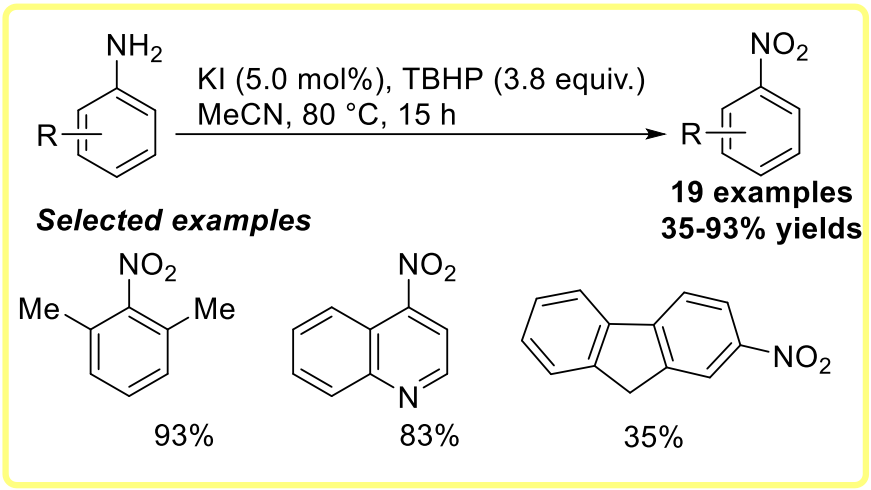

Scheme 1.11. Oxidative conversion of amines to nitro products accelerated by KI-TBHP.

In 2019, Sashidhara and co-workers demonstrated a practical method for oxidation of a variety of aromatic amines in the presence of H_2O_2 promoted by K_2CO_3 at room temperature, leading to various nitroarenes in good to excellent yields (65-94%) with a short span of time **(Scheme 1.12).**[46]

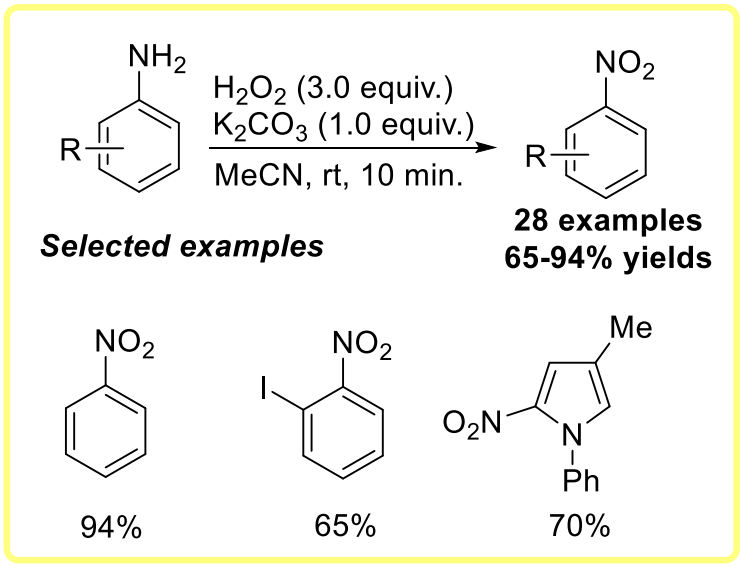

Scheme 1.12. Metal-free access to nitroarenes from aromatic amines.

1.3.2. Synthesis of functionalized pyridine derivatives

In 1876, Ramsay synthesized pyridine for the first time by combining hydrogen cyanide and acetylene in a red-hot tube furnace, leading to pyridine as shown in **Scheme 1.13.**[47]

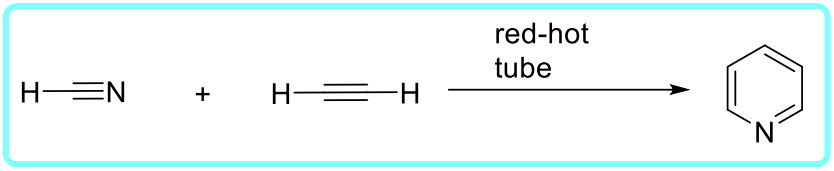

Scheme 1.13. First access to pyridine from hydrogen cyanide and acetylene.

1.3.2.1 Traditional methods:

Hantzsch pyridine synthesis

In 1881, Hantzsch discovered a rapid method for synthesizing densely substituted symmetrical pyridines involving 2.0 equiv of 1,3-dicarbonyl compounds, aromatic aldehydes, and NH_4OAc or ammonia as a source of N-atom for pyridine ring in EtOH. This pseudo-four-component pseudo-four-component reaction affords initially dihydropyridine moiety, which is subjected to oxidation in the presence of an oxidizing agent ($FeCl_3$, HNO_3, etc) to produce the pyridines **(Scheme 1.14).**[48]

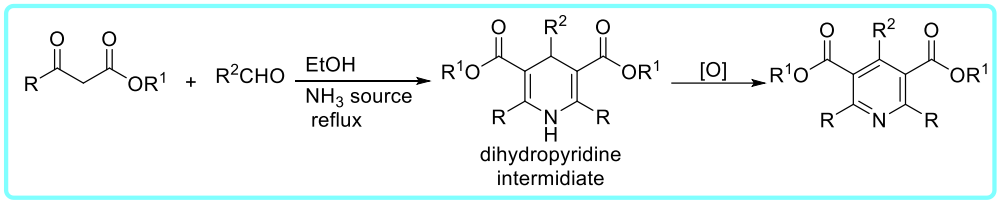

Scheme 1.14. Hantzsch pyridine synthesis.

Chichibabin pyridine synthesis

In 1924, Chichibabin revealed a pseudo-four-component reaction using enolizable aldehydes (3.0 equiv.) and ammonia at a high pressure with $NaNH_2$. This process allows for the synthesis of trisubstituted pyridines as shown in **Scheme 1.15.**[49]

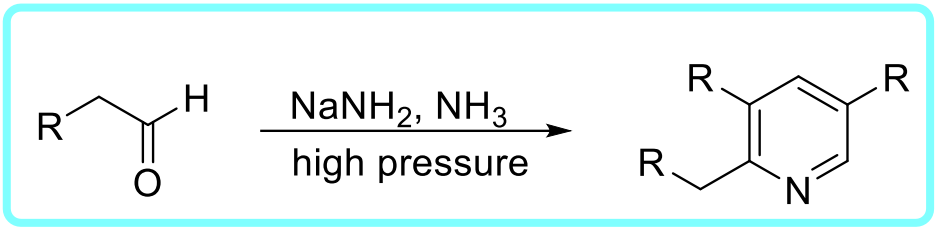

Scheme 1.15. Chichibabin reaction for the synthesis of pyridine derivatives.

Bohlmann-Rahtz Pyridine Synthesis

In 1957, Ferdinand Bohlmann and Dieter Rahtz invented a two-step process for making trisubstituted pyridines in good yields. This reaction involves the Michael addition reaction between enaminoesters with alkynones in EtOH at 50 °C to form addition products. They are subsequently converted into pyridine derivative at 150 °C under vacuum **(Scheme 1.16).**[50]

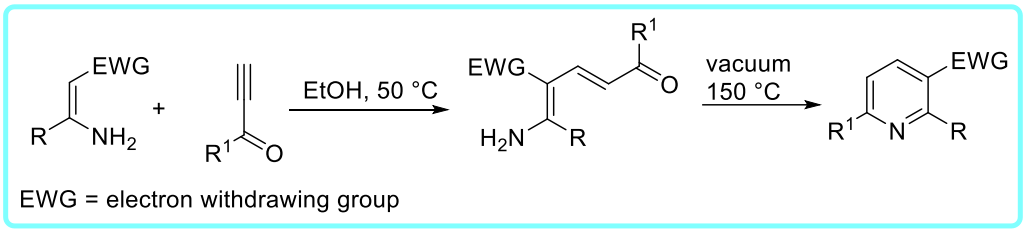

Scheme 1.16. Access to trisubstituted pyridines using the Bohlmann-Rahtz technique.

Kröhnke pyridine synthesis:

In 1976, Kröhnke and co-workers devised an innovative procedure for the synthesis of symmetric and unsymmetric 2,4,6-triarylpyridines (TAPs) by reacting N-phenacylpyridinium salts with α,β-unsaturated ketones in warm AcOH using NH_4OAc in **(Scheme 1.17).**[51]

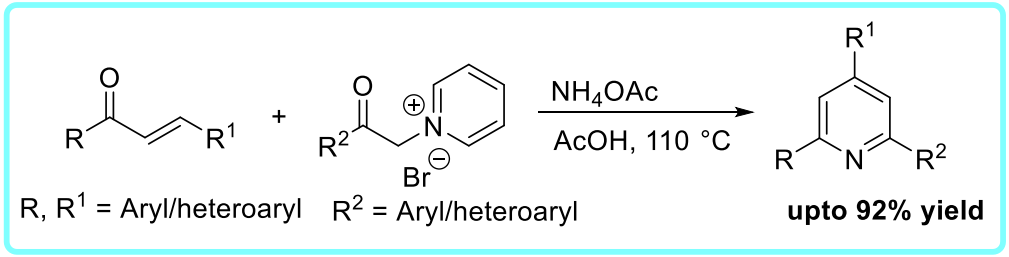

Scheme 1.17. Kröhnke's synthesis of 2,4,6-triarylpyridines.

Tu and co-workers reported a metal-solvent-free one-pot multicomponent reaction between aryl aldehydes, aryl ketones and NH_4OAc under microwave radiation. This process leads to various 2,4,6-triarylpyridines **(Scheme 1.18).**[52]

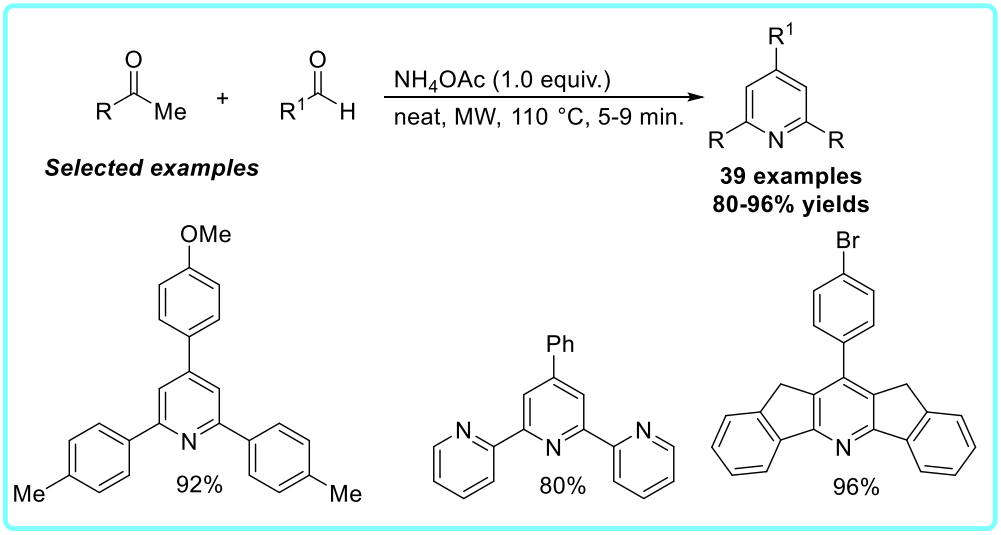

Scheme 1.18. A metal-solvent-free pyridine synthesis assisted by MW.

1.3.2.2 Modern strategies

In 2007, Arndt et al. revealed a hetero-Diels-Alder process that delivered tri-/tetra-substituted pyridines in modest to high yields (33-93%) using 1-azadienes (silylated enol oximes) and internal/terminal alkynes in a solvent-free environment at 150 ºC. However, this method suffers from a poor regioselectivity of the products **(Scheme 1.19).**[53]

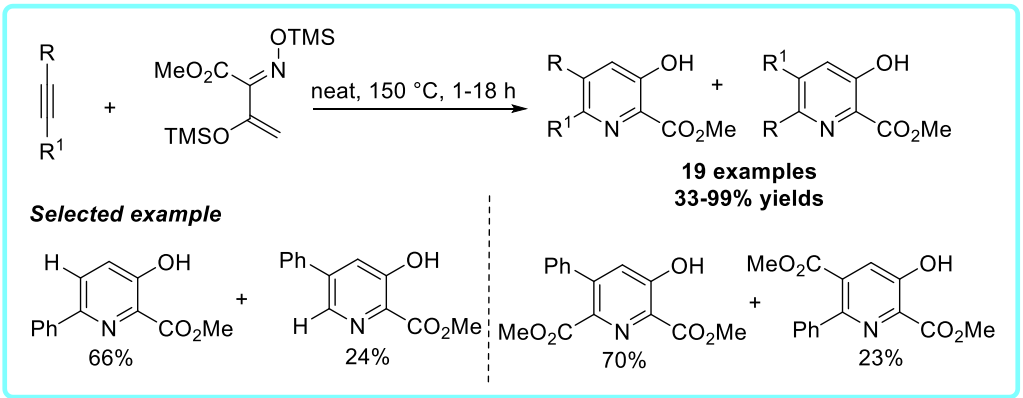

Scheme 1.19. Hetero-Diels-Alder process for the solvent-free synthesis of tri- and tetra-substituted pyridines.

In 2010, Tanaka *et al.* developed an efficient, mild Rh(I)-catalyzed regioselective cyclotrimerization of aryl/alkyl nitriles with aryl ethynyl ethers using BINAP (5.0 mol%) to afford a series of 2,4-diaryloxypyridines in a variable range of yields **(Scheme 1.20).**[54]

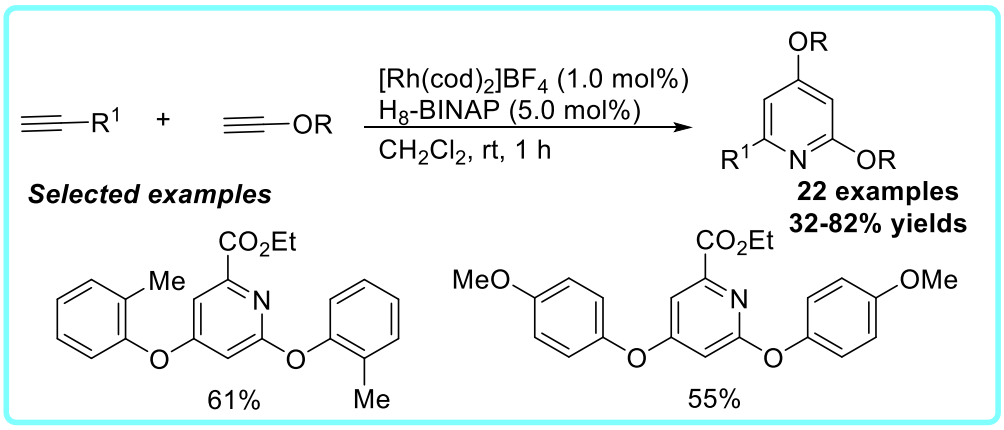

Scheme 1.20. Rh-catalyzed regioselective synthesis of 2,4,6-pyridines.

In 2016, Samanta *et al.* established a metal-free new domino technique for quick access to a significant class of 4,6-diarylpicolinates from a variety of 4-aryl-5*H*-1,2,3-oxathiazole-2,2-dioxides and MBH acetates of nitroalkenes/nitrodienes using DABCO as an inexpensive organobase at heating conditions. Furthermore, this metal-free domino method resulted in 82-93% yields **(Scheme 1.21).**[55]

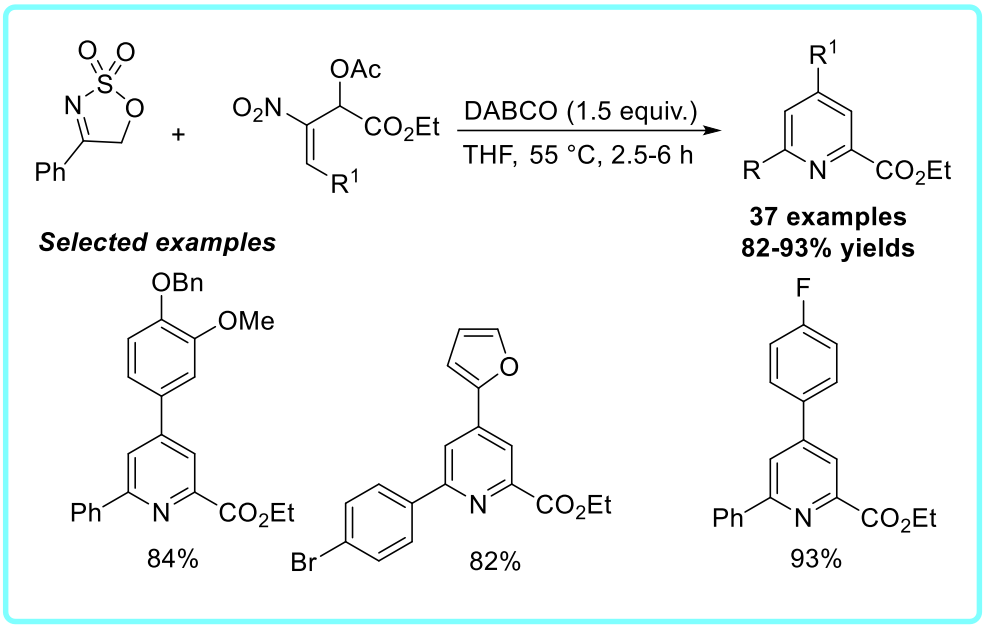

Scheme 1.21. One-pot metal-free approach to 4,6-Diarylpicolinates.

In 2020, Samanta *et al.* also developed a simple and efficient one-pot regioselective 1,6-addition elimination-6π-aza-electrocyclization-aromatization reaction of vinyl/dienyl-substituted para-quinone methides with an array of cyclic sulfamidate imines supported by DABCO as a solid organobase in an open atmosphere. This method enables 59-84% yields of symmetrical and unsymmetrical 2,4,6-trisubstituted pyridines with a phenolic moiety **(Scheme 1.22).**[56]

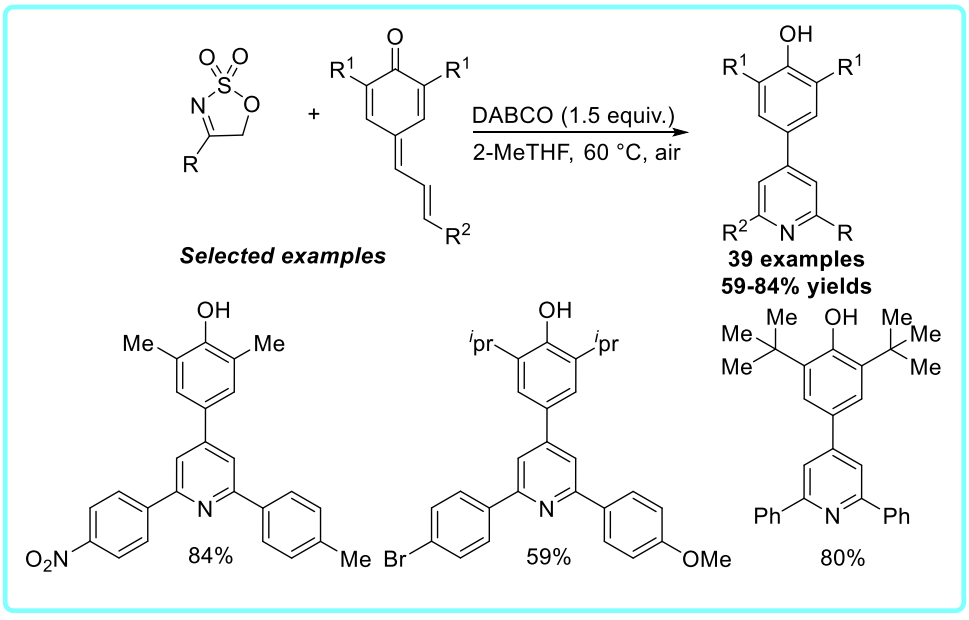

Scheme 1.22. One-pot synthesis of 2,4,6-trisubstituted pyridines.

In 2020, Qi and co-workers demonstrated a novel [3+3] cyclization process that involved the activation of alkynals using NHC as an organocatalyst in the presence of base followed by cyclization with N-tosyl-2-aminoacrylate in the presence of oxidant reaction followed by [3+3] cycloaddition with N-tosyl-2-aminoacrylates. This process concocts the trisubstituted pyridines in modest to good yields (33-73%. (**Scheme 1.23).**[57]

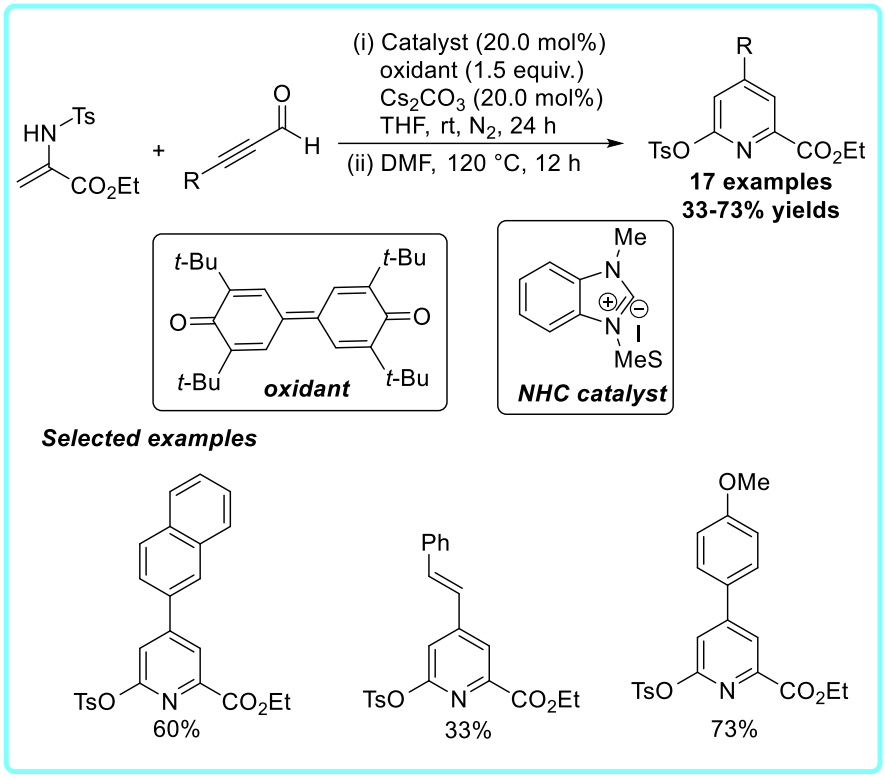

Scheme 1.23. NHC-catalyzed one-pot sequential synthesis of tri-substituted pyridines.

1.3.2.3 Synthesis of functionalized nicotinonitrile derivatives

Among pyridine derivatives, the synthesis of nicotinonitriles has piqued interest in the chemical community due to their wide range of biological actions. This section presents some of the significant methodologies for their efficient access.

A novel technique utilizing diphosphorus tetraiodide and ammonium carbonate in anhydrous carbon disulfide at room temperature has been devised for the

direct conversion of picolinic acid to nicotinonitrile in a 90% yield as disclosed by Telvekar *et al.* in **Scheme 1.24.**[58]

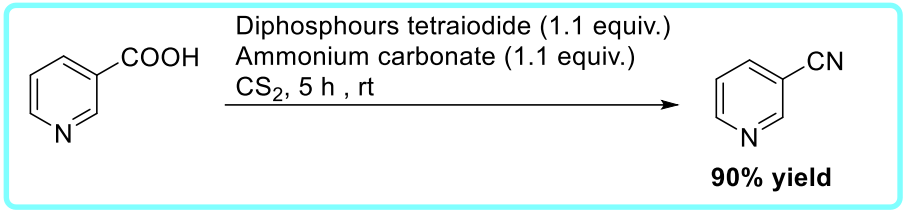

Scheme 1.24. A conversion of picolinic acid to nicotinonitrile.

In 2011, Weidauer *et al.* revealed a CuCl-catalyzed novel conversion of nicotinamide to nicotinonitrile in 99% yield utilizing N-methyl-N-(trimethylsilyl)trifluoroacetamide (MSTFA) as a silylating agent **(Scheme 1.25).**[59]

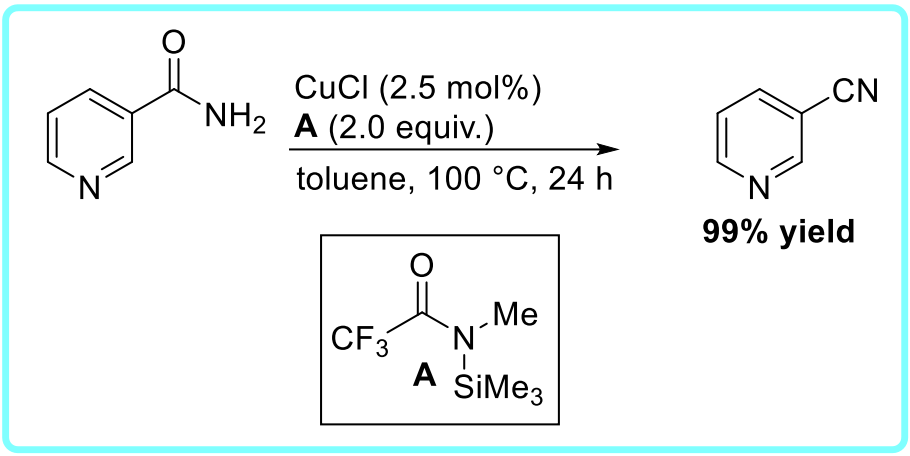

Scheme 1.25. Copper-catalyzed dehydration of nicotinamide.

In 2004, Yang *et al.* invented a novel palladium-catalyzed cyanation reaction of 3-bromopyridine with KCN using a catalytic amount of Bu_3SnCl under heating conditions to afford nicotinonitrile in a 93% yield **(Scheme 1.26)**[60]

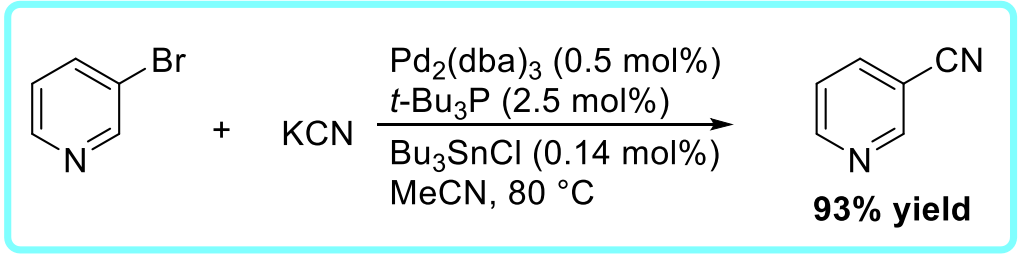

Scheme 1.26. Palladium-catalyzed cyanation of 3-bromopyridine.

In 2013, Msquade *et al.* disclosed a condensation reaction between DMF-DMA and alkylidene malononitriles in the presence of acetic anhydride to form enamine derivatives which are then subjected to cyclization using a mixture of HBr/AcOH at 55 °C. This sequential process affords 2-bromonicotinonitriles in combined yields ranging from 32% to 94% **(Scheme 1.27).**[61]

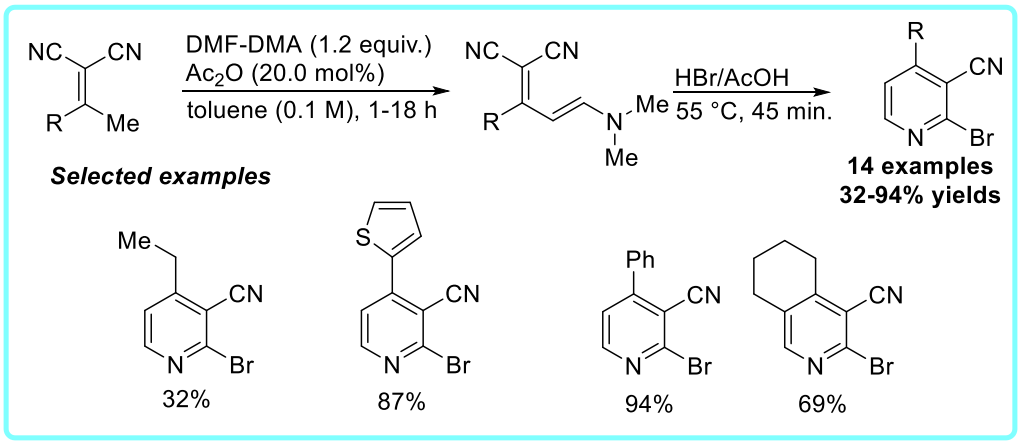

Scheme 1.27. One-pot sequential synthesis of 2-bromonicotinonitriles.

In the same year, Dong *et al.* also reported a quick and easy way to produce multi-substituted 2-aminopyridines with promising chemical yields of 61-79%. This [5C + 1N] cyclization process via intramolecular aza-cyclization-dehydration reaction involves using 2,4-pentadienenitriles and hydroxylamine

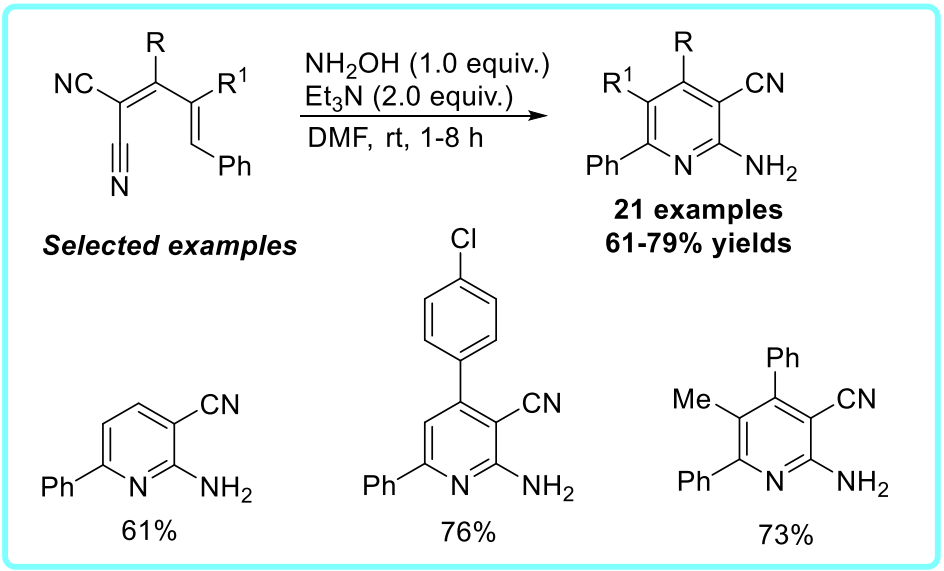

Scheme 1.28. Synthesis of 2-aminopyridines from 2,4-pentadienenitriles.

(NH_2OH) in the presence of triethyl amine at room temperature in **Scheme 1.28).**[62]

In 2015, Villemin and co-workers described a solvent-metal-free one-pot procedure involving arylidene malononitriles, acetophenones, and either ammonium acetate or ammonium carbonate as a N-sourcing agent to make high yields of 3-cyano-2-aminopyridines **(Scheme 1.29).**[63]

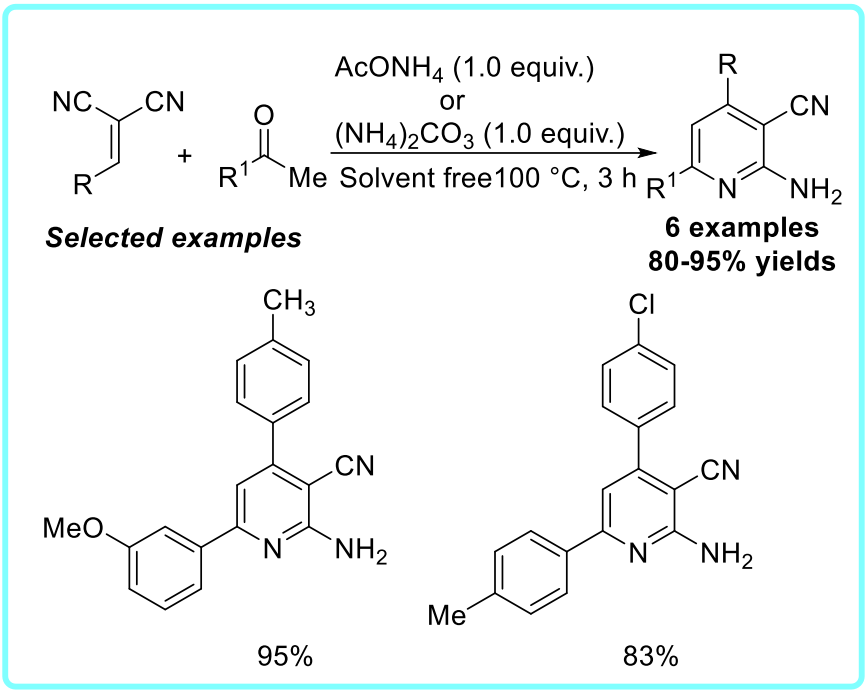

Scheme 1.29. A metal-solvent-free access to 3-cyano-2-aminopyridines.

In 2016, Khalili and co-workers reported a mild, efficient, multicomponent reaction of aldehydes, enolizable cyclic/acyclicketones, malononitrile, and ammonium acetate employing graphene oxide (GO) as a heterogeneous catalyst in water as a green medium., leading a series of 2-amino-3-cyanopyridine derivatives in 75-97% yields. In addition, graphene oxide catalysts could be recycled five times efficiently **(Scheme 1.30).**[64]

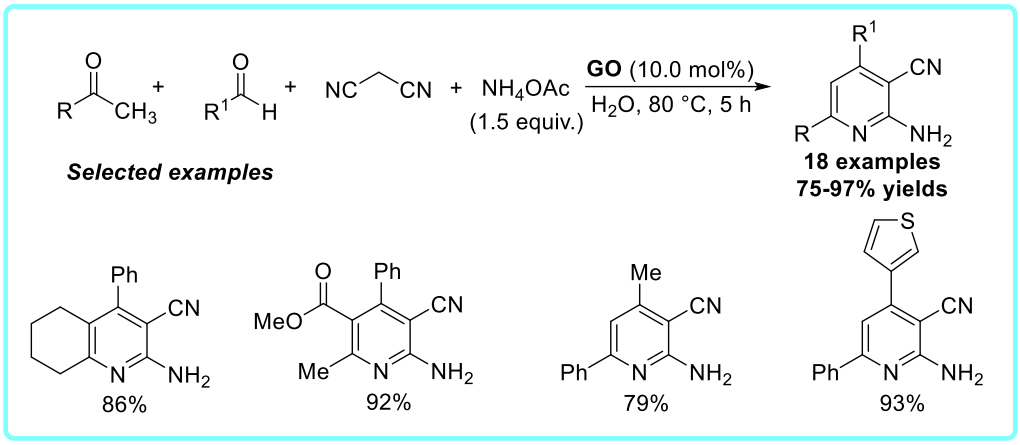

Scheme 1.30. Graphene oxide-catalyzed synthesis of derivatives of 2-amino-3-cyanopyridines.

In 2019, Rawat *et al.* devised a solvent-free CuI@Al_2O_3-nanocatalyzed one-pot three-component method between oxime acetates, aldehydes, and malononitrile at 60 °C. This green process delivers 71-89% yields of 2-aminonicotinonitriles under neat conditions without adding additives. This method has advantages regards to a broad substrate range, high yields, and shorter reaction time **(Scheme 1.31).**[65]

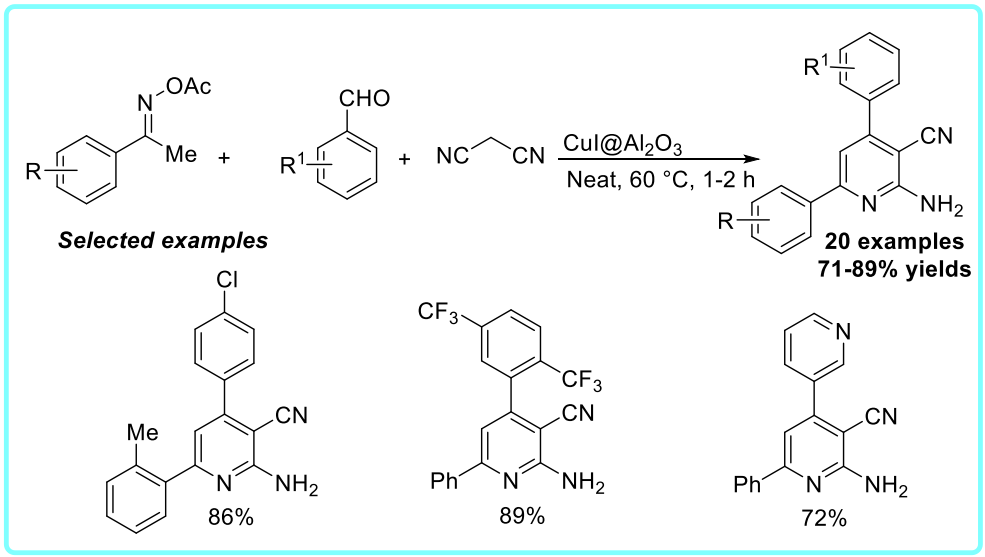

Scheme 1.31. MCR approach to 2-aminonicotinonitrile derivatives using a CuI@Al_2O_3 nanocatalyst.

In 2019, Zhang and his colleagues developed a simple Cu(I)-catalyzed cyclization of ketoximes with tetracyanoethylene (TCNE) in the presence of Na_2SO_4 in toluene at 120 °C, providing 2-amino-3,4-dicyanopyridines with a variable range of yields (28-61%). This cyclization technique tolerates smoothly a variety of functional groups **(Scheme 1.32).**[66]

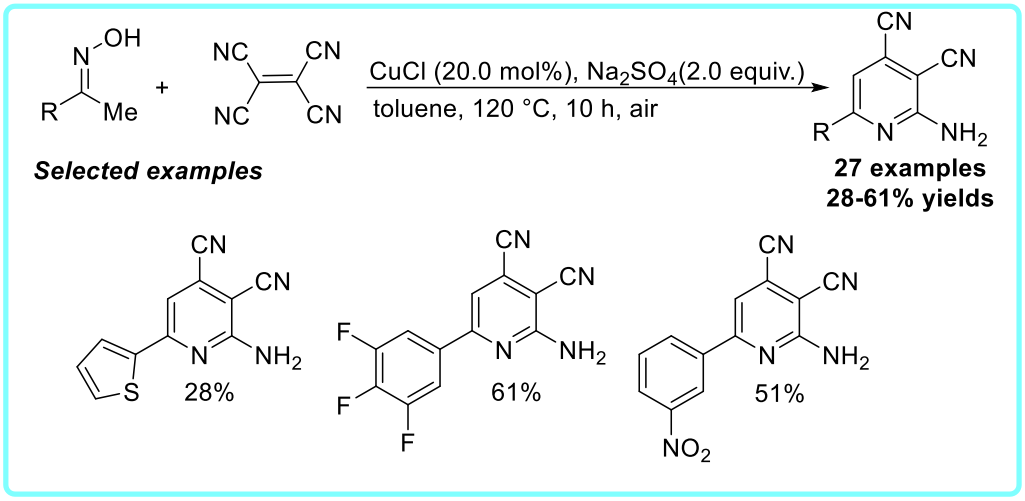

Scheme 1.32. CuCl-catalyzed one-pot synthesis of 2-amino-3,4-dicyanopyridines.

In 2021, Ghosh *et al.* utilized *β*-cyclodextrin as a bio-based catalyst for synthesizing 2-amino-4,6-diphenylnicotinonitrile derivatives from acetones, aldehydes, malononitrile, and NH_4OAc in water under heating conditions. This process has several benefits, such as no need for additional oxidants, metal-free, and avoiding toxic and volatile organic solvents, making it environmentally benign **(Scheme 1.33).**[67]

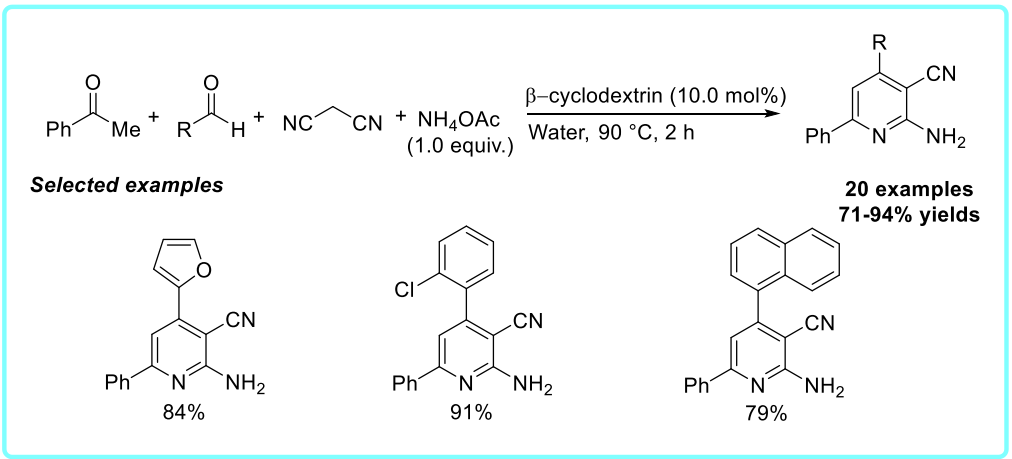

Scheme 1.33. Metal-free MCR approach to 2-amino-4,6-diphenylnicotinonitriles.

In 2021, Wang and co-workers invented a metal-free robust annulation method for accessing 5*H*-chromeno[2,3-*b*]pyridine-3-carbonitriles. The use of piperidine promotes Michael addition−cyclization-aromatization process between 2-amino-4*H*-chromen-4-ones and arylidene malononitriles in DMF at 120 °C, leading to fused pyridine derivatives in 76-88% yields **(Scheme 1.34).**[68]

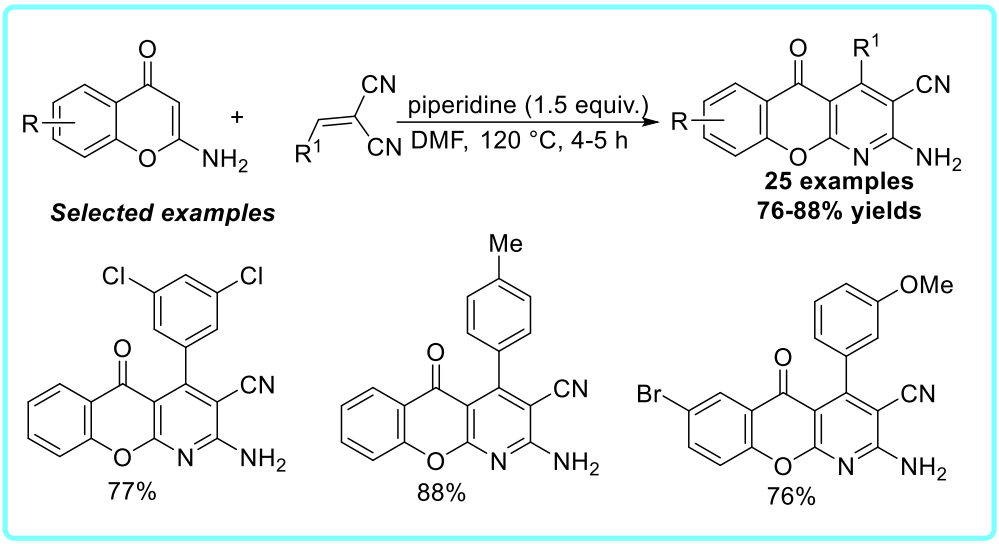

Scheme 1.34. Synthesis of 2-amino-5*H*-chromeno[2,3-*b*]pyridine-3-carbonitriles.

1.3.3. Synthesis of functionalized aziridine derivatives

1.3.3.1 Synthesis of aziridines by intramolecular cyclization of 2-aminoalcohols

In 2002, Bieber *et al.* presented base-promoted two complementary one-pot processes that led to (*S*)-N-tosyl aziridines from optically active (*S*)-2-amino alcohols using an excess amount of TsCl and K_2CO_3 or KOH in MeCN (method A) or aqueous CH_2Cl_2(method B). The obtained yields using method A are generally much higher than method B, as shown in **Scheme 1.35**.[69]

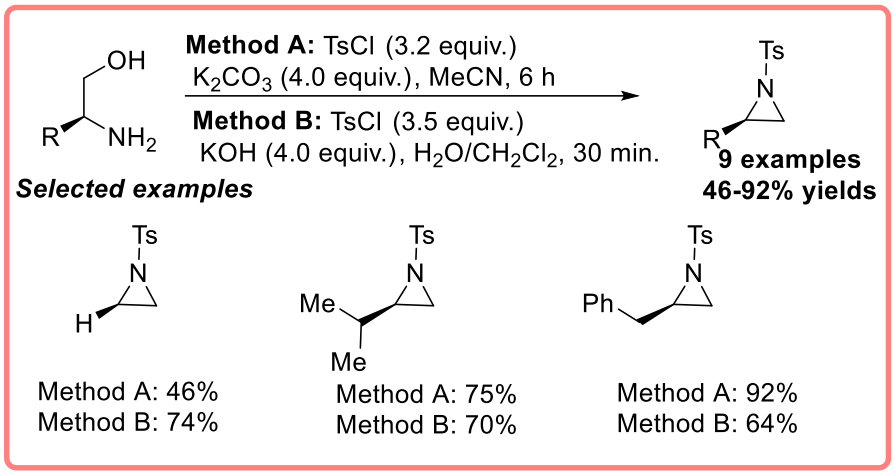

Scheme 1.35. Direct synthesis of (*S*)-N-tosyl aziridines using (*S*)-amino alcohols.

In 2010, Xu *et al.* erected a mild, one-pot, two-step aziridination process from vicinal amino alcohols in the presence of chlorosulfonic acid to form the corresponding sulfate esters, which are subsequently treated with inorganic base either NaOH or Na_2CO_3, resulting in substituted aziridines in moderate to high yields (12-81%) in **Scheme 1.36.**[70]

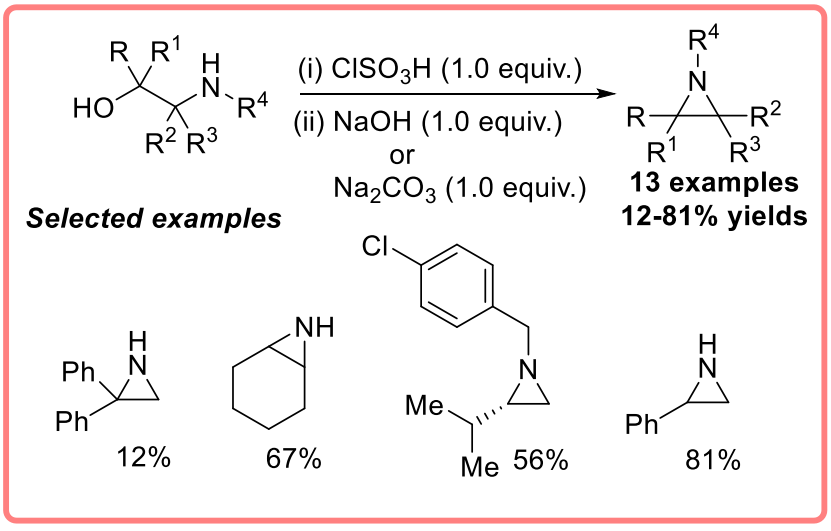

Scheme 1.36. Conversion of amino alcohols into aziridines.

1.3.3.2 Synthesis of aziridines by intramolecular cyclization of chloroamines

In 2007, Kimpe *et al.* synthesized a chiral aziridine in an excellent yield (88%) with high diastereoselectivity (98:2 dr) through the reduction of α-chloro (R_S)-*N*-*tert*-butanesulfinylimine using $NaBH_4$ in MeOH to form (R_S, *S*)-β-chloro sulfinamide, which was easily cyclized in the presence of KOH, leading to a targeted aziridine **(Scheme 1.37).**[71]

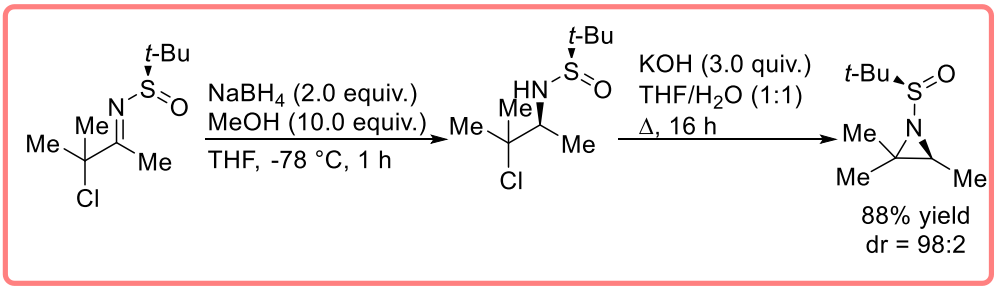

Scheme 1.37. Access to chiral aziridine from *N*-*tert*-butanesulfinyl α-chloro imine.

In 2011, Antilla *et al.* reported a biphenanthrol (VAPOL) magnesium phosphate salt-catalyzed asymmetric aza-Darzens reaction involving aldamines and 3-chloropentane-2,4-dione in THF, followed by intramolecular cyclization assisted by DMAP as a base. This sequential process leads to aziridines in 52-78% yields and moderate to high enantiomeric excess (57-92% ee) **(Scheme 1.38).**[72]

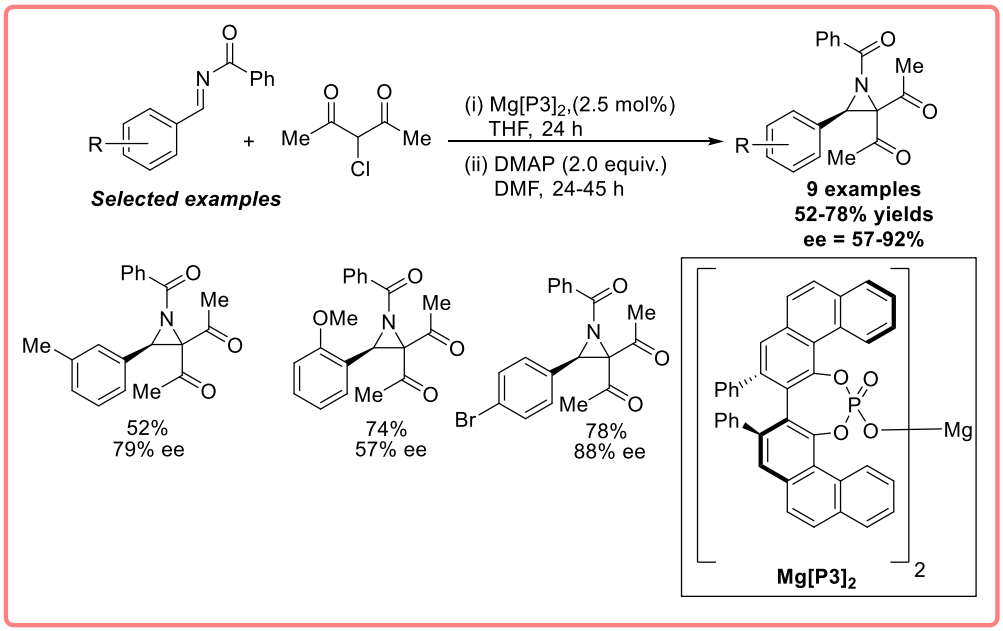

Scheme 1.38. Enantioselective synthesis of aziridines by using a biphenanthrol magnesium phosphate salt.

In 2017, Trost *et al.* invented a one-pot stereospecific aziridination process using optically active 1-chloro-2-amino derivative triggered by either Cs_2CO_3 (method A) or NaH (method B) as a base to obtain excellent yields of trisubstituted *cis*-aziridines with outstanding diastereoselectivities **(Scheme 1.39).**[73]

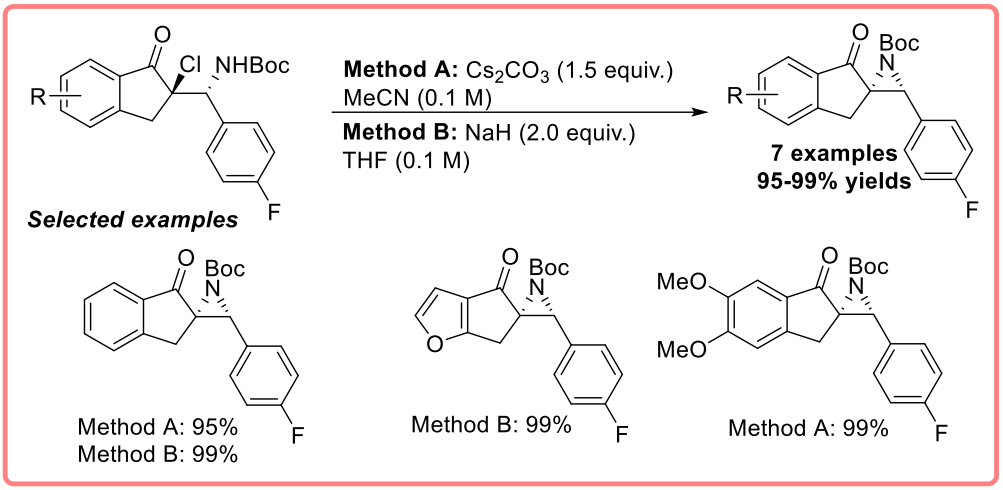

Scheme 1.39. Asymmetric synthesis of trisubstituted aziridines.

In 2001, Prabhakar *et al.* documented a mild aziridination reaction involving an array of olefins and bromamine T as the nitrogen atom transfer reagent using a catalytic amount of palladium(II), capable of producing N-tosyl-2-substituted aziridines with satisfactory yields **(Scheme 1.40).**[74]

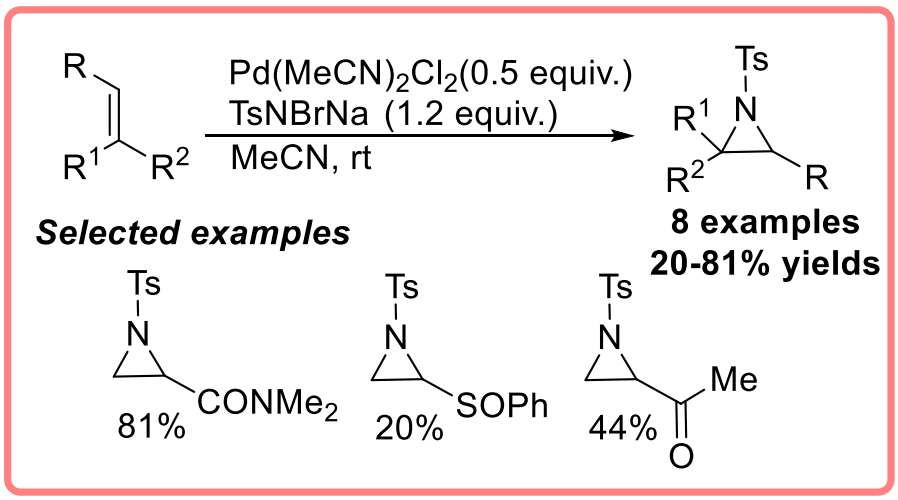

Scheme 1.40. Pd(II)-catalyzed aziridination of olefins with bromamine T.

In 2006, Shi *et al.* established a metal-free, efficient aziridination of chalcones using O-Mesitylenesulfonylhydroxylamine as an NH-transfer reagent in the presence of NMM and KOH at room temperature to produce aziridine derivatives in moderate to high yields. The tertiary amine might react with MSH to generate hydrazinium salt, followed by deprotonation in the presence of a base to form an anionic aminimide. Then, it undergoes addition-cyclization with chalcone, which leads to the aziridine derivative proposed by the authors **(Scheme 1.41).**[75]

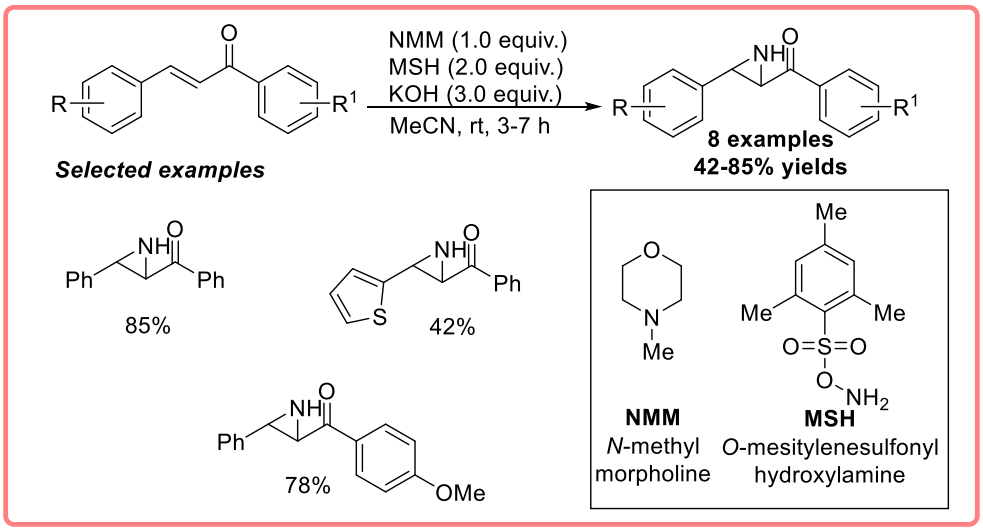

Scheme 1.41. Aziridination of chalcones.

In 2021, McLaughlin *et al.* developed an exciting method for synthesizing previously unknown functionalized aziridine derivatives in good to excellent yields (68-92%). At room temperature, this reaction proceeds at room temperature between allyl sulfonamides and *N*-iodosuccinamide (NIS), resulting in aziridine derivatives **(Scheme 1.42).**[76]

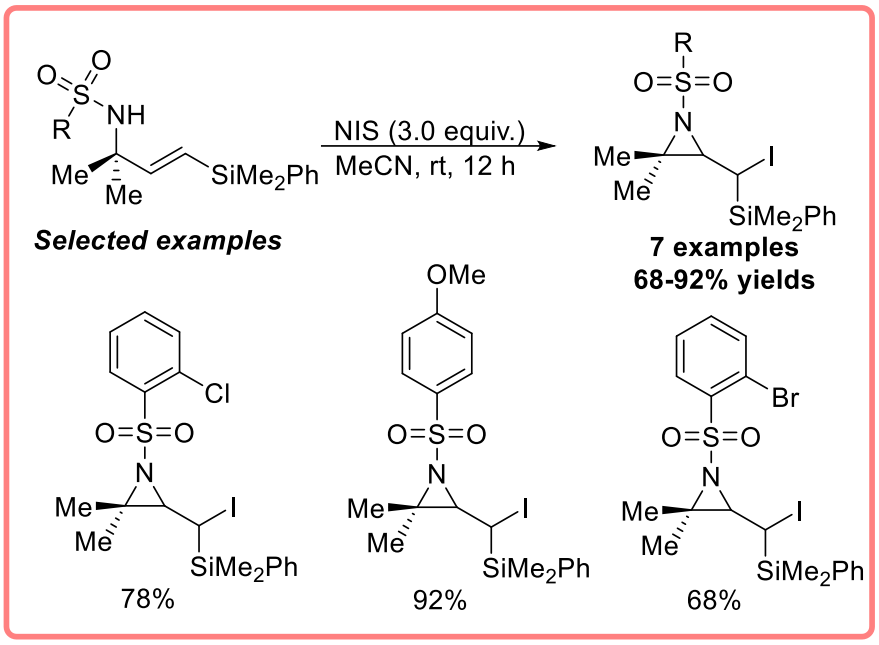

Scheme 1.42. NIS-promoted synthesis of N-protected aziridines.

In 2022, Powers *et al.* established a novel cross-coupling technique for making *N*-aryl aziridines from pyridinium aziridines and arylboronic acids catalyzed by Ni(II)-salt in the presence of 2,4,6-collidine. This cross-coupling reaction allows for the synthesis of aziridines in 24-87% yields with high tolerance of functionalities in **Scheme 1.43.**[77]

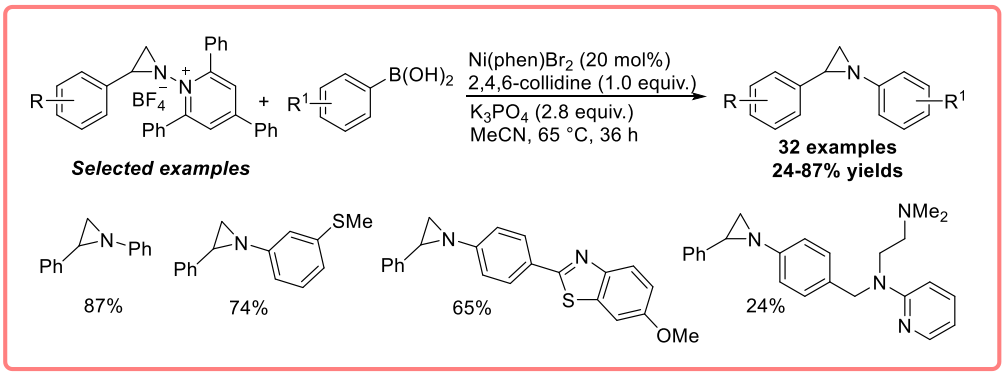

Scheme 1.43. Synthesis of *N*-aryl aziridines via Ni-catalyzed cross-coupling of *N*-pyridinium aziridines.

In 2003, Johnston *et al.* disclosed an atom economic procedure for making *N*-alkyl *cis*-aziridines from ethyl diazoacetate with Schiff base catalyzed by

Brønsted acid, leading to 40-89% yields of aziridines with a variable range of diastereomeric ratios (*cis: trans* = 60:40 to 95:5, **Scheme 1.44).**[78]

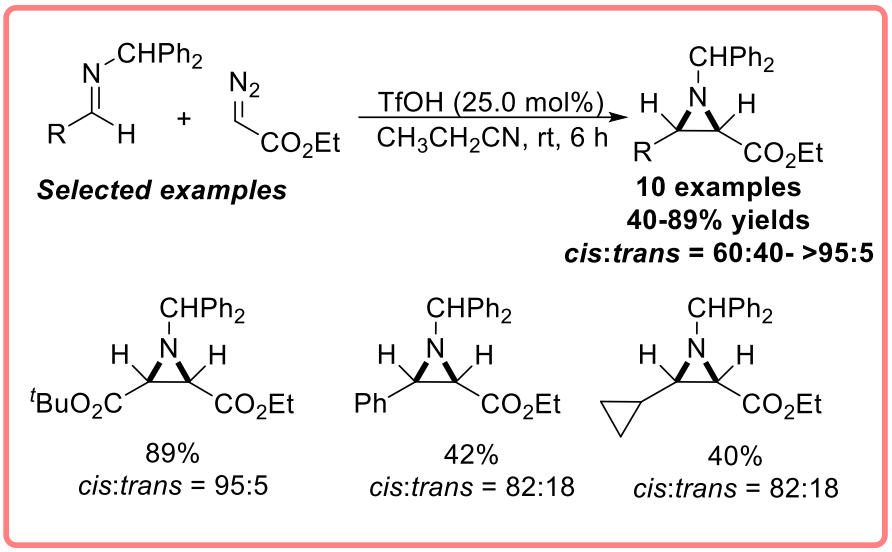

Scheme 1.44. Acid catalyzed aza-Darzens reaction for the synthesis of aziridines.

In 2009, Zhong *et al.* revealed an efficient chiral phosphoric acid-catalyzed, asymmetric aziridination reaction of diazoacetamides with *N*-Boc-imines to bestow various *trans*-aziridines in high to excellent yields (81-97%) and high diastereo- and enantioselectivities (dr>50:1; up to ≤96% ee). This method tolerates various functionalities including acid sensitive *N-Boc* group **(Scheme 1.45).**[79]

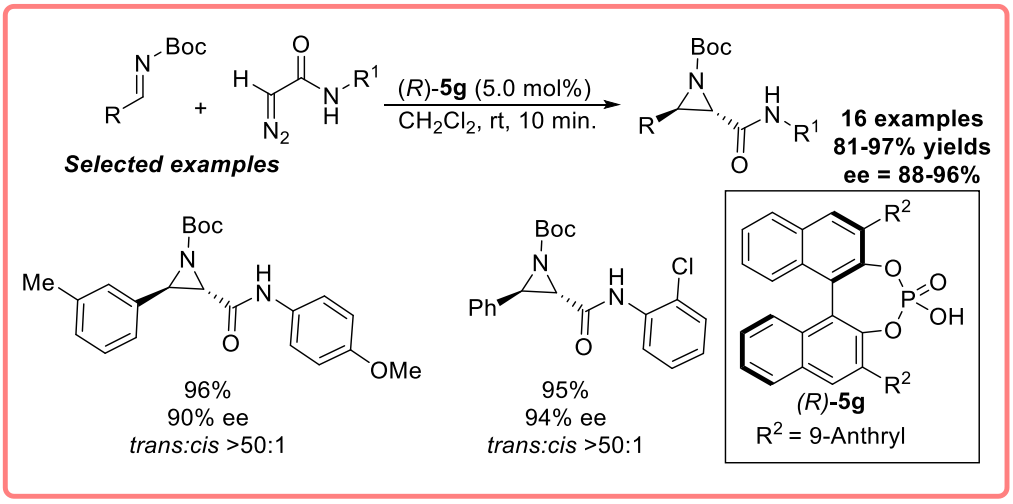

Scheme 1.45. Chiral phosphoric acid-catalyzed asymmetric *trans*-aziridination of diazoacetamides with *N*-Boc-imines.

In 2017, Xu *et al.* developed an efficient diastereoselective aziridination reaction using *N*-sulfonyl imines and α-ketoesters in the presence of $P(NMe_2)_3$ to afford substituted aziridines in 15-99% yields and diastereomeric ratios ranging from 27:73 to 99:1 **(Scheme 1.46).**[80]

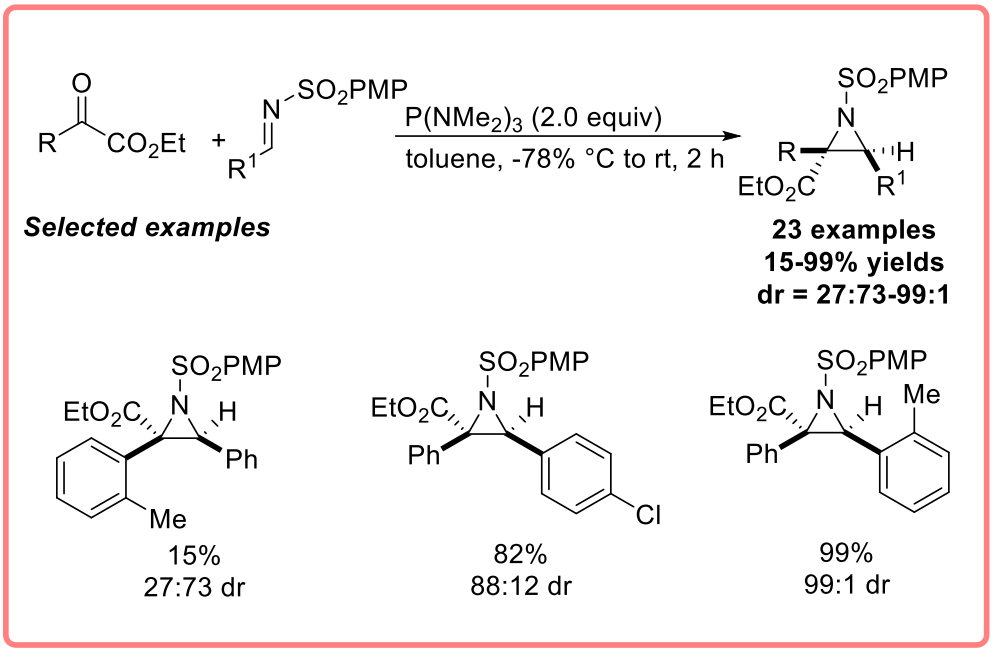

Scheme 1.46. $P(NMe_2)_3$-mediated aziridination of imines.

In 2006, Stockman *et al.* demonstrated a powerful aziridination reaction involving chiral *tert*-butyl-sulfinyl-ketimines and trimethylsulfonium iodide in the presence of NaH in DMSO, capable of making chiral aziridines in good yields (36-73%) with high diastereomeric excess (>95% de, **Scheme 1.47).**[81]

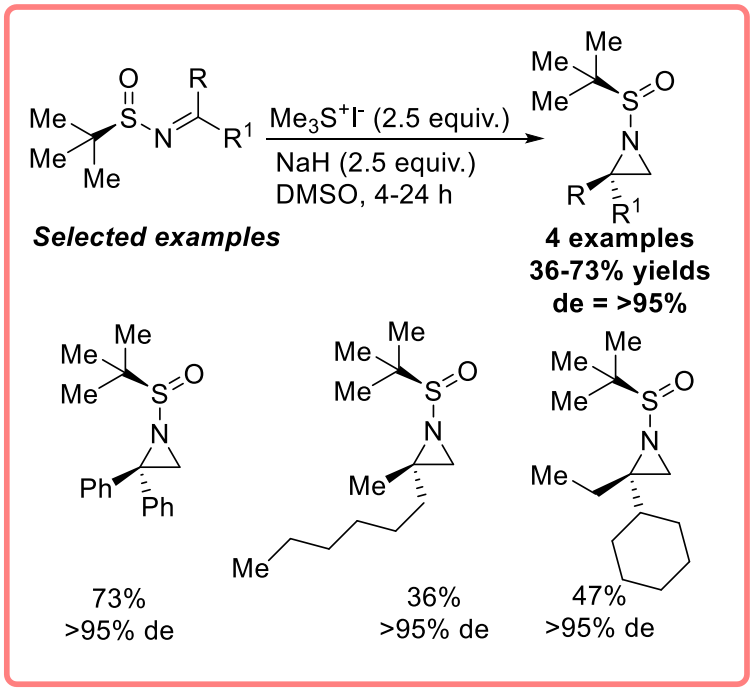

Scheme 1.47. One-pot access to optically active aziridines.

In 2016, Hajra *et al.* reported a highly efficient asymmetric aza-Corey-Chaykovsky reaction of chiral isatin-derived *tert*-butanesulfinyl ketimines with in situ generated benzyl sulfur ylides from benzyl tetrahydrothiophenium bromide in the presence of NaH. This process enables chiral spiro-aziridine

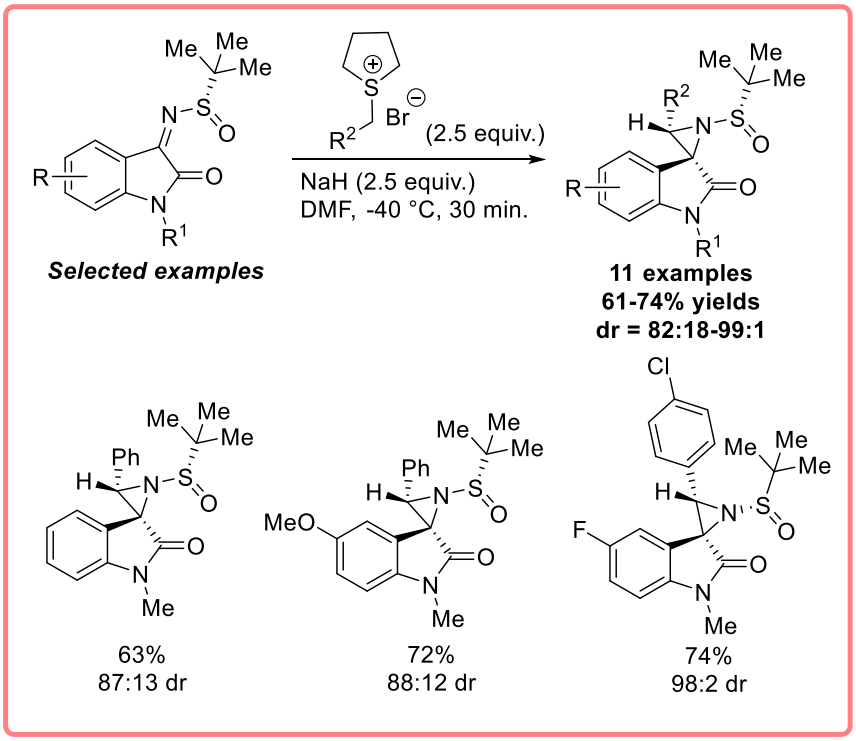

Scheme 1.48. Aza-Corey-Chaykovsky reaction for the synthesis of 3-substituted spiroaziridine oxides.

oxindoles in satisfactory chemical yields and good to excellent distereoselectivities (up to 99:1 dr) as shown in **Scheme 1.48**.[82]

1.4. Conclusion

A comprehensive and systematic review of the literature reveals that various sophisticated and traditional methods have been established to successfully synthesize numerous substituted nitroarenes, pyridine frameworks, and aziridines. While many of these techniques have their own advantages, some also have specific shortcomings. These include the use of harmful and toxic transition-metal catalysts, volatile and hazardous organic solvents, operational difficulties, multi-step procedures, unsatisfactory yields, generation of unwanted side products, need for additional external oxidants and ligands etc. Additionally, many approaches suffer from inherent challenges, including poor atom-economy, limited substrate scope, inadequate regio- and diastereoselectivities, and intrinsic substrate combinations. Therefore, searching for straightforward, practical, pot-economy methods for accessing pharmacologically and synthetically value-added compounds, particularly nitrobenzenes, pyridines, and aziridines under mild conditions is an crucial research object for organic and medicinal chemists. Thus, we are highly inspired to resolve the shortcomings above.

1.5 References

1. Nicolaou K. C., Chena J. S. (2009), The art of total synthesis through cascade reactions, *Chem. Soc. Rev.*, 38, 2993-3009 (DOI: 10.1039/b903290h).

2. Jeanty M., Enders D. Grondal C. (2010), Organocatalytic cascade reactions as a new tool in total synthesis. *Nat. Chem.,* 2, 167-178 (DOI: 10.1038/nchem.539).

3. Hayashi Y. (2016), Pot economy and one-pot synthesis, *Chem. Sci.,* 7, 866-880 (DOI: 10.1039/C5SC02913a).

4. Robinson R., (1917), A synthesis of tropinone, *J. Chem. Soc.*, Trans., 111, 762-768 (DOI: 10.1039/CT9171100762).

5. Walji A. M., MacMillan D. W. C. (2007), Strategies to bypass the taxol problem. enantioselective cascade catalysis, a new approach for the efficient construction of molecular complexity, *Synlett,* 10, 1477-1489 (DOI: 10.1055/s2007-980382).

6. Hunger K. (2003), *Industry Dyes: Chemistry, Properties and Applications*, Wiley-VCH, Weinheim.

7. Lawrence S. A. (2004) *Amines: Synthesis, Properties and Application*, Cambridge University Press, Cambridge.

8. Vogt P.F., Gerulis J. J. (2005), *Amines, Aromatic, in Ullmann's Encyclopedia of Industrial Chemistry,* Wiley-VCH, Weinheim.

9. Ju K.-S., Parales R. E. (2010), Nitroaromatic compounds, from synthesis to biodegradation, *Microbiol. Mol. Biol. Rev.*, 74, 250-272 (DOI: 10.1128/MMBR.00006-10).

10. Remennikov G. Y. (2017), Synthesis of fused pyrazoles *via* intramolecular cyclization of appropriately *ortho*-substituted nitroarenes and nitroheteroarenes, *Chem. Heterocycl. Compd.*, 53, 101-115 (DOI: 10.1007/s10593-017-2028-6).

11. Muto K., Okita T., Yamaguchi J. (2020), Transition-metal-catalyzed denitrative coupling of nitroarenes, *ACS Catal.*, 10, 9856-9871 (DOI: 10.1021/acscatal.0c02990).

12. Olender D., Zwawiak J., Zaprutko L. (2018), Multidirectional efficacy of biologically active nitro compounds included in medicines, *Pharmaceuticals*, 11, 54 (DOI: 10.3390/ph11020054).

13. Nepali K., Lee H.-Y., Liou J.-P. (2019), Nitro-group-containing drugs, *J. Med. Chem.*, 62, 2851-2893 (DOI: 10.1021/acs.jmedchem.8b00147).

14. Penning T. M., Su A. L., El-Bayoumy K. (2022), Nitroreduction: a critical metabolic pathway for drugs, environmental pollutants, and explosives, *Chem. Res. Toxicol.*, 35, 1747-1765 (DOI: 10.1021/acs.chemrestox.2c00175).

15. Henry G. D. (2004), De novo synthesis of substituted pyridines, *Tetrahedron*, 60, 6043-6061 (DOI: 10.1016/j.tet.2004.04.043).

16. Hill M. D. (2010), Recent strategies for the synthesis of syridine derivatives, *Chem. Eur. J.*, 16, 12052-12062 (DOI: 10.1002/chem.201001100).

17. Allais C., Grassot J.-M., Rodriguez J., Constantieux T. (2014), Metal-free multicomponent syntheses of pyridines, *Chem. Rev.*, 114, 10829-10868 (DOI: 10.1021/cr500099b).

18. Khan E. (2021), Pyridine derivatives as biologically active precursors; organics and selected coordination complexes, *ChemistrySelect*, 6, 3041-3064 (DOI: 10.1002/slct.202100332).

19. Baumann M., Baxendale I. R. (2013), An overview of the synthetic routes to the best selling drugs containing 6-membered heterocycles, *Beilstein J. Org. Chem.*, 9, 2265-2319 (DOI: 10.3762/bjoc.9.265).

20. Gholap A. R., Toti K. S., Shirazi F., Kumari R., Bhat M. K., Deshpande M. V., Srinivasan K. V. (2007), Synthesis and evaluation of antifungal properties of a series of the novel 2-amino-5-oxo-4-phenyl-5,6,7,8 tetrahydroquinoline-3-carbonitrile and its analogues, *Bioorg. Med. Chem.*, 15, 6705-6715 (DOI: 10.1016/j.bmc.2007.08.009).

21. Deng J., Sanchez T., Al-Mawsawi L. Q., Dayam R., Yunes R. A., Garofalo A., Bolger M. B., Neamati N. (2007), Discovery of structurally diverse HIV-1 integrase inhibitors based on a chalcone pharmacophore, *Bioorg. Med. Chem.*, 15, 4985-5002 (DOI: 10.1016/j.bmc.2007.04.041).

22. Fleming F. F., Yao L., Ravikumar P. C., Funk L., Shook B. C. (2010), Nitrile-containing pharmaceuticals: efficacious roles of the nitrile pharmacophore, *J. Med. Chem.*, 53, 7902-7917 (DOI: 10.1021/jm100762r).

23. Murata T., Shimada M., Sakakibara S., Yoshino T., Kadono H., Masuda T., Shimazaki M., Shintani T., Fuchikami K., Sakai K., Inbe H., Takeshita K., Niki T., Umeda M., Bacon K. B., Ziegelbauer K. B., Lowinger T. B. (2003), Discovery of novel and selective IKK-β serine-threonine protein kinase

inhibitors. Part 1, *Bioorg. Med. Chem. Lett.*, 13, 913-918 (DOI: 10.1016/S0960-894X(02)01046-6).

24. Kametani T., Honda T. (1986), Application of aziridines to the synthesis of natural products, *Adv. Heterocycl. Chem.*, 39, 181-236 (DOI: 10.1016/S0065-2725(08)60765-5).

25. Coleman R. S., Kong J.-S., Richardson T. E. (1999), Synthesis of naturally occurring antitumor agents: stereo controlled synthesis of the azabicyclic ring system of the azinomycins, *J. Am. Chem. Soc.*, 121, 9088-9095 (DOI: 10.1021/ja992274w).

26. Sweeney J. B. (2002), Aziridines: epoxides' ugly cousins?, *Chem. Soc. Rev.*, 31, 247-258 (DOI: 10.1039/b006015l).

27. Ismail F. M. D., Levitsky D. O., Dembitsky V. M. (2009), Aziridine alkaloids as potential therapeutic agents, *Eur. J. Med. Chem.*, 44, 3373-3387 (DOI: 10.1016/j.ejmech.2009.05.013).

28. Thibodeaux C. J., Chang W.-C., Liu H.-W. (2012), Enzymatic chemistry of cyclopropane, epoxide, and aziridine biosynthesis, *Chem. Rev.*, 112, 1681-1709 (DOI: 10.1021/cr200073d).

29. Zang H., Gates K. S. (2000), DNA Binding and alkylation by the "left half" of azinomycin B, *Biochemistry*, 39, 14968-14975 (DOI: 10.1021/bi001998d).

30. Dank C., Ielo L. (2023), Recent advances in the accessibility, synthetic utility, and biological applications of aziridines, *Org. Biomol. Chem.*, 21, 4553-4573 (DOI: 10.1039/d3ob00424d).

31. Aggarwal V. K., Vasse J.-L. (2003), Asymmetric sulfur ylide mediated aziridination: application in the synthesis of the side chain of taxol, *Org. Lett.*, 5, 3987-3990 (DOI: 10.1021/ol035554w).

32. Yeung Y.-Y., Hong S., Corey E. J. (2006), A short enantioselective pathway for the synthesis of the anti-influenza neuramidase inhibitor oseltamivir from 1,3-butadiene and acrylic acid, *J. Am. Chem. Soc.*, 128, 6310-6311 (10.1021/ja0616433).

33. Degennaro L., Trinchera P., Luisi R. (2014), Recent advances in the stereoselective synthesis of aziridines, *Chem. Rev.*, 114, 7881-7929 (DOI: 10.1021/cr400553c).

34. Booth G. (2000), Nitro compounds, aromatic, *Wiley-VCH Verlag GmbH & Co. KGaA, Weinheim*, (DOI: 10.1002/14356007.a17_411).

35. Olah G. A., Malhotra R., Narang S. C. (1990), Nitration methods and mechanisms, *Red. Trav. Chim. Pays-Bas*, 109, 594-594 (DOI: 10.1002/recl.19901091207).

36. Kulkarni A. K. (2014), Continuous flow nitration in miniaturized devices, *Beilstein J. Org. Chem.*, 10, 405-424 (DOI: 10.3762/bjoc.10.38).

37. Koskin A. P., Mishakov I. V., Vedyagin A. A. (2016), In search of efficient catalysts and appropriate reaction conditions for gas phase nitration of benzene, *Resour. Effic. Technol.*, 2, 118-125 (DOI: 10.1016/j.reffit.2016.07.004).

38. Saito S., Koizumi Y. (2005), Copper-catalyzed coupling of aryl halides and nitrite salts: a mild ullmann-type synthesis of aromatic nitro compounds, *Tetrahedron Lett.*, 46, 4715-4717 (DOI: 10.1016/j.tetlet.2005.05.033).

39. Fors B. P., Buchwald S. L. (2009), Pd-Catalyzed conversion of aryl chlorides, triflates, and nonaflates to nitroaromatics, *J. Am. Chem. Soc.*, 131, 12898-12899 (DOI: 10.1021/ja905768k).

40. Zarei M., Noroozizadeh E., Moosavi-Zare A. R., Zolfigol M. A. (2018), Synthesis of nitroolefins and nitroarenes under mild conditions, *J. Org. Chem.*, 83, 3645-3650 (DOI: 10.1021/acs.joc.7b03289).

41. Zhang K., Budinská A., Passera A., Katayev D. (2020), *N*-Nitroheterocycles: bench-stable organic reagents for catalytic *ipso*-nitration of aryl- and heteroarylboronic acids, *Org. Lett.*, 22, 2714-2719 (DOI: 10.1021/acs.orglett.0c00671).

42. Liu Y.-K., Lou S.-J., Xu D.-Q., Xu Z.-Y. (2010), Regiospecific synthesis of nitroarenes by palladium-catalyzed nitrogen-donor-directed aromatic C-H nitration, *Chem. Eur. J.*, 16, 13590-13593 (DOI: 10.1002/chem.201002581).

43. Lu Y., Li Y., Zhang R., Jin K., Duan C. (2013), Regioselective *ortho*-nitration of N-phenyl carboxamides and primary anilines using bismuth nitrate/acetic anhydride, *Tetrahedron*, 69, 9422-9427 (DOI: 10.1016/j.tet.2013.08.076).

44. Li Y.-X., Li L.-H., Yang Y.-F., Hua H.-L., Yan X.-B., Zhao L.-B., Zhang J.-B., Ji F.-J., Liang Y.-M. (2014), Direct oxidative nitration of aromatic sulfonamides under mild conditions, *Chem. Commun.*, 50, 9936-9938 (DOI: 10.1039/c4cc03784g).

45. Reddy K. R., Uma C., Venkateshwar M. M., Kantam M. L. (2009), Selective oxidation of aromatic amines to nitro derivatives using potassium iodide-*tert*-butyl hydroperoxide catalytic system, *Adv. Synth. Catal.*, 351, 93-96 (DOI: 10.1002/adsc.200800641).

46. Gupta S., Ansari A., Sashidhara K. V. (2019), Base promoted peroxide systems for the efficient synthesis of nitroarenes and benzamides, *Tetrahedron Lett.*, 60, 151076 (DOI: 10.1016/j.tetlet.2019.151076).

47. Henninger A. (1877) *Ber. Dtsch. Chem. Ges.*, 10, 727-737 (DOI: 10.1002/cber.187701001202).

48. Hantzsch A. (1881), Condensationsprodukte aus aldehydammoniak und ketonartigen verbindungen, *Ber. Dtsch. Chem. Ges.*, 14, 1637-1638 (DOI: 10.1002/cber.18810140214).

49. Chichibabin, A. E.; Zeide, O. A. J. (1906), Condensation of carbonyl compounds with ammonia or amines under pressure to form pyridine derivatives; the reaction is reversible and produces different pyridine derivatives along with byproducts, *Russ. Phys.-Chem. Soc.*, 37, 1229.

50. Bohlmann F., Rahtz D. (1957), Über eine neue pyridinsynthese, *Chem. Ber.*, 90, 2265-2272 (DOI: 10.1002/cber.19570901021).

51. Kröhnke F. (1976), The specific synthesis of pyridines and oligopyridines, *Synthesis*, 1-24 (DOI: 10.1055/s-1976-23941).

52. Tu S., Li T., Shi F., Fang F., Zhu S., Wei X., Zong Z. (2005), An efficient improve for the kröhnke reaction: one-pot synthesis of 2,4,6-triarylpyridines using raw materials under microwave Irradiation, *Chem. Lett.,* 34, 732-733. (DOI: 10.1246/cl.2005.732).

53. Lu J.-Y., Arndt H.-D. (2007), Hetero diels-alder synthesis of 3-hydroxypyridines: access to the nosiheptide core, *J. Org. Chem.,* 72, 4205-4212 (DOI: 10.1021/jo0703505).

54. Komine Y., Tanaka K. (2010), Rhodium-catalyzed complete regioselective intermolecular cross cyclotrimerization of aryl ethynyl ethers and nitriles or isocyanates at room temperature, *Org. Lett.,* 12, 1312-1315 (DOI:10.1021/ol100182u).

55. Majee D., Biswas S., Mobin S. M., Samanta S. (2016), Access to 4,6-diarylpicolinates via a domino reaction of cyclic sulfamidate imines with morita–baylis–hillman acetates of nitroolefins/nitrodienes, *J. Org. Chem.,* 10, 4378-4385 (DOI: 10.1021/acs.joc.6b00472).

56. Guin S., Gudimella S. K., Samanta S. (2020), 1,6-Addition of vinyl p-quinone methides with cyclic sulfamidate imines: access to 4-hydroxyaryl-2,6-diarylpyridines, *Org. Biomol. Chem.,* 18, 1337-1342 (DOI: 10.1039/c9ob02708d).

57. Li J.-H., Duan X.-Y., Tian Z.-H., Zheng Y.-F., Qi J. (2020), N-Heterocyclic carbene-catalyzed activation of ynals for the construction of functional pyridines, *Asian J. Org. Chem.,* 9, 385-389 (DOI: 10.1002/ajoc.201900693).

58. Telvekar V. N., Rane R. A. (2007), A novel system for the synthesis of nitriles from carboxylic acids, *Tetrahedron Lett.,* 48, 6051-6053 (DOI: 10.1016/j.tetlet.2007.06.108).

59. Enthaler S., Weidauer M. (2011), Copper-catalyzed dehydration of primary amides to nitriles, *Catal. Lett.,* 141, 1079-1085 (DOI 10.1007/s10562-011-0660-9).

60. Yang C., Williams J. M. (2004), Palladium-catalyzed cyanation of aryl bromides promoted by low-level organotin compounds, *Org. Lett.*, 6, 2837-2840 (DOI: 10.1021/ol049621d).

61. Longstreet A. R., Campbell B. S., Gupton B. F., McQuade D. T. (2013), Improved synthesis of mono- and disubstituted 2-halonicotinonitriles from alkylidene malononitriles, *Org. Lett.*, 2013, 15, 5298-5301 (DOI: 10.1021/ol4025265).

62. Xin X., Huang P., Xiang D., Zhang R., Zhao F., Zhang N., D. Dong. (2013), [5C + 1N] Annulation of 2,4-pentadienenitriles with hydroxylamine: a synthetic route to multi-substituted 2-aminopyridines, *Org. Biomol. Chem.*, 2013, 13, 1001-1006 (DOI: 10.1039/c2ob27053f).

63. Belhadj F., Kibou Z., Cheikh N., Choukchou-Braham N., Villemin D. (2015), Convenient access to new 4-substituted aminopyrido[2,3-d] pyrimidine derivatives, *Tetrahedron Lett.*, 56, 5999-6002 (DOI: 10.1016/j.tetlet.2015.09.042).

64. Khalili D. (2016), Graphene oxide: a reusable and metal-free carbocatalyst for the one-pot synthesis of 2-amino-3-cyanopyridines in water, *Tetrahedron Lett.*, 57, 1721-1723 (DOI: 10.1016/j.tetlet.2016.03.020).

65. Rawat M., Rawat D. S. (2019), CuI@Al_2O_3 catalyzed synthesis of 2-aminonicotinonitrile derivatives under solvent free condition, *Tetrahedron Let.t*, 60, 1153-1157 (DOI: 10.1016/j.tetlet.2019.03.048).

66. Han Z., Lv J., Zhang J. (2019), One-pot synthesis of 2-amino-3,4-dicyanopyridines from ketoximes and tetracyanoethylene via Cu(I)-catalyzed cyclization, *Tetrahedron*, 75, 2162-2168 (DOI: 10.1016/j.tet.2019.02.032).

67. Mitra B., Pariyar G. C., Ghosh P. (2021), β-Cyclodextrin: a supramolecular catalyst for metal-free approach towards the synthesis of 2- amino-4,6-diphenylnicotinonitriles and 2,3- dihydroquinazolin-4(1*H*)-one, *RSC Adv.*, 11, 1271-1281 (DOI: 10.1039/d0ra09562a).

68. Zhang D., Luo N., Gan J., Wan X., Wang C. (2021), Piperidine-mediated [3+3] Cyclization of 2-amino-4*H*-chromen-4-ones and

2-benzylidenemalononitriles: to access2-aminochromeno[2,3-*b*]pyridine derivatives, *J. Org. Chem.,* 86, 9218-9224 (DOI: 10.1021/acs.joc.1c00797).

69. Bieber L. W., De Araújo M. C. F. (2002), Short and efficient synthesis of optically active N-tosyl aziridines from 2-amino alcohols, *Molecules,* 7, 902-906 (DOI: 10.3390/71200902).

70. Li X., Chen N., Xu J. (2010), An improved and mild wenker synthesis of aziridines, *Synthesis,* 10, 3423-3428 (DOI: 10.1055/s-0030-1257913).

71. Denolf B., Leemans E., Kimpe N. De. (2007), Asymmetric synthesis of aziridines by reduction of *N-tert*-butanesulfinyl α-chloro imines, *J. Org. Chem.,* 72, 3211-3217 (DOI: 10.1021/jo0624795).

72. Larson S. E., Li G., Rowland G. B., Junge D., Huang R., Woodcock H. L., Antilla J. C. (2011), Catalytic asymmetric aza-darzens reaction with a vaulted biphenanthrol magnesium phosphate salt, *Org. Lett.,* 13, 2188-2191 (DOI: 10.1021/ol200407r).

73. Trost B. M., Saget T., Hung C.-I. (2017), Efficient access to chiral trisubstituted aziridines via catalytic enantioselective aza-darzens reactions, *Angew. Chem. Int. Ed.,* 56, 2440-2444 (DOI: 10.1002/anie.201607845).

74. Antunes A. M. M., Marto S. J. L., Branco P. S., Prabhakar S., Lobo A. M. (2001), Palladium(II)-promoted aziridination of olefins with bromamine T as the nitrogen transfer reagent, *Chem. Commun.,* 2001, 405-406 (DOI: 10.1039/b008701g).

75. Shen Y.-M., Zhao M.-X., Xu J., Shi Y. (2006), An amine-promoted aziridination of chalcones, *Angew. Chem. Int. Ed.,* 45, 8005-8008 (DOI: 10.1002/anie.200602586).

76. Roberts D. D., McLaughlin M. G. (2021), Regioselective synthesis of multifunctional allylic amines; access to ambiphilic aziridine scaffolds, *Org. Lett.,* 23, 4463-4467 (DOI: 10.1021/acs.orglett.1c01398).

77. Tan T., Samanta S., Maity A., Roychowdhury P., Powers D. C. (2022), *N*-aminopyridinium reagents as traceless activating groups in the synthesis of N-aryl aziridines, *Nat. Commun.,* 13, 3341 (DOI: 10.1038/s41467-022-31032-w).

78. Williams A. L., Johnston J. N. (2004), The brønsted acid-catalyzed direct aza-darzens synthesis of *N*-alkyl *cis*-aziridines, *J. Am. Chem. Soc.,* 126, 1612-1613 (DOI: 10.1021/ja0385282).

79. Zeng X., Zeng X., Xu Z., Lu M., Zhong G. (2009), Highly efficient asymmetric *trans*-selective aziridination of diazoacetamides and *N*-Boc-imines catalyzed by chiral brønsted acids, *Org. Lett.,* 11, 3036-3039 (DOI: 10.1021/ol901047w).

80. Jiang J., Liu H., Lu C.-D., Xu Y.-J. (2017), $P(NMe_2)_3$-Mediated aziridination of imines with α-ketoesters for synthesis of aziridine-2-carboxylates, *J. Org. Chem.,* 82, 811-818 (DOI: 10.1021/acs.joc.6b02669).

81. Morton D., Pearson D., Field R. A., Stockman R. A. (2006), Direct synthesis of chiral aziridines from *N*-*tert*-butyl-sulfinylketimines, *Chem. Commun.,* 2006,1833-1835 (DOI: 10.1039/b601527a).

82. Hajra S., Aziz S. M., Jana B., Mahish P., Das D. (2016), Synthesis of chiral spiro-aziridine oxindoles via aza-corey−chaykovsky reaction of isatin derived *N*-*tert*-butanesulfinyl ketimines, *Org. Lett.,* 18, 532-535 (DOI: 10.1021/acs.orglett.5b03564).

Chapter 2

Reversal reactivity of β-alkylnitroalkenes as 1,3-binucleophiles:

application to nitroarenes using organocatalysis

2.1 Introduction

The innovative design and synthesis of nitroarene molecular templates is a long-standing research goal and well-studied research topic in organic chemistry.[1-2] These popular moieties are heavily used to manufacture agrochemicals, dyes, pharmaceuticals, high explosives, plastics, pesticides, feedstocks, and ubiquitous commodities of organic molecules.[1-3] Most importantly, the nitro group on the aromatic ring can be smoothly converted into a wide array of functionalities[4-9] such as amine, azide, amide, hydroxylamine, sulfonamide, azo, nitrile, alkyl, alkenyl, alkynyl, halides as well as various complex heterocycles.[10]In addition, they can inherently participate in S_NAr reactions with various nucleophiles, leading to various functionalized arenes[11-12]**(Figure 2.1).**[13-16]

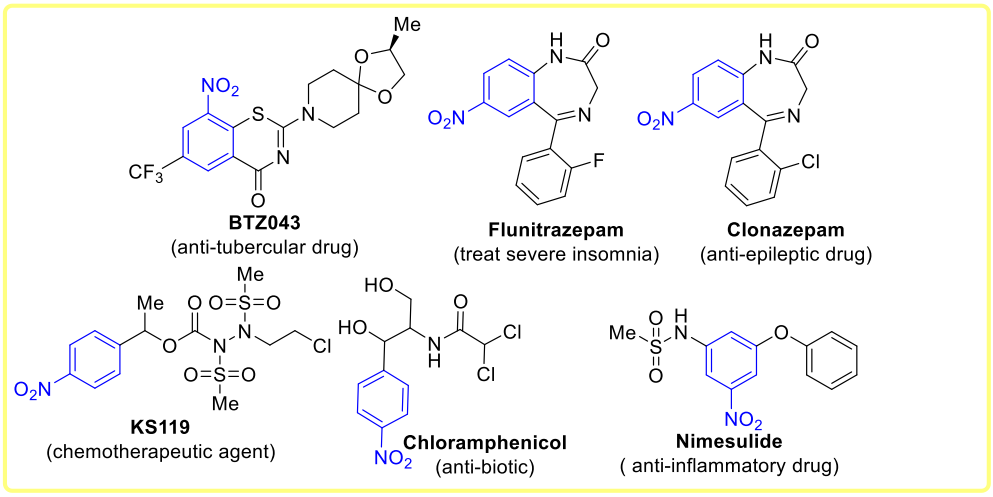

Figure 2.1 Representative examples of a few drugs and bioactive compounds containing nitroarenes molecular templates.

2.2 Review work

Owing to their rich applications as shown earlier section (**Figure 2.1)**, nitroarenes were generally synthesized *via* aromatic electrophilic nitration of arenes using a mixture of excess fuming HNO_3 and H_2SO_4.[17-20] Additionally, various advanced techniques have also been established for the construction of substituted nitroarenes. A few important methods are described in the next section.

2.2.1 Synthesis of nitroarenes

In 2004, Olah *et al.* developed an innovative *ipso*-nitration of arylboronicacids using a mixture of $AgNO_3$ and chlorotrimethylsilane. This process allows for the regioselective synthesis of nitroarenes in moderate to excellent yields (20-90%) **(Scheme 2.1).**[21]

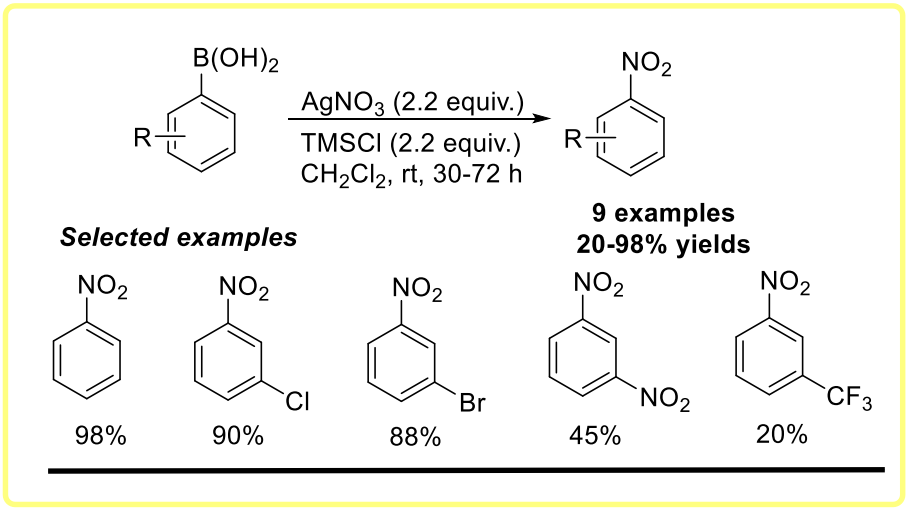

Scheme 2.1. *Ipso*-nitration of arylboronic acids using a mixture of $TMSCl/AgNO_3$.

In 2011, Beller *et. al* described a simple, highly regioselective *ipso*-nitration technique that led to various nitrobenzene derivatives in moderate to high yields (45-87%) involving arylboronic acids using inexpensive *tert*-butyl nitrite at 80 °C in an open-atmosphere in **(Scheme 2.2).**[22]

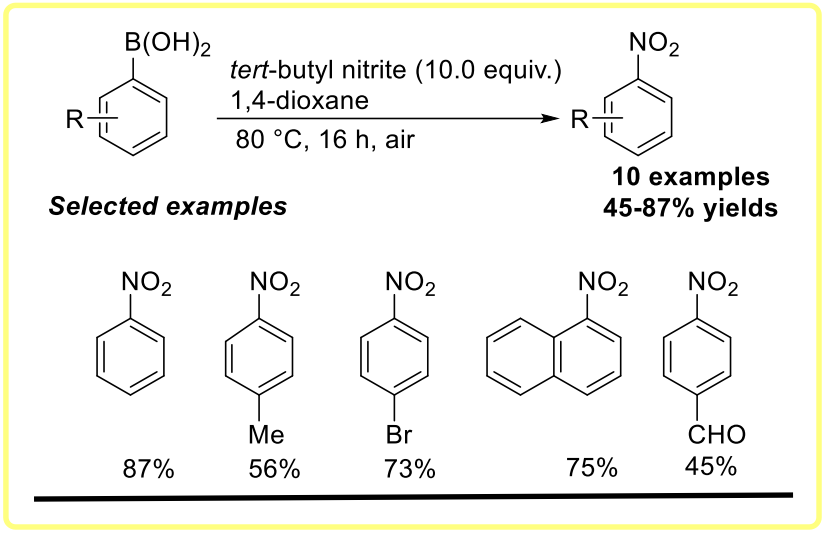

Scheme 2.2. *Ipso*-nitration of arylboronic acids using *tert*-butyl nitrite.

In 2015, Jiao *et al.* developed a Pd-catalyzed directing group directed *ortho*-selective C(sp^2)-H nitration of arenes possessing various directing groups (pyridine, pyrimidine, pyrazole etc.) using a simple and readily available *tert*-butyl nitrite (TBN) in toluene under one-atmosphere of O_2 to produce the corresponding nitroarene derivatives in 40-89% yields (**Scheme 2.3)**.[23]

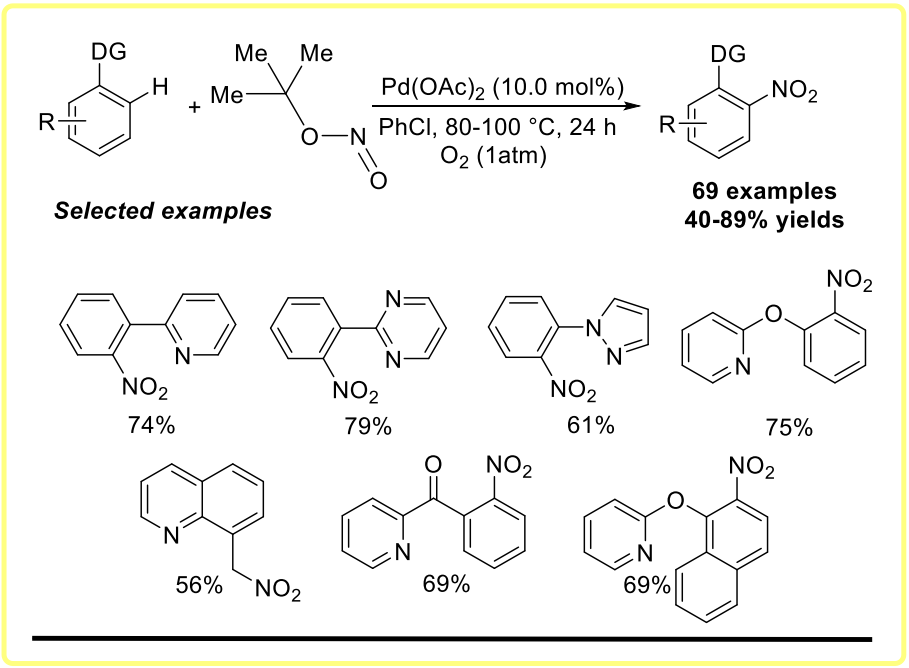

Scheme 2.3. Palladium-catalyzed C−H nitration of arenes.

The catalytic cycle of the above Pd-catalyzed C−H nitration is presented as shown in **Scheme 2.4** The reaction likely involves the synthesis of palladacycle intermediate **A** through directing group-assisted *ortho*-selective cyclometallation on the benzene ring with $Pd(OAc)_2$. Subsequently, the oxidative addition of active NO_2• radical and *t*-BuO• radical to intermediate **A** form the Pd^{IV} intermediate **B**. The latter undergoes C-NO_2 bond formation via reductive elimination to form a nitro compound and regenerations of Pd^{II} species for next cycle shown in **(Scheme 2.4).**[23]

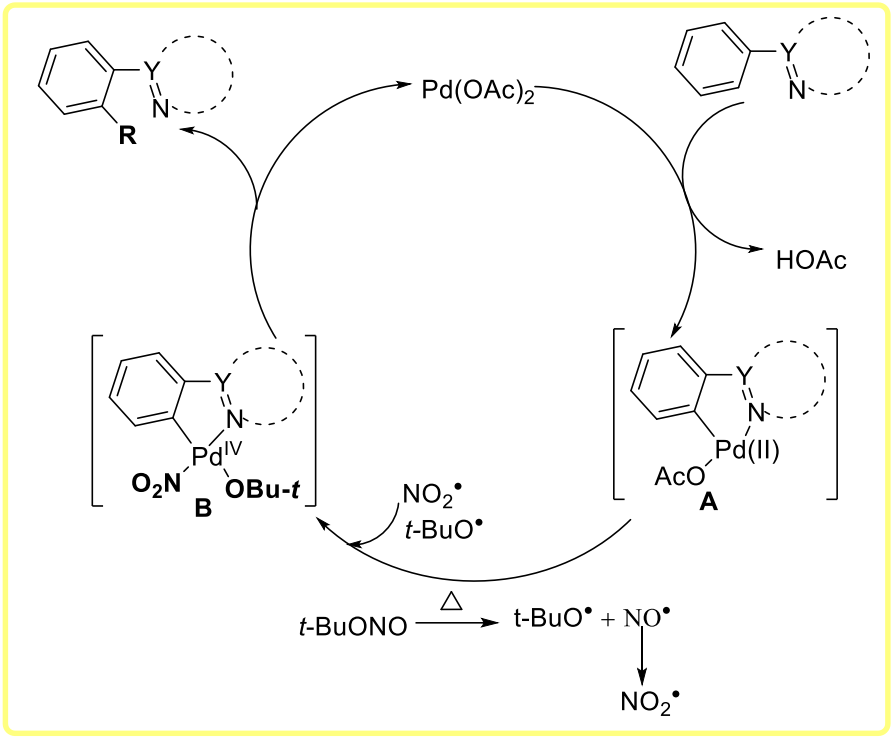

Scheme 2.4. A plausible mechanism for the palladium-catalyzed C−H nitration of arenes.

Later in 2016, Zhang and coworkers reported the first example of transition metal-catalyzed meta-selective C_{Ar}-H nitration of arenes is described With the use of $Ru_3(CO)_{12}$ as the catalyst and $Cu(NO_3)_2{\cdot}3H_2O$ as the nitro source. this approach provides a fast-track strategy for atom/step economical synthesis of many useful pharmaceutical molecules **(Scheme 2.5).**[24]

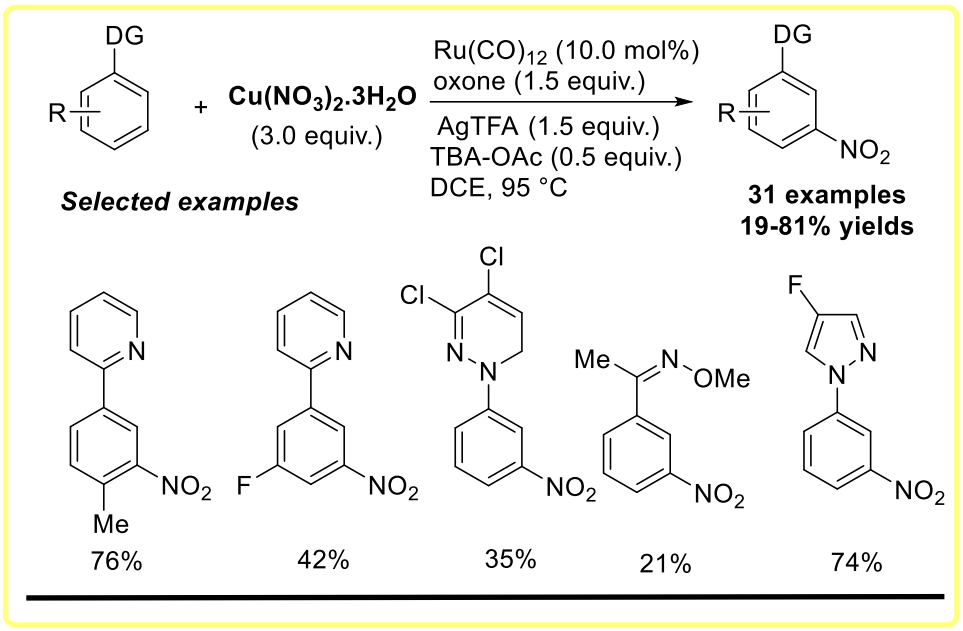

Scheme 2.5. Meta-Selective C_{Ar}-H nitration of arenes.

In 2003, Carmeli *et al.* demonstrated a novel methodology for the nitration of arlazides using in situ generated HOF:CH_3CN as a best oxygen-transfer agent. This method gives 65-98% yields of nitrobenzenes **(Scheme 2.6).**[25]

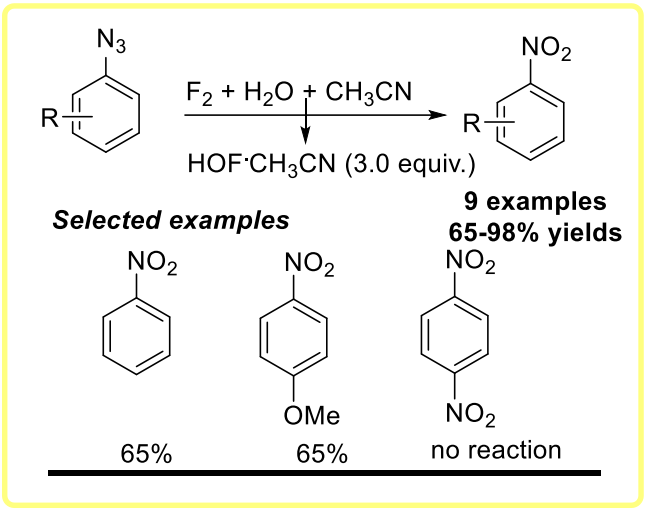

Scheme 2.6. Synthesis of nitroarenes from azides.

In 2007, Kim and his coworkers reported a sequential one-pot three-step synthesis of poly-substituted nitrobenzenes in satisfactory chemical yields. This reaction involves the cyclization reaction between Morita-Baylis-Hillman

acetates and 1,3-dinitroalkanes as 1,3-dinucleophiles in the presence of K_2CO_3 at room temperature, followed by acid-catalyzed dehydration and subsequent aromatization triggered by K_2CO_3 under heating conditions **(Scheme 2.7).**[26]

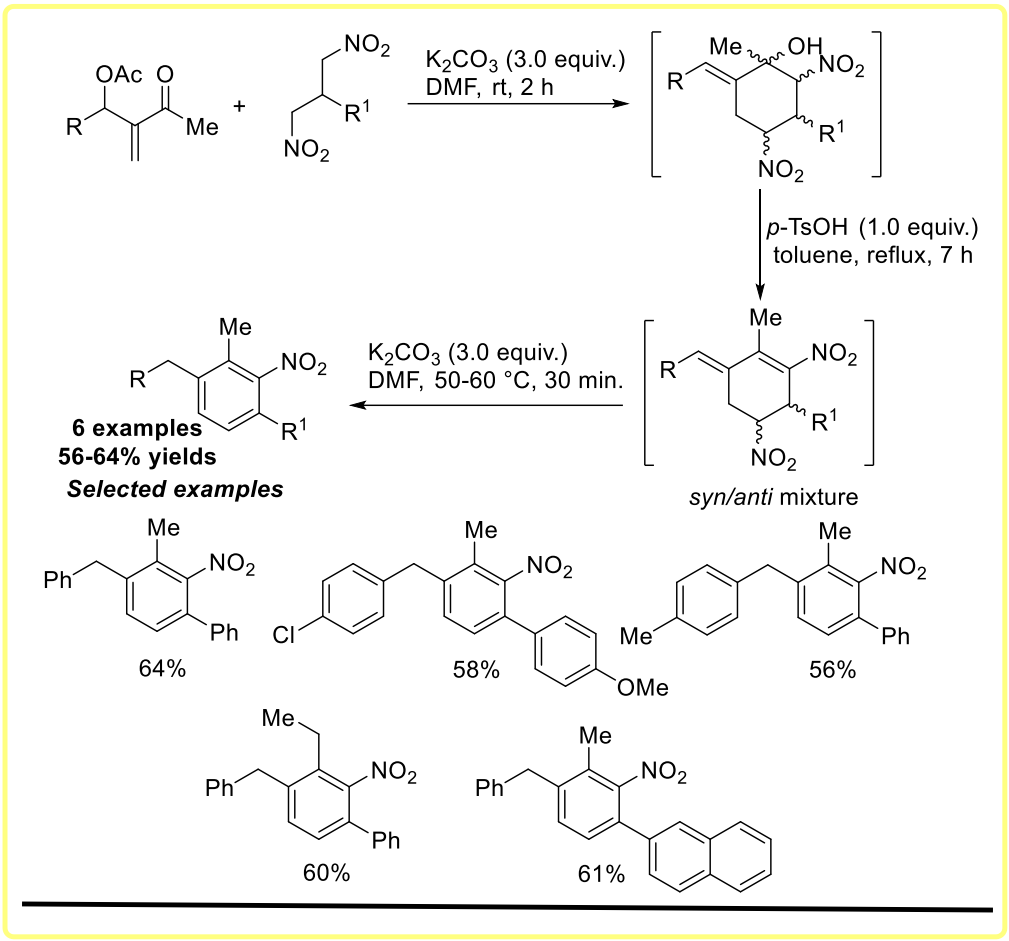

Scheme 2.7. One-pot sequential route to poly-substituted nitroarenes.

In 2016, Samanta *et al.* developed an interesting organocatalytic eco-friendly domino method for the assembly of nitroarenes in promising chemical yields

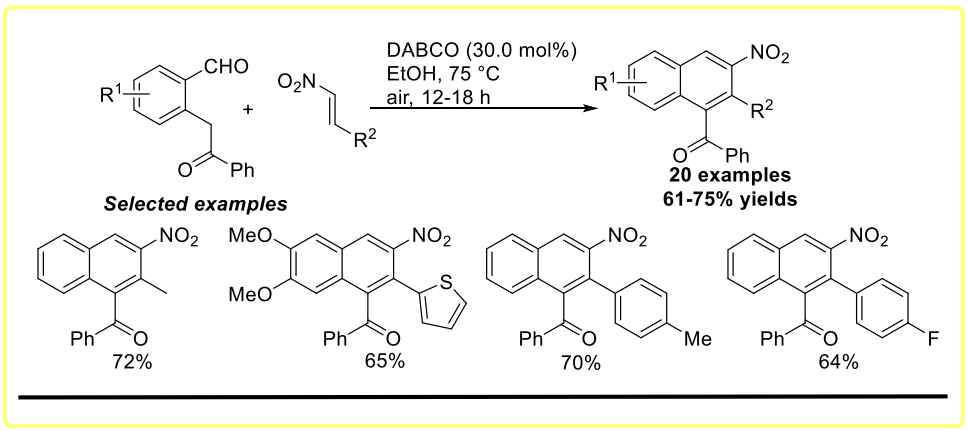

Scheme 2.8. DABCO-catalyzed one-pot synthesis of nitroarenes.

(61-75%). This cyclization reaction proceeds between 2-(2-formylaryl)acetophenones and aryl/heteroaryl-substituted 2-nitroolefins catalyzed by DABCO in EtOH as a green solvent in an open-atmosphere **(Scheme 2.8).**[27]

In 2022, Samanta *et al.* documented a novel DBU-promoted sequential one-pot reaction utilizing nitroalkenes as 1,3 binucleophiles with a variety of γ-aryl/alkenyl-substituted β,γ-unsaturated α-ketocarbonyls under ambient conditions, resulting in the formation of a wide range of valuable 2,5-diaryl-4-nitrobenzoates with moderate to good yields (50-70%, **Scheme 2.9).**[28]

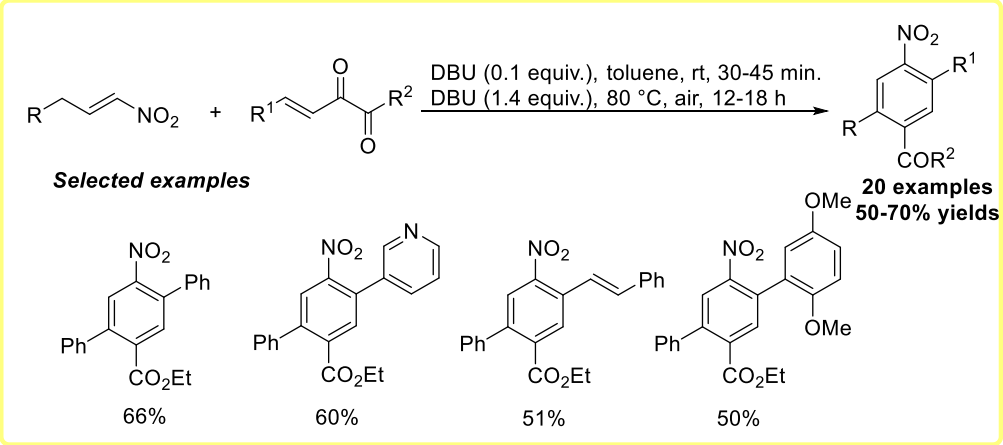

Scheme 2.9. DBU-promoted sequential one-pot access to 4-nitrobenzoates.

2.2.3 Conclusion

The literature study suggests that numerous synthetic methods are available to construct substituted nitroarenes. Although the reported methods are generally reliable, they still encounter many practical difficulties, such as using metal salts and oxidants, a requirement of pre-functionalized arenes, poor atom economy, specific substrate scope, difficulty in removing directing groups, etc. Therefore, there is ample opportunity to develop a robust organocatalytic, practical approach for synthesizing diverse nitroarenes involving adaptable starting materials.

2.3 Present work

Due to the importance of nitroarenes in pharmaceuticals, feedstocks, and the manufacture of agrochemicals and high-explosive materials, it remains desirable to synthesize nitroarenes derivatives from simple reactants using mild and eco-friendly conditions. Towards this goal, we seem that β-alkylnitroalkene, which possesses an active γ-methylene proton, may act as a pronucleophile. This may eventually participate in [3+3] cyclization reaction with an iminium species derived from α,β-unsaturated aldehyde using a secondary amine catalyst. Thus, this unique process may generate the targeted nitroarene product**.** As a part of continued research interest in the development of organocataltic new synthetic process, here in we further report a mild, organocatalytic domino method for making a series of nitroarenes from β-alkylnitroalkenes and α,β-unsaturated aldehyde catalyzed by pyrrolidine-acid sat **(Scheme 2.10).**

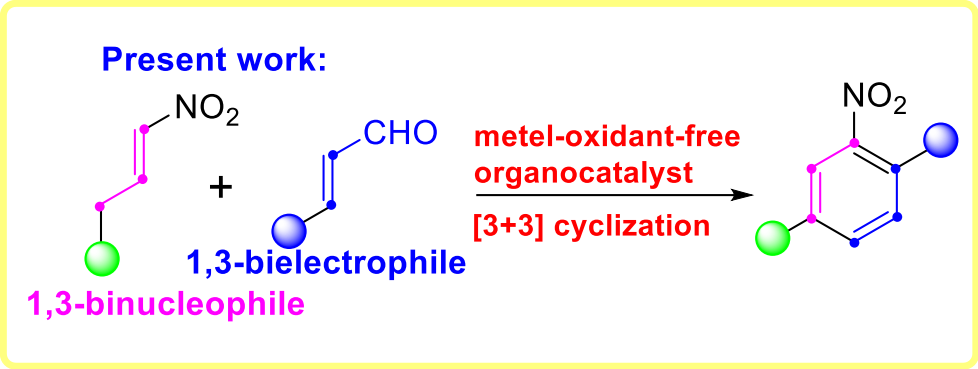

Scheme 2.10. Organocatalytic-mediated synthesis of nitroarenes.

2.4. Results and discussion

2.4.1 Screening of solvents and catalysts

We began our optimization reaction by choosing the model reaction of (2*E*)-3-nitro-2-propen-1-ylbenzene (**1a**) with *trans*-cinnamaldehyde (**2a**) in the presence of L-proline (20 mol%) as the catalyst in CH_2Cl_2 in an open-flask at 45 °C. To our delight, after 18h, 41% yield of a novel class of 2′-nitro-1,1′ :4′,1″-terphenyl (**3aa**) was obtained (entry 1, **Table 2.1**). The chemical structure of **3aa** was assigned by its spectroscopic data (^{1}H NMR, ^{13}C NMR, and HRMS). The ^{1}H NMR spectrum **3aa** exhibits 13 aromatic protons in the range of 7.37-8.07 ppm. Moreover, ^{13}C NMR spectrum of **3aa** shows a total of 14 peaks at 150.0, 141.9, 138.7, 137.5, 135.2, 132.7, 130.9, 129.5, 129.1, 128.9, 128.6,

128.3, 127.4, 122.9 ppm. In addition, the molecular ion peak $[M+Na]^+$ at 298.0834 in the HRMS spectrum corresponds to the molecular weight 275.0946 of the desired compound **3aa.**

Next, we investigate the effect of solvents and catalysts on the yield of the **3aa**. The results are summarized below in **Table 2.1.** To know the effects of improving the productivity of this reaction, several pyrrolidine-acid salts (20 mol%) were screened for the above cyclization reaction. Intriguingly, the equimolecular combination of pyrrolidine and 4-chlorobenzoic acid (pKa= 3.98) (i. e. catalyst **IV**) afforded 65% yield of **3aa**, which is higher than other catalysts (**II-III**, **V-X;** 10–60% yields) applied for this reaction. It is noteworthy to mention that the acidity of the additive has a significant role in the rate of the cyclization reaction. For example, when the catalysts (**IX** and **X**) were made by either a strong aromatic acid [such as 3,5-dinitrobenzoic acid (pKa= 2.82, entry 9), PTSA (pKa= -2.8, entry 10)] or use of excess acid (entries 11 and 12), the unsatisfactory yields (10-37%) of **3aa** were obtained. Therefore, considering the yield (65%, entry 4), catalyst **IV** (pyrrolidine:4-ClBzOH) was considered the best catalyst for this cyclization reaction. Among various organic solvents (MeOH, EtOH, 2-MeTHF, $CHCl_3$, toluene, MeCN and DMF), particularly MeOH (entry 13) produced a better yield (74%) compared to others (48-67%, entries 14-19). It is noted that using 10 mol% of catalyst **IV**, the yield (41%, entry 20) dropped significantly. Moreover, little effect was observed when the reaction was carried out under an O_2 atmosphere (entry 21). It should be noted that 61% yield of **3aa** was obtained in MeOH when the reaction was used L-proline as a catalyst under identical conditions (entry 22).

Table 2.1. Optimization of the reaction.[a]

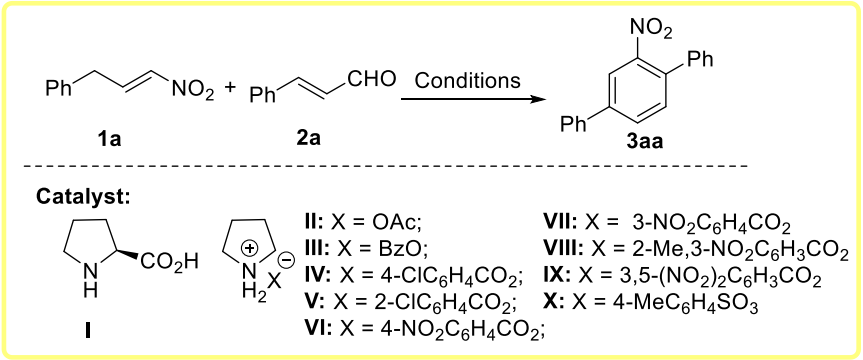

Entry	Catalyst [loading mol%]	Solvent	Yield [%] [b]
1[d]	L-Proline (20 mol%)	CH_2Cl_2	41
2[d]	**II** (20 mol%)	CH_2Cl_2	32
3	**III** (20 mol%)	CH_2Cl_2	50
4	**IV** (20 mol%)	CH_2Cl_2	65
5	**V** (20 mol%)	CH_2Cl_2	60
6	**VI** (20 mol%)	CH_2Cl_2	57
7	**VII** (20 mol%)	CH_2Cl_2	56
8	**VIII** (20 mol%)	CH_2Cl_2	60
9	**IX** (20 mol%)	CH_2Cl_2	37
10	**X** (20 mol%)	CH_2Cl_2	10
11	**IV**/4-ClBzOH (1 :1)	CH_2Cl_2	30
12	**IV**/3-NO_2BzOH (1 :1)	CH_2Cl_2	27
13	**IV** (20 mol%)	MeOH	74
14	**IV** (20 mol%)	EtOH	65
15	**IV** (20 mol%)	2-MeTHF	63
16	**IV** (20 mol%)	$CHCl_3$	60
17	**IV** (20 mol%)	toluene	52
18	**IV** (20 mol%)	MeCN	67
19	**IV** (20 mol%)	DMF	48
20	**IV** (10 mol%)	MeOH	41
21[c]	**IV** (20 mol%)	MeOH	75
22	L-Proline (20 mol%)	MeOH	61

[a]All the reactions were carried out with **1a** (0.20 mmol) and **2a** (0.24 mmol) in dry solvent (1.0 mL) at 45 °C for 12h in an open atmosphere. [b]Yield of the isolated product. [c]Under an O_2-atmosphere. [d]Reaction time was 18h.

2.4.2 Possible mechanism

We propose a reasonable reaction pathway for the construction of nitrobenzene scaffold **3aa** using catalyst **IV** as outlined in **(Scheme 2.11).** First, the catalyst

IV reacts with a *trans*-cinnamaldehyde **(2a)** to generate a reactive iminium ion intermediate **2a′** as a LUMO lowering energy species. After that, the counter anion (conjugate of a base) of the resulting iminium ion would capture an active methylene proton at the γ-position of nitroalkene **1a** to form an α-carbonucleophilic synthon, which involves the Michael addition with **2a′**, followed by a protonation to give an iminium adduct **5**. Subsequently, the sequence of deprotonation-tautomerization-intramolecular Mannich reaction may generate cyclohexene **6**. Next, the latter eliminates a pyrrolidine-acid salt to form cyclohexadiene **8**. Finally, the aerial oxidation of **8** leads to **3aa**. Alternatively, the intermediate **5** could be generated through a concerted ene-type of reaction between LUMO of enophile **2a′** and **1a** as a HOMO. Even though this transition state is unlikely to follow due to the energetically less favorable,[29] it cannot be ruled out completely as shown in **(Scheme 2.11).**

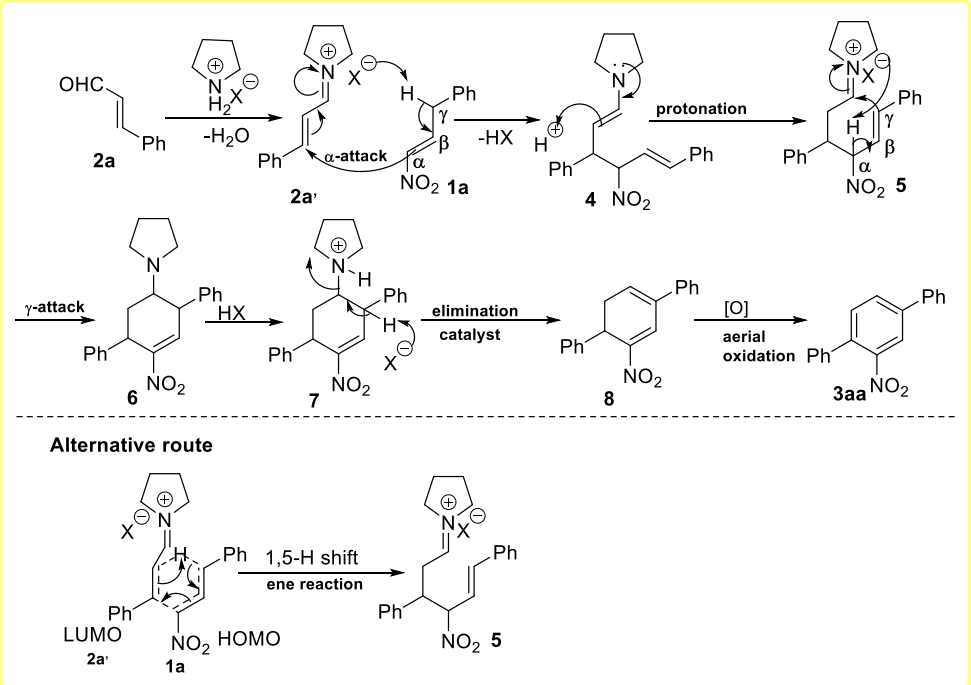

Scheme 2.11. A possible reaction mechanism.

2.4.3 Substrate scope

2.4.3.1 Synthesis of nitroarenes

Having optimal reaction conditions in hand, we then turned our attention to examining the generality and scope of the [3+3] cyclization reaction by varying several 3-nitroallylbenzenes (**1a-1f**) and β-aryl/heteroaryl/alkyl-substituted acroleins using 20 mol% of a catalyst **IV**. As illustrated in **Table 2.2,** several Michael acceptors like β-aryl-substituted acroleins bearing both electron-rich (Me, MeO, and OBn) and electron-poor (F, Cl, Br, and NO_2) substituents on the aryl-rings at *ortho, meta,* and *para* positions showed good reactivity, while making C-C and C=C bonds with **1a.** These reactions produced the corresponding 2,5-diarylnitrobenzenes in good yields. Moreover, we were pleased to observe that acroleins with a sterically hindered aryl moiety such as 2,6- dichlorobenzene, 2,6-difluorobenzene, 1-naphthyl or pyrenyl also provided pretty good yields (50-67%) of the corresponding 2,5-disubstituted nitroarenes. However, these substrates took additional time for the accomplishment of the products. Excitingly, alkyl-substituted acroleins (**2s** and **2t**) are poor Michael acceptors due to the propensity to form the dienamine species in the presence of an iminium catalyst. Greatly, by the present catalytic system, the corresponding 2-alkyl substituted nitroarenes were isolated in 51% yield for **3as** and 50% yield for **3at**. In addition, heteroaryl-substituted acroleins (**2q** and **2r**) were subjected to cyclization with **1a** that delivered the corresponding nitrobenzenes **3aq** and **3ar** in 70% and 74% yields. Moreover, acrolein with a CO_2Et group provided a 54% yield of ethyl benzoate derivative **3au**. Next, the incorporation of several electron donating (Me, MeO, and *t*-Bu) and electron-poor halogen (Cl and Br) substituents on the aryl rings of nitroalkenes did not create any problem toward the cyclization with β-aryl/alkyl/heteroaryl-substituted acroleins to give the corresponding nitroarenes (**3ba-3gr**) in 59-76% yields. In addition, many valuable substituents Me, MeO, BnO, *t*-Bu, CO_2Et, Cl, Br, F, NO_2, furan, thiophene, etc were tolerated under the present conditions.

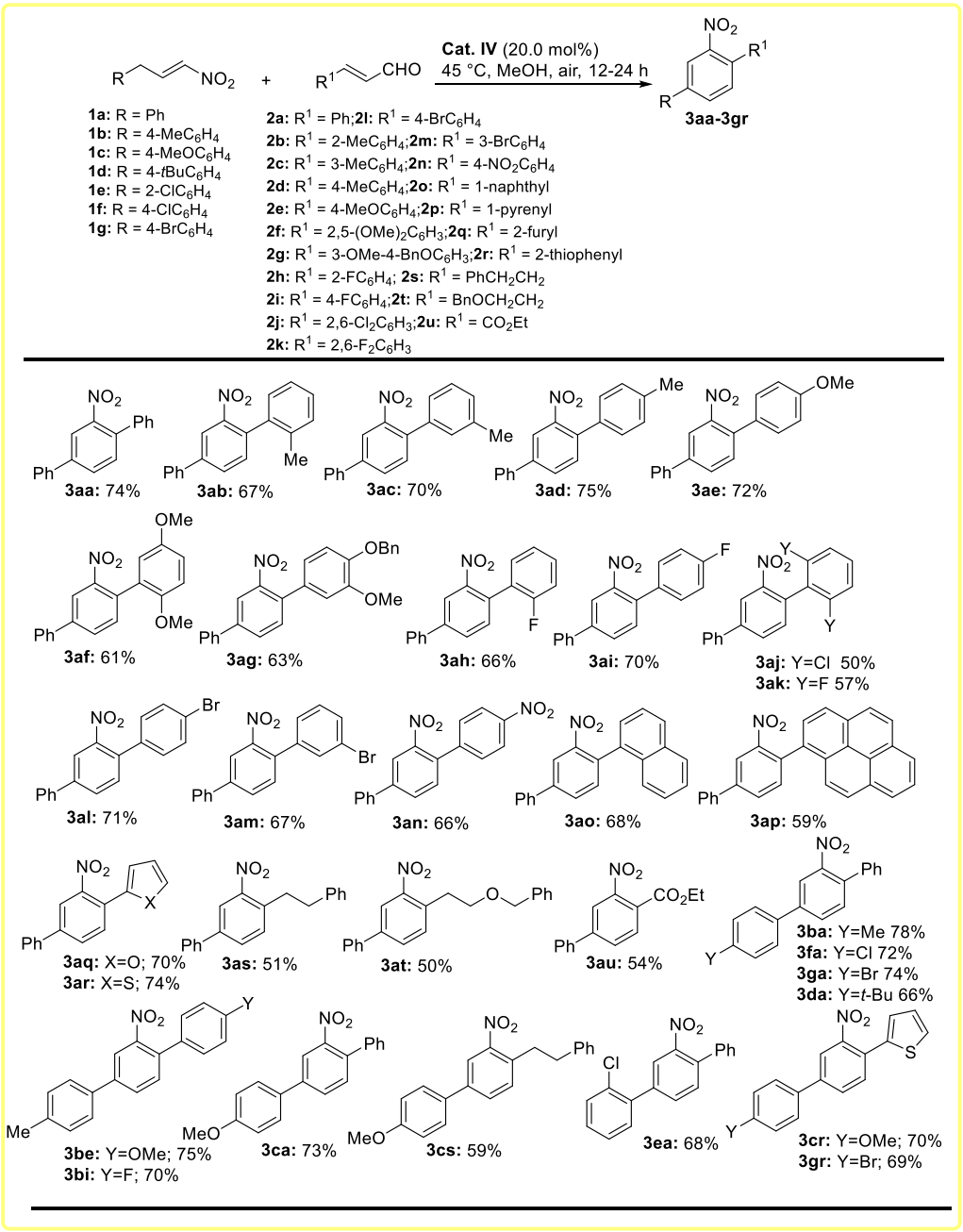

Table 2.2. Substrate scope of the [3+3] cyclization reaction.

Enthused by previous successes, α,β,γ,δ-unsaturated aldehydes have been used as challenging Michael acceptors in this cyclization reaction. Interestingly, catalyst **IV** was capable of activating δ-aryl-substituted α,β,γ,δ-unsaturated aldehydes, which underwent 1,4-Michael addition with 1,3-binucleophiles like β-benzyl-substituted nitroethylenes **1a** and **1f**. Consequently, after 18 h, we isolated good yields (50-60%, **Table 2.3**.) of a synthetically valuable (*E*)-styryl-substituted nitrobenzene derivatives were obtained. Notably, this represents the

first successful synthetic report to access the molecules described above under metal-oxidant-free conditions.

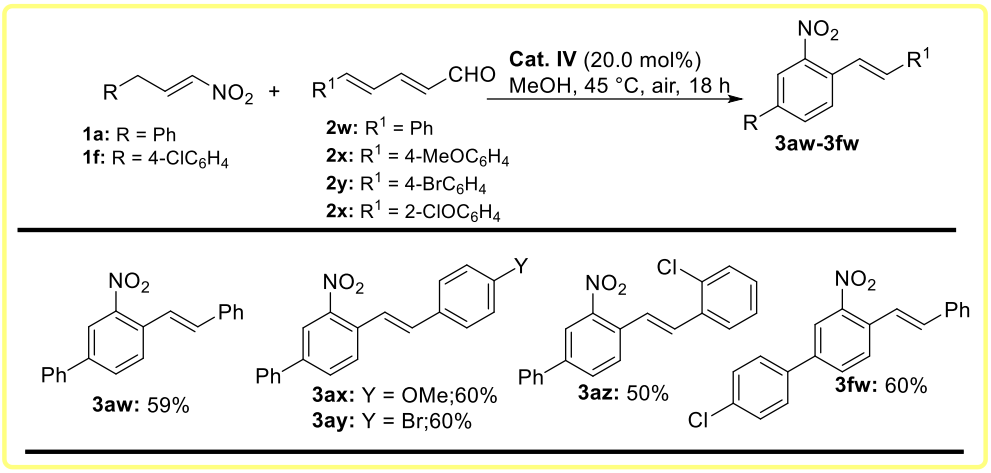

Table 2.3. Pot-economy approach to (*E*)-styryl-substituted nitrobenzene derivatives.

To highlight the synthetic potential of prepared scaffolds, we performed the Cadogan cyclization[30] of **3aa** using PPh_3 in 1,2-dichlorobenzene at 180 °C, producing a valuable 2-phenyl carbazole (**11**) in 81% yield after 5h (**Table 2.4**.). Furthermore, the nitro group of **3aa** was efficiently reduced to compound **9** by employing an excess amount of Fe in AcOH:H_2O at 110 °C for 24h. Furthermore, the resulting aniline derivative **9** was treated with $NaNO_2$ in HCl at 0–5 °C followed by CuCl at 70 °C, resulting in 86% yield of 2′-chloro-1,1′:4′,1″-terphenyl (**12**) as a well-known starting material for nanoribbon structure synthesis.[31] To our surprise, the treatment of compound **9** with $NaNO_2$/NCS or NBS in DMF at room temperature afforded 90% yield of simple deaminated 1,1′:4′,1″-terphenyl (**10**) instead of a 2-chloro/bromo-1,1′:4′,1″-terphenyl. Interestingly, the reductive cyclization[32] of nitrostyrene derivative **3aw** in the presence of B_2pin_2 and KF in EtOH produced a valuable 2,6-diphenyl-1*H*-indole (**13**) in 86% yield.

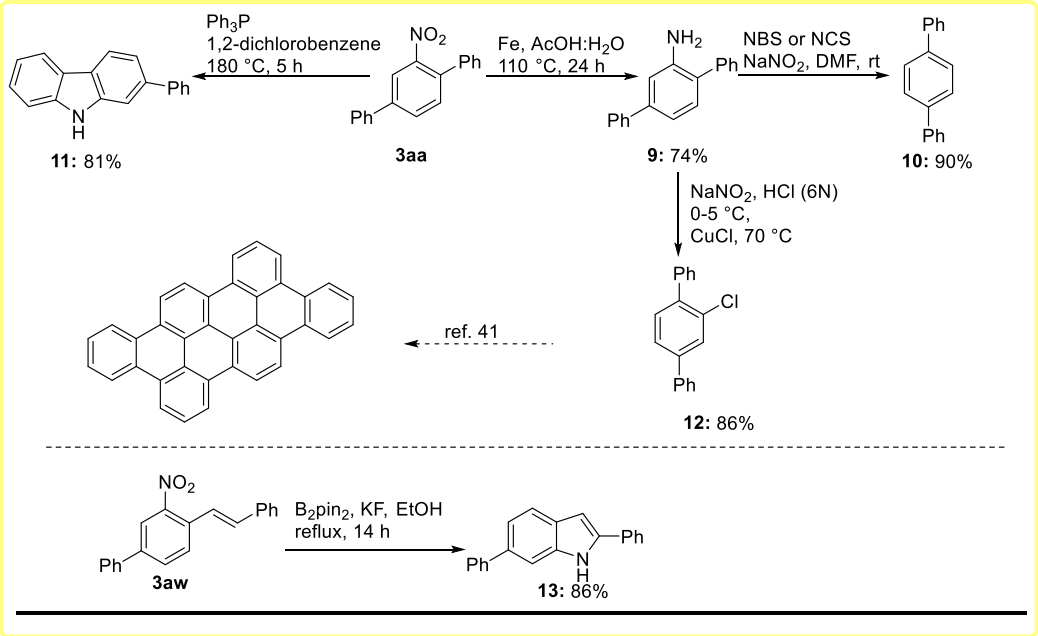

Table 2.4. Some important synthetic applications of nitrobenzene derivatives.

2.5. Conclusion

In this chapter, a simple organocatalytic [3+3] domino technique to synthesize a diverse set of 2,5-disubstituted nitrobenzene building blocks in satisfactory yields under mild conditions was developed. This reaction involves a Michael-initiated cyclization from β-alkyl-substituted nitroalkenes as 1,3-binucleophiles and a family of structurally varied β-aryl/alkyl/alkenyl-substituted acroleins in the presence of pyrrolidine:4-ClBzOH salt as a powerful organocatalyst in an open-atmosphere. Interestingly, this metal-oxidant-nitration-free process bestows many positive features such as no need for toxic metal salts, highly atom-economical, exceptional tolerance of functionalities, broad substrate scope, no toxic by-product (just water), user-friendliness process, etc. Moreover, this technique enables the synthesis of several valuable molecules such as 2-arylcarbazole, 2,6-diphenylindole, 2′-chloro-1,1′:4′,1″-terphenyl, and 1,1′:4′,1″-terphenyl derivatives from nitroarenes by simple synthetic operations.

2.6. Experimental

General procedure for the synthesis of compounds 1 and 2: All the nitroalkenes (**1a-g**) and unsaturated aldehydes (**2a-2z**) were either synthesized by literature known procedures or purchased from commercial sources.

Preparation of catalyst IV: To a stirred solution of 4-chlorobenzoic acid (20 mmol) in dry DCM (20 mL) at 10 °C was added slowly distilled pyrrolidine (20 mmol) under nitrogen atmosphere. After that, the reaction mixture was stirred at room temperature for 6 h. Then the DCM was removed completely by rotary evaporator under low pressure, followed by high vacuum pump to give a white powder pyrrolidine:4-ClBzOH salt (catalyst **IV**).

General procedure for the synthesis of nitrobenzene derivatives (3aa-3fw): To a stirred solution of appropriate β-substituted acrolein (0.24 mmol, 1.2 equiv.) and catalyst **IV** (0.04 mmol, 20 mol%) in dry methanol (1.0 mL) was added nitroalkene (0.2 mmol) at room temperature. The reaction mixture was heated at 45 °C in an open-atmosphere for 12-24h (monitored by TLC). After the completion of the reaction, the solvent was evaporated under reduced pressure to give the crude mass which was purified by flash column chromatography using hexane/EtOAc (100:0 to 95:5), leading to the desired nitrobenzene derivative. All the products were characterized by their spectroscopic data (^{1}H NMR and ^{13}C NMR, HRMS).

Preparation of carbazole derivative (11): A mixture of compound **3aa** (0.3 mmol) and triphenyl phosphine 0.75 mmol in 1,2-dichlorobenzene (2.0 mL) was heated to reflux at 180 °C under nitrogen atmosphere. After completion of the reaction, it was directly purified by silica-gel column chromatography using 10-15% hexane/ethyl acetate as a mixture of solvent to give the targeted carbazole derivative **11**.

Reduction of nitrobenzene 3aa to aniline 9: To a stirred solution of nitro compound (0.3 mmol) and Fe-powder (2.4 mmol) in AcOH:H_2O (1:1) 3.0 mL was refluxed at 110 ˚C for 24 h. The reaction was cooled and quenched by saturated $NaHCO_3$ solution. Afterwards, the reaction mixture was extracted with ethyl acetate (3x10 mL), washed with water, and dried over Na_2SO_4. The

combined organic phase was evaporated under reduced pressure to provide the crude product. Finally, it was purified by silica-gel column chromatography using a mixture of hexane/ethyl acetate (9:1) to lead the pure aniline derivative **9**.

Synthesis of compound 10: A mixture of aniline derivative **9** (0.1 mmol), $NaNO_2$ (0.2 mmol), and N-chlorosuccinimide or N-bromosuccinimide (0.15) in DMF (1.0 mL) at room temperature was stirred for 14 h. Afterwards, the reaction mixture was extracted with ethyl acetate (3x10 mL), washed with water, and dried over Na_2SO_4. The combined organic phase was evaporated under reduced pressure to provide the crude product. After that it was purified by silica-gel column chromatography using a mixture of hexane/ethyl acetate (99:1) to provide compound **10** (90% yield).

Synthesis of compound 12: The compound **9** (0.1 mmol) was taken in 6N HCl (2.0 mL) at 0-5 °C. After that $NaNO_2$ (0.2 mmol) was added portion wise to the above solution. The reaction mixture was stirred for 45 min at the same temperature. Then the CuCl (0.3 mmol) in 2.0 mL water was added at room temperature, followed by heating at 70 °C for 3h. Afterwards, the reaction mixture was extracted with ethyl acetate (3x10 mL) before being neutralized with aqueous $NaHCO_3$ solution, washed with water, and dried over Na_2SO_4. The combined organic phase was evaporated under reduced pressure to provide the crude product. After that it was purified by silica-gel column chromatography using a mixture of hexane/ethyl acetate (99:1) to provide compound **12** (86% yield).

Reductive cyclization of *ortho*-nitrostyrene derivative 3aw to indole derivative (13): A mixture of **3aw** (0.1 mmol), B_2pin_2 (0.2 mmol), and KF (0.3 mmol) in dry EtOH (3.0 mL) was heated at 90 °C in a sealed tube for 14h. After the removal of ethanol, the reaction mixture was extracted with ethyl acetate, washed with water, and dried Na_2SO_4 to give the crude mass. The pure product was obtained after column chromatographic purification.

Characterization data:

2′-Nitro-1,1′:4′,1′′-terphenyl (3aa): Colorless solid; mp 128-130 °C; yield 74% (40.7 mg); ^{1}H NMR (400 MHz, $CDCl_3$) δ 8.07 (d, *J* = 1.9 Hz, 1H), 7.84(dd,

J = 8.0, 1.9 Hz, 1H), 7.67-7.63 (m, 2H), 7.52 (d, *J* = 7.9 Hz, 3H), 7.48- 7.41 (m, 4H), 7.37 (dd, *J* = 7.6, 1.9 Hz, 2H) ppm; ^{13}C NMR (100 MHz, $CDCl_3$) δ 150.0, 141.9, 138.7, 137.5, 135.2, 132.7, 130.9, 129.5, 129.1, 128.9, 128.6, 128.3, 127.4, 122.9 ppm; HRMS (ESI-TOF) *m/z* calcd for $C_{18}H_{13}NNaO_2$ $[M+Na]^+$: 298.0838, found 298.0834.

2-Methyl-2′-nitro-1,1′:4′,1″-terphenyl (3ab): Colorless solid**;** mp 118-120 °C; yield 67 % (38.7 mg); ^{1}H NMR (400 MHz, $CDCl_3$) δ 8.17 (s, 1H), 7.81 (d, *J* = 7.9 Hz, 1H), 7.63 (d, *J* = 7.5 Hz, 2H), 7.47 (t, *J* = 7.4 Hz, 2H), 7.43- 7.38 (m, 1H), 7.35 (d, *J* = 7.9 Hz, 1H), 7.30-7.16 (m, 3H), 7.11 (d, *J* = 7.4 Hz, 1H), 2.12 (s, 3H) ppm; ^{13}C NMR (100 MHz, $CDCl_3$) δ 149.8, 142.0, 138.7, 137.6, 136.1, 135.5, 133.0, 131.2, 130.4, 129.5, 128.9, 128.7, 128.6, 127.4, 126.1, 122.8, 20.3 ppm; HRMS (ESI-TOF) *m/z* calcd for $C_{19}H_{15}NNaO_2$ $[M+Na]^+$: 312.0995, found 312.0996.

3-Methyl-2′-nitro-1,1′:4′,1″-terphenyl (3ac): Colorless solid**;** mp 116-118 °C; yield 70% (40.5 mg); ^{1}H NMR (400 MHz, $CDCl_3$) δ 7.96 (s, 1H), 7.72 (d, *J* = 7.9 Hz, 1H), 7.56-7.54 (m, 2H), 7.42-7.39 (m, 3H), 7.36-7.32 (m, 1H), 7.24 (t, *J* = 7.5 Hz, 1H), 7.15-7.13 (m, 1H), 7.09-7.06 (m, 2H), 2.32 (s, 3H) ppm; ^{13}C NMR (100 MHz, $CDCl_3$) δ 150.0, 141.8, 138.8, 138.7, 137.4, 135.3, 132.7, 130.8, 129.5, 129.4, 129.0, 128.9, 128.8, 127.4, 125.3, 122.8, 21.8 ppm; HRMS (ESI-TOF) *m/z* calcd for $C_{19}H_{15}NNaO_2$ $[M+Na]^+$: 312.0995, found 312.0995.

4-Methyl-2′-nitro-1,1′:4′,1″-terphenyl (3ad): Colorless solid; mp 123-125 °C; yield 75% (43.3 mg); mp 130-132 °C; ^{1}H NMR (400 MHz, $CDCl_3$) δ 8.04 (s, 1H), 7.82 (dd, *J* = 7.9, 1.1 Hz, 1H), 7.64 (d, *J* = 7.4 Hz, 2H), 7.52-7.48 (m, 3H), 7.45-7.43 (m, 1H), 7.24-7.26 (m, 4H), 2.41 (s, 3H) ppm; ^{13}C NMR (100 MHz, $CDCl_3$) δ 150.1, 141.7, 138.7, 138.6, 135.2, 134.5, 132.7, 130.9, 129.9, 129.5, 128.8, 128.1, 127.4, 122.8, 21.6 ppm; HRMS (ESI-TOF) *m/z* calcd for $C_{19}H_{15}NNaO_2$ $[M+Na]^+$: 312.0995, found 312.1024.

4-Methoxy-2′-nitro-1,1′:4′,1″-terphenyl (3ae): Colorless solid; mp 136-138 °C; yield 72% (43.9 mg); ^{1}H NMR (400 MHz, $CDCl_3$) δ 8.02 (s, 1H), 7.81 (d, *J* = 7.8 Hz, 1H), 7.64 (d, *J* = 7.5 Hz, 2H), 7.54-7.47 (m, 3H), 7.44 (d, *J* = 7.2 Hz, 1H), 7.30 (d, *J* = 8.4 Hz, 2H), 6.98 (d, *J* = 8.4 Hz, 2H), 3.86 (s, 3H) ppm; ^{13}C NMR (100 MHz, $CDCl_3$) δ 160.1, 150.1, 141.5, 138.7, 134.8, 132.7, 130.8,

129.53, 129.51 (2C, one peak overlap), 128.8, 127.4, 122.8, 114.6, 55.7 ppm; HRMS (ESI) *m/z* calcd for $C_{19}H_{15}NNaO_3$ $[M+Na]^+$: 328.0944, found 328.0949.

2,5-Dimethoxy-2′-nitro-1,1′:4′,1′′-terphenyl (3af): Colorless solid; mp 128-130 °C; yield 61% (40.8 mg); ^{1}H NMR (400 MHz, $CDCl_3$) δ 8.15 (s, 1H), 7.85 (d, *J* = 7.9 Hz, 1H), 7.66-7.64 (m, 2H), 7.51-7.47 (m, 3H), 7.45-7.40 (m, 1H), 6.94-6.83 (m, 3H), 3.84 (s, 3H), 3.68 (s, 3H) ppm; ^{13}C NMR (100 MHz, $CDCl_3$) δ 154.3, 150.5, 150.4, 141.9, 138.9, 133.1, 131.8, 131.3, 129.5, 128.8, 127.9, 127.4, 122.8, 116.3, 114.3, 111.9, 56.2, 56.0 ppm; HRMS (ESI-TOF) *m/z* calcd for $C_{20}H_{17}NNaO_4$ $[M+Na]^+$: 358.1050, found 358.1056.

4-(Benzyloxy)-3-methoxy-2′-nitro-1,1′:4′,1′′-terphenyl (3ag): Pale yellow solid; mp 124-126 °C; yield 63% (51.8 mg); ^{1}H NMR (400 MHz, $CDCl_3$) δ 8.00 (s, 1H), 7.80 (d, *J* = 7.9 Hz, 1H), 7.64-7.62 (m, 2H), 7.52-7.42 (m, 6H), 7.39 (t, *J* = 7.4 Hz, 2H), 7.34-7.30 (m, 1H), 6.96-6.94 (m, 1H), 6.89-6.85 (m, 2H), 5.20 (s, 2H), 3.90 (s, 3H) ppm; ^{13}C NMR (100 MHz, $CDCl_3$) δ 150.2, 150.0, 148.9, 141.6, 138.7, 137.3, 134.8, 132.6, 130.7, 130.3, 129.5, 129.0, 128.9, 128.3, 127.7, 127.4, 122.7, 120.8, 114.3, 112.0, 71.4, 56.5. HRMS (ESI-TOF) *m/z* calcd for $C_{26}H_{21}NNaO_4$ $[M+Na]^+$:434.1363, found 434.1375.

2-Fluoro-2′-nitro-1,1′:4′,1′′-terphenyl (3ah): Colorless solid**;** mp 106-108°C; yield 66% (38.7 mg); ^{1}H NMR (400 MHz, $CDCl_3$) δ 8.26 (s, 1H), 7.89 (d, *J* = 7.7 Hz, 1H), 7.67-7.65 (m, 2H), 7.51-7.37 (m, 6H), 7.29-7.27 (m, 1H), 7.15 (t, *J* = 8.9 Hz, 1H) ppm; ^{13}C NMR (100 MHz, $CDCl_3$) δ 159.7 (d, J_{C-F} = 246.0 Hz), 149.8, 142.7, 138.6, 133.3, 131.5, 130.6 (d, J_{C-F} = 8.0 Hz), 130.4, 129.6, 129.5 129.0, 127.4, 125.7 (d, J_{C-F} = 1.6 Hz), 125.0, 123.3, 115.9 (d, J_{C-F} = 22.2 Hz) ppm; HRMS (ESI-TOF) *m/z* calcd for $C_{18}H_{12}FNNaO_2$ $[M+Na]^+$: 316.0744, found 316.0747.

4-Fluoro-2′-nitro-1,1′:4′,1′′-terphenyl (3ai): Colorless solid**;** mp 114-116 °C; yield 70% (41.0 mg)**;** ^{1}H NMR (500 MHz, $CDCl_3$) δ 8.07 (d, *J* =1.65 Hz, 1H), 7.83 (dd, *J* = 7.95, 1.65 Hz, 1H), 7.64 (d, *J* = 7.4 Hz, 2H), 7.52-7.43 (m, 4H), 7.33 (dd, *J* = 8.6, 2.0 Hz, 2H), 7.14 (d, *J*= 8.6 Hz, 2H) ppm; ^{13}C NMR (100 MHz, $CDCl_3$) δ 163.1 (d, J_{C-F} = 247.0 Hz) 150.0, 142.2, 138.6, 134.2, 133.5, 132.7, 131.0, 130.1 (d, J_{C-F} =8.0 Hz) 129.6, 129.0, 127.4, 122.9, 116.1

(d, J_{C-F} = 22.0 Hz) ppm; HRMS (ESI-TOF) *m/z* calcd for $C_{18}H_{12}FNNaO_2$ $[M+Na]^+$: 316.0744, found 316.0743.

2,6-Difluoro-2′-nitro-1,1′:4′,1′′-terphenyl (3ak): Colorless solid; mp 110-112 °C; yield 57% (37.4 mg); ^{1}H NMR (500 MHz, $CDCl_3$) δ 8.36 (d, *J* = 1.9 Hz, 1H), 7.90 (dd, *J* = 8.0, 1.9 Hz, 1H), 7.66-7.65 (m, 2H), 7.56-7.48 (m, 3H), 7.45-7.46 (m, 1H), 7.40-7.34 (m, 1H), 7.05-6.98 (m, 2H) ppm; ^{13}C NMR (125 MHz, $CDCl_3$) δ 160.0 (dd, J_{C-F} = 246.9, 6.46 Hz), 149.6, 143.4, 138.5, 133.9, 131.6, 130.5 (t, J_{C-F} = 10.15 Hz), 129.6, 129.1, 127.5, 123.6, 123.1, 115.1 (t, J_{C-F} = 19.4 Hz), 112.0 (dd, J_{C-F} = 5.4, 20.1 Hz) ppm; HRMS (ESI-TOF) *m/z* calcd for $C_{18}H_{11}F_2NNaO_2[M+Na]^+$: 334.0650, found 334.0651.

2,6-Dichloro-2′-nitro-1,1′:4′,1′′-terphenyl (3aj): Colorless solid; mp 136-138 °C; yield 50%; 34.4 mg); ^{1}H NMR (500 MHz, $CDCl_3$) δ 8.45 (d, *J* = 1.8 Hz, 1H), 7.96 (dd, *J* = 8.0, 1.8 Hz, 1H), 7.73-7.68 (m, 2H), 7.58 – 7.55 (m, 2H), 7.48 -7.38 (m, 4H), 7.32-7.28 (m, 1H) ppm; ^{13}C NMR (125 MHz, $CDCl_3$) δ 143.5, 138.2, 133.3, 131.6, 129.4, 127.9, 127.1, 125.9, 124.9, 124.4, 124.0, 123.2, 122.4, 118.3 ppm; HRMS (ESI-TOF): m/z $[M+ Na]^+$ calcd for $C_{18}H_{11}Cl_2NNaO_2$ 366.0059, found 366.0064.

4-Bromo-2′-nitro-1,1′:4′,1′′-terphenyl (3al): Colorless solid; mp 141-143 °C; yield 71% (50.3 mg); ^{1}H NMR (400 MHz, $CDCl_3$) δ 8.10 (s, 1H), 7.84 (d, *J* = 7.9 Hz, 1H), 7.64 (d, *J* = 7.5 Hz, 2H), 7.58 (d, *J* = 7.9 Hz, 2H), 7.53-7.43 (m, 4H), 7.23 (d, *J* = 8.0 Hz, 2H) ppm; ^{13}C NMR (100 MHz, $CDCl_3$) δ 149.7, 142.4, 138.5, 136.5, 134.1, 132.5, 132.3 (2C, one overlap peak), 131.1, 129.9, 129.6, 129.0, 127.4, 123.1 ppm; HRMS (ESI-TOF) *m/z* calcd for $C_{18}H_{12}{}^{79}BrNO_2Na$ $[M+Na]^+$: 375.9944, found 375.9984; HRMS (ESI) *m/z* calcd for $C_{18}H_{12}{}^{81}BrNO_2Na$ $[M+Na]^+$: 377.9923, found 377.9938.

3-Bromo-2′-nitro-1,1′:4′,1′′-terphenyl (3am): Colorless solid; mp 144-146 °C; yield 67% (47.4 mg); ^{1}H NMR (500 MHz, $CDCl_3$) δ 8.05 (d, *J* = 1.5 Hz, 1H), 7.77 (dd, *J* = 8.0, 1.5 Hz, 1H), 7.56 (d, *J* = 7.0 Hz, 2H), 7.48-7.36 (m, 6H) 7.23 (t, *J* = 7.5 Hz, 1H), 7.19 (d, *J* = 9.0 Hz, 1H) ppm; ^{13}C NMR (100 MHz, $CDCl_3$) δ 149.7, 142.6, 139.6, 138.4, 133.8, 132.6, 131.6, 131.3, 131.1, 130.5, 129.6, 129.1, 127.4, 127.0, 123.1, 123.0 ppm; HRMS (ESI-TOF) *m/z* calcd for

$C_{18}H_{12}{}^{79}BrNO_2Na$ $[M+Na]^+$: 375.9944, found 375.9964; HRMS (ESI) *m/z* calcd for $C_{18}H_{12}{}^{81}BrNO_2Na$ $[M+Na]^+$: 377.9923, found 377.9945.

2′,4-Dinitro-1,1′:4′,1′′-terphenyl (3an): Colorless solid; mp 152-154 °C; yield 65% (41.6 mg); ^{1}H NMR (400 MHz, $CDCl_3$) δ 8.32 (d, *J* = 8.3 Hz, 2H), 8.22 (s, 1H), 7.91 (d, *J* = 7.9 Hz, 1H), 7.66 (d, *J* = 7.6 Hz, 2H), 7.54-7.45 (m, 6H) ppm; ^{13}C NMR (100 MHz, $CDCl_3$) δ 149.4, 148.1, 144.5, 143.4, 138.2, 133.3, 132.4, 131.5, 129.7, 129.4, 129.3, 127.5, 124.3, 123.5 ppm; HRMS (ESI-TOF) *m/z* calcd for $C_{18}H_{12}N_2NaO_4$[M+Na]$^+$: 343.0689, found 343.0717.

1-(3-Nitro-[1,1′-biphenyl]-4-yl)naphthalene (3ao): Pale yellow solid; mp 161-163°C; yield 68% (44.2 mg); ^{1}H NMR (500 MHz, $CDCl_3$) δ 8.30 (s, 1H), 7.92 (d, *J* = 7.75 Hz, 3H), 7.71 (d, *J* = 7.0 Hz, 2H), 7.56-7.51 (m, 6H), 7.49-7.38 (m, 3H) ppm; ^{13}C NMR (100 MHz, $CDCl_3$) δ 150.5, 142.4, 138.7, 135.6, 134.2, 133.9, 133.8, 131.9, 131.2, 130.2, 129.6, 129.0, 128.9, 127.5, 127.0, 126.5, 126.4, 125.6, 125.2, 123.0 ppm; HRMS (ESI-TOF) *m/z* calcd for $C_{22}H_{15}NNaO_2$ $[M+Na]^+$: 348.0995, found 348.1022.

1-(3-Nitro-[1,1′-biphenyl]-4-yl)pyrene (3ap): Light green solid, mp 230-232 °C: yield 59% (47.1 mg)**;** ^{1}H NMR (500 MHz, $CDCl_3$) δ 8.36 (s, 1H),8.24 (t, *J* = 7.0 Hz, 2H), 8.19 (d, *J* = 7.5 Hz, 1H), 8.13 (br s, 2H), 8.05-8.02 (m, 2H), 7.98 (dd, *J* = 7.8, 1.5 Hz, 1H), 7.91 (d, *J*= 7.8 Hz, 1H), 7.80 (d, *J* = 9.15 Hz, 1H), 7.76 (d, *J* = 7.5 Hz, 2H), 7.67 (d, *J* = 7.9 Hz, 1H), 7.56 (7, *J* = 7.9Hz, 2H), 7.48 (t, *J* = 7.3 Hz, 1H) ppm; ^{13}C NMR (100 MHz, $CDCl_3$) δ 150.8, 142.5, 138.7, 134.7, 134.4, 132.7, 131.7, 131.6, 131.2, 131.2, 129.6, 129.1, 129.0, 128.6, 128.3, 127.7, 127.5, 126.7, 126.5, 125.9, 125.7, 125.1, 125.1, 125.0, 124.4, 123.1 ppm; HRMS (ESI-TOF) *m/z* calcd for $C_{28}H_{17}NNaO_2$ $[M+Na]^+$: 422.1151, found 422.1178.

2-(3-Nitro-[1,1′-biphenyl]-4-yl)thiophene (3ar): Colorless solid; mp 80-82°C; yield 74% (41.6 mg); ^{1}H NMR (400 MHz, $CDCl_3$) δ 7.96 (s, 1H), 7.79 (d, *J* = 7.8 Hz, 1H), 7.63 (d, *J* = 7.5 Hz, 3H), 7.50 (t, *J* = 7.3 Hz, 2H), 7.45-7.43 (m, 2H), 7.13-7.10 (m, 2H) ppm; ^{13}C NMR (100 MHz, $CDCl_3$) δ 150.1, 142.3, 138.5, 137.3, 133.0, 130.5, 129.6, 129.0, 128.2, 127.6, 127.5, 127.4, 127.2, 122.6 ppm; HRMS (ESI-TOF) *m/z* calcd for $C_{16}H_{11}NNaO_2S$ $[M+Na]^+$: 304.0403, found 304.0403.

2-(3-Nitro-[1,1'-biphenyl]-4-yl)furan (3aq): Colorless solid; mp 120-122 °C; yield 70% (37.1 mg); ^{1}H NMR (500 MHz, $CDCl_3$) δ 7.89 (s, 1H), 7.79 (s, 2H), 7.61 (d, *J* = 7.5 Hz, 2H), 7.53 (s, 1H), 7.49 (t, *J*= 7.5 Hz, 2H),7.44-7.41 (m, 1H), 6.71 (d, *J* = 3.4 Hz, 1H), 6.52 (dd, *J*=3.4, 1.75 Hz, 1H) ppm; ^{13}C NMR (100 MHz, $CDCl_3$) δ 148.6, 148.2, 144.2, 141.8, 138.5, 130.4, 129.5 (2C), 128.9, 127.3, 123.0, 122.6, 112.3, 110.2 ppm; HRMS (ESI-TOF) *m/z* calcd for $C_{16}H_{11}NNaO_3$ $[M+Na]^+$: 288.0631, found 288.0635.

3-Nitro-4-phenethyl-1,1′-biphenyl (3as): Colorless solid; mp 94-96 °C; yield 51% (30.9 mg)**;** ^{1}H NMR (400 MHz, $CDCl_3$) δ 8.18 (s, 1H), 7.73 (s, 1H), 7.62 (s, 2H), 7.50 (s, 2H), 7.43 (s, 1H), 7.32 (d, *J* = 5.9 Hz, 3H), 7.26 (s, 3H), 3.24 (br s, 2H), 3.02 (br s, 2H) ppm; ^{13}C NMR (100 MHz, $CDCl_3$) δ 150.0, 141.3, 141.0, 138.8, 135.6, 133.0, 131.6, 129.5, 128.9, 128.8, 128.7, 127.3, 126.6, 123.4, 37.4, 35.5 ppm; HRMS (ESI-TOF) *m/z* calcd for $C_{20}H_{17}NNaO_2$ $[M+Na]^+$: 326.1151, found 326.1153.

4-(2-(Benzyloxy)ethyl)-3-nitro-1,1′-biphenyl (3at): Colorless solid; mp 80-82 °C; 50% yield (33.4 mg); ^{1}H NMR (400 MHz, $CDCl_3$) δ 8.12 (d, *J* = 2.0 Hz, 1H), 7.73 (dd, *J* = 8.0, 2.0 Hz, 1H), 7.61-7.56 (m, 2H), 7.47 (t, *J* = 8.0 Hz, 3H), 7.43-7.37 (m, 1H), 7.29 (d, *J* = 6.8 Hz, 5H), 4.52 (s, 2H), 3.79 (t, *J* = 6.4 Hz, 2H), 3.25 (t, *J* = 6.4 Hz, 2H) ppm; ^{13}C NMR (100 MHz, $CDCl_3$) δ 150.4, 141.1, 138.8, 138.5, 133.6, 133.1, 131.4, 129.5, 128.7, 128.7, 127.9, 127.9, 127.3, 123.4, 73.3, 70.0, 33.5 ppm; HRMS (ESI-TOF) *m/z* calcd for $C_{21}H_{19}NNaO_3$ $[M+Na]^+$: 356.1257, found 356.1272.

4′′-Methyl-2′-nitro-1,1′:4′,1′′-terphenyl(3ba): Colorless solid; mp 105-107 °C; yield 76% (43.9 mg); ^{1}H NMR (500 MHz, $CDCl_3$) δ 8.05 (d, *J* = 1.55 Hz, 1H), 7.82 (dd, *J* = 8.0, 1.55 Hz, 1H), 7.54 (d, *J* = 8.0 Hz, 2H), 7.49 (d, *J* = 8.0 Hz, 1H), 7.46-7.39 (m, 3H), 7.36-7.35 (m, 2H), 7.31 (d, *J* = 8.0 Hz, 2H), 2.42 (s, 3H) ppm; ^{13}C NMR (100 MHz, $CDCl_3$) δ 150.0, 141.9, 138.9, 137.5, 135.7, 134.9, 132.7, 130.7, 130.3, 129.1, 128.6, 128.3, 127.2, 122.6, 21.5 ppm; HRMS (ESI-TOF) *m/z* calcd for $C_{19}H_{15}NNaO_2$ $[M+Na]^+$: 312.0995, found 312.1000.

4-Methoxy-4′′-Methyl-2′-nitro-1,1′:4′,1′′-terphenyl (3be): Colorless solid; mp 120-122 °C; yield 75% (47.8 mg); ^{1}H NMR (400 MHz, $CDCl_3$) δ 8.00 (d, *J* = 2.0 Hz, 1H), 7.79 (dd, *J* = 8.0, 1.9 Hz, 1H), 7.54 (d, *J* = 7.9 Hz, 2H), 7.48

(d, *J* = 8.0 Hz, 1H), 7.30 (dd, *J* = 8.3, 4.6 Hz, 4H), 6.97 (d, *J* = 8.8 Hz, 2H), 3.86 (s, 3H), 2.43 (s, 3H) ppm; ^{13}C NMR (100 MHz, $CDCl_3$) δ 160.0, 150.1, 141.4, 138.8, 135.8, 134.4, 132.6, 130.6, 130.2, 129.5 (2C, one overlap peak), 127.2, 122.5, 114.6, 55.7, 21.5 ppm; HRMS (ESI-TOF) *m/z* calcd for $C_{20}H_{17}NNaO_3[M+Na]^+$: 342.1101, found 342.1095.

4-Fluoro-4′′-methyl-2′-nitro-1,1′:4′,1′′-terphenyl (3bi): Colorless solid: mp 106-108 °C; yield 70% (42.9 mg); ^{1}H NMR (400 MHz, $CDCl_3$) δ 8.06 (d, *J* = 2.0 Hz, 1H), 7.82 (dd, *J* = 7.9, 1.9 Hz, 1H), 7.54 (d, *J* = 7.9 Hz, 2H), 7.46 (d, *J* = 8.0 Hz, 1H), 7.36-7.30 (m, 4H), 7.13 (t, *J* = 8.7 Hz, 2H), 2.43 (s, 3H) ppm; ^{13}C NMR (100 MHz, $CDCl_3$) δ 163.1 (d, J_{C-F}= 247.0 Hz) 149.9, 142.1, 139.0, 135.6, 133.8, 133.5 (d, J_{C-F} = 4.0 Hz*)*, 132.6, 130.7, 130.3, 130.1 (d, J_{C-F} = 8.0 Hz*)*, 127.2, 122.6, 116.1 (d, J_{C-F} = 21.0 Hz), 21.5 ppm; HRMS (ESI-TOF) *m/z* calcd for $C_{19}H_{14}FNNaO_2[M+Na]^+$: 330.0901, found: 330.0911.

4′′-Methoxy-2′-nitro-1,1′:4′,1′′-terphenyl (3ca): colorless solid; mp 100-102 °C; yield 73% (44.5 mg); ^{1}H NMR (400 MHz, $CDCl_3$) δ 8.02 (s, 1H), 7.79 (d, *J* = 6.6 Hz, 1H), 7.59 (d, *J* = 7.0 Hz, 2H), 7.52-7.32 (m, 6H), 7.03 (d, *J* = 7.1 Hz, 2H), 3.88 (s, 3H) ppm; ^{13}C NMR (100 MHz, $CDCl_3$) δ 155.3, 144.9, 136.4, 132.4, 129.4, 127.5, 125.9, 125.3, 123.9 , 123.5, 123.4, 123.2, 117.1, 109.9, 50.6 ppm; HRMS (ESI-TOF) *m/z* calcd for $C_{19}H_{15}NNaO_3$ $[M+Na]^+$: 328.0944, found 328.0973.

4′-Methoxy-3-nitro-4-phenethyl-1,1′-biphenyl (3cs): Colorless solid; mp 80-82 °C; yield 59% (39.3 mg); ^{1}H NMR (400 MHz, $CDCl_3$) δ 8.11 (d, *J* = 1.7 Hz, 1H), 7.67 (dd, *J* = 8.0, 1.8 Hz, 1H), 7.54 (d, *J* = 8.7 Hz, 2H), 7.30 (d, *J* = 7.8 Hz, 3H), 7.23 (d, *J* = 7.6 Hz, 3H), 7.00 (d, *J* = 8.7 Hz, 2H), 3.87 (s, 3H), 3.20 (dd, *J* = 9.4, 6.6 Hz, 2H), 2.99 (dd, *J* = 9.4, 6.5 Hz, 2H) ppm; ^{13}C NMR (100 MHz, $CDCl_3$) δ 160.3, 150.0, 141.3, 140.6, 134.9, 132.9, 131.3, 131.1, 128.9, 128.8, 128.4, 126.6, 122.9, 114.9, 55.8, 37.4, 35.5 ppm; HRMS (ESI-TOF) *m/z* calcd for $C_{21}H_{19}NNaO_3$ $[M+Na]^+$: 356.1257, found 356.1244.

2-(4′-Methoxy-3-nitro-[1,1′-biphenyl]-4-yl)thiophene (3cr): Colorless solid; mp 90-92 °C; yield 70% (43.5 mg); ^{1}H NMR (400 MHz, $CDCl_3$) δ 7.91 (d, *J* = 1.7 Hz, 1H), 7.74 (dd, *J* = 8.1, 1.8 Hz, 1H), 7.60-7.54 (m, 3H), 7.46-7.38 (m, 1H), 7.14-7.06 (m, 2H), 7.02 (d, *J* = 8.7 Hz, 2H), 3.87 (s, 3H) ppm; ^{13}C NMR

(100 MHz, $CDCl_3$) δ 160.5, 150.1, 141.9, 137.5, 132.9, 130.8, 129.9, 128.5, 128.1, 127.4, 127.4, 126.5, 122.0, 115.0, 55.8 ppm; HRMS (ESI-TOF) *m/z* calcd for $C_{17}H_{13}NNaO_3S$ $[M+Na]^+$: 334.0508, found 334.0511.

4′′-(*tert*-Butyl)-2′-nitro-1,1′:4′,1′′-terphenyl (3da): Colorless solid; mp128-130 °C; yield 66% (43.7 mg); ^1H NMR (500 MHz, $CDCl_3$) δ 8.06 (t, *J* = 2.8 Hz, 1H), 7.87-7.77 (m, 1H), 7.59 (d, *J* = 7.9 Hz, 2H), 7.56-7.48 (m, 3H), 7.47-7.39 (m, 3H), 7.37 (d, *J* = 6.7 Hz, 2H), 1.38 (d, *J* = 3.4 Hz, 9H) ppm; ^{13}C NMR (125 MHz, $CDCl_3$) δ 152.1, 150.0, 141.8, 137.5, 135.7, 134.9, 132.6, 130.7, 129.0, 128.6, 128.3, 127.1, 126.5, 122.6, 35.04, 31.65 ppm; HRMS (ESI-TOF) *m/z* calcd for $C_{22}H_{21}NNaO_2[M+Na]^+$: 354.1465, found 354.1466.

2-Chloro-3′-nitro-1,1′:4′,1′′-terphenyl (3ea): Colorless solid; mp 115-117 °C; yield 68% (42.1 mg); ^1H NMR (400 MHz, $CDCl_3$) δ 7.96 (d, *J* = 1.8 Hz, 1H), 7.72 (dd, *J* = 8.0, 1.8 Hz, 1H), 7.51 (d, *J* = 7.9 Hz, 2H), 7.45-7.37 (m, 8H) ppm; ^{13}C NMR (100 MHz, $CDCl_3$) δ 149.3, 139.9, 138.1, 137.4, 135.8, 133.6, 132.8, 132.0, 131.5, 130.7, 130.0, 129.1, 128.7, 128.3, 127.6, 125.4 ppm; HRMS (ESI-TOF) *m/z* calcd for $C_{18}H_{12}ClNNaO_2$ $[M+Na]^+$: 332.0449, found 332.0459.

2-(4′-Bromo-3-nitro-[1,1′-biphenyl]-4-yl)thiophene (3gr): Colorless solid; mp 100-102 °C; yield 69% (49.7 mg); ^1H NMR (400 MHz, $CDCl_3$) δ 7.92 (s, 1H), 7.75 (d, *J* = 7.7 Hz, 1H), 7.63 (d, *J* = 7.9 Hz, 3H), 7.52-7.41 (m, 3H), 7.17 -7.05 (m, 2H) ppm; ^{13}C NMR (100 MHz, $CDCl_3$) δ 150.1, 141.0, 137.3, 137.1, 133.1, 132.7, 130.2, 129.1, 128.9, 128.3, 127.7, 127.6, 123.5, 122.4 ppm; HRMS (ESI-TOF) *m/z* calcd for $C_{16}H_{10}{}^{79}BrNNaO_2S[M+Na]^+$: 381.9508, found 381.9526; HRMS (ESI-TOF) *m/z* calcd for $C_{16}H_{10}{}^{81}BrNNaO_2S[M+Na]^+$: 383.9487, found 383.9499.

4′′-Bromo-2′-nitro-1,1′:4′,1′′-terphenyl (3ga): Colorless solid; mp 109-111 °C; yield 74%(52.4 mg); ^1H NMR (500 MHz, $CDCl_3$) δ 8.03 (d, *J* = 1.9 Hz, 1H), 7.80 (dd, *J* = 8.0, 2.0 Hz, 1H), 7.64 (d, *J* = 8.5 Hz, 2H), 7.52 (dd, *J* = 8.2, 4.9 Hz, 3H), 7.48-7.40 (m, 3H), 7.38-7.33 (m, 2H) ppm; ^{13}C NMR (125 MHz, $CDCl_3$) δ 150.0, 140.7, 137.5, 137.2, 135.6, 132.9, 132.7, 130.7, 129.1, 128.9, 128.7, 128.2, 123.3, 122.6 ppm; **HRMS** (ESI-TOF): m/z $[M + Na]^+$ calcd for

$C_{18}H_{12}{}^{79}BrNNaO_2$ 375.9944, found 375.9968; **HRMS** (ESI-TOF): m/z [M + Na]$^+$ calcd for $C_{18}H_{12}{}^{81}BrNNaO_2$ 377.9923, found 377.9949.

Ethyl 4′-chloro-3-nitro-[1,1′-biphenyl]-4-carboxylate (3au): Gummy liquid**;** yield 54% (29.3 mg); ^{1}H NMR (500 MHz, $CDCl_3$) δ 8.07 (d, *J* = 1.6 Hz, 1H), 7.88 – 7.82 (m, 2H), 7.63-7.59 (m, 2H), 7.51 (t, *J* = 7.3 Hz, 2H), 7.49-7.45 (m, 1H), 4.41 (q, *J* = 7.2 Hz, 2H), 1.38 (t, *J* = 7.2 Hz, 3H) ppm; ^{13}C NMR (125 MHz, $CDCl_3$) δ 165.5, 149.5, 145.6, 138.0, 131.1, 130.9, 129.6, 129.5, 127.5, 126.1, 122.6, 62.8, 14.2 ppm; HRMS (ESI-TOF) *m/z* calcd for $C_{15}H_{13}NNaO_4$[M+Na]$^+$: 294.0737, found 294.0719.

4′′-Chloro-2′-nitro-1,1′:4′,1′′-terphenyl (3fa); colorless solid; mp 98-100 °C; yield 72% (44.6 mg); ^{1}H NMR (500 MHz, $CDCl_3$) δ 8.03 (d, *J* = 2.0 Hz, 1H), 7.80 (dd, *J* = 8.0, 1.9 Hz, 1H), 7.58 (d, *J* = 8.5 Hz, 2H), 7.52 (d, *J* = 8.0 Hz, 1H), 7.49-7.42 (m, 5H), 7.36 (dd, *J* = 7.8, 1.8 Hz, 2H) ppm; ^{13}C NMR (125 MHz, $CDCl_3$) δ 150.0, 140.6, 137.2, 137.0, 135.5, 135.1, 132.8, 130.7, 129.7, 129.1, 128.7, 128.6, 128.2, 122.6 ppm; HRMS (ESI-TOF) *m/z* calcd for $C_{18}H_{12}ClNNaO_2$[M+Na]$^+$: 332.0449, found 332.0446.

(*E*)-3-Nitro-4-styryl-1,1′-biphenyl (3aw): colorless solid; mp 116-118 °C; yield 59% (35.5 mg); ^{1}H NMR (500 MHz, $CDCl_3$) δ 8.19 (d, *J* = 1.7 Hz, 1H), 7.88-7.80 (m, 2H), 7.67-7.60 (m, 3H), 7.59-7.55 (m, 2H), 7.50 (t, *J* = 7.5 Hz, 2H), 7.45-7.37 (m, 3H), 7.36-7.30 (m, 1H), 7.15 (d, *J* = 16.1 Hz, 1H); ^{13}C NMR (125 MHz, $CDCl_3$) δ 148.7, 141.5, 138.6, 136.9, 134.1, 131.8, 131.6, 129.5, 129.2, 129.0, 128.8, 128.8, 127.4, 127.2, 123.4, 123.3; HRMS (ESI-TOF) *m/z* calcd for $C_{20}H_{15}NNaO_2$ [M+Na]$^+$: 324.0995, found 324.0998.

(*E*)-4′-Chloro-3-nitro-4-styryl-1,1′-biphenyl (3fw): colorless solid; mp 132-134 °C; yield 60% (40.2 mg); ^{1}H NMR (500 MHz, $CDCl_3$) δ 8.15 (d, *J* = 1.9 Hz, 1H), 7.86 (d, *J* = 8.2 Hz, 1H), 7.79 (dd, *J* = 8.3, 2.0 Hz, 1H), 7.62 (d, *J* = 16.1 Hz, 1H), 7.57 (dd, *J* = 8.9, 2.4 Hz, 4H), 7.47 (d, *J* = 8.5 Hz, 2H), 7.40 (t, *J* = 7.6 Hz, 2H), 7.36-7.30 (m, 1H), 7.15 (d, *J* = 16.1 Hz, 1H) ppm; ^{13}C NMR (125 MHz, $CDCl_3$) δ 148.7, 140.2, 137.0, 136.8, 135.1, 134.4, 132.2, 131.4, 129.7, 129.2, 129.1, 129.0, 128.5 (2C), 127.5, 123.2; HRMS (ESI-TOF) *m/z* calcd for $C_{20}H_{14}ClNNaO_2$ [M+Na]$^+$: 358.0605, found 358.0580.

(*E*)-4-(4-Methoxystyryl)-3-nitro-1,1′-biphenyl (3ax): colorless solid; mp 128-130 °C; yield 60% (39.7 mg); ^{1}H NMR (500 MHz, $CDCl_3$) δ 8.16 (d, *J* = 2.0 Hz, 1H), 7.82-7.81 (m, 2H), 7.63 (d, *J* = 9.0 Hz, 2H), 7.51-7.47 (m, 5H), 7.43-7.41 (m, 1H), 7.12 (d, *J* = 16.0 Hz, 1H), 6.94-6.91 (m, 2H), 3.85 (s, 3H); ^{13}C NMR (125 MHz, $CDCl_3$) δ 160.4, 148.6, 141.0, 138.7, 133.8, 132.1, 131.5, 129.7, 129.5, 128.8, 128.8, 128.5, 127.2, 123.3, 121.0, 114.6, 55.7 ppm; HRMS (ESI-TOF) *m/z* calcd for $C_{21}H_{17}NNaO_3[M+Na]^+$: 354.1101, found 354.1104.

(*E*)-4-(2-Chlorostyryl)-3-nitro-1,1′-biphenyl (3az): Colorless solid; mp 152-154 °C; yield 50% (33.5 mg); ^{1}H NMR (500 MHz, $CDCl_3$) δ 8.22 (d, *J* = 1.8 Hz, 1H), 7.88 (q, *J* = 8.1 Hz, 2H), 7.75 (d, *J* = 7.4 Hz, 1H), 7.67 – 7.55 (m, 4H), 7.50 (t, *J* = 7.6 Hz, 2H), 7.43 (t, *J* = 8.1 Hz, 2H), 7.37-7.26 (m, 2H) ppm; ^{13}C NMR (125 MHz, $CDCl_3$) δ 148.8, 142.0, 138.5, 135.0, 134.1, 131.8, 131.7, 130.2, 130.0, 129.8, 129.5, 129.3, 128.9, 127.5, 127.5, 127.3, 126.1, 123.4 ppm; HRMS (ESI-TOF) *m/z* calcd for $C_{20}H_{14}ClNNaO_2$ $[M+Na]^+$: 358.0605 , found 358.0609.

(*E*)-4-(4-Bromostyryl)-3-nitro-1,1′-biphenyl (3ay): Colorless solid; mp 126-128 °C; yield 56% (42.5 mg); ^{1}H NMR (500 MHz, $CDCl_3$) δ 8.20 (s, 1H), 7.83 (s, 2H), 7.64-7.59 (m, 3H), 7.52-7.48 (m, 4H), 7.44-7.41 (m, 3H), 7.07 (d, *J* = 16.1 Hz, 1H) ppm; ^{13}C NMR (125 MHz, $CDCl_3$) δ 143.6, 136.7, 133.4, 130.7, 127.6, 127.2, 126.6, 126.4, 124.4, 123.9, 123.8, 123.7, 122.1, 119.1, 118.3, 117.8 ppm; HRMS (ESI) *m/z* calcd for $C_{20}H_{14}{}^{79}BrNNaO_2$ $[M+Na]^+$: 402.0100, found 402.0128; HRMS (ESI-TOF) *m/z* calcd for $C_{20}H_{14}{}^{81}BrNNaO_2$ $[M+Na]^+$: 404.0080, found 404.0102.

2-Phenyl-9*H*-carbazole (11):[4] yield 81%; ^{1}H NMR (400 MHz, DMSO-d_6) δ 11.32 (s, 1H), 8.18 (d, *J* = 8.0 Hz, 1H), 8.13 (d, *J* = 8.0 Hz, 1H), 7.75 (d, *J* = 6.8 Hz, 2H), 7.72 (s, 1H), 7.52-7.45 (m, 4H), 7.40-7.37 (m, 2H), 7.17 (t, *J* = 6.8 Hz) ppm; ^{13}C NMR (100 MHz, DMSO-d_6) δ 140.86, 140.78, 138.32, 129.41, 127.53, 127.48, 126.11, 122.66, 122.31, 121.08, 120.73, 119.18, 111.48, 109.35 ppm.

[1,1′:4′,1′′-Terphenyl]-2′-amine (9): yield 74%; ^{1}H NMR (400 MHz, $CDCl_3$) δ 7.66-7.57 (m, 2H), 7.55-7.40 (m, 6H), 7.36 (t, *J* = 7.2 Hz, 2H), 7.21 (d, *J* = 7.8 Hz, 1H), 7.07 (dd, *J* = 7.8, 1.8 Hz, 1H), 7.01 (d, *J* = 1.8 Hz, 1H) ppm; ^{13}C

NMR (100 MHz, $CDCl_3$) δ 144.12, 141.95, 141.43, 139.55, 131.24, 129.42, 129.21, 129.02, 127.60, 127.58, 127.40, 127.1, 118.0, 114.6 ppm.

Compound 10: ^{1}H NMR (500 MHz, $CDCl_3$) δ 7.68 (s, 4H), 7.65 (d, *J* = 6.5 Hz, 4H), 7.49-7.42 (m, 4H), 7.39-7.34 (m, 2H) ppm**;** ^{13}C NMR (125 MHz, $CDCl_3$) δ 140.7, 140.1, 128.8, 127.5, 127.3, 127.0 ppm.

Compound 12:^{1}H NMR (400 MHz, $CDCl_3$) δ 7.63 (d, *J* = 1.4 Hz, 1H), 7.53 (d, *J* = 7.3 Hz, 2H), 7.47-7.30 (m, 10H) ppm; ^{13}C NMR (100 MHz, $CDCl_3$) δ 141.8, 139.4, 139.2, 139.1, 132.9, 131.7, 129.5, 128.9, 128.5, 128.0, 127.9, 127.6, 127.0, 125.5 ppm.

2,6-Diphenyl-1*H*-indole (13): yield 86%; ^{1}H NMR (500 MHz, DMSO-d_6) δ 11.64 (s, 1H), 7.89 (d, *J* = 7.4 Hz, 2H), 7.69 (d, *J* = 7.3 Hz, 2H), 7.62 (d, *J* = 8.5 Hz, 2H), 7.49-7.46 (m, 4H), 7.34 (t, *J* = 7.1 Hz, 3H), 6.95 (d, *J* = 1.5 Hz, 1H) ppm; ^{13}C NMR (125 MHz, DMSO-d_6) δ 141.8, 138.9, 138.2, 134.4, 132.5, 129.4, 129.3, 128.6, 127.9, 127.1, 127.0, 125.4, 120.9, 119.4, 109.6, 99.1 ppm.

2.7. Copies of ^{1}H and ^{13}C NMR spectra of some important compounds described in chapter 2

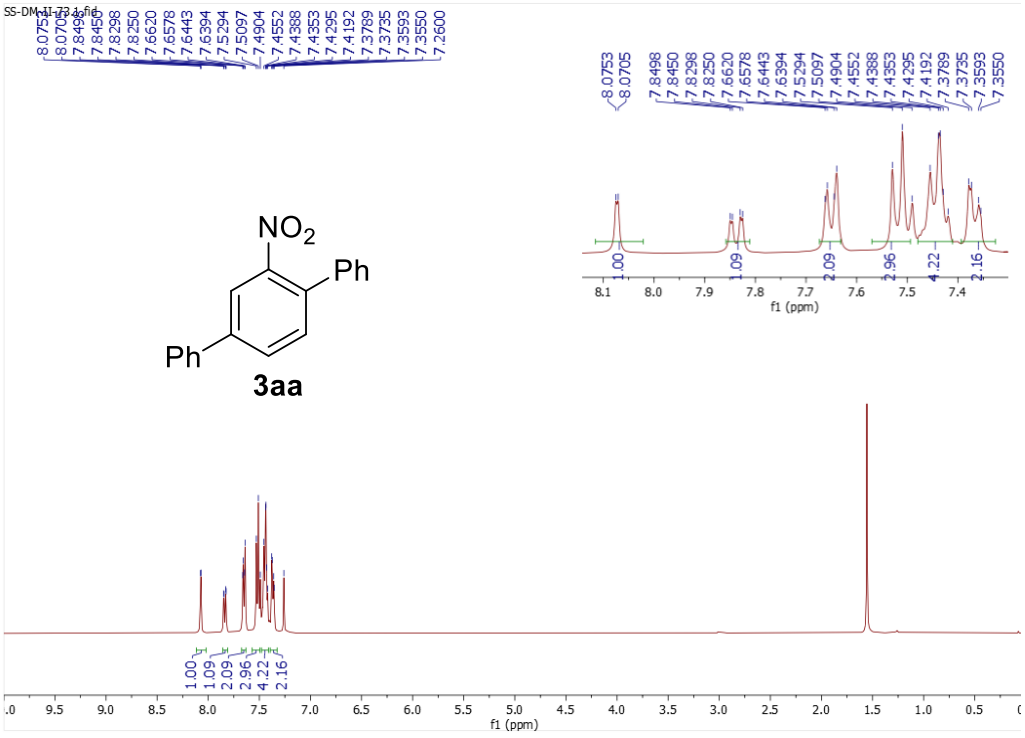

Figure 2.2 400 MHz ^{1}H NMR spectrum of **3aa** in $CDCl_3$.

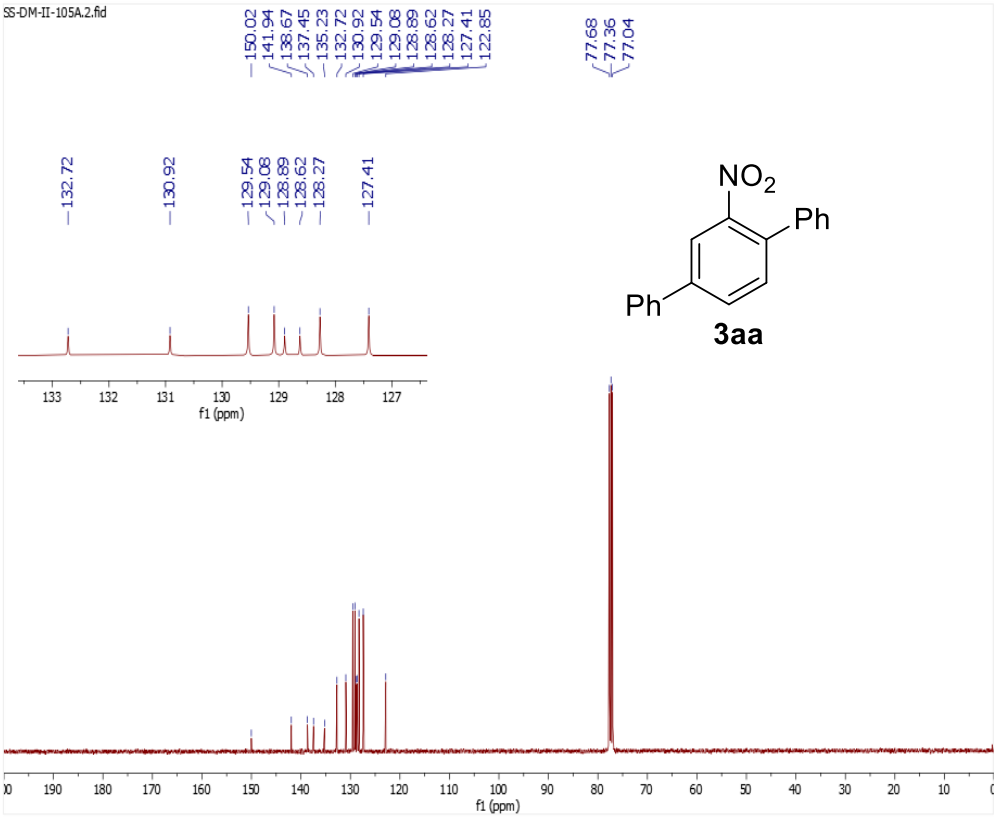

Figure 2.3 100 MHz ^{13}C NMR spectrum of **3aa** in $CDCl_3$.

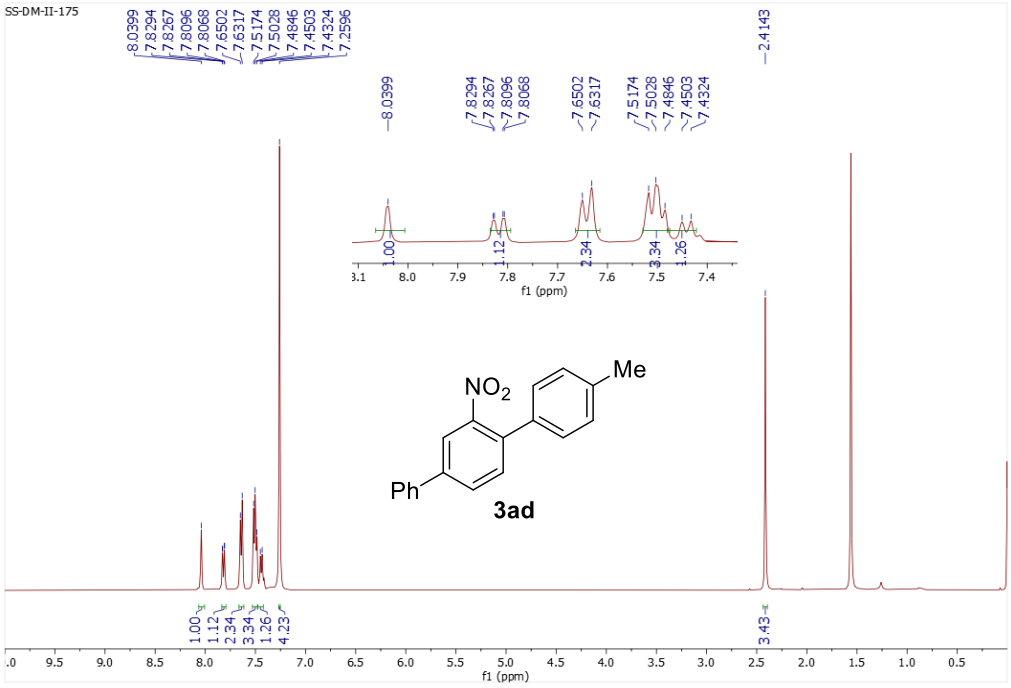

Figure 2.4 400 MHz ^{1}H NMR spectrum of **3ad** in $CDCl_3$.

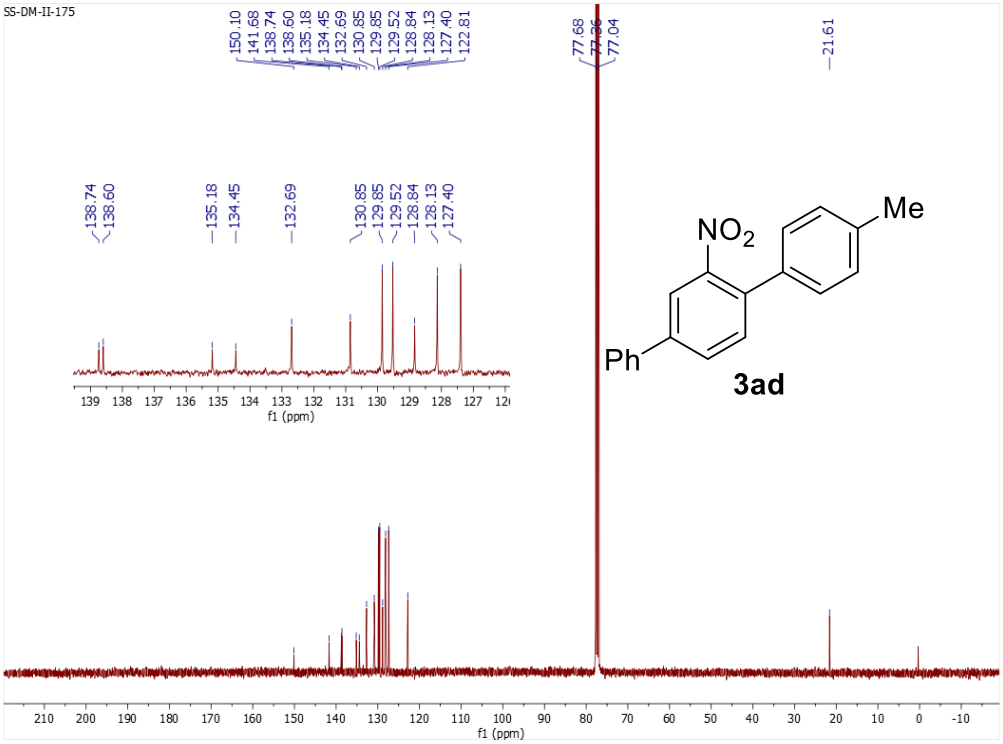

Figure 2.5 100 MHz ^{13}C NMR spectrum of **3ad** in $CDCl_3$.

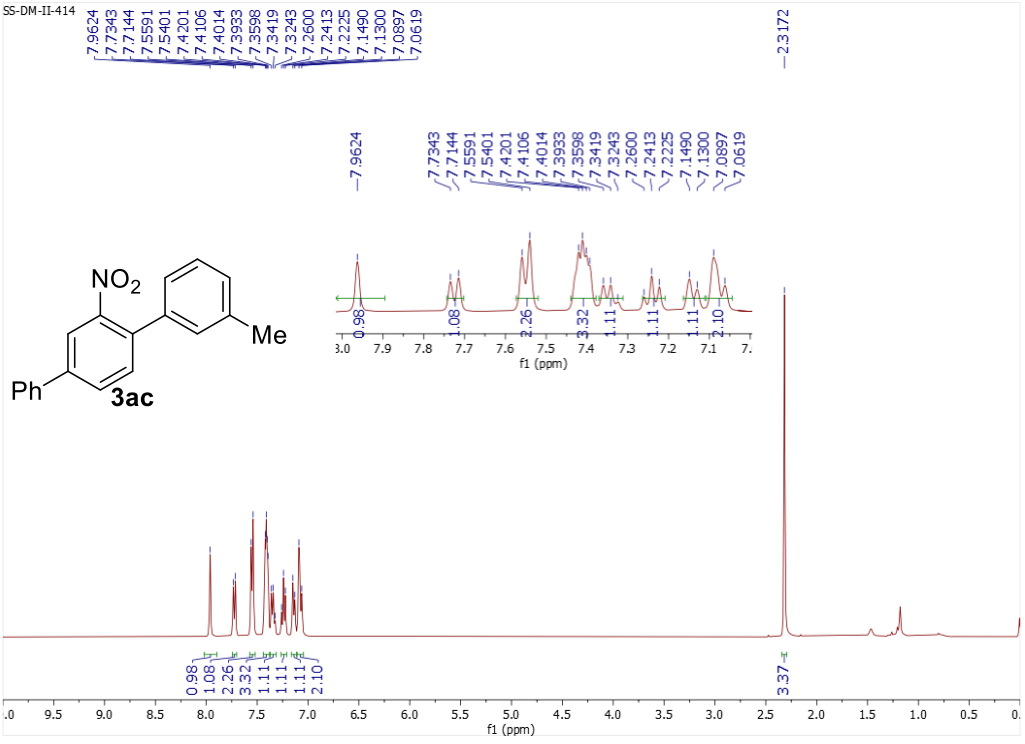

Figure 2.6 400 MHz ^{1}H NMR spectrum of **3ac** in $CDCl_3$.

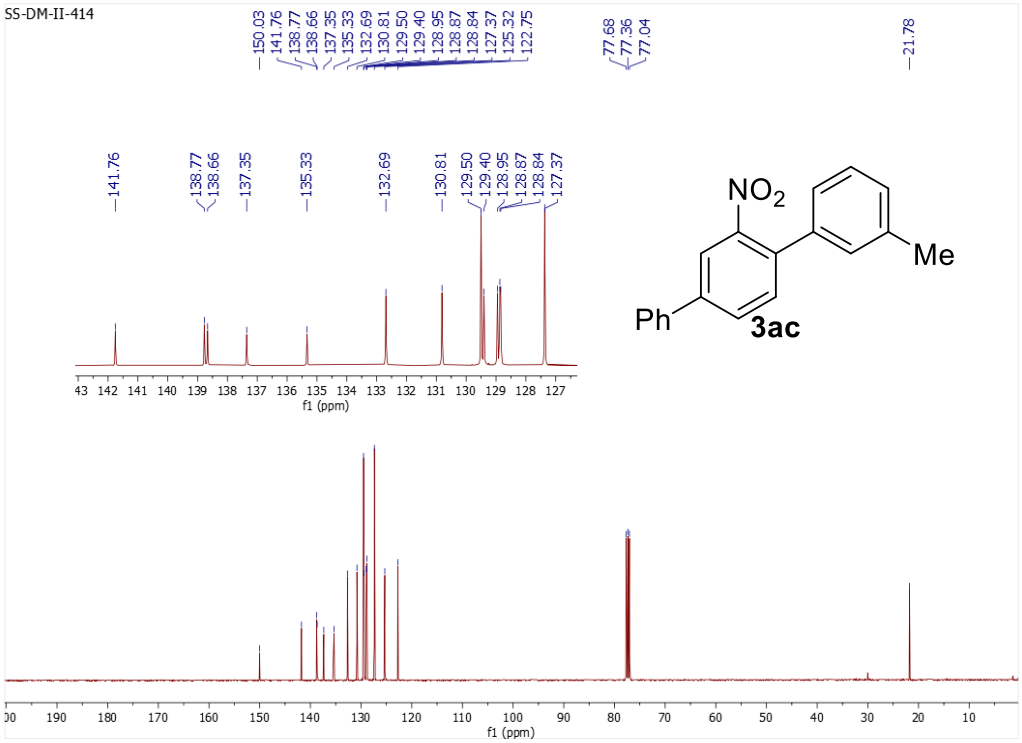

Figure 2.7 100 MHz ^{13}C NMR spectrum of **3ac** in $CDCl_3$.

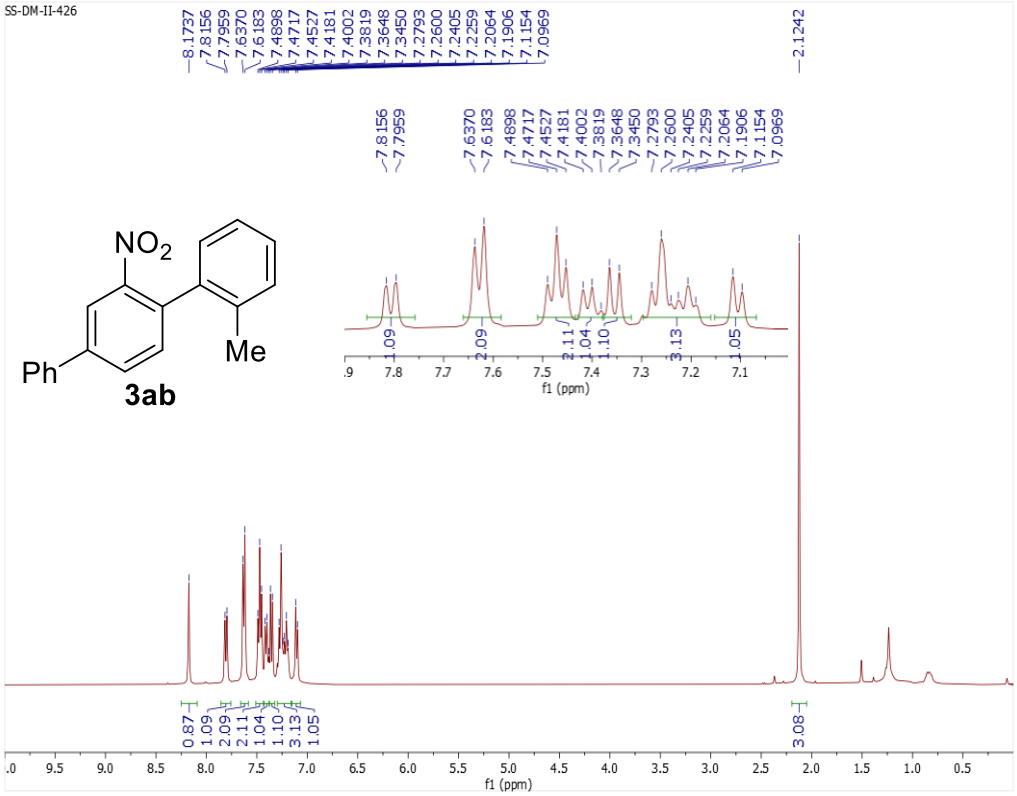

Figure 2.8 400 MHz ^{1}H NMR spectrum of **3ab** in $CDCl_3$.

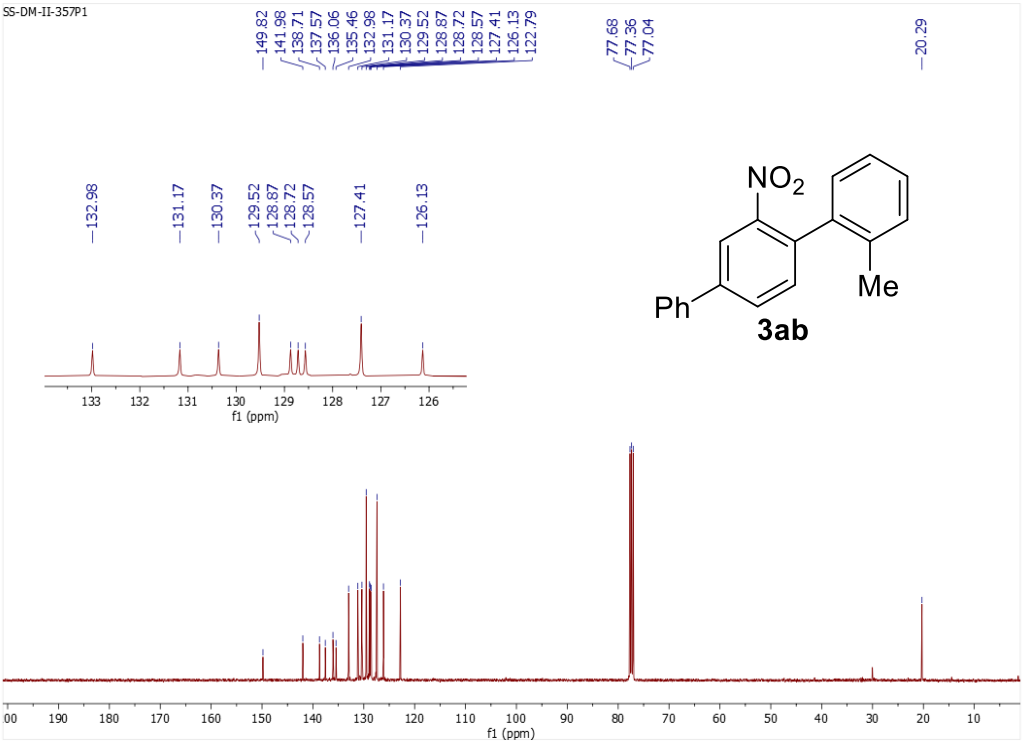

Figure 2.9 100 MHz ^{13}C NMR spectrum of **3ab** in $CDCl_3$.

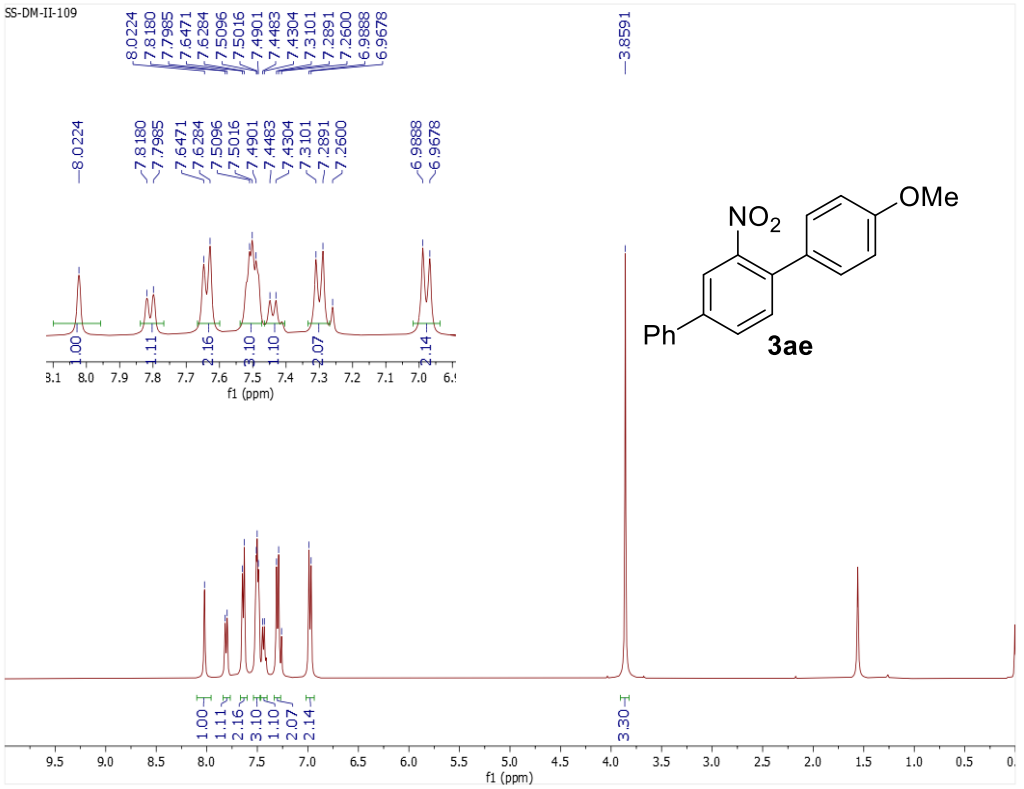

Figure 2.10 400 MHz ^{1}H NMR spectrum of **3ae** in $CDCl_3$.

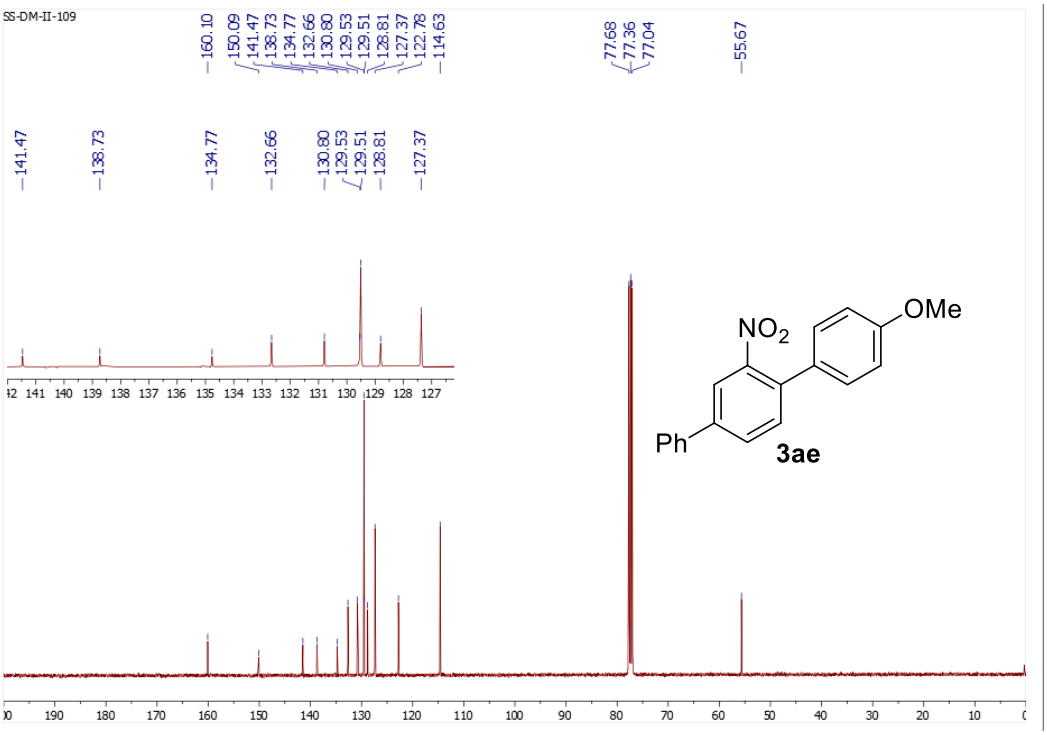

Figure 2.11 100 MHz ^{13}C NMR spectrum of **3ae** in $CDCl_3$.

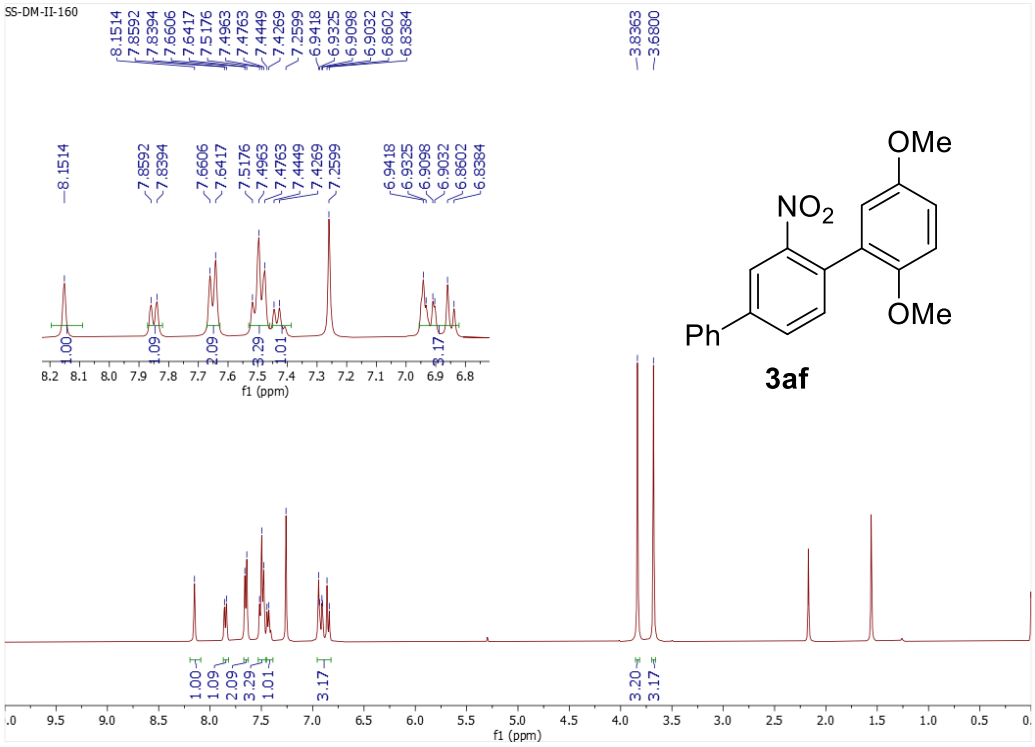

Figure 2.12 400 MHz ^{1}H NMR spectrum of **3af** in $CDCl_3$.

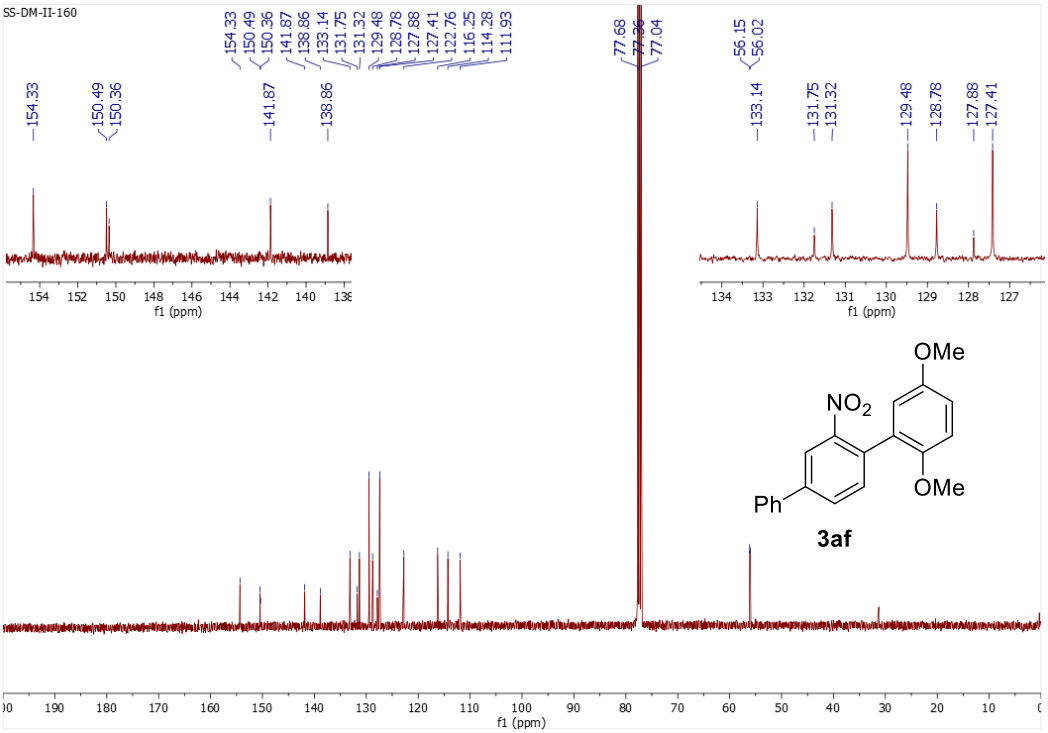

Figure 2.13 100 MHz ^{13}C NMR spectrum of **3af** in $CDCl_3$.

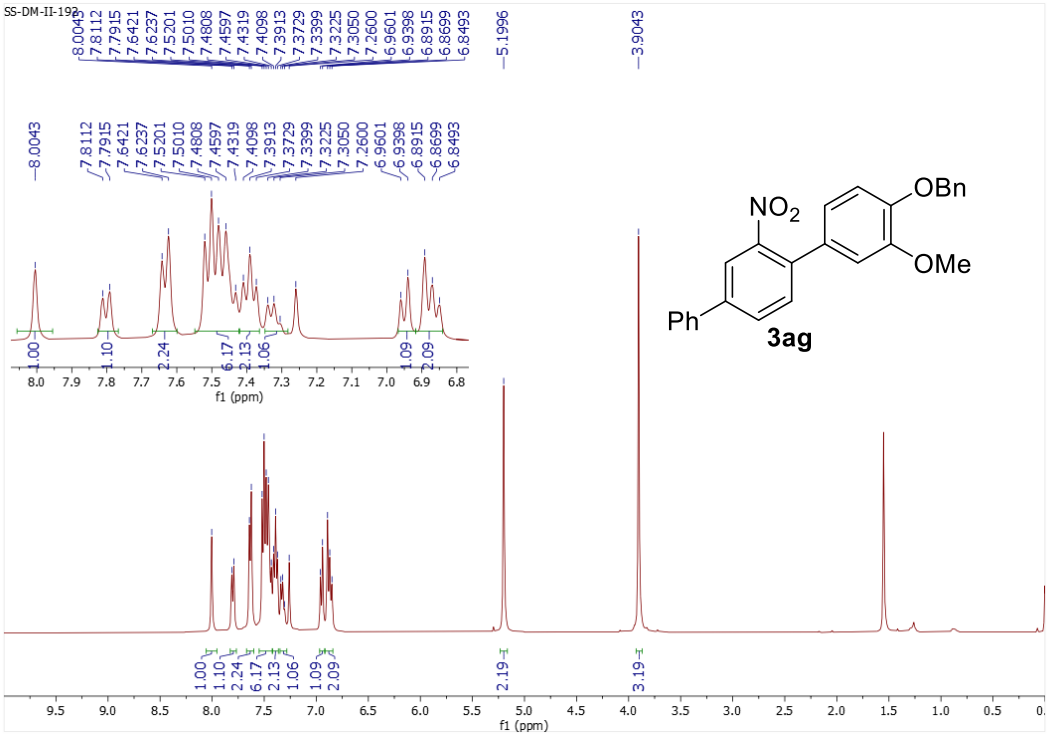

Figure 2.14 400 MHz ^{1}H NMR spectrum of **3ag** in $CDCl_3$.

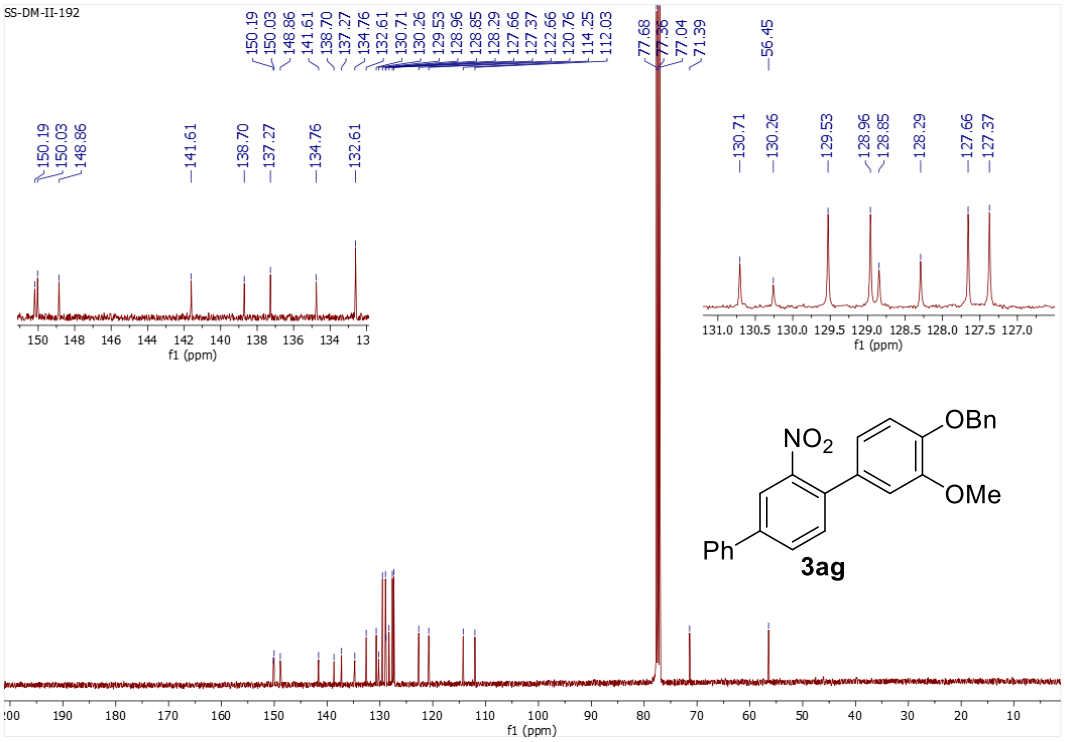

Figure 2.15 100 MHz ^{13}C NMR spectrum of **3ag** in $CDCl_3$.

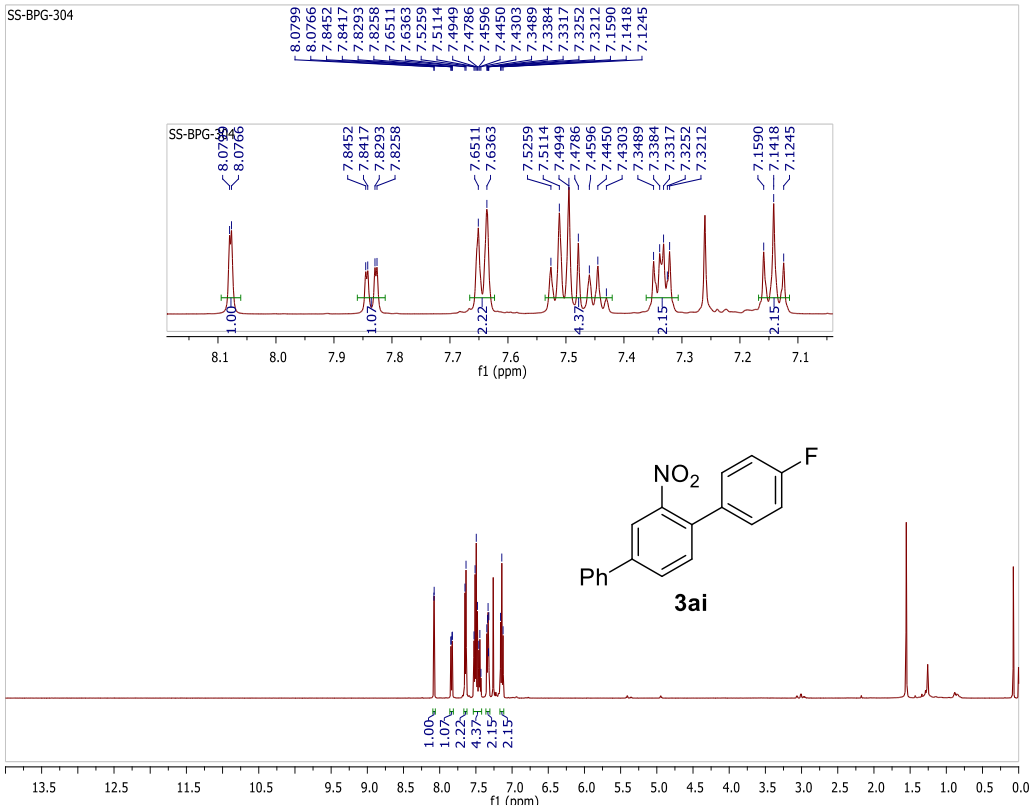

Figure 2.16 500 MHz ^{1}H NMR spectrum of **3ai** in $CDCl_3$.

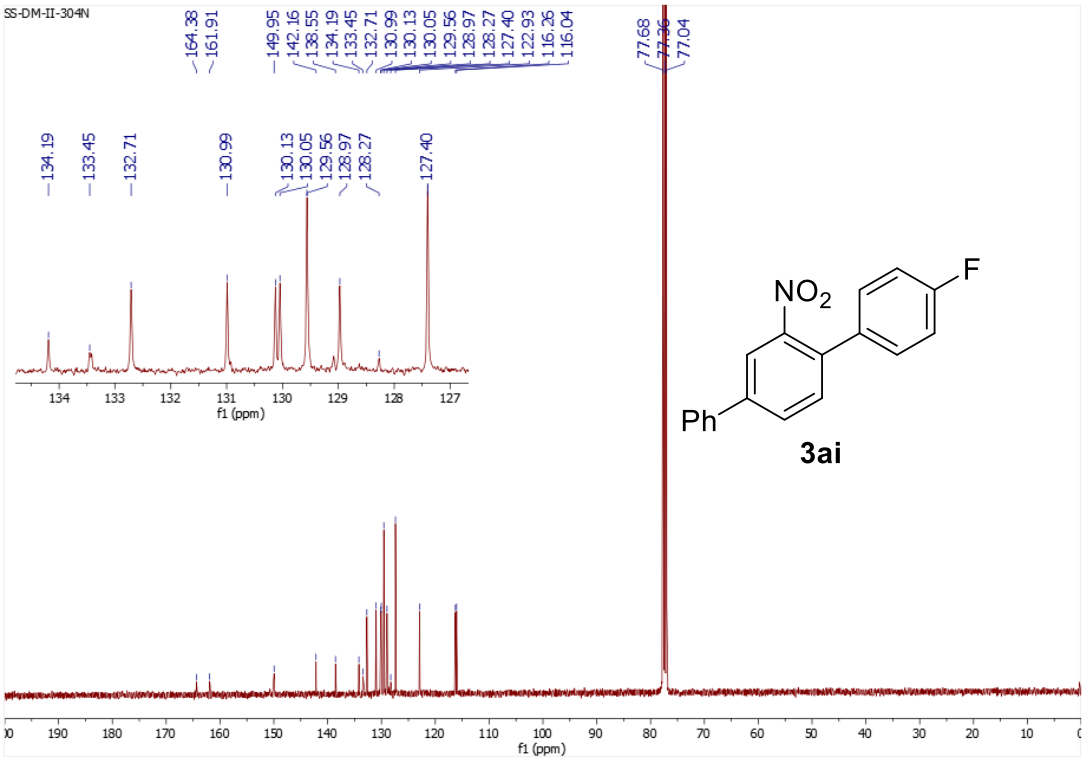

Figure 2.17 125 MHz ^{13}C NMR spectrum of **3ai** in $CDCl_3$.

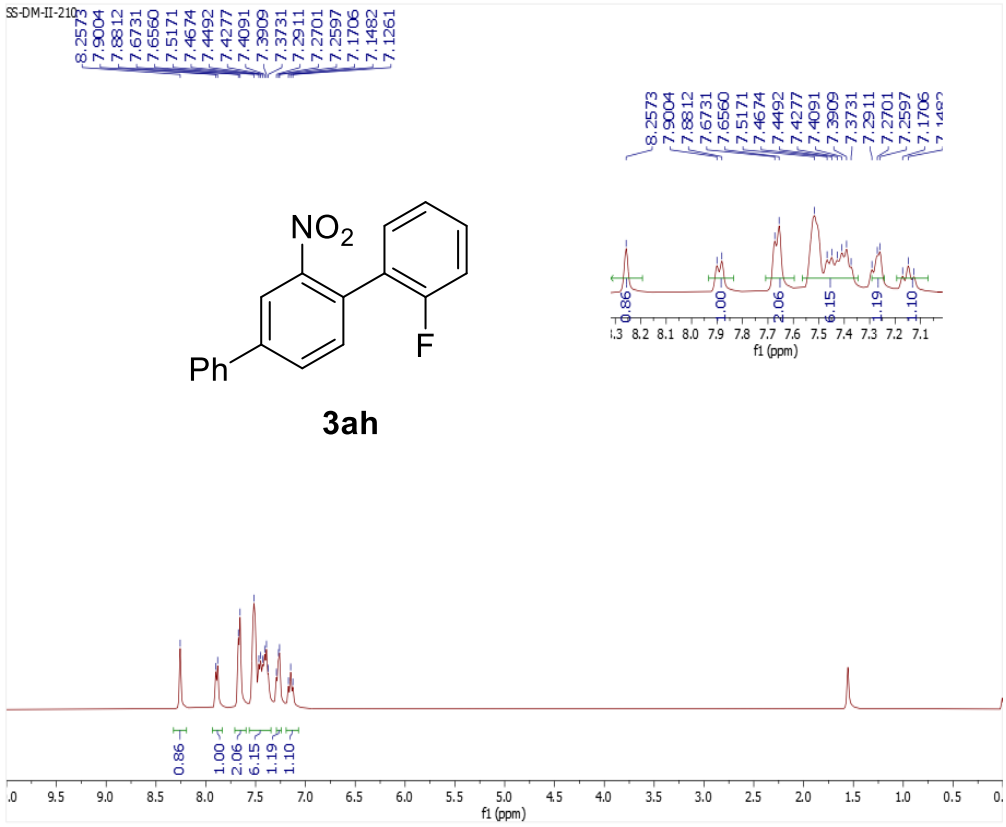

Figure 2.18 400 MHz ^{1}H NMR spectrum of **3ah** in $CDCl_3$.

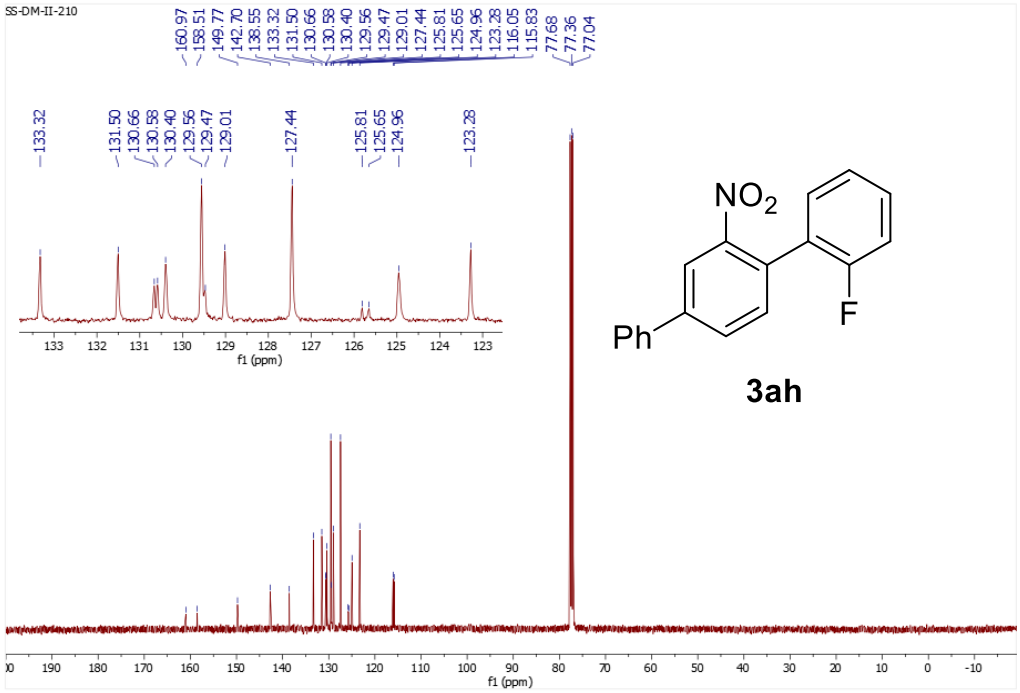

Figure 2.19 100 MHz ^{13}C NMR spectrum of **3ah** in $CDCl_3$.

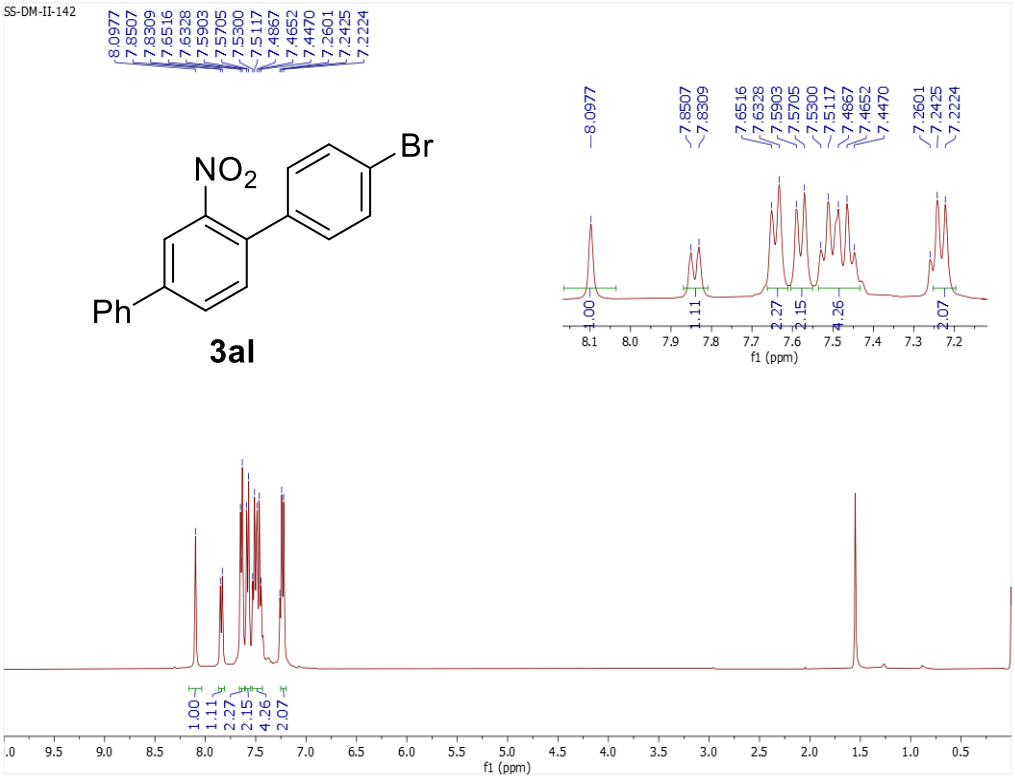

Figure 2.20 400 MHz ^{1}H NMR spectrum of **3al** in $CDCl_3$.

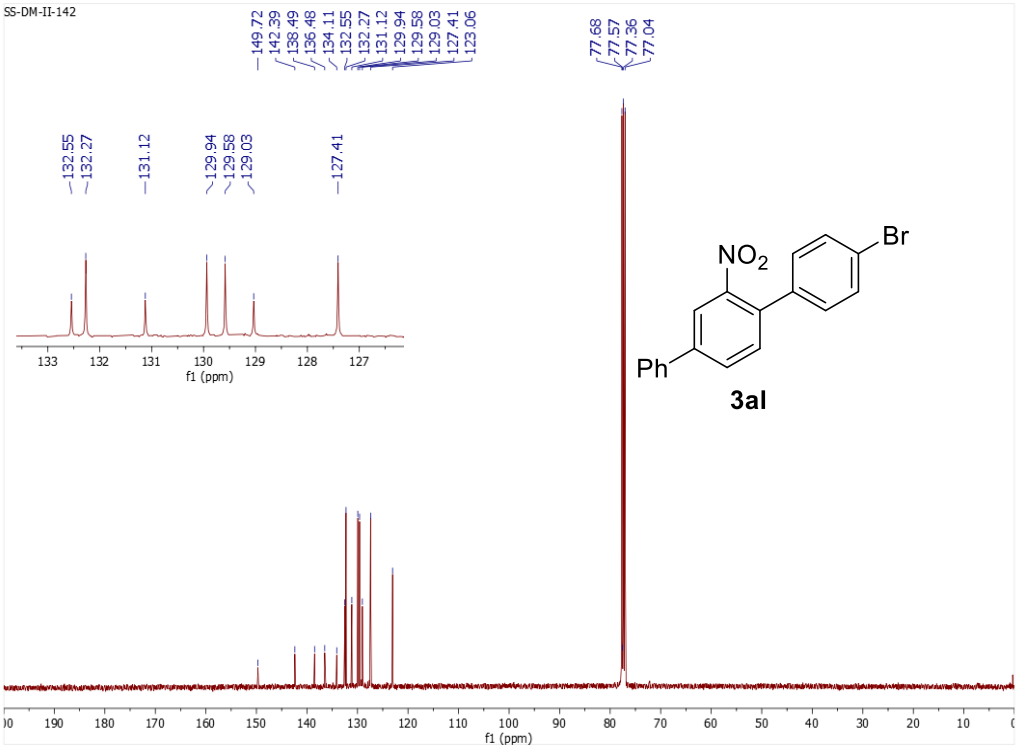

Figure 2.21 100 MHz ^{13}C NMR spectrum of **3al** in $CDCl_3$.

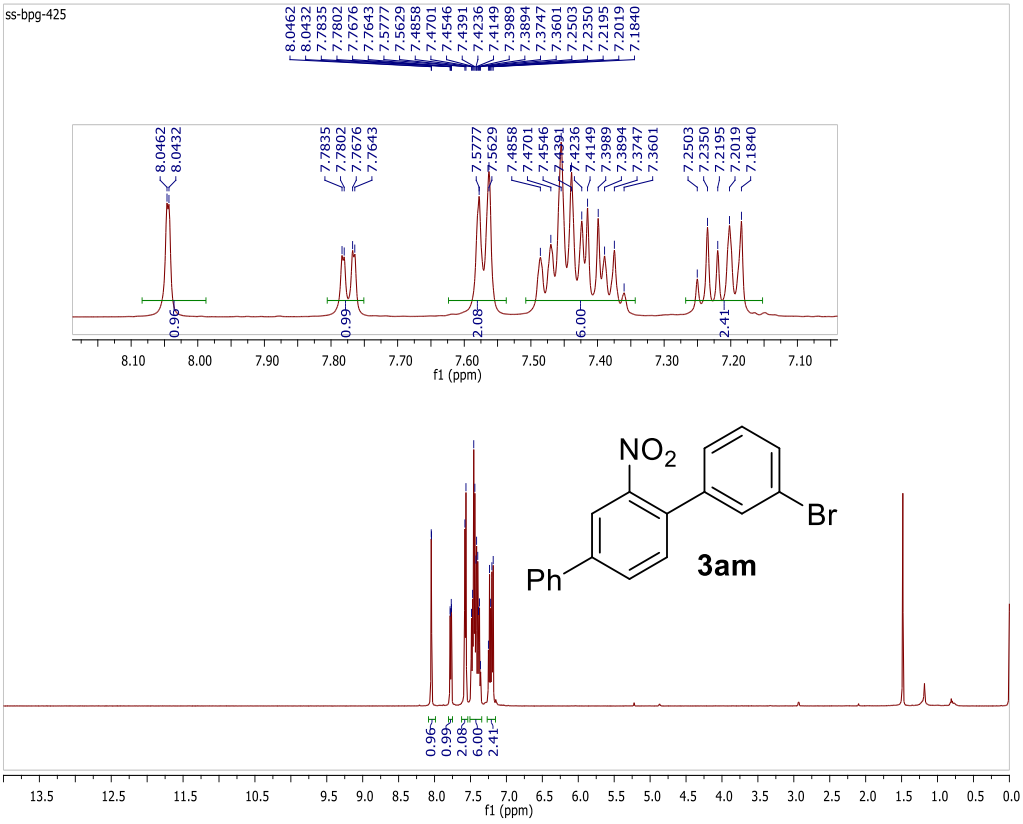

Figure 2.22 500 MHz ^{1}H NMR spectrum of **3am** in $CDCl_3$.

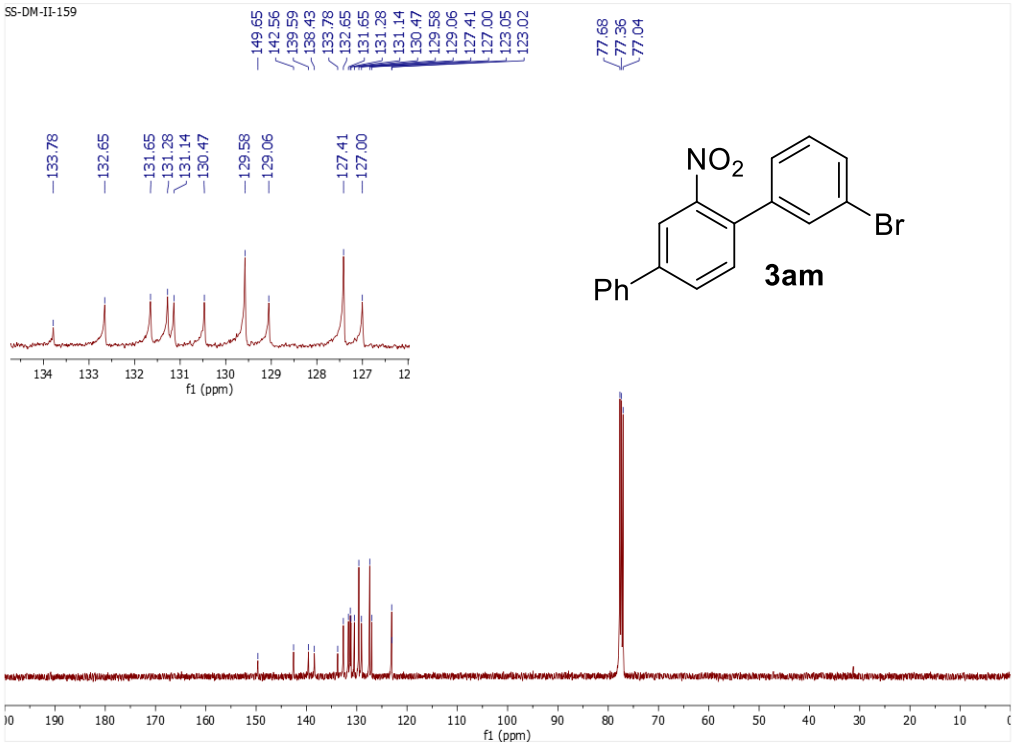

Figure 2.23 125 MHz ^{13}C NMR spectrum of **3am** in $CDCl_3$.

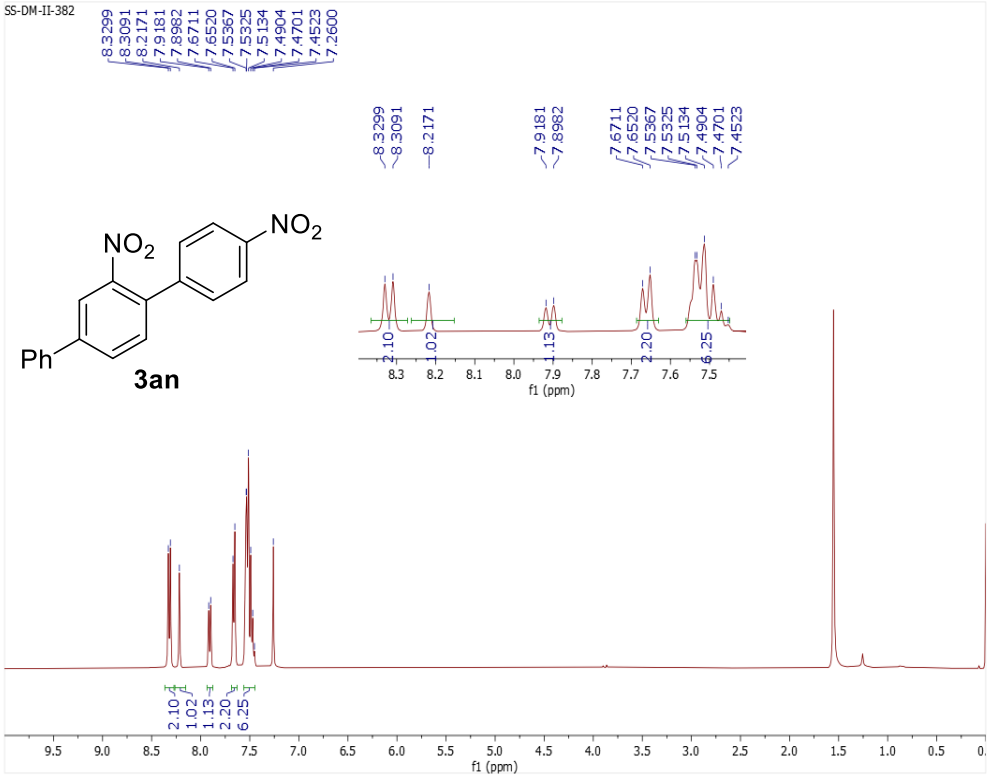

Figure 2.24 400 MHz ^{1}H NMR spectrum of **3an** in $CDCl_3$.

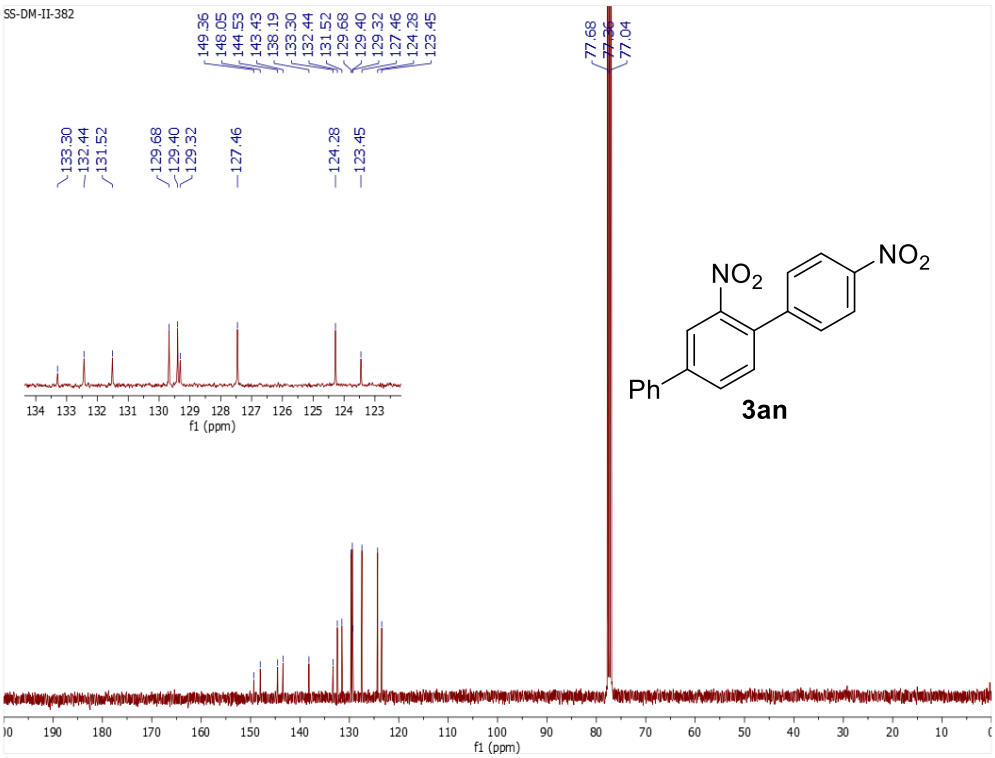

Figure 2.25 100 MHz ^{13}C NMR spectrum of **3an** in $CDCl_3$.

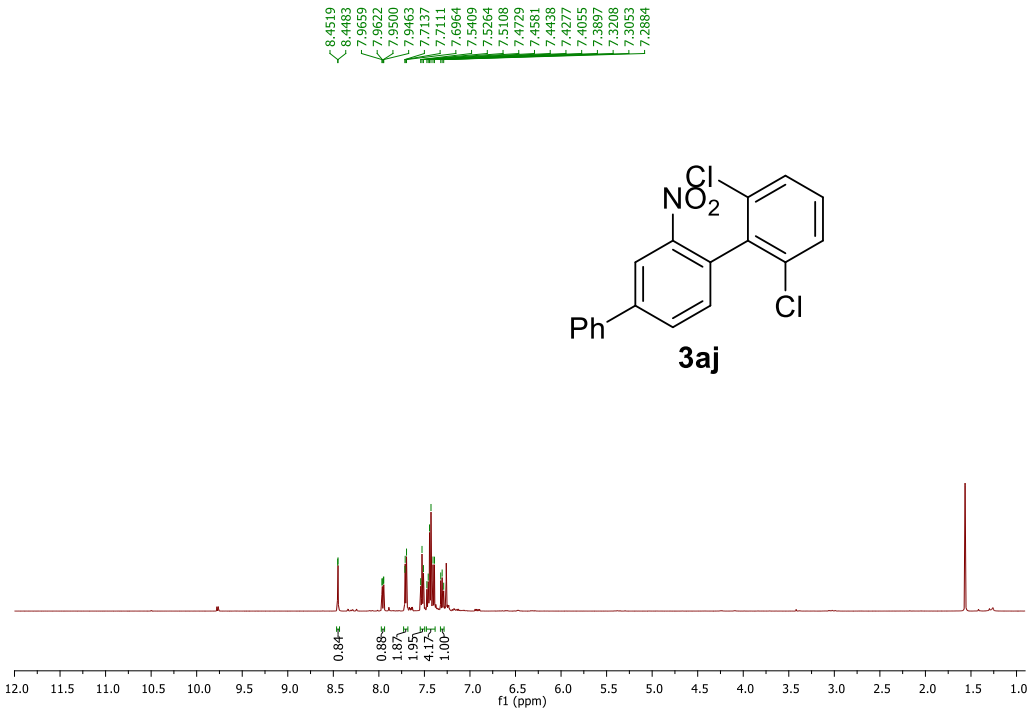

Figure 2.26 500 MHz ^{1}H NMR spectrum of **3aj** in $CDCl_3$.

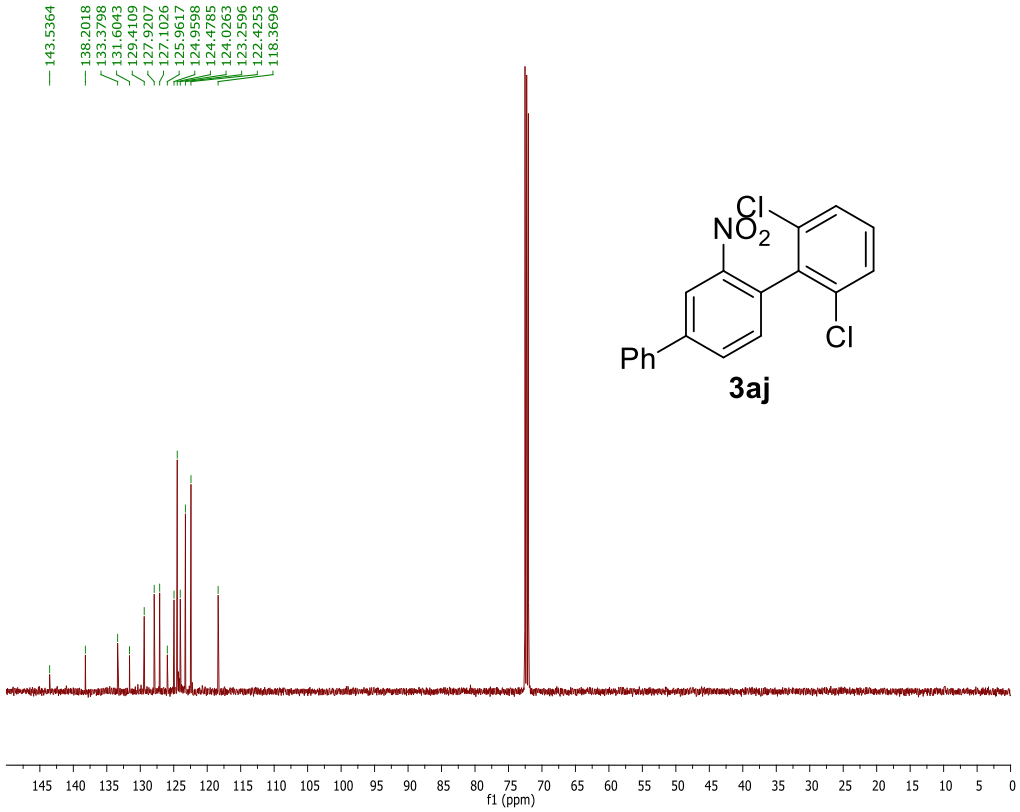

Figure 2.27 125 MHz ^{13}C NMR spectrum of **3aj** in $CDCl_3$.

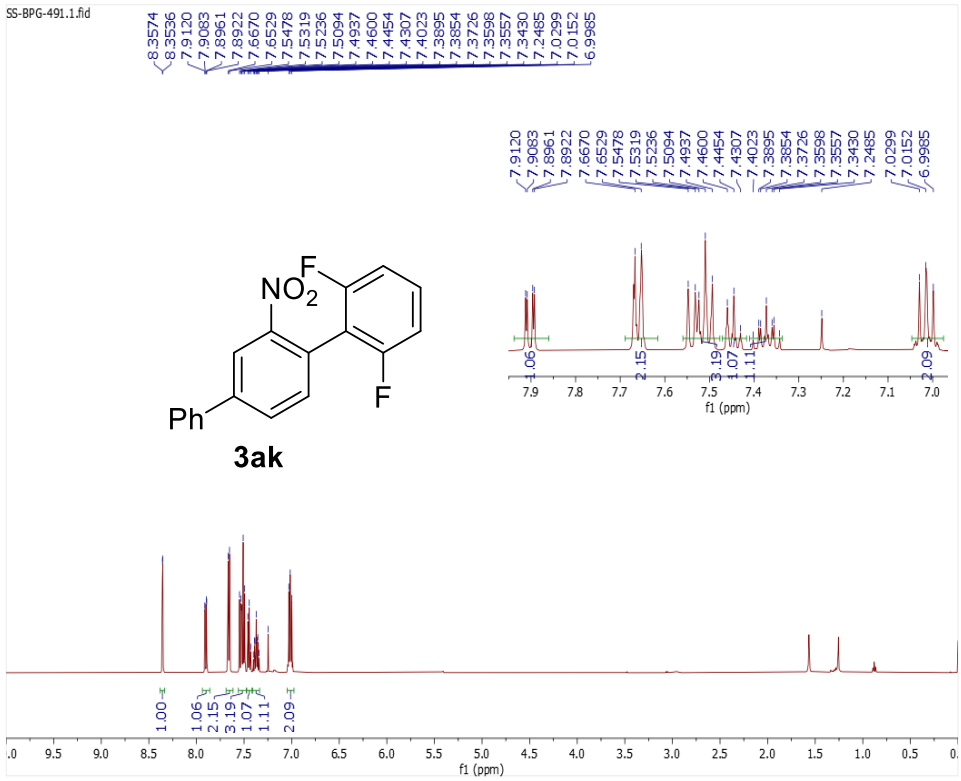

Figure 2.28 500 MHz ^{1}H NMR spectrum of **3ak** in $CDCl_3$.

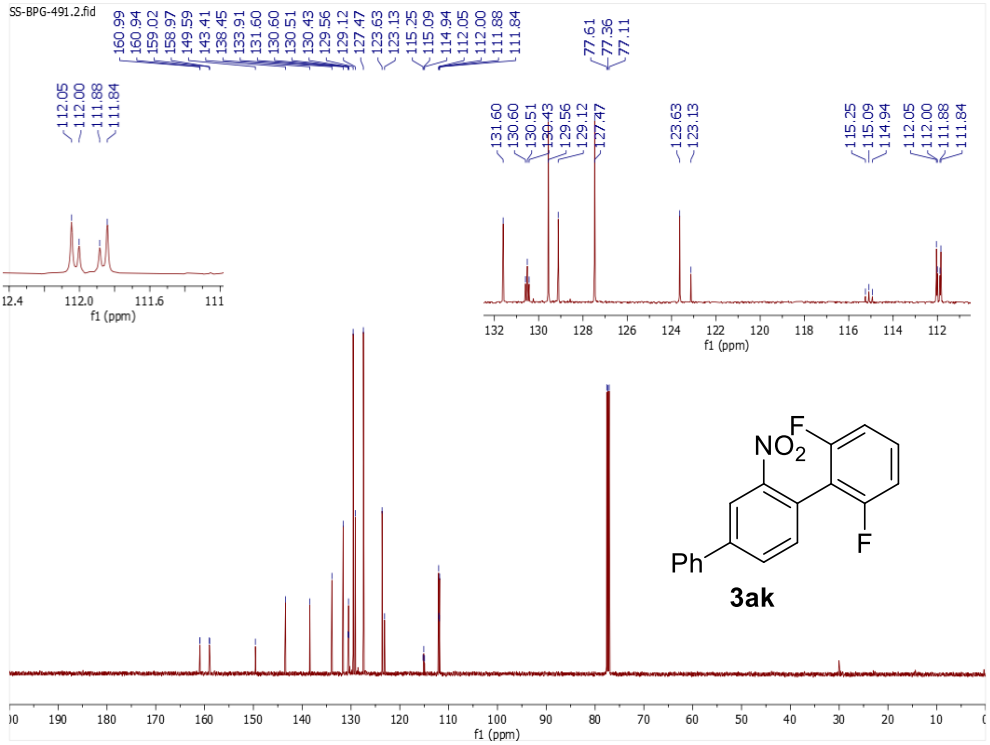

Figure 2.29 125 MHz ^{13}C NMR spectrum of **3ak** in $CDCl_3$.

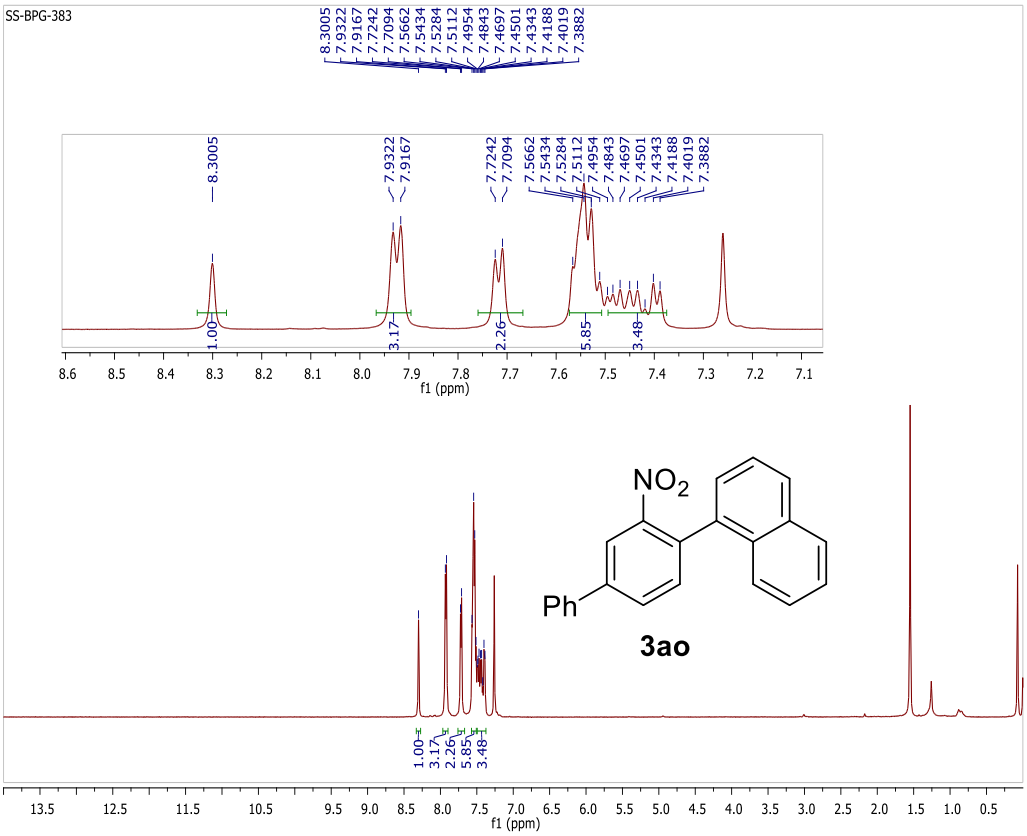

Figure 2.30 500 MHz ^{1}H NMR spectrum of **3ao** in $CDCl_3$.

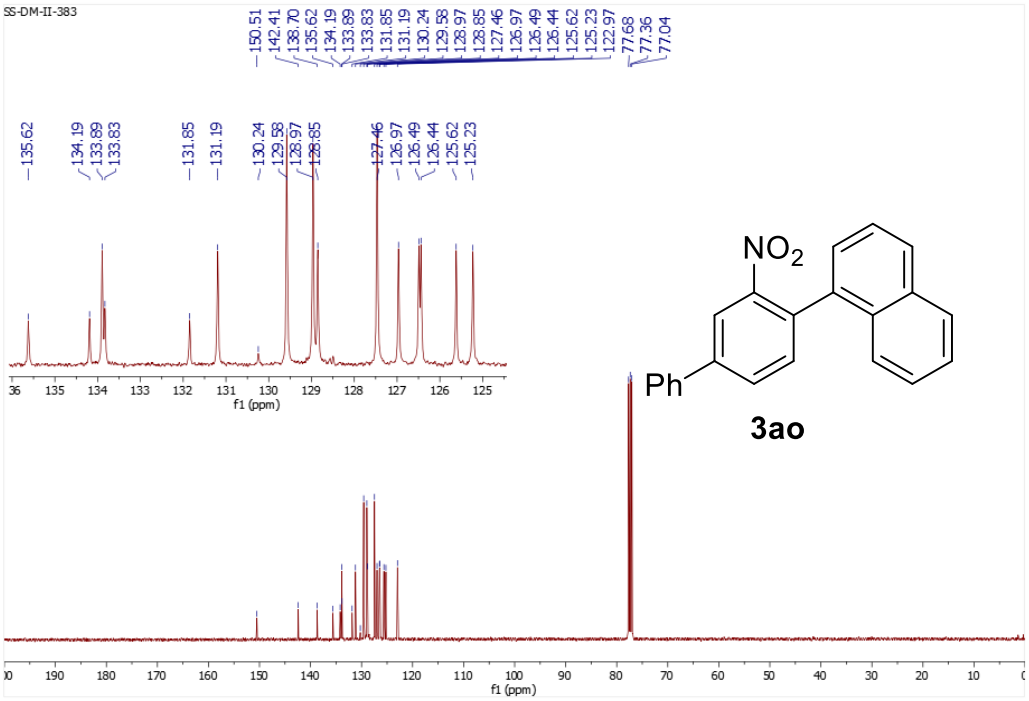

Figure 2.31 125 MHz ^{13}C NMR spectrum of **3ao** in $CDCl_3$.

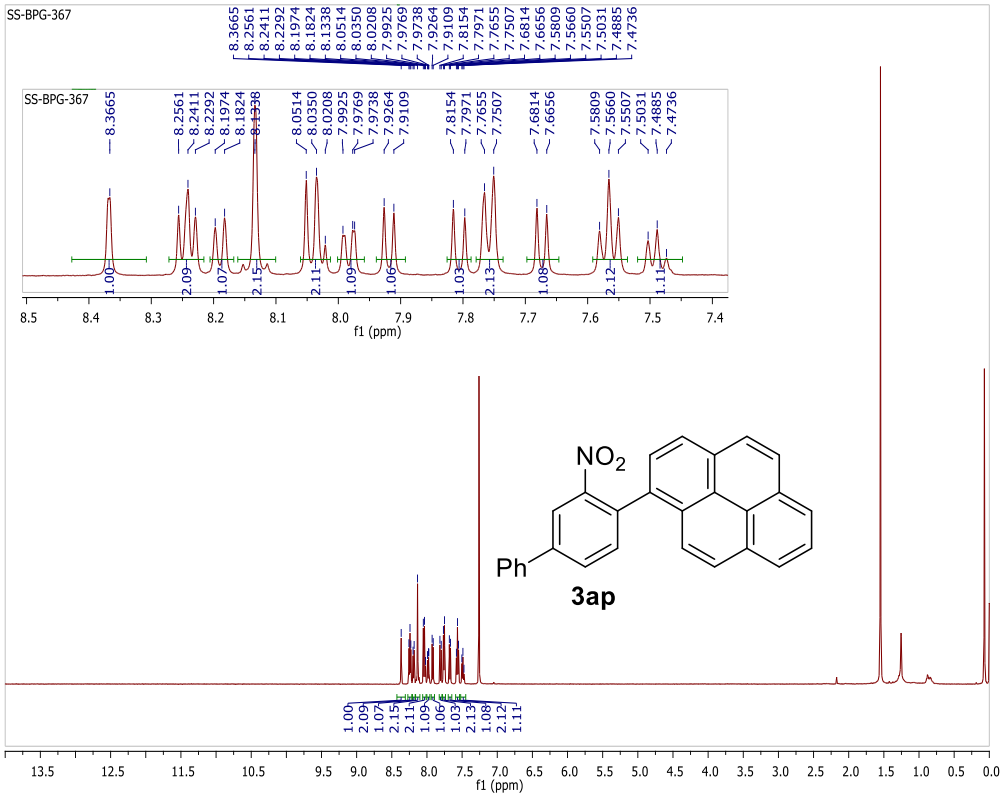

Figure 2.32 500 MHz ^{1}H NMR spectrum of **3ap** in $CDCl_3$.

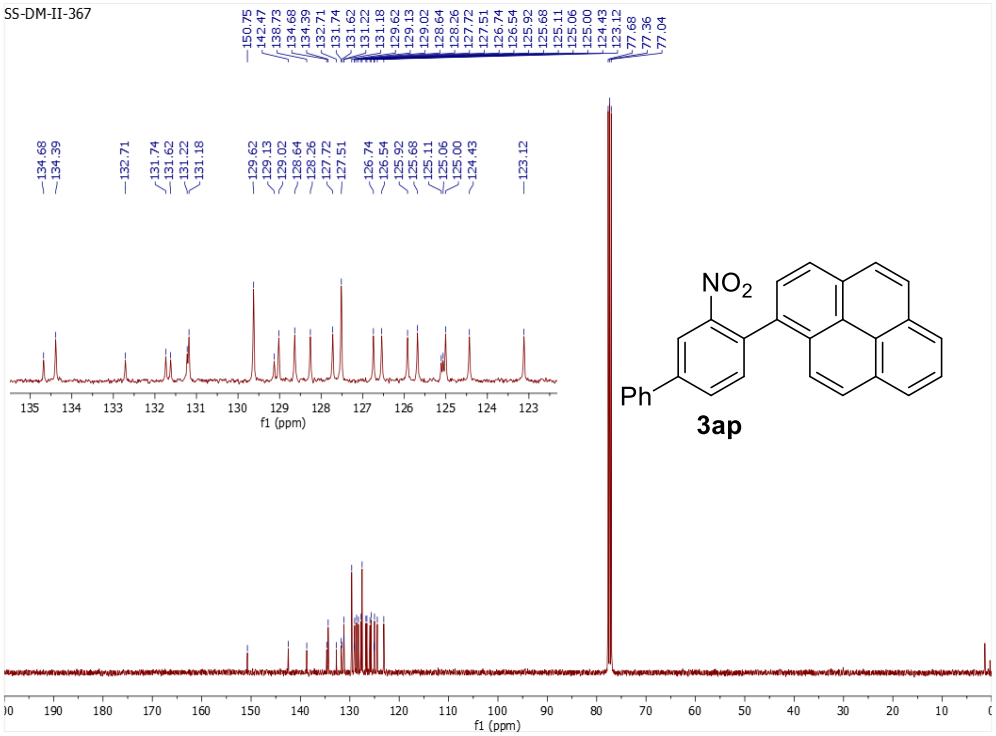

Figure 2.33 125 MHz ^{13}C NMR spectrum of **3ap** in $CDCl_3$.

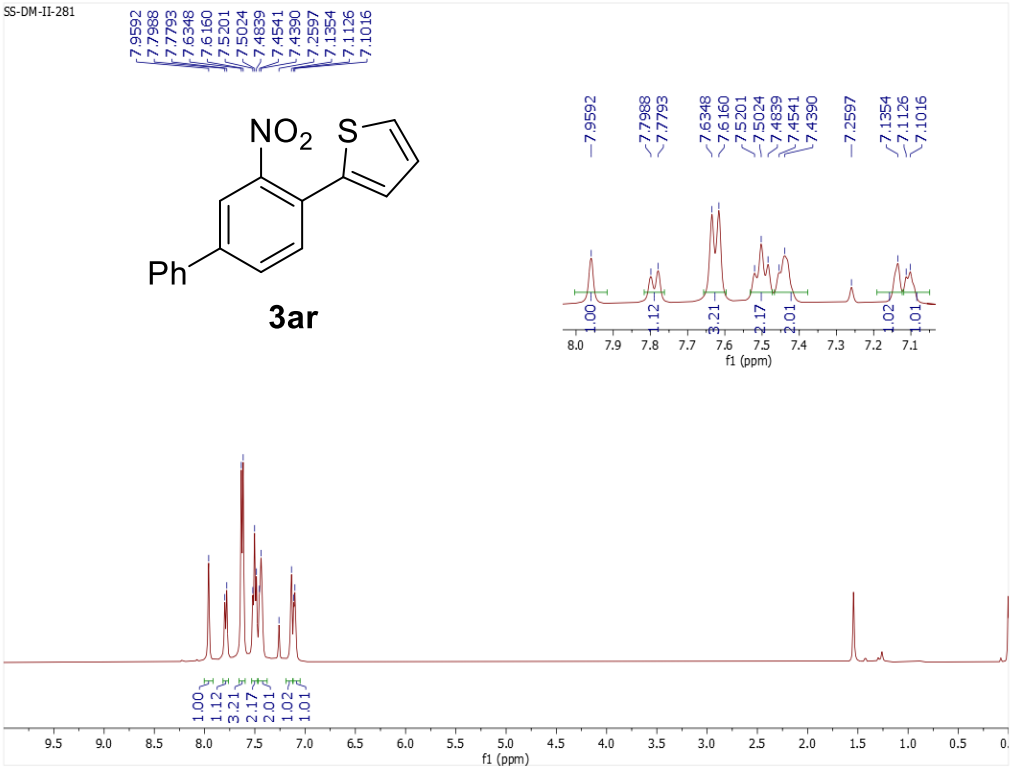

Figure 2.34 500 MHz ^{1}H NMR spectrum of **3ar** in $CDCl_3$.

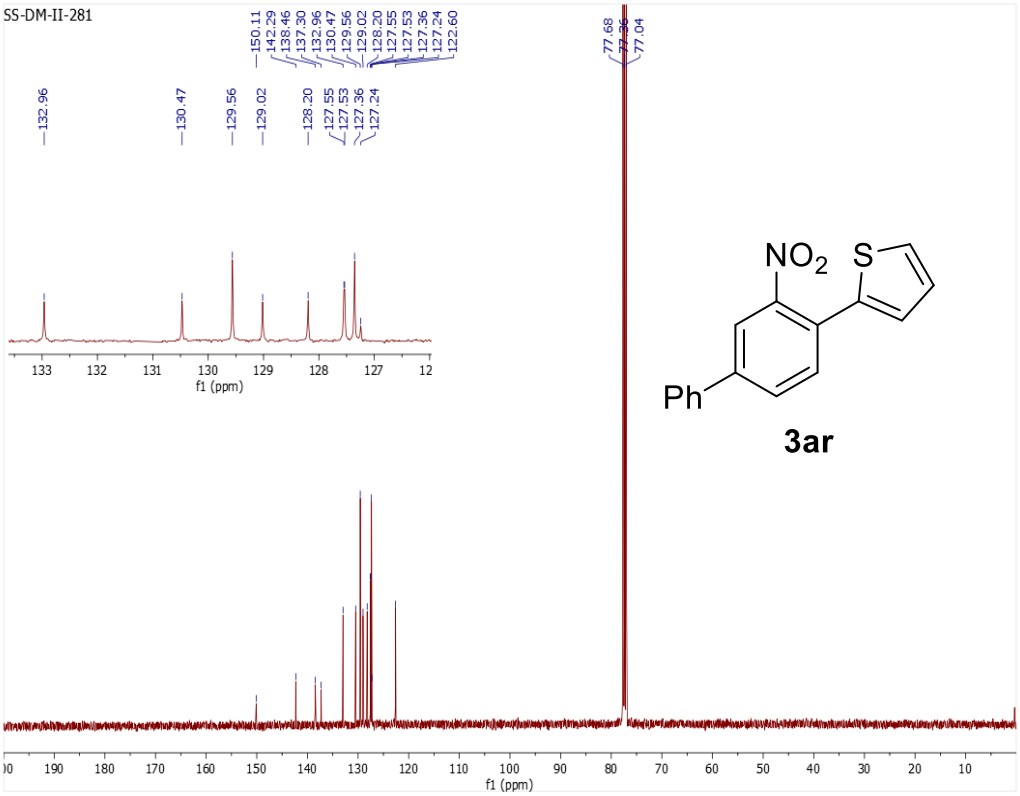

Figure 2.35 125 MHz ^{13}C NMR spectrum of **3ar** in $CDCl_3$.

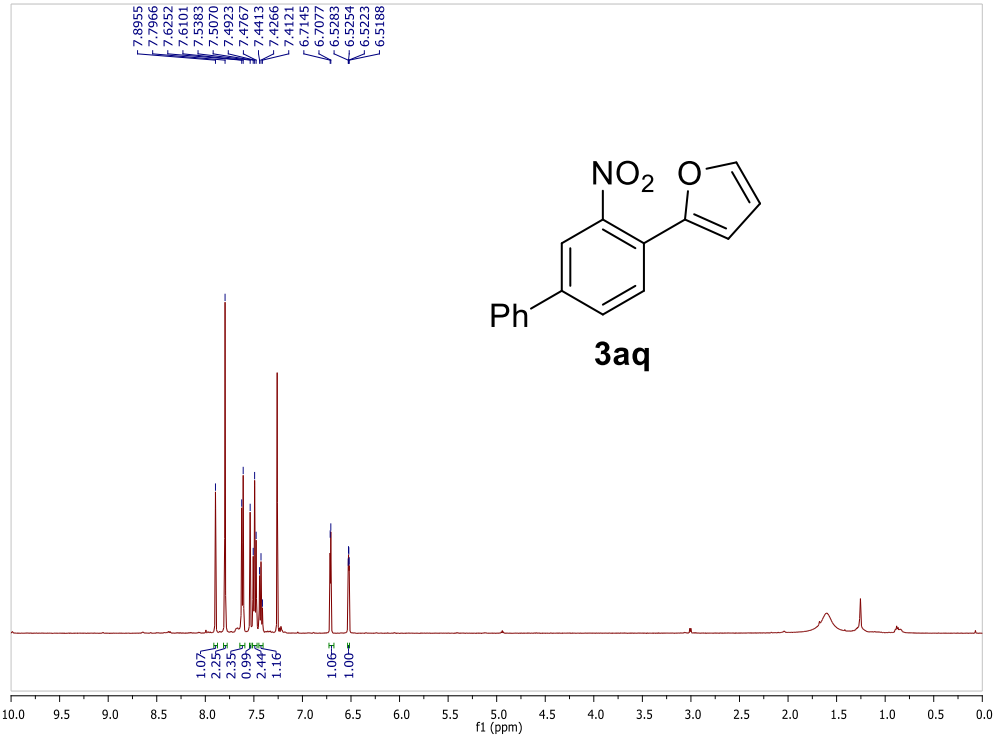

Figure 2.36 400 MHz ^{1}H NMR spectrum of **3aq** in $CDCl_3$.

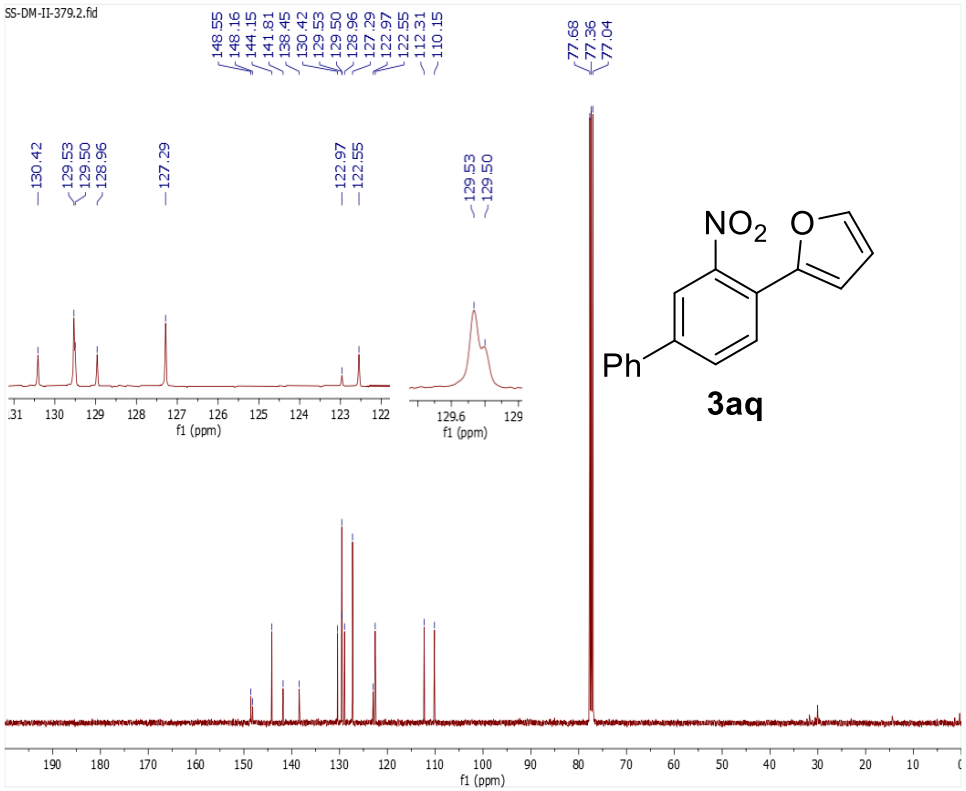

Figure 2.37 100 MHz ^{13}C NMR spectrum of **3aq** in $CDCl_3$.

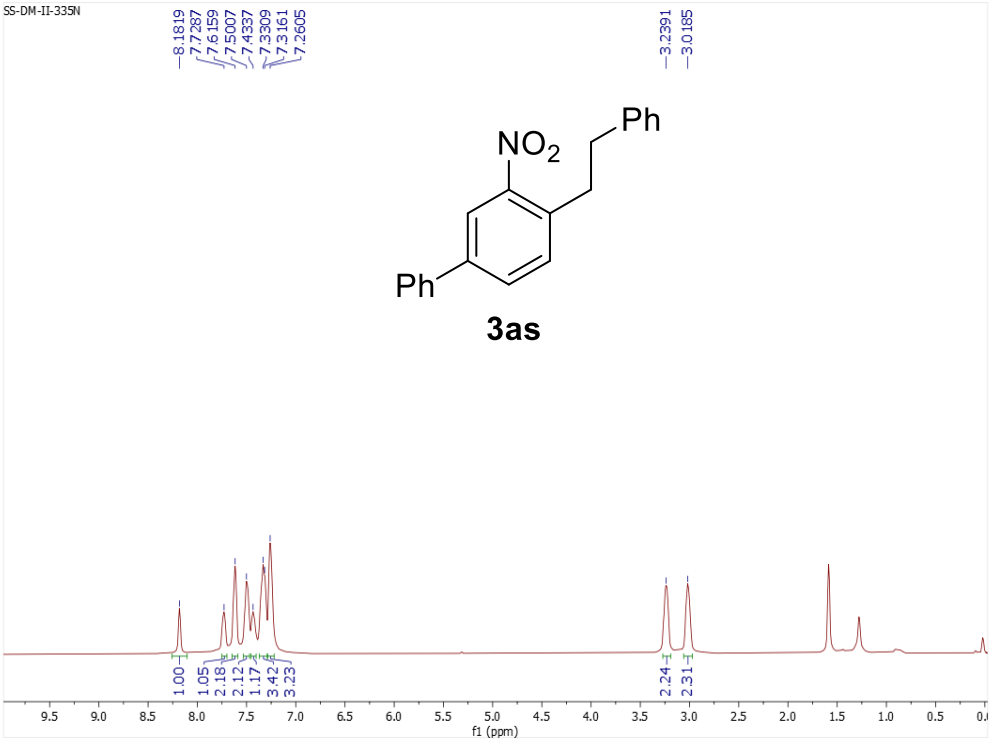

Figure 2.38 400 MHz ^{1}H NMR spectrum of **3as** in $CDCl_3$.

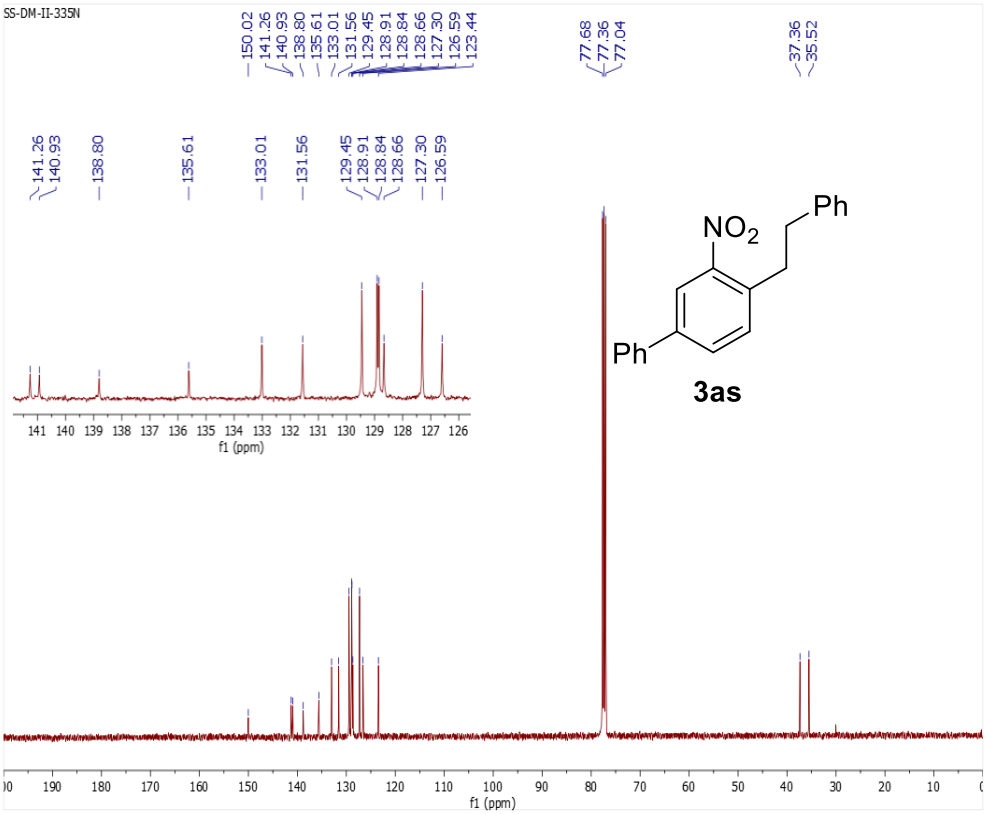

Figure 2.39 100 MHz ^{13}C NMR spectrum of **3as** in $CDCl_3$.

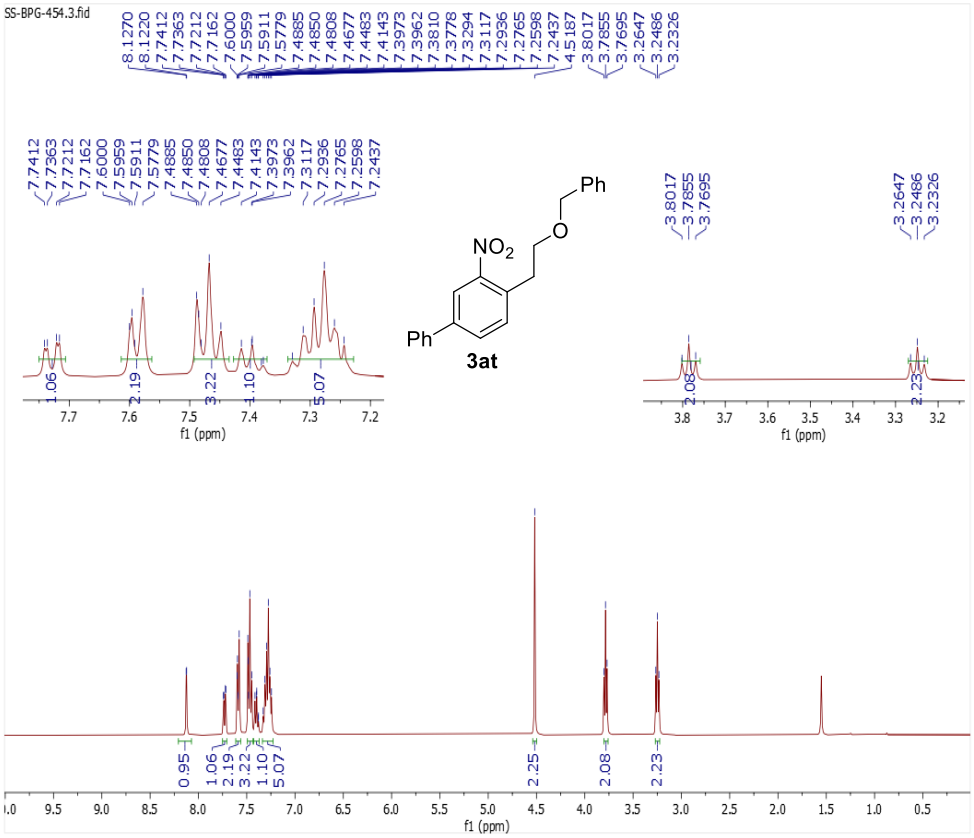

Figure 2.40 400 MHz ^{1}H NMR spectrum of **3at** in $CDCl_3$.

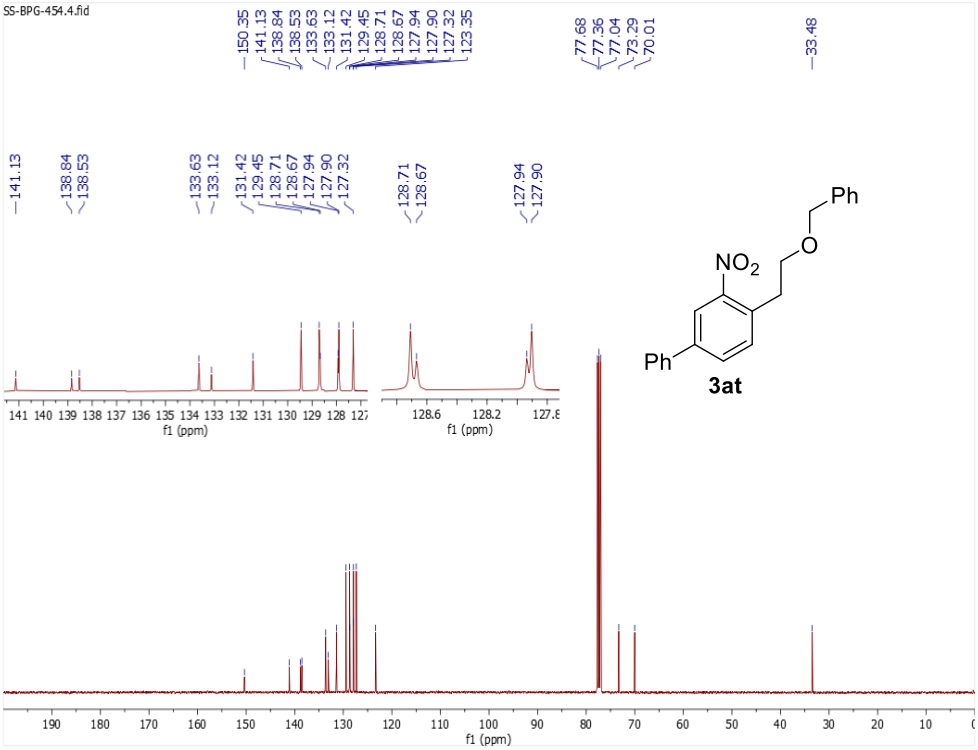

Figure 2.41 100 MHz ^{13}C NMR spectrum of **3at** in $CDCl_3$.

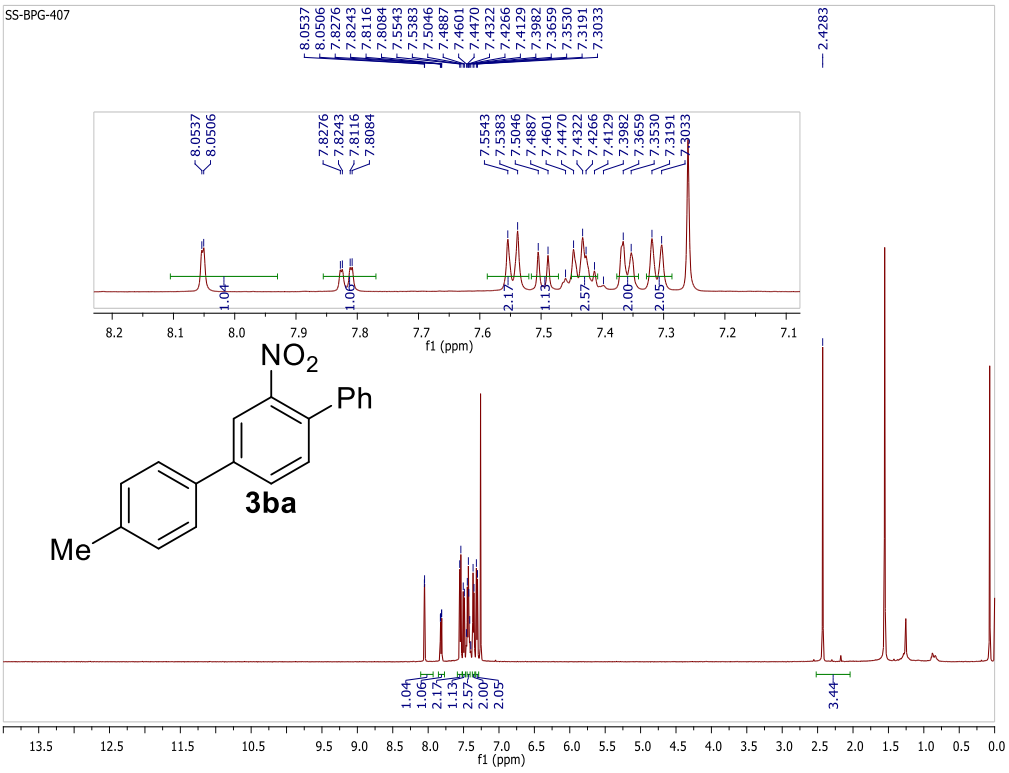

Figure 2.42 500 MHz ^{1}H NMR spectrum of **3ba** in $CDCl_3$.

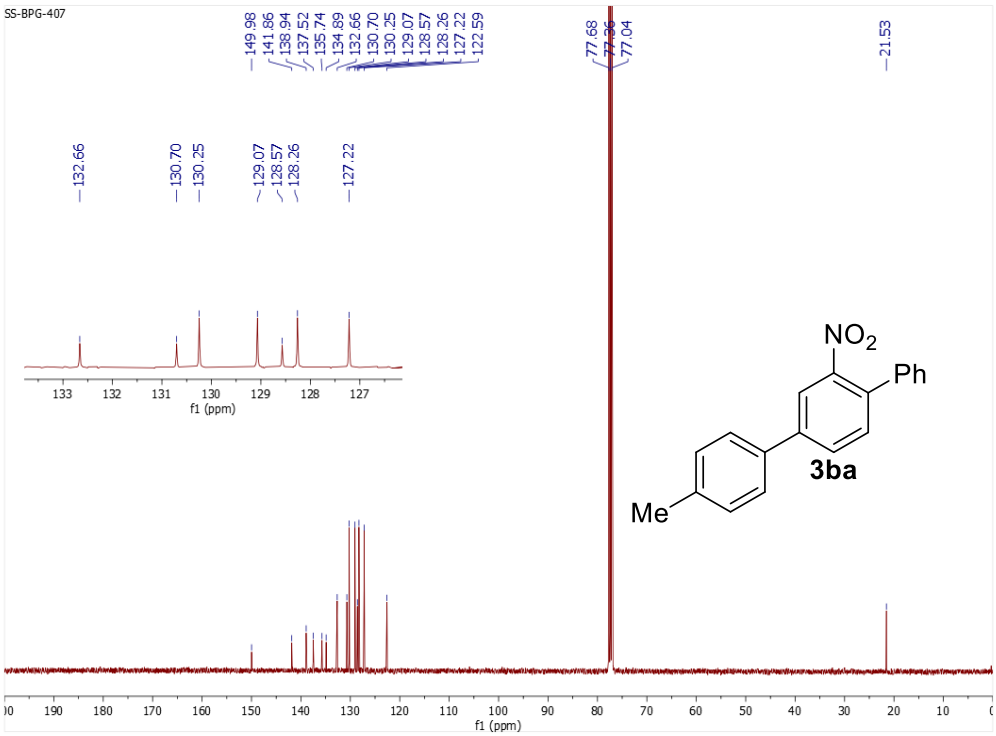

Figure 2.43 125 MHz ^{13}C NMR spectrum of **3ba** in $CDCl_3$.

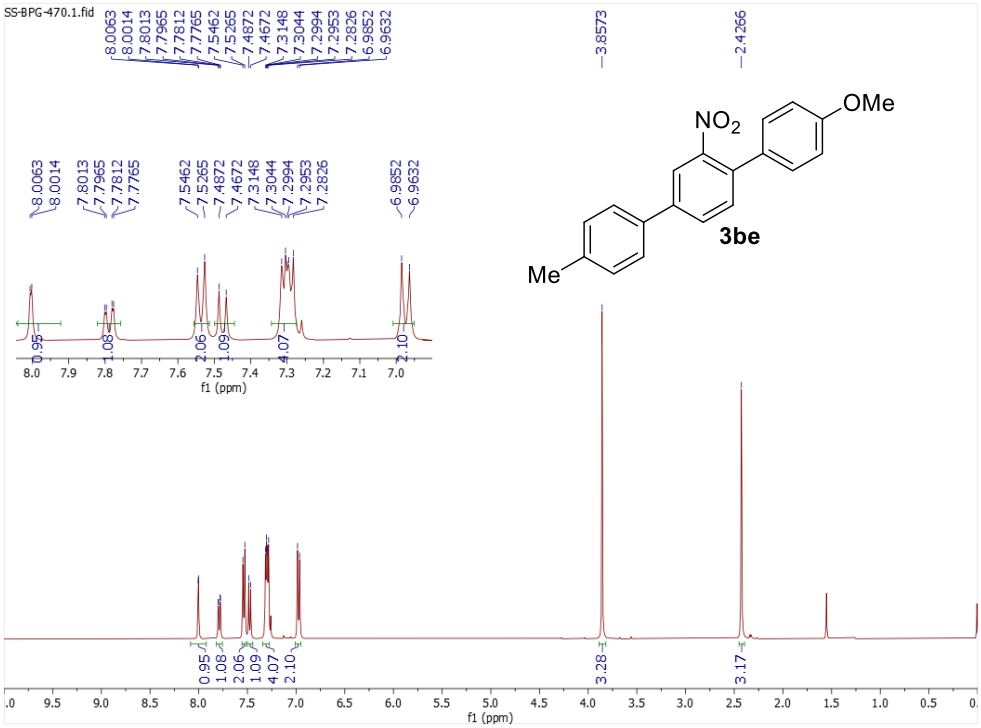

Figure 2.44 400 MHz ^{1}H NMR spectrum of **3be** in $CDCl_3$.

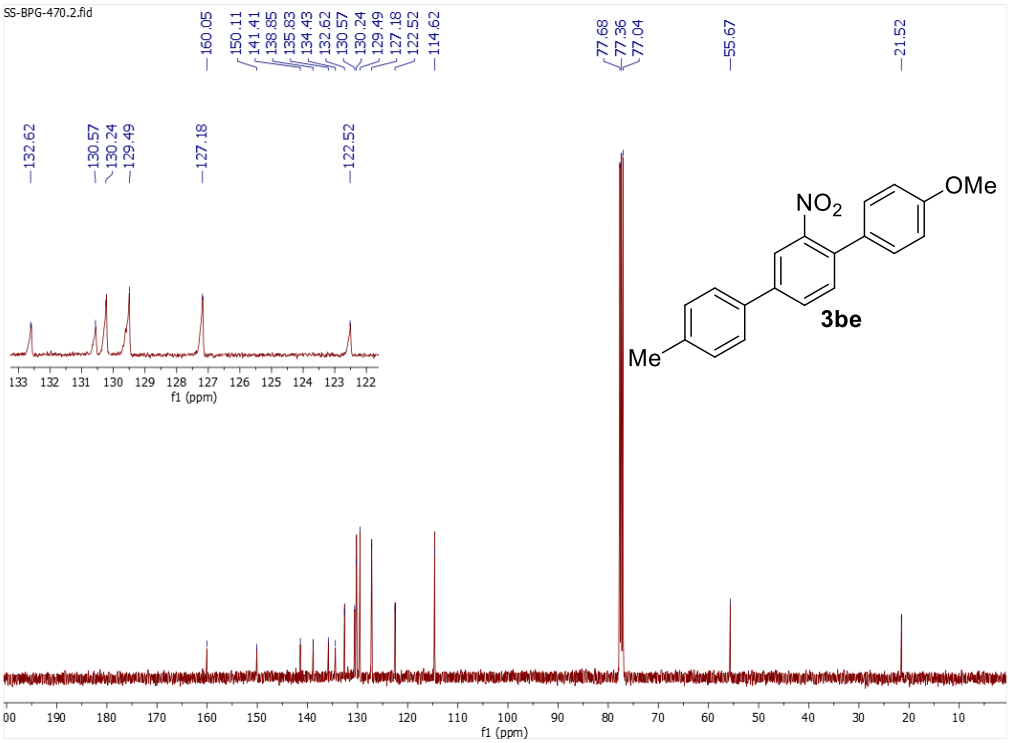

Figure 2.45 100 MHz ^{13}C NMR spectrum of **3be** in $CDCl_3$.

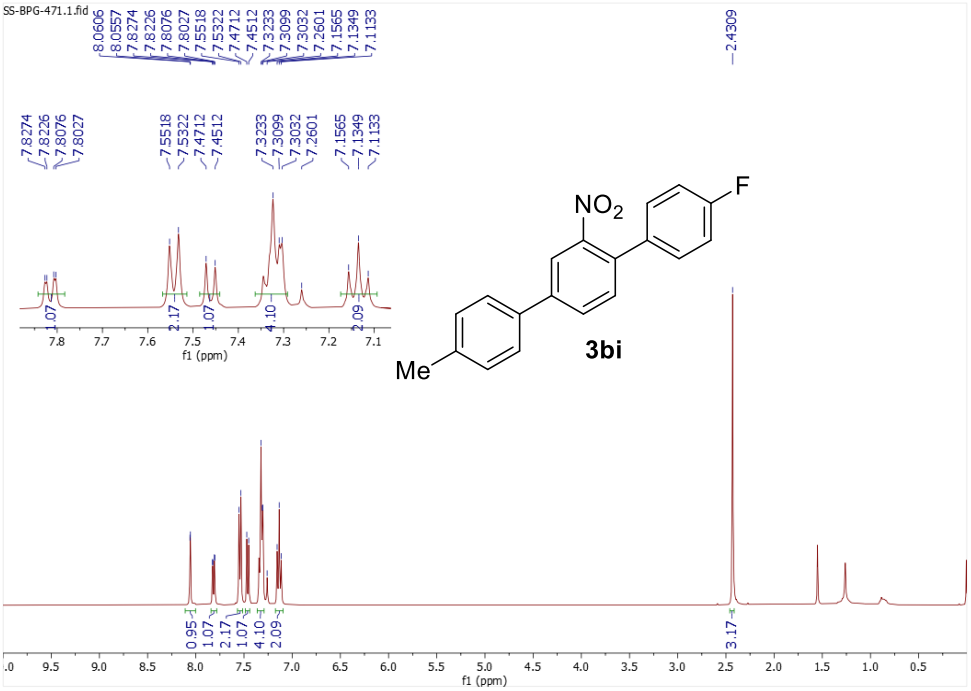

Figure 2.46 400 MHz ^{1}H NMR spectrum of **3bi** in $CDCl_3$.

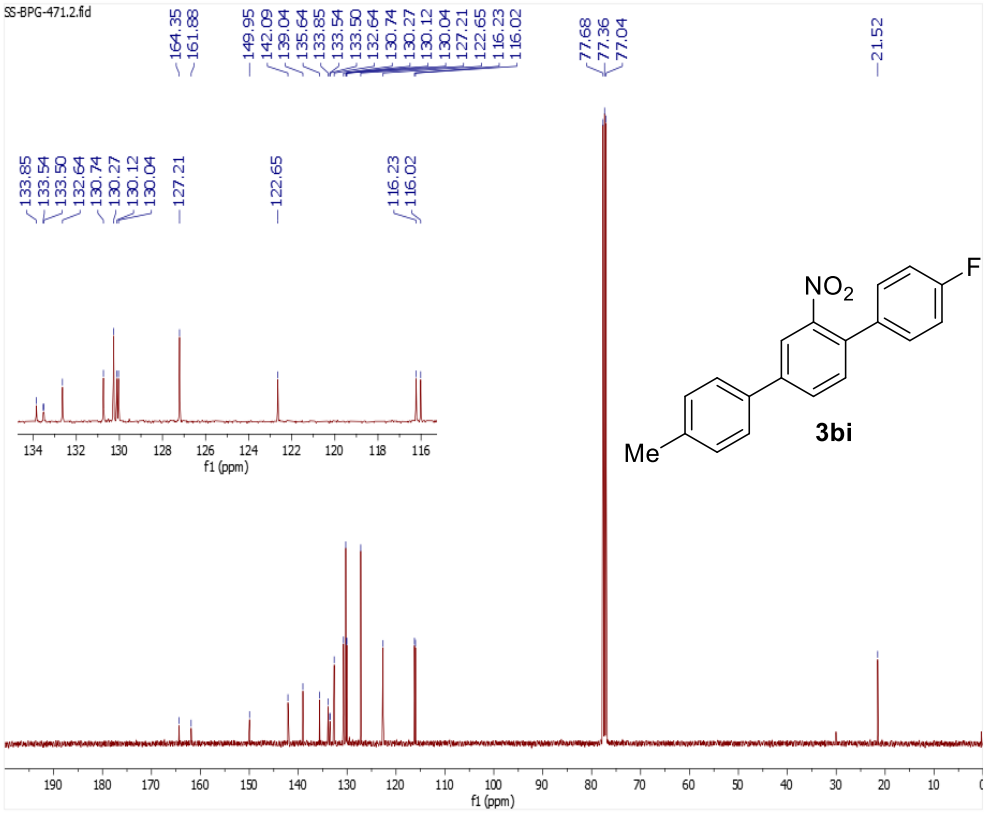

Figure 2.47 100 MHz ^{13}C NMR spectrum of **3bi** in $CDCl_3$.

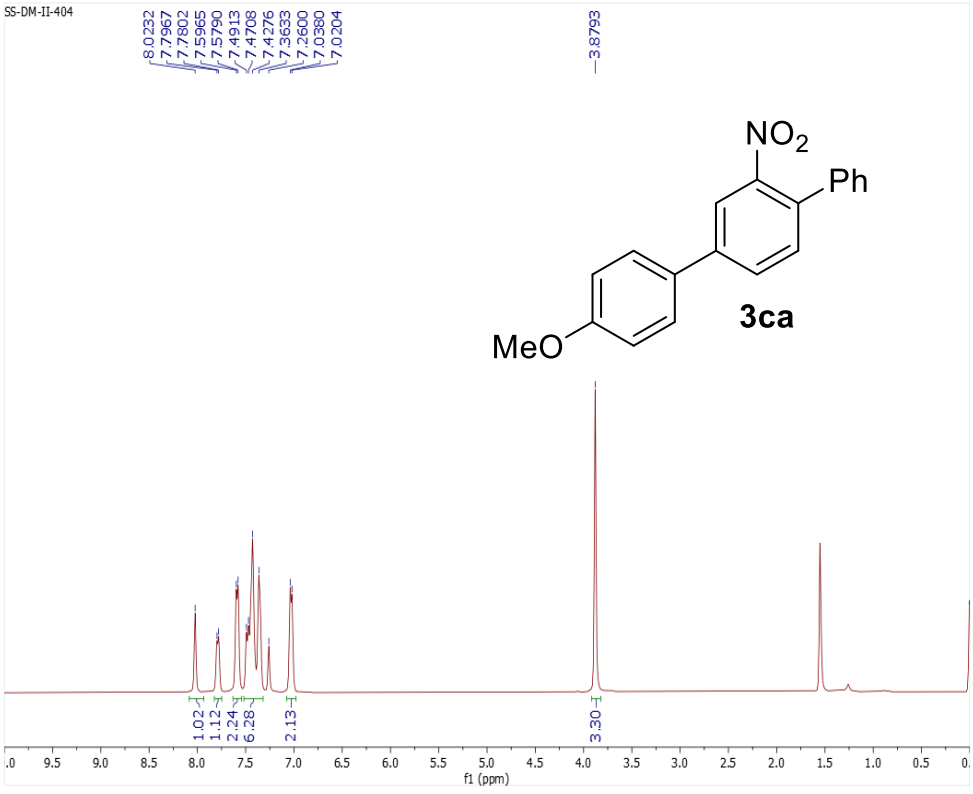

Figure 2.48 400 MHz ^{1}H NMR spectrum of **3ca** in $CDCl_3$.

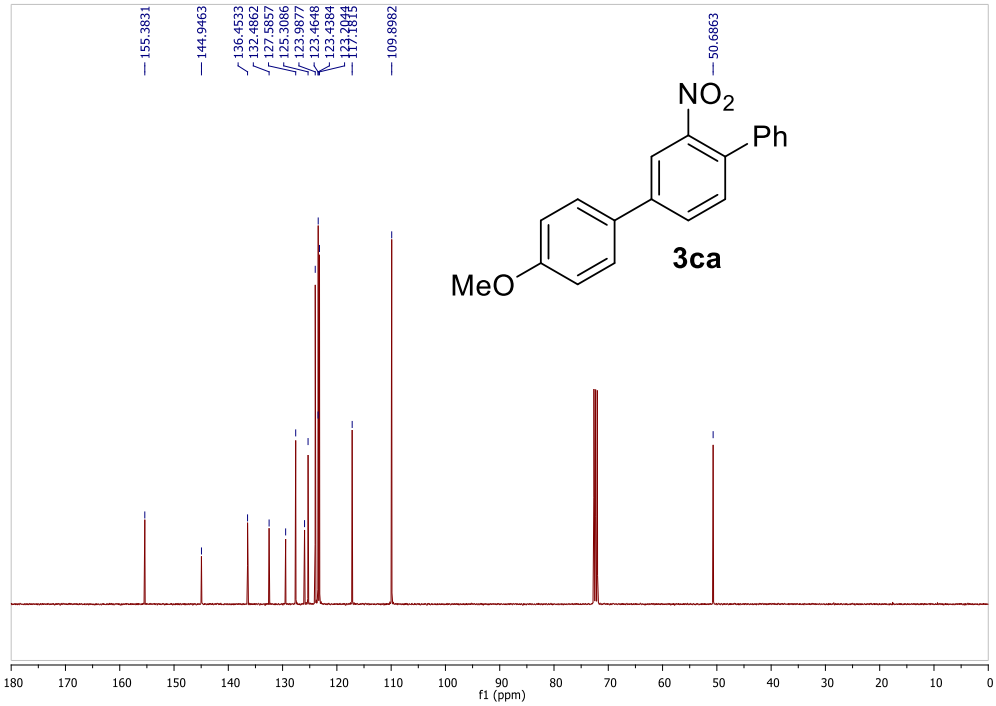

Figure 2.49 100 MHz ^{13}C NMR spectrum of **3ca** in $CDCl_3$.

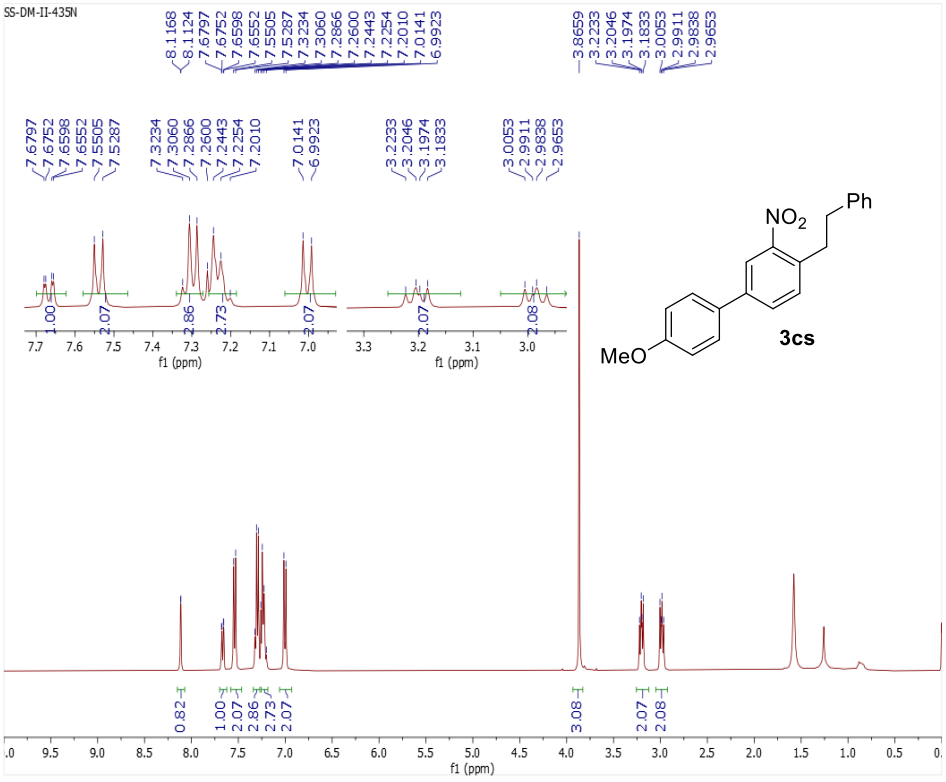

Figure 2.50 400 MHz ^{1}H NMR spectrum of **3cs** in $CDCl_3$.

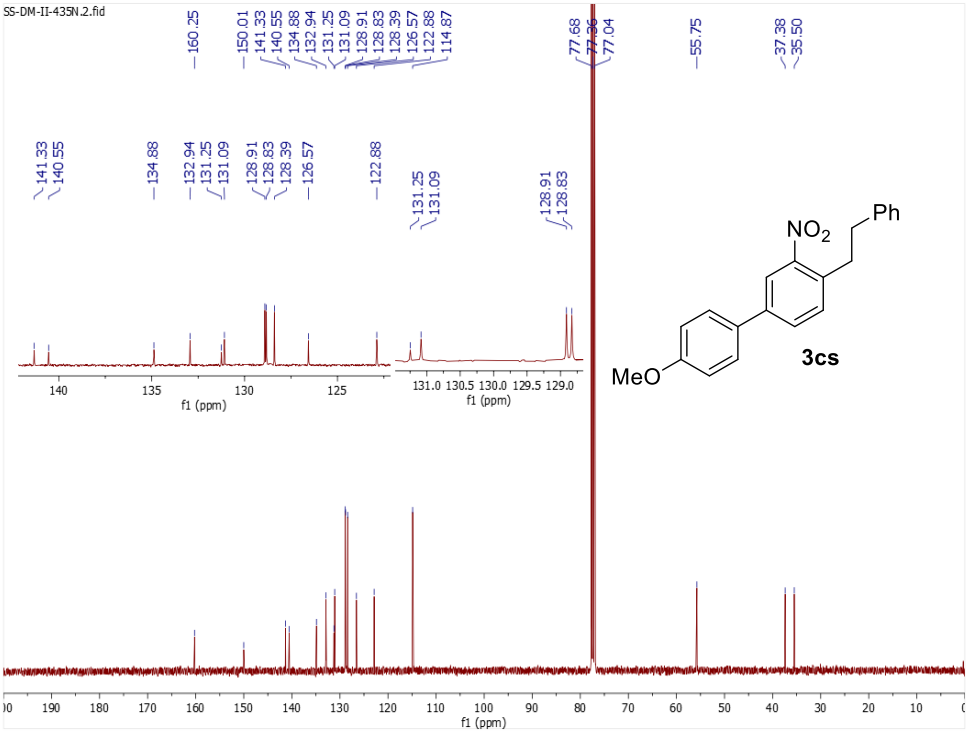

Figure 2.51 100 MHz ^{13}C NMR spectrum of **3cs** in $CDCl_3$.

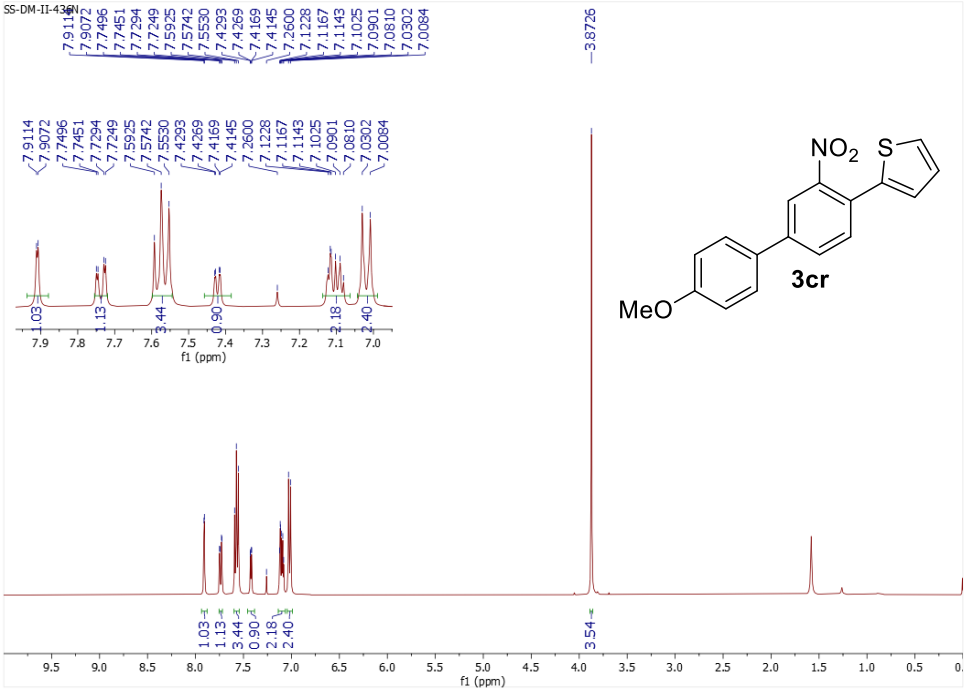

Figure 2.52 400 MHz ^{1}H NMR spectrum of **3cr** in $CDCl_3$.

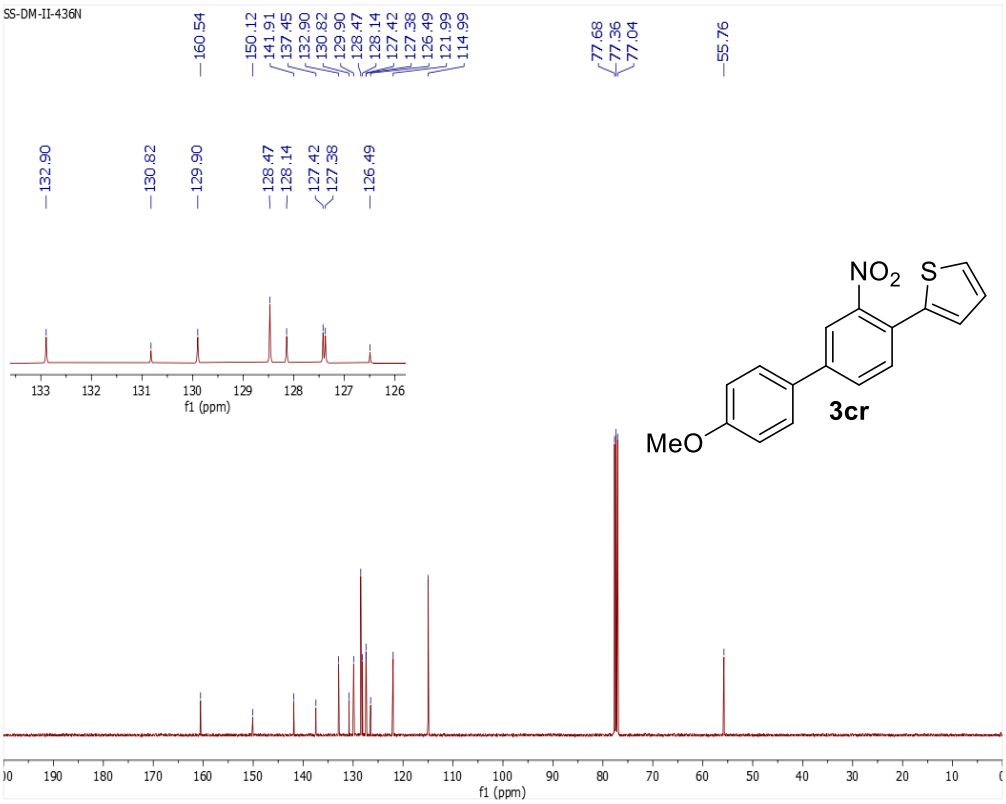

Figure 2.53 100 MHz ^{13}C NMR spectrum of **3cr** in $CDCl_3$.

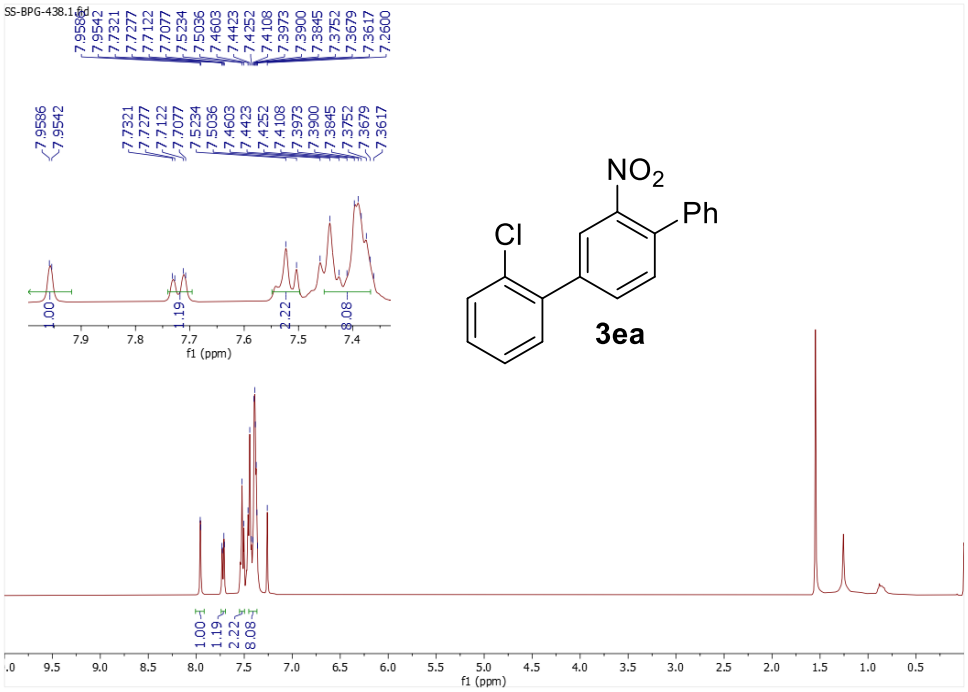

Figure 2.54 400 MHz ^{1}H NMR spectrum of **3ea** in $CDCl_3$.

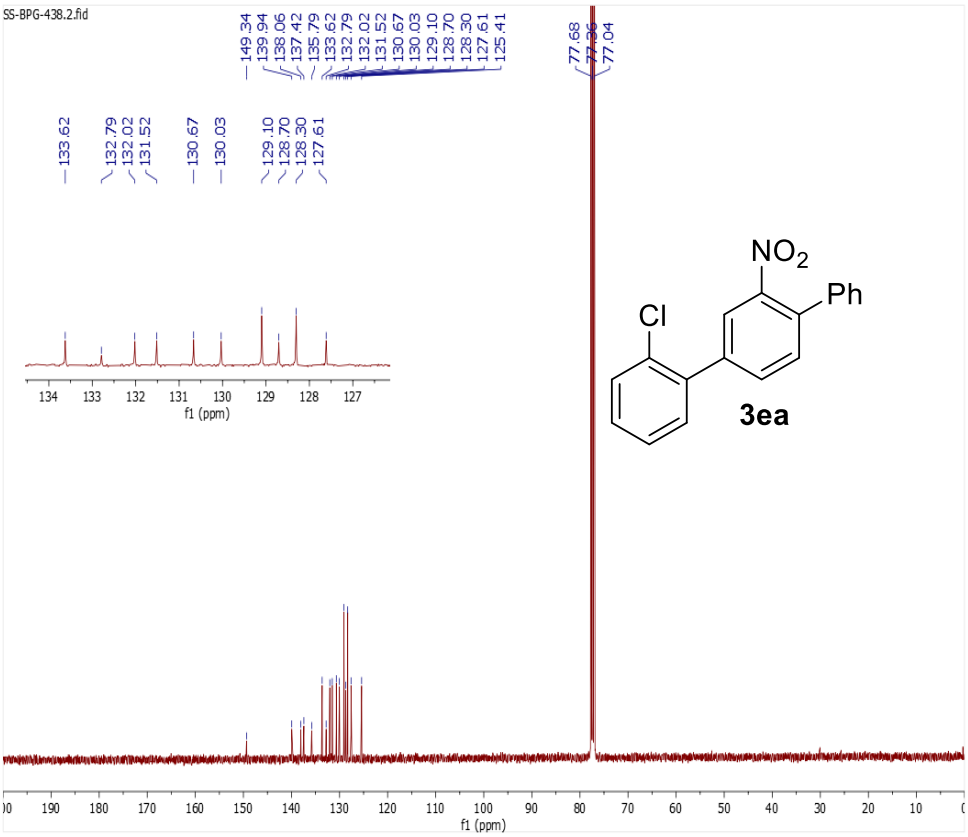

Figure 2.55 100 MHz ^{13}C NMR spectrum of **3ea** in $CDCl_3$.

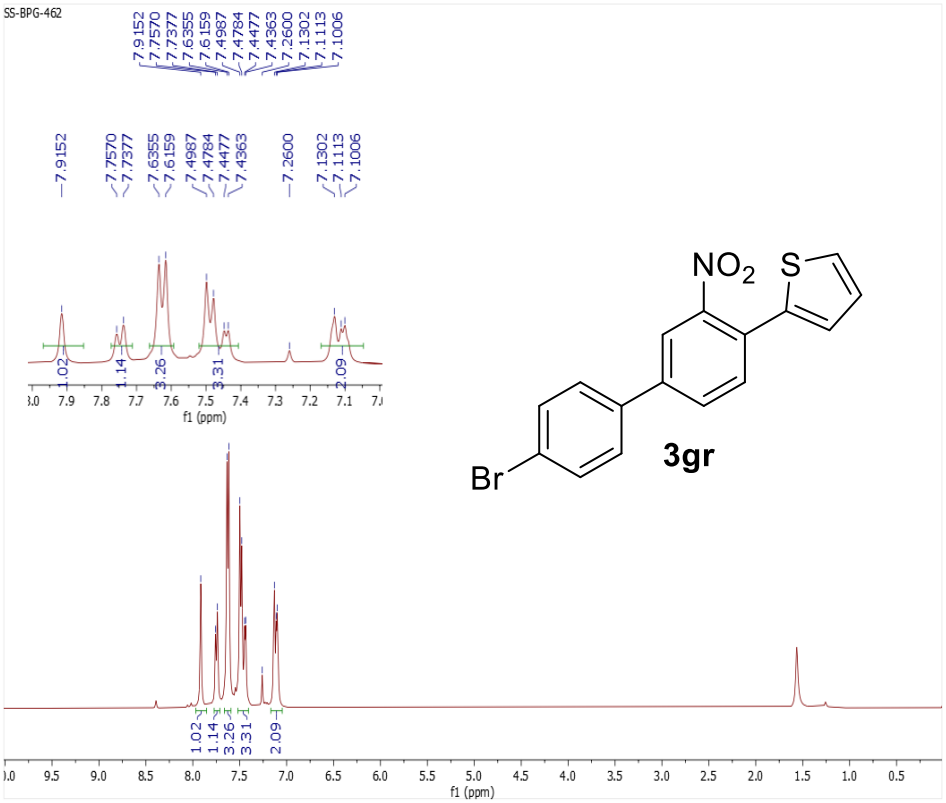

Figure 2.56 400 MHz ^{1}H NMR spectrum of **3gr** in $CDCl_3$.

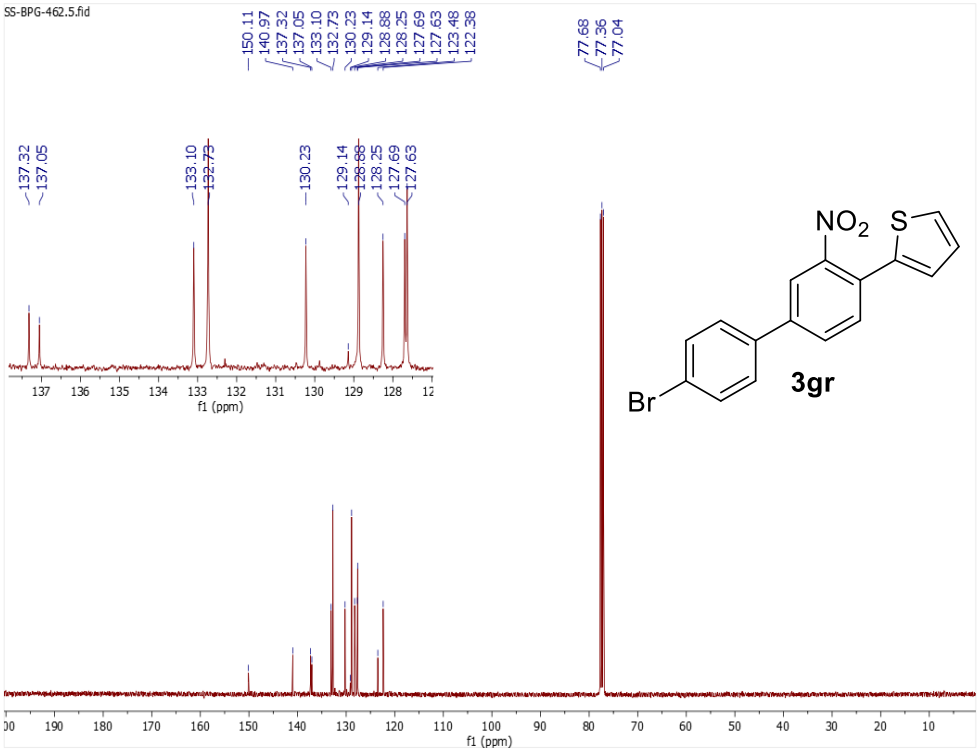

Figure 2.57 100 MHz ^{13}C NMR spectrum of **3gr** in $CDCl_3$.

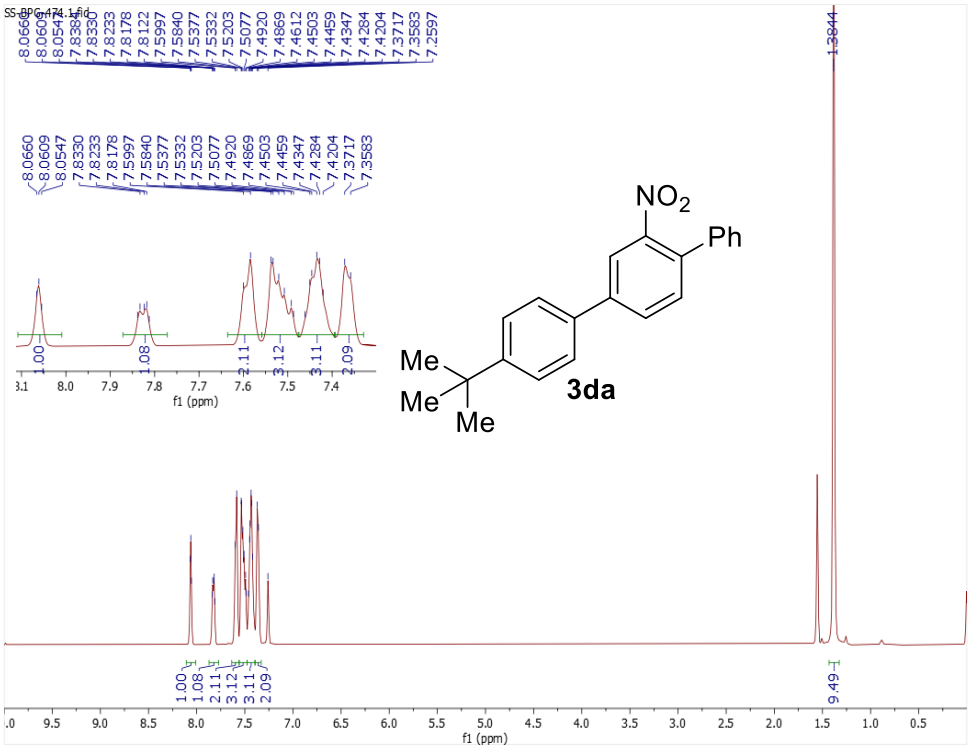

Figure 2.58 500 MHz ^{1}H NMR spectrum of **3da** in $CDCl_3$.

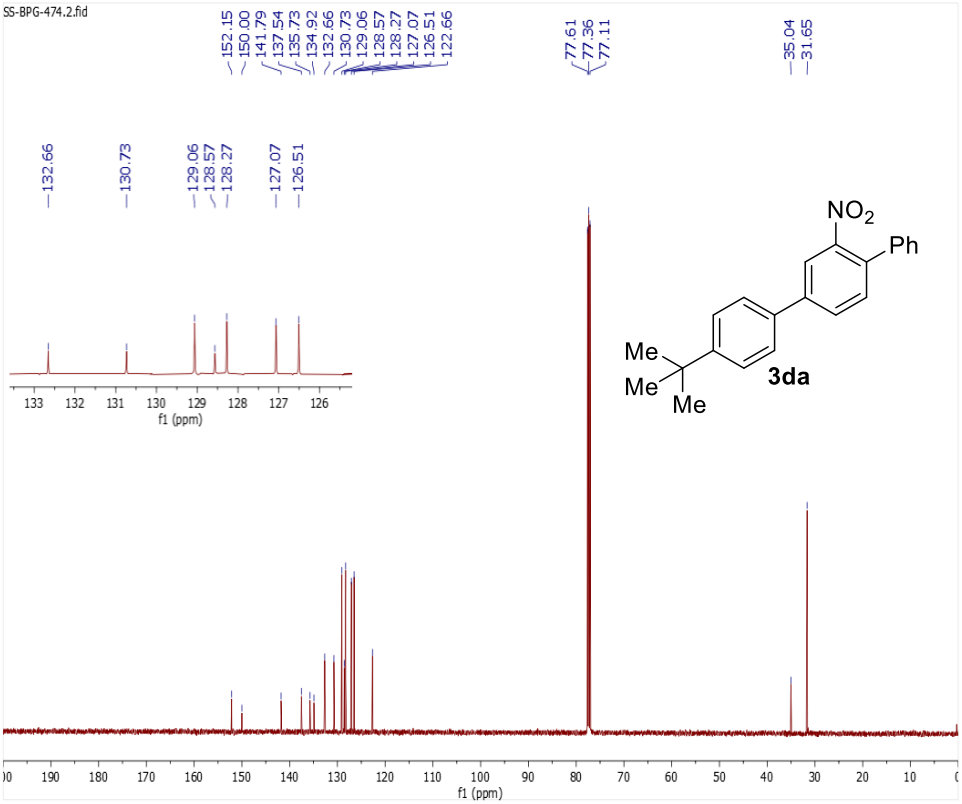

Figure 2.59 125 MHz ^{13}C NMR spectrum of **3da** in $CDCl_3$.

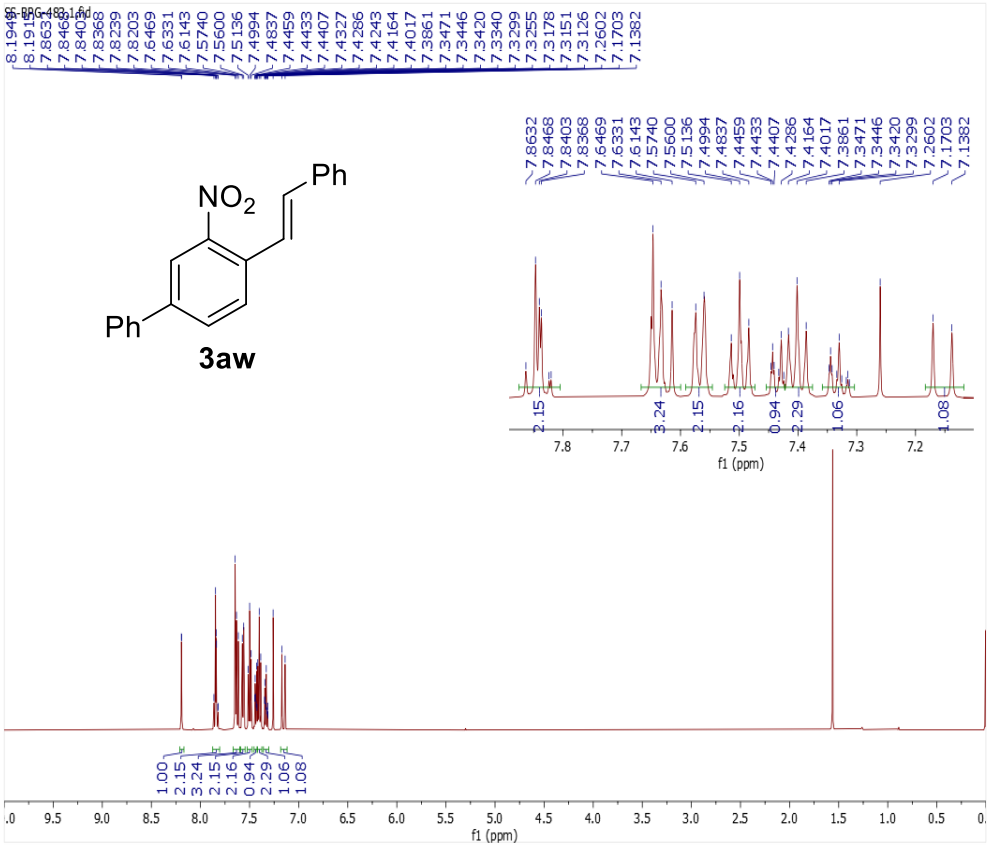

Figure 2.60 500 MHz ^{1}H NMR spectrum of **3aw** in $CDCl_3$.

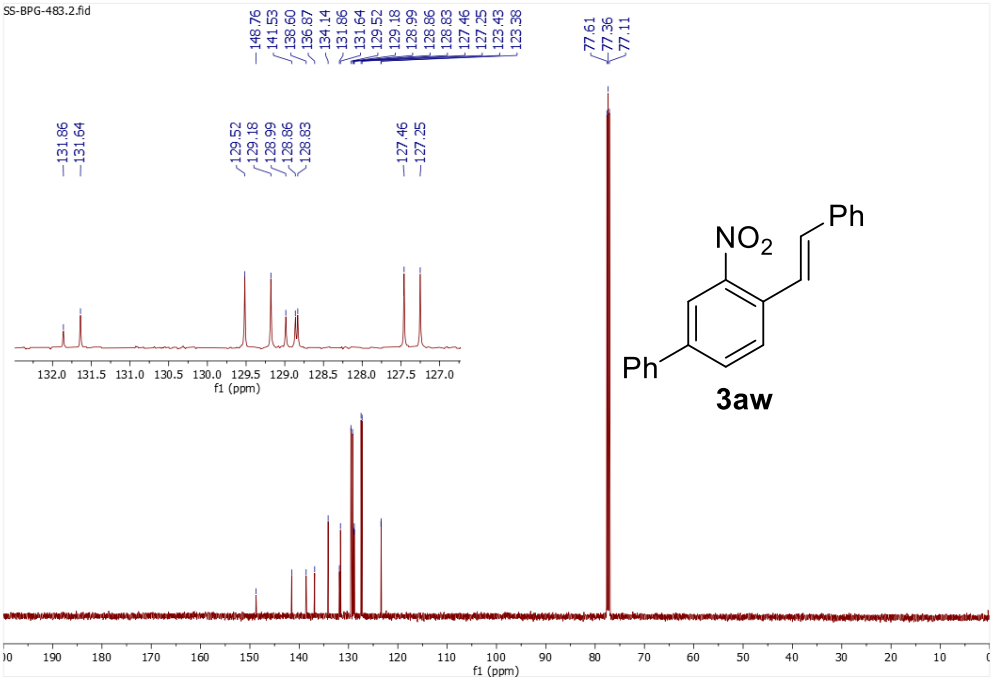

Figure 2.61 125 MHz ^{13}C NMR spectrum of **3aw** in $CDCl_3$.

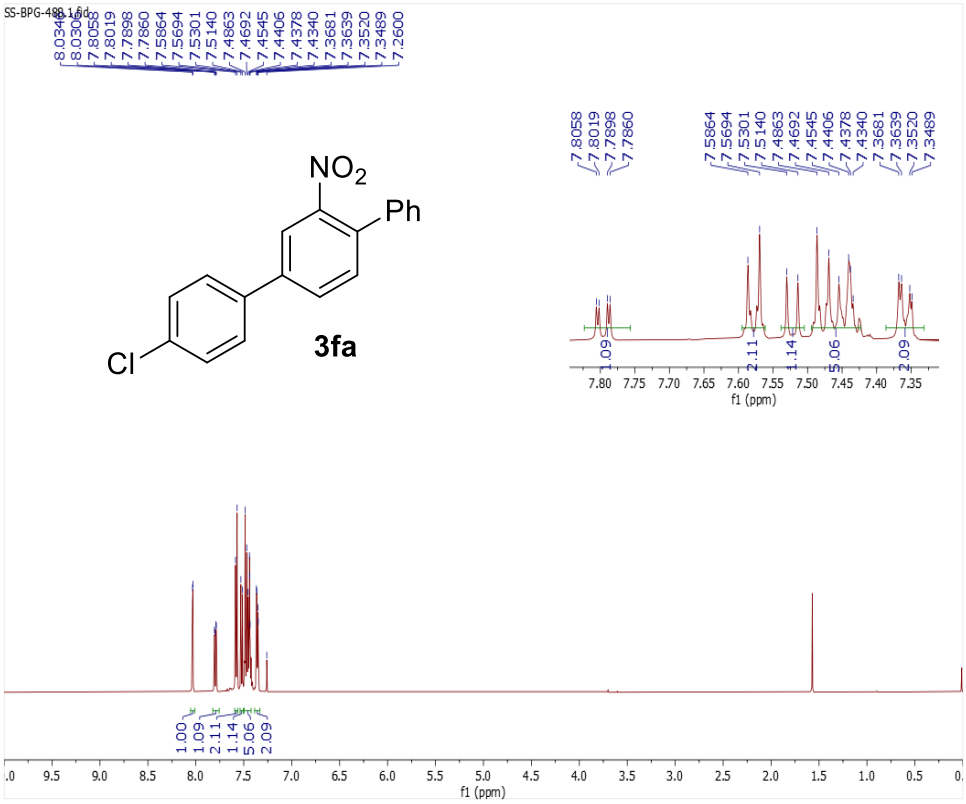

Figure 2.62 500 MHz ^{1}H NMR spectrum of **3fa** in $CDCl_3$.

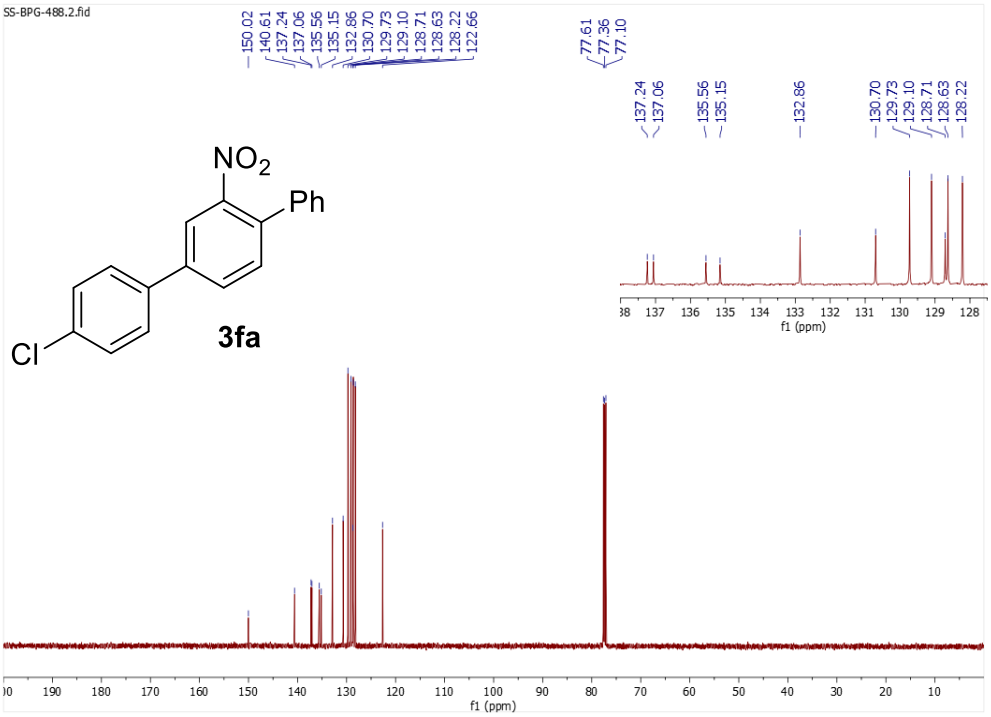

Figure 2.63 125 MHz ^{13}C NMR spectrum of **3fa** in $CDCl_3$.

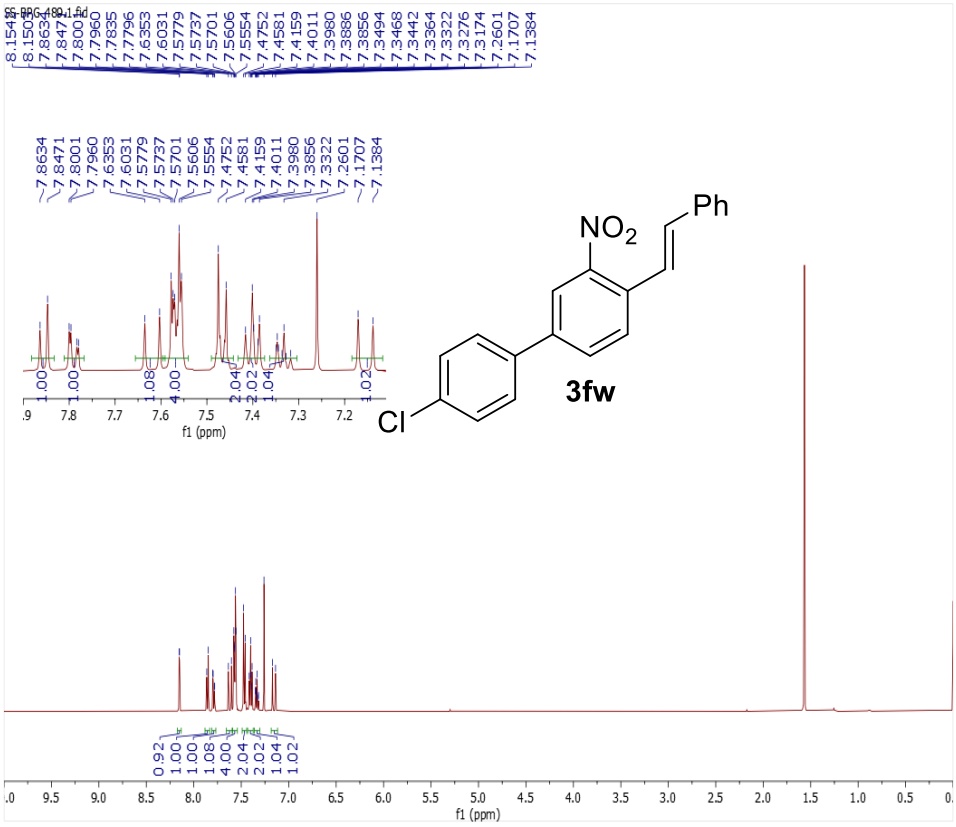

Figure 2.64 500 MHz ^{1}H NMR spectrum of **3fw** in $CDCl_3$.

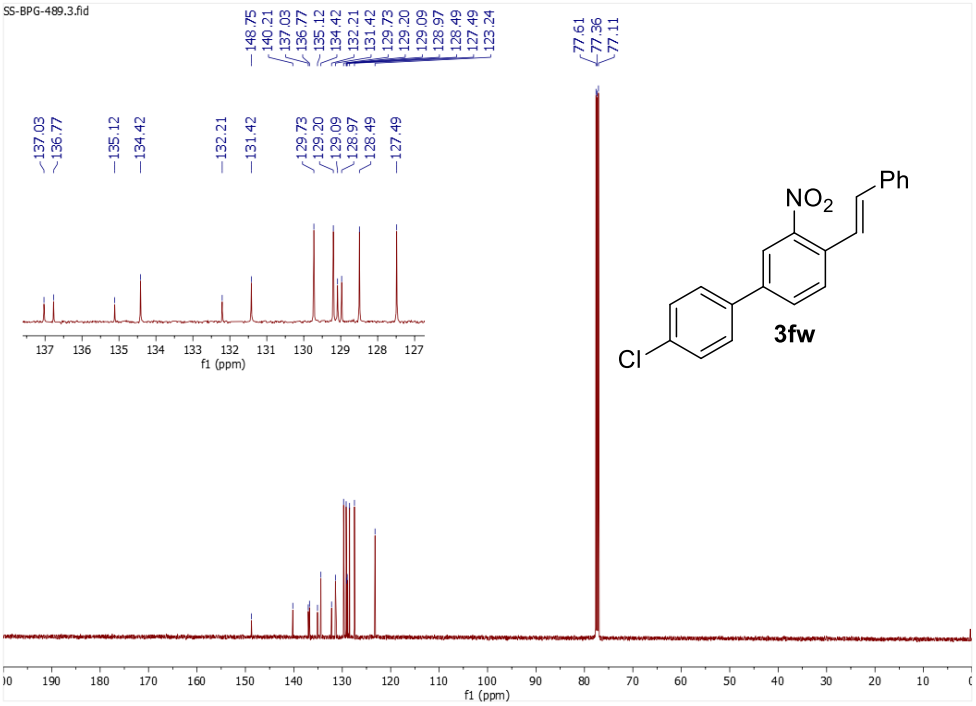

Figure 2.65 125 MHz ^{13}C NMR spectrum of **3fw** in $CDCl_3$.

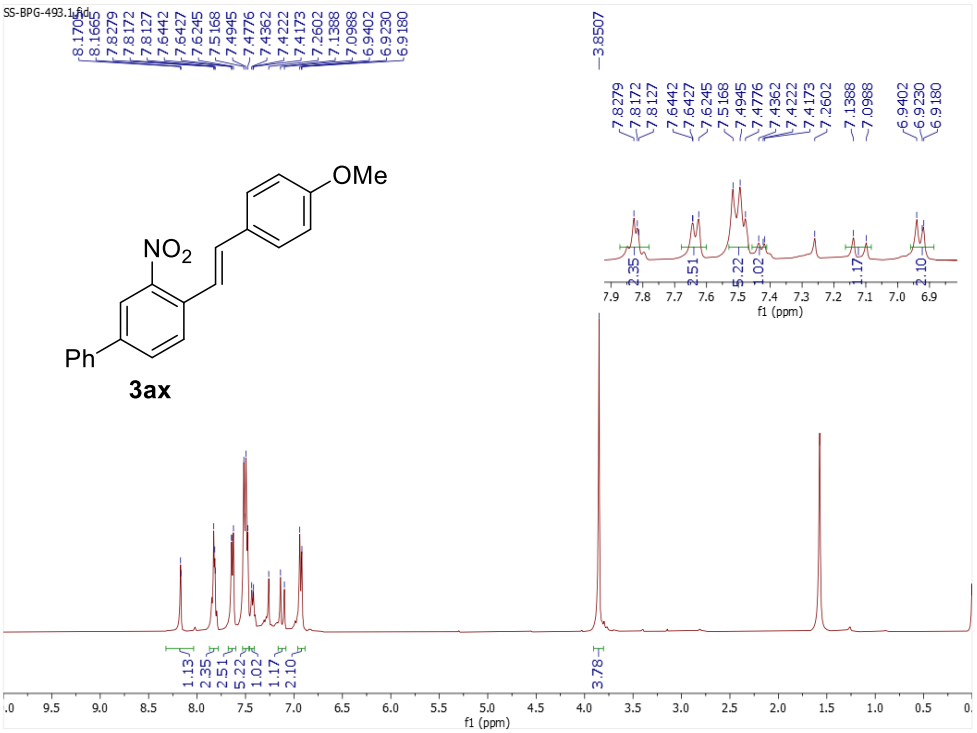

Figure 2.66 500 MHz ^{1}H NMR spectrum of **3ax** in $CDCl_3$.

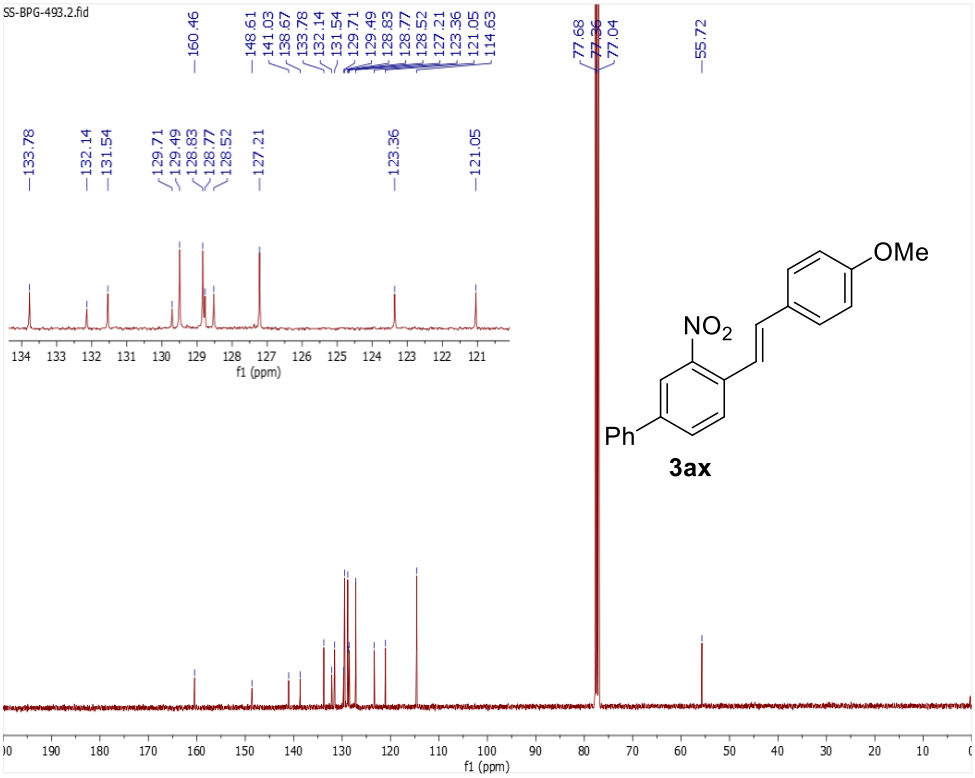

Figure 2.67 125 MHz ^{13}C NMR spectrum of **3ax** in $CDCl_3$.

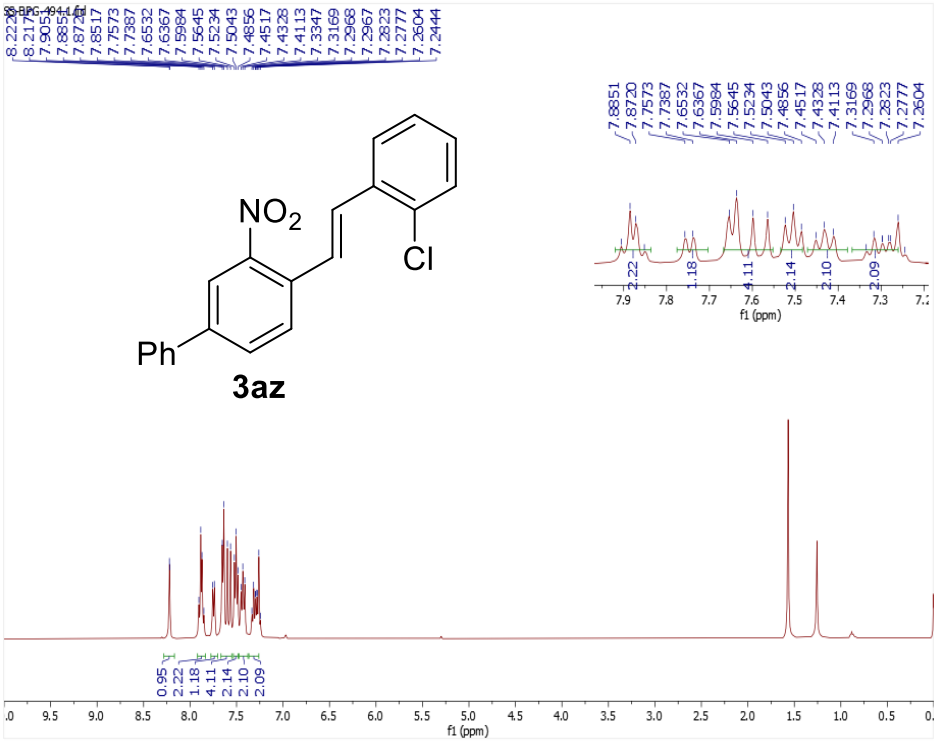

Figure 2.68 500 MHz ^{1}H NMR spectrum of **3az** in $CDCl_3$.

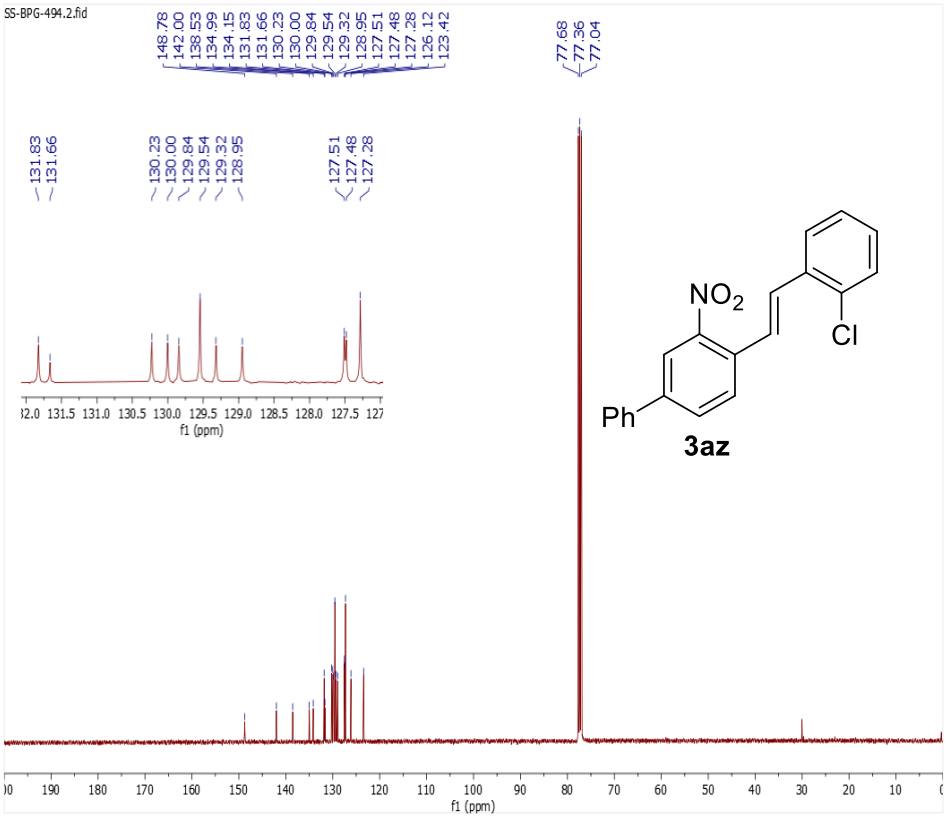

Figure 2.69 125 MHz ^{13}C NMR spectrum of **3az** in $CDCl_3$.

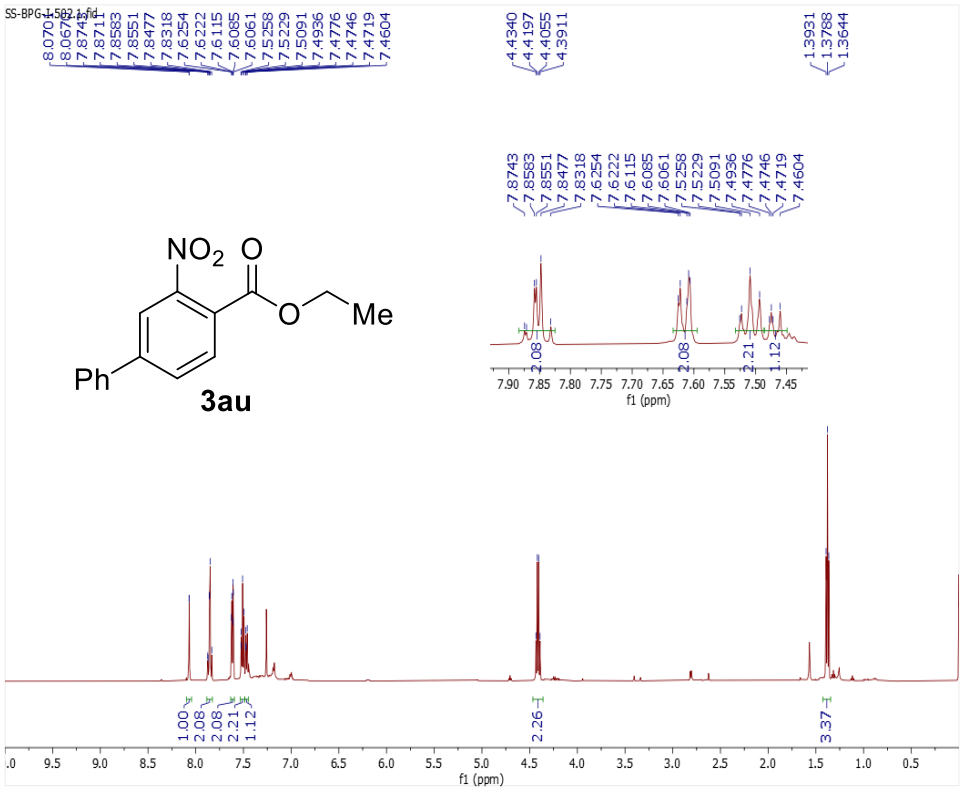

Figure 2.70 500 MHz ^{1}H NMR spectrum of **3au** in $CDCl_3$.

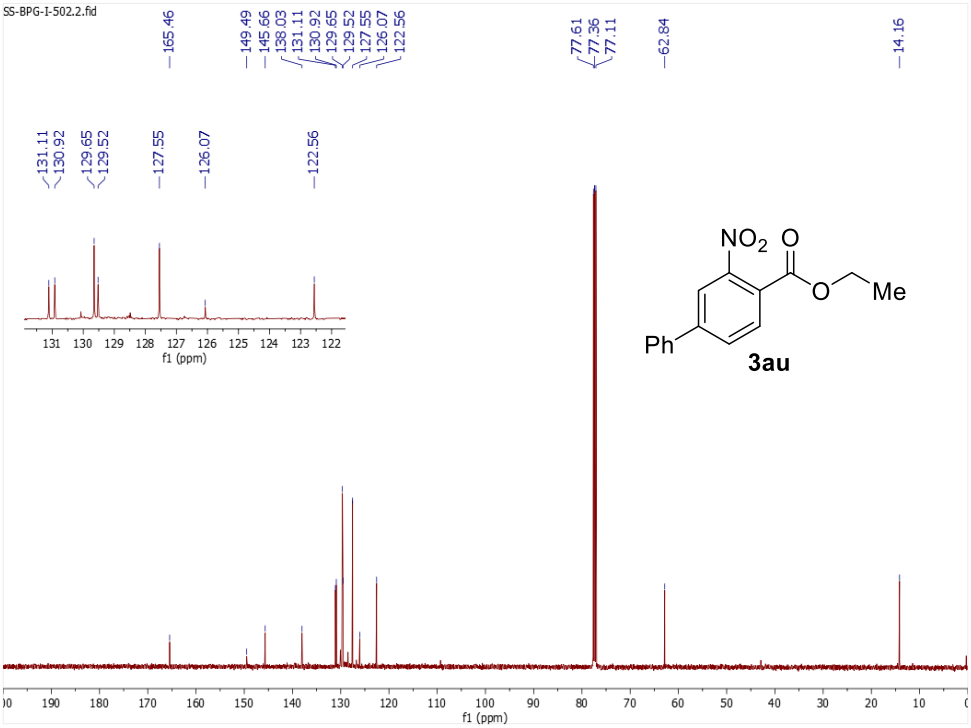

Figure 2.71 125 MHz ^{13}C NMR spectrum of **3au** in $CDCl_3$.

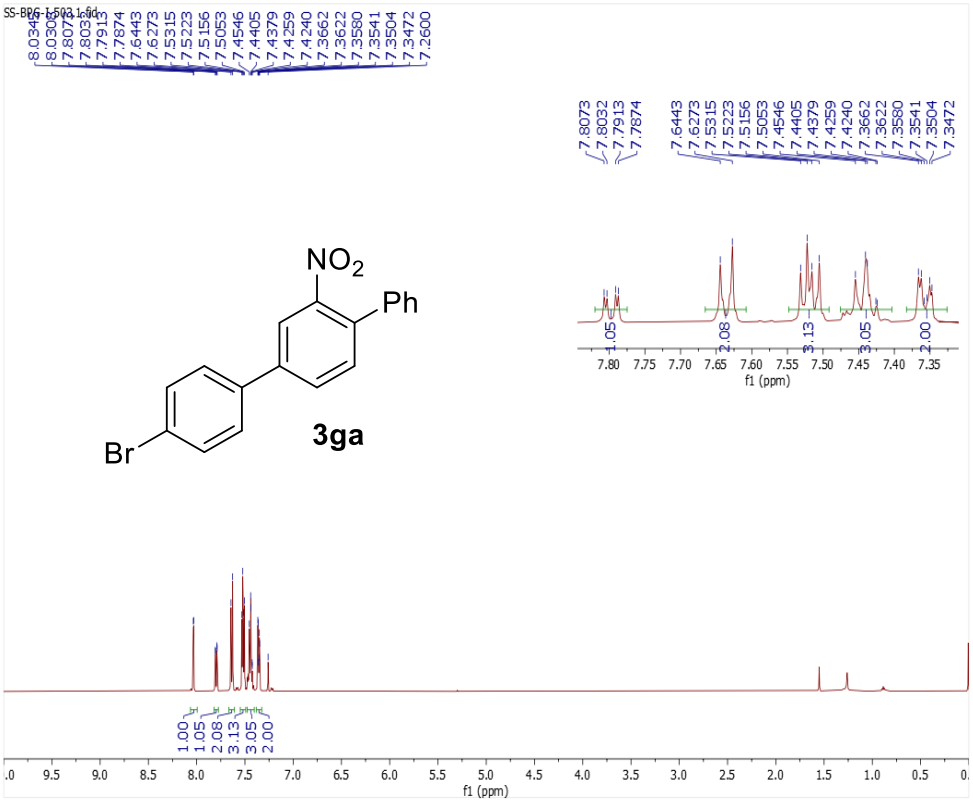

Figure 2.72 500 MHz ^{1}H NMR spectrum of **3ga** in $CDCl_3$.

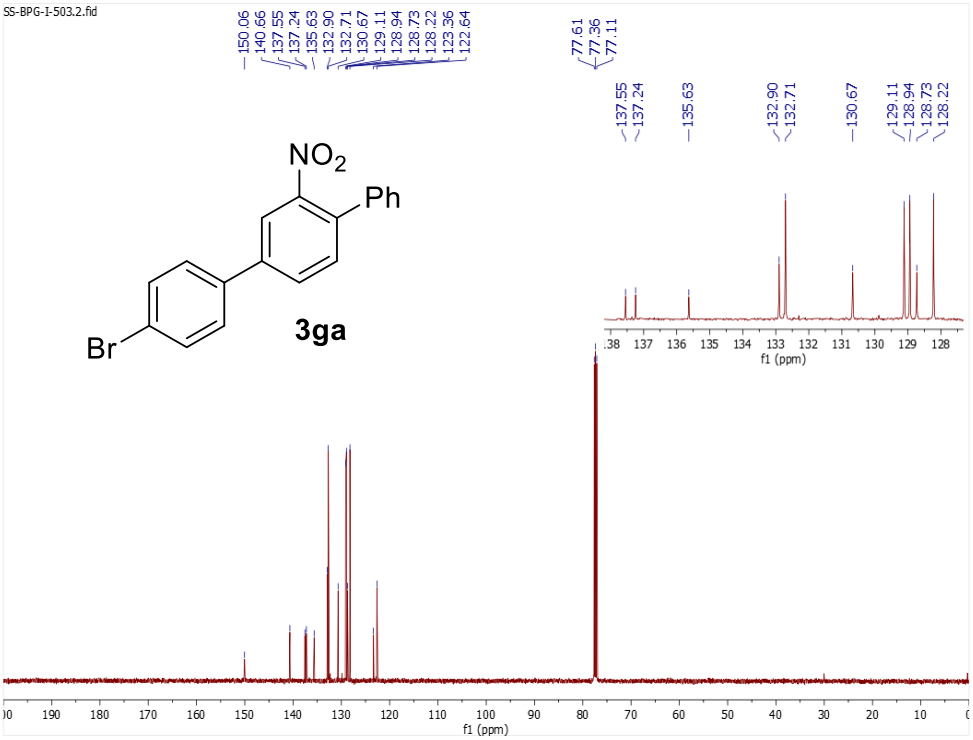

Figure 2.73 125 MHz ^{13}C NMR spectrum of **3ga** in $CDCl_3$.

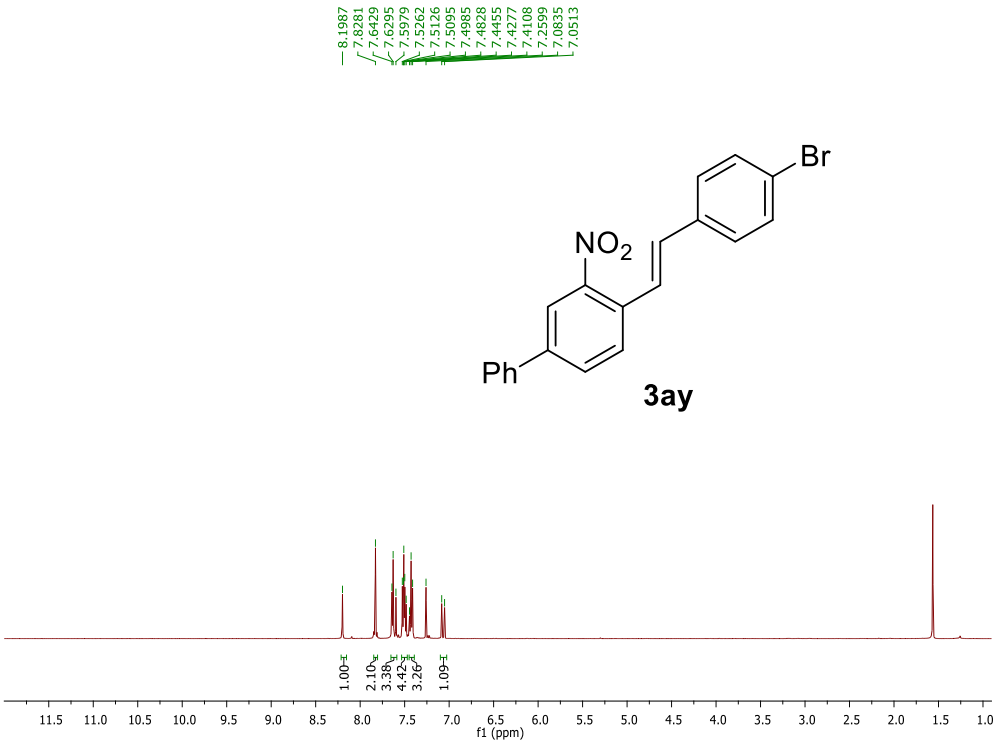

Figure 2.74 500 MHz ^{1}H NMR spectrum of **3ay** in $CDCl_3$.

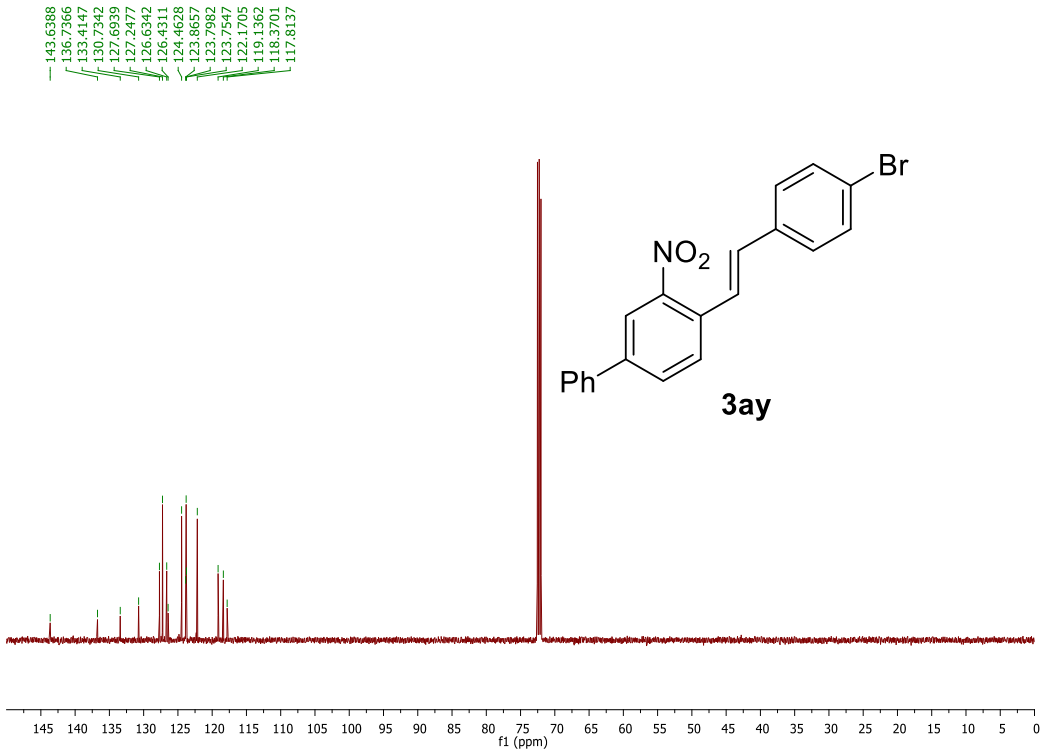

Figure 2.75 125 MHz ^{13}C NMR spectrum of **3ay** in $CDCl_3$.

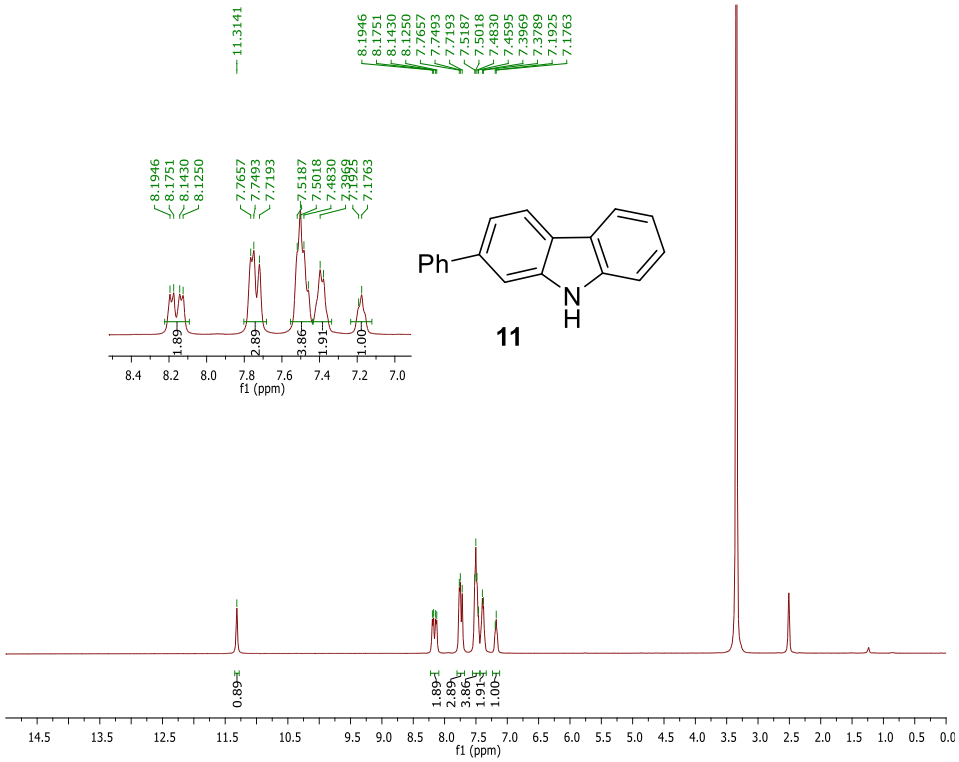

Figure 2.76 400 MHz ^{1}H NMR spectrum of **11** in DMSO-d_6.

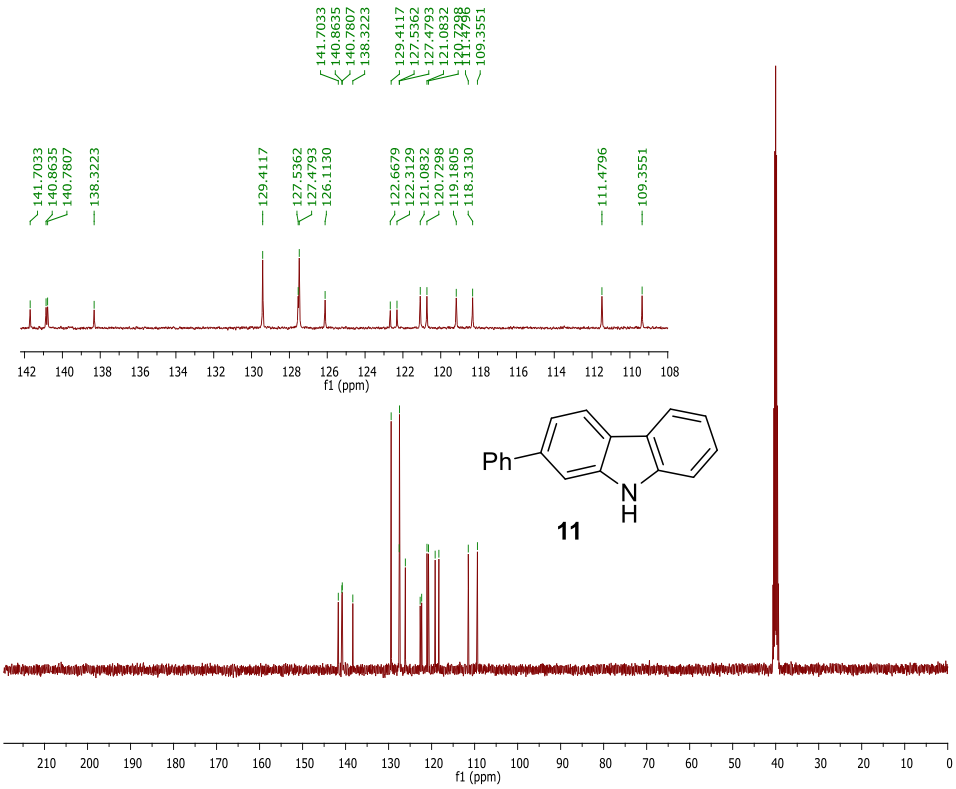

Figure 2.77 100 MHz ^{13}C NMR spectrum of **11** in DMSO-d_6.

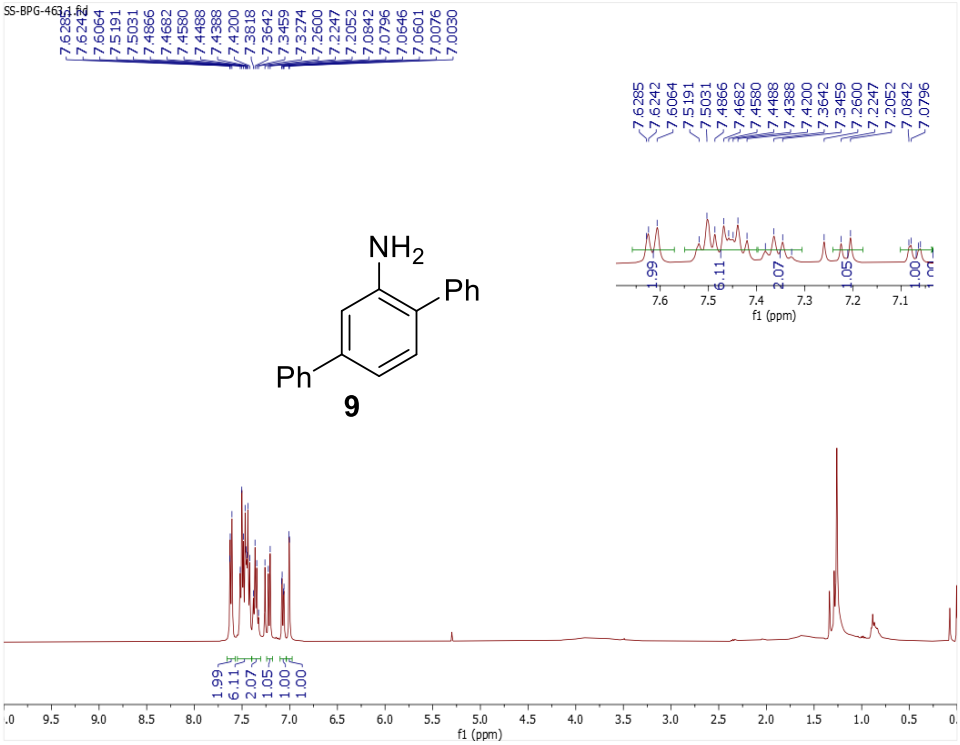

Figure 2.78 400 MHz ^{1}H NMR spectrum of **9** in $CDCl_3$.

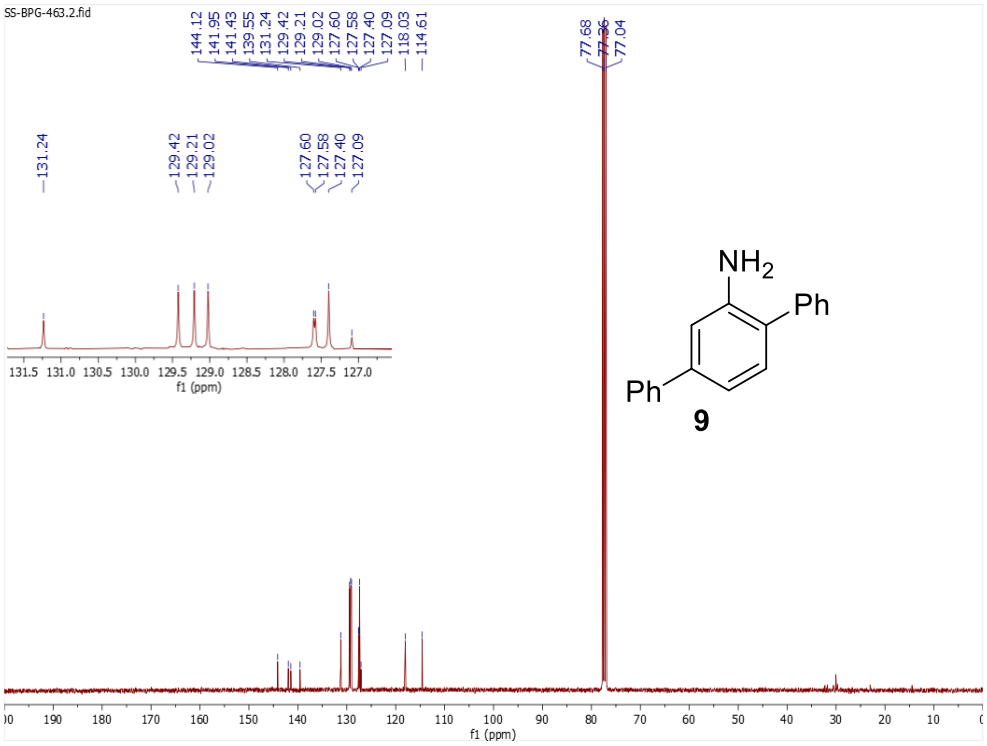

Figure 2.79 100 MHz ^{13}C NMR spectrum of **9** in $CDCl_3$.

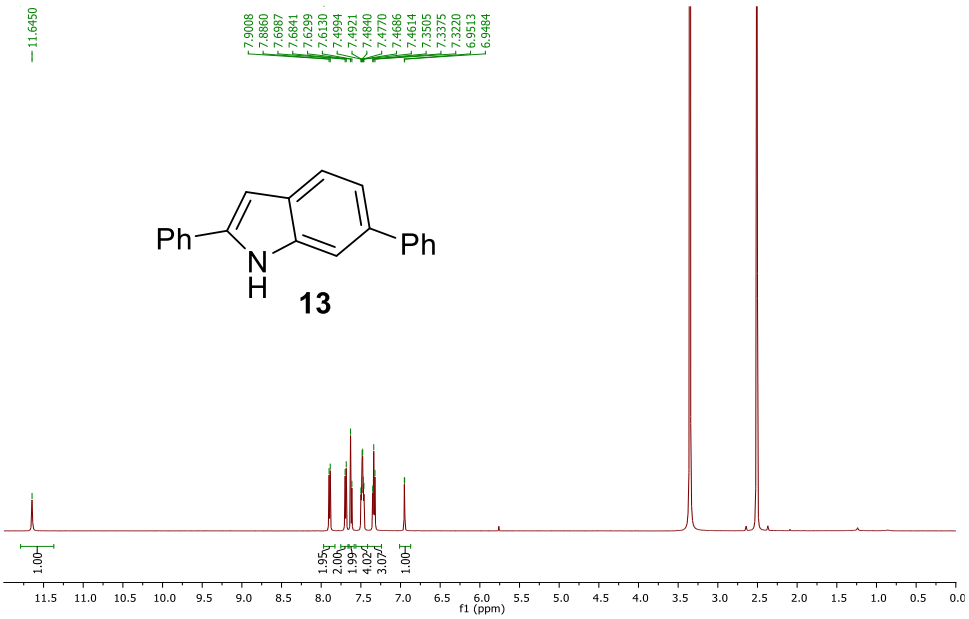

Figure 2.80 500 MHz ^{1}H NMR spectrum of **13** in DMSO-d_6.

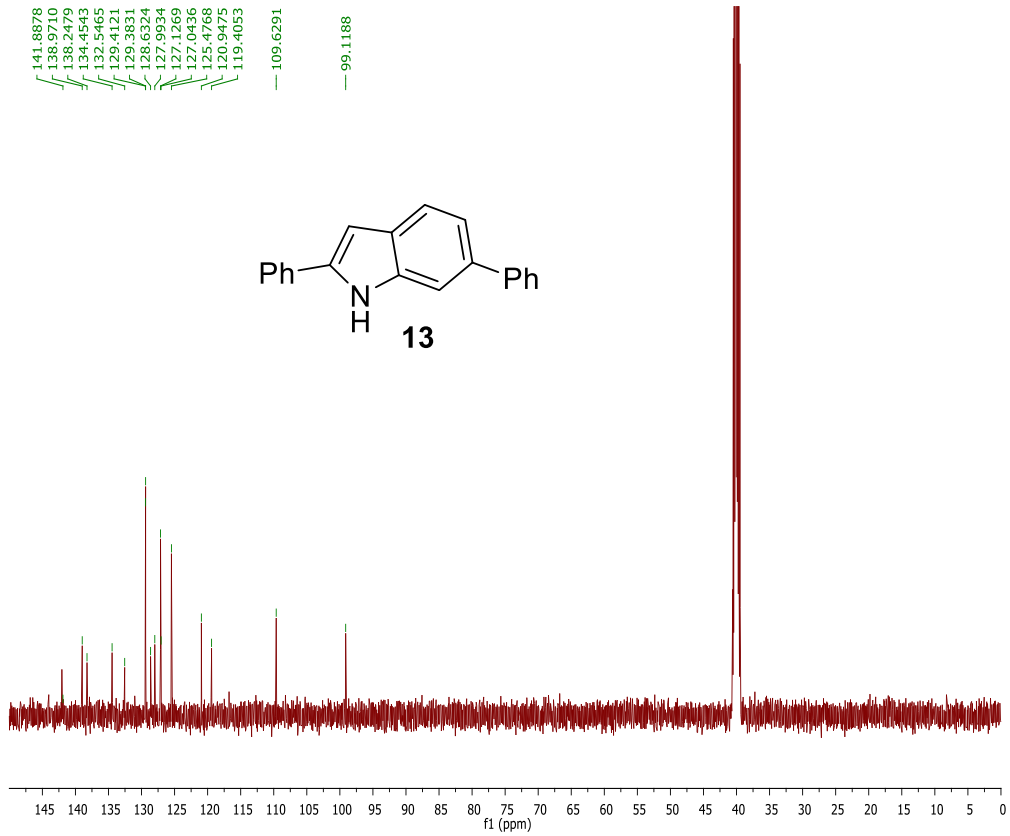

Figure 2.81 125 MHz ^{13}C NMR spectrum of 1**3** in DMSO-d_6.

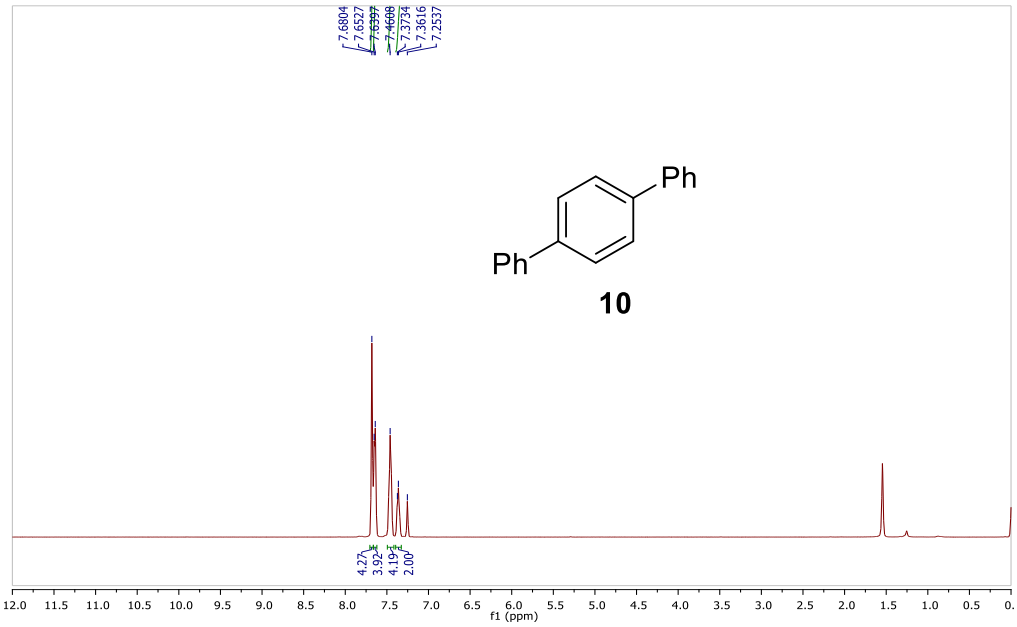

Figure 2.82 500 MHz ^{1}H NMR spectrum of **10** in $CDCl_3$.

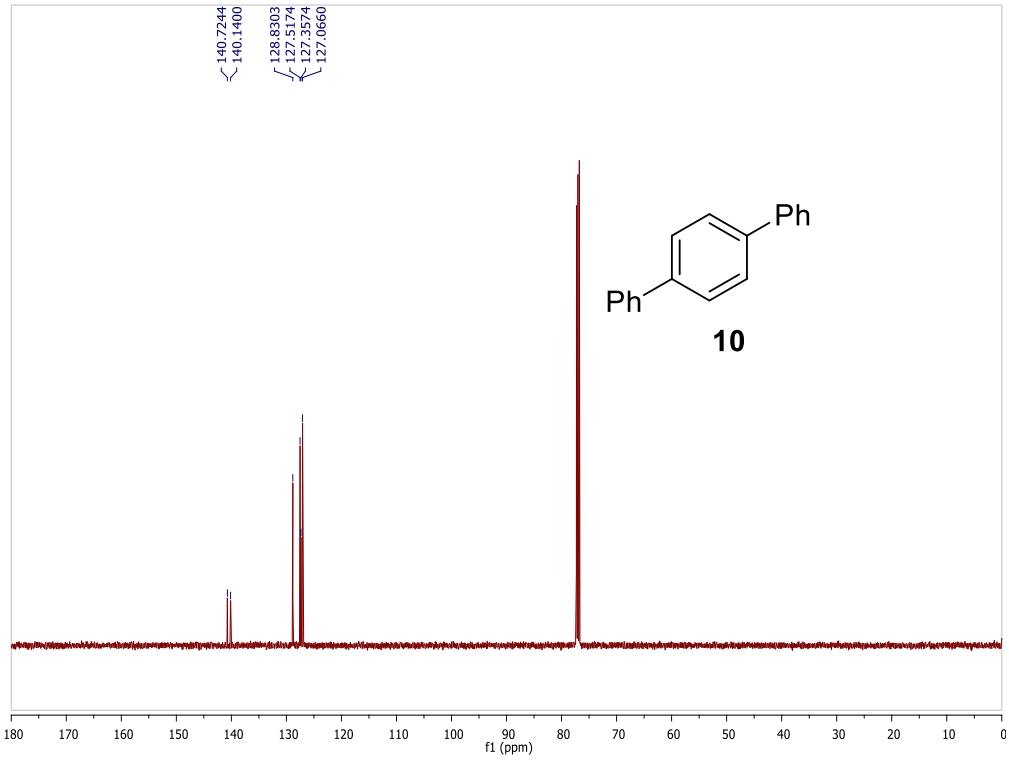

Figure 2.83 125 MHz ^{13}C NMR spectrum of **10** in $CDCl_3$.

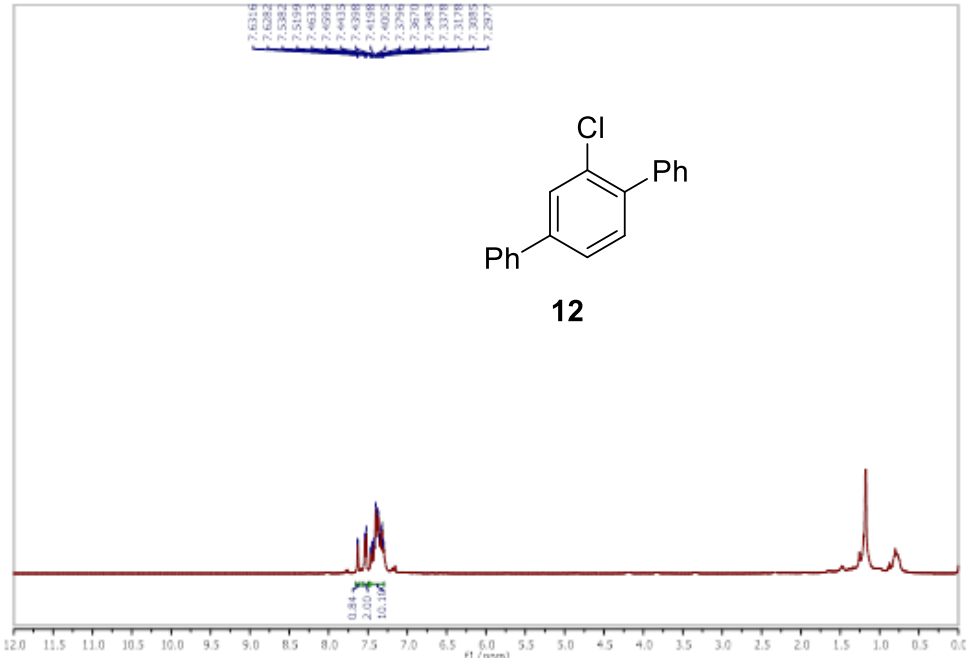

Figure 2.84 400 MHz ^{1}H NMR spectrum of **12** in $CDCl_3$.

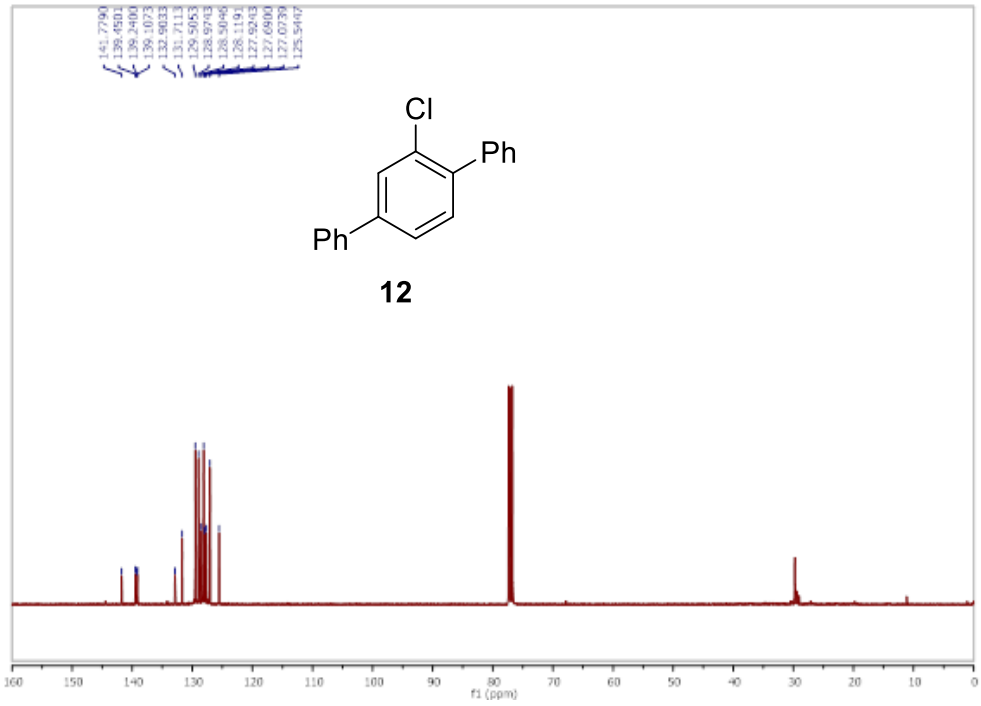

Figure 2.85 100 MHz ^{13}C NMR spectrum of **12** in $CDCl_3$.

2.8. References

1. Muto K., Okita T., Yamaguchi T. (2020), Transition-metal-catalyzed denitrative coupling of nitroarenes, *ACS Catal.*, 10, 9856-9871 (DOI: 10.1021/acscatal.0c02990).

2. Klaus H. (2003) Industry dyes: chemistry, properties, and applications, Wiley VCH, Weinheim, 2003.

3. Ju K.-M., Parales R. E. (2010), Nitroaromatic compounds from synthesis to biodegradation, *Microbiol. Mol. Biol. Rev.*, 74, 250-272 (DOI: 10.1128/MMBR.00006-10).

4. Feng B., Yang Y., You J. (2020), A methylation platform of unconventional inert aryl electrophiles: trimethylboroxine as a universal methylating reagent, *Chem. Sci.*, 11, 6031-6035 (DOI: 10.1039/D0SC01641A).

5. Shen N., Zhai S.-J., Cheung C.W., Ma J.-A. (2020), Direct N-formylation of nitroarenes with CO_2, *Chem. Commun.*, 56, 9620-9623 (DOI: 10.1039/D0CC03098H).

6. Okita T., Asahara K. K., Muto K., Yamaguchi J. (2020), Palladium-catalyzed mizoroki–heck reaction of nitroarenes and styrene derivatives, *Org. Lett.*, 22, 3205-3208 (DOI: 10.1021/acs.orglett.0c00983).

7. Li G., Nykaza T. V., Cooper J. C., Ramirez A., Luzung M.R., Radosevich A.T. (2020), An improved P^{III}/P^{V}═O-catalyzed reductive C–N coupling of nitroaromatics and boronic acids by mechanistic differentiation of rate- and product-determining steps, *J. Am. Chem. Soc.*, 142, 6786-6799 (DOI: 10.1021/jacs.0c01666).

8. Yadav M. R., Nagaoka M., Kashihara M., Zhong R.-L., Miyazaki T., Sakaki S., Nakao Y. (2017), The suzuki–miyaura coupling of nitroarenes, *J. Am. Chem. Soc.*, 139, 9423-9426 (DOI: 10.1021/jacs.7b03159).

9. Gui J., Pan C.-M., Jin Y., Qin T., Lo J. C., Lee B. J., Spergel S. H., Mertzman M. E., Pitts W. J., Cruz T. E., Schmidt M. A., Darvatkar N., Natarajan S. R., Baran P. S. (2015), Practical olefin hydroamination with nitroarenes, *Science*, 348, 886-891 (DOI: 10.1126/science.aab0245).

10. Remennikov G. Y. (2017), Synthesis of fused pyrazoles *via* intramolecular cyclization of appropriately ortho-substituted nitroarenes and nitroheteroarenes, *Chem. Heterocycl. Compd.*, 53, 101-115 (DOI: 10.1007/s10593-017-2028-6).

11. Ando S., Tsuzaki M., Ishizuka T. (2020), Aryl ether syntheses *via* aromatic substitution proceeding under mild conditions, *J. Org. Chem.*, 85, 11181-11189 (DOI: 10.1021/acs.joc.0c01250).

12. Bunnett J. F., Zahler R.E. (1951), Aromatic nucleophilic substitution reactions, *Chem. Rev.*, 49, 274-412 (DOI: 10.1021/cr60153a002).

13. Nepali K., Lee H.-Y., Liou J.-P. (2019), Nitro-group-containing drugs, *J. Med. Chem.*, 62, 2851-2893 (DOI: 10.1021/acs.jmedchem.8b00147).

14. Jorge R., Oliveira D. (2017), Metabolic profile of flunitrazepam: clinical and forensic toxicological aspects, *Drug Metab. Lett.*, 1, 14-20 (DOI: 10.2174/1872312811666170407164216).

15. Hansch C., Nakamoto K., Gorin M., Denisevich P., Garrett E. R., Heman-Ackah S. M., Won C. H. (1973), Structure-activity relation of chloramphenicols, *J. Med. Chem.*, 16, 917-922 (DOI: 10.1021/jm00266a011).

16. Renard J.-F., Arslan D., Garbacki N., Pirotte B., Leval X. D. (2009), Pyridine analogues of nimesulide: design, synthesis, and in vitro and in vivo pharmacological evaluation as promising cyclooxygenase 1 and 2 inhibitors, *J. Med. Chem.*, 19, 5864-5871 (DOI: 10.1021/jm900702b).

17. Schofiled K. (1980), Aromatic nitration, cambridge university press, *Cambradge,* (DOI: 10.1002/ange.19810930846).

18. Olah G. A., Malhotra R., Narang S. C. (1989), Nitration: methods and mechanism, VCH publishers, Weinheim, (DOI: 10.1002/recl.19901091207).

19. Hughes E. D., Ingold C. K., Reed R. I. (1946), Kinetics of aromatic nitration: the nitronium ion, *Nature*, 448-449 (DOI: 10.1038/158448c0).

20. Kulkarni A. K. (2014), Continuous flow nitration in miniaturized devices,

21. Prakash G. K. S., Panja C., Mathew T., Surampudi V., Petasis N. A., Olah G. A. (2004), *ipso*-Nitration of arylboronic acids with chlorotrimethylsilane−nitrate salts, *Org. Lett.*, 6, 2205-2207 (DOI: 10.1021/ol0493249).

22. Wu X.-F., Schranck J., Neumannb H., Beller M. (2011), Convenient and mild synthesis of nitroarenes by metal-free nitration of arylboronic acids, *chem. Commun.*, 47, 12462-12463 (DOI: 10.1039/C1CC15484B).

23. Liang Y.-F., Li X., Wang X., Yan Y., Feng P., Jiao N. (2015), Aerobic oxidation of Pd^{II} to Pd^{IV} by active radical reactants: direct C–H nitration and acylation of arenes *via* oxygenation process with molecular oxygen, *ACS Catal.*, 5, 1956-1963 (DOI: 10.1021/cs502126n).

24. Fan Z., Ni J., Zhang A. (2016), Meta-selective C_{Ar}–H nitration of arenes through a $Ru_3(CO)_{12}$-catalyzed ortho-metalation strategy, *J. Am. Chem. Soc.*, 138, 8470-8475 (DOI: 10.1021/jacs.6b03402).

25. Rozen S., Carmeli M. (2003), From azides to nitro compounds in a few seconds using HOF·CH_3CN, *J. Am. Chem. Soc.*, 125, 8118-8119 (DOI: 10.1021/ja035616d).

26. Park D. Y., Lee K. Y., Kim J. N. (2007), Synthesis of poly-substituted nitrobenzene derivatives from baylis–hillman adducts *via* [3+3] annulation protocol, *Tetrahedron Lett.*, 48, 1633-1636 (DOI: 10.1016/j.tetlet.2006.12.146).

27. Dagar A., Biswas S., Mobin S. M., Samanta S. (2016), Access to densely functionalized naphthalenes by organobase catalyzed domino reaction of 2-(2-formyl aryl)acetophenones with nitroolefins, *Tetrahedron Lett.*, 57, 3326-3329 (DOI: 10.1016/j.tetlet.2016.06.062).

28. Rathor S. S., Majee D., Samanta S. (2022), DBU- and DABCO-Promoted selective access to 2,5-diarylnitrobenzoates and cyclohexenones via one-pot reactions, *Synlett*, 33, 1052-1058 (10.1055/a-1817-0882).

29. Gotoh H., Uchimaru T., Hayashi Y. (2015), Two reaction mechanisms *via* iminium ion intermediates: the different reactivities of diphenylprolinol silyl ether and trifluoromethyl-substituted diarylprolinol silyl ether, *Chem. Eur. J.*, 21, 12337-12346 (DOI: 10.1002/chem.201500326).

30. Freeman A. W., Urvoy M., Criswell M. E. (2005), Triphenylphosphine-mediated reductive cyclization of 2-nitrobiphenyls: a practical and convenient synthesis of carbazoles, *J. Org. Chem.*, 70, 5014-5019 (DOI: 10.1021/jo0503299).

31. Koga Y., Kaneda T., Saito Y., Murakami K., Itami K. (2018), Synthesis of partially and fully fused polyaromatics by annulative chlorophenylene dimerization, *Science*, 359, 435-439 (DOI: 10.1126/science.aap9801).

32. Yang K., Zhou F., Kuang Z., Gao G., Driver T. G., Song Q. (2016), Diborane-mediated deoxygenation of *o*-nitrostyrenes to form indoles, *Org. Lett.*, 18, 4088-4091 (DOI: 10.1021/acs.orglett.6b01934).

Chapter 3

$Cu(OAc)_2$/DABCO-mediated domino reaction of vinyl malononitriles with cyclic sulfamidate imines: access to 6-hydroxyaryl-2-aminonicotinonitriles

3.1 Introduction

Developing a new synthetic method for pyridine with valuable functionalities is considered one of the most reputed and extensive studied areas within heterocyclic chemistry.[1-2] *T*hese moieties are omnipresent in a large number of biologically active natural alkaloids, vitamins (B_6 and B_3), enzymes, *etc*.[1-4] Considering their great significance, the synthesis of pyridines with important functionalities continues to be a thriving research field in organic and medicinal chemistry.[1–10] Among various pyridine derivatives, access to 2-amino-3-cyanopyridines stand out as a lucrative target for chemists due to their diverse biological activities **(Fig. 3. 1)**[11-13] such as an antifungal,[11] protein (IKK-β) inhibitory activity,[12] potent inhibitor of HIV-1 integrase,[13] anti-cardiovascular,[14] A_{2A}adenosine receptor antagonists,[15] *etc*.

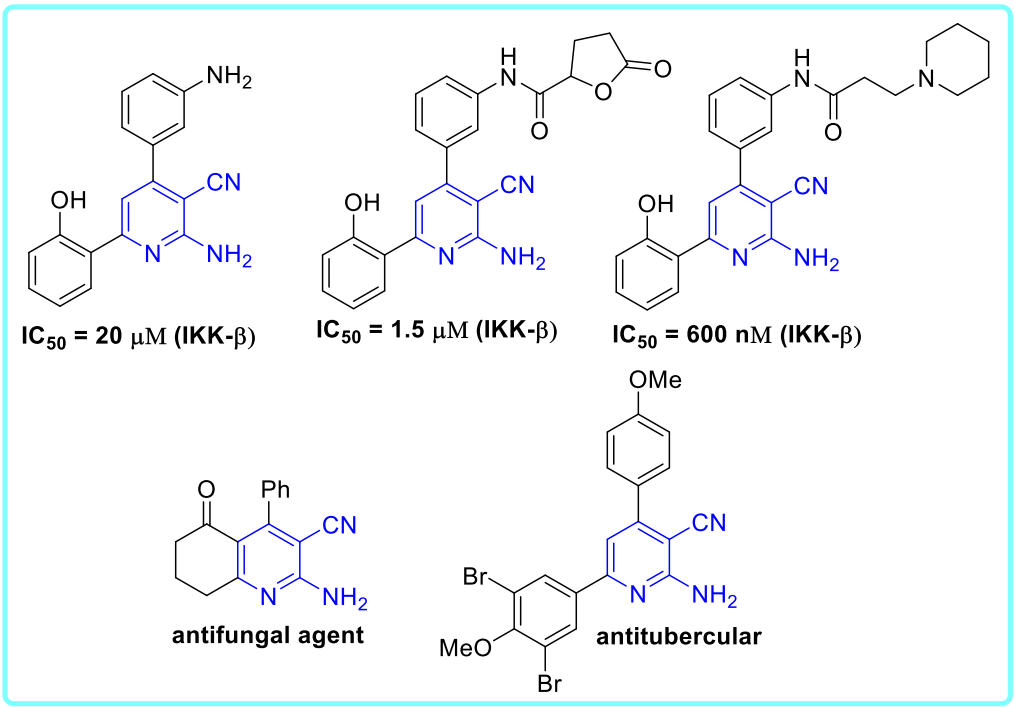

Figure 3.1 A few examples of biologically active 2-aminonicotinonitriles.

3.2 Review work

On account of their comprehensive applications, enormous attempts have been practiced over the decades towards synthesizing 2-amino-3-cyanopyridines, including several effective techniques such as condensation reactions, multicomponent reactions, etc.[16-17] Some of the relevant literature reports have been discussed in the next section.

In 1980, Kambe *et al.* developed a metal-free four-component reaction between enolizable ketones, arylaldehydes, malononitrile, and ammonium acetate as an N-source in refluxing benzene to give a series of 2-Amino-4-aryl-3-cyanopyridines.[18] This methodology offers moderate yields of the mentioned derivatives (44-68% yields) in **(Scheme 3.1).**

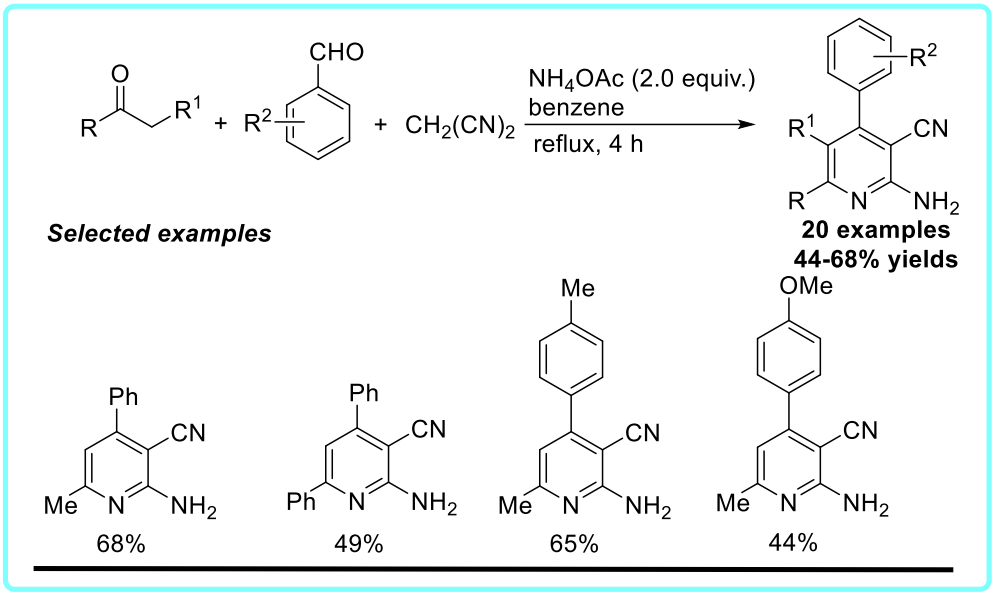

Scheme 3.1. Metal-free synthesis of 2-amino-4-aryl-3-cyanopyridines.

Wang *et al.* accomplished a one-pot four-component reaction aldehydes, ketones, malononitrile, and ammonium acetate catalyzed by ytterbium perfluorooctanoate [$Yb(PFO)_3$] to produce a family of 2-amino-3-cyanopyridine derivatives in good to high yields (60-95%) in **(Scheme 3.2).**[19]

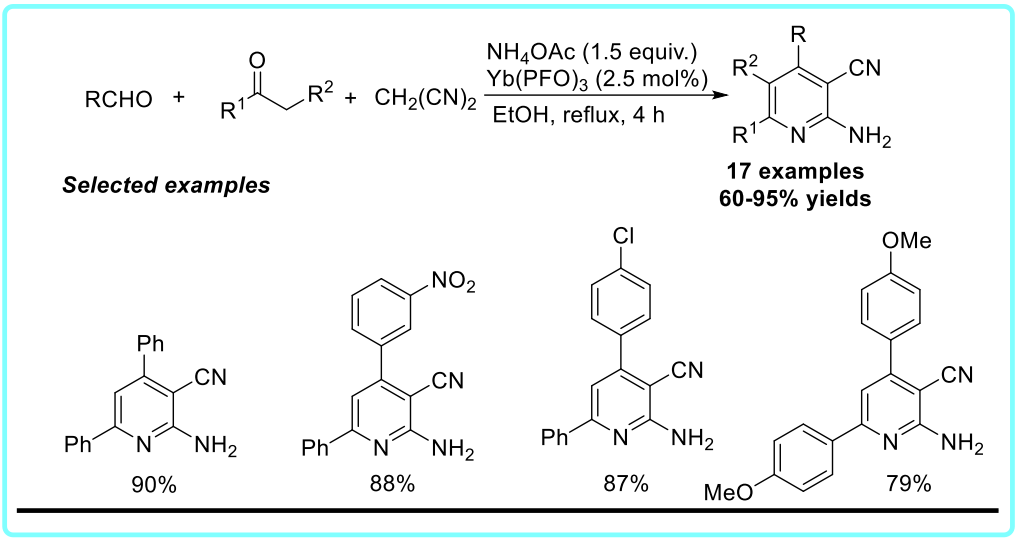

Scheme 3.2. $Yb(PFO)_3$-catalyzed one-pot synthesis of 2-amino-3-cyanopyridines.

Based on the proposed mechanism **(Scheme 3.3)** reported by the authors, the reaction may occur via Yb(III)-catalyzed Michael reaction between an in situ generated enamine **3** from ketone and ammonium acetate and alkylidenemalononitrile **2** (obtained from the condensation of aldehyde with malononitrile) to form intermediate **4**, which undergoes sequence of cyclization, isomerization, and aromatization process to produce the final pyridine.[19]

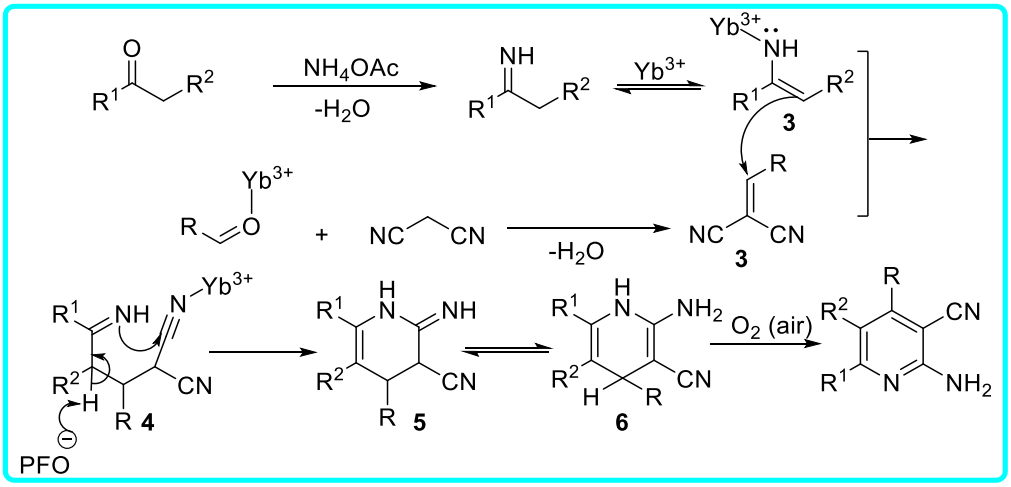

Scheme 3.3. A possible mechanism for the formation of 2-amino-3-cyanopyridines catalyzed by $Yb(PFO)_3$.

In 2014, Cui and co-workers demonstrated a divergent synthesis of 2-amino nicotinonitriles *via* copper-catalyzed three-component reaction between oxime esters malononitrile and arylaldehydes in the presence of piperidine base at 60 °C. The cyclization reaction proceeds through a conversion of pivaloyl oxime esters to copper enamides in the presence of copper(I), which can undergo Michael addition to in situ generated 2-benzylidenemalonitriles, followed by intramolecular cyclization to give 2-amino nicotinonitriles in good to high yields **(Scheme 3.4).**[20]

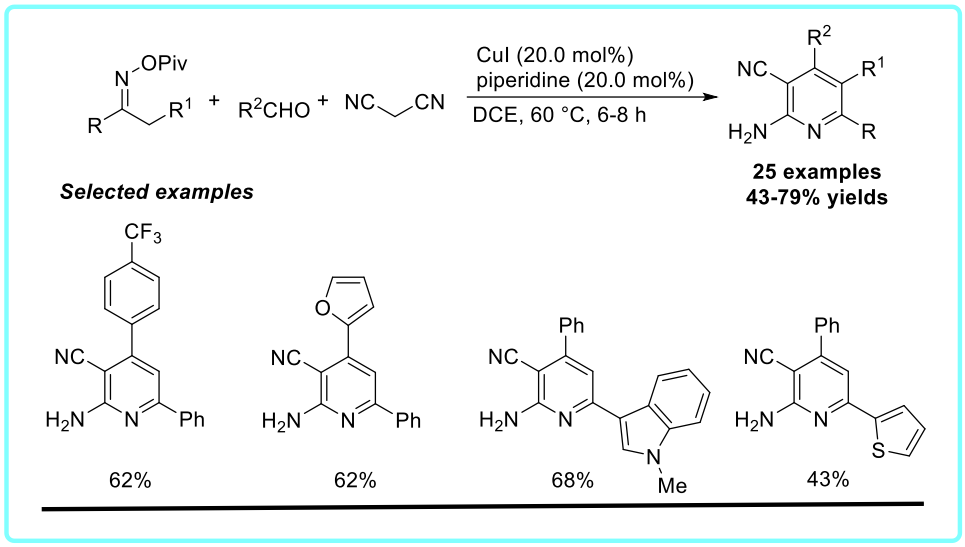

Scheme 3.4. Copper-catalyzed three-component route to 2-aminonicotinonitriles.

Shang *et al.* also revealed an efficient MCR technique for synthesizing highly substituted 2-aminopyridine derivatives in moderate to good yields. This four-component reaction involves the use of $FeCl_3$ catalysis to facilitate the reaction between arylaldehdes, 2-arylacetonitriles, ethyl acetoacetate and anilines via a sequence of nucleophilic addition/intermolecular cyclization process as shown in **(Scheme 3.5)**.[21]

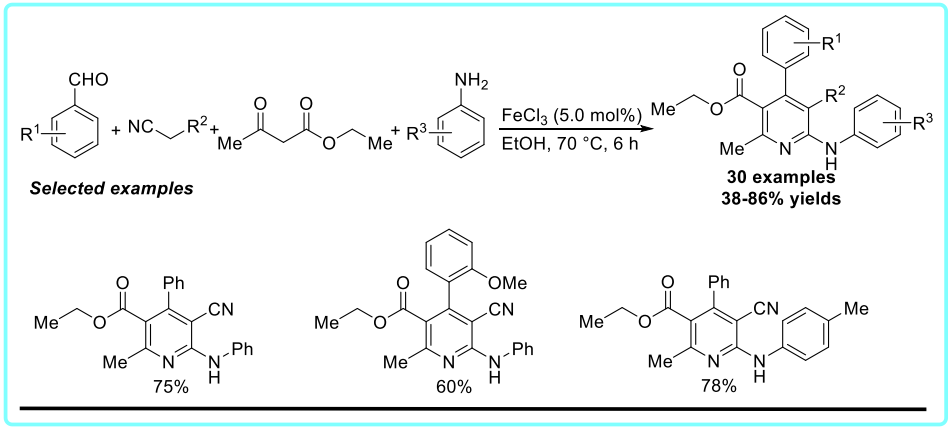

Scheme 3.5. $FeCl_3$-catalyzed four-component reaction for the formation of poly substituted pyridines.

Ponticello *et al.* reported a convenient, metal-free one-pot sequential method for the preparation of 2-bromonicotonitriles in poor to moderate yields (15-42%) *via* a condensation of alkylidenemalononitriles with DMF acetal, followed by the cyclization of resulting α,β-unsaturated aldehydes with a mixture of HBr/AcOH at 55 °C **(Scheme 3.6).**[22]

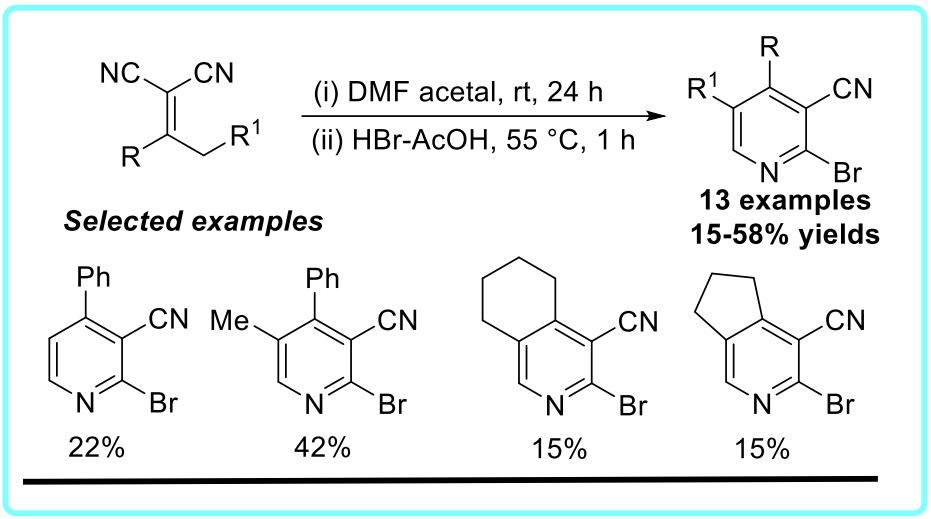

Scheme 3.6. One-pot two-step sequential access to 2-bromonicotinonitriles.

A metal-solvent-free sequential one-pot for accessing to 4-substituted-3-cyano-2-aminopyridines using enaminonitriles and various primary amines under microwave irradiation was established by Lohier *et al.* This simple technique bestows high yields of substituted pyridines (50-84%) **(Scheme 3.7)**.[23]

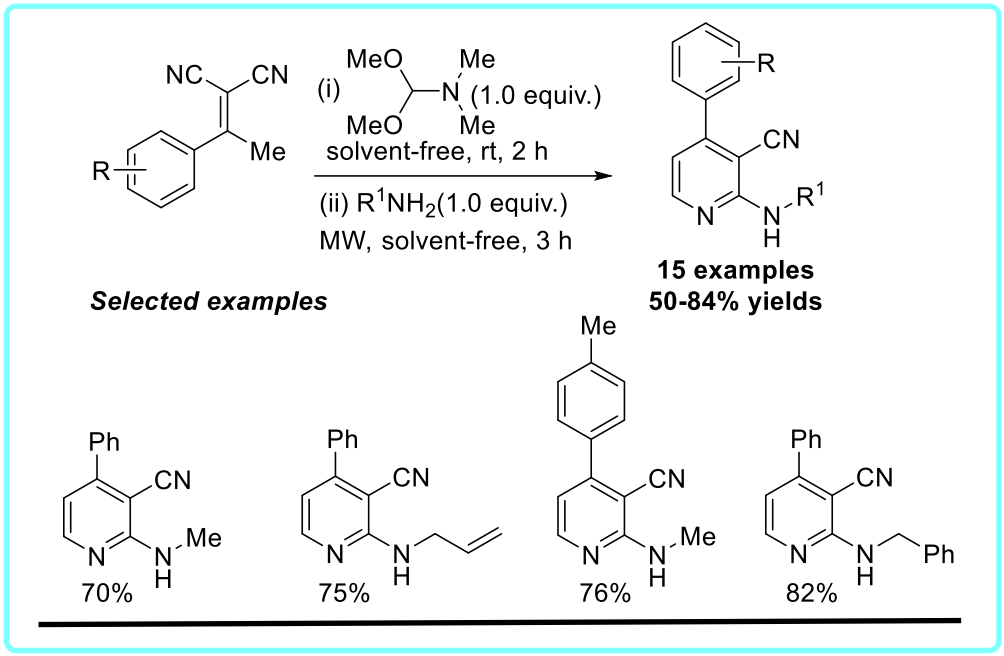

Scheme 3.7. Synthesis of 4-substituted-3-cyano-2-aminopyridines.

Soon after, Yu *et al.* also disclosed a powerful strategy for the synthesis of fully substituted 2-aminonicotinonitriles involving vinyl malononitriles and α-keto vinyl azides using NaOMe at 120 °C. This cyclization process proceeds smoothly *via* a base-mediated ring-opening, followed by intramolecular rearrangement to afford 2-aminonicotinonitriles in good to high yields (74-85%) **(Scheme 3.8).**[24]

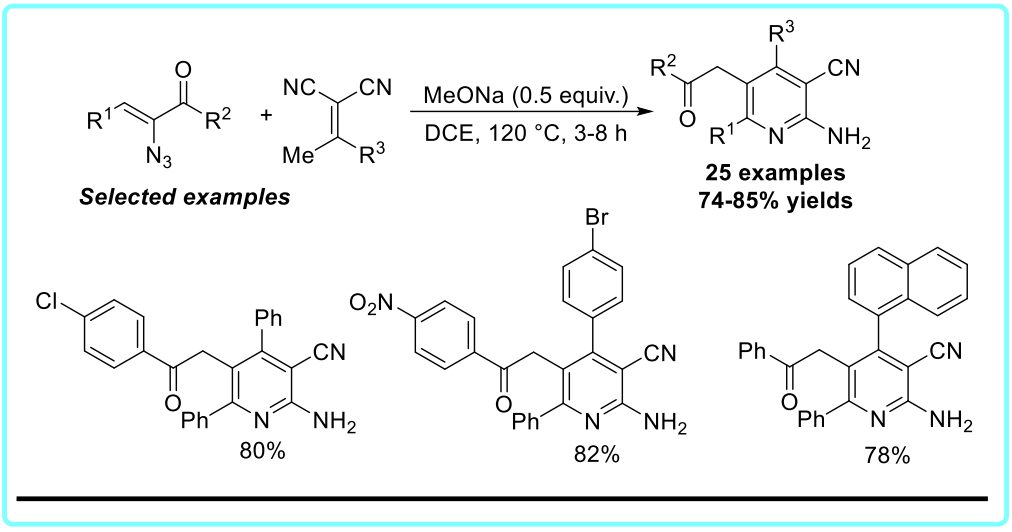

Scheme 3.8. Synthesis of 2-aminonicotinonitriles from vinyl azides and α,α-dicyanoalkenes.

Shimazaki *et al.* illustrated an appealing two-step synthetic reaction involving Wang-resin protected hydoxyacetophenones, aldehydes, malononitrile, and ammonium acetate, followed by the removal of resin in TFA medium. This process gives 3-cyano-6-(2-hydroxyphenyl)pyridines in quantitative yields **(Scheme 3.9)**.[25]

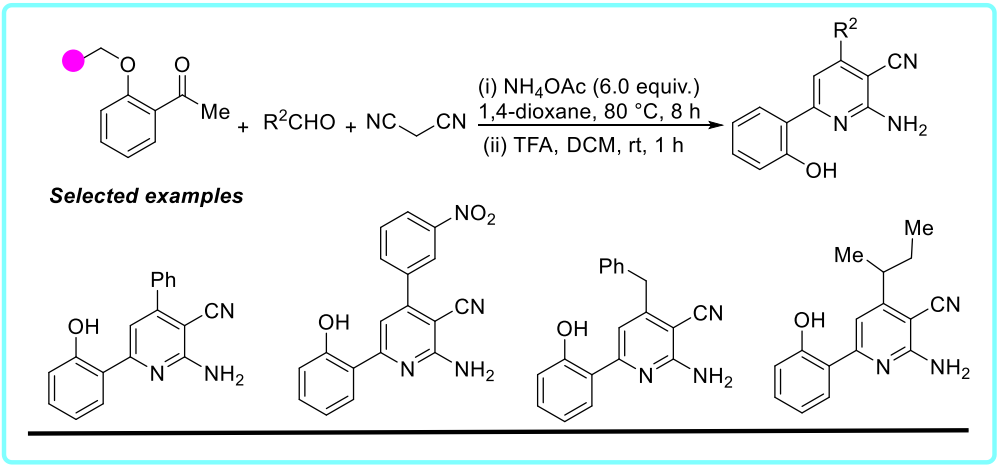

Scheme 3.9. Synthesis of 3-cyano-6-(2-hydroxyphenyl)pyridines by multi-component condensations.

3.2.1 Conclusion

A literature survey hints that a vast number of synthetic methods have been developed to construct functionalized pyridines due to their diverse applications in different fields. However, the practical access to 2-aminonicotinonitriles derivatives with value-added 6-hydroxyarylated moieties, an area that has been highly overlooked, presents a unique opportunity for discovery and innovation. These derivatives, with their promising applications in medicinal chemistry, are underexplored and have a great potential for new drug discoveries. Moreover, the preparation of functionalized 6-hydroxyarylated 2-aminonicotinonitriles still requires multistep operations. Therefore, there is a great interest in developing an experimentally simple, convenient, one-pot method that would produce a series of functionalized 6-hydroxyarylated 2-aminonicotinonitriles from simple reactants.

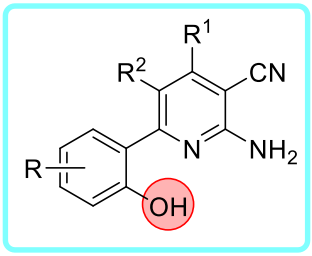

Figure 3.2. Representative structure of functionalized 6-hydroxyarylated 2-aminonicotinonitriles.

3.3 Present work

Pyridines are historically recognized aza-heterocyclic molecules that have valuable applications in various domains, including organic, medicinal, and materials chemistry, as described earlier. Therefore, developing new synthetic processes for accessing pyridines with valuable functionalities, such as hydoxyaryl and CN groups at the appropriate positions on the pyridine ring, continues to be a challenging target for chemists. In this context, we are pleased to report a one-pot method that utilizes cyclic sulfamidate imines as 1C1N sources and different kinds of acyclic/cyclic vinyl malononitriles as sources of 4C to deliver pyridine derivatives *via* a vinylogous Mannich-cycloaromatization sequence process under mild conditions.

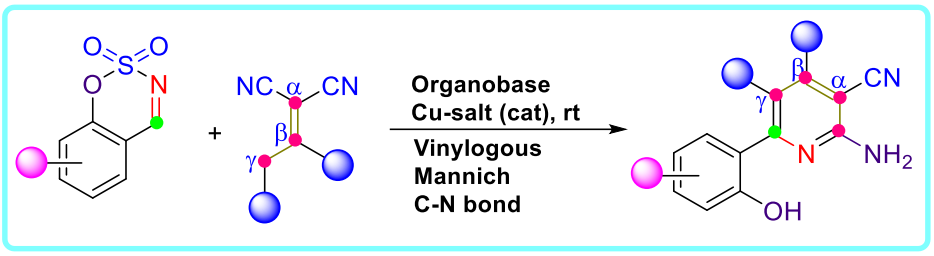

Scheme 3.10. One-pot access to 6-hydroxyaryl-2-aminonicotinonitriles.

3.4 Results and discussion

3.4.1 Optimization of the reaction conditions

The optimization reaction was commenced by selecting cyclic sulfamidate imine (1.0 equiv., **1a**), 2-(1 phenylethylidene)malononitrile (1.1 equiv., **2a**), and 1.5 equiv. of DABCO (1,4-diazobicyclo[2.2.2]octane) at room temperature in MeCN. Unfortunately, after 4 h, this reaction produced a trace amount of targeted product **3aa** (7% yield) along with an unwanted α,β,γ,δ-unsaturated

malononitrile **4** in 71% yield (entry 1, **Table 3.1**). Using Et_3N (10% and 61% yields of **3aa** and **4,** respectively) led to a similar result (entry 2). At this point, we surmised that a Lewis acid might activate the nitrile group through coordination, which helps the cyclization process, resulting in enhancement of yield of **3aa**. For this purpose, $Cu(OAc)_2$ (10 mol%) was employed in the above reaction. Satisfactorily, **3aa** was isolated in a 74% yield (entry 3). The chemical structure of **3aa** was assigned by its spectroscopic data (^{1}H NMR, ^{13}C NMR, HRMS, and SC-XRD data). In the ^{1}H NMR spectrum of **3aa**, the presence of a singlet at 13.40 ppm, corresponds to the phenolic O-H group and 12 aromatic protons in the range of 6.78-8.07 ppm. In addition, the ^{13}C NMR spectrum of **3aa** shows a total of 16 peaks at 160.1, 159.5, 159.4, 155.8, 137.2, 132.9, 130.2, 129.2, 128.8, 128.7, 119.3, 118.7, 118.5, 117.0, 108.6, 86.6 ppm. The molecular ion peak $[M+Na]^+$ at 310.0951 in the HRMS spectrum corresponds to the molecular weight 287.1059 of the desired compound **3aa.**

Next, we scrutinized several Cu salts ($Cu(OTf)_2$, $CuBr_2$, CuI, and CuCl) and other metal salts ($Zn(OTf)_2$, $Gd(OTf)_3$, $Nd(OTf)_3$, $In(OTf)_3$, $FeCl_3$ and $ZnCl_2$) to act as catalysts for this transformation. Among the various additives (entries 4-13), only $Cu(OTf)_2$ produces **3aa** with a promising yield of 76% (entry 4). However, $Cu(OAc)_2$ was chosen as the best additive due to its affordability.

Table 3.1 Optimization of the reaction conditions.[a,b]

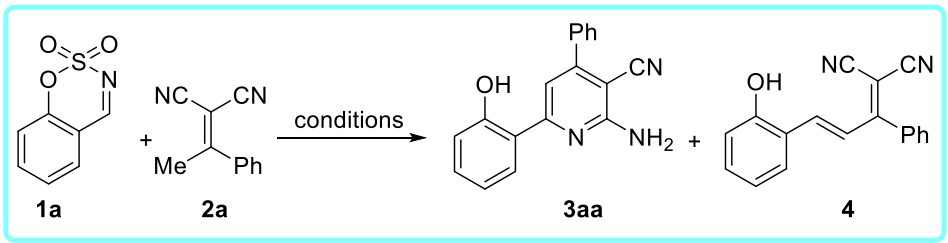

Entry	Base (1.5 equiv.)	Catalyst (10 mol%)	Solvent	*T*/h	Yield[b] 3aa	Yield[b] 4
1	DABCO	-	MeCN	4	7	71
2	Et_3N	-	MeCN	6	10	61
3	DABCO	$Cu(OAc)_2.H_2O$	MeCN	3	74	5
4	DABCO	$Cu(OTf)_2$	MeCN	3	76	5
5	DABCO	$CuBr_2$	MeCN	3	55	21
6	DABCO	CuI	MeCN	3	37	36

7	DABCO	CuCl	MeCN	3	39	27
8	DABCO	$Zn(OTf)_2$	MeCN	3	19	57
9	DABCO	$Gd(OTf)_3$	MeCN	3	16	52
10	DABCO	$Nd(OTf)_3$	MeCN	3	18	56
11	DABCO	$In(OTf)_3$	MeCN	3	13	65
12	DABCO	$FeCl_3$	MeCN	3	10	23
13	DABCO	$ZnCl_2$	MeCN	3	15	41
14	DBU	$Cu(OAc)_2.H_2O$	MeCN	3	5	65
15	Et_3N	$Cu(OAc)_2.H_2O$	MeCN	3	65	7
16	DMAP	$Cu(OAc)_2.H_2O$	MeCN	3	63	10
17	DIPEA	$Cu(OAc)_2.H_2O$	MeCN	3	54	18
18	Cs_2CO_3	$Cu(OAc)_2.H_2O$	MeCN	3	5	27
19	DABCO	$Cu(OAc)_2.H_2O$	toluene	3	70	7
20	DABCO	$Cu(OAc)_2.H_2O$	CH_2Cl_2	3	66	4
21	DABCO	$Cu(OAc)_2.H_2O$	DMF	3	59	6
22	DABCO	$Cu(OAc)_2.H_2O$	2-MeTHF	3	57	8
23	DABCO	$Cu(OAc)_2.H_2O$	EtOH	6	42	9
24	DABCO	$Cu(OAc)_2.H_2O$	PEG-400	6	13	3
25[c,d]	–	$Cu(OAc)_2.H_2O$	MeCN	12	ND	

[a]Unless otherwise noted, all the reactions were conducted using **1a** (0.2 mmol), **2a** (0.22 mmol), base (0.3 mmol, 1.5 equiv.), and additive (0.02 mmol) in a dry solvent (1.5 mL) at room temperature at the mentioned time. [b]Isolated yield after column chromatography. [c]ND indicates not detected. [d]Reaction did not happen at room temperature and under refluxing conditions.

Moreover, several bases (DBU, Et_3N, DMAP, DIPEA, and Cs_2CO_3, entries 14-18) with 10 mol% $Cu(OAc)_2$ as combined systems were tested in an MeCN solvent. Results show that the DABCO/$Cu(OAc)_2$ system provided a better yield (74% *vs.* 5-65%) of **3aa** than the other ones. Notably, strong bases like DBU (entry 14) and Cs_2CO_3 (entry 18) led to inferior outcomes. Switching from the MeCN solvent to other solvents like toluene, DCM, DMF, 2-MeTHF, EtOH, and PEG-400 resulted in inferior to good yields (5-70%, entries 19-24) of **3aa**. It should be noted that in the absence of DABCO, $Cu(OAc)_2$ was unable to promote this domino reaction at room temperature as well as under refluxing conditions (entry 25).

3.4.2 Plausible mechanism

Based on the above experimental results and literature precedents,[26] we present a logical mechanism for this domino reaction as shown in **Scheme 3.11.** First, the base abstracts a methyl proton from **2a** to form a carbanion intermediate **2a′**. Then, the latter reacts with cyclic sulfamidate imine **1a** via Mannich reaction, giving anionic intermediate **5.** Afterwards, $Cu(OAc)_2$ may coordinate with the two cyano groups of **5** to make a more reactive species **7** which is subsequently cyclized (Pinner type) *via* a C–N bond formation as shown in path **B**, resulting in tricyclic imine intermediate **8**. Finally, it tautomerizes to form dihydropyridine intermediate **9**, which is subjected to the elimination of SO_2 under the influence of a base to make pyridine derivative **3aa.** On the other hand, in the absence of a copper salt, the intermediate **5** may transform into another carbanion intermediate **6** *via* intramolecular proton transformation which in turn eliminates N-sulfonyl amine (SO_2=NH), producing α,β,γ,δ-unsaturated malononitrile **4** as shown in path **A**. **(Scheme 3. 11)**

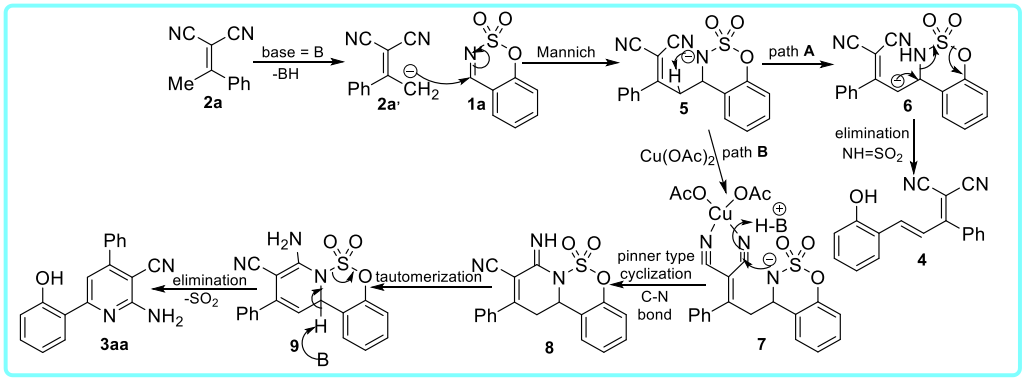

Scheme 3.11. A plausible mechanism for this domino reaction.

3.4.3 Substrate scope

With the optimal reaction parameters in hand, we studied the generality and scope of this protocol using a set of cyclic sulfamidate imines and various vinyl malononitriles snthesized from acyclic ketones as 4C units for the pyridine synthesis promoted by DABCO/$Cu(OAc)_2$ as a combined system at room temperature. It was evident from **Table 3.2** that several 2-(1 arylethylidene)malononitriles (**2b–2l**) bearing electron-donating (Me, MeO and

OCH_2O) and electron-withdrawing substituents (Cl, Br, F and NO_2) on the aryl rings at *ortho, meta* and *para* positions cyclized nicely with **1a**. They delivered the corresponding biologically active 2-aminonicotinonitrile derivatives **3ab–3al**; a few of them (**3ab, 3ac, 3ai, 3aj, 3ah and 3al**) showed good anti-inflammatory activity.[27] Notably, the electron-donating groups gave slightly more favorable yields than the electron-withdrawing ones (76-77% vs. 69-73%). Interestingly, the α,α-dicyanoolefins with heteroaryl rings (**2n** and **2o**) at the β-positions showed good reactivities towards the vinylogous Mannich-cycloaromatization reaction with **1a,** leading to 4-heteroaryl-substituted pyridines **3an** and **3ao** in 80% and 81% yields, respectively. Moreover, a bulky naphthyl moiety attached to vinyl malononitrile produced **3am** in a 73% yield. Pleasantly, when the vinyl malononitriles derived from aliphatic ketones (**2p** and **2q**) were employed as 4C precursors, they produced tetra- and fully-substituted pyridines **3ap** and **3aq** in high yields (82-84%). Next, this method is not only applicable for β-methyl vinyl malononitriles but also equally valid for β-ethyl/ butyl groups. For instance, the substrates **2r** and **2s** ran smoothly with **1a** in a spotless manner to give fully substituted **3ar** and **3as** in 86% and 81% yields, respectively, after 7h. To our pleasure, a number of electron-donating (Me and MeO) and electron-poor halogen atoms (Cl and Br) on the aryl parts of the cyclic sulfamidate imines also led to the corresponding hydroxyarylated pyridines (**3ba-3cr**) in 62-78% yields. It should be pointed that generally, cyclic imines possessing electron withdrawing halogen atoms (**1e**, **1f** and **1h**) irrespective of their positions gave slightly lower yields of the targeted pyridines (**3ea**, **3fa,** and **3ha**; 62-67% yields) than the electron donating ones (**3ba**, **3da** and **3ga**, 70-73% yields). Importantly, β-naphthol-substituted pyridine **3ia** could be synthesized with 61% yield when a cyclic imine **1i** reacted with **2a**. The developed conditions are sufficiently mild, allowing for diverse functionalities: Me, Et, propyl, MeO, OCH_2O, F, Cl, Br, NO_2, NH_2, CN, OH, furan, thiophene, cyclopropane, *etc.*

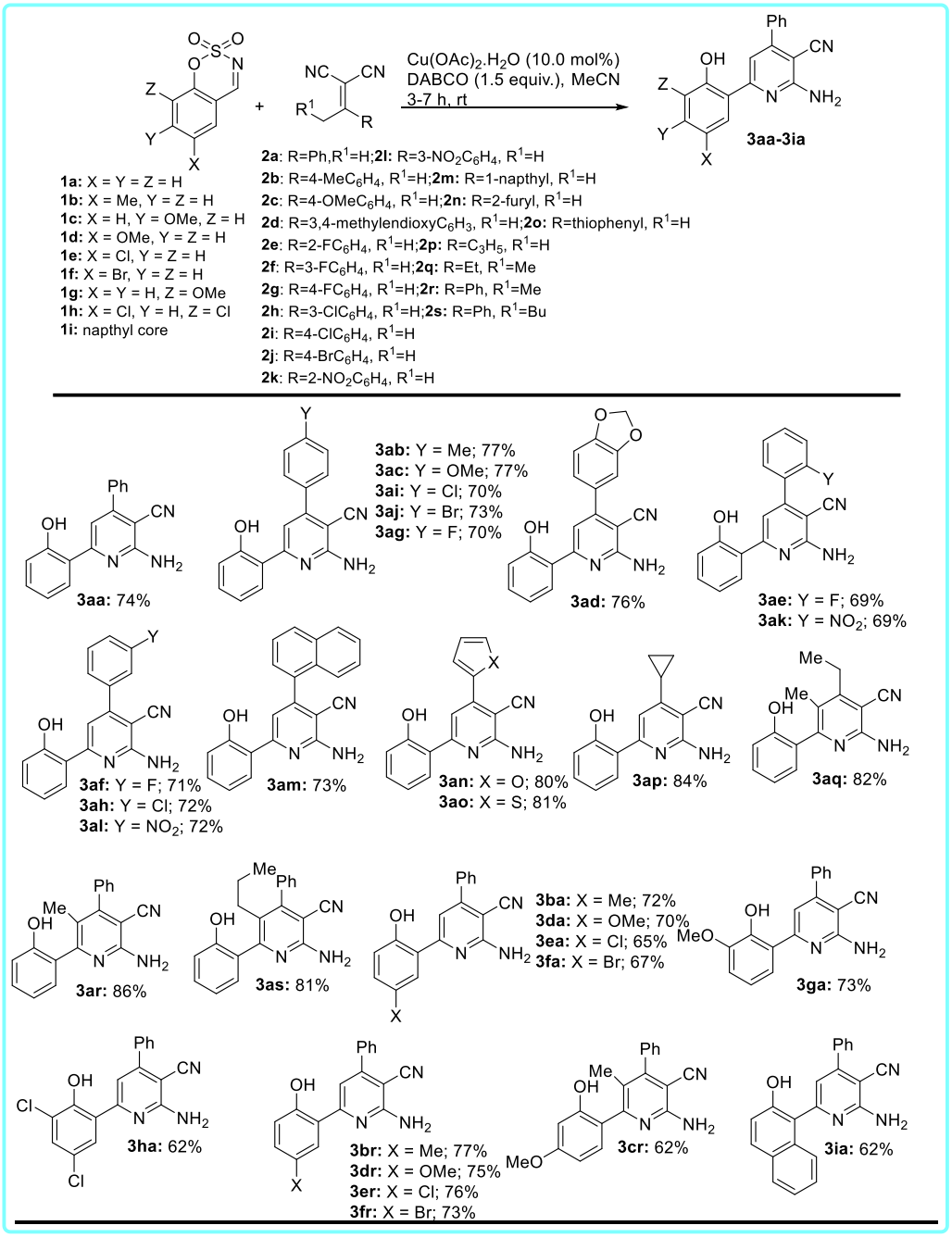

Table 3.2 One-pot synthesis of 6-(2-hydroxyaryl)-2-amino-3-cyanopyridines (**3aa-3ia**).

After successfully employing acyclic vinyl malononitriles as 4C sources for accessing to tetra- and fully-substituted pyridines, we then focused on sterically demanding cyclic α, α-dicyanoolefins as challenging carbonucleophiles in this domino reaction. We examined a bunch of α, α-dicyanoolefins (**2t-2w**) derived from several cyclic ketones such as cyclohexanone, cycloheptanone, α-

indanone and α-tetralone. These compounds were subjected to annulation with a family of cyclic sulfamidate imines (**1a**, **1d-1f**) under the present system, which led to the corresponding bi- and tri-carbocyclic-fused nicotinonitriles (**3at-3ft**) in good to high yields (74-85%, **Table 3.3).** Furthermore, six-membered heterocycle-substituted α,α-dicyanoolefins **2x** and **2y** underwent neat and clean cyclization with **1a**, giving the corresponding pyranyl and chromanyl-fused pyridines **3ax** and **3ay** in 77% and 79% yields, respectively. We were pleased to find that this domino approach also yielded an enantiomerically pure steroidal-A-ring-fused nicotinonitrile as a single isomer (**3az**) in 71% yield when α,α-dicyanoalkene derived from 5α-cholestan-3-one was employed as a carbonucleophile. Notably, all the prepared fused pyridines are challenging to access by the established methods **(Table 3.3)**

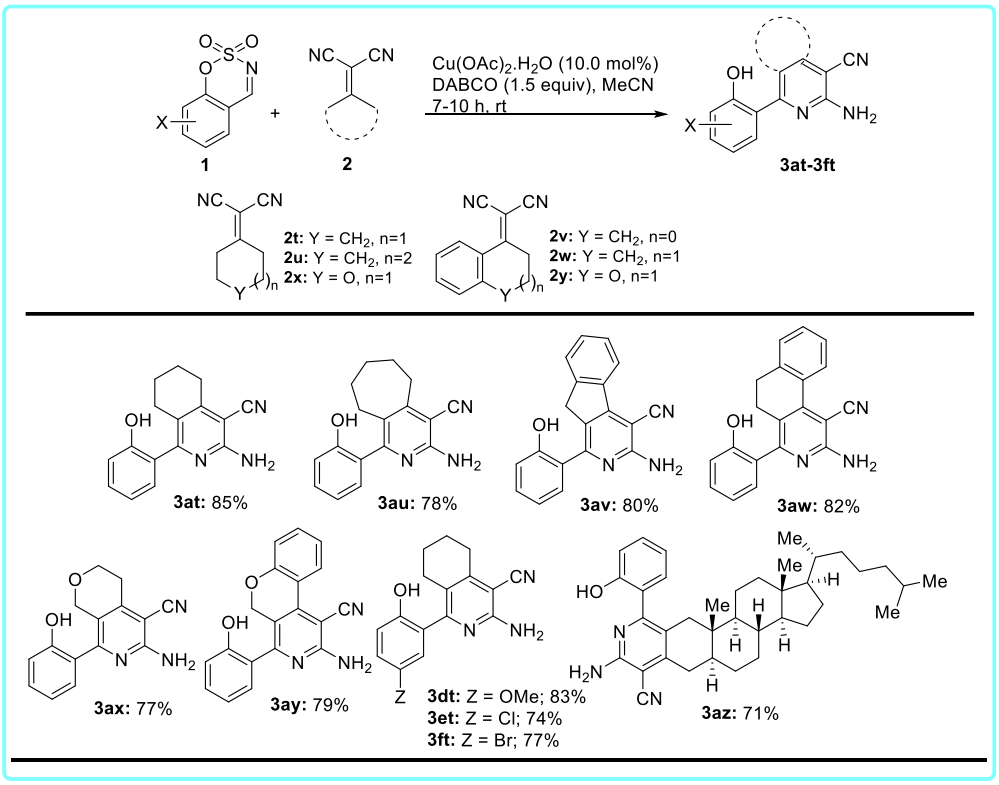

Table 3.3 One-pot synthesis of carbo- and heterocyclic fused nicotinonitriles (**3at-3ft**).

To further highlight the synthetic practicability of the current protocol, we scaled up the Cu(II)-catalyzed and DABCO-mediated domino reactions of the cyclic sulfamidate imine **1a** (1.09 g, 6 mmol) with **2a** (1.1 g, 6.6 mmol) in dry

MeCN (10 mL) at room temperature using DABCO (9.0 mmol, 1.0 g) and $Cu(OAc)_2 \cdot H_2O$ (0.6 mmol, 119.8 mg) for 5h. The desired product **3aa** could be isolated in 69% yield (1.19 g) without a loss of productivity (**Scheme 3.12)**

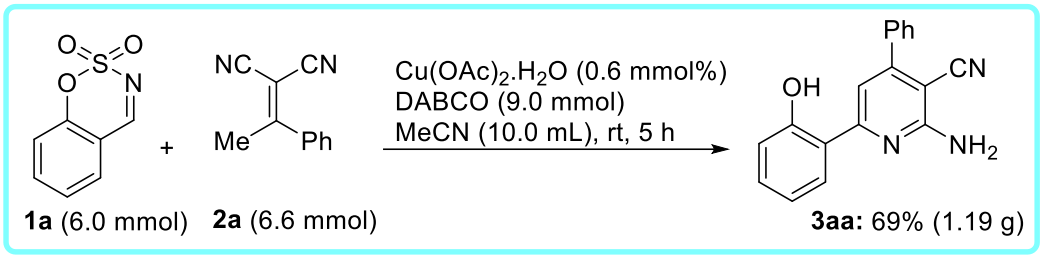

Scheme 3.12. Gram-scale synthesis.

To show the versatility of the synthesized pyridines, compound **3al** was efficiently transmuted into 4-(3-aminophenyl)-2-aminonicotinonitrile **10** in 82% yield. This conversion involves the reduction of the nitro group of **3al** using 8.0 equiv. of Fe-powder, NH_4Cl (in excess) in EtOH: H_2O (1:1) at 100 °C for 18 h. This skeleton exhibited promising selective IKK-β serine-threonine protein kinase inhibitor activity (IC_{50} = 20 μM). Additionally, the phenolic OH group of **3al** was protected using TBSCl, imidazole, and triethylamine in DMF to provide an 88% yield of OTBS protected nicotinonitrile **11** (shown in **Scheme 3.13)**, which is a well-known starting material for synthesizing the highly potent selective IKK-β kinase inhibitor **12** with IC_{50} value 1.5 μM.[12]

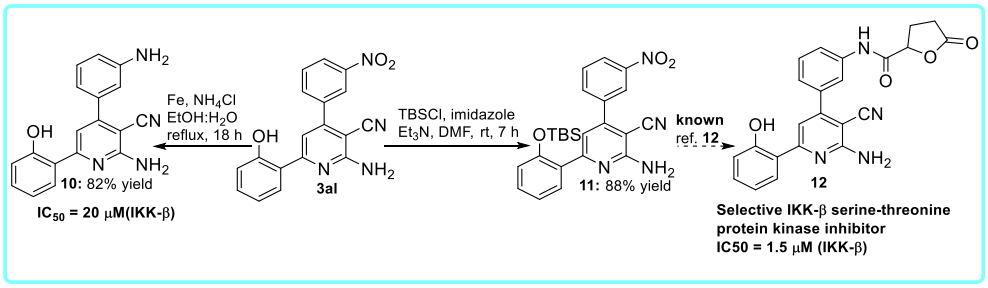

Scheme 3.13. Important synthetic application of a 2-aminonicotinitrile derivative.

3.5. Conclusion

This chapter established a mild, convenient, and efficient domino method for synthesizing a diverse set of pharmacologically exciting hydroxyarylated 2-aminonicotinonitriles and their fused analogs with good to high yields. The above vinylogous Mannich-cycloaromatization process involves an array of cyclic sulfamidate imines and various acyclic/cyclic vinyl malononitiles as carbon pronucleophiles promoted by DABCO/$Cu(OAc)_2$ as a robust system. Moreover, this domino process has several advantages, such as broad substrate scope, excellent functional group tolerance, the creation of two new C–N bonds, and applying a gram-scale synthesis, which highlights the protocol's practicability. Significantly, our method modified the prepared building block towards highly selective IKK-β serine-threonine protein kinase inhibitors.

3.6. Experimental Section

Preparation of starting materials: The vinyl malononitriles (**2a-z**)[28-30] and cyclic sulfamidate imines (**1a-i**)[31-33] were prepared according to the literature procedures. The products were characterized by ^{1}H NMR and ^{13}C NMR spectroscopic data. All chemicals were purchased from commercial suppliers and used without further purification unless otherwise stated.

Representative procedure for the synthesis of (3aa-3ft): To a stirred solution of compounds **1** (0.2 mmol), **2** (0.22 mmol) and $Cu(OAc)_2.H_2O$ (10 mol%) in dry MeCN (1.5 mL) was added DABCO (0.3 mmol) slowly at room temperature for 3 h. Upon completion of the reaction (monitored by TLC), the reaction mixture was extracted with ethyl acetate (3 × 10 mL), washed with brine and dried over Na_2SO_4. The combined organic phases were concentrated under reduced pressure to leave the crude residue. Finally, the product **3aa-3ft** was isolated in a pure form through column chromatography over silica gel using a mixture of EtOAc/hexane (10:90, v/v) as the eluent. The product was fully characterized by its spectroscopic data (^{1}H NMR, ^{13}C NMR, and HRMS).

Characterization data:

2-Amino-6-(2-hydroxyphenyl)-4-phenylnicotinonitrile(3aa): Yellow colour solid; mp 238-240 °C; yield 74% (42.5 mg); ^{1}H NMR (400 MHz, DMSO-d_6) δ 13.40 (s, 1H), 8.07 (d, *J* = 7.7 Hz, 1H), 7.69 (d, *J* = 3.3 Hz, 2H), 7.57 (s, 3H), 7.49 (s, 2H), 7.41 (s, 1H), 7.35 (t, *J* = 7.4 Hz, 1H), 6.93-6.78 (m, 2H) ppm; ^{13}C NMR (100 MHz, DMSO-d_6) δ 160.1, 159.5, 159.4, 155.8, 137.2, 132.9, 130.2, 129.2, 128.8, 128.7, 119.3, 118.7, 118.5, 117.0, 108.6, 86.6 ppm; HRMS (ESI-TOF) *m/z* calcd for $C_{18}H_{13}N_3NaO[M+Na]^+$: 310.0951, found 310.0950.

2-Amino-6-(2-hydroxyphenyl)-4-(4-methylphenyl)nicotinonitrile(3ab): Yellow colour solid; mp 228-230 °C; yield 77% (46.3 mg); ^{1}H NMR (500 MHz, DMSO-d_6) δ 13.42 (s, 1H), 8.06 (d, *J* = 7.9 Hz, 1H), 7.60 (d, *J* = 7.9 Hz, 2H), 7.46 (s, 2H), 7.41-7.32 (m, 4H), 6.92-6.87 (m, 2H), 2.41 (s, 3H) ppm; ^{13}C NMR (125 MHz, DMSO-d_6) δ 160.1, 159.4, 159.4, 155.7, 140.0, 134.3, 132.8, 129.7, 128.8, 128.7, 119.3, 118.7, 118.5, 117.1, 108.4, 86.5, 21.3 ppm; HRMS (ESI-TOF) *m/z* calcd for $C_{19}H_{15}N_3NaO[M+Na]^+$: 324.1107, found 324.1128.

2-Amino-6-(2-hydroxyphenyl)-4-(4-methoxyphenyl)nicotinonitrile(3ac): Yellow colour solid; mp 240-242 °C; yield 77% (48.8 mg); ^{1}H NMR (500 MHz, DMSO-d_6) δ 13.46 (s, 1H), 8.07 (dd, *J* = 8.0, 1.0 Hz, 1H), 7.68 (d, *J* = 8.7 Hz, 2H), 7.44 (s, 2H), 7.38 (s, 1H), 7.36-7.32 (m, 1H), 7.12 (d, J = 8.8 Hz, 2H), 6.92-6.87 (m, 2H), 3.85 (s, 3H) ppm; ^{13}C NMR (125 MHz, DMSO-d_6) δ 161.0, 160.1, 159.5, 159.3, 155.3, 132.8, 130.4, 129.3, 128.6, 119.3, 118.7, 118.5, 117.3, 114.6, 108.3, 86.3, 55.8 ppm; HRMS (ESI-TOF) *m/z* calcd for $C_{19}H_{16}N_3O_2[M+H]^+$: 318.1237, found 318.1239.

2-Amino-4-(benzo[*d*][1,3]dioxol-5-yl)-6-(2-hydroxyphenyl)nicotinonitrile(3ad): Yellow colour solid; mp 260-262 °C; yield 76% (50.3 mg); ^{1}H NMR (400 MHz, DMSO-d_6) δ 13.42 (s, 1H), 8.07 (d, *J* = 7.9 Hz, 1H), 7.44 (s, 2H), 7.41-7.26 (m, 3H), 7.22 (d, *J* = 8.0 Hz, 1H), 7.10 (d, *J* = 8.1 Hz, 1H), 6.92-6.87 (m, 2H), 6.14 (s, 2H) ppm; ^{13}C NMR (100 MHz, DMSO-d_6) δ 160.1, 159.4, 159.3, 155.2, 149.1, 148.0, 132.8, 130.9, 128.7, 123.2, 119.3, 118.7, 118.5 117.1, 109.3, 108.9, 108.5, 102.1, 86.47 ppm; HRMS (ESI-TOF) *m/z* calcd for $C_{19}H_{13}N_3NaO_3$ [M+Na]$^+$: 354.0849, found 354.0852.

2-Amino-4-(2-fluorophenyl)-6-(2-hydroxyphenyl)nicotinonitrile(3ae):

Yellow colour solid; mp 226-228 °C; yield 69% (42.1mg); ^{1}H NMR (500 MHz, DMSO-d_6) δ 13.25 (s, 1H), 7.96 (d, *J* = 7.9 Hz, 1H), 7.55-7.51 (m, 2H), 7.49 (s, 2H), 7.40-7.31 (m, 3H), 7.28 (t, *J* = 7.6 Hz, 1H), 6.86 (d, *J* = 8.2 Hz, 1H), 6.82 (t, *J* = 7.5 Hz, 1H) ppm; ^{13}C NMR (100 MHz, DMSO-d_6) 160.0, 159.7, 159.0 (d, J_{C-F} = 245.83 Hz) 158.9, 150.5, 133.0, 132.4 (d, J_{C-F} = 8.3 Hz), 131.4, 128.7, 125.3 (d, J_{C-F} = 3.0 Hz), 125.2, 125.0, 119.4, 118.6, 116.5 (d, J_{C-F} = 21.6 Hz), 116.3, 109.5, 88.1 ppm; HRMS (ESI-TOF) *m/z* calcd for $C_{18}H_{13}FN_3O$ $[M+H]^+$: 306.1037, found 306.1042.

2-Amino-4-(3-fluorophenyl)-6-(2-hydroxyphenyl)nicotinonitrile(3af):

Yellow colour solid; mp 190-192 °C; yield 71% (43.3 mg); ^{1}H NMR (500 MHz, DMSO-d_6) δ 13.34 (s, 1H), 8.10-8.04 (m, 1H), 7.64-7.48 (m, 5H), 7.43 (s, 1H), 7.41-7.37 (m, 1H), 7.36-7.31 (m, 1H), 6.91-6.86 (m, 2H) ppm; ^{13}C NMR (125 MHz, DMSO-d_6) δ 162.3 (d, J_{C-F} = 242.9 Hz), 160.1, 159.7, 159.4, 154.3, 139.5 (d, J_{C-F} = 8.05 Hz), 133.0, 131.30 (d, J_{C-F} = 8.4 Hz), 128.8, 125.1 (d, J_{C-F} = 2.6 Hz), 119.4, 118.6 (d, J_{C-F} = 6.5 Hz), 117.1, 116.9, 116.8, 115.9 (d, J_{C-F} = 22.7 Hz), 108.6, 86.5; ^{19}F NMR (471 MHz, DMSO-d_6) δ -112.40 (s) ppm; HRMS (ESI-TOF) *m/z* calcd for $C_{18}H_{13}FN_3O$ $[M+H]^+$: 306.1037, found 306.1049.

2-Amino-4-(4-fluorophenyl)-6-(2-hydroxyphenyl)nicotinonitrile(3ag):

Yellow colour solid; mp 242-244 °C; yield 70% (42.7 mg); ^{1}H NMR (500 MHz, DMSO-d_6) δ 13.37 (s, 1H), 8.07 (d, *J* = 8.0 Hz, 1H), 7.77-7.52 (m, 2H), 7.49 (s, 2H), 7.42 (t, *J* = 8.6 Hz, 3H), 7.35 (t, *J* = 7.7 Hz, 1H), 6.93-6.88 (m, 2H) ppm; ^{19}F NMR (471 MHz, DMSO-d_6) δ -111.50 (s) ppm; ^{13}C NMR (125 MHz, DMSO-d_6) δ 163.5 (d, J_{C-F} = 245.6 Hz), 160.1, 159.6, 159.4, 154.7, 133.7 (d, J_{C-F} = 2.7 Hz), 132.9, 131.3 (d, J_{C-F} = 8.6 Hz), 128.8, 119.4, 118.6 (d, J_{C-F} = 10.2 Hz), 116.9, 116.3, 116.1, 108.6, 86.6 ppm; HRMS (ESI-TOF) *m/z* calcd for $C_{18}H_{12}FKN_3O$ $[M+K]^+$: 344.0596, found 344.0590.

2-Amino-4-(3-chlorophenyl)-6-(2-hydroxyphenyl)nicotinonitrile(3ah):

Yellow colour solid; mp 256-258 °C; yield 72% (46.3 mg); ^{1}H NMR (500 MHz, DMSO-d_6) δ 13.29 (s, 1H), 8.03 (d, *J* = 7.4 Hz, 1H), 7.70 (s, 1H), 7.59- 7.51 (m, 3H), 7.47 (s, 2H), 7.38 (s, 1H), 7.32-7.24 (m, 1H), 6.85-6.80 (m, 2H) ppm; ^{13}C NMR (100 MHz, DMSO-d_6) δ 160.1, 159.7, 159.3, 154.1, 139.2, 133.8, 133.0,

131.0, 130.0, 128.8, 128.7, 127.70, 119.3, 118.6, 118.5, 116.7, 108.7, 86.56 ppm; HRMS (ESI-TOF) *m/z* calcd for $C_{18}H_{13}ClN_3O$ $[M+H]^+$: 322.0742, found 322.0750.

2-Amino-4-(4-chlorophenyl)-6-(2-hydroxyphenyl)nicotinonitrile(3ai):
Yellow colour solid; mp 300-302 °C; yield 70% (45.0 mg); ^{1}H NMR (500 MHz, DMSO-d_6) δ 13.36 (s, 1H), 8.07 (d, *J* = 7.9 Hz, 1H), 7.73 (d, *J* = 8.4 Hz, 2H), 7.65 (d, *J* = 8.3 Hz, 2H), 7.53 (s, 2H), 7.43 (s, 1H), 7.36 (t, *J* = 7.5 Hz, 1H), 6.93-6.88 (m, 2H) ppm; ^{13}C NMR (125 MHz, DMSO-d_6) δ 160.1, 159.6, 159.4, 154.5, 136.0, 135.1, 133.0, 130.8, 129.2, 128.8, 119.3, 118.6, 118.5 116.8, 108.5, 86.4 ppm; HRMS (ESI-TOF) *m/z* calcd for $C_{18}H_{12}ClKN_3O[M+K]^+$: 360.0300, found 360.0330.

2-Amino-4-(4-bromophenyl)-6-(2-hydroxyphenyl)nicotinonitrile(3aj):
Yellow colour solid; mp 280-282 °C; yield 73% (53.5mg); ^{1}H NMR (400 MHz, DMSO-d_6) δ 13.35 (s, 1H), 8.07 (d, *J* = 7.5 Hz, 1H), 7.78 (d, *J* = 7.6 Hz, 2H), 7.65 (d, *J* = 7.6 Hz, 2H), 7.53 (S, 2H), 7.42 (s, 1H), 7.35 (t, *J* = 14.2 Hz, 1H), 6.93-6.87 (m, 2H) ppm; ^{13}C NMR (125 MHz, DMSO-d_6) δ 160.1, 159.6, 159.4, 154.5, 136.4, 133.0, 132.1, 131.0, 128.8, 123.9, 119.3, 118.6, 118.5 116.8, 108.5, 86.3 ppm; HRMS (ESI) *m/z* calcd for $C_{18}H_{12}{}^{79}BrKN_3O[M+K]^+$: 403.9795, found 403.9783; HRMS (ESI-TOF) *m/z* calcd for $C_{18}H_{12}{}^{81}BrKN_3O$ $[M+K]^+$: 405.9775, found 403.9745.

2-Amino-6-(2-hydroxyphenyl)-4-(2-nitrophenyl)nicotinonitrile(3ak):
Yellow colour solid; mp 264-266 °C; yield 69% (45.8 mg); ^{1}H NMR (500 MHz, DMSO-d_6) δ 13.35 (s, 1H), 8.29 (d, *J* = 7.8 Hz, 1H), 7.99-7.91 (m, 2H), 7.86-7.79 (m, 1H), 7.68 (dd, *J* = 7.5, 0.9 Hz, 1H), 7.59 (s, 2H), 7.43 (s, 1H), 7.39-7.31 (m, 1H), 6.93 (d, *J* = 8.2 Hz, 1H), 6.87 (t, *J* = 7.4 Hz, 1H) ppm; ^{13}C NMR (125 MHz, DMSO-d_6) δ 160.1, 159.8, 158.5, 153.8, 147.5, 134.8, 133.2, 132.3, 132.0, 131.4, 128.7, 125.4, 119.4, 118.6, 118.4, 115.9, 108.1, 87.1 ppm; HRMS (ESI-TOF) *m/z* calcd for $C_{18}H_{13}N_4O_3$ $[M+H]^+$: 333.0982, found 333.1008.

2-Amino-6-(2-hydroxyphenyl)-4-(3-nitrophenyl)nicotinonitrile(3al): light brown solid; yield 73% (48.0 mg); mp 262-264 °C; ^{1}H NMR (500 MHz, DMSO-d_6) δ 13.32 (s, 1H), 8.53-8.46 (m, 1H), 8.39 (dd, *J* = 8.2, 1.4 Hz, 1H), 8.14 (d, *J* = 7.8 Hz, 1H), 8.11-8.03 (m, 1H), 7.86 (t, *J* = 8.0 Hz, 1H), 7.57 (s,

2H), 7.52 (s, 1H), 7.40-7.30 (m, 1H), 6.92-6.88 (m, 2H) ppm; ^{13}C NMR (125 MHz, DMSO-d_6) δ 160.0, 159.9, 159.3, 153.4, 148.3, 138.6, 135.6, 133.1, 130.9, 128.8, 124.9, 123.8, 119.4, 118.6, 118.5, 116.6, 108.8, 86.5 ppm; HRMS (ESI-TOF) *m/z* calcd for $C_{18}H_{12}N_4NaO_3[M+Na]^+$: 355.0802, found 355.0797.

2-Amino-6-(2-hydroxyphenyl)-4-(naphthalen-1-yl)nicotinonitrile(3am): Yellow colour solid; mp 258-260 °C; yield 73% (49.2 mg); ^{1}H NMR (500 MHz, DMSO-d_6) δ 13.50 (s, 1H), 8.09 (dd, *J* = 15.5, 8.1 Hz, 2H), 7.98 (dd, *J* = 10.4, 3.1 Hz, 1H), 7.70-7.65 (m, 2H), 7.63-7.54 (m, 5H), 7.45 (s, 1H), 7.35-7.32 (m, 1H), 6.94 (d, *J* = 8.2 Hz, 1H), 6.87-6.82 (m, 1H) ppm; ^{13}C NMR (125 MHz, DMSO-d_6) δ 160.2, 159.4, 159.0, 155.3, 135.3, 133.6, 132.9, 130.5, 129.8, 128.9, 128.8, 127.5, 127.0, 126.9, 125.8, 125.3, 119.4, 118.6, 118.5, 116.4, 110.0, 89.1 ppm; HRMS (ESI-TOF) *m/z* calcd for $C_{22}H_{15}N_3NaO$ $[M+Na]^+$: 360.1107, found 360.1107.

2-Amino-4-(furan-2-yl)-6-(2-hydroxyphenyl)nicotinonitrile (3an): Yellow colour solid; mp 236-238 °C; yield 80% (44.3 mg); ^{1}H NMR (500 MHz, DMSO-d_6) δ 13.34 (s, 1H), 8.06 (d, *J* = 9.2 Hz, 2H), 7.66 (s, 1H), 7.61 (d, *J* = 2.4 Hz, 1H), 7.47 (s, 2H), 7.36 (t, *J* = 7.5 Hz, 1H), 6.93 (t, *J* = 7.8 Hz, 2H), 6.82 (s, 1H) ppm; ^{13}C NMR (125 MHz, DMSO-d_6) δ 160.0, 159.8, 159.6, 148.9, 146.3, 141.9, 132.9, 128.5, 119.4, 118.6, 118.6, 117.2, 114.3, 113.3, 103.7, 81.35 ppm; HRMS (ESI-TOF) *m/z* calcd for $C_{16}H_{12}N_3O_2$ $[M+H]^+$: 278.0924, found 278.0907.

2-Amino-6-(2-hydroxyphenyl)-4-(thiophen-2-yl)nicotinonitrile(3ao): Yellow colour solid; mp 242-244 °C; yield 81% (47.5 mg); ^{1}H NMR (500 MHz, DMSO-d_6) δ 13.26 (s, 1H), 8.07 (d, *J* = 8.4 Hz, 1H), 8.00-7.85 (m, 2H), 7.50 (d, *J* = 10.1 Hz, 3H), 7.36 (t, *J* = 7.7 Hz, 1H), 7.32-7.30 (m, 1H), 7.00-6.86 (m, 2H) ppm; ^{13}C NMR (125 MHz, DMSO-d_6) δ 160.0, 159.9, 159.6, 147.2, 138.0, 133.0, 130.6, 130.1, 128.9, 128.7, 119.4, 118.6, 118.6, 117.3, 107.3, 84.4 ppm; HRMS (ESI-TOF) *m/z* calcd for $C_{16}H_{12}N_3OS$ $[M+H]^+$: 294.0696, found 294.0723.

2-Amino-4-cyclopropyl-6-(2-hydroxyphenyl)nicotinonitrile(3ap): Yellow colour solid; mp 278-280 °C; yield 84% (42.2 mg); ^{1}H NMR (500 MHz, DMSO-d_6) δ 13.50 (s, 1H), 7.93 (d, *J* = 7.9 Hz, 1H), 7.30-7.16 (m, 3H), 6.80-

6.78 (m, 2H), 6.71 (s, 1H), 2.05-1.99 (m, 1H), 1.12 (dd, *J* = 10.2, 4.6 Hz, 2H), 1.03 (dd, *J* = 6.8, 3.4 Hz, 2H) ppm; ^{13}C NMR (100 MHz, DMSO-d_6) δ 160.9, 160.0, 159.4, 158.4, 132.6, 128.5, 119.1, 118.5, 118.4, 116.6, 102.2, 88.5, 15.0, 11.0 ppm; HRMS (ESI-TOF) *m/z* calcd for $C_{15}H_{14}N_3O$ [M+H]+ : 252.1131, found 252.1107.

2-Amino-4-ethyl-6-(2-hydroxyphenyl)-5-methylnicotinonitrile(3aq):

Yellow colour solid; mp 186-188 °C; yield 82% (41.5 mg); ^{1}H NMR (500 MHz, DMSO-d_6) δ 9.64 (s, 1H), 7.19-7.11 (m, 1H), 7.02 (dd, *J* = 7.5, 1.5 Hz, 1H), 6.88-6.74 (m, 2H), 6.38 (s, 2H), 2.65 (q, *J* = 7.5 Hz, 2H), 1.88 (s, 3H), 1.09 (t, *J* = 7.6 Hz, 3H) ppm; ^{13}C NMR (125 MHz, DMSO-d_6) δ 160.6, 158.5, 156.5, 154.5, 130.3, 129.9, 127.8, 119.2, 119.0, 117.1, 115.9, 88.9, 25.7, 14.2, 13.7 ppm; HRMS (ESI-TOF) *m/z* calcd for $C_{15}H_{16}N_3O$ $[M+H]^+$: 254.1288, found 254.1293.

2-Amino-6-(2-hydroxyphenyl)-4-phenyl-5-propylnicotinonitrile(3as):

Yellow colour solid; mp 196-198 °C; yield 81% (53.3 mg); ^{1}H NMR (500 MHz, DMSO-d_6) δ 9.31 (s, 1H), 7.30 (t, *J* = 7.2 Hz, 2H), 7.27-7.23 (m, 1H), 7.11 (d, *J* = 7.0 Hz, 2H), 7.03-6.97 (m, 1H), 6.89 (d, *J* = 7.4 Hz, 1H), 6.69 (d, *J* = 8.1 Hz, 1H), 6.64 (t, *J* = 7.4 Hz, 1H), 6.46 (s, 2H), 1.91 (t, *J* = 7.7 Hz, 2H), 0.70-0.78 (m, 2H), 0.13 (t, *J* = 7.3 Hz, 3H) ppm; ^{13}C NMR (125 MHz, DMSO-d_6) δ 161.3, 158.4, 154.6, 154.3, 137.5, 130.3, 129.7, 128.9, 128.6, 127.9, 123.8, 119.0, 117.0, 116.0, 89.6, 30.7, 23.3, 14.4 ppm; HRMS (ESI-TOF) *m/z* calcd for $C_{21}H_{20}N_3O$ $[M+H]^+$: 330.1601, found 330.1601.

2-Amino-6-(2-hydroxyphenyl)-5-methyl-4-phenylnicotinonitrile(3ar):

Yellow colour solid; mp 202-204 °C; yield 86% (51.8 mg); ^{1}H NMR (500 MHz, $CDCl_3$) δ 10.38 (s, 1H), 7.55-7.49 (m, 3H), 7.44 (dd, *J* = 7.8, 1.4 Hz, 1H), 7.35 -7.31 (m, 3H), 7.06 (dd, *J* = 8.1, 0.5 Hz, 1H), 6.95-6.90 (m, 1H), 5.18 (s, 2H), 2.10 (s, 3H) ppm; ^{13}C NMR (125 MHz, $CDCl_3$) δ 159.2, 158.0, 156.7, 155.8, 136.7, 131.4, 130.4, 129.2, 128.9, 128.1, 121.9, 120.1, 119.0, 117.9, 116.0, 91.2, 18.5 ppm; HRMS (ESI-TOF) *m/z* calcd for $C_{19}H_{15}N_3NaO$ $[M+Na]^+$: 324.1107, found 324.1113.

2-Amino-6-(2-hydroxy-5-methylphenyl)-4-phenylnicotinonitrile(3ba):

Yellow colour solid; mp 262-264 °C; yield 72% (43.3 mg); ^{1}H NMR (500 MHz,

DMSO-d_6) δ 13.15 (s, 1H), 7.87 (s, 1H), 7.68-7.66 (m, 2H), 7.61-7.53 (m, 3H), 7.44 (s, 2H), 7.40 (s, 1H), 7.15 (dd, *J* = 8.3, 1.3 Hz, 1H), 6.82 (d, *J* = 8.3 Hz, 1H), 2.26 (s, 3H) ppm; ^{13}C NMR (125 MHz, DMSO-d_6) δ 159.6, 159.4, 157.8, 155.7, 137.2, 133.7, 130.2, 129.2, 128.8, 128.5, 128.0, 118.3, 118.2, 117.0, 108.6, 86.4, 20.4 ppm; HRMS (ESI-TOF) *m/z* calcd for $C_{19}H_{16}N_3O$ $[M+H]^+$: 302.1288, found 302.1288.

2-Amino-6-(2-hydroxy-5-methoxyphenyl)-4-phenylnicotinonitrile(3da):

Yellow colour solid; mp 198-200 °C; yield 70% (44.4 mg); ^{1}H NMR (500 MHz, DMSO-d_6) δ 12.88 (s, 1H), 7.73-7.62 (m, 2H), 7.56 (d, *J* = 5.0 Hz, 3H), 7.48 (d, *J* = 2.7 Hz, 1H), 7.42 (s, 3H), 6.98 (dd, *J* = 8.9, 2.8 Hz, 1H), 6.86 (d, *J* = 8.9 Hz, 1H), 3.74 (s, 3H) ppm; ^{13}C NMR (125 MHz, DMSO-d_6) δ 159.4, 159.3 155.9, 154.0, 152.3, 137.2, 130.2, 129.2, 128.8, 120.3, 119.4, 118.6, 117.0, 111.9, 109.0, 86.7, 56.1 ppm; HRMS (ESI-TOF) *m/z* calcd for $C_{19}H_{16}N_3O_2$ $[M+H]^+$: 318.1237, found 318.1233.

2-Amino-6-(5-chloro-2-hydroxyphenyl)-4-phenylnicotinonitrile(3ea):

Yellow colour solid; mp 210-212 °C; yield 65% (41.7 mg); ^{1}H NMR (500 MHz, DMSO-d_6) δ 9.15 (s, 1H), 8.41 (d, *J* = 2.2 Hz, 1H), 7.69 (dd, *J* = 8.8, 2.3 Hz, 2H), 7.58-7.54 (m, 3H), 7.53-7.51 (m, 2H), 7.50 (s, 1H), 7.21 (d, *J* = 8.8 Hz, 1H), 6.74 (d, *J* = 8.9 Hz, 1H); ^{13}C NMR (125 MHz, DMSO-d_6) δ 155.9, 153.3, 150.4, 149.6, 138.3, 136.0, 131.8, 129.1, 128.9, 125.0, 119.4, 118.4, 117.4, 110.1, 104.1, 94.6 ppm; HRMS (ESI-TOF) *m/z* calcd for $C_{18}H_{13}ClN_3O$ $[M+H]^+$: 322.0742, found 322.0747.

2-Amino-6-(5-bromo-2-hydroxyphenyl)-4-phenylnicotinonitrile(3fa):

Yellow colour solid; mp 216-218 °C; yield 67% (49.0 mg); ^{1}H NMR (500 MHz, DMSO-d_6) δ 9.14 (s, 1H), 8.50 (d, *J* = 1.7 Hz, 1H), 7.66 (d, *J* = 6.3 Hz, 2H), 7.62 (dd, *J* = 8.8, 1.9 Hz, 1H), 7.57-7.51 (m, 3H), 7.50 (d, *J* = 4.0 Hz, 2H), 7.13 (d, *J* = 8.7 Hz, 1H), 6.71 (d, *J* = 6.4 Hz, 1H) ppm; ^{13}C NMR (125 MHz, DMSO-d_6) δ 155.8, 153.3, 150.8, 149.7, 138.3, 136.0, 134.6, 129.2, 128.9, 127.9, 120.0, 118.7, 116.4, 110.2, 104.1, 94.6 ppm; HRMS (ESI-TOF) *m/z* calcd for $C_{18}H_{13}{}^{79}BrN_3O[M+H]^+$: 366.0237, found 366.0242; HRMS (ESI-TOF) *m/z* calcd for $C_{18}H_{13}{}^{81}BrN_3O[M+H]^+$: 368.0216, found 368.0216.

2-Amino-6-(2-hydroxy-3-methoxyphenyl)-4-phenylnicotinonitrile(3ga): Yellow colour solid; mp 200-202 °C; yield 73% (46.0 mg); ^{1}H NMR (500 MHz, DMSO-d_6) δ 13.50 (s, 1H), 7.62-7.60 (m, 2H), 7.56 (d, *J* = 8.2 Hz, 1H), 7.51-7.49 (m, 3H), 7.42 (s, 2H), 7.30 (s, 1H), 6.98 (d, *J* = 7.9 Hz, 1H), 6.75 (t, *J* = 8.1 Hz, 1H), 3.74 (s, 3H) ppm; ^{13}C NMR (100 MHz, DMSO-d_6) δ 159.7, 159.3, 155.8, 150.5, 149.3, 137.2, 130.2, 129.2, 128.8, 120.1, 118.6, 118.5, 116.9, 114.9, 108.9, 86.6, 56.3 ppm; HRMS (ESI-TOF) *m/z* calcd for $C_{19}H_{16}N_3O_2$ $[M+H]^+$: 318.1237, found 318.1231.

2-Amino-6-(3,5-dichloro-2-hydroxyphenyl)-4-phenylnicotinonitrile(3ha): Yellow colour solid; mp 222-224 °C; yield 62% (44.1mg); ^{1}H NMR (500 MHz, DMSO-d_6) δ 14.81 (s, 1H), 8.24 (d, *J* = 2.4 Hz, 1H), 7.70-7.68 (m, 2H), 7.64 (d, *J* = 2.3 Hz, 2H), 7.60-7.53 (m, 4H); ^{13}C NMR (125 MHz, DMSO-d_6) δ 158.9, 157.2, 156.6, 155.0, 136.7, 131.8, 130.4, 129.1, 129.0, 126.8, 123.0, 122.8, 120.4, 116.6, 109.1, 88.1 ppm: HRMS (ESI-TOF) *m/z* calcd for $C_{18}H_{11}Cl_2N_3NaO$ $[M+Na]^+$: 378.0171, found 378.0162.

2-Amino-6-(2-hydroxy-4-methoxyphenyl)-5-methyl-4-phenylnicotinonitrile(3cr): Yellow colour solid; mp 168-170 °C; yield 78% (51.6 mg); ^{1}H NMR (500 MHz, DMSO-d_6) δ 10.12 (s, 1H), 7.51 (t, *J* = 7.2 Hz, 2H), 7.49-7.43 (m, 1H), 7.32 (d, *J* = 7.2 Hz, 2H), 7.13 (d, *J* = 8.4 Hz, 1H), 6.63 (s, 2H), 6.46 (d, *J* = 7.4 Hz, 2H), 3.72 (s, 3H), 1.74 (s, 3H) ppm; ^{13}C NMR (125 MHz, DMSO-d_6) δ 161.0, 160.6, 158.2, 156.3, 154.8, 137.6, 131.4, 129.1, 129.0, 128.7, 119.8, 118.9, 117.2, 105.2, 101.6, 88.9, 55.5, 16.56 ppm; HRMS (ESI-TOF) *m/z* calcd for $C_{20}H_{18}N_3O_2$ $[M+H]^+$: 332.1394, found 332.1394.

2-Amino-6-(2-hydroxy-5-methoxyphenyl)-5-methyl-4-phenylnicotinonitrile(3dr): Yellow colour solid; mp 184-186 °C; yield 75% (49.6 mg); ^{1}H NMR (500 MHz, DMSO-d_6) δ 9.34 (s, 1H), 7.54-7.51 (m, 2H), 7.48 (t, *J* = 7.3 Hz, 1H), 7.33 (d, *J* = 7.1 Hz, 2H), 6.82 (s, 2H), 6.71 (s, 1H), 6.59 (s, 2H), 3.76 (s, 3H), 1.72 (s, 3H) ppm; ^{13}C NMR (125 MHz, DMSO-d_6) δ 160.7, 158.43, 154.6, 152.2, 148.4, 137.3, 129.1, 128.7, 128.6, 128.0, 119.0, 117.2, 116.9, 115.8, 115.0, 89.4, 55.9, 16.0 ppm; HRMS (ESI-TOF) *m/z* calcd for $C_{20}H_{18}N_3O_2$ $[M+H]^+$: 332.1394, found 332.1394.

2-Amino-6-(2-hydroxy-5-methylphenyl)-5-methyl-4-phenylnicotinonitrile(3br): Yellow colour solid; mp 198-200 °C; yield 77% (48.4 mg); ^{1}H NMR (500 MHz, DMSO-d_6) δ 9.42 (s, 1H), 7.54 (t, *J* = 7.3 Hz, 2H), 7.48 (t, *J* = 7.3 Hz, 1H), 7.37-7.32 (m, 2H), 7.03 (dd, *J* = 8.2, 1.6 Hz, 1H), 6.97 (s, 1H), 6.80 (d, *J* = 8.2 Hz, 1H), 6.67 (s, 2H), 2.23 (s, 3H), 1.73 (s, 3H) ppm; ^{13}C NMR (125 MHz, DMSO-d_6) δ 161.1, 158.5, 154.4, 152.4, 137.6, 130.7, 130.4, 129.1, 129.0, 128.7, 127.6, 127.4, 118.8, 117.1, 116.0, 89.1, 20.4, 16.0 ppm; HRMS (ESI-TOF) *m/z* calcd for $C_{20}H_{18}N_3O$ $[M+H]^+$: 316.1444, found 316.1451.

2-Amino-6-(5-bromo-2-hydroxyphenyl)-5-methyl-4-phenylnicotinonitrile(3fr): Yellow colour solid; mp 190-192 °C; yield 73% (55.5 mg); ^{1}H NMR (500 MHz, DMSO-d_6) δ 10.02 (s, 1H), 7.52 (t, *J* = 7.3 Hz, 2H), 7.50-7.45 (m, 1H), 7.38 (dd, *J* = 8.7, 2.6 Hz, 1H), 7.35-7.31 (m, 2H), 7.29 (d, *J* = 2.5 Hz, 1H), 6.87 (d, *J* = 8.7 Hz, 1H), 6.71 (s, 2H), 1.70 (s, 3H) ppm; ^{13}C NMR (125 MHz, DMSO-d_6) δ 159.3, 158.5, 154.7, 154.0, 137.3, 132.6, 132.5, 130.1, 129.1, 128.7, 118.8, 118.3, 117.0, 110.2, 89.7, 15.9 ppm; HRMS (ESI-TOF) *m/z* calcd for $C_{19}H_{15}{}^{79}BrN_3O$ $[M+H]^+$: 380.0393, found 380.0384; HRMS (ESI-TOF) *m/z* calcd for $C_{19}H_{15}{}^{81}BrN_3O$ $[M+H]^+$: 382.0373, found 382.0359.

2-Amino-6-(5-chloro-2-hydroxyphenyl)-5-methyl-4-phenylnicotinonitrile(3er): Yellow colour solid; mp 194-196 °C; yield 76% (51.0 mg); ^{1}H NMR (500 MHz, DMSO-d_6) δ 9.97 (s, 1H), 7.52 (t, *J* = 7.3 Hz, 2H), 7.49-7.44 (m, 1H), 7.33 (d, *J* = 7.0 Hz, 2H), 7.26 (dd, *J* = 8.7, 2.6 Hz, 1H), 7.18 (d, *J* = 2.5 Hz, 1H), 6.92 (d, *J* = 8.7 Hz, 1H), 6.72 (s, 2H), 1.70 (s, 3H) ppm; ^{13}C NMR (100 MHz, DMSO-d_6) δ 159.3, 158.6, 154.7, 153.6, 137.3, 129.8, 129.6, 129.5, 129.1, 128.7, 122.7, 118.8, 117.8, 117.0, 89.72, 15.9 ppm; HRMS (ESI-TOF) *m/z* calcd for $C_{19}H_{15}ClN_3O$ $[M+H]^+$: 336.0898, found 336.0901.

2-Amino-6-(2-hydroxynaphthalen-1-yl)-4-phenylnicotinonitrile(3ia): Yellow colour solid; mp 230-232 °C; yield 61% (41.1 mg); ^{1}H NMR (500 MHz, DMSO-d_6) δ 10.05 (s, 1H), 7.93 (t, *J* = 11.6 Hz, 2H), 7.87 (d, *J* = 7.3 Hz, 1H), 7.74 (d, *J* = 6.8 Hz, 2H), 7.57 (t, *J* = 6.9 Hz, 2H), 7.53-7.49 (m, 2H), 7.48-7.43 (m, 1H), 7.43-7.38 (m, 1H), 7.34 (t, *J* = 8.8 Hz, 2H), 7.29 (d, *J* = 8.2 Hz, 1H)

ppm; ^{13}C NMR (125 MHz, DMSO-d_6) δ 152.9, 146.6, 144.8, 143.2, 138.7, 138.5, 133.5, 130.6, 129.6, 129.4, 129.1, 128.6, 128.2, 127.8, 127.4, 123.7, 123.3, 118.7, 118.2, 111.9 ppm; HRMS (ESI-TOF) *m/z* calcd for $C_{22}H_{16}N_3O$ $[M+H]^+$: 338.1288, found 338.1297.

3-Amino-1-(2-hydroxyphenyl)-5,6,7,8-tetrahydroisoquinoline-4-carbonitrile(3at): Yellow colour solid; mp 200-202 °C; yield 85% (45.0 mg); ^{1}H NMR (500 MHz, DMSO-d_6) δ 9.65 (s, 1H), 7.21 (t, *J* = 7.6 Hz, 1H), 7.06 (d, *J* = 7.4 Hz, 1H), 6.89 (d, *J* = 8.1 Hz, 1H), 6.85 (t, *J* = 7.4 Hz, 1H), 6.52 (s, 2H), 2.77 (t, *J* = 6.3 Hz, 2H), 2.32 (t, *J* = 6.1 Hz, 2H), 1.76-1.69 (m, 2H), 1.64-1.55 (m, 2H) ppm; ^{13}C NMR (125 MHz, DMSO-d_6) δ 160.5, 158.4, 154.6, 151.1, 130.0, 129.8, 127.2, 120.8, 119.16, 116.8, 116.0, 88.3, 28.4, 25.3, 22.5, 21.9 ppm; HRMS (ESI-TOF) *m/z* calcd for $C_{19}H_{16}N_3O$ $[M+H]^+$: 266.1288, found 266.1295.

3-Amino-1-(2-hydroxyphenyl)-6,7,8,9-tetrahydro-5*H*-cyclohepta[*c*]pyridine-4-carbonitrile(3au): Yellow colour solid; mp 182-184 °C; yield 78 % (43.6 mg); ^{1}H NMR (500 MHz, DMSO-d_6) δ 9.44 (s, 1H), 7.12 (t, *J* = 7.4 Hz, 1H), 6.96 (d, *J* = 7.2 Hz, 1H), 6.80 (d, *J* = 8.0 Hz, 1H), 6.76 (t, *J* = 7.3 Hz, 1H), 6.45 (s, 2H), 2.88-2.80 (m, 2H), 2.42-2.35 (m, 2H), 1.66 (s, 2H), 1.56 (s, 2H), 1.37 (s, 2H) ppm; ^{13}C NMR (125 MHz, DMSO-d_6) δ 158.9, 158.4, 157.5, 154.7, 130.3, 129.6, 127.8, 126.4, 119.0, 117.2, 115.8, 89.2, 33.7, 31.8, 29.7, 27.6, 26.8 ppm; HRMS (ESI-TOF) *m/z* calcd for $C_{17}H_{17}N_3NaO$ $[M+Na]^+$: 302.1264, found 302.1236.

3-Amino-1-(2-hydroxyphenyl)-9*H*-indeno[2,1-*c*]pyridine-4-carbonitrile(3av): Yellow colour solid; mp 236-238 °C; yield 80% (47.8 mg); ^{1}H NMR (500 MHz, DMSO-d_6) δ 12.48 (s, 1H), 8.27 (d, *J* = 7.1 Hz, 1H), 7.82 (d, *J* = 7.8 Hz, 1H), 7.66 (d, *J* = 6.8 Hz, 1H), 7.57-7.46 (m, 2H), 7.29 (t, *J* = 7.6 Hz, 1H), 7.19 (s, 2H), 6.96-6.85 (m, 2H), 4.09 (s, 2H) ppm; ^{13}C NMR (100 MHz, DMSO-d_6) δ 158.6, 158.5, 155.8, 153.5, 146.8, 137.0, 131.8, 131.0, 130.2, 127.8, 126.0, 124.4, 122.6, 121.9, 119.2, 117.9, 116.9, 80.6, 36.9 ppm; HRMS (ESI-TOF) *m/z* calcd for $C_{19}H_{14}N_3O$ $[M+H]^+$: 300.1131, found 300.1131.

2-Amino-4-(2-hydroxyphenyl)-5,6-dihydrobenzo[*f*]isoquinoline-1-carbonitrile(3aw): Yellow colour solid; mp 192-194 °C; yield 82% (51.3 mg); ^{1}H NMR (500 MHz, DMSO-d_6) δ 9.90 (s, 1H), 8.39-8.03 (m, 1H), 7.46-7.39 (m, 2H), 7.39-7.34 (m, 1H), 7.26-7.21 (m, 2H), 6.91-6.87 (m, 2H), 6.70 (s, 2H), 2.67-2.60 (m, 2H), 2.46-2.40 (m, 2H) ppm; ^{13}C NMR (125 MHz, DMSO-d_6) δ 160.2, 158.9, 155.2, 146.1, 140.6, 131.0, 130.7, 130.4, 128.57, 127.0, 127.0, 126.4, 121.5, 119.2, 118.6, 116.2, 84.0, 28.9, 24.7 ppm; HRMS (ESI-TOF) *m/z* calcd for $C_{20}H_{16}N_3O$ $[M+H]^+$: 314.1288, found 314.1315.

3-Amino-1-(5-chloro-2-hydroxyphenyl)-5,6,7,8-tetrahydroisoquinoline-4-carbonitrile(3et): Yellow colour solid; mp 196-198 °C; yield 74% (44.2 mg); ^{1}H NMR (500 MHz, DMSO-d_6) δ 9.91 (s, 1H), 7.24 (dd, *J* = 8.7, 2.6 Hz, 1H), 7.06 (d, *J* = 2.6 Hz, 1H), 6.89 (d, *J* = 8.7 Hz, 1H), 6.55 (s, 2H), 2.75 (t, *J* = 6.3 Hz, 2H), 2.29 (t, *J* = 6.1 Hz, 2H), 1.72-1.67 (m, 2H), 1.60-1.57 (m, 2H) ppm; ^{13}C NMR (125 MHz, DMSO-d_6) δ 158.9, 158.4, 153.6, 151.4, 129.5, 129.4, 129.1, 122.6, 120.8, 117.7, 116.72, 88.7, 28.4, 25.0, 22.4, 21.8 ppm; HRMS (ESI-TOF) *m/z* calcd for $C_{16}H_{15}ClN_3O$ $[M+H]^+$: 300.0898, found 300.0909.

3-Amino-1-(5-bromo-2-hydroxyphenyl)-5,6,7,8-tetrahydroisoquinoline-4-carbonitrile(3ft): Yellow colour solid; mp 202-204 °C; yield 77% (53.0 mg); ^{1}H NMR (500 MHz, DMSO-d_6) δ 9.99 (s, 1H), 7.36 (dd, *J* = 8.6, 1.5 Hz, 1H), 7.20-7.12 (m, 1H), 6.84 (d, *J* = 8.7 Hz, 1H), 6.52 (s, 2H), 2.75 (t, *J* = 6.2 Hz, 2H), 2.28 (t, *J* = 6.1 Hz, 2H), 1.72-1.67 (m, 2H), 1.59-1.55 (m, 2H) ppm; ^{13}C NMR (125 MHz, DMSO-d_6) δ 158.4, 156.8, 154.0, 151.4, 132.3, 129.7, 120.8, 118.6, 118.2, 116.7, 110.1, 88.8, 28.4, 25.0, 22.4, 21.8 ppm; HRMS (ESI-TOF) *m/z* calcd for $C_{16}H_{15}{}^{79}BrN_3O$ $[M+H]^+$: 344.0393, found 344.0393; HRMS (ESI-TOF) *m/z* calcd for $C_{16}H_{15}{}^{81}$BrN3O $[M+H]^+$: 346.0373, found 346.0378.

3-Amino-1-(2-hydroxy-5-methoxyphenyl)-5,6,7,8-tetrahydroisoquinoline-4- carbonitrile(3dt): Yellow colour solid; mp 184-186 °C; yield 83% (49.0 mg); ^{1}H NMR (500 MHz, DMSO-d_6) δ 9.14 (s, 1H), 6.80 (s, 2H), 6.62 (s, 1H), 6.53 (s, 2H), 2.76 (t, *J* = 6.2 Hz, 2H), 2.33 (t, *J* = 6.1 Hz, 2H), 1.74-1.66 (m, 2H), 1.65-1.55 (m, 2H) ppm; ^{13}C NMR (125 MHz, DMSO-d_6) δ 160.3, 158.4, 152.2, 151.1, 150.1, 148.3, 127.6, 120.8, 116.8, 115.5, 114.7, 88.4, 55.8, 28.4,

25.2, 22.5, 21.9 ppm; HRMS (ESI-TOF) *m/z* calcd for $C_{17}H_{18}N_3O_2$ $[M+H]^+$: 296.1394, found 296.1394.

6-Amino-8-(2-hydroxyphenyl)-3,4-dihydro-1*H*-pyrano[3,4-*c*]pyridine-5-carbonitrile(3ax):Yellow colour solid; mp 214-216 °C; yield 77% (44.2 mg); ^{1}H NMR (500 MHz, DMSO-d_6) δ 9.92 (s, 1H), 7.26-7.23 (m, 1H), 7.08 (dd, *J* = 7.6, 1.5 Hz, 1H), 6.91 (d, *J* = 8.0 Hz, 1H), 6.87 (t, *J* = 7.4 Hz, 1H), 6.75 (s, 2H), 4.31 (s, 2H), 3.87 (t, *J* = 5.8 Hz, 2H), 2.83 (t, *J* = 5.7 Hz, 2H) ppm; ^{13}C NMR (125 MHz, DMSO-d_6) δ 158.8, 157.4, 154.7, 148.5, 130.5, 130.2, 125.5, 119.3, 118.9, 116.3, 116.2, 88.1, 65.25, 63.8, 27.4 ppm; HRMS (ESI-TOF) *m/z* calcd for $C_{15}H_{15}N_3O_2$ $[M+H]^+$: 268.1081, found 268.1094.

2-Amino-4-(2-hydroxyphenyl)-5*H*-chromeno[3,4-*c*]pyridine-1-carbonitrile(3ay): Yellow colour solid; mp 210-212 °C; yield = 79% (49.8 mg); ^{1}H NMR (500 MHz, DMSO- d_6) δ 10.02 (s, 1H), 8.35 (d, *J* = 7.8 Hz, 1H), 7.49 (t, *J* = 7.7 Hz, 1H), 7.34-7.29 (m, 1H), 7.27 (d, *J* = 7.6 Hz, 1H), 7.23 (t, *J* = 7.6 Hz, 1H), 7.11 (d, *J* = 8.1 Hz, 1H), 7.03-6.90 (m, 4H), 4.72 (s, 2H) ppm; ^{13}C NMR (125 MHz, DMSO-d_6) δ 161.2, 157.0, 156.6, 155.3, 141.2, 133.1, 131.0, 130.9, 126.6, 125.0, 122.6, 120.5, 119.5, 118.1, 118.1, 116.2, 116.0, 82.1, 65.9 ppm; HRMS (ESI-TOF) *m/z* calcd for $C_{19}H_{14}N_3O_2$ $[M+H]^+$: 316.1081, found 316.1081.

(1*R*,3a*S*,3b*R*,5a*S*,11a*S*,13a*R*)-8-amino-10-(2-hydroxyphenyl)-11a,13a-dimethyl-1-((*R*)-6-methylheptan-2-yl)-2,3,3a,3b,4,5,5a,6,11,11a,11b,12,13,13a-tetradecahydro-1*H*-cyclopenta[5,6]naphtho[2,1 *g*]isoquinoline-7- carbonitrile(3az): Yellow colour solid; mp 262- 264 °C; yield 71% (78.6 mg); $[\alpha]^{27}{}_D$ = + 90° ($CHCl_3$); ^{1}H NMR (500 MHz, DMSO-d_6) δ 9.68 (s, 1H), 7.16 (t, *J* = 7.1 Hz, 1H), 6.99 (d, *J* = 6.8 Hz, 1H), 6.85 (d, *J* = 7.9 Hz, 1H), 6.78 (t, *J* = 6.9 Hz, 1H), 6.46 (s, 2H), 2.69 (d, *J* = 14.8 Hz, 1H), 2.32 (d, *J* = 15.7 Hz, 2H), 1.96 (d, *J* = 15.4 Hz, 1H), 1.83-1.81 (m, 1H), 1.71-1.70 (m, 1H), 1.60-1.59 (m, 1H), 1.49-1.43 (m, 4H), 1.24-1.13 (m, 8H), 1.04-0.98 (m, 6H), 0.90 (s, 3H), 0.79-0.78 (m, 9H), 0.65 (s, 1H), 0.55 (s, 6H) ppm; ^{13}C NMR (125 MHz, DMSO-d_6) δ 161.0, 158.2, 154.5, 150.0, 129.9, 129.8, 127.1, 120.0, 119.0, 116.7, 116.0, 87.7, 56.2, 56.1, 53.2, 42.3, 40.6, 36.1, 35.6, 35.3, 34.8, 32.8, 31.4, 28.2, 28.1, 28.0, 27.8, 24.2, 23.7,

23.0, 22.8, 21.1, 21.0, 18.8, 12.1, 11.5 ppm; HRMS (ESI-TOF) *m/z* calcd for $C_{37}H_{52}N_3O[M+H]^+$: 554.4105, found 554.4105.

(*E*)-2-(3-(2-hydroxyphenyl)-1-phenylallylidene)malononitrile(4): Yellow colour solid; mp 216-218 °C; ^{1}H NMR (500 MHz, $CDCl_3$) δ 7.92 (d, *J* = 15.6 Hz, 1H), 7.58-7.52 (m, 3H), 7.41 (dd, *J* = 15.3, 7.3 Hz, 3H), 7.29-7.25 (m, 1H), 7.12 (d, *J* = 15.6 Hz, 1H), 6.94 (t, *J* = 7.5 Hz, 1H), 6.80 (d, *J* = 8.1 Hz, 1H), 6.18 (s, 1H) ppm; ^{13}C NMR (125 MHz, $CDCl_3$) δ 172.8, 155.9, 145.6, 133.1, 132.8, 131.1, 130.5, 129.0, 128.98 , 125.6, 121.8, 121.2, 116.5, 113.7, 81.0 ppm; HRMS (ESI-TOF) *m/z* calcd for $C_{18}H_{12}N_2NaO$ $[M+Na]^+$: 295.0842, found 295.0853.

2-Amino-6-[2-(tert-butyldimethylsilyloxyphenyl)-4-(3-nitrophenyl)nicotinonitrile (11): Colourless solid; mp 78-80 °C; yield 88% ; ^{1}H NMR (500 MHz, DMSO-d_6) δ 8.40-8.22 (m, 2H), 8.05-7.91 (m, 1H), 7.87-7.72 (m, 1H), 7.65-7.63 (m, 1H), 7.31 (d, *J* = 0.9 Hz, 1H), 7.18-6.79 (m, 5H), 0.65 (s, 9H), 0.00 (s, 6H) ppm; ^{13}C NMR (125 MHz, DMSO-d_6) δ 161.3, 159.4, 153.3, 151.6, 148.3, 138.8, 135.2, 131.3, 131.2, 131.0, 130.4, 124.7, 123.1, 122.0, 120.7, 117.0, 114.5, 86.1, 25.7, 18.1, -4.0 ppm; HRMS (ESI-TOF) *m/z* calcd for $C_{24}H_{27}N_4O_3Si[M+H]^+$: 447.1847, found 447.1842.

2-Amino-4-(3-aminophenyl)-6-(2-hydroxyphenyl)nicotinonitrile(10): Light yellow solid; mp 206-208 °C; yield 82%; ^{1}H NMR (500 MHz, DMSO-d_6) δ 13.40 (s, 1H), 7.99 (d, *J* = 7.9 Hz, 1H), 7.39 (br s, 2H), 7.36-7.30 (m, 1H), 7.29 (s, 1H), 7.17 (t, *J* = 7.7 Hz, 1H), 6.95-6.83 (m, 2H), 6.79 (s, 1H), 6.75-6.70 (m, 2H), 5.32 (s, 2H) ppm; ^{13}C NMR (125 MHz, DMSO-d_6) δ 160.0, 159.4, 159.2, 156.7, 149.4, 138.0, 132.8, 129.7, 128.5, 119.4, 118.6, 118.5, 117.0, 116.0, 115.6, 113.7, 108.3, 86.5 ppm; HRMS (ESI-TOF) *m/z* calcd for $C_{18}H_{14}NO[M+H]^+$: 303.1240, found 303.1840.

Crystallographic data: Single crystal X-ray structural of compound **3aq** was measured on the Bruker D8 Quest Single Crystal-XRD at 150(2) K using graphite monochromated Mo Kα radiation (λα = 0.71073 Å). The strategy for the Data collection was evaluated by using the CrysAlisPro CCD software. The data were collected by the standard 'phi-omega scan techniques, and were scaled and reduced using CrysAlisPro RED software. The structure was solved by

direct methods using SHELXS-97, and refined by full matrix least-squares with SHELXL-97, refining on *F*2. The positions of all the atoms were obtained by direct methods. All non-hydrogen atoms were refined anisotropically. The remaining hydrogen atoms were placed in geometrically constrained positions, and refined with isotropic temperature factors, generally 1.2*Ueq* of their parent atoms. The crystal data are summarized in **Table 3.4**. The CCDC number of compound **3aq** (**2122234**) can be obtained free of charge via www.ccdc.cam.ac.uk (or from the Cambridge Crystallographic Data Centre,12 union Road, Cambridge CB21 EZ, UK; Fax: (+44) 1223-336-033; or deposit@ccdc.cam.ac.uk).

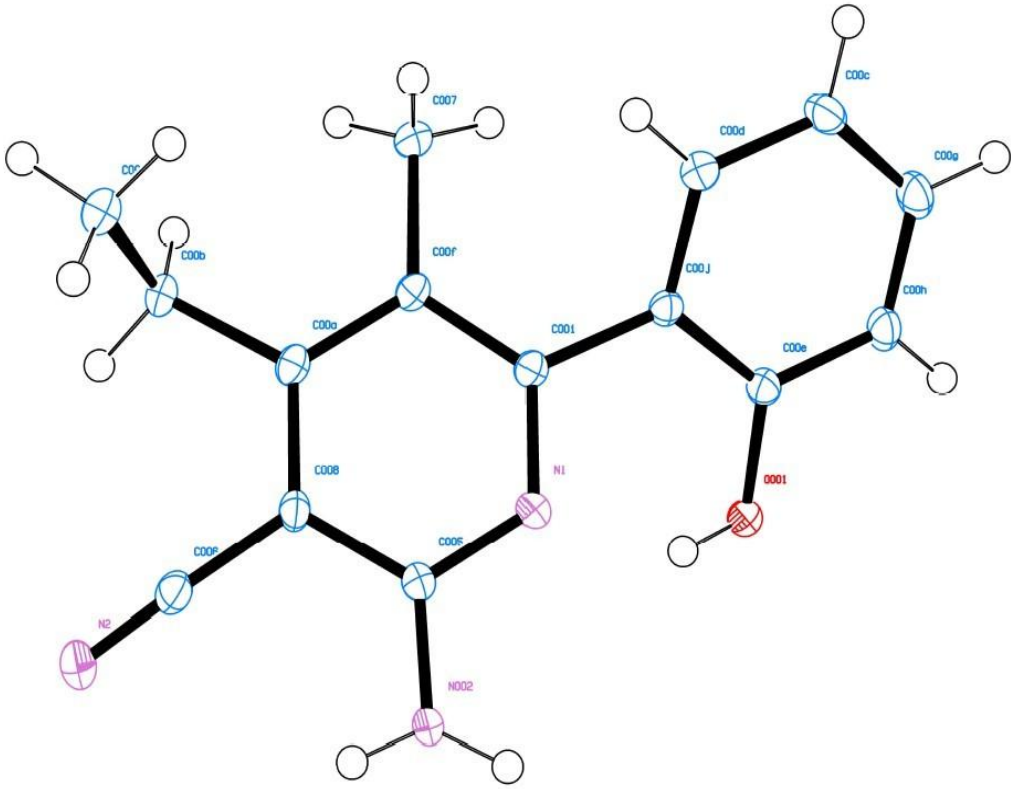

Figure 3.3. ORTEP diagram of compound **3aq** (**CCDC 2122234**), thermal ellipsoids drawn at the 50% probability level.

Table 3.4. Crystal data for compound 3aq.

Compound	**3aq**
Empirical formula	$C_{15}H_{15}N_3O$
Formula weight	253.3
Temperature	273 K
Wave length (Å)	1.54184 Å
Crystal system, space group	Orthorhombic, P 21 21 21, P 2ac 2ab
a (Å) *b* (Å) *c* (Å) *α* (°) *β* (°) *γ* (°)	a = 7.2949(2) b = 11.9167(2) c = 14.4321(3) alpha = 90 deg. beta = 90 deg. gamma = 90 deg.
Volume ($Å^3$)	1254.60(5)A^3
Z, Calculated density (mg/m^3)	4, 1.341 Mg/m^3
Absorption coefficient (mm^{-1})	1.341 mm^-1
F(000)	536
Θ range (deg)	3.129 to 28.298 deg.
Limiting indices	-9<=h<=9, -15<=k<=15, -19<=l<=19
Reflections collected / unique	20258 / 3111 [R(int) = 0.0386]
Completeness to Θ	96.8%
Max. and min. transmission	0.698 and 0.746
Absorption correction	none
Data / restrains / parameters	3111 / 0 / 180
Goodness-of-fit on F^2	0.998
Final R indices [I>2sigma(I)]	R1 = 0.0367, wR2 = 0.0646
R indices (all data)	R1 = 0.0393, wR2 = 0.1470
Extinction coefficient	n/a
Largest diff. peak and hole ($e.A^{-3}$)	0.382 and -0.246 e.A^-3
CCDC	**2122234**

3.7 Copies of ^{1}H and ^{13}C NMR spectra of some important compounds described in chapter 3

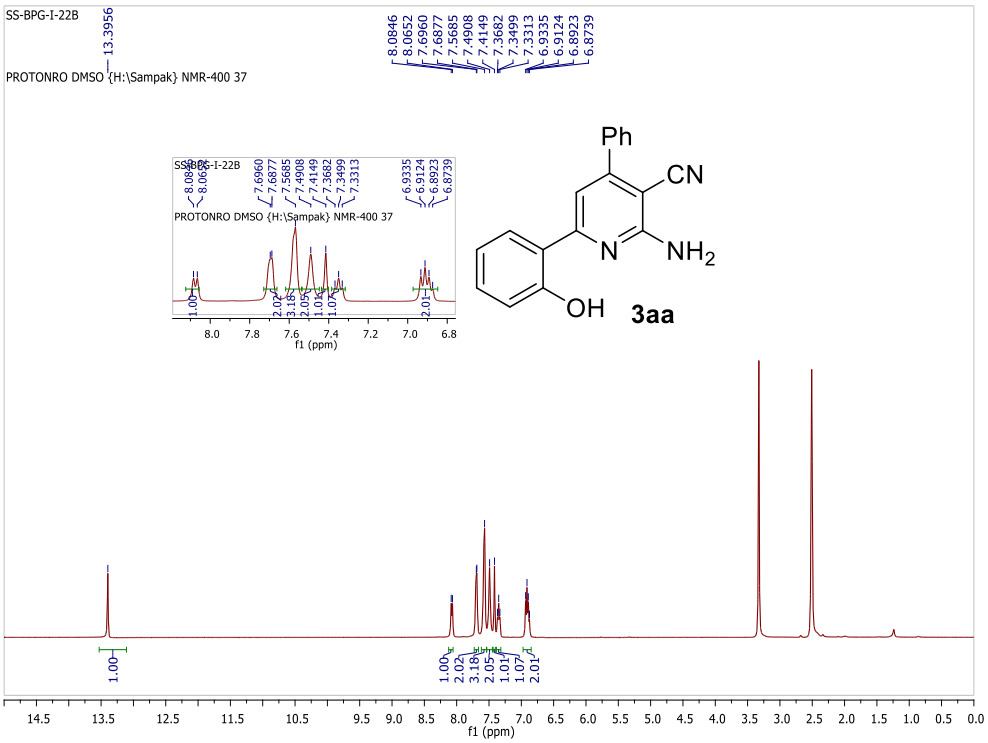

Figure 3.4 400 MHz ^{1}H NMR spectrum of **3aa** in DMSO-d_6.

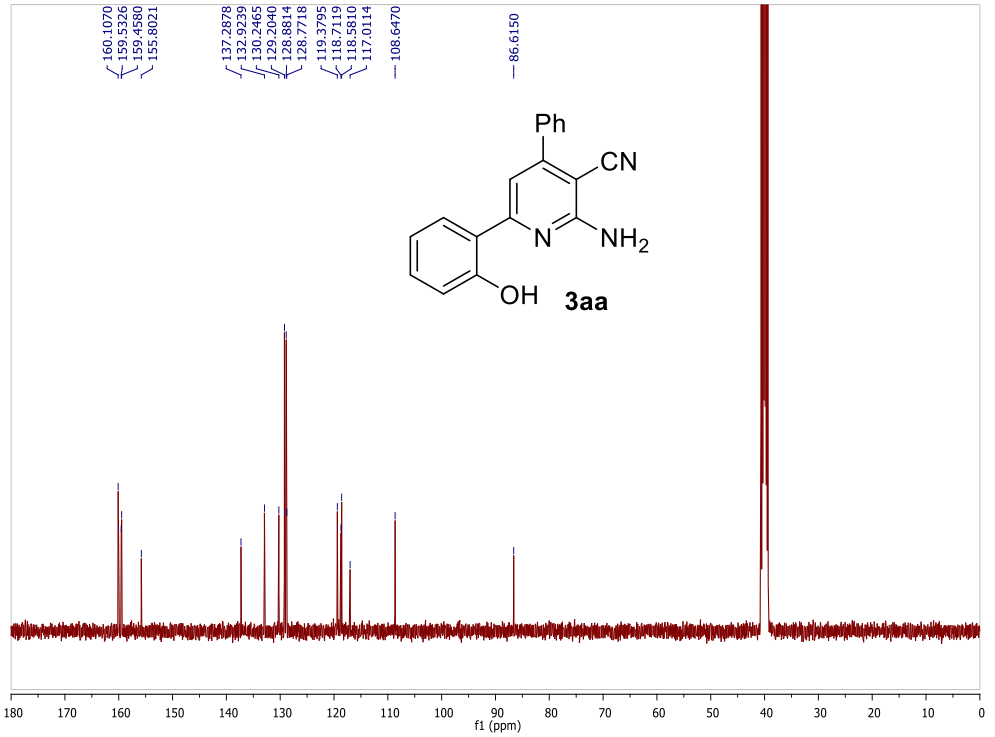

Figure 3.5 100 MHz ^{13}C NMR spectrum of **3aa** in DMSO-d_6.

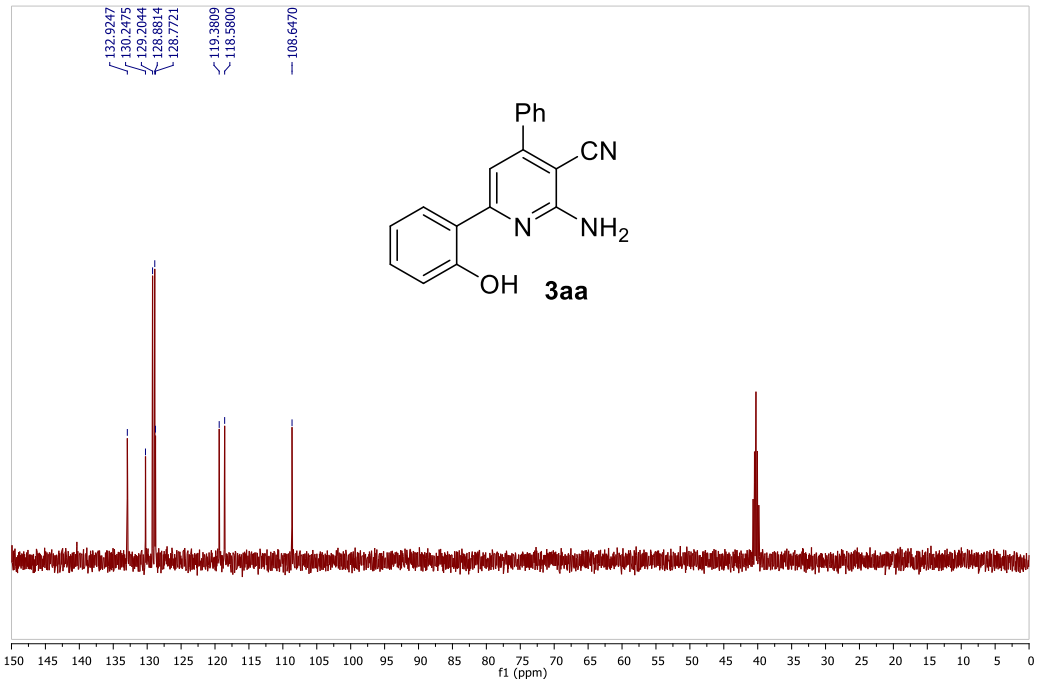

Figure 3.6 100 MHz DEPT-135 NMR spectrum of **3aa** in DMSO-d_6.

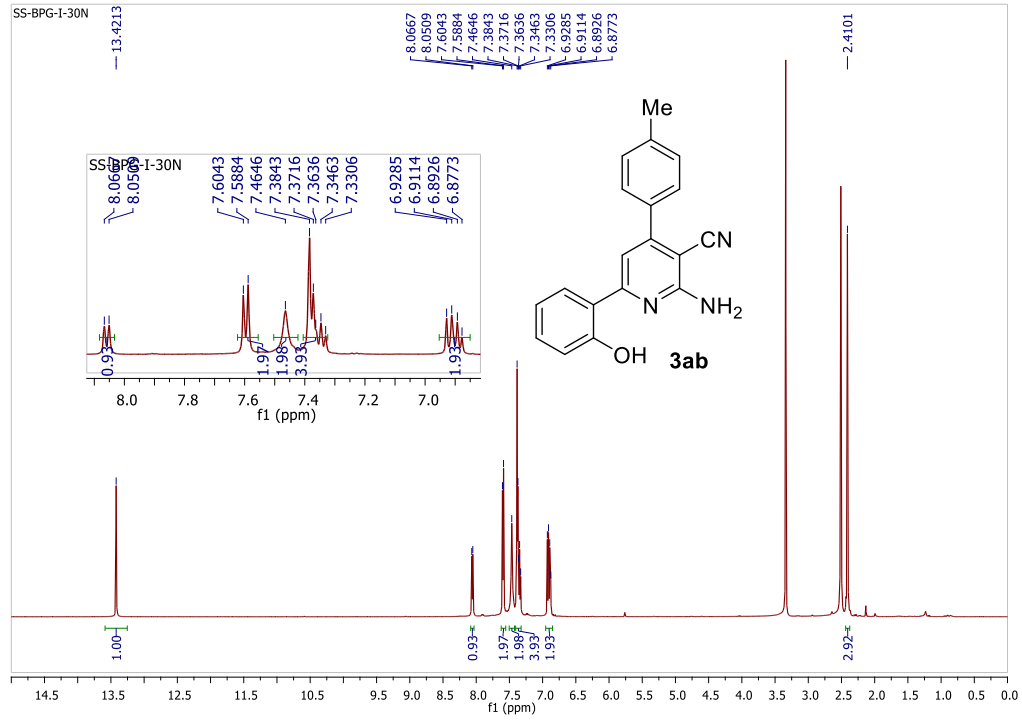

Figure 3.7 500 MHz ^{1}H NMR spectrum of **3ab** in DMSO-d_6.

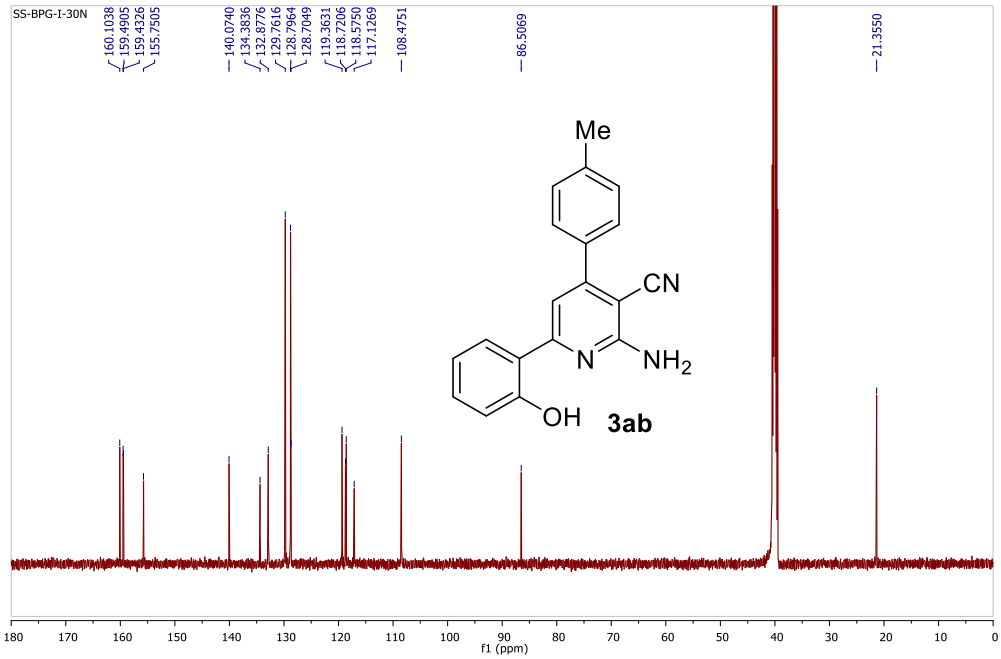

Figure 3.8 125 MHz ^{13}C NMR spectrum of **3ab** in DMSO-d$_6$.

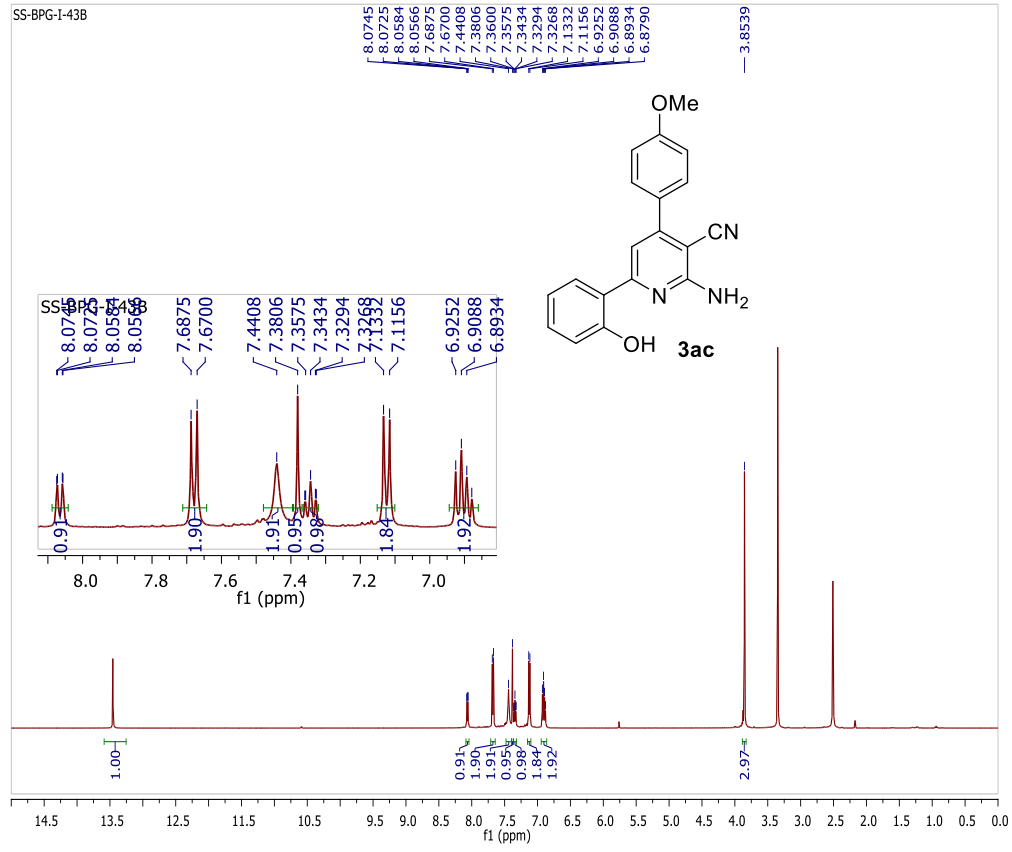

Figure 3.9 500 MHz ^{1}H NMR spectrum of **3ac** in DMSO-d$_6$.

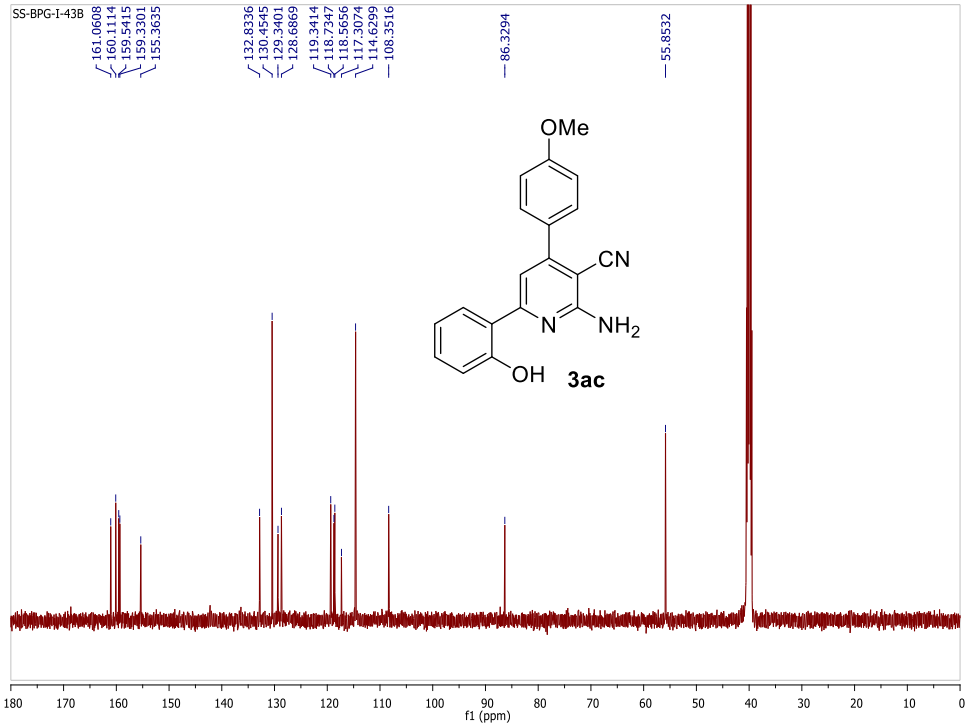

Figure 3.10 125 MHz ^{13}C NMR spectrum of **3ac** in DMSO-d$_6$.

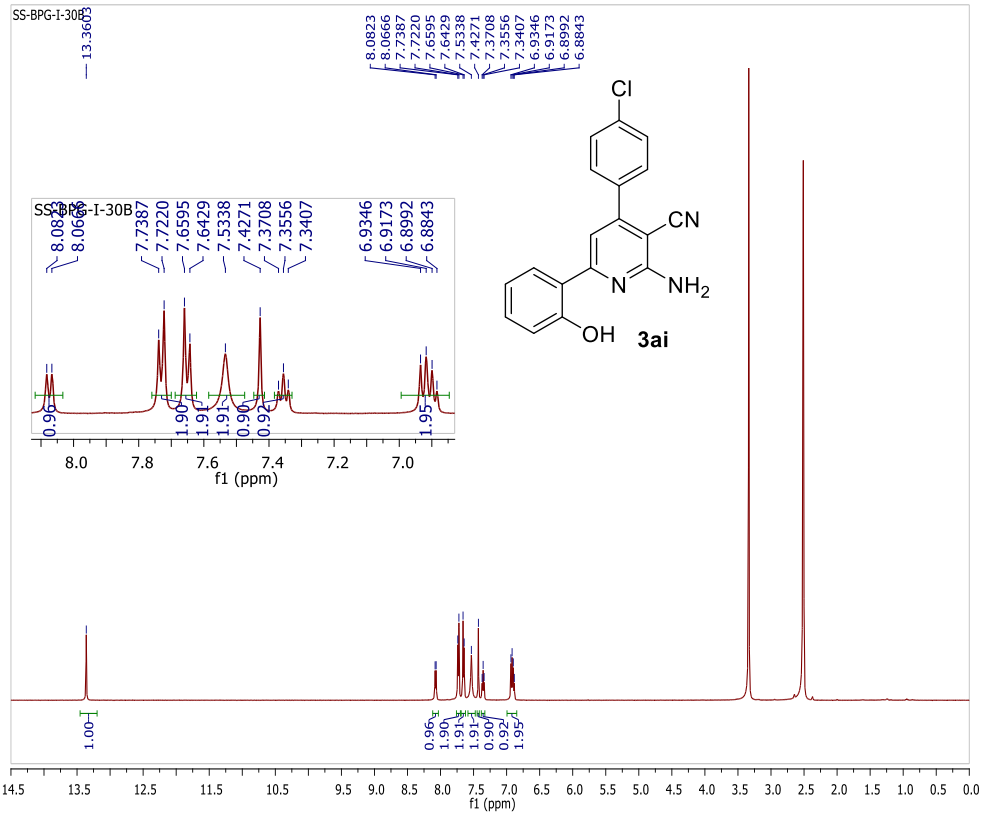

Figure 3.11 500 MHz ^{1}H NMR spectrum of **3ai** in DMSO-d$_6$.

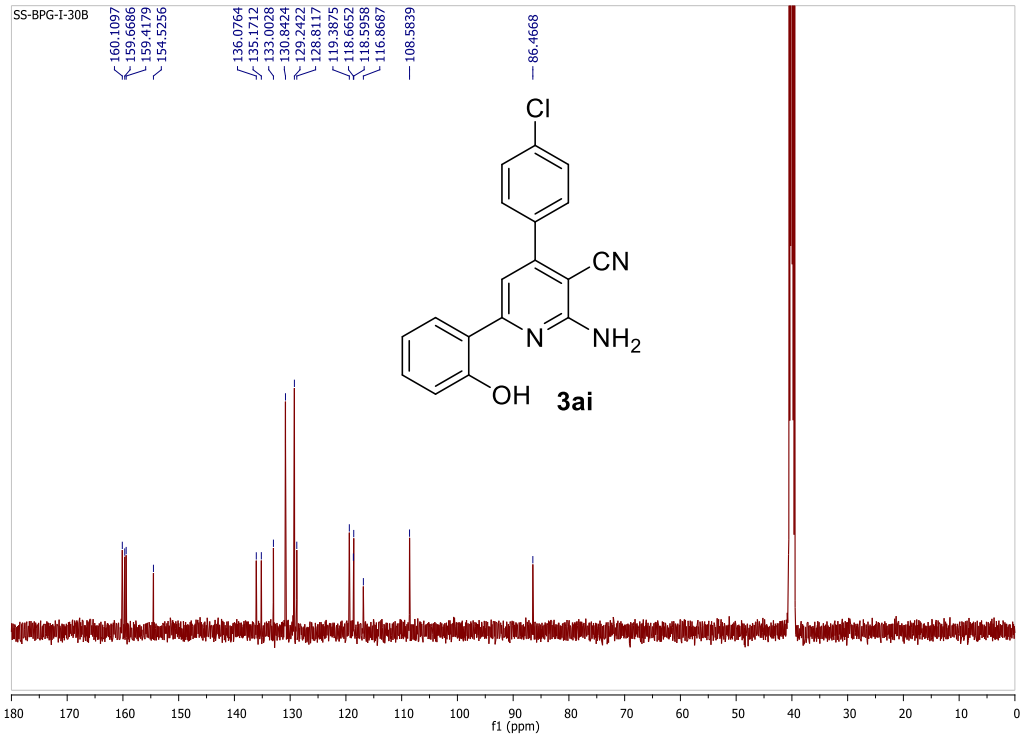

Figure 3.12 125 MHz ^{13}C NMR spectrum of **3ai** in DMSO-d$_6$.

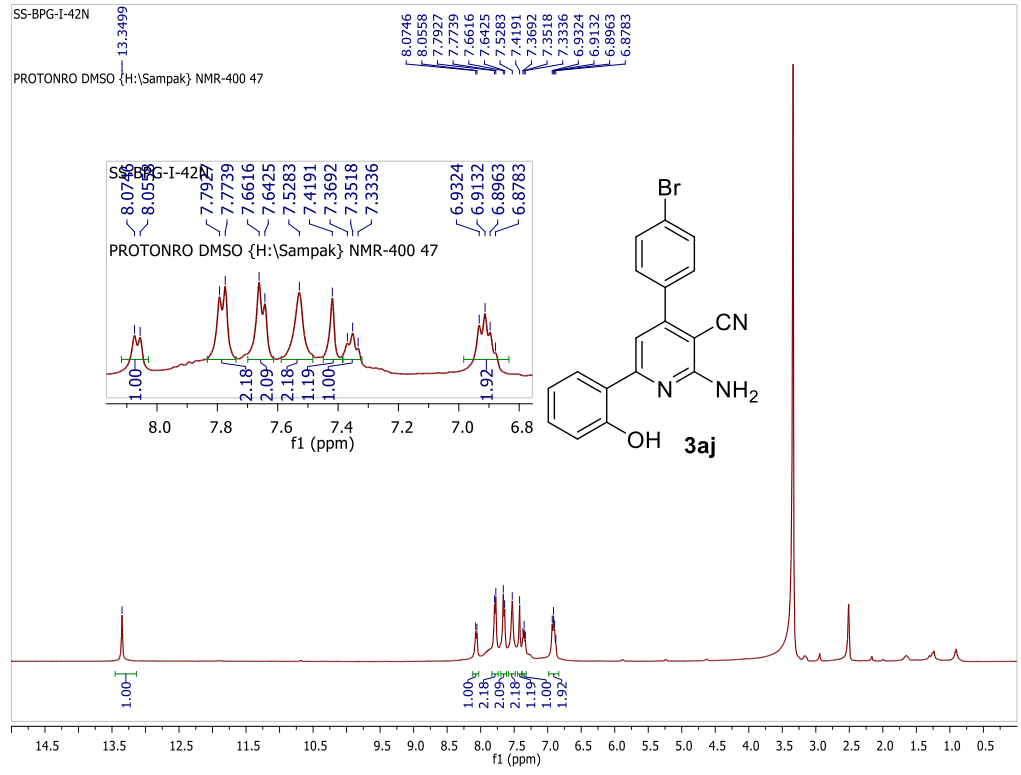

Figure 3.13 400 MHz ^{1}H NMR spectrum of **3aj** in DMSO-d$_6$.

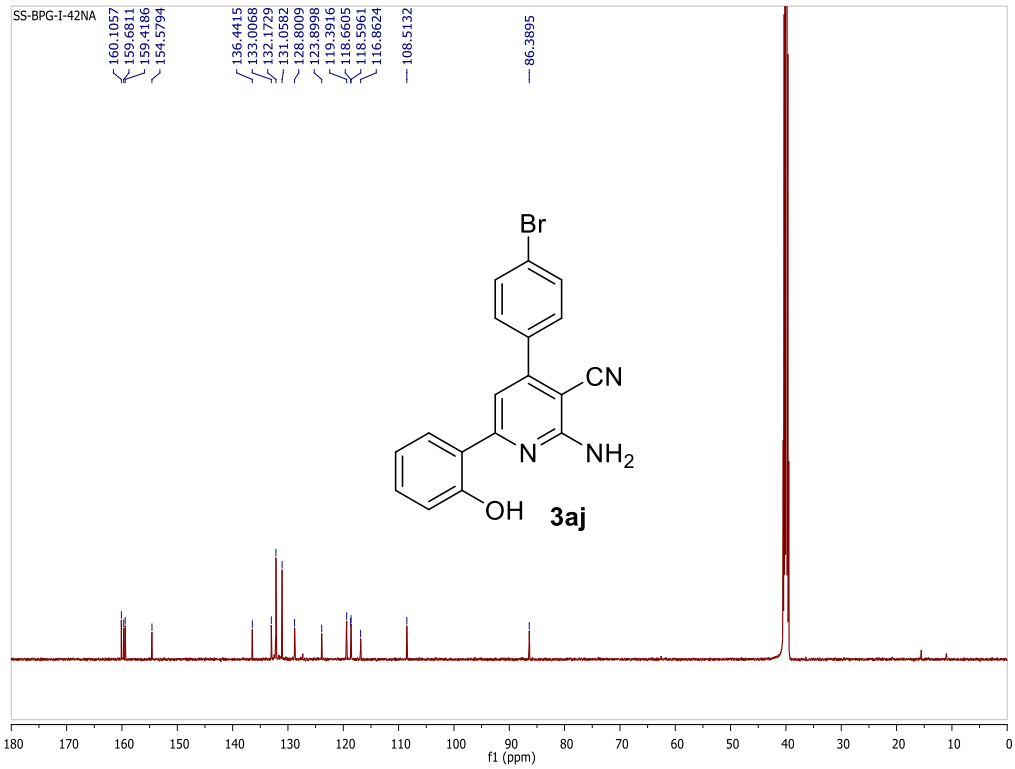

Figure 3.14 100 MHz ^{13}C NMR spectrum of **3aj** in DMSO-d$_6$.

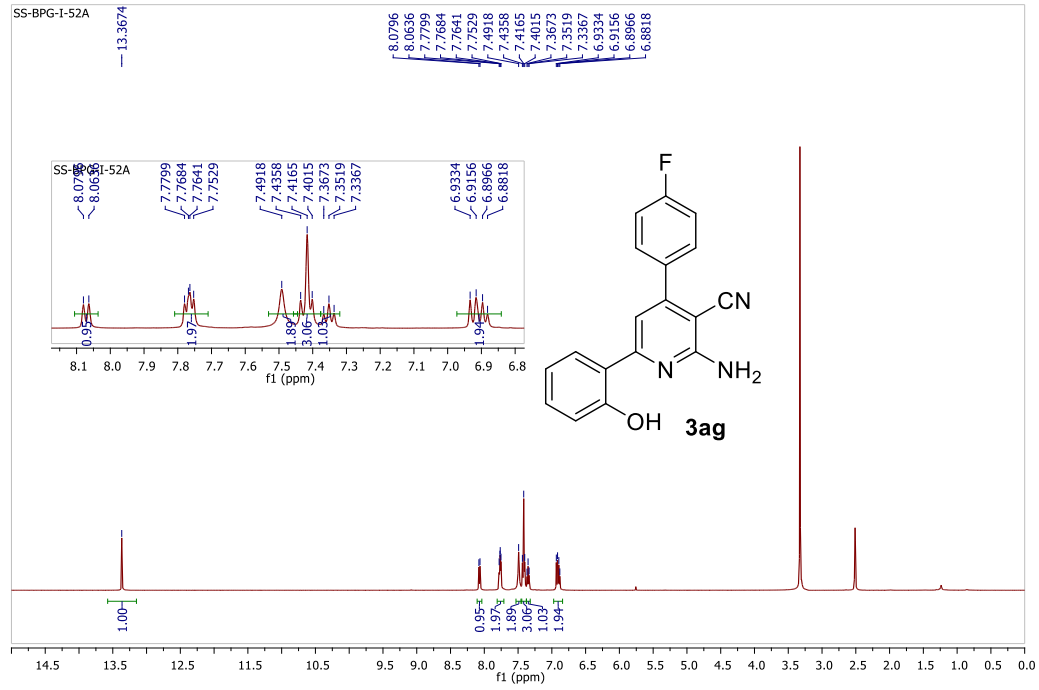

Figure 3.15 500 MHz ^{1}H NMR spectrum of **3ag** in DMSO-d$_6$.

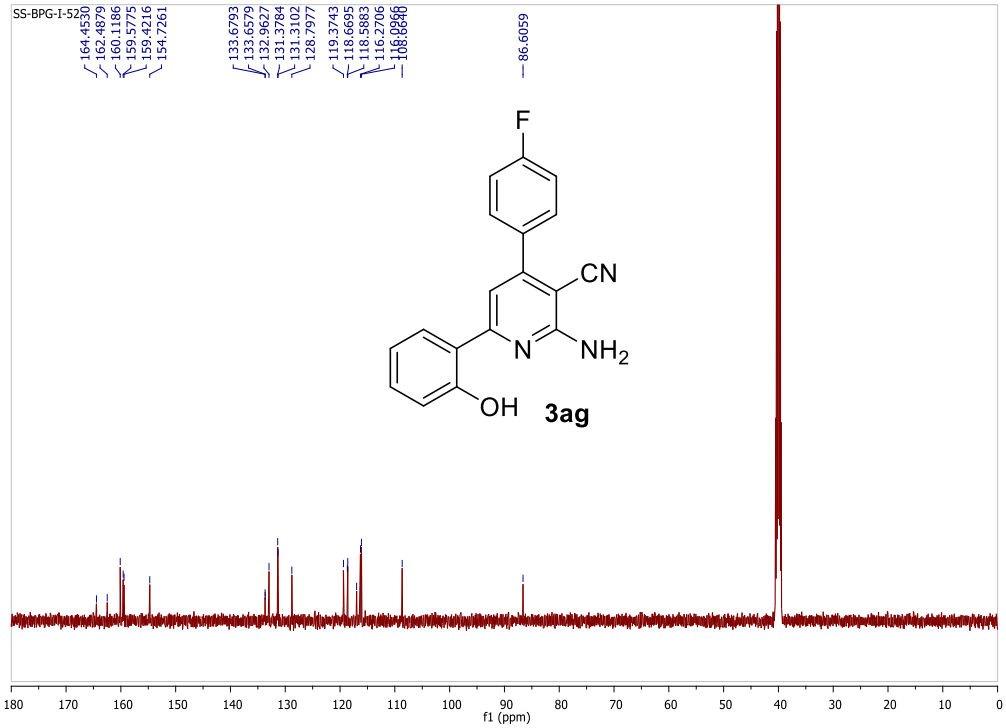

Figure 3.16 125 MHz ^{13}C NMR spectrum of **3ag** in DMSO-d_6.

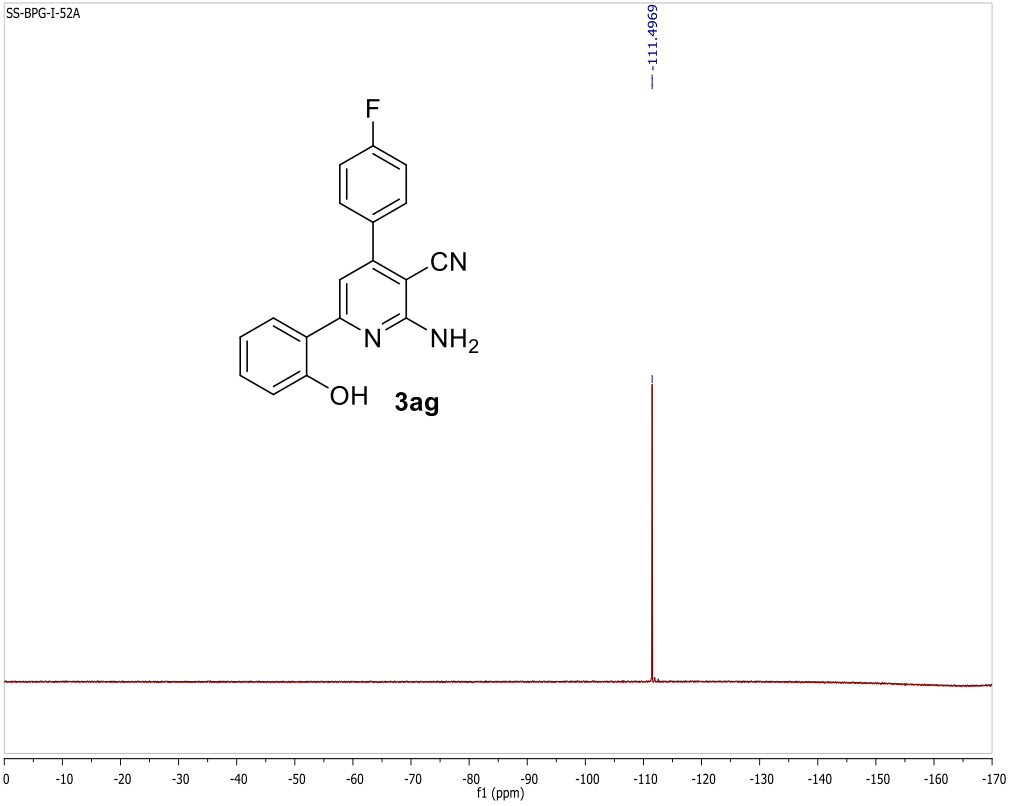

Figure 3.17 470 MHz ^{19}F NMR spectrum of **3ag** in DMSO-d_6.

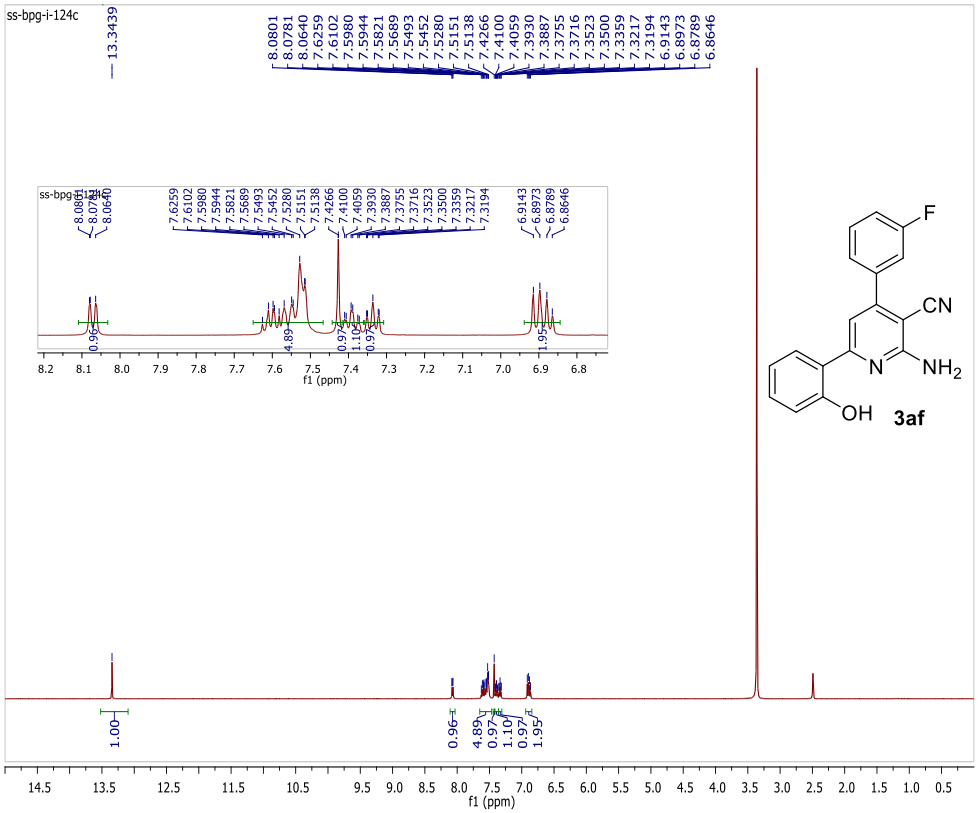

Figure 3.18 500 MHz ^{1}H NMR spectrum of **3af** in DMSO-d_6.

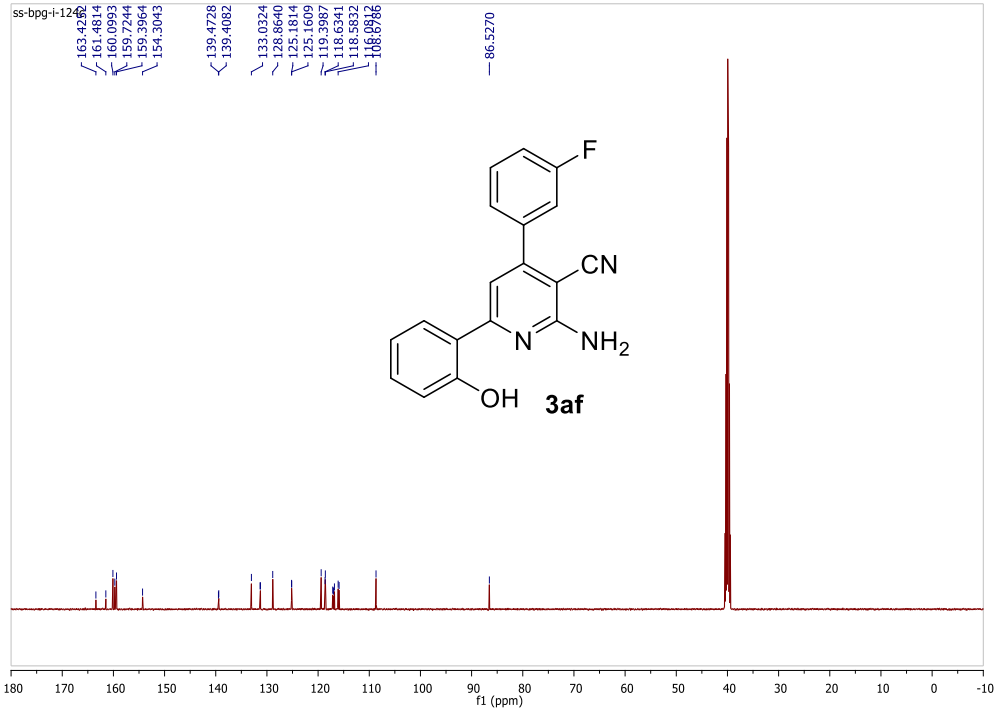

Figure 3.19 125 MHz ^{13}C NMR spectrum of **3af** in DMSO-d_6.

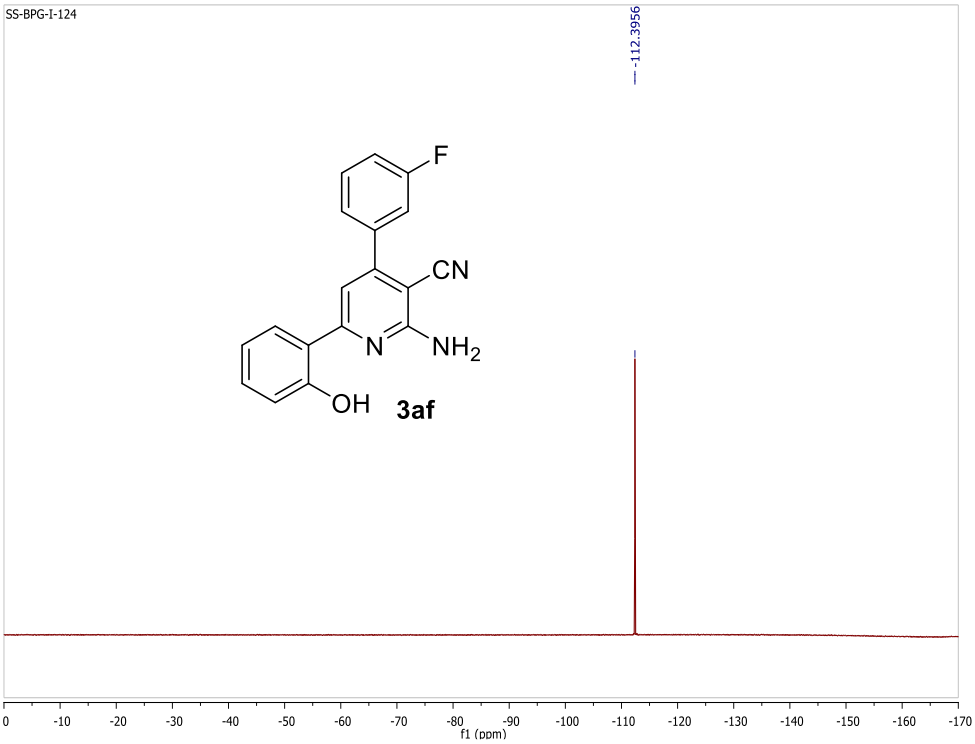

Figure 3.20 470 MHz ^{19}F NMR spectrum of **3af** in DMSO-d$_6$.

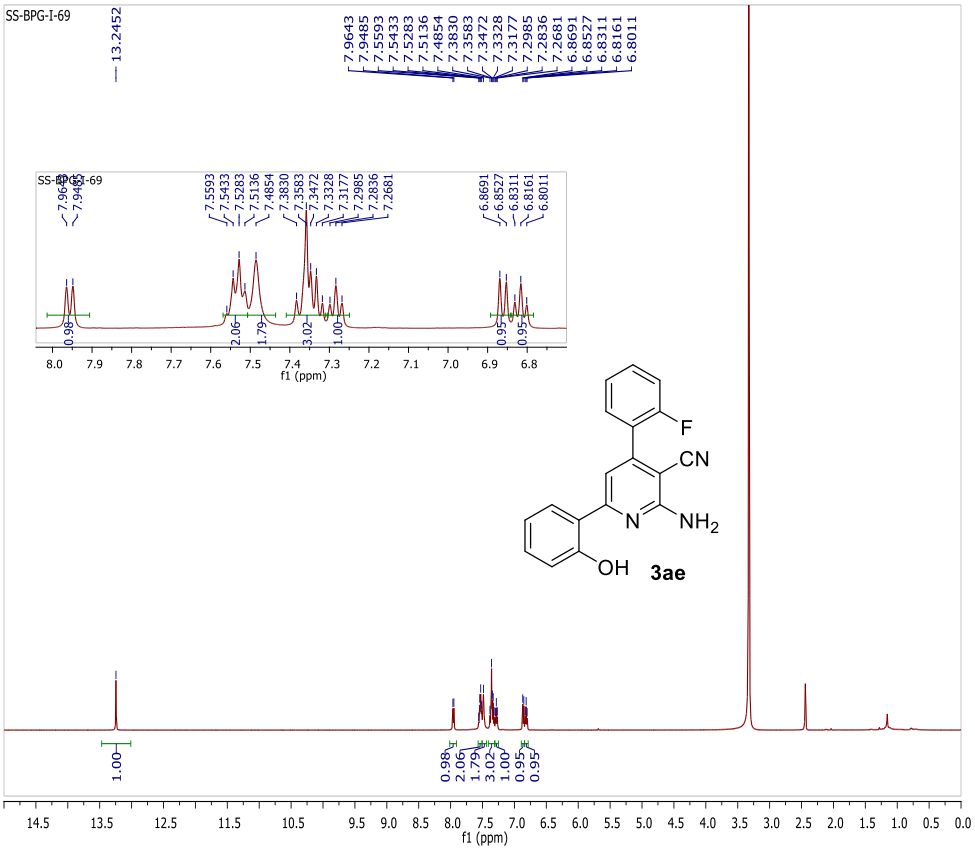

Figure 3.21 500 MHz ^{1}H NMR spectrum of **3ae** in DMSO-d$_6$.

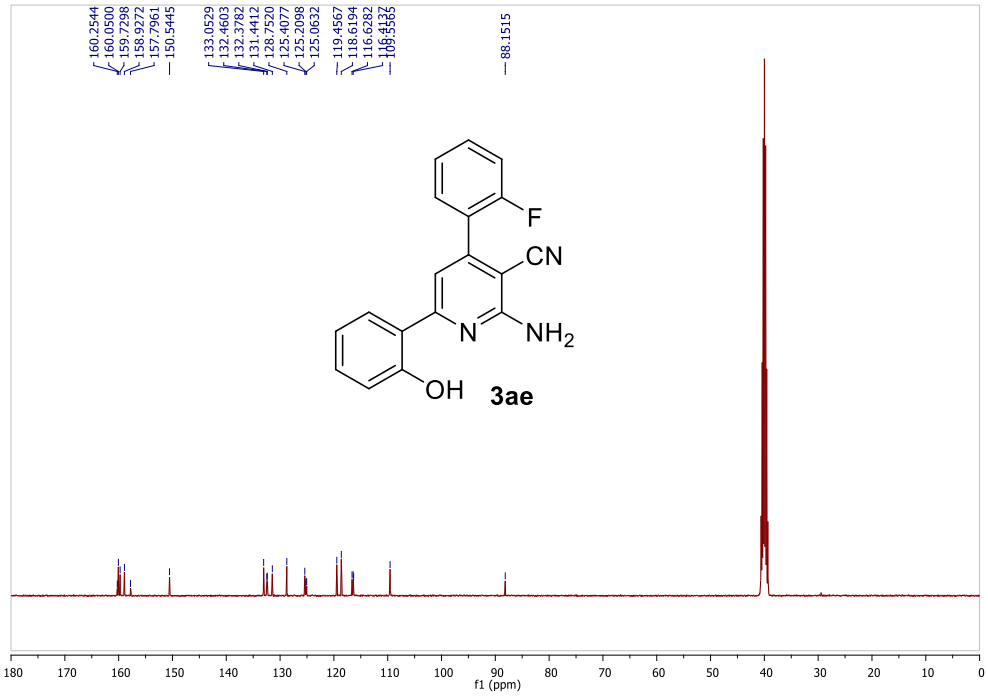

Figure 3.22 125 MHz ^{13}C NMR spectrum of **3ae** in DMSO-d_6.

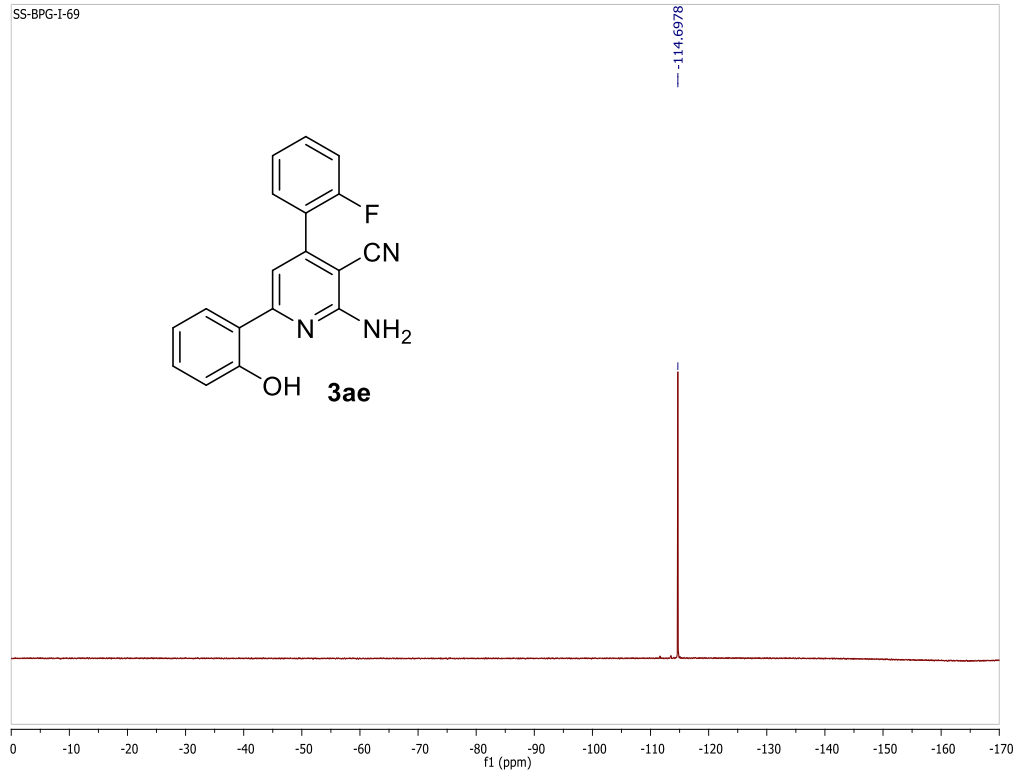

Figure 3.23 470 MHz ^{19}F NMR spectrum of **3ae** in DMSO-d_6.

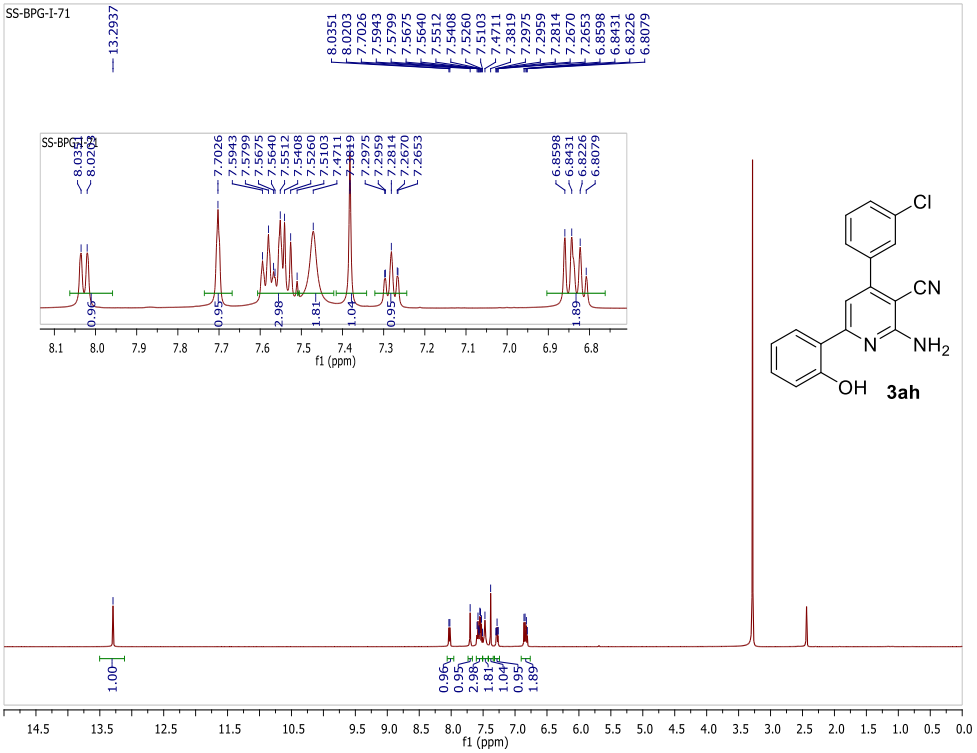

Figure 3.24 500 MHz ^{1}H NMR spectrum of **3ah** in DMSO-d$_6$.

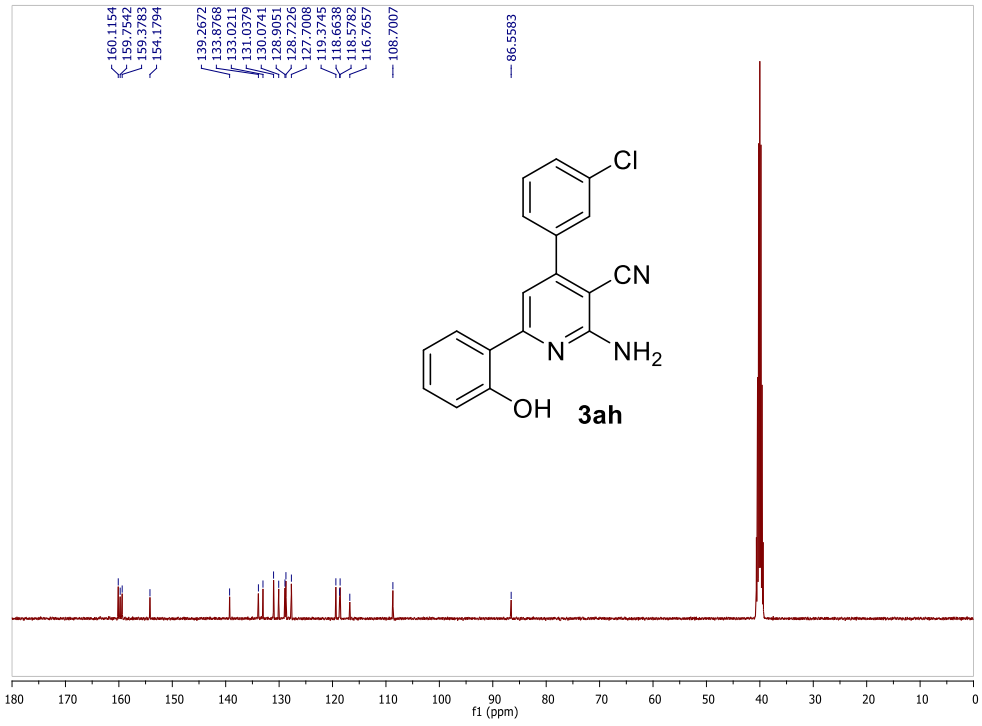

Figure 3.25 125 MHz ^{13}C NMR spectrum of **3ah** in DMSO-d$_6$.

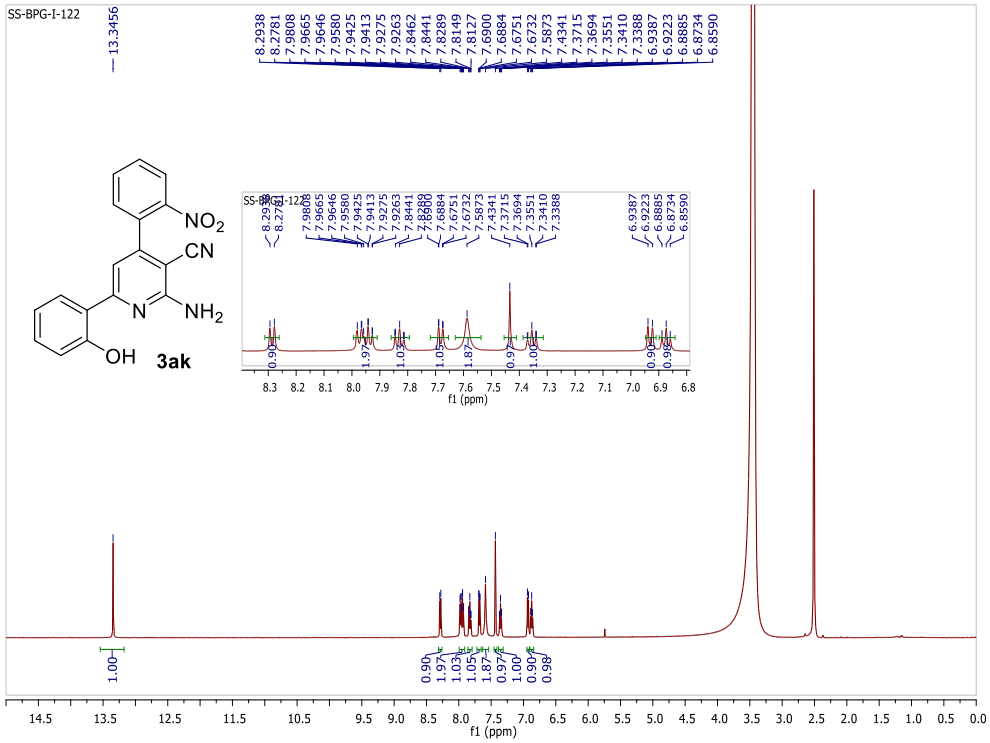

Figure 3.26 500 MHz ^{1}H NMR spectrum of **3ak** in DMSO-d$_6$.

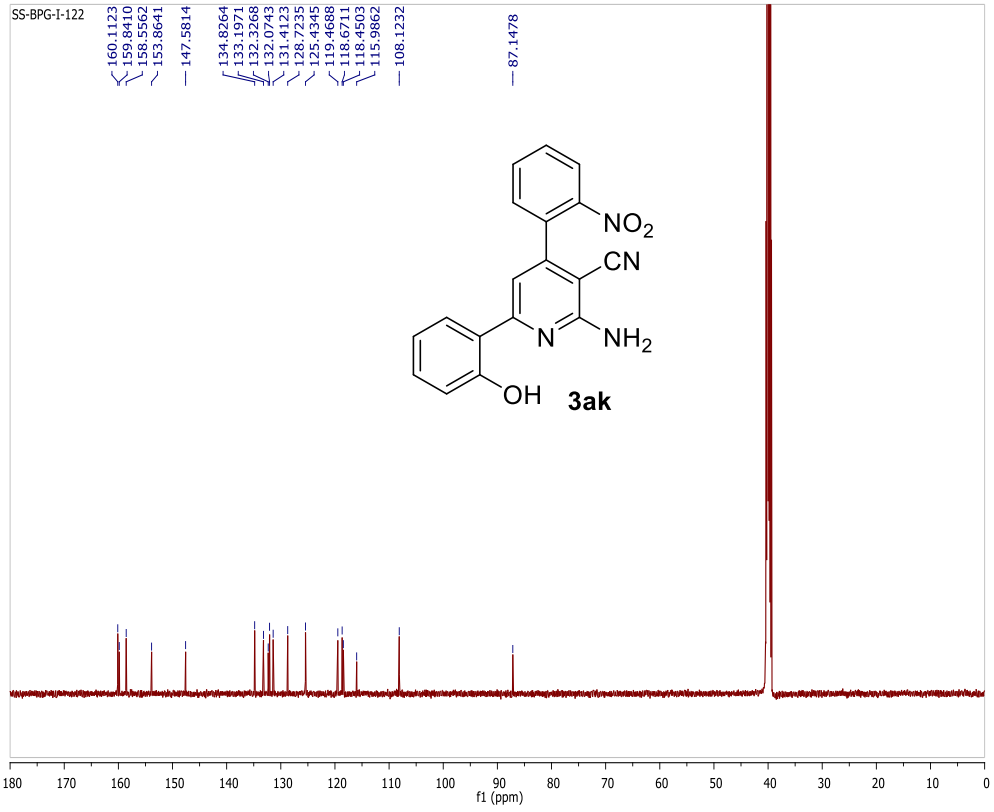

Figure 3.27 125 MHz ^{13}C NMR spectrum of **3ak** in DMSO-d$_6$.

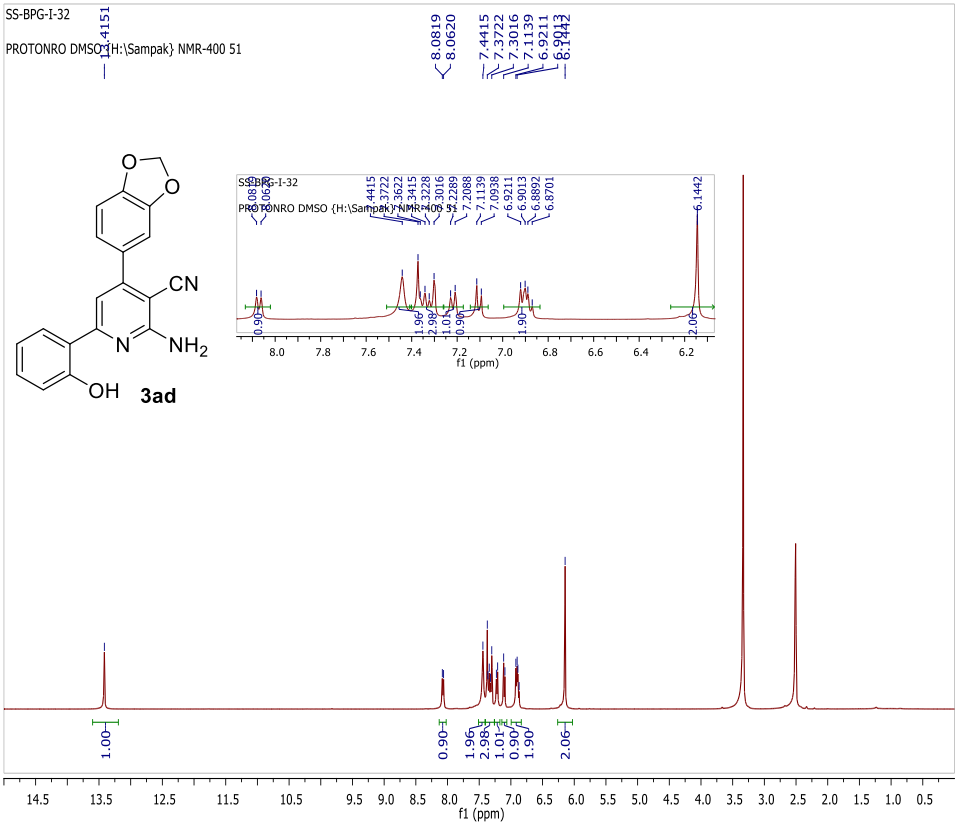

Figure 3.28 400 MHz ^{1}H NMR spectrum of **3ad** in DMSO-d_6.

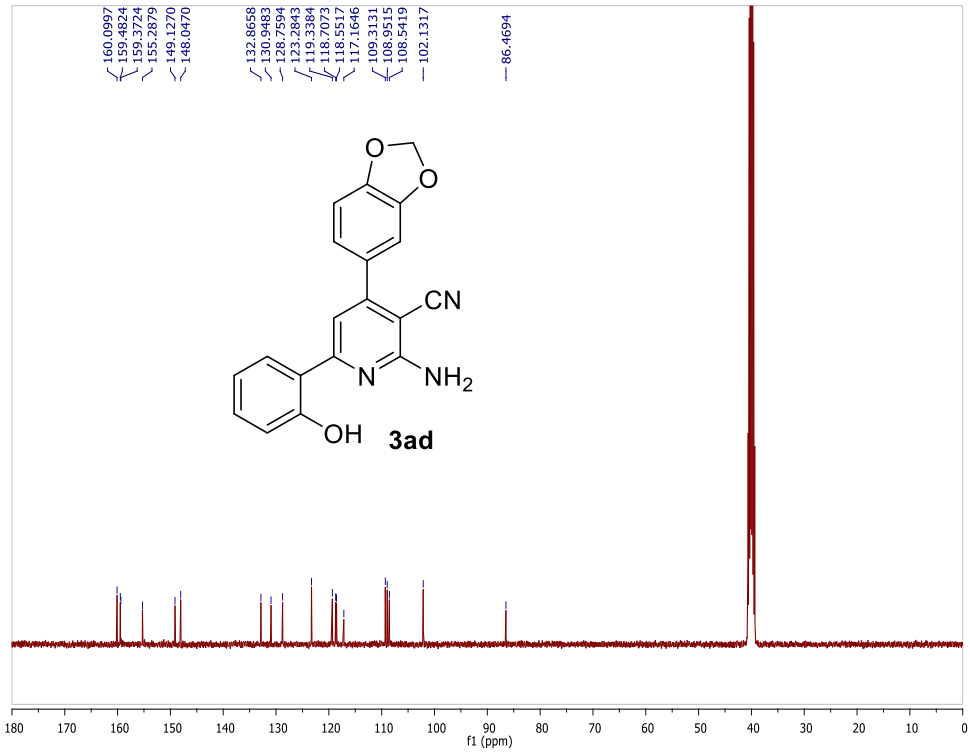

Figure 3.29 100 MHz ^{13}C NMR spectrum of **3ad** in DMSO-d_6.

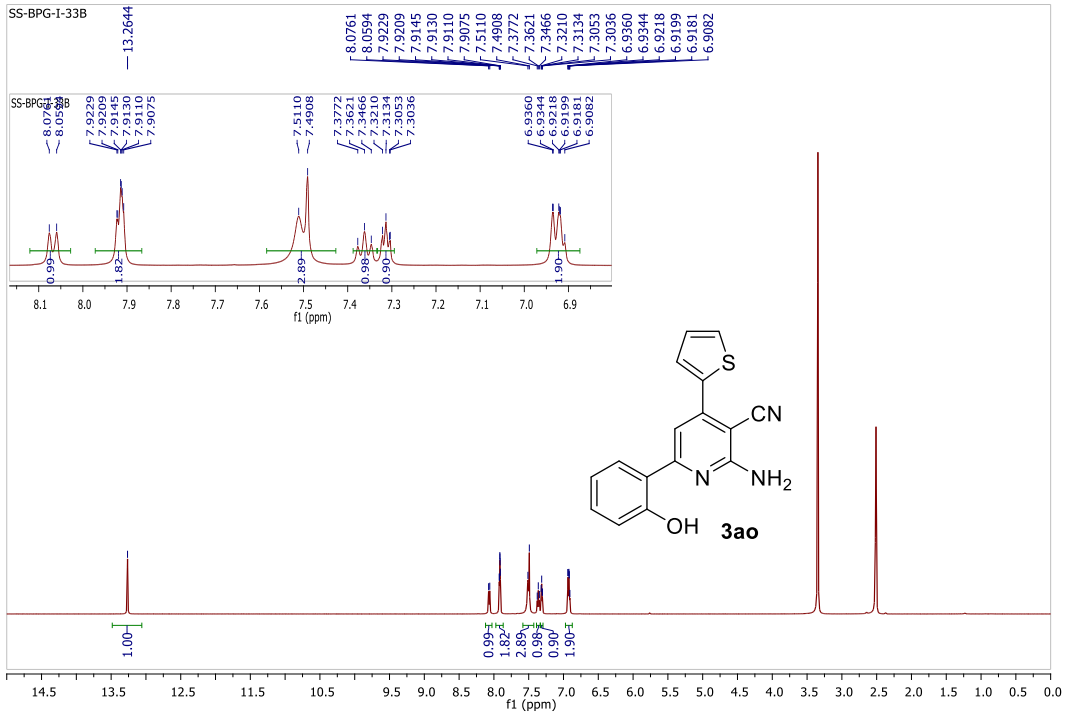

Figure 3.30 500 MHz ^{1}H NMR spectrum of **3ao** in DMSO-d$_6$.

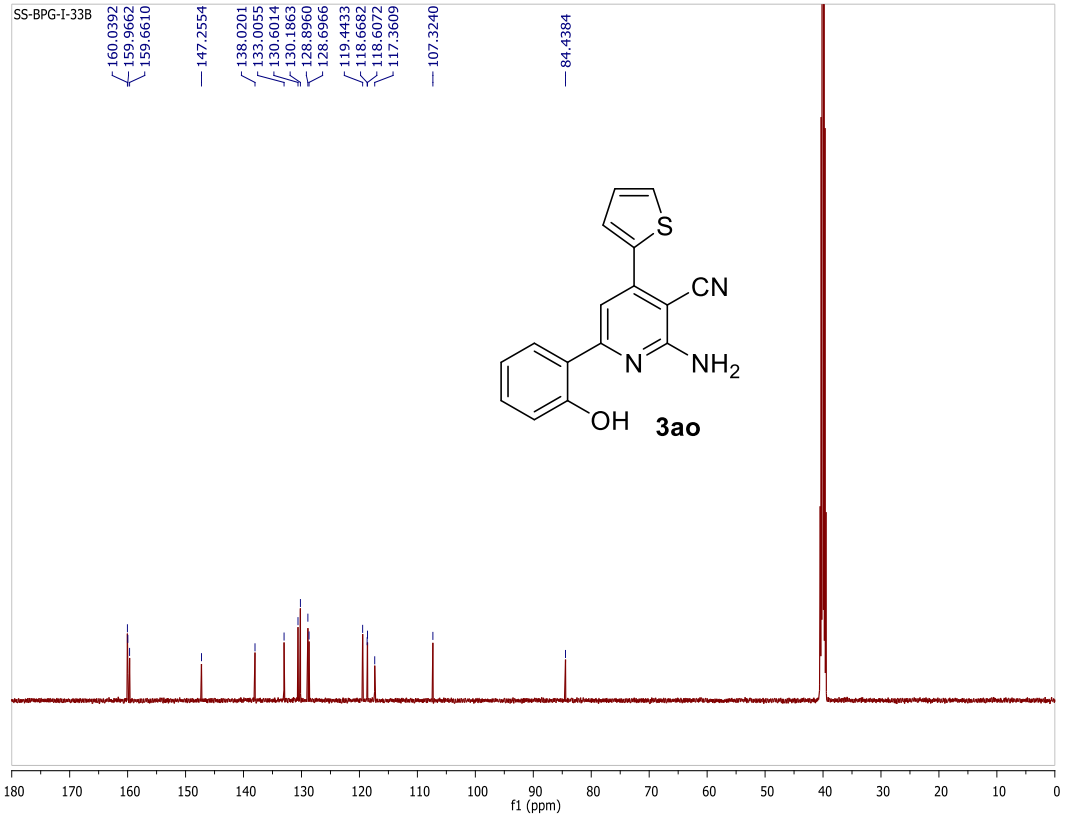

Figure 3.31 125 MHz ^{13}C NMR spectrum of **3ao** in DMSO-d$_6$.

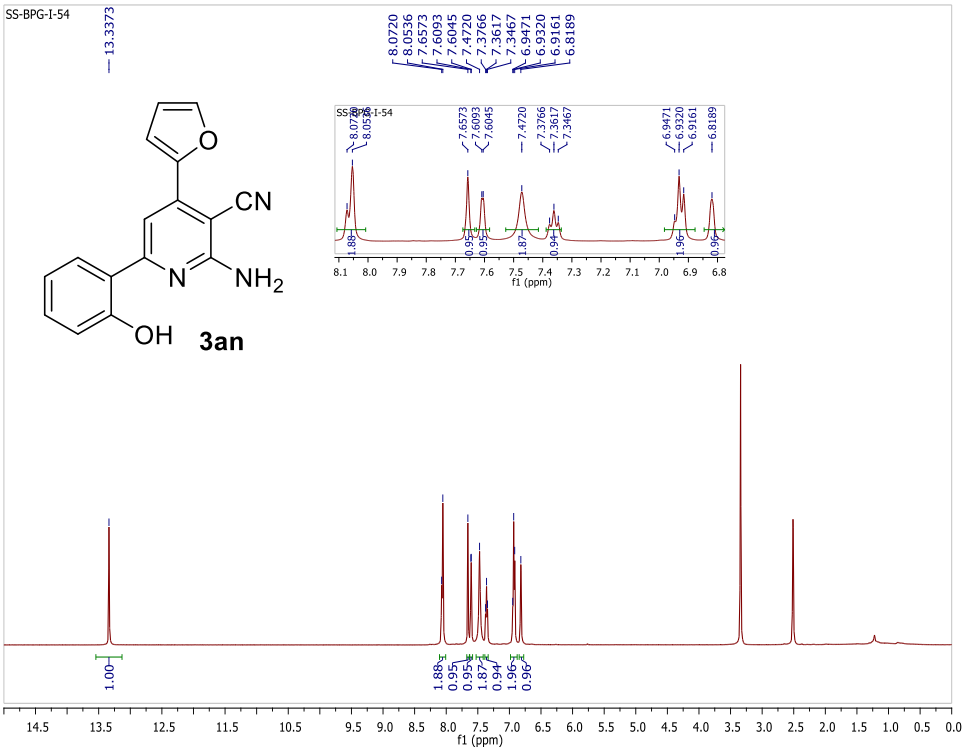

Figure 3.32 500 MHz ^{1}H NMR spectrum of **3an** in DMSO-d$_6$.

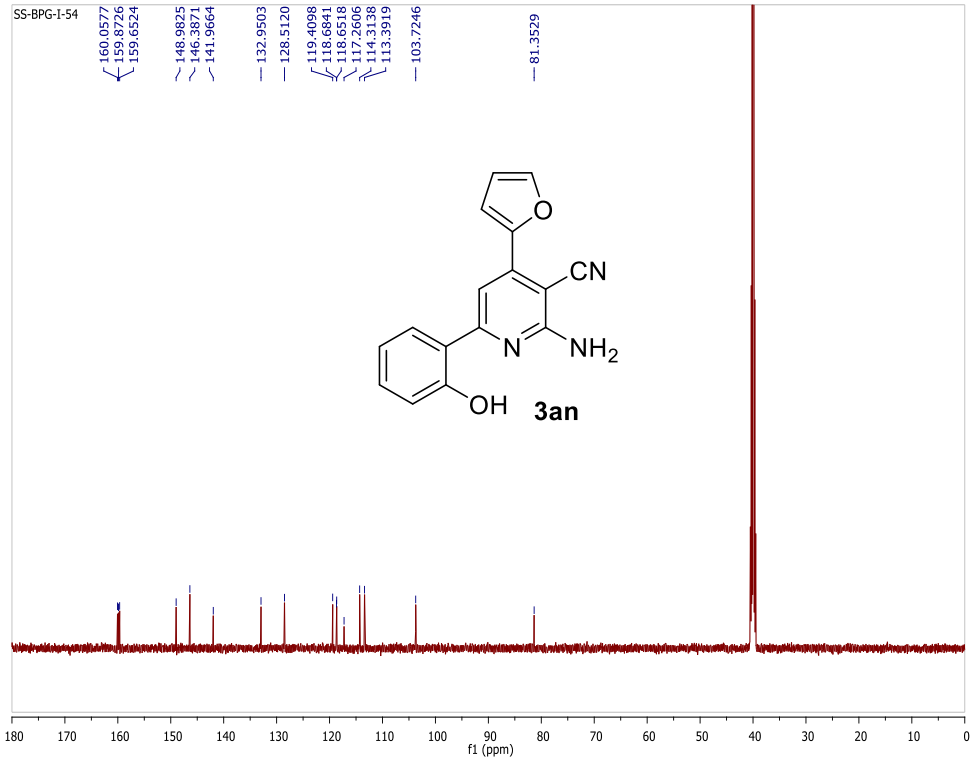

Figure 3.33 125 MHz ^{13}C NMR spectrum of **3an** in DMSO-d$_6$.

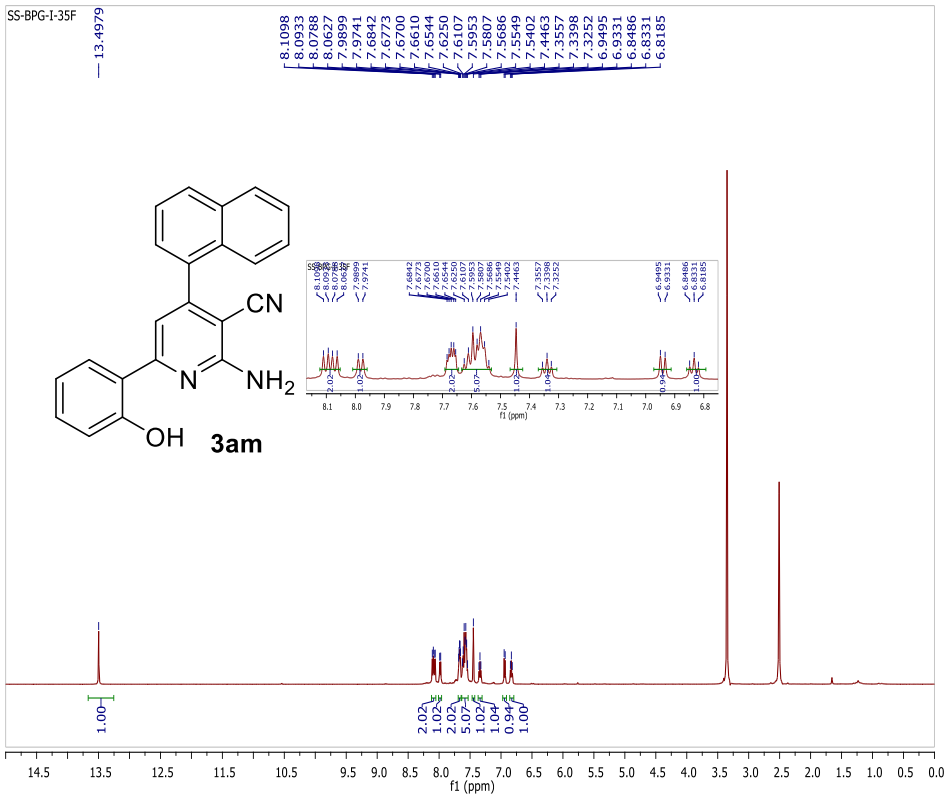

Figure 3.34 500 MHz ^{1}H NMR spectrum of **3am** in DMSO-d$_6$.

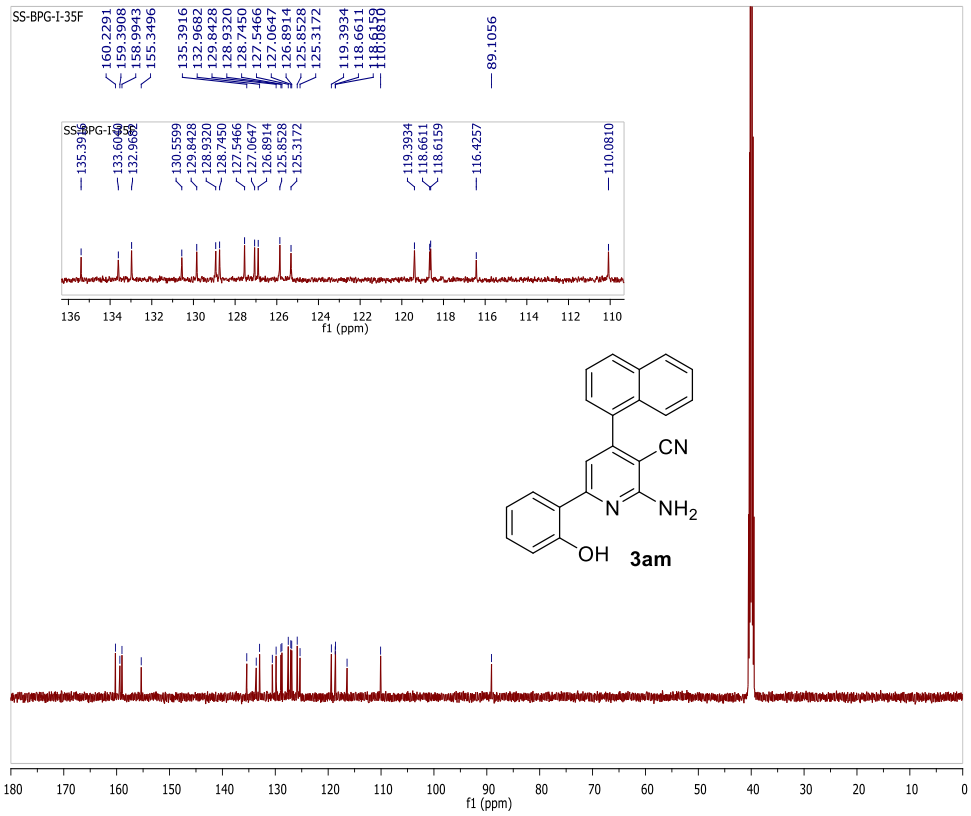

Figure 3.35 125 MHz ^{13}C NMR spectrum of **3am** in DMSO-d$_6$.

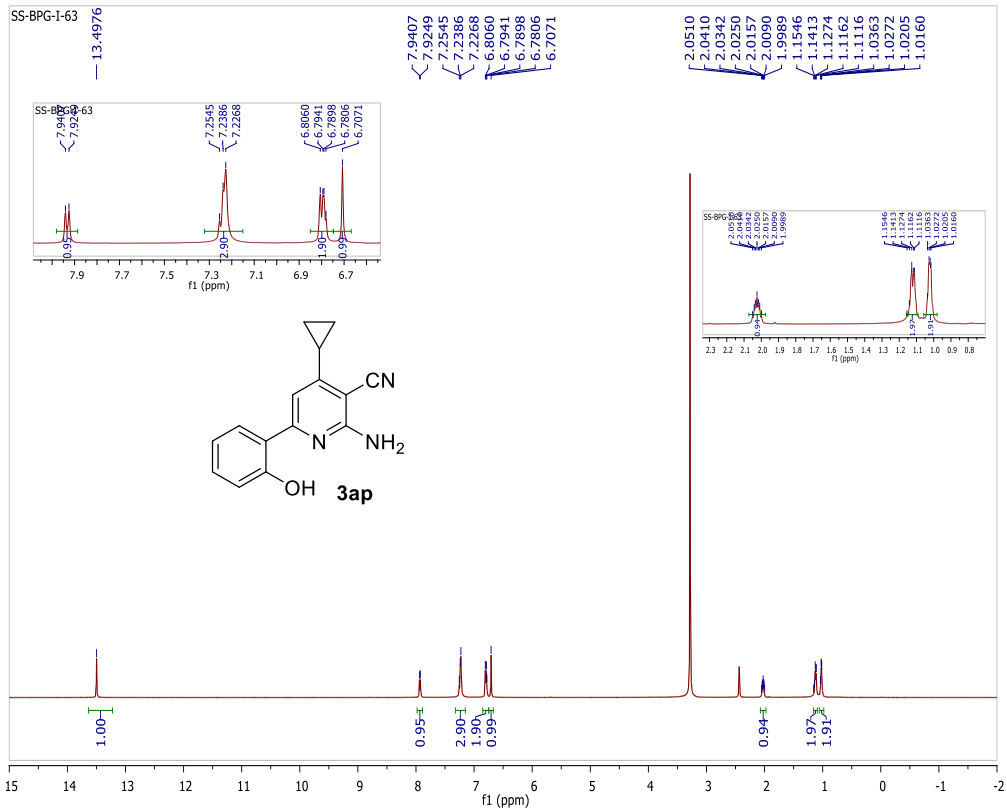

Figure 3.36 500 MHz ^{1}H NMR spectrum of **3ap** in DMSO-d$_6$.

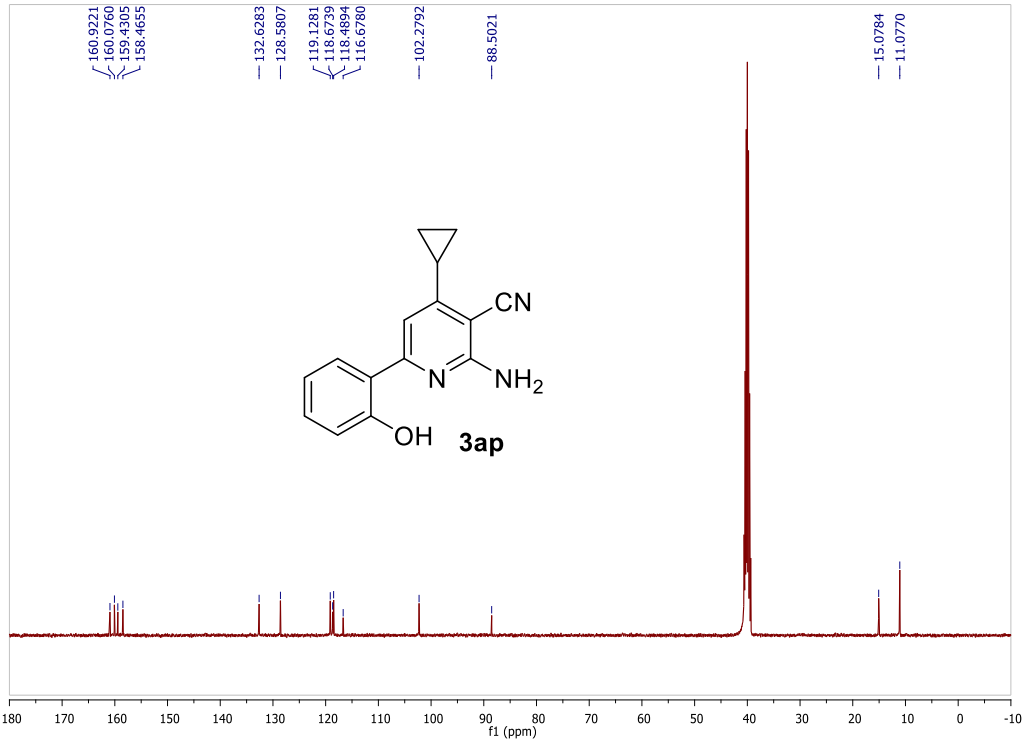

Figure 3.37 125 MHz ^{13}C NMR spectrum of **3ap** in DMSO-d$_6$.

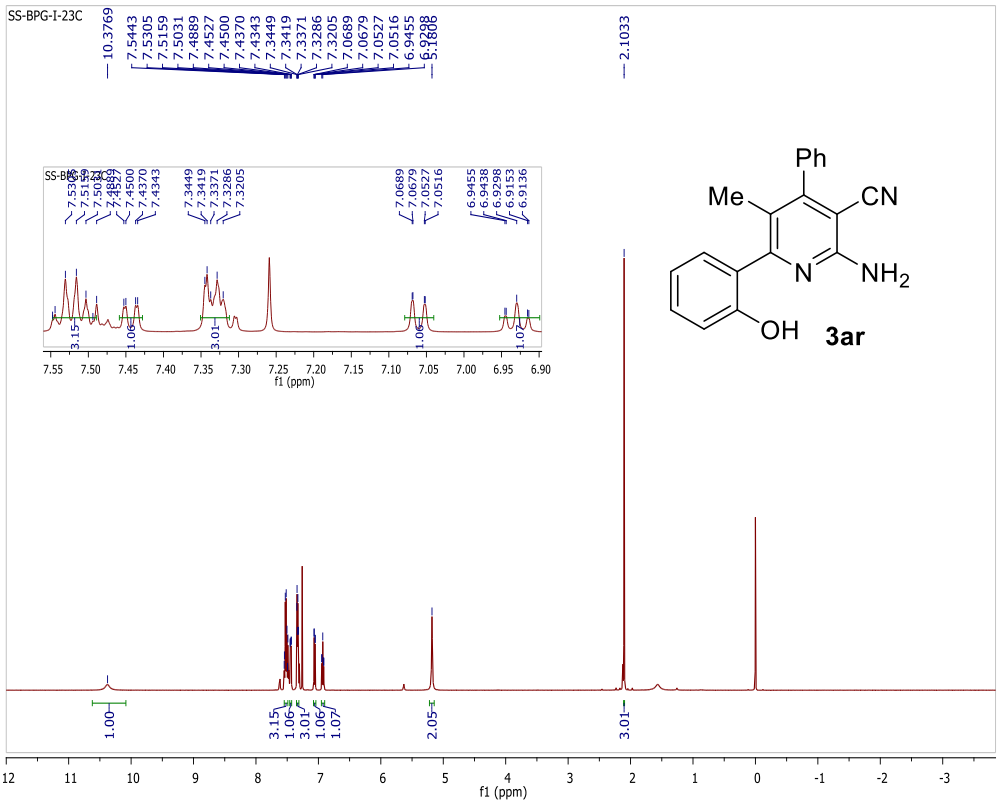

Figure 3.38 500 MHz ^{1}H NMR spectrum of **3ar** in $CDCl_3$.

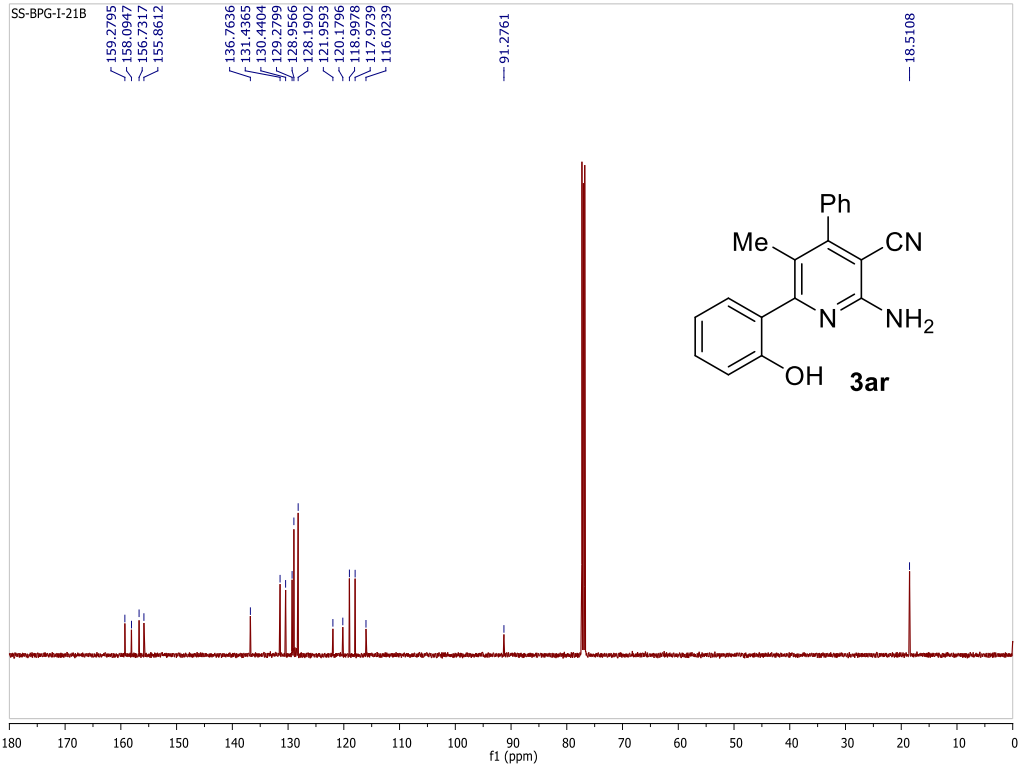

Figure 3.39 125 MHz ^{13}C NMR spectrum of **3ar** in $CDCl_3$.

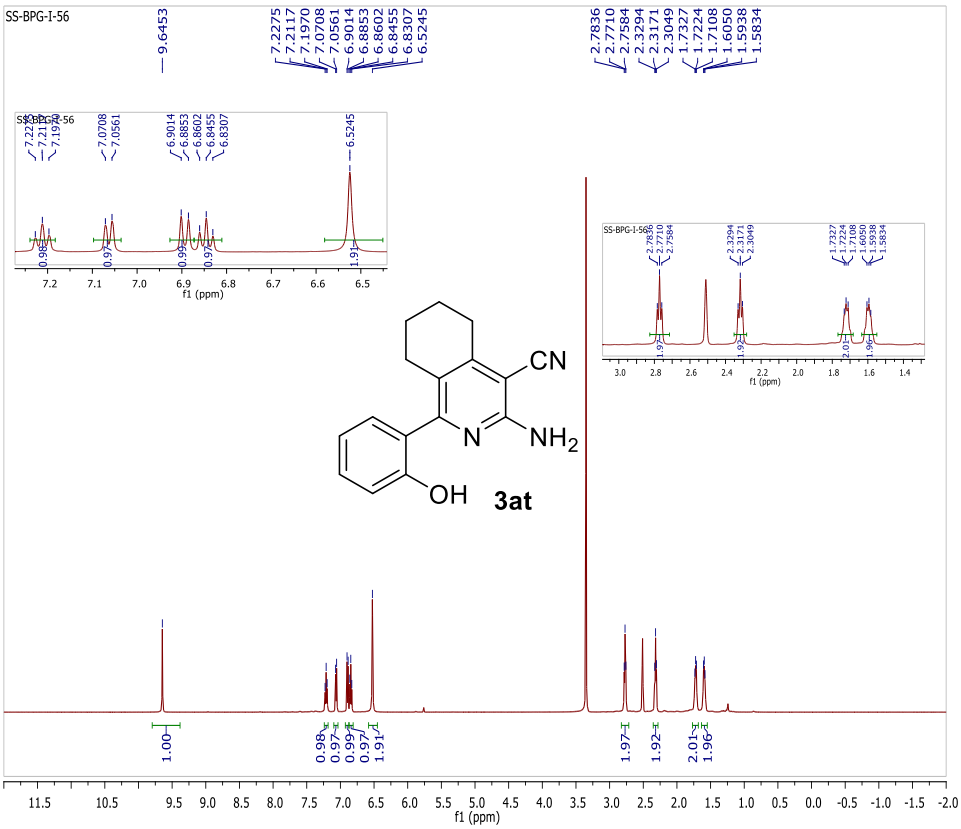

Figure 3.40 500 MHz ^{1}H NMR spectrum of **3at** in DMSO-d$_6$.

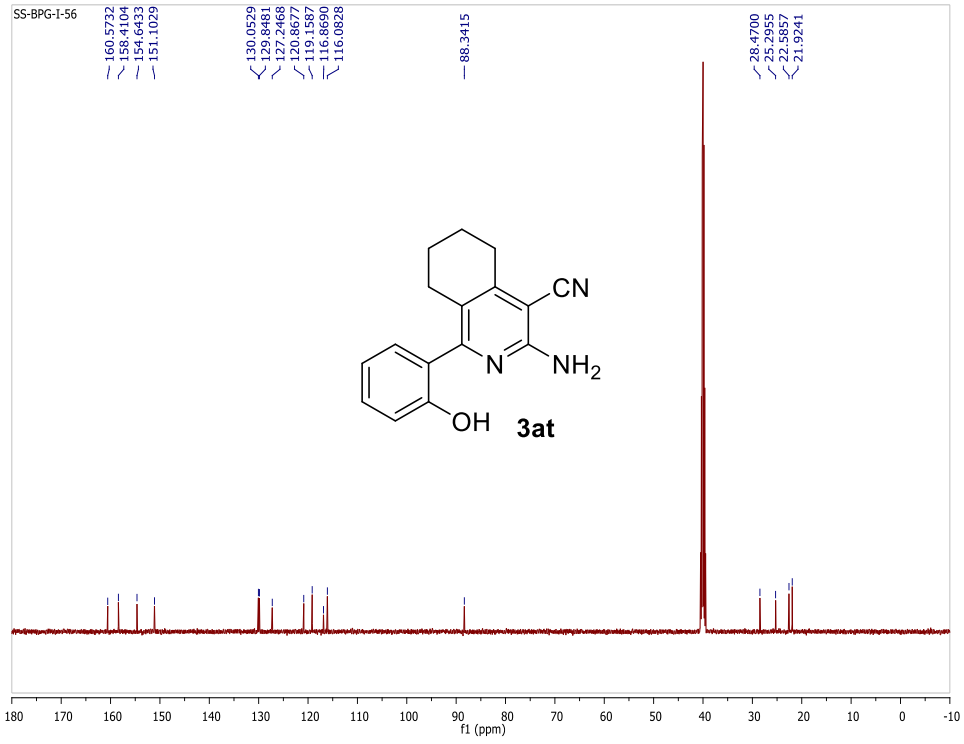

Figure 3.41 125 MHz ^{13}C NMR spectrum of **3at** in DMSO-d$_6$.

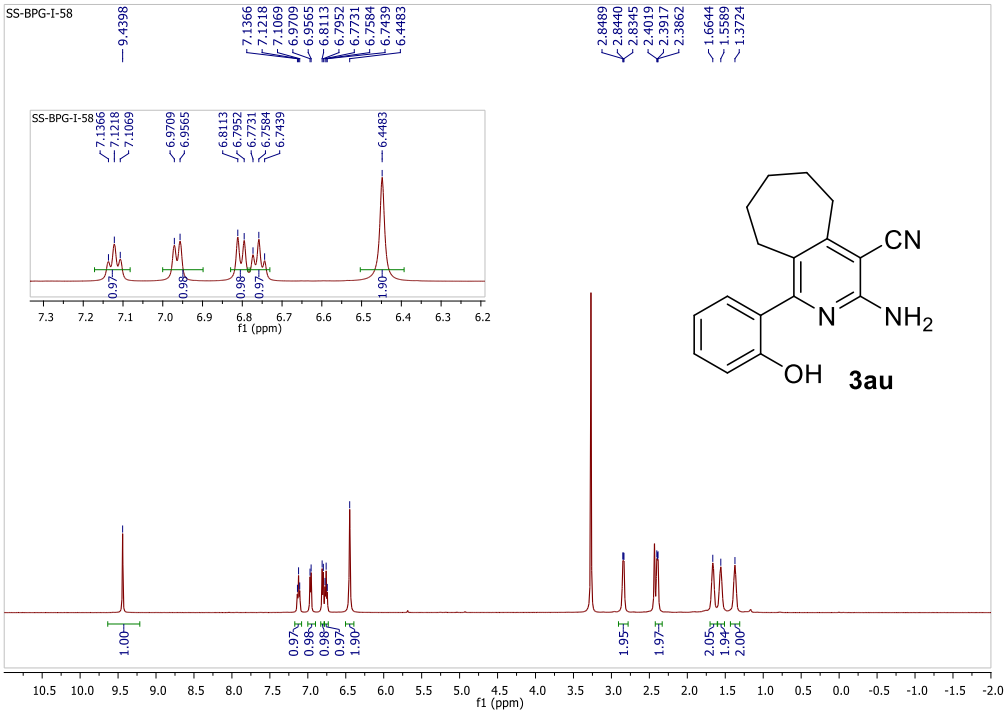

Figure 3.42 500 MHz ^{1}H NMR spectrum of **3au** in DMSO-d$_6$.

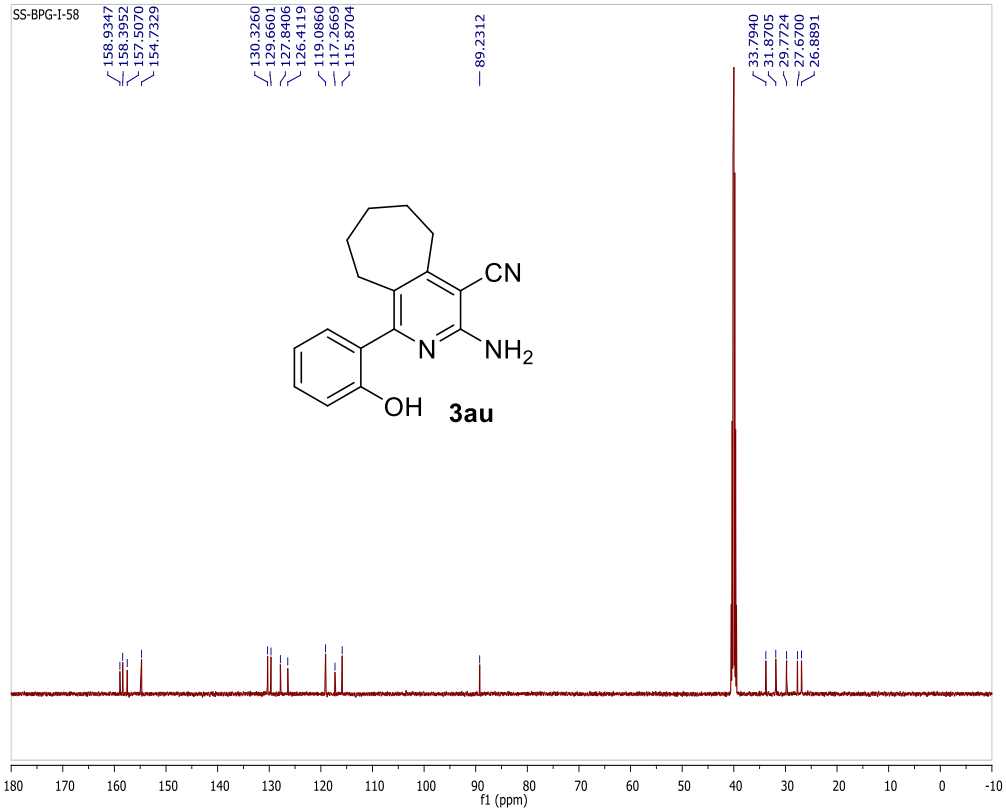

Figure 3.43 125 MHz ^{13}C NMR spectrum of **3au** in DMSO-d$_6$.

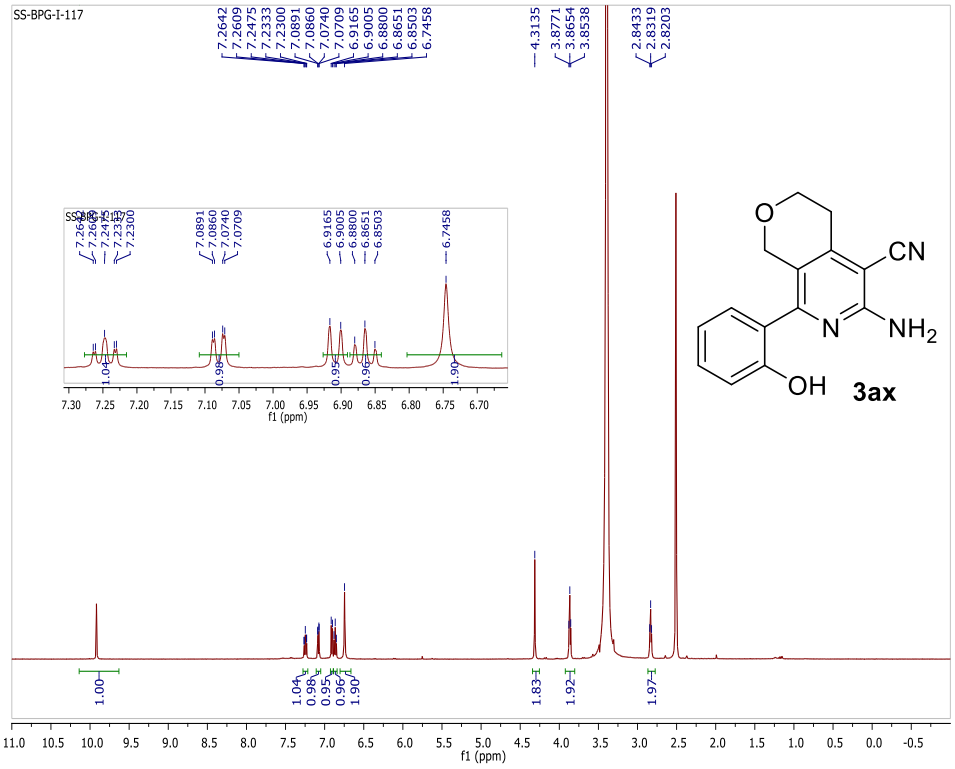

Figure 3.44 500 MHz ^{1}H NMR spectrum of **3ax** in DMSO-d$_6$.

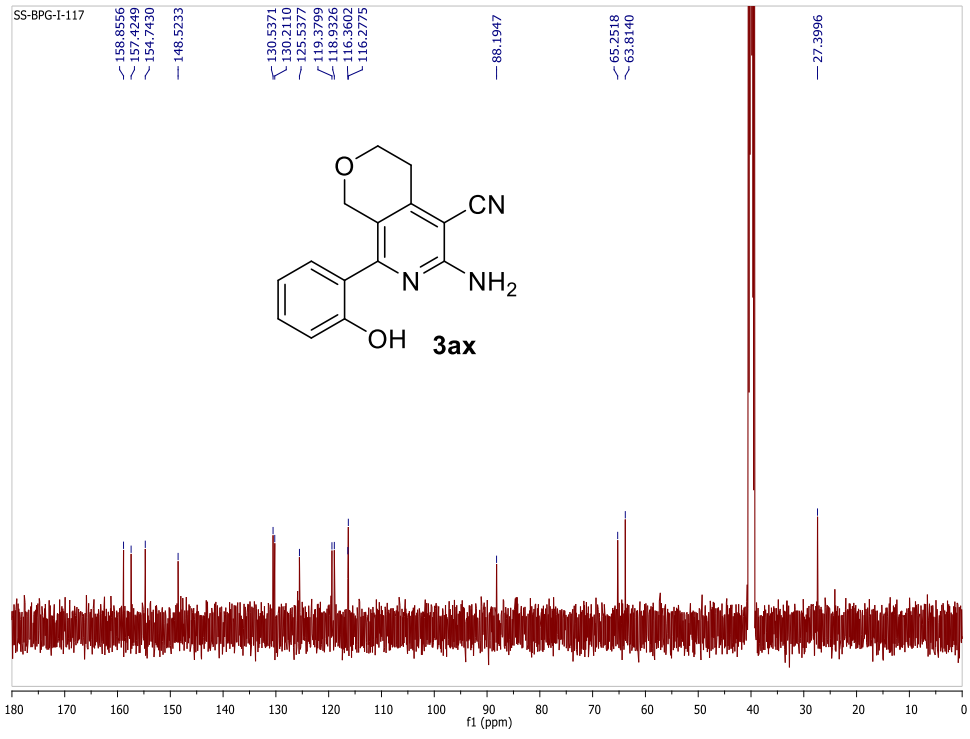

Figure 3.45 125 MHz ^{13}C NMR spectrum of **3ax** in DMSO-d$_6$.

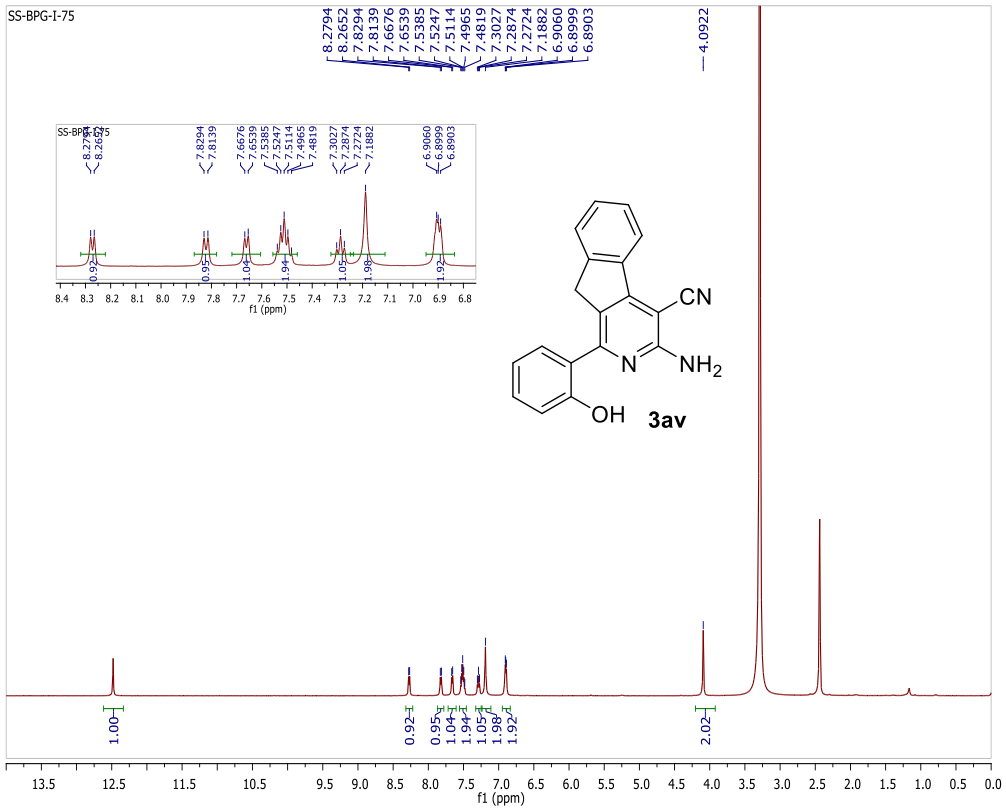

Figure 3.46 500 MHz ^{1}H NMR spectrum of **3av** in DMSO-d$_6$.

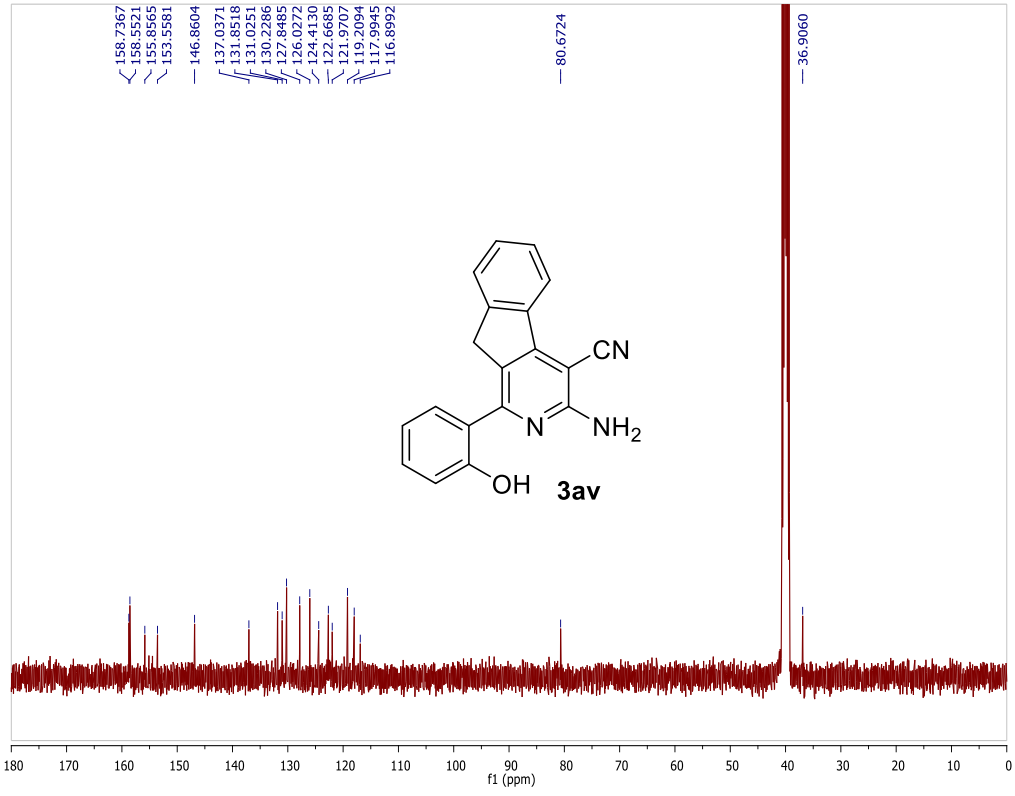

Figure 3.47 125 MHz ^{13}C NMR spectrum of **3av** in DMSO-d$_6$.

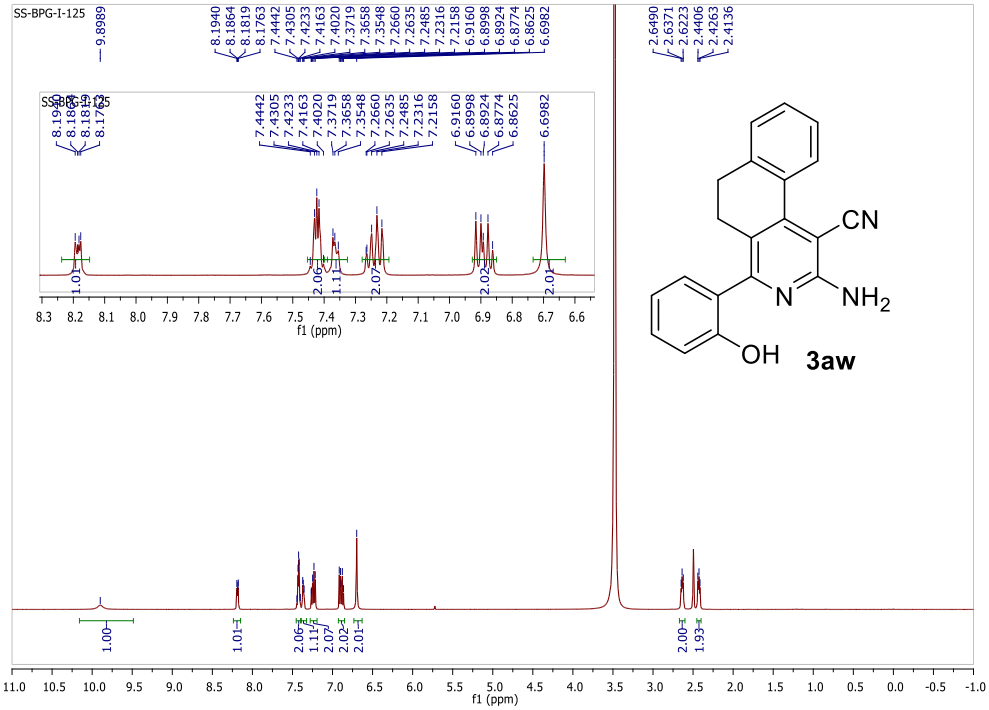

Figure 3.48 500 MHz ^{1}H NMR spectrum of **3aw** in DMSO-d$_6$.

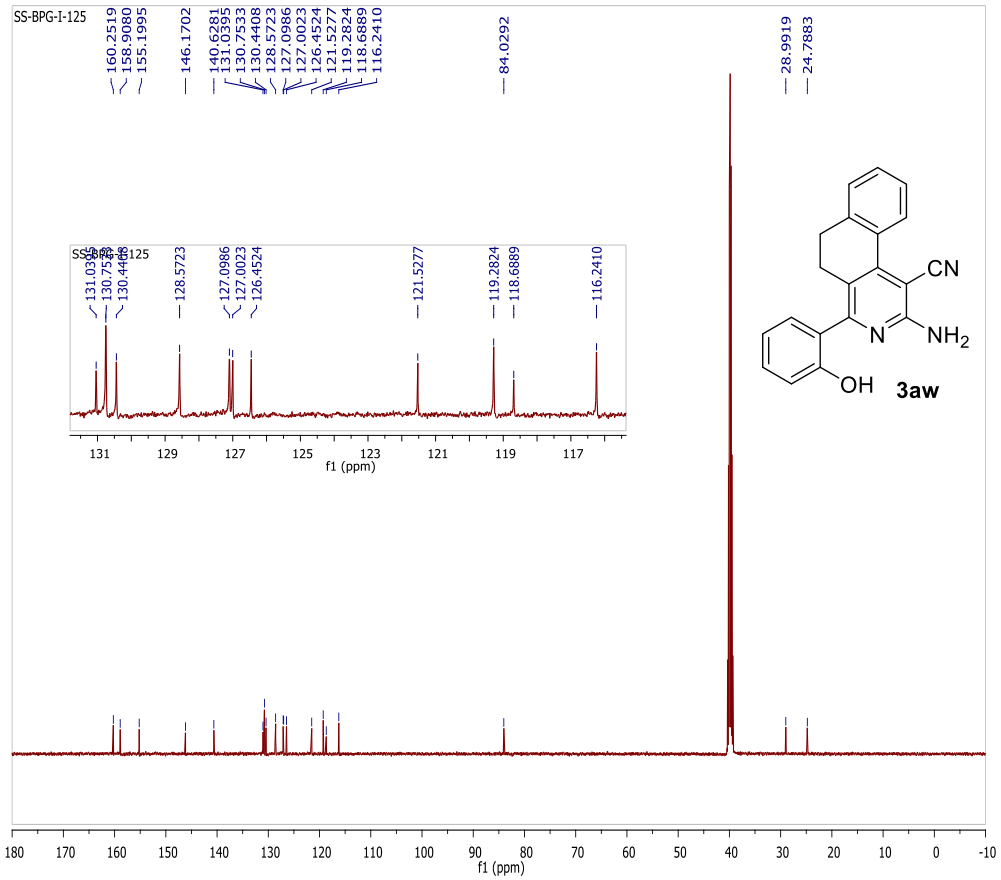

Figure 3.49 125 MHz ^{13}C NMR spectrum of **3aw** in DMSO-d$_6$.

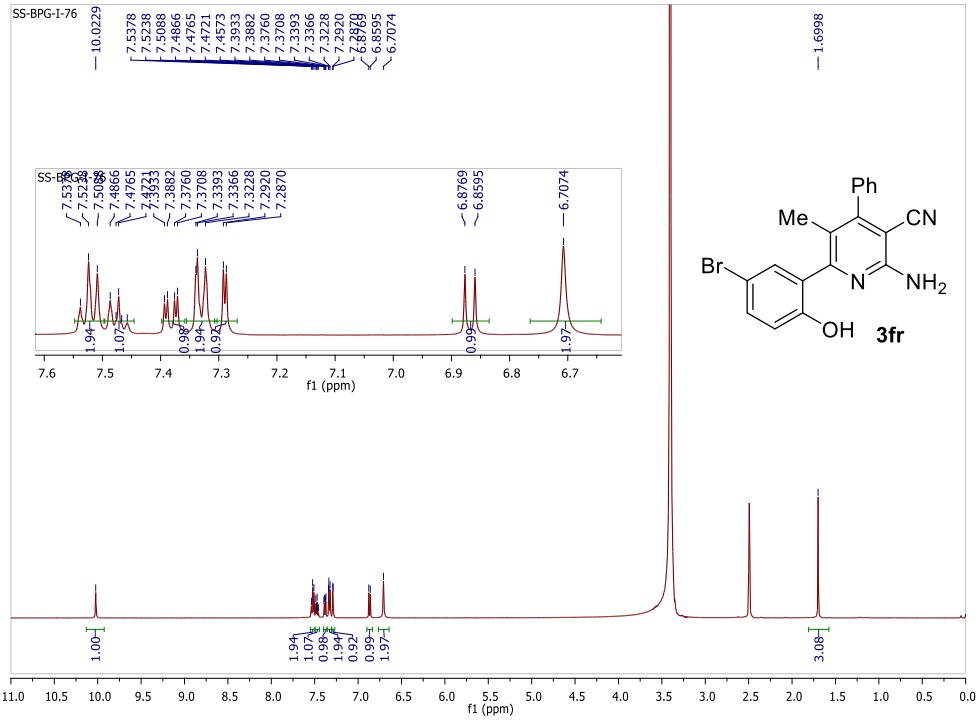

Figure 3.50 500 MHz ^{1}H NMR spectrum of **3fr** in DMSO-d$_6$.

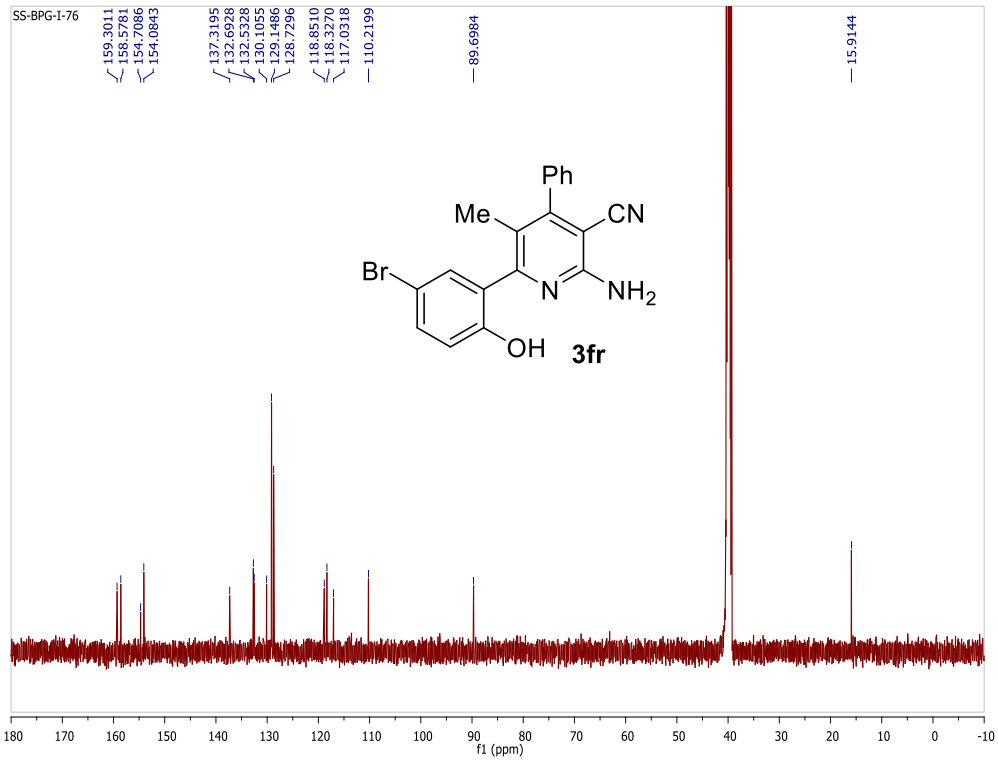

Figure 3.51 125 MHz ^{13}C NMR spectrum of **3fr** in DMSO-d$_6$.

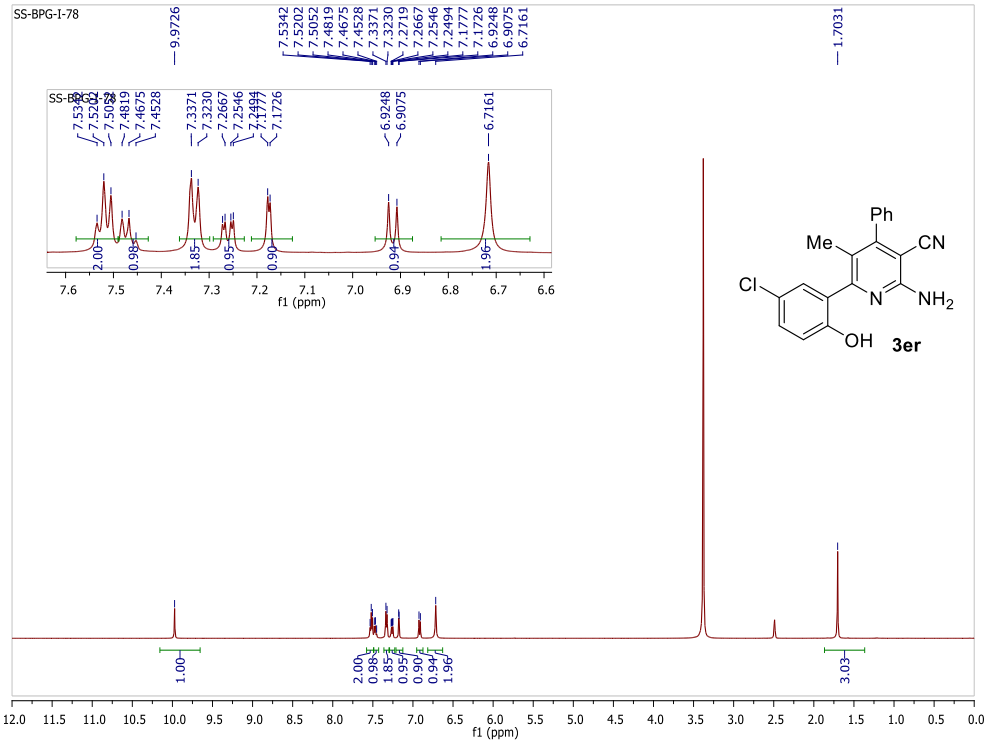

Figure 3.52 500 MHz ^{1}H NMR spectrum of **3er** in DMSO-d$_6$.

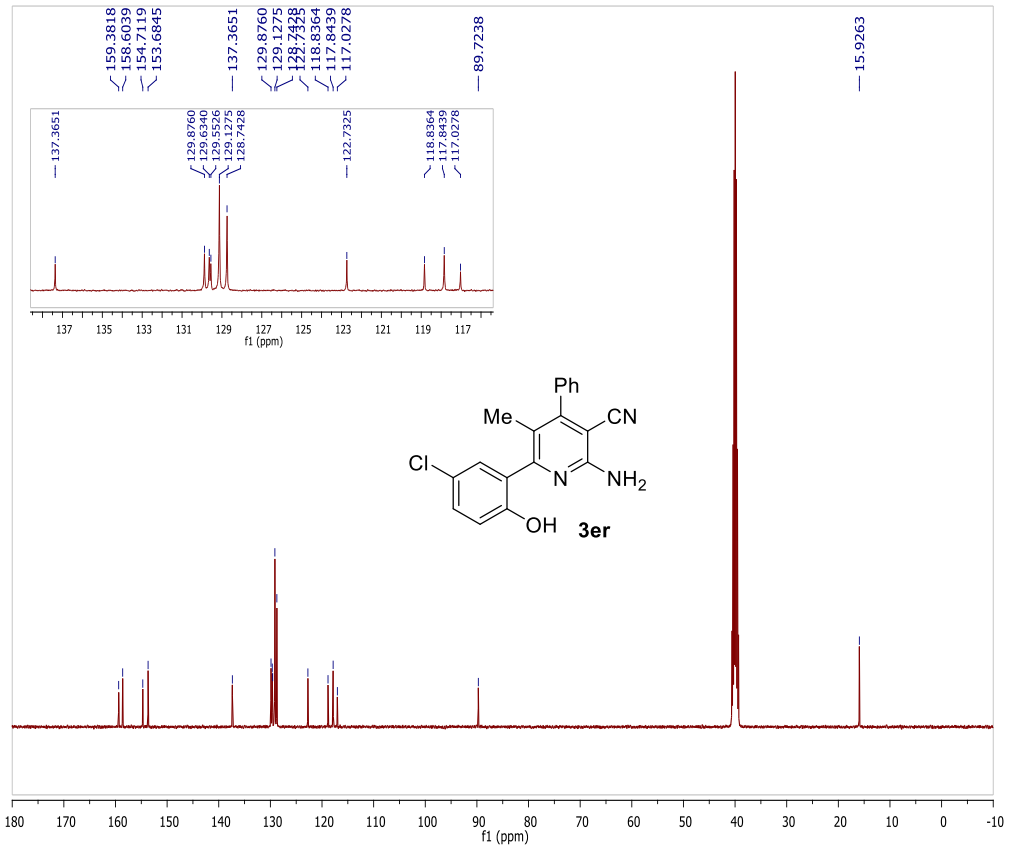

Figure 3.53 125 MHz ^{13}C NMR spectrum of **3er** in DMSO-d$_6$.

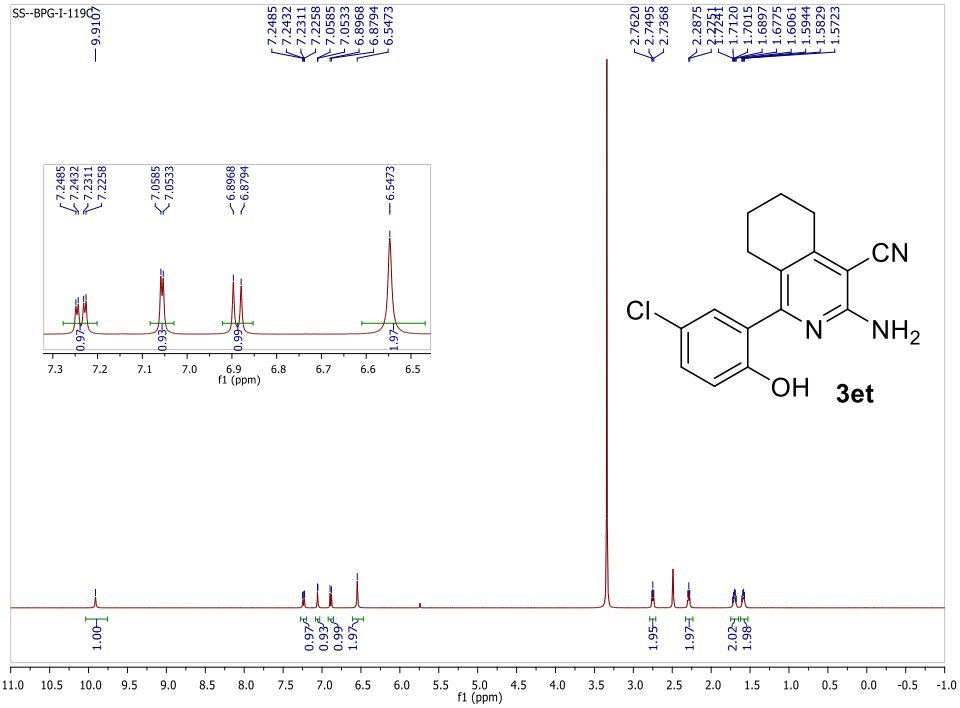

Figure 3.54 500 MHz ^{1}H NMR spectrum of **3et** in DMSO-d_6.

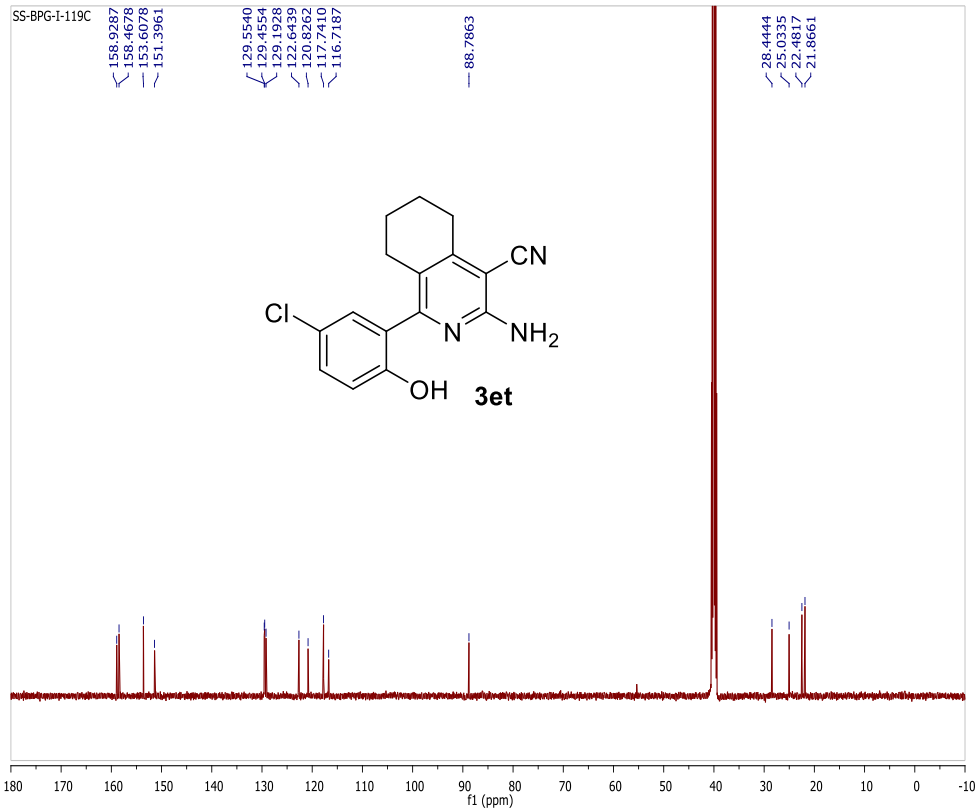

Figure 3.55 125 MHz ^{13}C NMR spectrum of **3et** in DMSO-d_6.

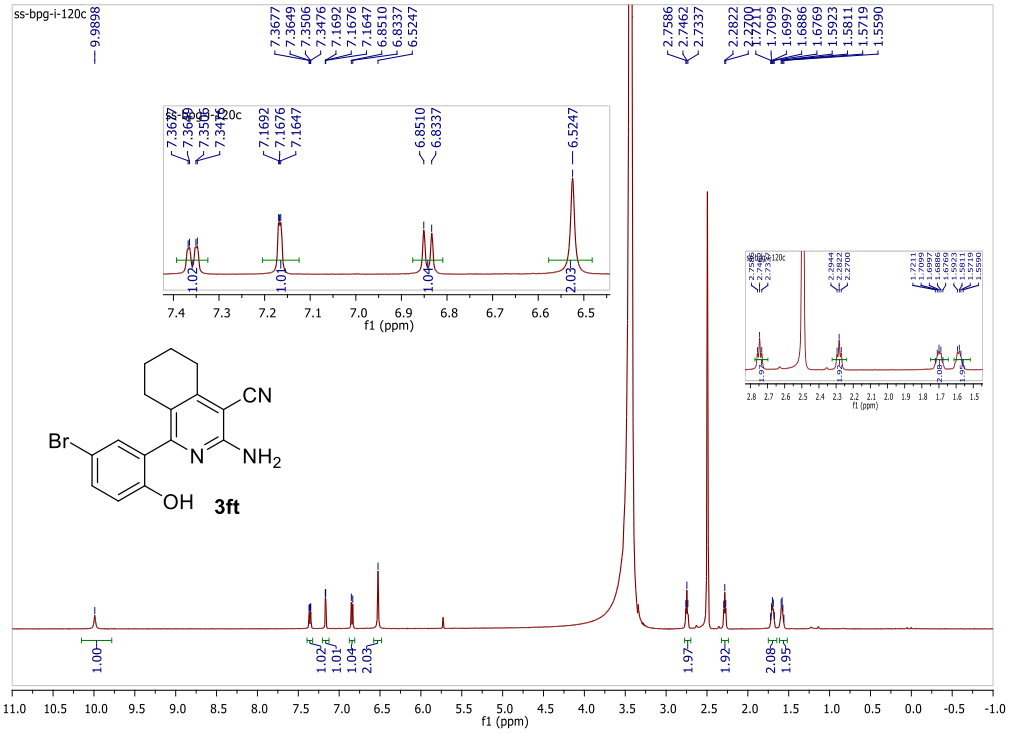

Figure 3.56 500 MHz ^{1}H NMR spectrum of **3ft** in DMSO-d$_6$.

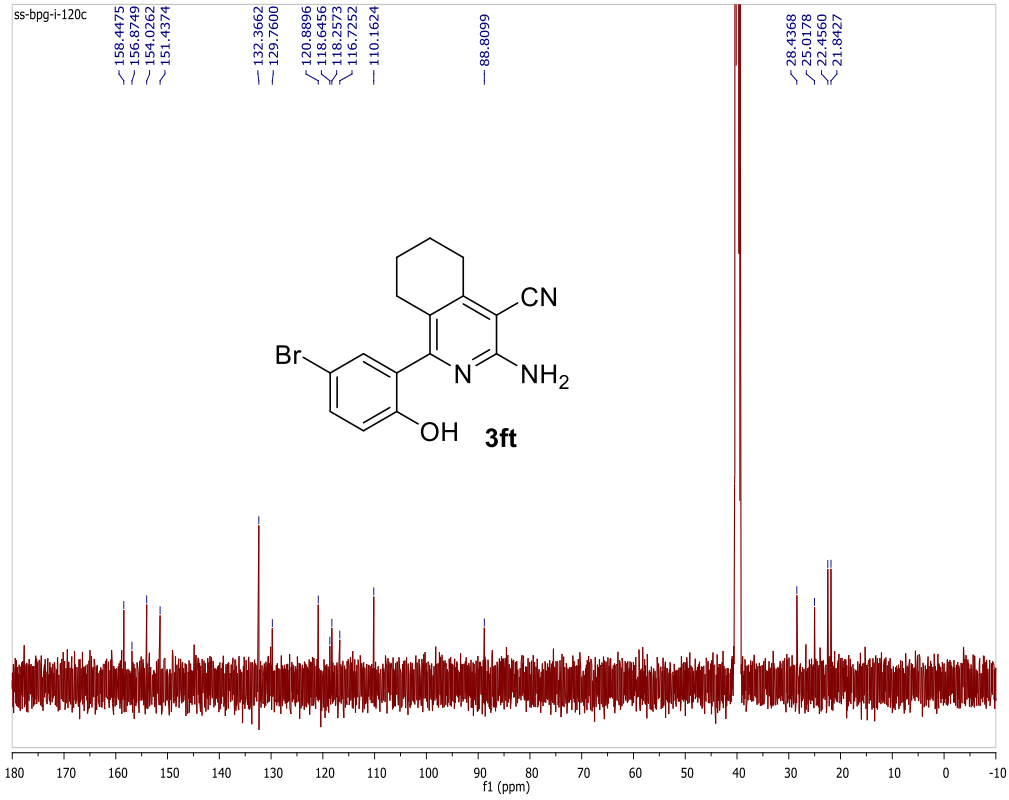

Figure 3.57 125 MHz ^{13}C NMR spectrum of **3ft** in DMSO-d$_6$.

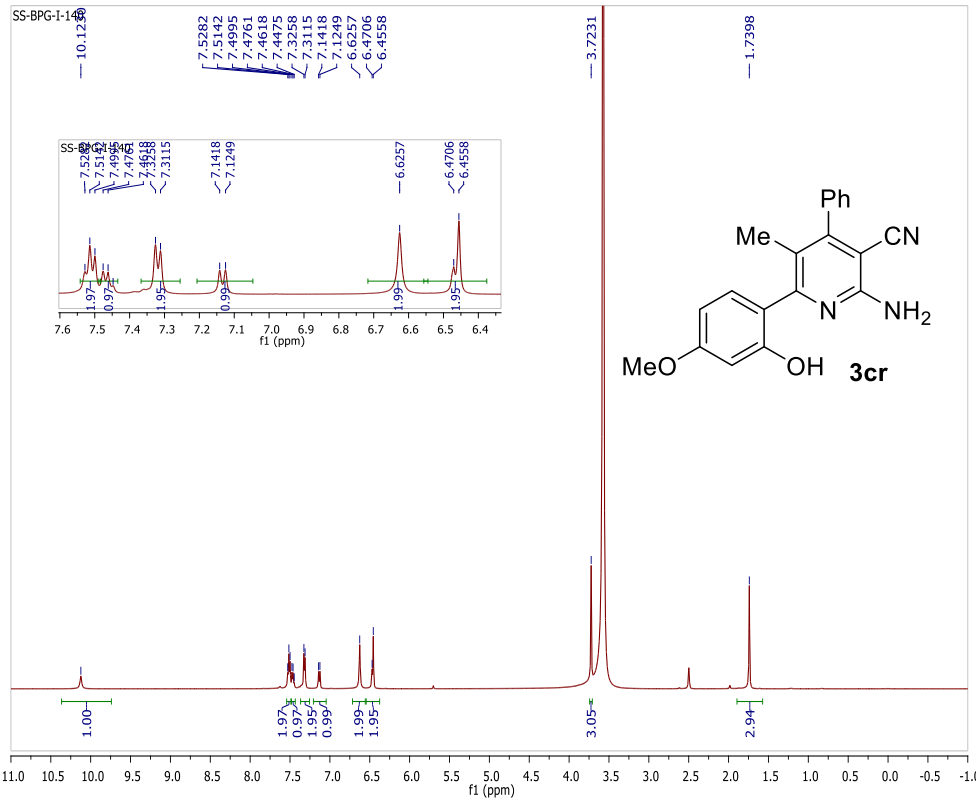

Figure 3.58 500 MHz ^{1}H NMR spectrum of **3cr** in DMSO-d$_6$.

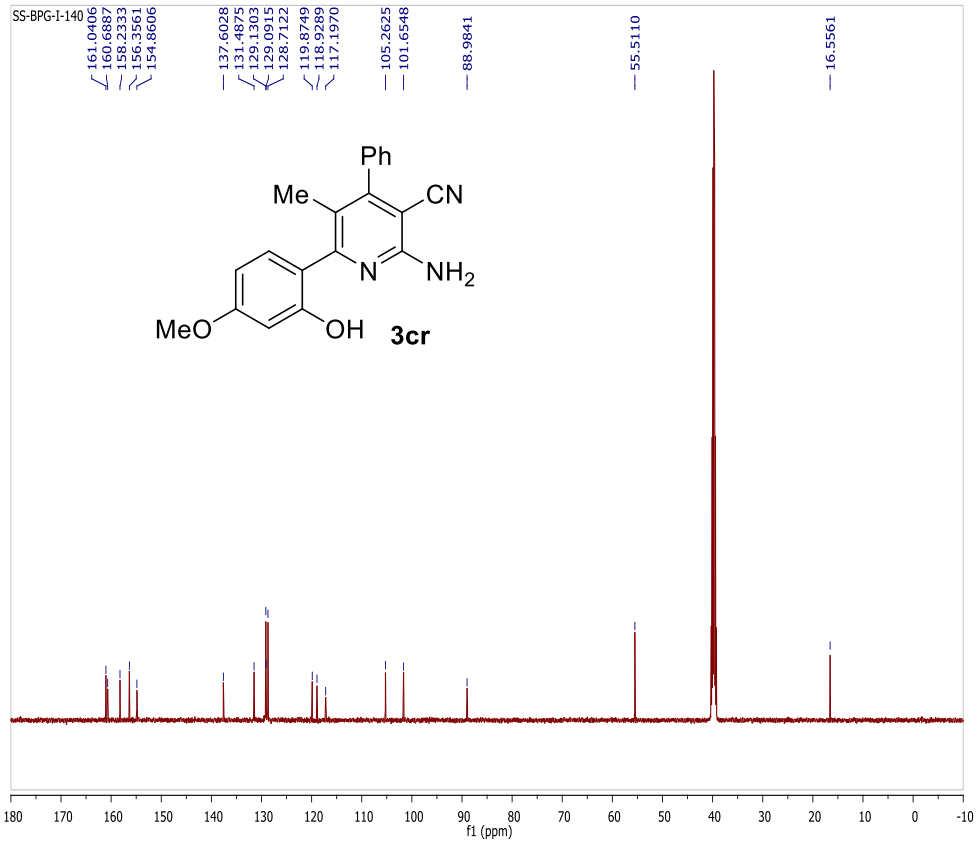

Figure 3.59 125 MHz ^{13}C NMR spectrum of **3cr** in DMSO-d$_6$.

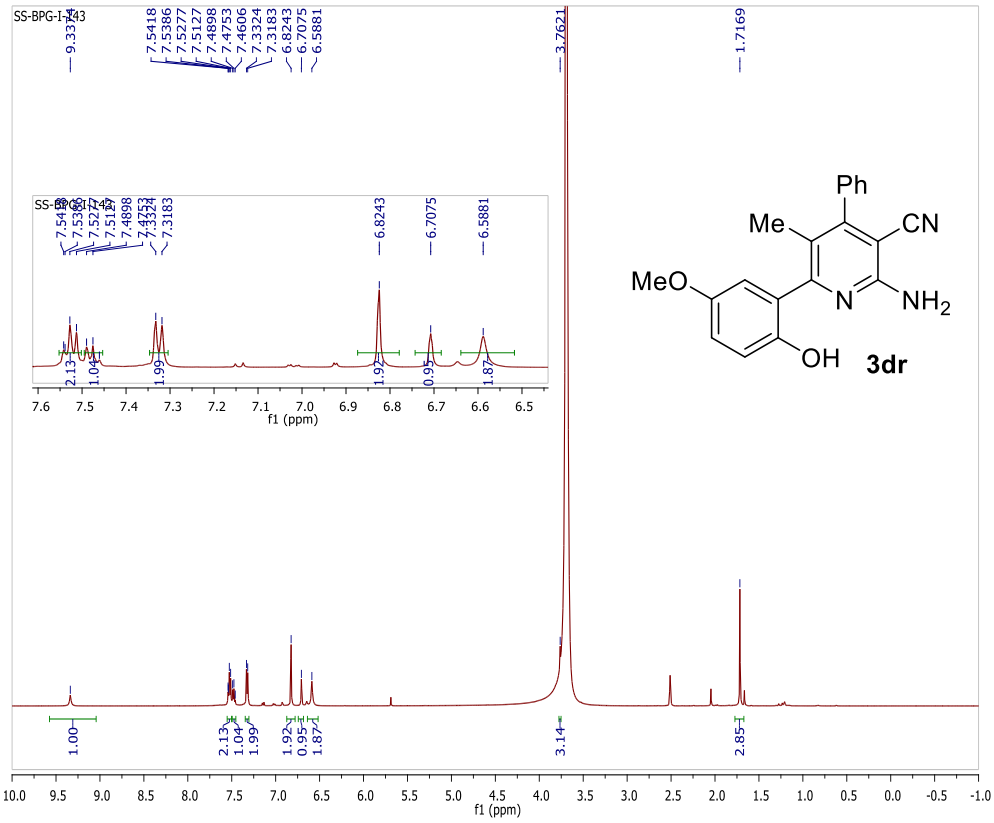

Figure 3.60 500 MHz ^{1}H NMR spectrum of **3dr** in DMSO-d_6.

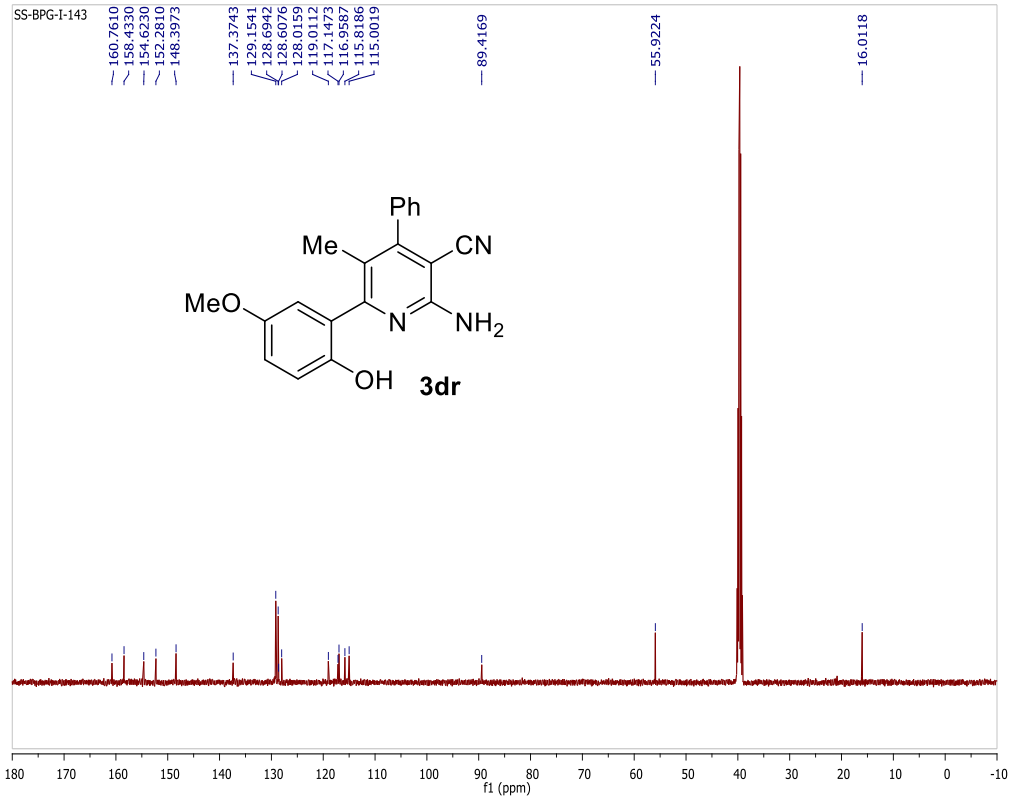

Figure 3.61 125 MHz ^{13}C NMR spectrum of **3dr** in DMSO-d_6.

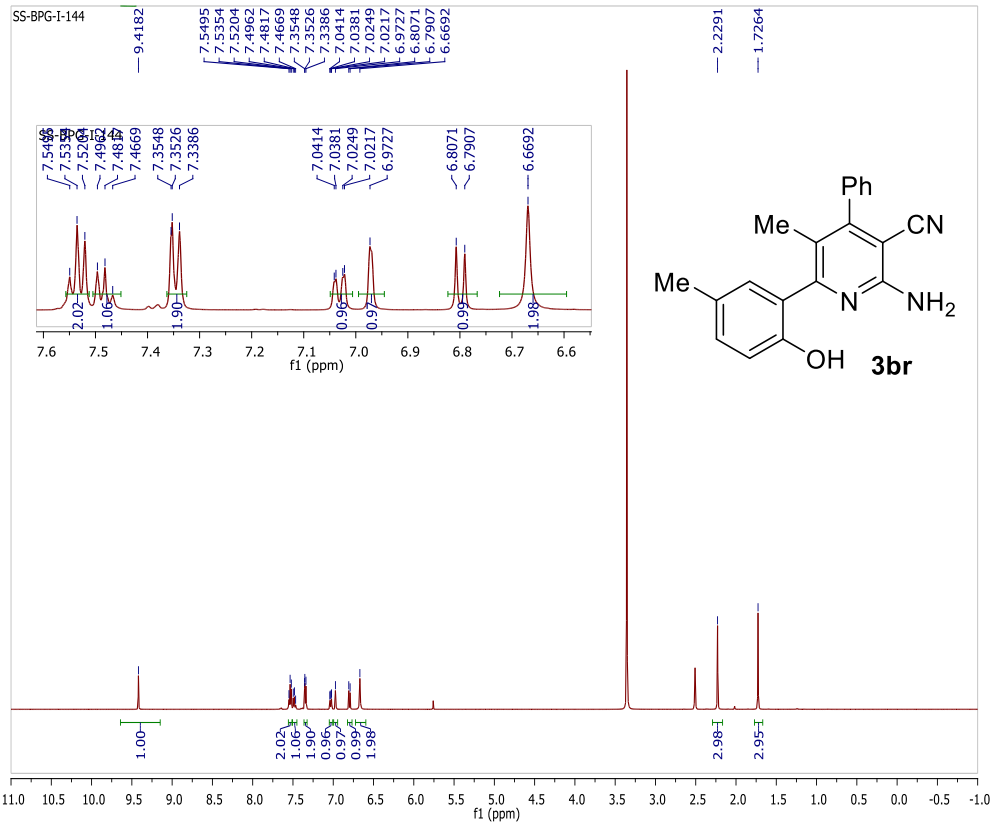

Figure 3.62 500 MHz ^{1}H NMR spectrum of **3br** in DMSO-d_6.

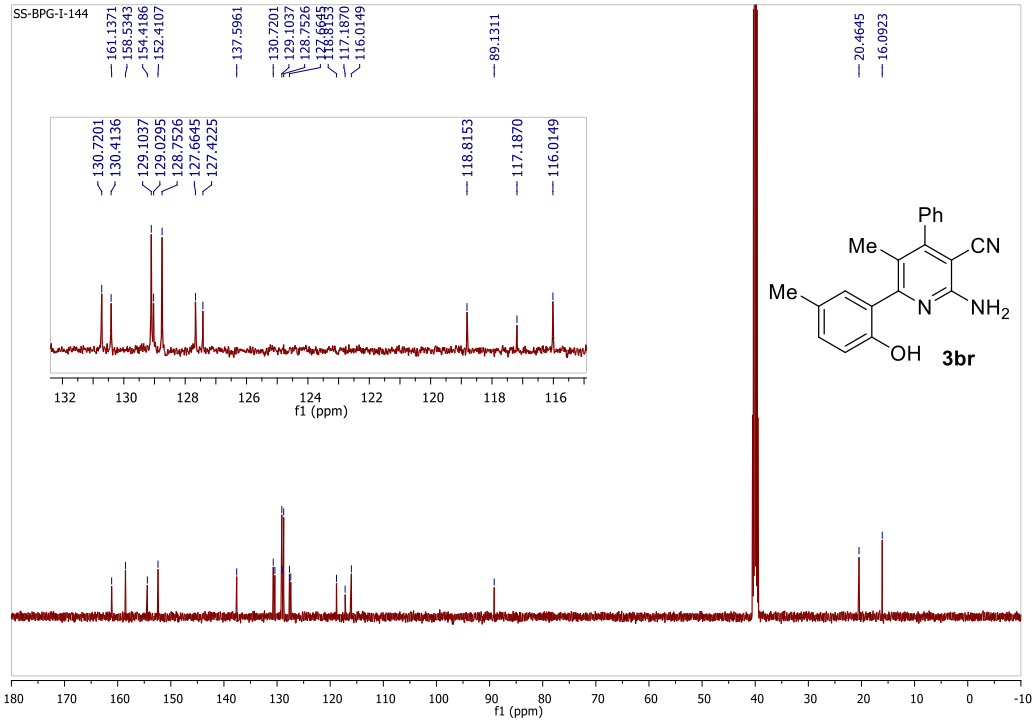

Figure 3.63 125 MHz ^{13}C NMR spectrum of **3br** in DMSO-d_6.

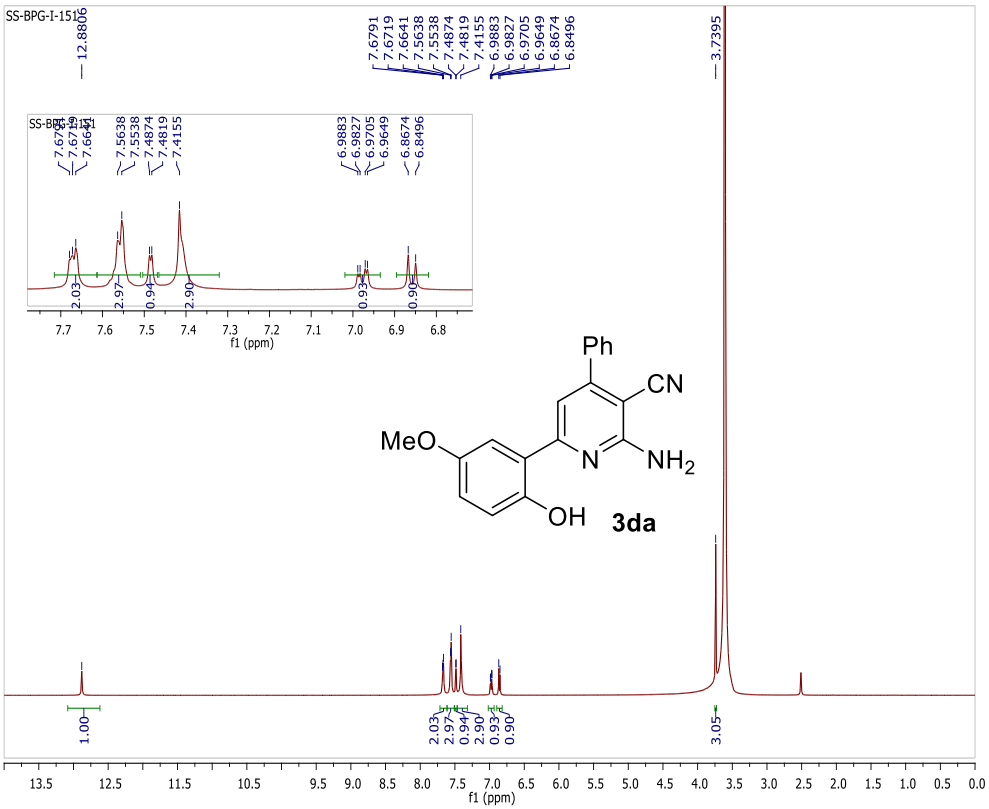

Figure 3.64 500 MHz ^{1}H NMR spectrum of **3da** in DMSO-d_6.

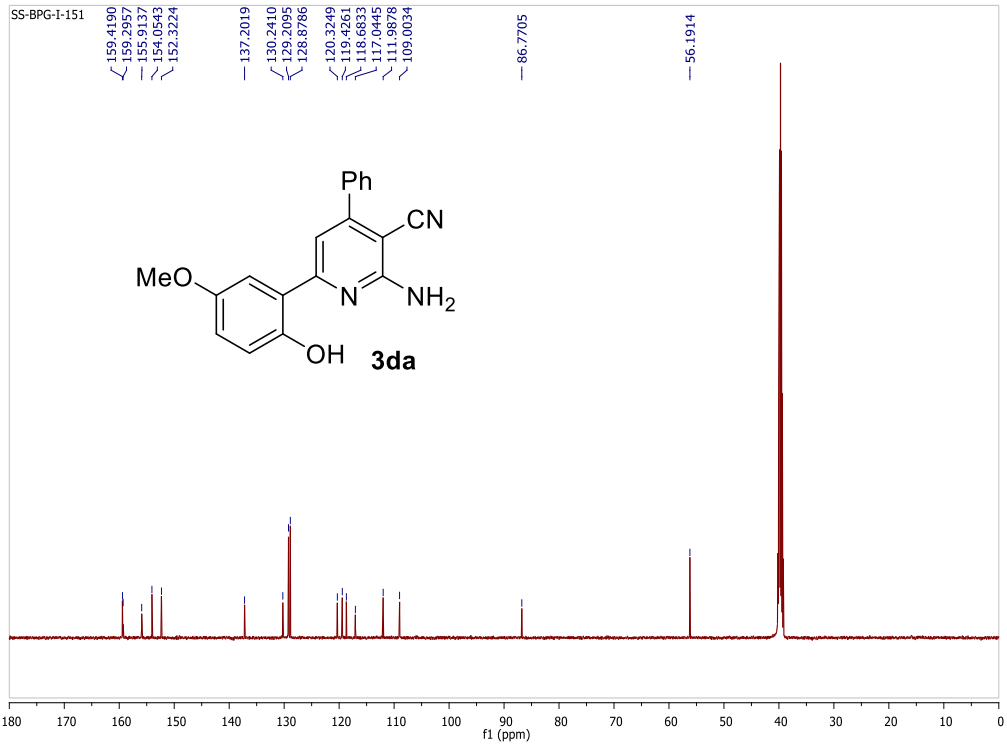

Figure 3.65 125 MHz ^{13}C NMR spectrum of **3da** in DMSO-d_6.

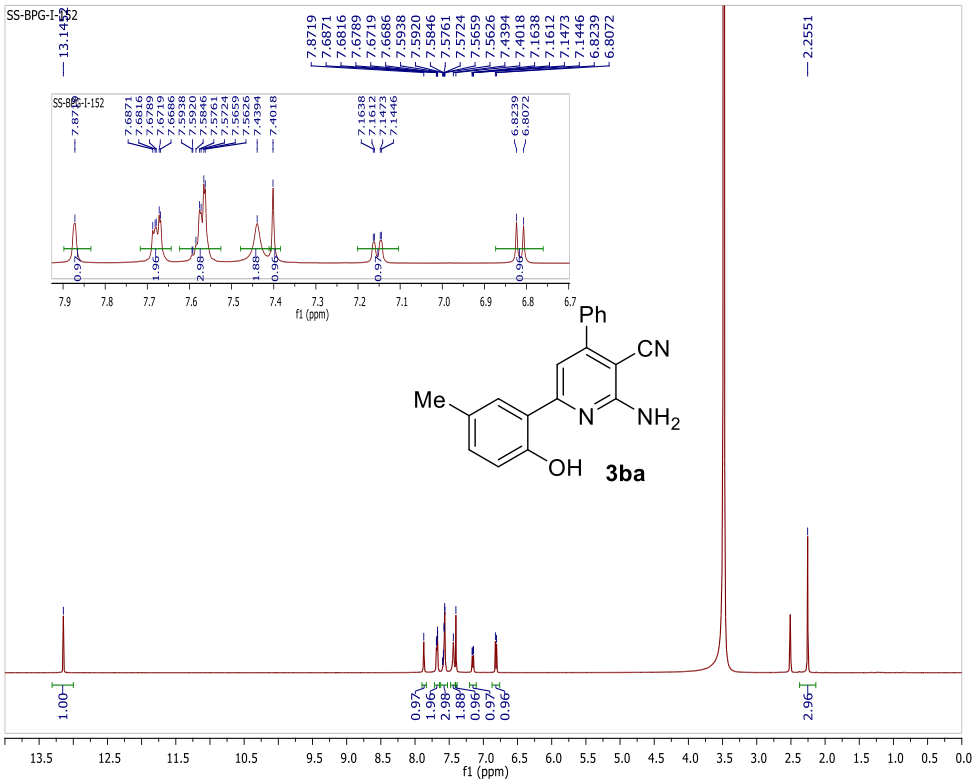

Figure 3.66 500 MHz ^{1}H NMR spectrum of **3ba** in DMSO-d$_6$.

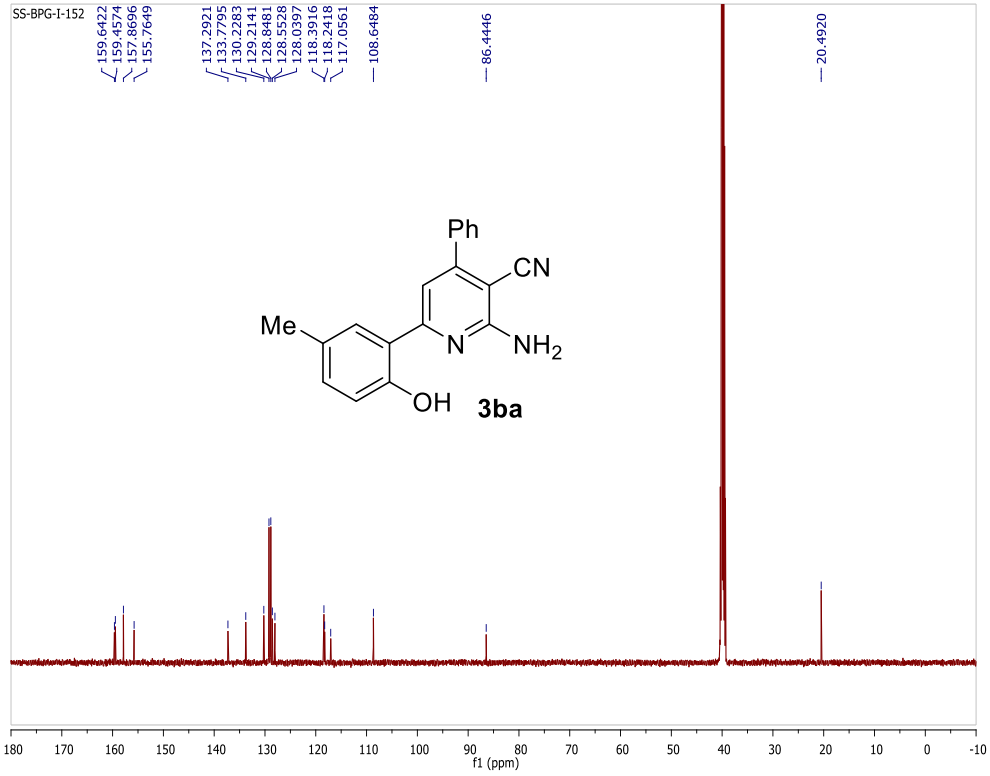

Figure 3.67 125 MHz ^{13}C NMR spectrum of **3ba** in DMSO-d$_6$.

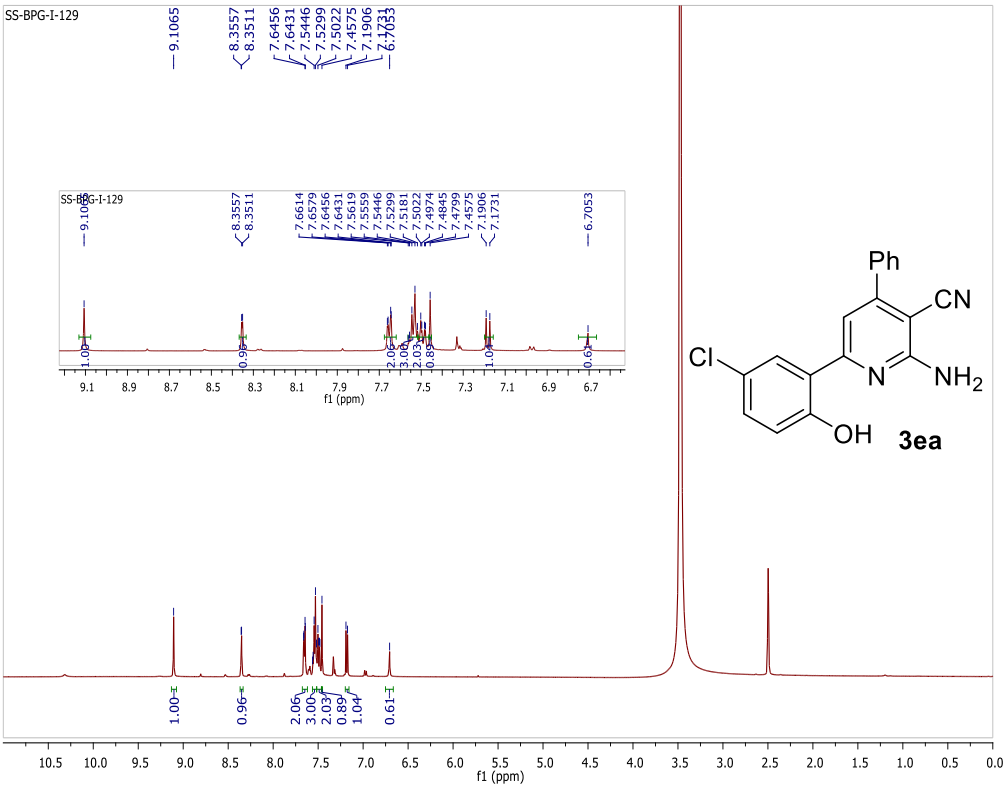

Figure 3.68 500 MHz ^{1}H NMR spectrum of **3ea** in DMSO-d_6.

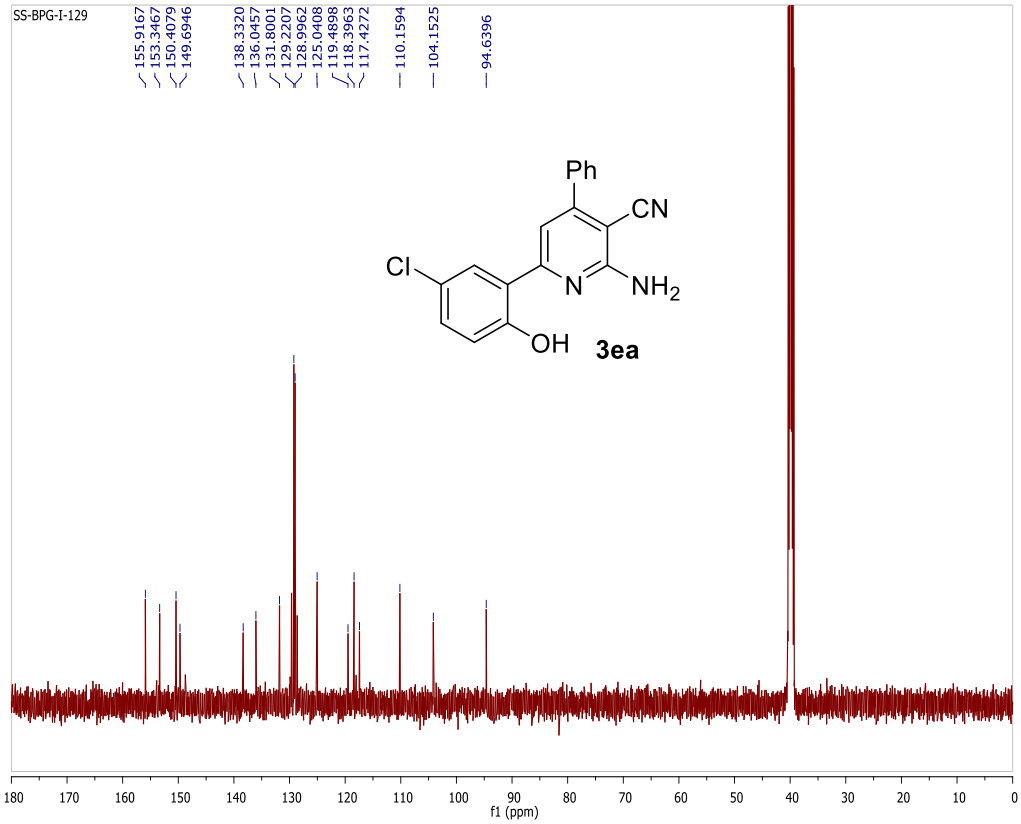

Figure 3.69 125 MHz ^{13}C NMR spectrum of **3ea** in DMSO-d_6.

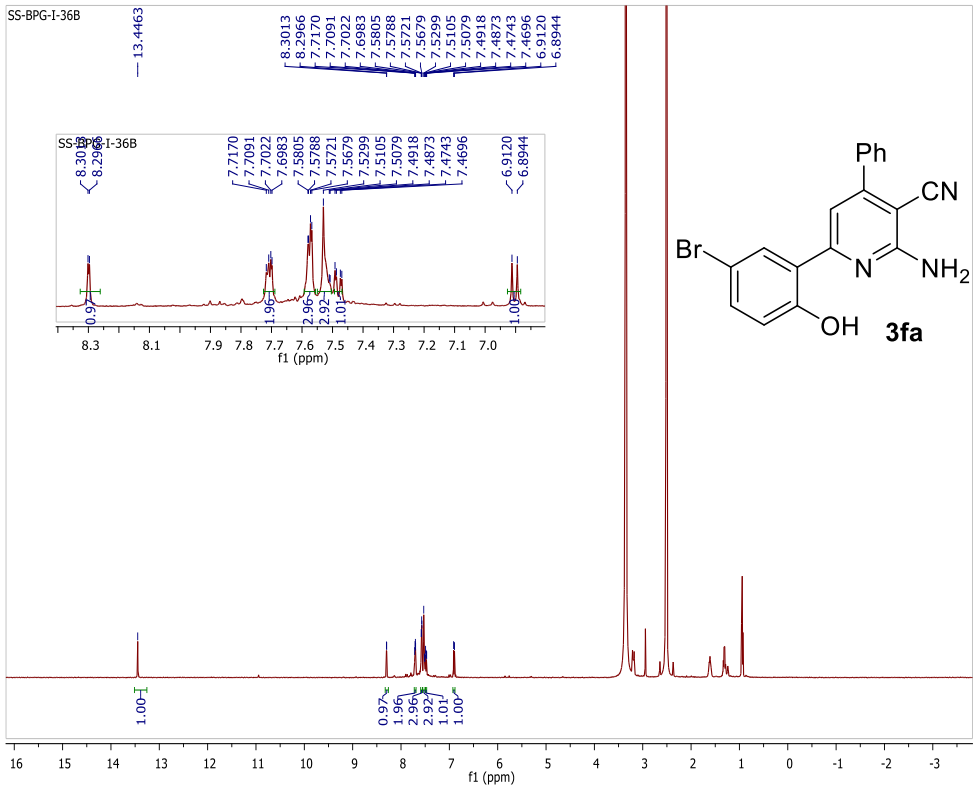

Figure 3.70 500 MHz ^{1}H NMR spectrum of **3fa** in DMSO-d_6.

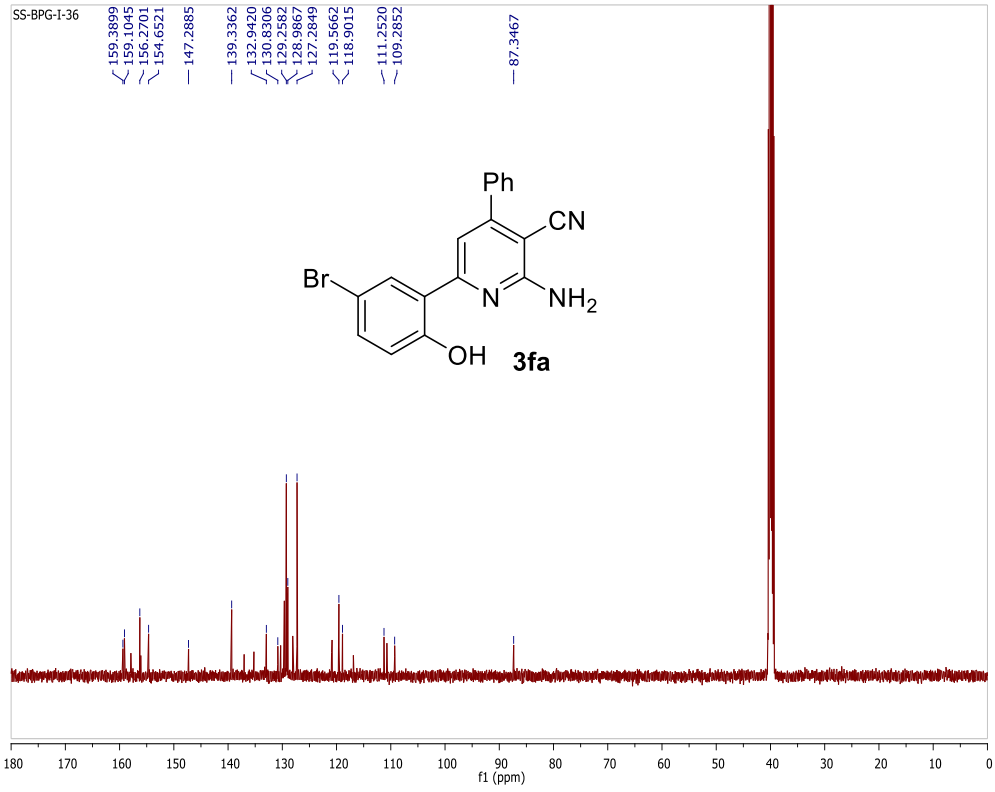

Figure 3.71 125 MHz ^{13}C NMR spectrum of **3fa** in DMSO-d_6.

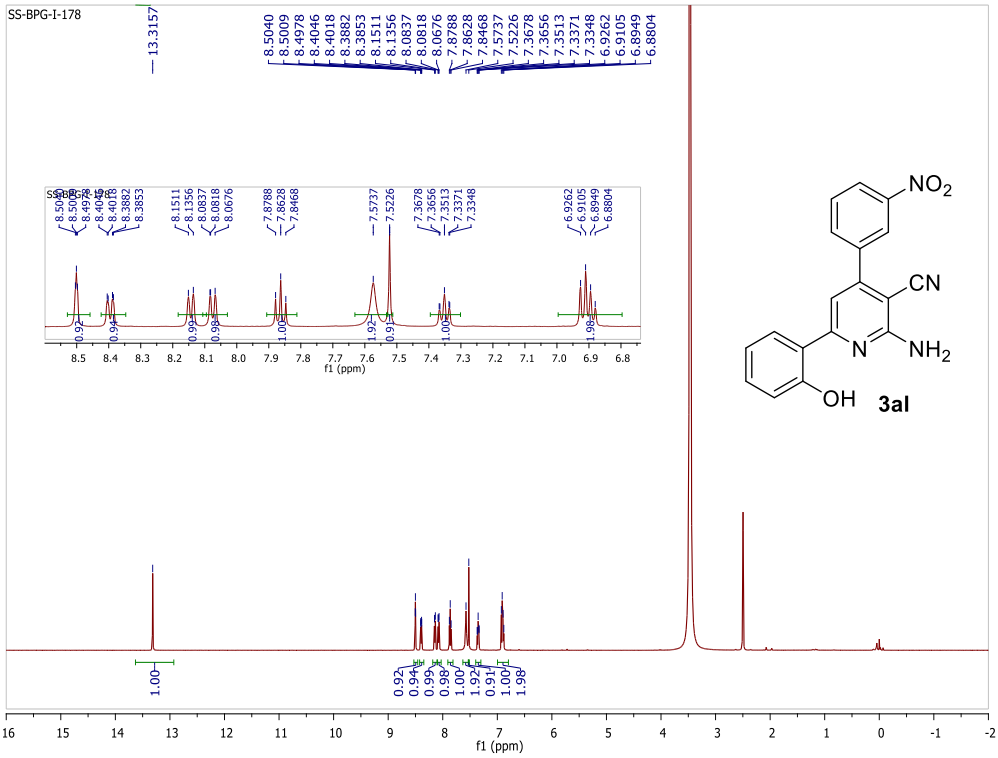

Figure 3.72 500 MHz ^{1}H NMR spectrum of **3al** in DMSO-d_6.

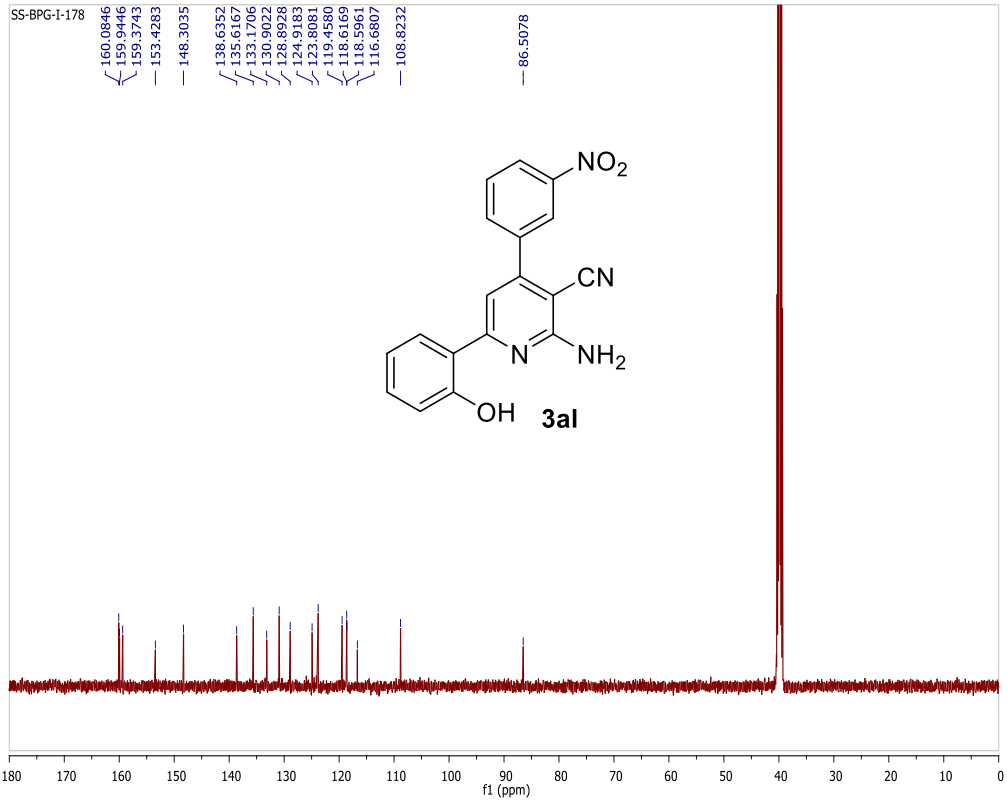

Figure 3.73 125 MHz ^{13}C NMR spectrum of **3al** in DMSO-d_6.

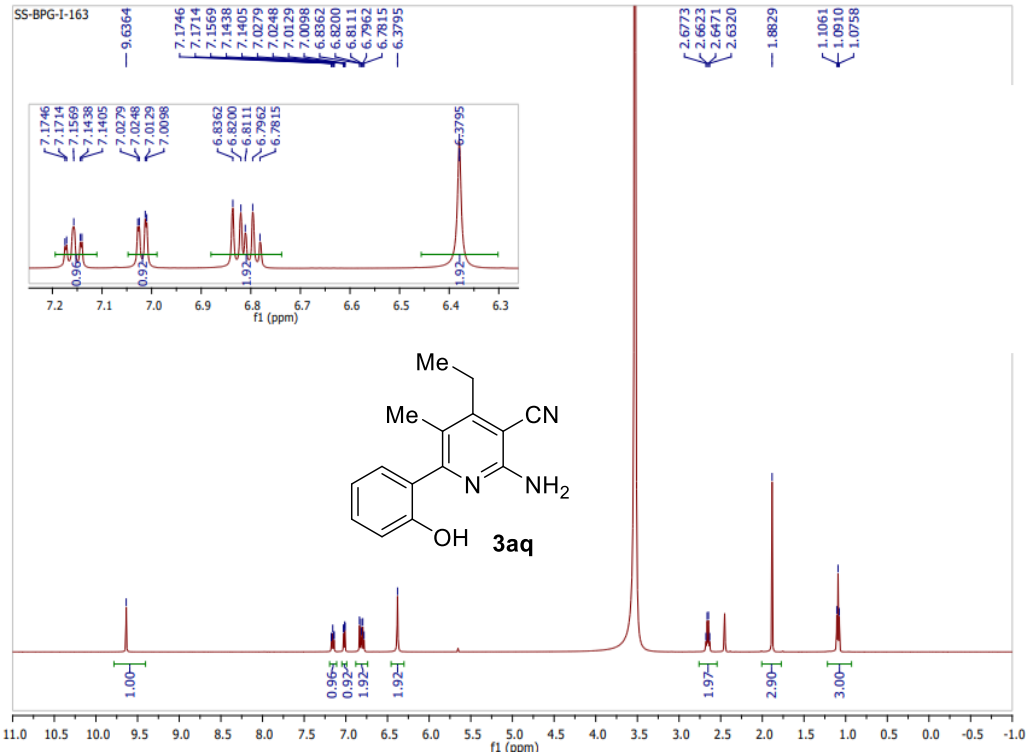

Figure 3.74 500 MHz ^{1}H NMR spectrum of **3aq** in DMSO-d$_6$.

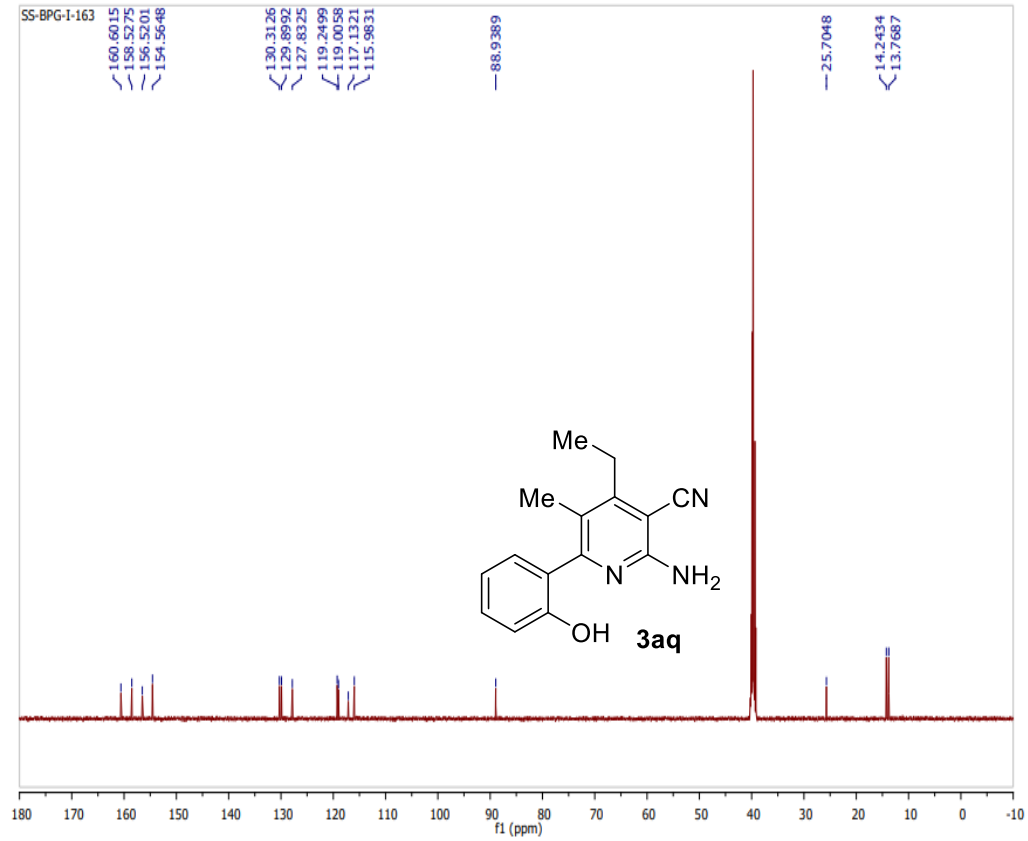

Figure 3.75 125 MHz ^{13}C NMR spectrum of **3aq** in DMSO-d$_6$.

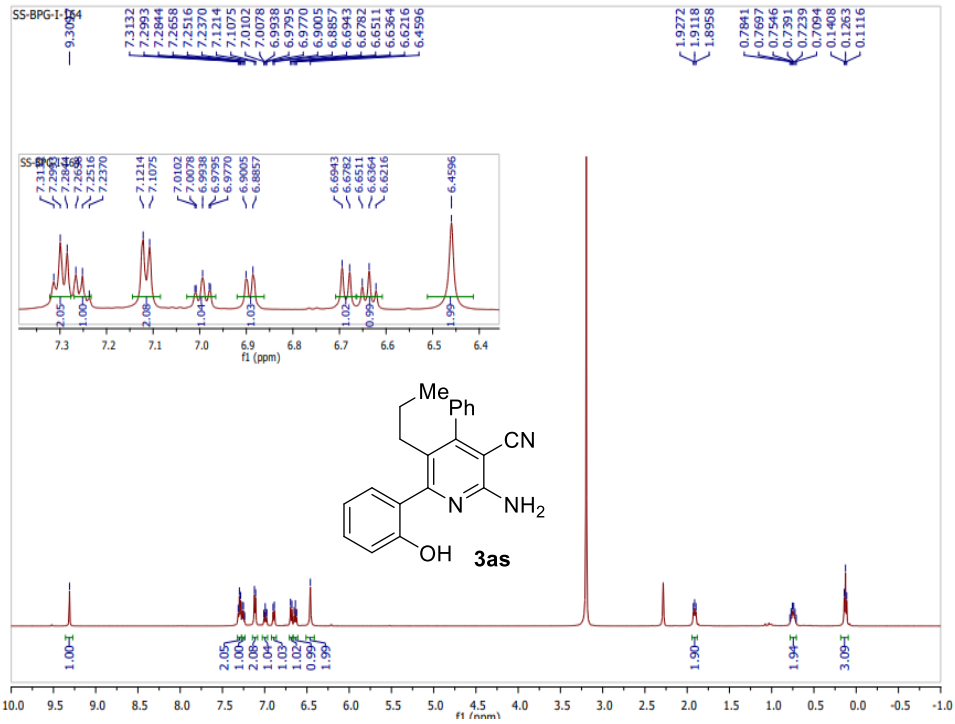

Figure 3.76 500 MHz ^{1}H NMR spectrum of **3as** in DMSO-d$_6$.

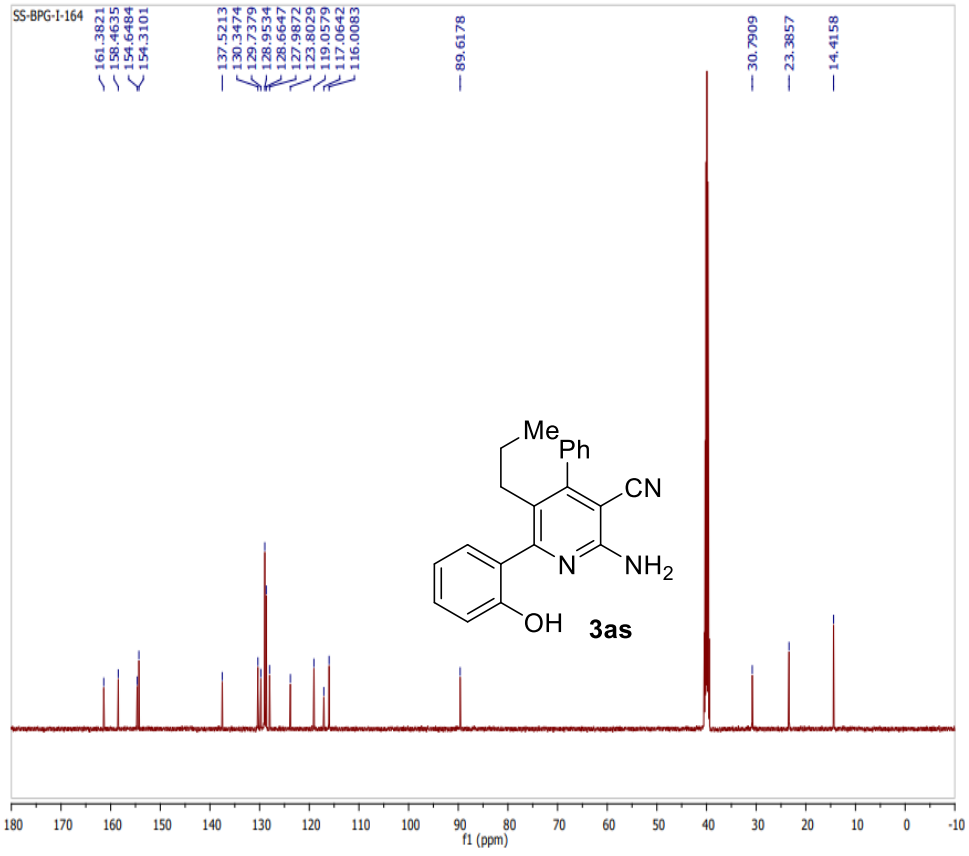

Figure 3.77 125 MHz ^{13}C NMR spectrum of **3as** in DMSO-d$_6$.

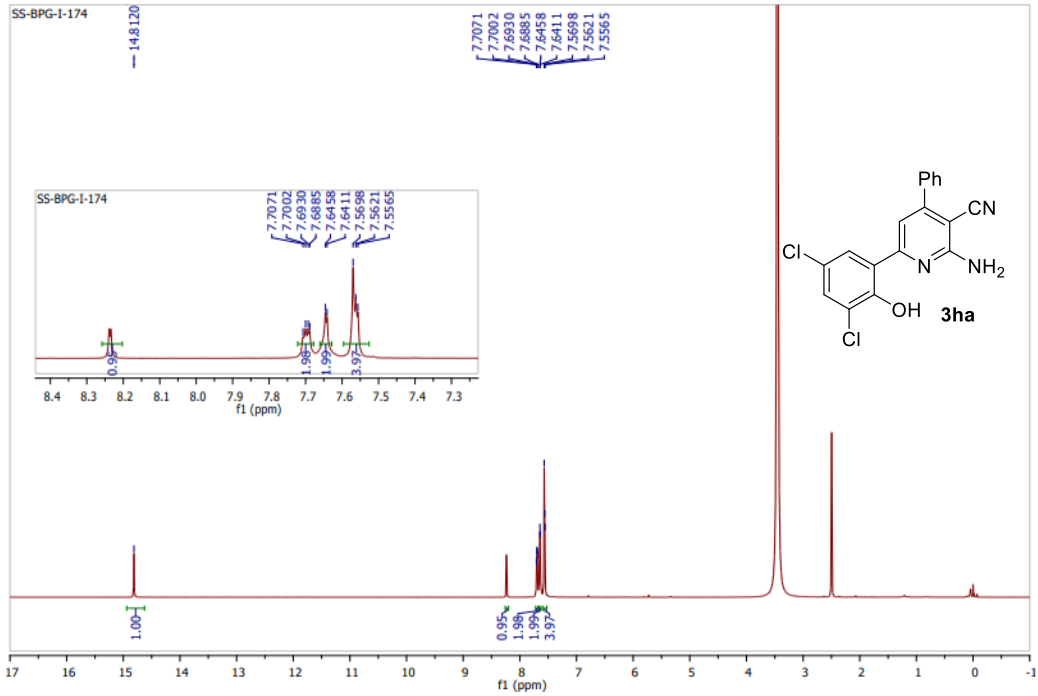

Figure 3.78 500 MHz ^{1}H NMR spectrum of **3ha** in DMSO-d_6.

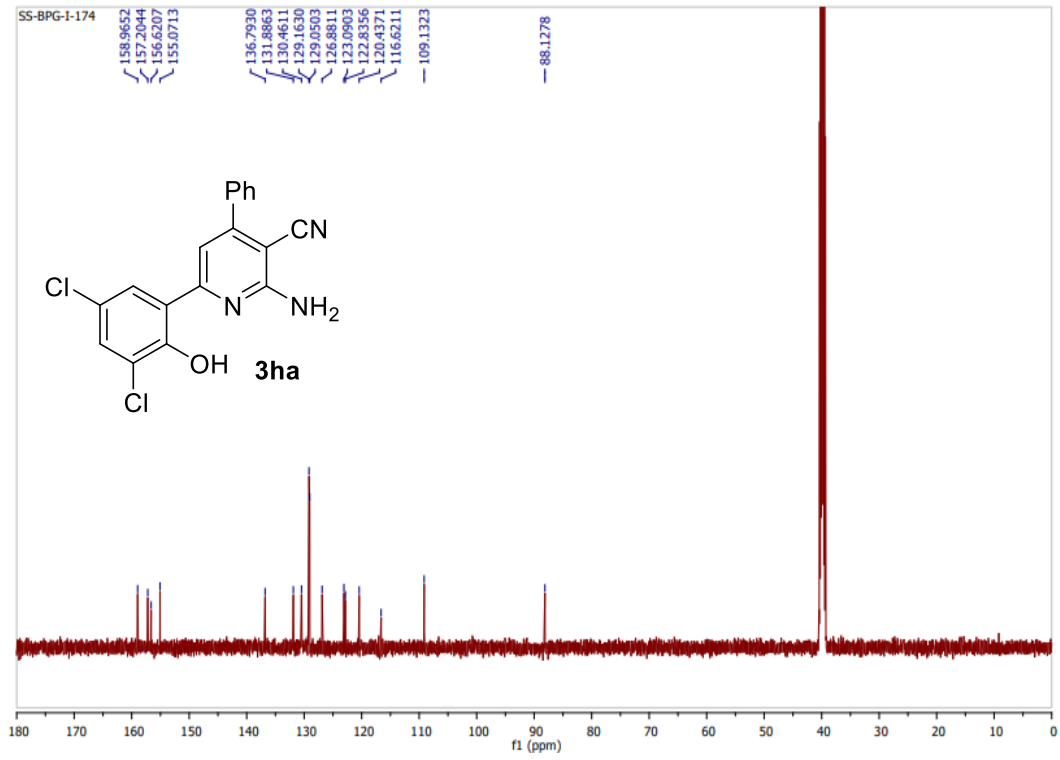

Figure 3.79 125 MHz ^{13}C NMR spectrum of **3ha** in DMSO-d_6.

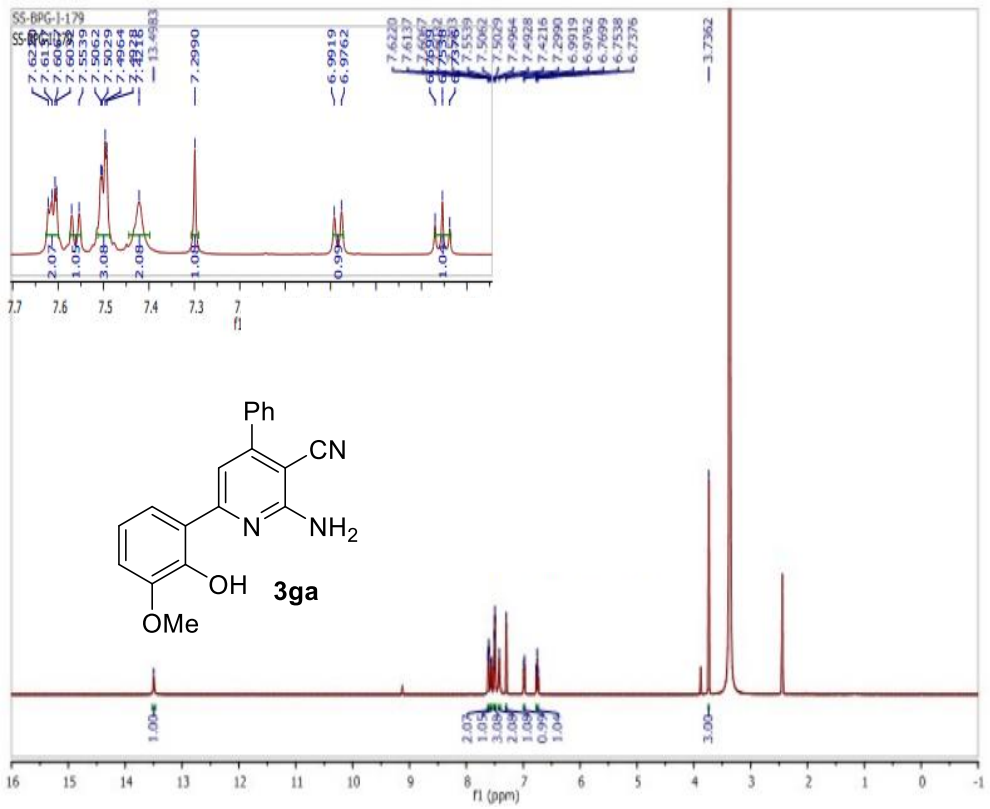

Figure 3.80 500 MHz ^{1}H NMR spectrum of **3ga** in DMSO-d_6.

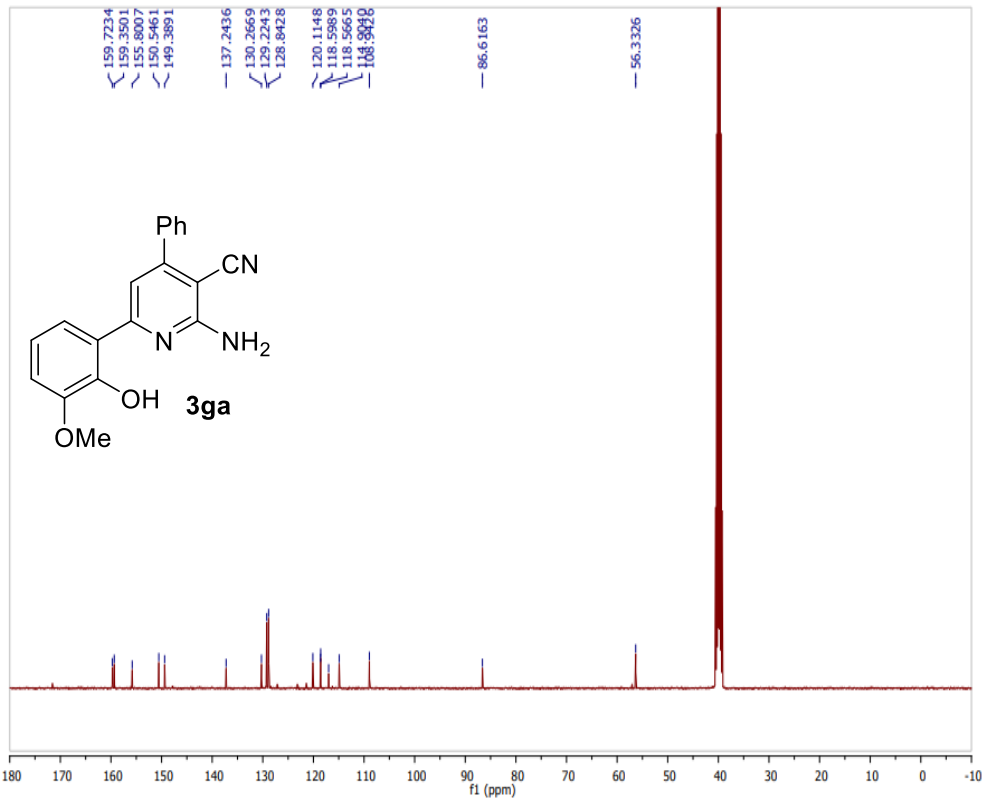

Figure 3.81 125 MHz ^{13}C NMR spectrum of **3ga** in DMSO-d_6.

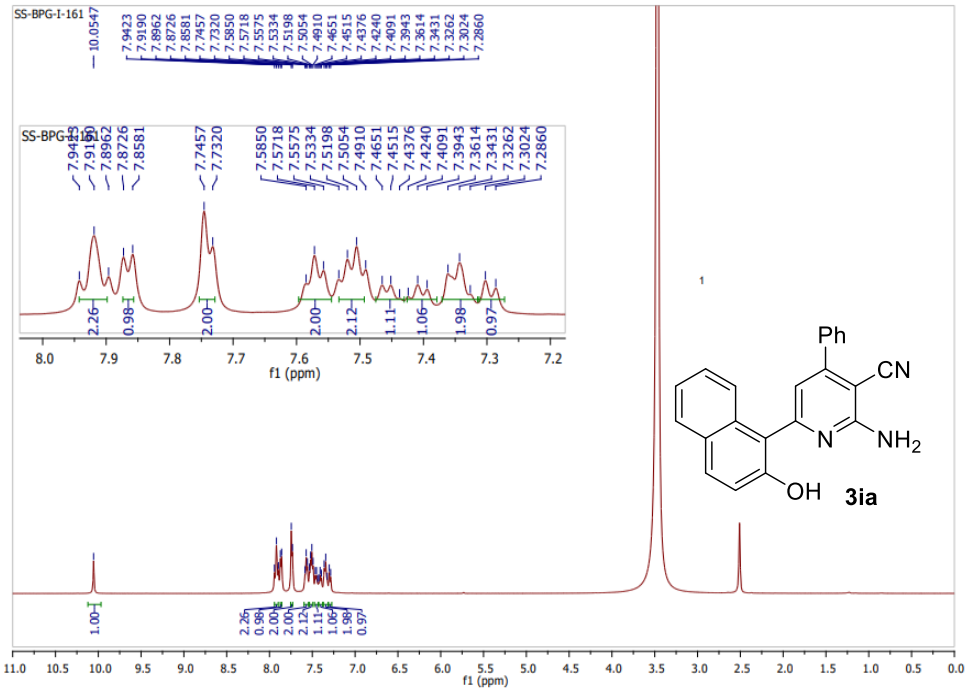

Figure 3.82 500 MHz ^{1}H NMR spectrum of **3ia** in DMSO-d_6.

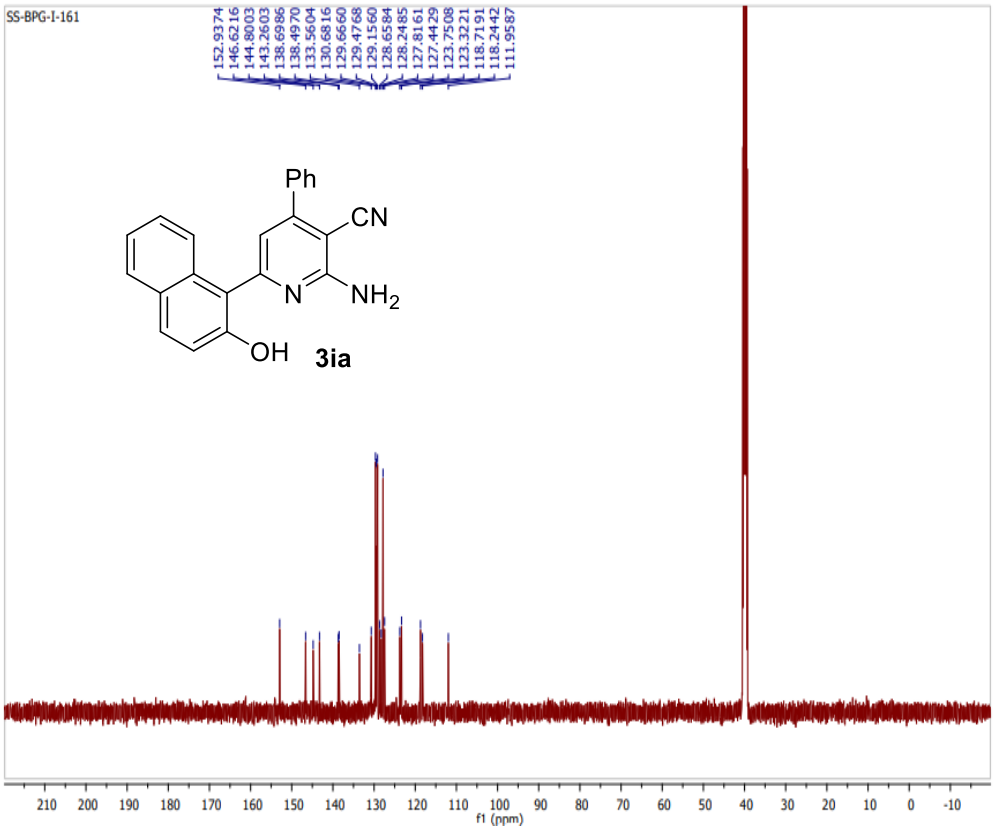

Figure 3.83 125 MHz ^{13}C NMR spectrum of **3ia** in DMSO-d_6.

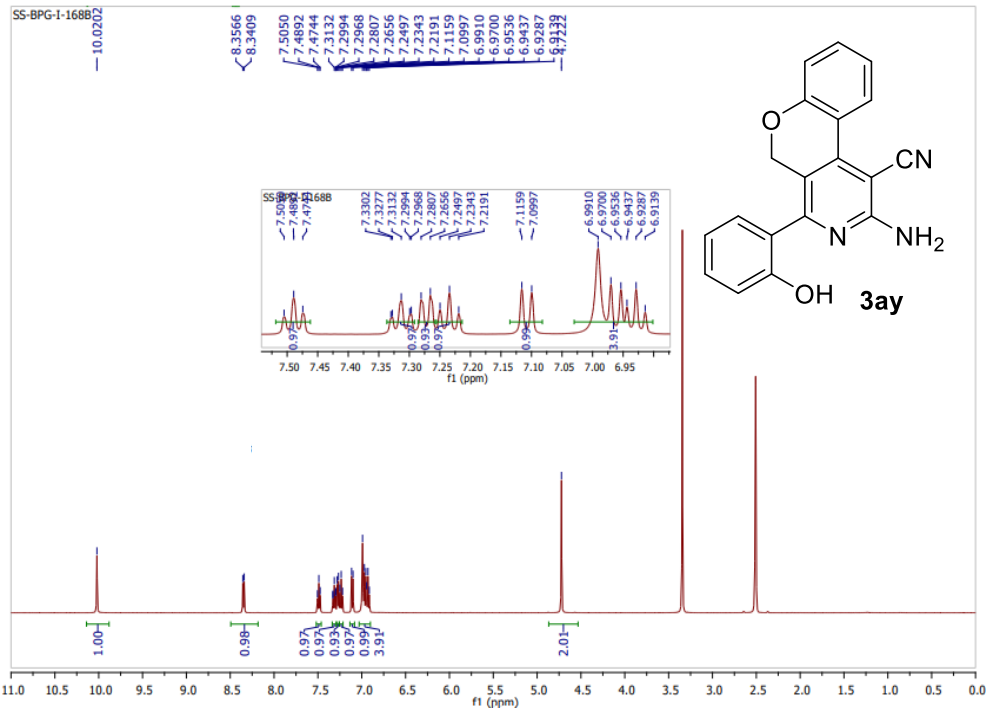

Figure 3.84 500 MHz ^{1}H NMR spectrum of **3ay** in DMSO-d$_6$.

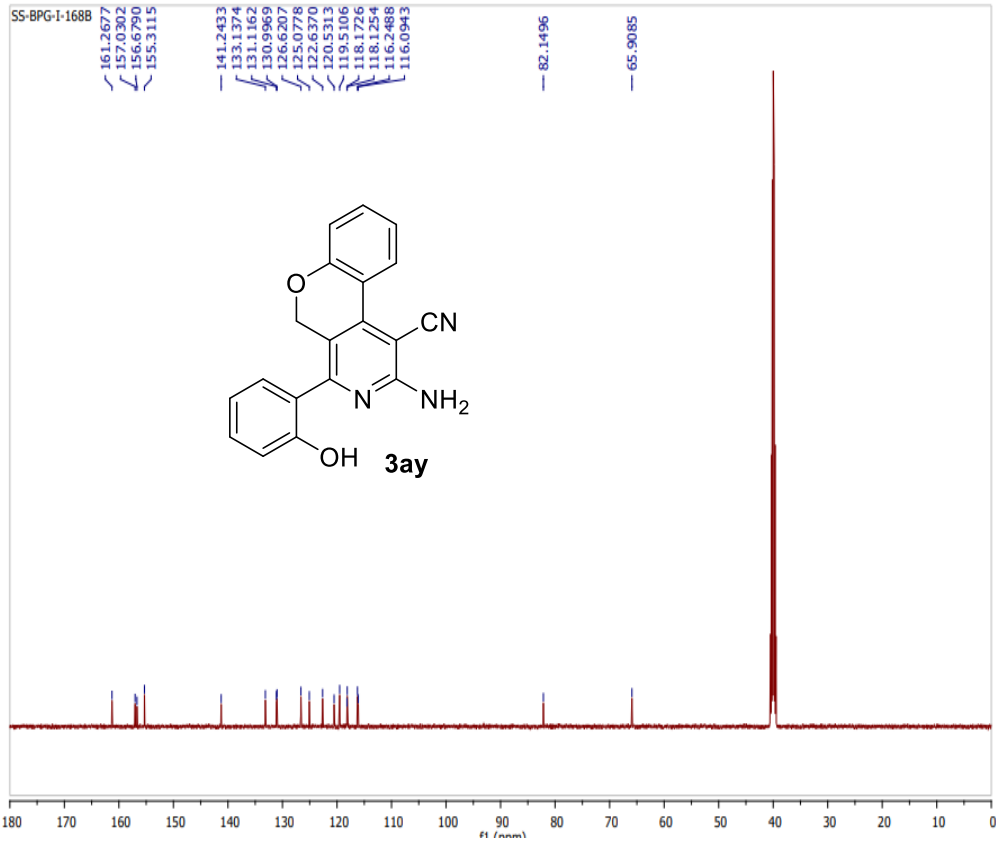

Figure 3.85 125 MHz ^{13}C NMR spectrum of **3ay** in DMSO-d$_6$.

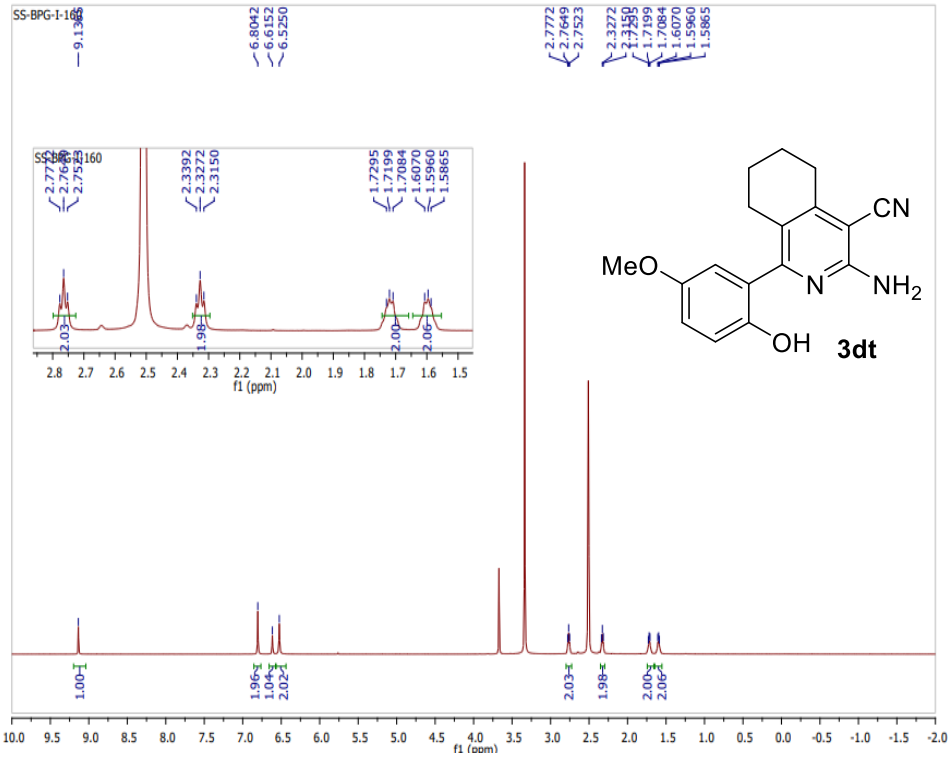

Figure 3.86 500 MHz ^{1}H NMR spectrum of **3dt** in DMSO-d_6.

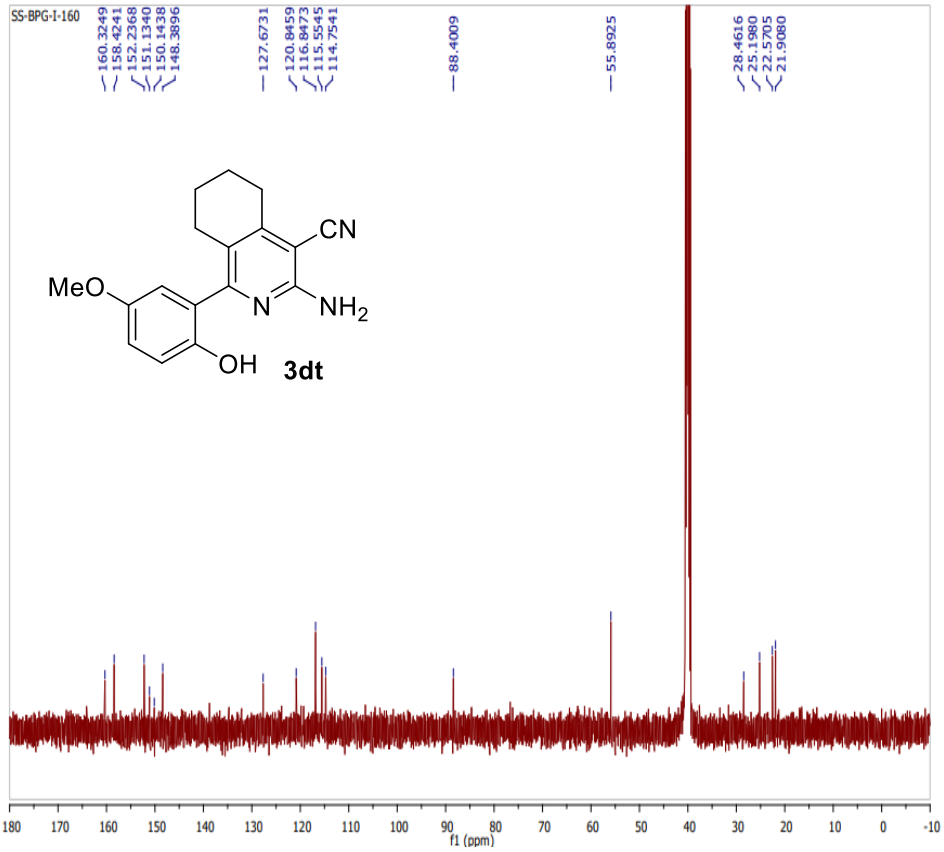

Figure 3.87 125 MHz ^{13}C NMR spectrum of **3dt** in DMSO-d_6.

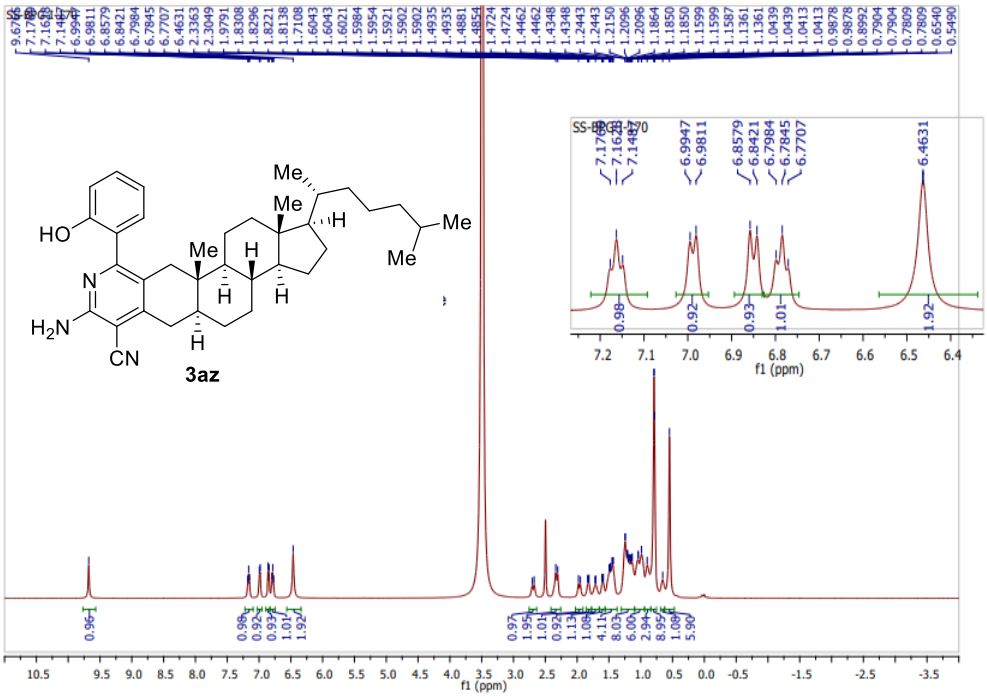

Figure 3.88 500 MHz ^{1}H NMR spectrum of **3az** in DMSO-d$_6$.

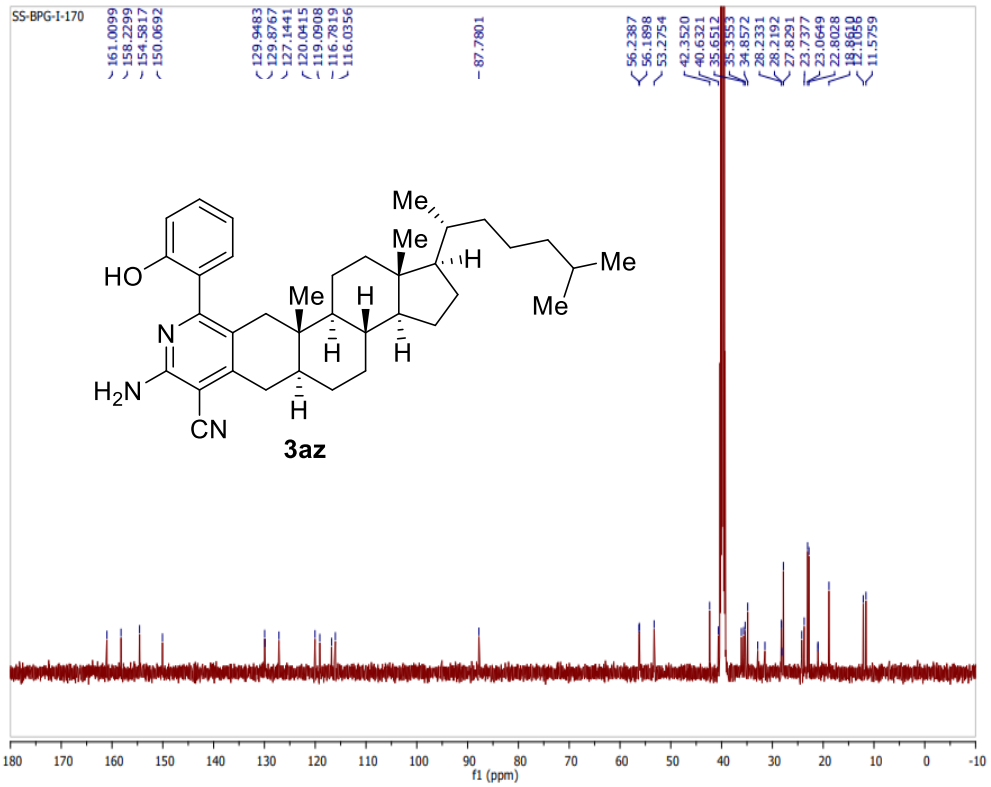

Figure 3.89 125 MHz ^{13}C NMR spectrum of **3az** in DMSO-d$_6$.

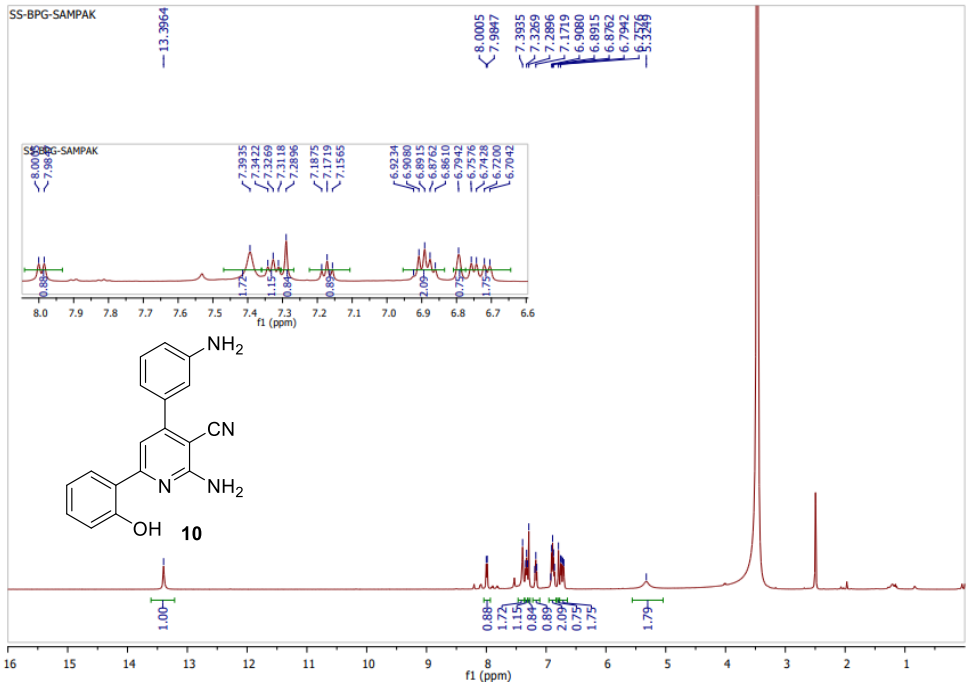

Figure 3.90 500 MHz ^{1}H NMR spectrum of **10** in DMSO-d_6.

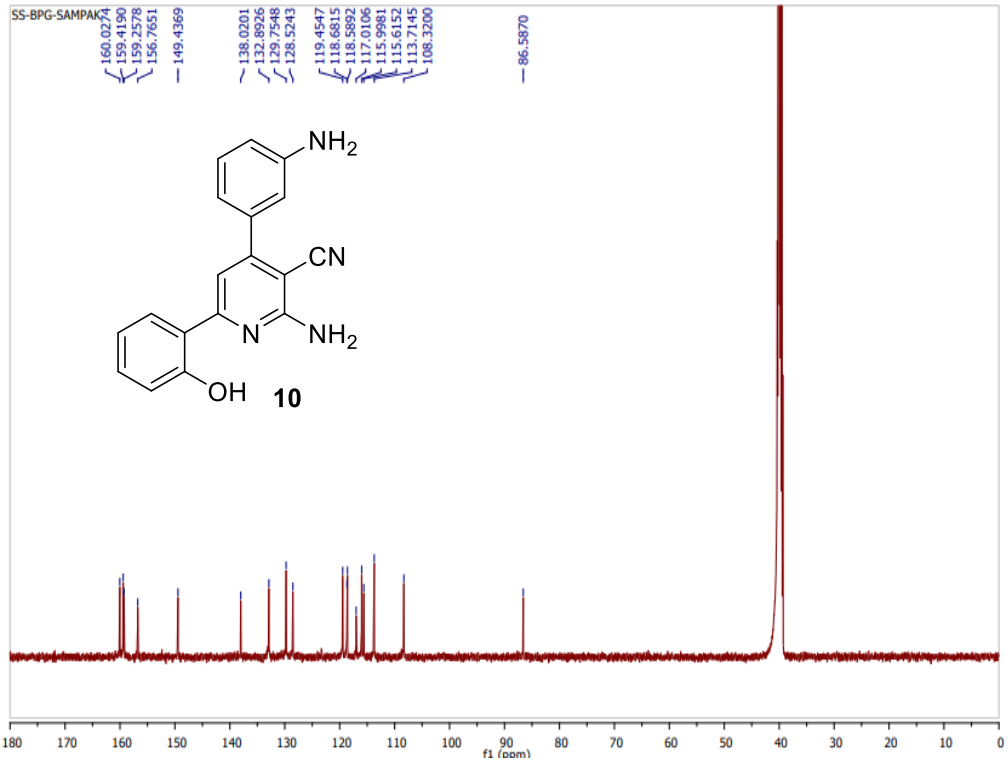

Figure 3.91 125 MHz ^{13}C NMR spectrum of **10** in DMSO-d_6.

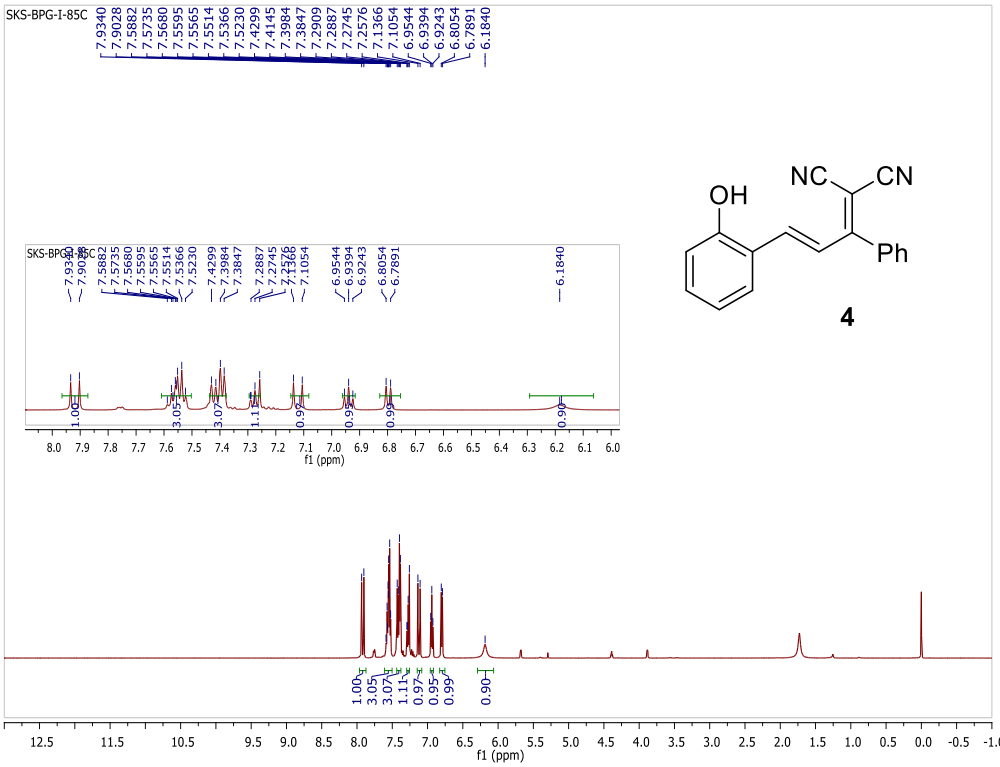

Figure 3.92 400 MHz ^{1}H NMR spectrum of **4** in $CDCl_3$.

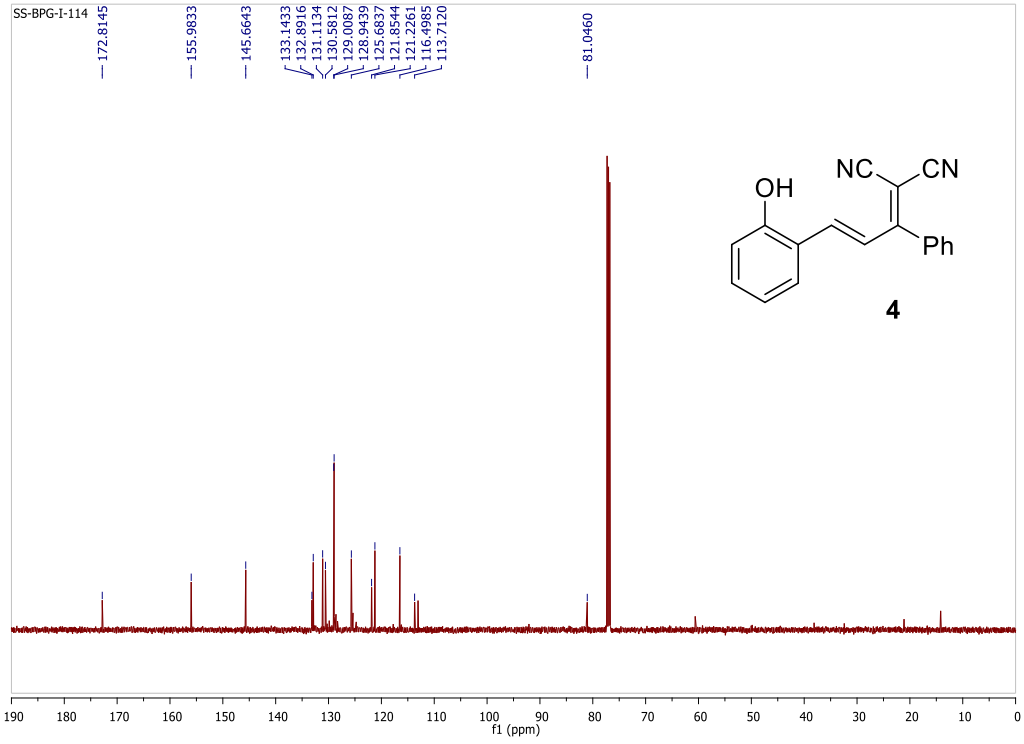

Figure 3.93 100 MHz ^{13}C NMR spectrum of **4** in $CDCl_3$.

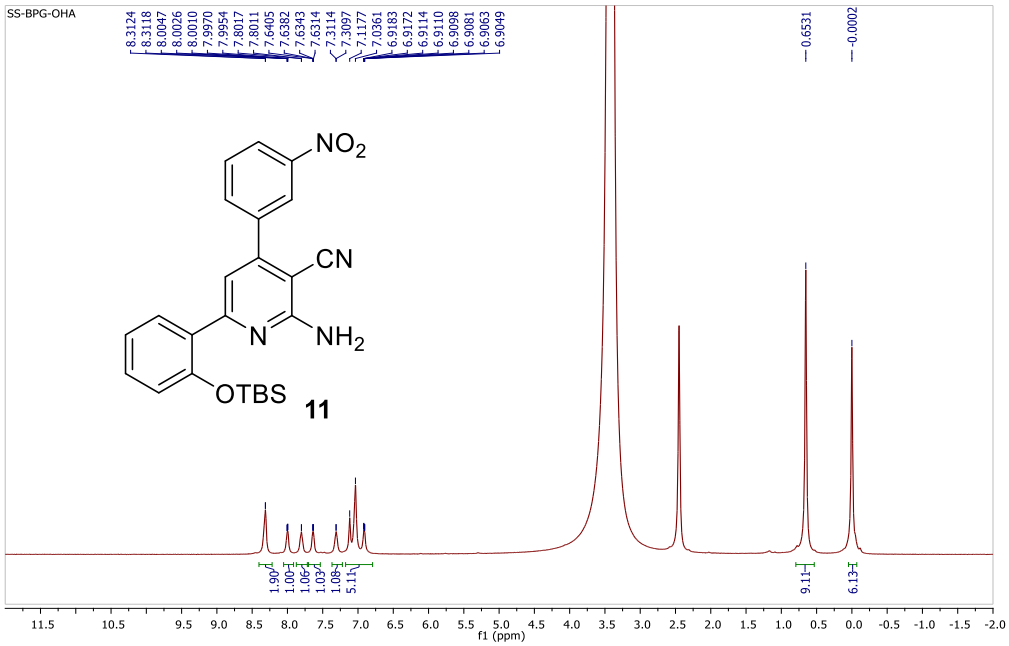

Figure 3.94 500 MHz ^{1}H NMR spectrum of **11** in DMSO-d$_6$.

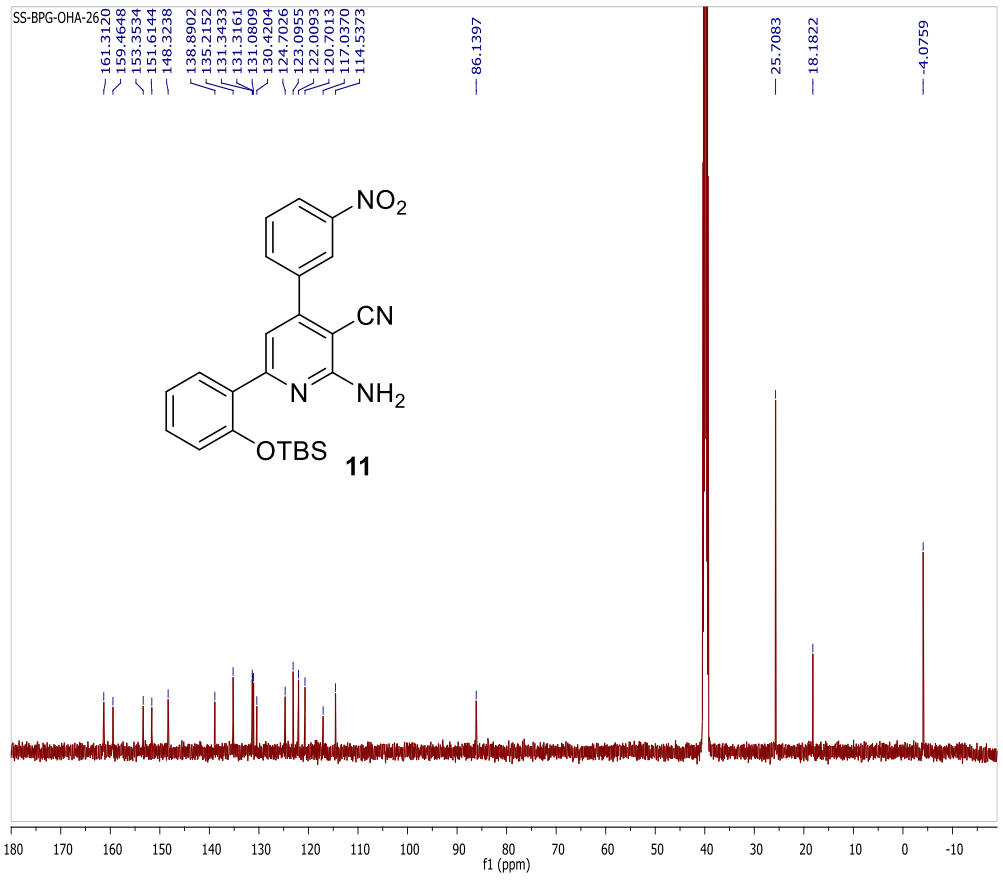

Figure 3.95 125 MHz ^{13}C NMR spectrum of **11** in DMSO-d$_6$.

3.8. References

1. Henry G. D. (2004), De novo synthesis of substituted pyridines, *Tetrahedron*, 60, 6043-6061 (DOI: 10.1016/j.tet.2004.04.043).

2. Hill M. D. (2010), Recent strategies for the synthesis of pyridine derivatives, *Chem. Eur. J.,* 16, 12052-12062 (DOI: 10.1002/chem.201001100).

3. Allais C., Grassot J.-M., Rodriguez J., Constantieux T. (2014), Metal-free multicomponent synthesis of pyridines, *Chem. Rev.,* 114, 10829-10868 (DOI: 10.1021/cr500099b).

4. Khan E. (2021), Pyridine derivatives as biologically active precursors; organics and selected coordination complexes, *Chemistryselect,* 6, 3041-3064 (DOI: 10.1002/slct.202100332).

5. Baumann M., Baxendale I. R. (2013), An overview of the synthetic routes to the best selling drugs containing 6-membered heterocycles, *Beilstein J. Org. Chem.,* 9, 2265-2319 (DOI: 10.3762/bjoc.9.265).

6. Sinthupoom N., Prachayasittikul V., Prachayasittikul S., Ruchirawat S., Prachayasittikul V. (2015), Nicotinic acid and derivatives as multifunctional pharmacophores for medical applications, *Eur. Food Res. Technol.,* 240, 1-17 (DOI: 10.1007/s00217-014-2354-1).

7. Sasabe H., Kido J. (2011), Multifunctional materials in high-performance OLEDs: challenges for solid-state lighting, *Chem. Mater.,* 23, 621-630 (DOI: 10.1021/cm1024052).

8. Hirai S., Horikawa Y., Asahara H., Nishiwaki N. (2017), Tailor-made synthesis of fully alkylated/arylated nicotinates by $FeCl_3$-mediated condensation of enamino esters with enones, *Chem. Commun.,* 53, 2390-2393 (DOI: 10.1039/C7CC00051K).

9. Xie L.-G., Shaaban S., Chen X., Maulide N. (2016), Metal-free synthesis of highly substituted pyridines by formal [2+2+2] cycloaddition under mild conditions, *Angew. Chem., Int. Ed.,* 55, 12864-12867 (DOI: 10.1002/anie.201606604).

10. Jianga Y., Park C.-M. (2014), A catalyst-controlled selective synthesis of pyridines and pyrroles, *Chem. Sci.*, 5, 2347-2351 (DOI: 10.1039/C4SC00125G).

11. Gholap A. R., Toti K. S., Shirazi F., Kumari R., Bhat M. K., Deshpande M. V., Srinivasan K. V. (2007), Synthesis and evaluation of antifungal properties of a series of the novel 2-amino-5-oxo-4-phenyl-5,6,7,8- tetrahydroquinoline-3-carbonitrile and its analogues, *Bioorg. Med. Chem.*, 15, 6705-6715 (DOI: 10.1016/j.bmc.2007.08.009).

12. Murata T., Shimada M., Sakakibara S., Yoshino T., Kadono H., Masuda T., Shimazaki M., Shintani T., Fuchikami K., Sakai K., Inbe H., Takeshita K., Niki T., Umeda M., Bacon K. B., Ziegelbauer K. B., Lowinger T. B. (2003), Discovery of novel and selective IKK- β serine-threonine protein kinase inhibitors. Part 1, *Bioorg. Med. Chem. Lett.*, 13, 913-918 (DOI: 10.1016/S0960-894X(02)01046-6).

13. Deng J., Sanchez T., Al-Mawsawi L. Q., Dayam R., Yunes R. A., Garofalo A., Bolger M. B., Neamati N. (2007), Discovery of structurally diverse HIV-1 integrase inhibitors based on a chalcone pharmacophore, *Bioorg. Med. Chem.*, 15, 4985-5002 (DOI: 10.1016/j.bmc.2007.04.041).

14. Vyas D. H., Tala S. D., Akbari J. D., Dhaduk M. F., Joshi K. A., Joshi H. S. (2009), Synthesis and antimicrobial activity of some new cyanopyridine and cyanopyrans towards mycobacterium tuberculosis and other microorganisms, *Indian J. Chem., Sect. B: Org. Chem. Incl. Med. Chem.*, 48, 833-833 (DOI: 10.1002/chin.200942024).

15. Mantri M., Graaf O. D., Veldhoven J. V., Göblyös A., Von Frijtag Drabbe Künzel J. K., Mulder-Krieger T., Link R., De Vries H., Beukers M. W., Brussee J., Ijzerman A. P. (2008), 2-Amino-6-furan-2-yl-4-substituted nicotinonitriles as A_{2A} adenosine receptor antagonists, *J. Med. Chem.*, 51, 4449-4455 (DOI: 10.1021/jm701594y).

16. Zhang D., Luo N., Gan J., Wan X., Wang C. (2021), Piperidine-mediated [3 + 3] Cyclization of 2-amino-4*H*-chromen-4-ones and 2-

benzylidenemalononitriles: to access 2-aminochromeno[2,3-*b*]pyridine derivatives, *J. Org. Chem.,* 86, 9218-9224 (DOI: 10.1021/acs.joc.1c00797).

17. Xin X., Huang P., Xiang D., Zhang R., Zhao F., Zhang N., Dong D. (2013), [5C + 1N] Annulation of 2,4-pentadienenitriles with hydroxylamine: a synthetic route to multi-substituted 2-aminopyridines, *Org. Biomol. Chem.,* 13, 1001-1006 (DOI: 10.1039/C2OB27053F).

18. Kambe S., Saito K., Sakurai A., Midorikawa H. (1980), A simple method for the preparation of 2-amino-4-aryl-3-cyanopyridines by the condensation of malononitrile with aromatic aldehydes and alkyl ketones in the presence of ammonium acetate, *Synthesis,* 1980, 366-368 (DOI: 10.1055/s-1980-29021).

19. Tang J., Wang L., Yao Y., Zhang L., Wang W. (2011), One-pot synthesis of 2-amino-3-cyanopyridine derivatives catalyzed by ytterbium perfluorooctanoate [$Yb(PFO)_3$], *Tetrahedron Lett.,* 52, 509-511 (DOI: 10.1016/j.tetlet.2010.11.102).

20. Wu Q., Zhang Y., Cui S. (2014), Divergent syntheses of 2-aminonicotinonitriles and pyrazolines by copper-catalyzed cyclization of oxime ester, *Org. Lett.,* 16, 1350-1353 (DOI: 10.1021/ol500094w).

21. He X., Shang Y. J., Yu Z., Fang M., Zhou Y., Han G., Wu F. (2014), $FeCl_3$-Catalyzed four-component nucleophilic addition/intermolecular cyclization yielding polysubstituted pyridine derivatives, *J. Org. Chem.,* 79, 8882-8888 (DOI: 10.1021/jo5014383).

22. Baldwin J. J., Raab A. W., Ponticello G. S. (1978), Utilization of *β,γ,* -unsaturated aldehyde equivalents in the synthesis of substituted 2-halonicotinic acid derivatives, *J. Org. Chem.,* 43, 2529-2535 (DOI: 10.1021/jo00406a052).

23. Villemin D., Belhadj Z., Cheikh N., Choukchou-Braham N., Bar N., Lohier J.-F. (2013), Solventless convenient synthesis of new cyano-2-aminopyridine derivatives from enaminonitriles, *Tetrahedron Lett.,* 54, 1664-1668 (DOI: 10.1016/j.tetlet.2013.01.021).

24. Shu K., Shao J., Li H., Chen B., Tang P., Liu X., Chen W., Yu Y. (2016), Base-mediated synthesis of highly functionalized 2-aminonicotinonitriles from

α-keto vinyl azides and α,α-dicyanoalkenes, *RSC Adv.*, 6, 49123-49126 (DOI: 10.1039/C6RA04669J).

25. Shintani T., Kadono H., Kikuchi T., Schubert T., Shogase Y., Shimazaki M. (2003), Efficient synthesis of 3-cyano-6-(2-hydroxyphenyl)pyridines by multi-component condensations on beads, *Tetrahedron Lett.*, 44, 6567-6569 (DOI: 10.1016/S0040-4039(03)01695-2).

26. Su W., Ding K., Chen Z. (2009), $Cu(OTf)_2/Et_3N$-promoted cyclocondensation of activated α-methylene alkenes and nitroolefins: a novel one-pot synthesis of polysubstituted benzenes, *Tetrahedron Lett.*, 50, 636-639 (DOI: 10.1016/j.tetlet.2008.11.081).

27. Manna F., Chimenti F., Bolasco A., Bizzarri B., Filippelli W., Filippelli A., Gagliardi L. (1999), Anti-inflammatory, analgesic and antipyretic 4,6-disubstituted 3-cyano-2-aminopyridines, *Eur. J. Med. Chem.*, 34, 245-254 (DOI: 10.1016/S0223-5234(99)80057-9).

28. Wu H.-C., Wang C., Chen Y.-H., Liu Y.-K. (2021), Asymmetric organocatalytic vinylogous michael addition triggered triple-cascade reactions of 2-hydroxycinnamaldehydes and vinylogous nucleophiles: construction of benzofused oxabicyclo[3.3.1]nonane scaffolds, *Chem. Commun.*, 57, 1762-1765 (DOI: 10.1039/D0CC07761E).

29. Wang H., Zhao Y. L., Ren C. Q., Diallo A., Liu Q. (2011), Tandem [5+1] annulation–isocyanidecyclization: efficient synthesis of hydroindolones, *Chem. Commun.*, 47, 12316-12318 (DOI: 10.1039/C1CC14916D).

30. Longstreet A. R., Campbell B. S., Gupton B. F., McQuade D. T. (2013), Improved synthesis of mono- and disubstituted 2-halonicotinonitriles from alkylidene malononitriles, *Org. Lett.*, 15, 5298-5301 (DOI: 10.1021/ol4025265).

31. Reddy M. K., Bhajammanavar V., Baidya M. (2021), Annulation cascade of sulfamate-derived cyclic imines with glycine aldimino esters: synthesis of 1,3-benzoxazepine scaffolds, *Org. Lett.*, 23, 3868-3872 (DOI: 10.1021/acs.orglett.1c01001).

32. Jethava K. P., Fine J., Chen Y., Hossain A., Chopra G. (2020), Accelerated reactivity mechanism and interpretable machine learning model of N-sulfonylimines toward fast multicomponent reactions, *Org. Lett.*, 22, 8480-8486 (DOI: 10.1021/acs.orglett.0c03083).

33. Zhou J., Zhang H., Chen X.-L., Qu Y.-L., Zhu Q., Feng C.-G., Chen Y.-J. (2019), Regio- and diastereoselective access to 4-imidazolidinones via an aza-mannich initiated cyclization of sulfamate-derived cyclic imines with α-halo hydroxamates, *J. Org. Chem.*, 84, 9179-9187 (DOI: 10.1021/acs.joc.9b01128).

Chapter 4

Copper(I)-photocatalyzed diastereoselective aziridination of N-sulfonyl imines with vinyl azides: application to benzo[*f*][1,2,3]oxathiazepines dioxides and fused isoxazolines

4.1 Introduction

The three-membered aziridines represent a reputable class of N-containing heterocyclic molecules which are omnipresent in many bioactive natural molecules,[1-3] active pharmaceutical ingredients,[4-6] and synthetic molecules with great biological significance,[7] (**Figure 4. 1**). [7-9] Most importantly, owing to their intrinsic ring strain, they create a unique opportunity to serve as multifaceted, highly reactive intermediates for rapidly accessing a variety of value-added N-containing compounds for drug discovery programs.[8-11]

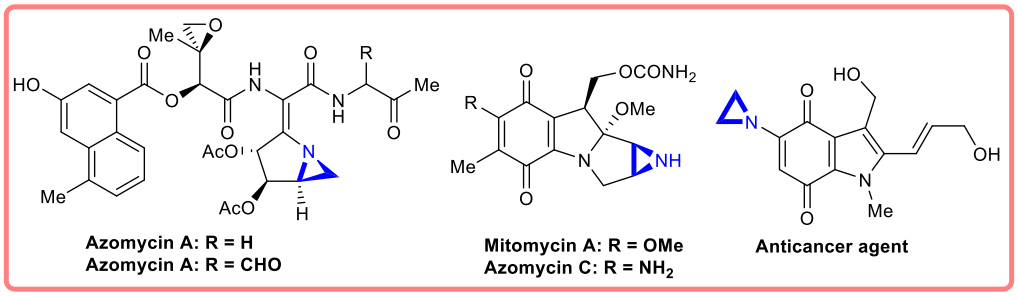

Figure 4.1. Selected examples of biologically relevant compounds having an aziridine moiety.

4.2 Review work

On account of their significant applications, tremendous efforts have been made by chemists worldwide to develop various catalytic and noncatalytic techniques which include visible-light-induced photoactive catalysis, olefin aziridination, multicomponent reactions, sequential one-pot reactions, etc. to construct a wide breadth of aziridine derivatives.[12-14] Some of the relevant literature reports have been discussed in the next section (**4.2.1**).

4.2.1. Synthesis of aziridine derivatives

Zhou *et al.* in 2016 demonstrated a metal-free, Rose-Bengal-catalyzed and visible-light induced decarboxylative cyclization between N-aryl glycines as the imine sources and diazo compounds, affording various N-arylated aziridines in moderate to excellent yields (**Scheme 4.1**).[15]

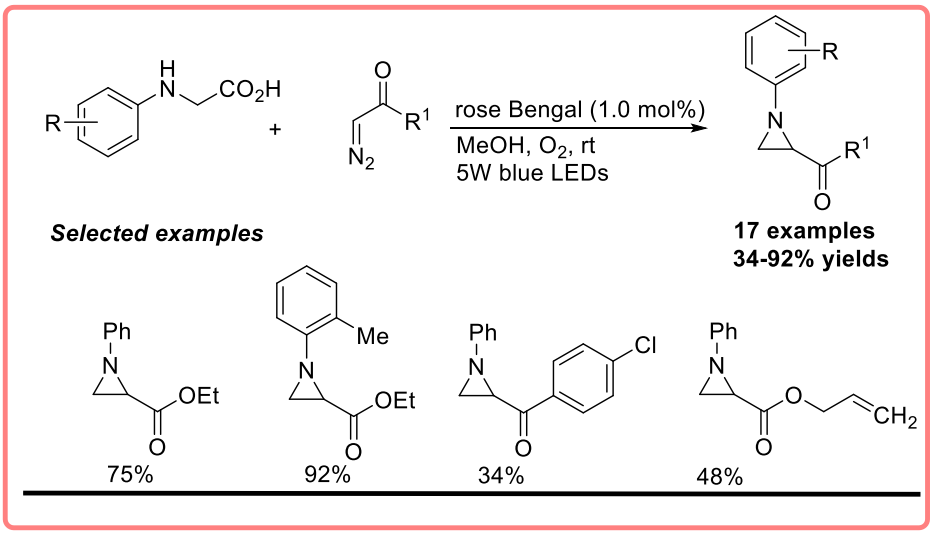

Scheme 4.1. Visible-light induced decarboxylative cyclization of N-aryl glycines with diazo compounds.

A plausible mechanism for the above **(Scheme 4.1)** visible-light induced decarboxylative cyclization of N-aryl glycines and diazo compounds has been presented in **Scheme 4.2.** Initially, photoexcitation of RB by visible light produces excited RB*, which is promptly quenched by N-aryl glycine to provide the cation radical **A**. Decarboxylation of **A** results in the formation of α-amino alkyl radical **B**. The continued oxidation of **B** by the superoxide radical produces iminium ion **C**, which then deprotonates to form active imine **D**. Aziridines **3** were ultimately synthesized through the nucleophilic addition of diazo compounds to the C=N bond, succeeded by an intramolecular nucleophilic attack by the nitrogen atom on an adjacent carbon atom, with N_2 acting as the leaving group.[15]

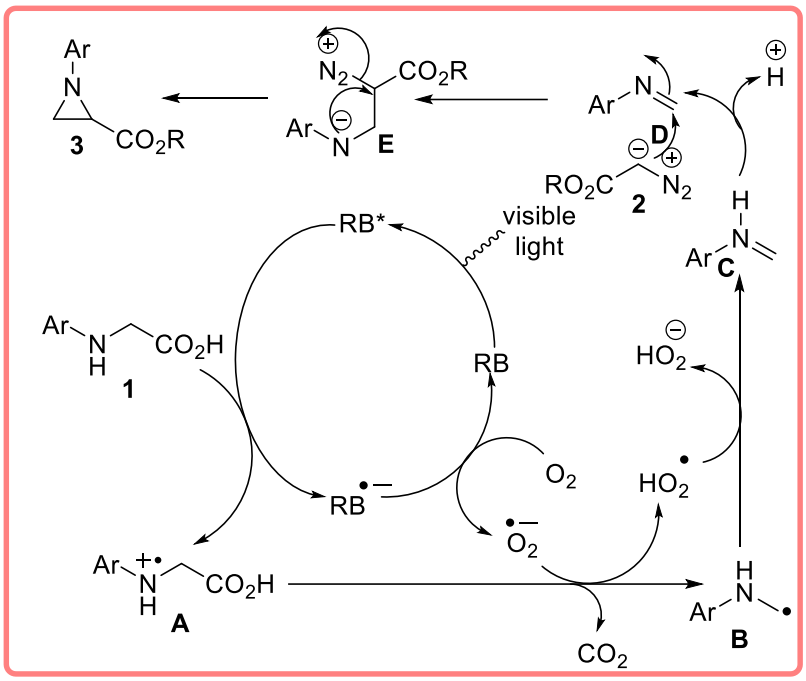

Scheme 4.2. Plausible mechanism of decarboxylative cyclization of N-aryl glycines with diazo compounds.

Xuan *et al.* (2021) also developed a photocatalyst-free, visible light-promoted cycloaddition of α-diazo esters with hexahydro-1,3,5-triazines under blue-LEDs (24 W) at room temperature. This novel technique leads to a series of aziridine frameworks in a variable range of yields (33-95%) **(Scheme 4.3).**[16]

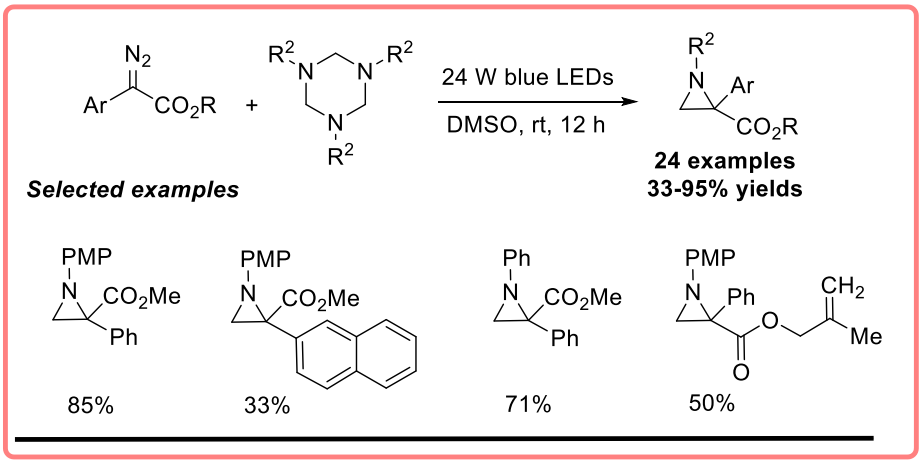

Scheme 4.3. Synthesis of aziridines from α-diazo esters and hexahydro-1,3,5-triazines.

Yoon *et al.* (2016) demonstrated an efficient photoactive Ir(III)-complex-catalyzed olefin aziridination reaction of alkenes with azidoformates irradiated by a 15 W blue LED flood lamp at 464 nm to endow a series of aziridine derivatives in satisfactory chemical yields and diastereoselectivities. This transition-metal based photocatalytic system holds several positive points such as applicable to cyclic/acyclic alkenes, excellent catalytic activity (2.5 mol%) and good tolerance of functionalities **(Scheme 4.4).**[17]

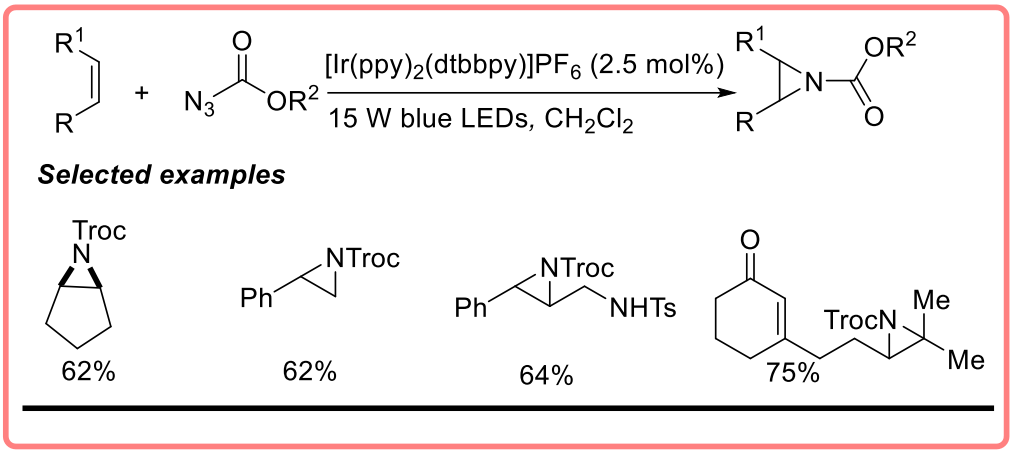

Scheme 4.4. Ir(III)-catalyzed and visible-light driven olefin aziridination reaction.

A similar study, Xu *et al.* (2018) reported an appealing diastereoselective method for the synthesis of substituted aziridines adorned with various functionalities from alkenes and N-protected 1-aminopyridinium salts as the source of N-centered radicals catalyzed by Ir(III)-complex under the irradiation of blue LED strip at room temperature. This SET-process implies to various alkenes and affords good to high yields and excellent diastereomeric ratios (up to 20:1 dr) under mild conditions **(Scheme 4.5).**[18]

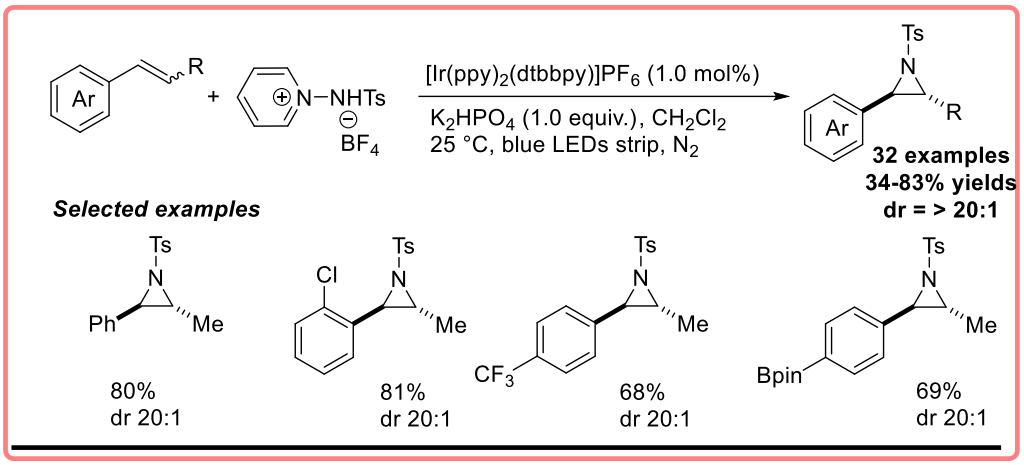

Scheme 4.5. Ir(III)-catalyzed and visible-light induced olefin aziridination reaction.

A seminal work's by Koenigs *et al.* developed a powerful method for the rapidly synthesis of trifluoromethylated aziridines in moderate to excellent yields (37-95%). This photocatalytic method proceeds between α-trifluoromethylstyrenes and iminoiodanes as the nitrenes in the presence of $Ru(bpy)_3Cl_2$ as a photocatalyst irradiated by blue-LED at 470 nm via a single-electron-transfer process. in **(Scheme 4.6).**[19]

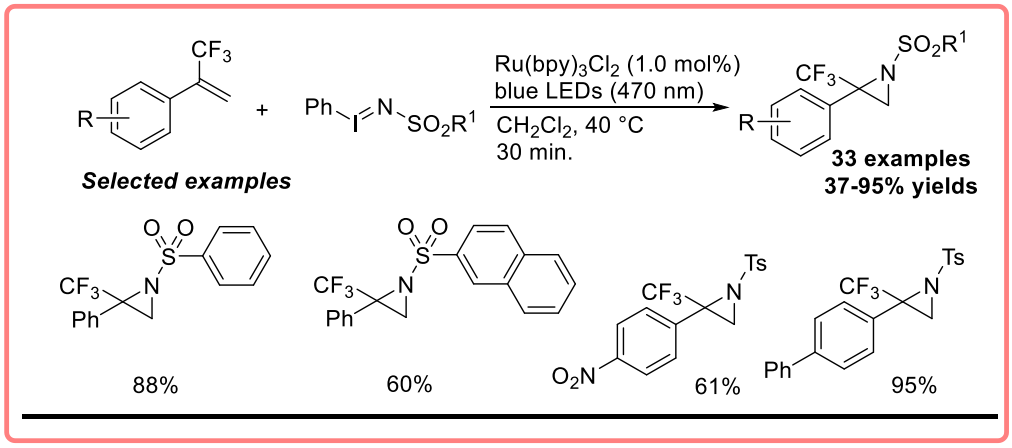

Scheme 4.6. Ru(II)-catalyzed and visible-light assisted aziridination reaction for accessing trifluoromethylated aziridines.

Rastogi *et al.* (2023) also applied above photocatalytic method (**Scheme 4.5**) for the highly diastereoselective synthesis of aziridine derivatives in poor to good yields (18-62%) involving chalcones instead of α-trifluoromethyl styrenes

and iminoiodinanes catalyzed by Ru(II)-complex. This double C-N bond-making process excels with a variety of substrates and tolerates various functionalities as shown in (**Scheme 4.7**).[20]

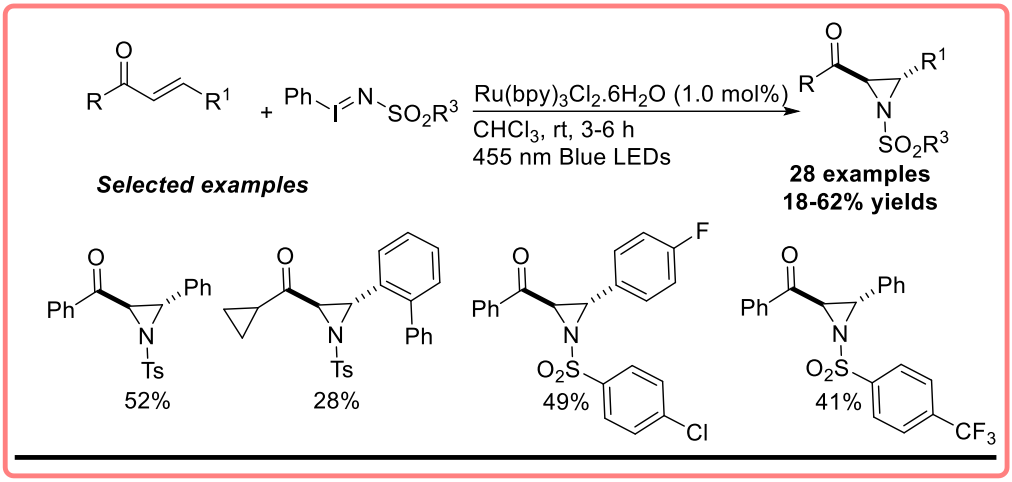

Scheme 4.7. Photoactive Ru(II)-complex-catalyzed aziridination reaction using chalcones and iminoiodinanes.

In 2013, Cho *et al.* synthesized an interesting class of perfluoroalkylated aziridines by using allylic amines and alkyl fluorides in the presence of 0.5 mol% of $Ru(bpy)_3Cl_2$ induced by visible-light. This photocatalytic reaction resulted in average to good yields (55-65%) **(Scheme 4.8).**[21]

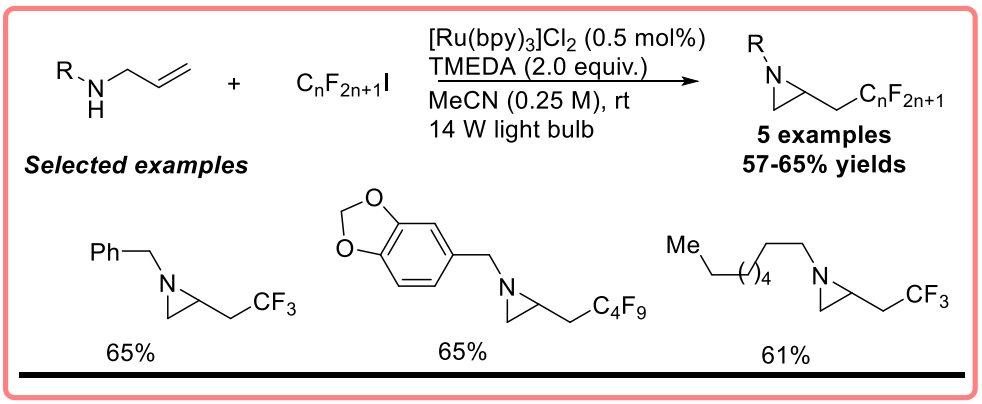

Scheme 4.8. Synthesis of perfluoroalkylated aziridines.

Tang *et al.* accomplished a highly diastereoselective one-pot two-step sequential protocol that constructed *cis*-sulfamidate-fused aziridines in moderate to high yields by combining allylic ylide and cyclic N-sulfonyl

ketimines in the presence of *t*-BuOK, followed by Pd(0)-catalyzed isomerization in moderate to high yields in **(Scheme 4.9).**[22]

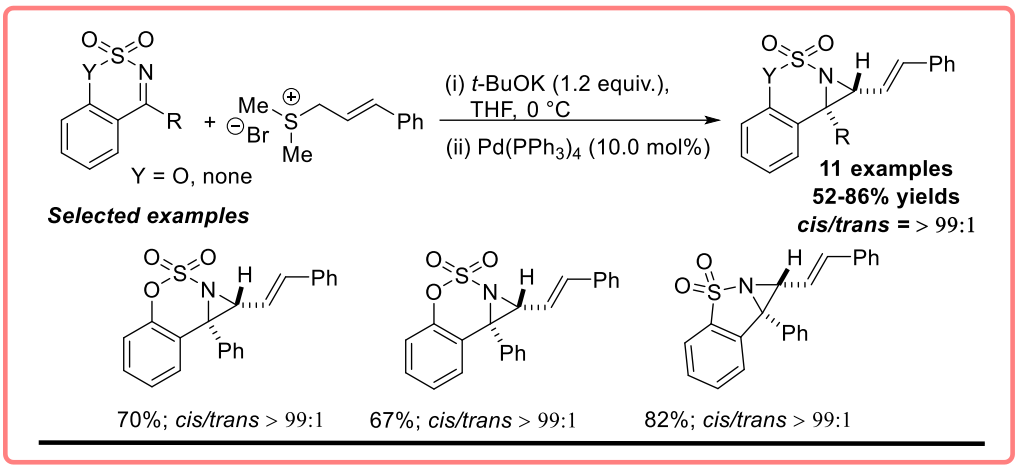

Scheme 4.9. Sequential one-pot two-step sequential approach to aziridinations.

In 2016, Ma *et al.* developed a highly enantio- and diastereoselective sequential one-pot two-step reaction between cyclic N-sulfonyl imines and β-keto acids catalyzed by CuI/Ph-Box as a combined catalytic system via the decarboxylative Mannich reaction, followed by the oxidative C-H amination using KI and TBHP as an oxidant, leading to fused aziridine derivatives in good to high yields (46-83%) **(Scheme 4.10).**[23]

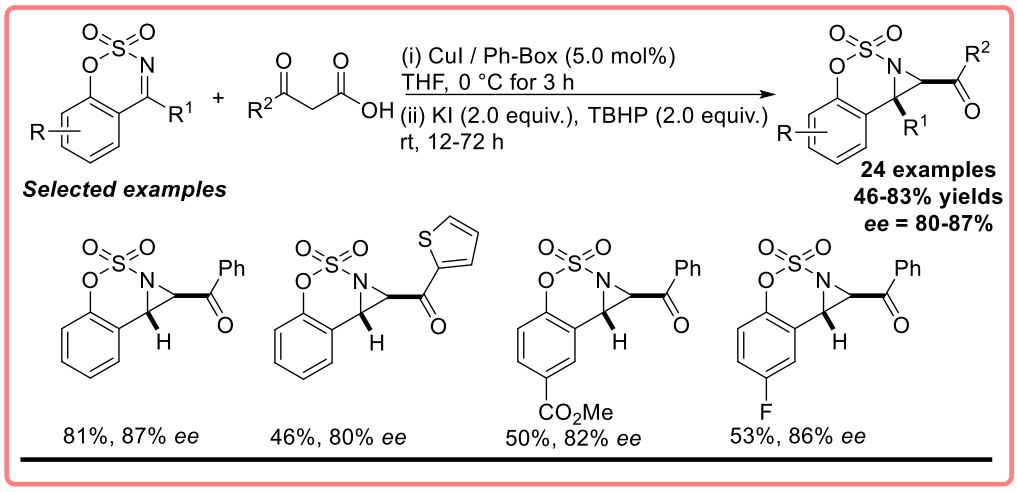

Scheme 4.10. Copper(I)-catalyzed one-pot enantioselective access to fused aziridines.

In 2017, Xu *et al*. reported a sequential one-pot two-step enantioselective method involving N-sulphonyl ketimines with unfunctionalized ketones via asymmetric Mannich reaction using 20 mol% organocatalyst, followed by intramolecular C-H amination catalyzed by $CuBr_2$ in the presence of KI and TBHP as an oxidant to deliver multi-substituted chiral fused aziridines in good to excellent yields (72-93%) in **Scheme (4.11).**[24]

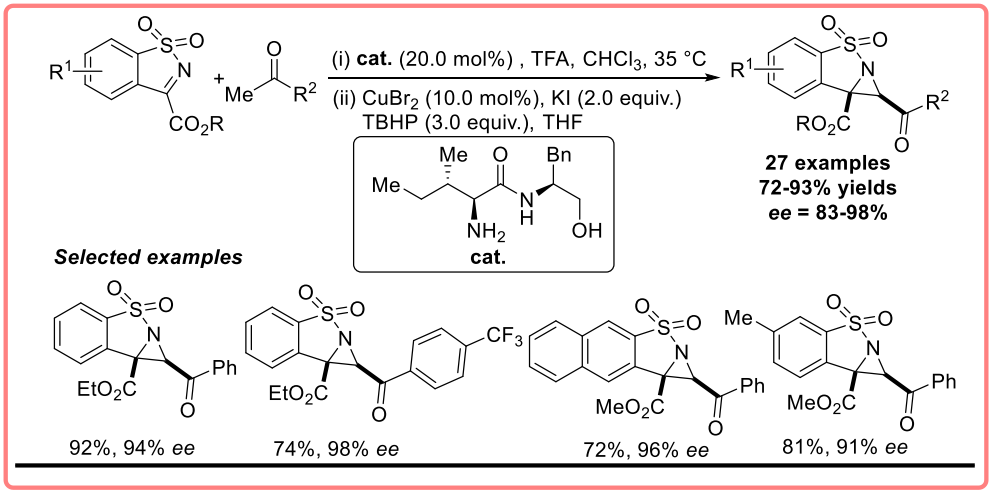

Scheme 4.11. Asymmetric aziridination reaction of N-sulphonyl ketimines and ketones.

4.2.2 Conclusion

The above discussion highlighted that the synthesis of substituted aziridines utilizing Ir(III)/Ru(II)-based photocatalysts often presents challenges, including high costs, limited availability, and reduced efficacy in terms of reduction capabilities. These factors may hinder the realization of their extensive potential, practicality, and scalability. Additionally, the methods outlined face several issues, such as the need for excess base and additional oxidants, lower atom economy, multi-step processes, and prolonged reaction times. Furthermore, the synthesis of functionalized aziridines is crucial for the structural integrity of bioactive natural products and pharmaceutical compounds. Consequently, developing an efficient one-pot strategy to generate a diverse library of sulfamidate-fused aziridines is both relevant and highly compelling.

4.3 Present work

Given the importance of aziridine moieties, developing an efficient, environmentally benign, photoactive copper-complex catalyzed one-pot technique for the highly diastereoselective access to a diverse set of sulfamidate-fused aziridines is a substantial challenge in the organic and medicinal chemistry. Towards this goal, we surmised that the synthetically useful α-aryl vinyl azides [25–26] may generate nucleophilic iminyl radicals in the presence of photoactive copper-salt under visible light irradiation which would involve Mannich reaction with cyclic N-sulfonyl imines, followed by an intramolecular oxidative C-H amination of the resultant Mannich adducts to give the targeted fused aziridines.

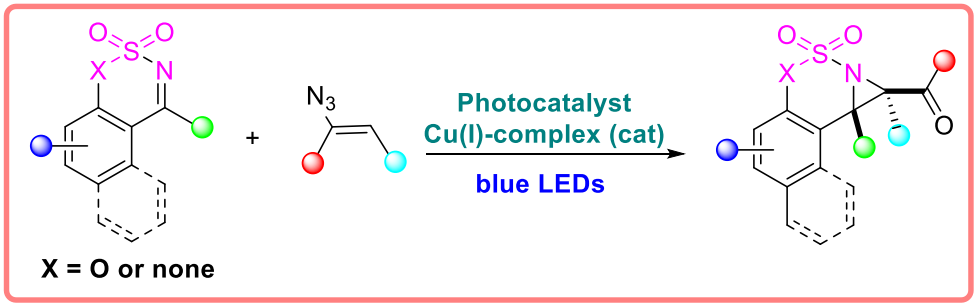

Scheme 4.12. Copper(I)-photocatalyzed synthesis of substituted sulfamidate fused aziridines.

As part of our ongoing research interest towards the development of sustainable methods for preparing pharmacologically reputable aza-heterocycles using cyclic N-sulfonyl imines, [27-28] herein we wish to report a visible-light-induced and Cu(I)-photocatalyzed diastereoselective aziridination reaction of cyclic N-sulfonyl imines with vinyl azides, leading to substituted sulfamidate fused aziridines via a selective C-C/C-N/C=O bond-making event. **(Scheme 4.11)**

4.4 Results and discussion

4.4.1 Optimization of the reaction conditions

We initiated the optimization reaction between N-sulfonyl imine **1a** and vinyl azide **2a** as model substrates using 10 mol% of CuI irradiated by 5W of blue light-emitting diode (LED) at 450 nm in MeCN:H_2O (50:1) at room

temperature. Amazingly, after 24 h, this process led to an exciting class of sulfamidate-fused aziridine **3aa** in 32% yield with excellent diastereoselectivity (99:1 dr, **Table 4.1** entry 1). The chemical structure of 3aa was assigned by its spectroscopic data (^{1}H NMR, ^{13}C NMR, HRMS, and SC-XRD data). The ^{1}H NMR spectrum of **3aa** exhibits 2 aliphatic protons in the range of 4.29-4.71 ppm and 9 aromatic protons in the range of 7.18-8.11 ppm. ^{13}C NMR spectrum of **3aa** shows 1 carbonyl carbon peak at $\delta_{C=O}$ = 189.1 ppm, 2 aliphatic carbon peaks at 47.7 and 45.1 ppm, and 10 aromatic carbon peaks (149.8, 135.0, 134.8, 130.7, 129.6, 129.1, 129.0, 127.0, 119.5, 118.1 ppm). The molecular ion peak $[M+Na]^{+}$ at 302.0484 in the HRMS spectrum corresponds to the molecular weight 301.0409 of the desired compound **3aa.** The relative stereochemistry of **3aa** was *trans* to be assigned by its single-crystal-X-ray diffraction data (CCDC number **2264093**, for the details, see **Figure 4.2** and **Table 4.5**).

The above outcomes exhilarated us to delve into this aziridination reaction in more detail. Interestingly, using 10 mol% of CuI with 10 mol% of several pyridine-based ligands such as 2,2′-bpy (**L1**), 4,4′-bpy (**L2**), 1,10-phenanthroline (**L3**), neocuproine (**L4**) and pyridine (**L5**), significant enhancement rate of this aziridination reaction was observed in the case of **L1**, **L3** and **L4** to afford **3aa** in 74% (entry 2), 75% (entry 4) and 72% (entry 5) yields, respectively, after 16h. However, **L2** and **L5** did not affect the annulation reaction rate much, leading to moderate yields (45% and 42%, respectively) of **3aa**. Thus, considering the cost of **L1** (2,2′-bpy) as a ligand, it was chosen for further transformation. Further examination of different copper salts (CuCl, CuBr, $Cu(OAc)_2$, $CuCl_2$, and $CuBr_2$) ligand **L1** led to unsatisfactory results (13-59% yields of **3aa**, entries 7-11). Furthermore, other photocatalysts such as $Ru(bpy)_3Cl_2$, eosin Y, and rose Bengal failed to promote this reaction (entries 12-14). Therefore, merging CuI and **L1** (1:1) showed the best photocatalyst compared to others tested for this reaction. Next, we focused on examining the common solvent effect in the reaction. Results indicated that the reaction proceeded nicely in acetone (71%, entry), THF (70%), CH_2Cl_2 (65%), except DMSO (9%) and DMF (10%). Moreover, when the reaction was irradiated by either a white LED light (WL), green LED light (GL), or sunlight (SL), unsatisfactory yields (35%, 55%, or 28%, respectively, entries 20-22) of product

3aa were obtained. It should be noted that using 5 mol% of CuI/**L1**, the reaction led to **3aa** in 52% yield (entry 23). Moreover, when the reaction was carried out in dry MeCN, the yield of **3aa** was dropped to 25% (entry 24, **Table 4. 1**).

Table 4.1. Optimization of the reaction conditions.[a-c]

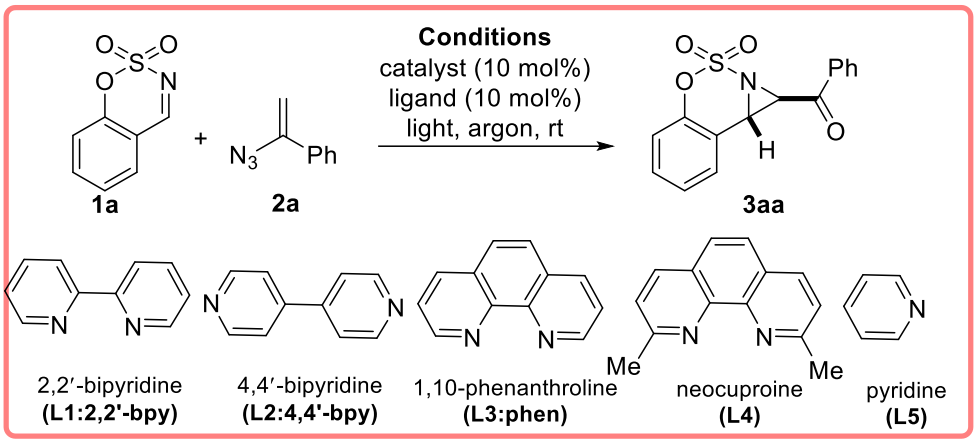

Entry	Catalyst	Ligand	Light	Solvent	Yield (%)[b,c]
1[d]	CuI	-	BL	MeCN : H_2O	32
2	CuI	L1	BL	MeCN : H_2O	74
3	CuI	L2	BL	MeCN : H_2O	45
4	CuI	L3	BL	MeCN : H_2O	75
5	CuI	L4	BL	MeCN : H_2O	72
6	CuI	L5	BL	MeCN : H_2O	42
7	CuCl	L1	BL	MeCN : H_2O	13
8	CuBr	L1	BL	MeCN : H_2O	59
9	$Cu(OAc)_2$	L1	BL	MeCN : H_2O	trace
10	$CuCl_2$	L1	BL	MeCN : H_2O	10
11	$CuBr_2$	L1	BL	MeCN : H_2O	45
12[f]	Ru(II)-	-	BL	MeCN : H_2O	trace
13	Eosin Y	-	BL	MeCN : H_2O	trace
14	RB	-	BL	MeCN : H_2O	trace
15	CuI	L1	BL	DMSO : H_2O	9
16	CuI	L1	BL	DMF : H_2O	10
17	CuI	L1	BL	acetone : H_2O	71
18	CuI	L1	BL	THF : H_2O	70

19	CuI	L1	BL	CH_2Cl_2 : H_2O	65
20	CuI	L1	WL	MeCN : H_2O	35
21	CuI	L1	GL	MeCN : H_2O	55
22	CuI	L1	SL	MeCN : H_2O	28
23[e]	CuI	L1	BL	MeCN : H_2O	52
24[g]	CuI	L1	BL	MeCN	25

[a]Unless otherwise noted, all the reaction was carried out with **1a** (0.2 mmol), **2a** (0.4 mmol), catalyst (10 mol%), and ligand (10 mol%) in specified solvent: H_2O (2.0 mL, 50:1) under four 5W blue LEDs light (450 nm) irradiation at room temperature in an argon atmosphere for 16h. [b]Isolated yield after column chromatography. [c]Diastereomeric ratio (dr = 99:1) was determined by the integration of the corresponding ^{1}H NMR peaks attached C1(sp^3)- and C2(sp^3)-H of the crude product **3aa**. [d]Reaction time was 24 h. [e]5 mol% of CuI and **L1** used. [f]$Ru(bpy)_3Cl_2$ was used. [g]Reaction was carried out in dry MeCN.

Next, we performed several control experiments to better understand the mechanism as depicted in **Scheme 4.13** For instance, when the reaction is conducted without CuI (**Scheme 4.13a**) or in the absence of light (dark) (**Scheme 4.13b**), it does not lead to product **3aa** or gives an inferior result. Therefore, both the catalyst and light are essential for this transformation. Next, the replacement of vinyl azide **2a** with azirine **3a** makes the cyclization reaction sluggish, producing **3aa** in a low yield (19%) under standard conditions (**Scheme 4.13c**). Moreover, using acetophenone and cyclic imine **1a** as coupling partners, the reaction did not happen (**Scheme 4.13d**). Therefore, the above results indicate that the target product **3aa** is unlikely to originate from either **3a** or acetophenone during the reaction. Furthermore, the aziridination reaction was completely inhibited by using an excess amount of TEMPO (5.0 equiv) or BHT (6.0 equiv) as the radical scavenger. Instead, the formations of radical trapped TEMPO adduct **7** (m/z=$(M+H)^+$ =276.1954, **Scheme 4.13e**) and BHT-adduct **8** $(M+H)^+$ =339.2357, **Scheme 4.13f**) were detected by LC-MS. It suggests that photoinduced Cu(I)-catalyzed C-C/C-N bond-forming reaction

may proceed through a radical pathway. It is fruitful to note that under an O_2 atmosphere, product **3aa** was obtained with a diminished yield (55%). Thus, the current protocol is more compatible with an inert condition than an O_2 atmosphere (**Scheme 4.13g**). Moreover, the light ON-OFF experiment indicates that continuous visible light irradiation is required for this photochemical conversion (See **Table 4.7**).

4.4.2 Control experiments

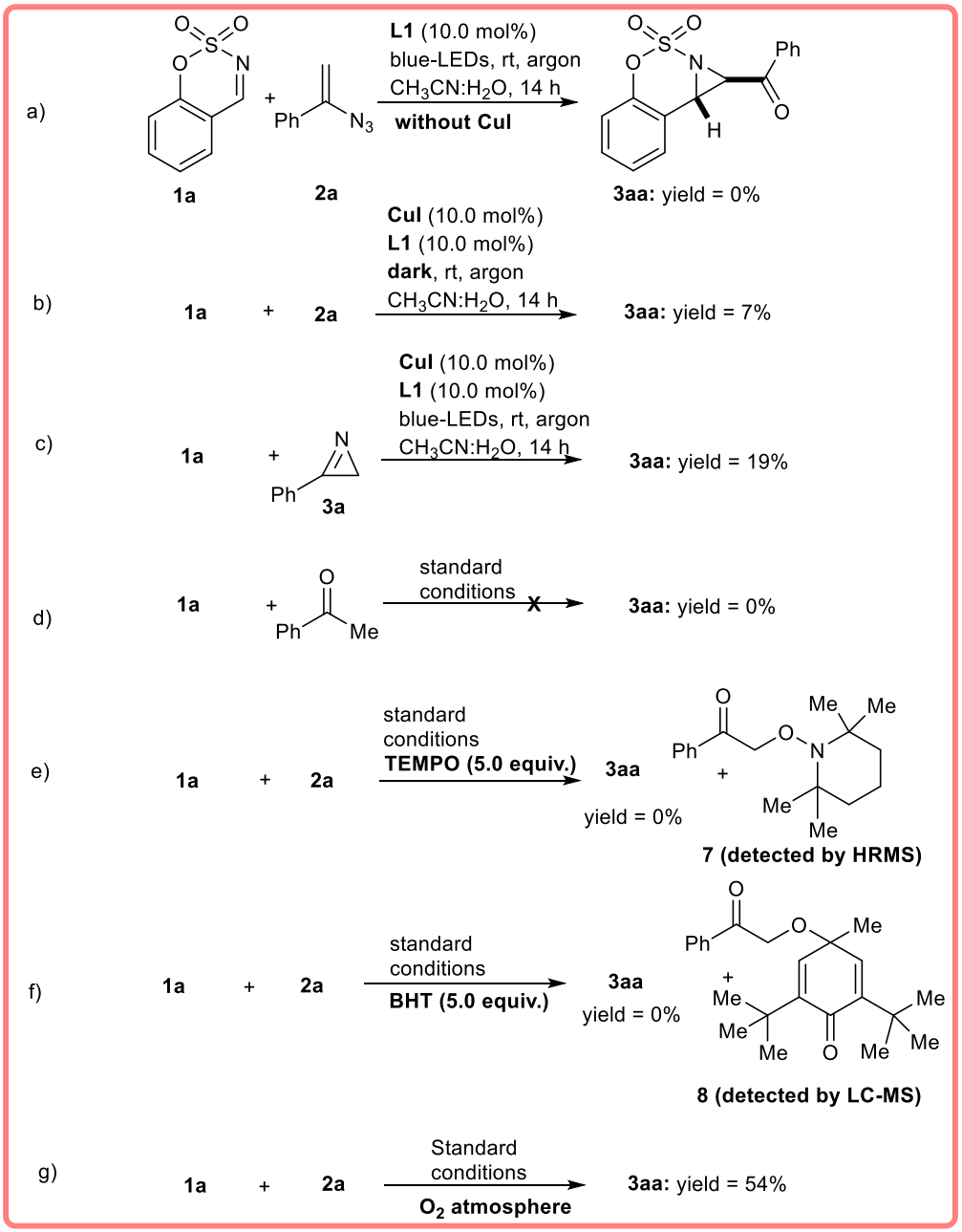

Scheme 4.13. Control experiments.

4.4.3 plausible mechanism

Based on the control experiments, a plausible mechanism for this aziridination reaction is depicted in **Scheme 4.14.** The first step may involve the complexation between CuI and ligand **L1** to form a Cu(I)L1-complex [see the color-changing experiment (**Figure 4.6**) and UV-vis spectra (**Figures 4.7-4.8**). Then, the in situ generated Cu(I)L1-complex absorbs blue LEDs light to form an electron-rich photoexcited Cu(I)L1* species ($E_{Cu}{}^{I}/_{Cu}{}^{II}$= 0.75 V), which triggers a single electron transfer (SET) that may reduce vinyl azide **2a** (E_{red} = -0.53 V) to vinyl azide anion radical **9**. The latter undergoes a denitrogenative decomposition to form an iminyl-Cu(II) radical **10**. This nucleophilic carboncentered radical attacks the C=N bond of **1a** to form another iminyl-copper(II) radical **11**. Next, the intramolecular 1,3-Cu(II) migration and HAT (hydrogen-atom-transfer) of **11** may lead to an organocopper(II) species **12** and subsequent hydrolysis to give a radical intermediate **13**. The latter prone to the oxidative cyclization to afford aziridine **3aa** and regeneration of Cu(I)- complex for the next cycle. The outcome of excellent diastereoselectivity may be explained by the possible four-membered organocopper(III) transition states **TS1** and **TS2** (path **A**). In the case of **TS1**, the orientation of benzoyl and aryl part of sulfamidate is opposite, stabilizing the **TS1** due to the minimum steric repulsion compared to unfavorable **TS2**, which leads to **3aa** with the desired

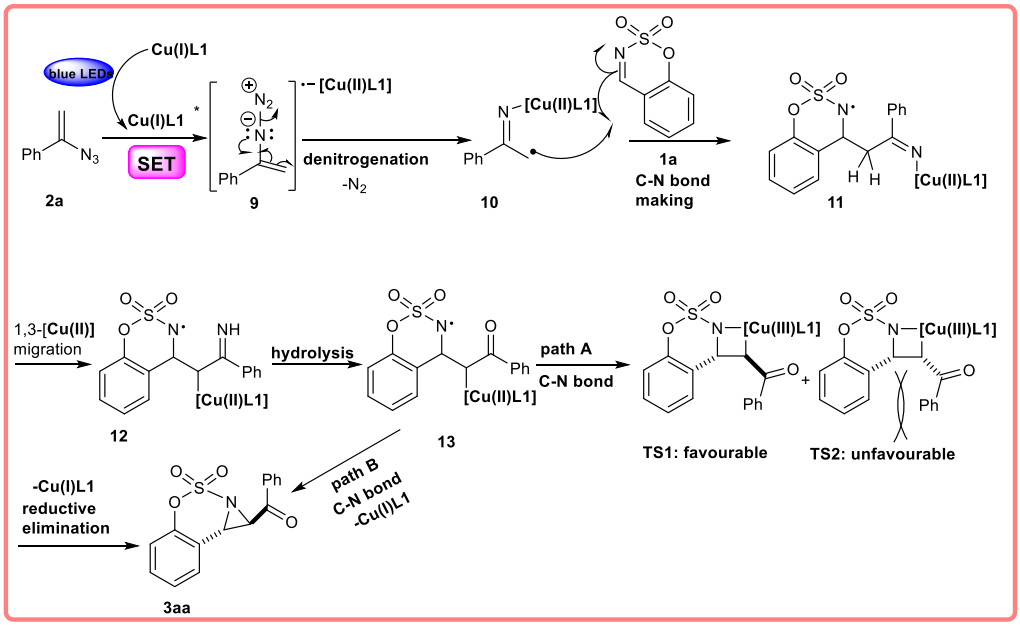

Scheme 4.14. A plausible mechanism.

trans-isomer. Alternatively, without forming a four-membered Cu(III)-complex, the desired **3aa** may be generated directly from Cu(II)-complex 13 via a reductive elimination in path **B**.

4.4.4 Substrate scope

Having optimal reaction conditions in hand, we next delved the generality and scope of this [1C1N+1C] aza-cyclization reaction by reacting a set of cyclic N-sulfonyl aldimines and α-aryl vinyl azides as one carbon atom units for aziridine ring synthesis catalyzed by in situ generated photoinduced Cu(I)-complex irradiated by blue LEDs light. As shown in **Table 4.2,** azides (**2b-2o**) having electron-donating (Me, MeO and *t*-Bu) and electron-withdrawing (Ph, F, Cl, Br, and CF_3) substituents on the aryl rings at *ortho*-, *meta*- and *para* positions smoothly cyclized with **1a**, producing the corresponding aroyl-substituted fused aziridines (**3ab**-**3ao**) with excellent diastereoselectivities (up to 99:1 dr). Notably, the obtained yields of electron-donating substituted aziridines **3ab, 3ac, 3ad, 3aj** and **3am** (76%, 75%, 68%, 68% and 73% yields, respectively) are slightly higher than those electron withdrawing ones (**3ae**-**3ao**; 57-67% yields). Furthermore, vinyl azide with a bulky naphthyl group can also participate in this C-C/C-N/C=O bond-forming reaction, affording a good yield (72%) of **3ap**. Next, cyclic imines (**1b-1l**) adorned with electron-poor halogen atoms (F, Cl and Br) and a number of electron-donating (Me, MeO and EtO) and at C6, C7 and C8 positions on the benzene rings showed good reactivitiy towards the aziridination reactions with a wide array of vinyl azides under the enriched photocatalytic system, resulting in the corresponding aziridines (**3ba-3kg**) with excellent diastereoselectivities However, the acquired yields in the case of electron-withdrawing substituents are, to some extent, higher than those of donating ones. Moreover, N-sulfonyl imine derived from a sizeable 1-hydroxy-2-naphthaldehyde was also a suitable substrate that resulted in 70% yield of **3ma**. It should be noted that alkyl-substituted vinyl azide (**2r**) did not react with cyclic imine **1a** under present conditions. Furthermore, the introduction of a strong electron-withdrawing NO_2 group on the aryl part of vinyl azide or cyclic imine did not participate in this azacyclization reaction. Nevertheless, not only a strained aziridine moiety but also other valuable substituents such as Me, *t*-

Bu, MeO, EtO, F, Cl, Br, CF_3, aryl, Bz, and N-SO_3 were achieved by this method.

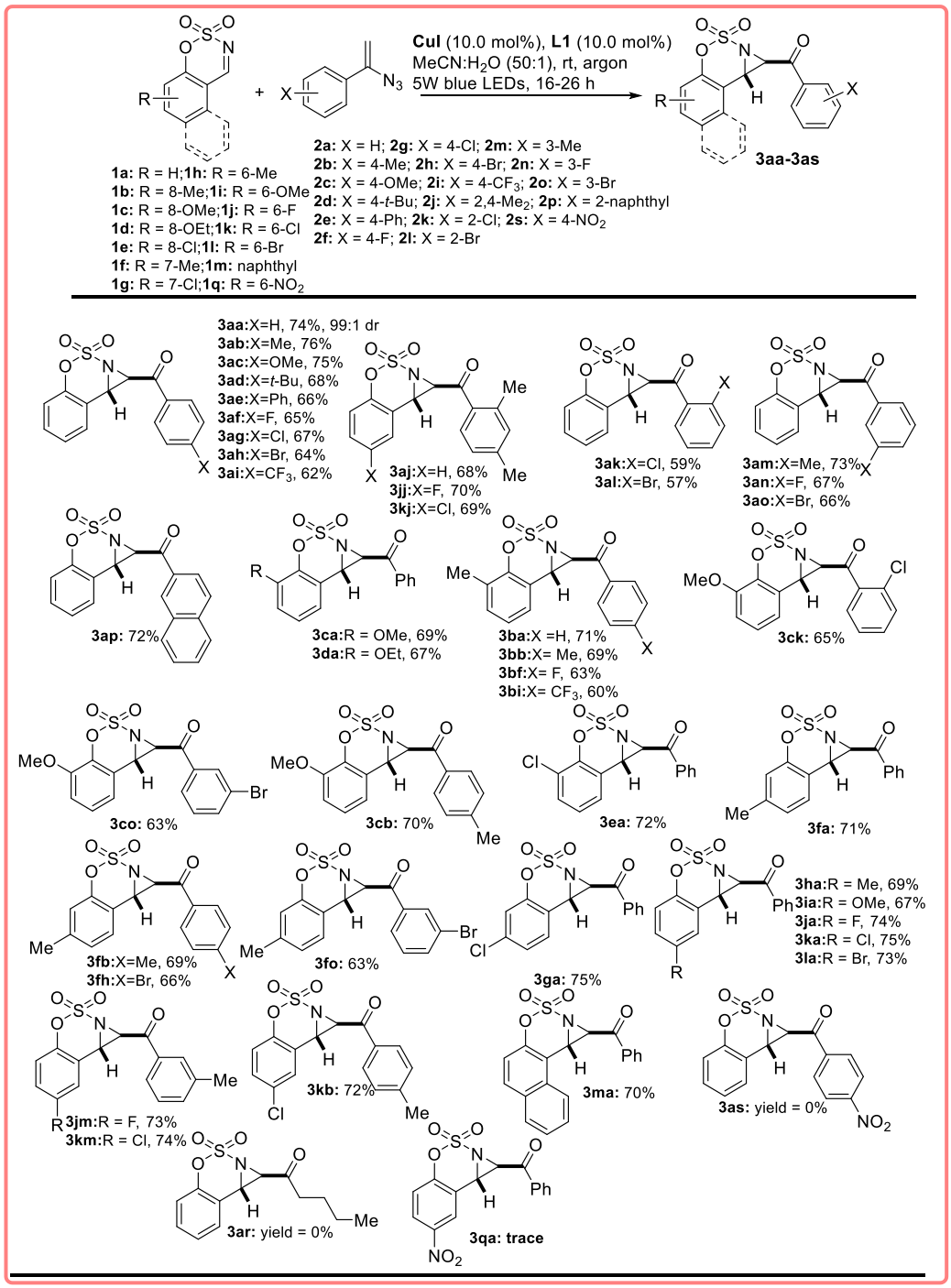

Table 4.2. One-pot access to fused aziridines (**3aa-3as**).

Next, a challenging coupling partner like α-aryl-β-substituted vinyl azide **2q** also underwent aziridination reaction with **1c** under standard conditions to give a lower yield (33%) of **3cq** bearing a tetrasubstituted chiral carbon center after 30 h (**Scheme 4.15**).

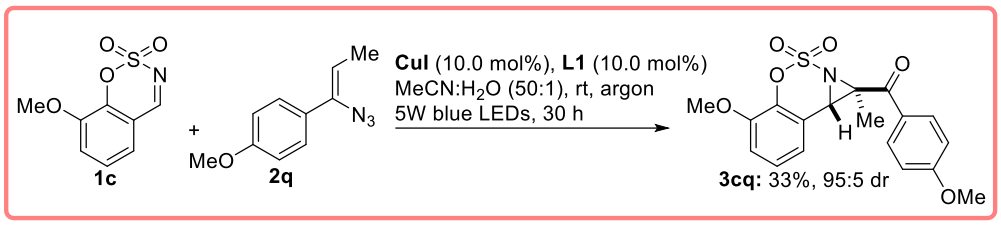

Scheme 4.15. Aziridination reaction using a β-methyl-α-aryl vinyl azide.

To further expand this robust photocatalytic reaction, we chose 5-membered cyclic N-sulfonyl imine (**1n**) as the 1C1N source to carry out the cyclization reaction with vinyl azide **2a**, capable of delivering fused aziridine in 78% yield and 99:1 diastereomeric ratio (**Scheme 4.16**). Gratifyingly, a sterically hindered six-membered N-sulfonyl ketimine **1o** was employed in the aziridination reaction with **2a** that led to 36% yield of a targeted aziridine **3oa** together with the Mannich adduct **6oa** (21% yield) after 32 h. However, replacing the CO_2Et group of **1o** with a methyl one failed to give the product **3pa**.

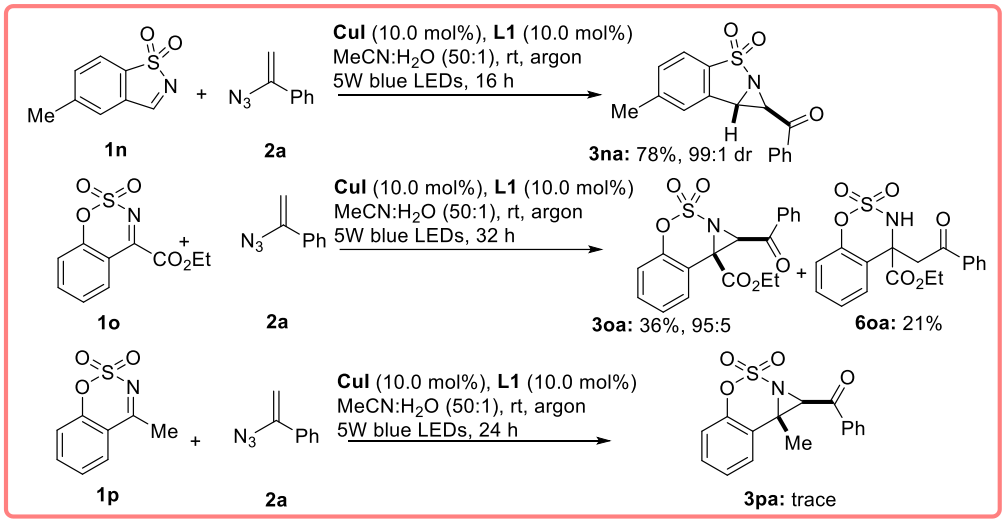

Scheme 4.16. Aziridination reaction using 5- and 6-membered N-sulfonyl imines.

To highlight the synthetic potential of highly strained fused aziridines, we began the reaction between **3aa** and $NH_2OH.HCl$ in the presence of NaOAc in EtOH at room temperature for 48 h. Surprisingly, this reaction concocted 73% yield of a vital class of benzo[*f*]isoxazolo[4,5-*d*][1,2,3]oxathiazepine 5,5-dioxide **4aa** with a single diastereomer (**Table 4.3**). Interestingly, the obtained bis-heterocycle containing important classes of isoxazoline[29-30] and benzo[*f*][1,2,3]oxathiazepine 2,2-dioxide[31-32] may show individual ring's unprecedented biological action or synergistic bioactivity. Therefore, this novel ring expansion concept was applied to other sulfamidate-fused aziridines (**3ae-3fo**) under identical conditions. Pleasantly, they converted into the corresponding 6-7-5 tricyclic products **4ae-4fo** in 66-78% yields with outstanding diastereoselectivities via a selective *endo* C-N bond scission of aziridine ring. Moreover, the *trans*-configuration of **4fa** was unequivocally determined by its single-crystal X-ray diffraction data (CCDC **2264094** for more details **Figure 4.3** and **Table 4.6**). As noted, synthesizing the above bis-heterocyclic building blocks is either difficult to access or inaccessible by the reported methods. Therefore, the current transition-metal-free method would affirmatively pave the way for their practical access.

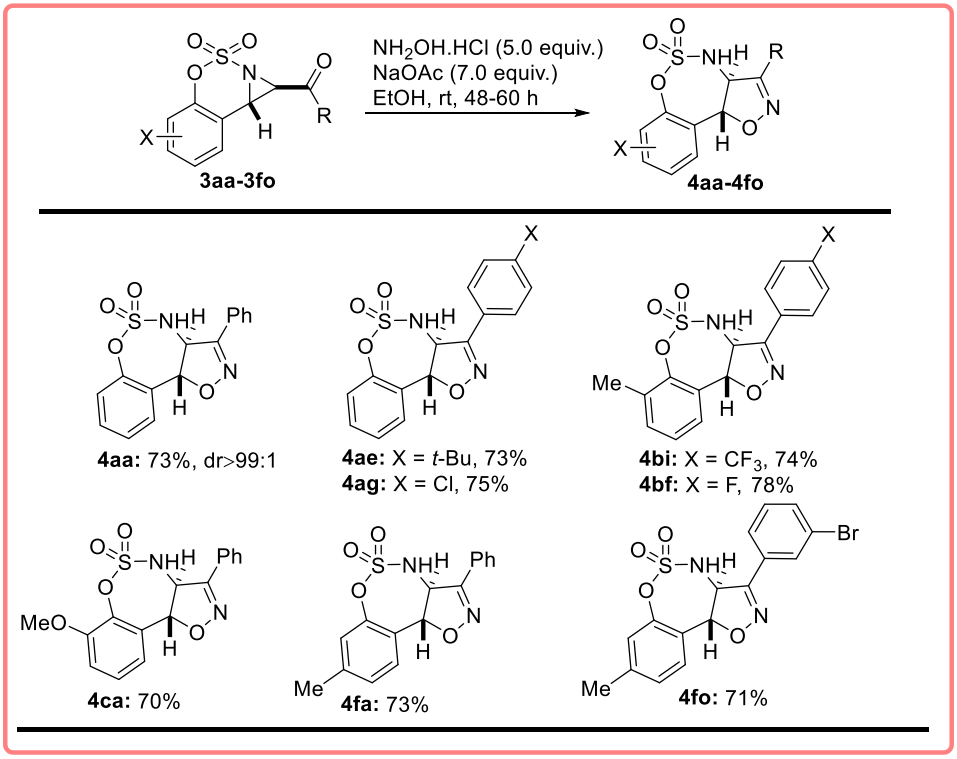

Table 4.3. Transition-metal-free access to benzo[*f*]isoxazolo[4,5-*d*][1,2,3]oxathiazepine 5,5-dioxides (**4aa-4fo**).

We further highlighted the synthetic usefulness of acquired aziridines. The compound **3aa** was treated with Et_3N (2.0 equiv) in MeCN at 55°C (**Method A**, **Table 4.4**). Pleasantly, after 12h, an exciting class[33-34] of seven-membered ene-sulfonamide **5aa** in 79% yield was achieved via a selective cleavage of the *endo* C-N bond. Similarly, this ring-elongation method could convert other aziridines **3ba, 3bb, 3ca,** and **3fa** into the corresponding ene-sulfonamides **5ba, 5bb, 5ca**, and **5fa** in 79-83% yields with 100% atom-economy. Interestingly, at 80°C, 5-membered sulfonamide-fused aziridine **3na** was also transmuted into the desired 6-membered ene-sulfonamide **5na** in a moderated yield of 34%. Alternatively, this ring expansion reaction also succeeded using 1.0 equivalent $LiAlH_4$ (acting as a base) in dry THF at 55 °C (**method B**). Results indicated that the obtained yields by method **B** were somewhat lower (61% and 66% for **5aa** and **5af**, respectively) than those achieved by **method A**. It should be noted

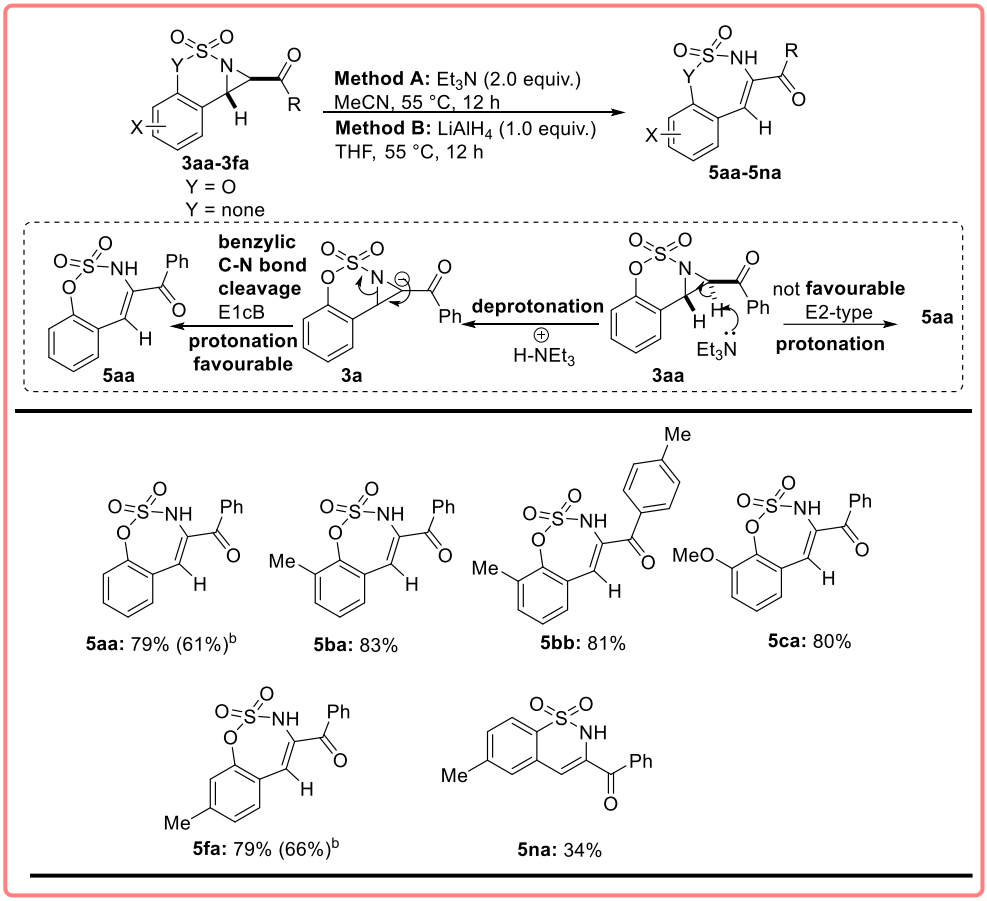

Table 4.4. Base-assisted ring-expansion strategy to 3*H*-benzo[*f*]1,2,3]oxathiazepine 2,2-dioxides (**5aa-5na**).

that the ring expansion reaction may proceed through an abstraction of C(sp^3)-H proton attached to the benzoyl group of **3aa** to generate a stable carbanion intermediate (**3a**), followed by the cleavage of the benzylic C-N bond (E1cB pathway). This *endo* C-N bond cleavage may not be possible through the E2 mechanism due to the non-fulfillment of anti-coplanar orientation between the C-H sigma and C-N bonds of **3aa.**

For the continuation of the synthetic utility of fused-aziridine, the compound **3fa** was selectively hydrogenated external C-N bond of aziridine ring in the presence of 10 mol% Pd/C under H_2-balloon at room temperature for 20 min. This process delivered 91% yield of **6fa** having a pharmacologically attractive β-keto sulfonamide moiety[35-36] **Scheme 4.17.**

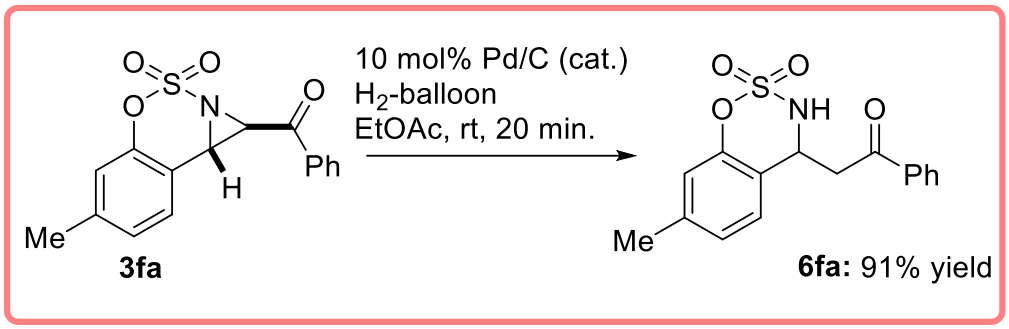

Scheme 4.17. Pd/C-catalyzed hydrogenation of *exo*-C-N bond of aziridine **3fa**.

4.5 Conclusion

In this chapter, a facile visible-light assisted diastereoselective [2+1] aza-cyclization reaction between cyclic N-sulfonyl imines and α-aryl-substituted vinyl azides using in-situ generated Cu(I)-complex as a photocatalyst was developed. This radical-initiated C-C/C-N/C=O bond-making process offers a new strategy for enabling a series of sulfamidate-fused aziridine building blocks. Overall, this technique has several positive features such as easy to handle, use of cheap earth-abundant copper(I)-photocatalyst, room temperature, excellent tolerance of functionality, broad substrate scope, satisfactory chemical yields, excellent diastereoselectivities, and environmentally benign. Intriguingly, the versatility of the resultant aziridines has been demonstrated by

synthesizing historically unexplored benzo[*f*][1,2,3]oxathiazepine dioxides and fused isoxazolines through a metal-free based ring elongation method.

4.6 Experimental Section

General procedure for the synthesis of compounds 1 and 2: All the cyclic sulfamidates (**1a-1o**)[37-39] and vinyl azides (**2a-p**)[40-42] were synthesized by literature known procedures. All the starting materials were known in the literatures. All the catalysts were purchased from commercial suppliers.

Representative procedure for the synthesis of 3aa-3pa: A mixture of **1** (0.2 mmol), **2** (0.4 mmol), and 2,2′-bpy (10 mol%) in MeCN:H_2O (2.0 mL, 50:1) was taken in a screw-capped test tube (25 mL), followed by degassing with argon (four times). Then CuI (10 mol%) was added to this solution. The mixture was further stirred under the irradiation of blue LEDs (4×5W, 460 nm) at room temperature for 24h. After the completion of the reaction, the reaction mixture was extracted with ethyl acetate (3 × 10 mL) and dried over Na_2SO_4. The combined organic phases were evaporated under reduced pressure to give the crude mass which was purified by flash column chromatography using 5 to 10% EtOAc in hexane, affording aziridine **3aa-3pa** as a white solid. The products were characterized by their spectroscopic data (^1H, ^{13}C NMR, and HRMS data).

Representative experimental procedure for the synthesis of Benzo[*f*]isoxazolo[4,5-*d*][1,2,3]oxathiazepine 5,5-dioxides (4aa-4fo): The aziridine (0.1 mmol), $NH_2OH.HCl$ (0.5 mmol) and NaOAc (0.7 mmol) in EtOH (5.0 mL) were taken in a round bottom flask under an argon atmosphere. The reaction mixture was stirred at room temperature. After completion of the starting material, ethanol was removed by a rotary evaporator under reduced pressure to leave the crude product, which was extracted by ethyl acetate (3 × 10 mL), washed with brine solution, and dried over Na_2SO_4. All the extracted solvents were evaporated to give the impure product. Then, it was purified by column chromatography over silica-gel using a mixture of EtOAc/hexane (85:15), providing the expected dihydro-4*H*-benzo[*f*]isoxazolo[4,5-*d*][1,2,3]oxathiazepine 5,5-dioxide. All the products were characterized by ^1H, ^{13}C NMR and HRMS data.

Typical procedure for the synthesis of compound 5aa-5na: To a stirred solution of aziridine **3** (0.1 mmol) in dry MeCN (1.0 mL) was added Et_3N (0.2 mmol) at 60 °C under an argon atmosphere. The reaction mixture was continued stirring for 12h. Afterwards, the reaction mixture was extracted with ethyl acetate (3 × 10 mL), washed with brine solution, and dried over Na_2SO_4. All the combined organic phases were evaporated to give the crude product which was purified by column chromatography over silica-gel using a mixture of EtOAc/hexane (1:15), providing the expected ring expansion product **5**. their spectroscopic data (^1H, ^{13}C NMR and HRMS) characterized the product.

Procedure for the synthesis of compound 6fa: The compound **3fa** (0.12 mmol) in ethyl acetate (5.0 mL) was taken in a two-neck round-bottom flask, followed by the addition of 10% of Pd/C (10 mg) at room temperature under H_2-balloon. Then, the reaction mixture was degassed two times. Then the reaction mixture was vigorously stirred for 20 min. After that, it was filtered off through a celite 545 and washed with EtOAc (3 × 15 mL). Then, the filtrate was concentrated to give the crude product. The residue was purified by column chromatography over silica-gel using a mixture of EtOAc/hexane to give a pure product **6fa**.

Photochemical reaction set-up:

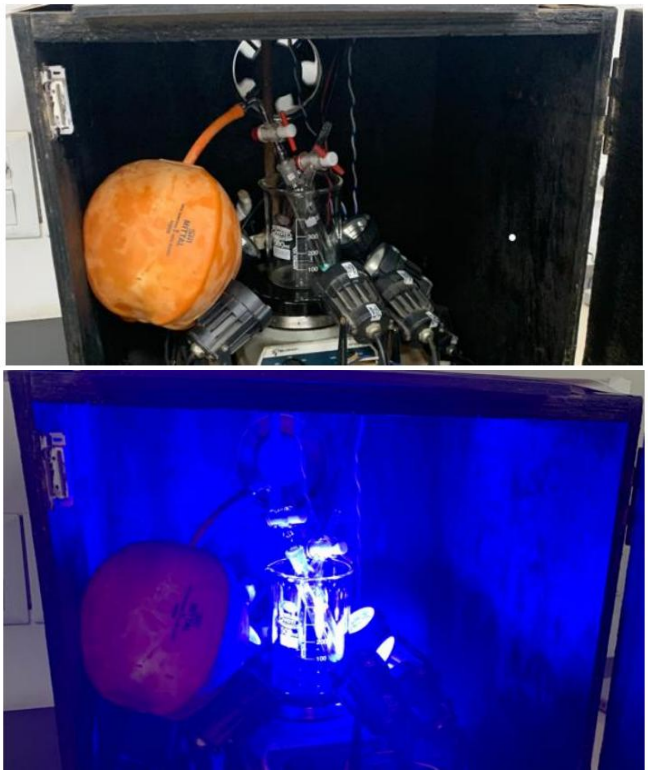

Characterization data:

((1*R,8b*S**)-3,3-Dioxido-1,8b-dihydroazirino[1,2-*c*]benzo[*e*][1,2,3]oxathiazin-1-yl)(phenyl)methanone (3aa):** Colorless solid; mp 142-144 °C; yield = 74% (44.6 mg); dr = 99:1; R_f = 0.22 (EtOAc/Hexane = 15:85); ^{1}H NMR (500 MHz, $CDCl_3$) δ 8.11 (d, *J* = 7.5 Hz, 2H), 7.68 (t, *J* = 7.2 Hz, 1H), 7.56-7.52 (m, 3H), 7.45 (t, *J* = 7.6 Hz, 1H), 7.34 (t, *J* = 7.4 S4 Hz, 1H), 7.18 (d, *J* = 8.1 Hz, 1H), 4.71 (d, *J* = 3.2 Hz, 1H), 4.30 (d, *J* = 3.0 Hz, 1H) ppm; ^{13}C NMR (125 MHz, $CDCl_3$) δ 189.1, 149.8, 135.0, 134.8, 130.7, 129.6, 129.1, 129.0, 127.0, 119.5, 118.1, 47.7, 45.1 ppm; HRMS (ESI-TOF) *m/z* calcd for $C_{15}H_{12}NO_4S$ $[M+H]^+$: 302.0482, found 302.0484.

((1R*,8bS*)-3,3-Dioxido-1,8b-dihydroazirino[1,2-c]benzo[e][1,2,3]oxathiazin-1-yl)(4-methylphenyl)methanone (3ab): Colorless solid; mp 140-142 °C; yield = 76% (47.9 mg); dr = 99:1; R_f = 0.33 (EtOAc/Hexane = 15:85); ^{1}H NMR (500 MHz, $CDCl_3$) δ 8.01 (d, *J* = 8.2 Hz, 2H), 7.52 (dd, *J* = 7.6, 1.3 Hz, 1H), 7.48-7.42 (m, 1H), 7.34-7.31 (m, 3H), 7.17 (d, *J* = 8.1 Hz, 1H), 4.69 (d, *J* = 3.6 Hz, 1H), 4.29 (d, *J* = 3.6 Hz, 1H), 2.45 (s,

3H) ppm; ^{13}C NMR (125 MHz, $CDCl_3$) δ 188.6, 149.8, 146.1, 132.6, 130.6, 129.8, 129.5, 129.1, 127.0, 119.5, 118.2, 47.7, 45.1, 21.8 ppm; HRMS (ESI-TOF) *m/z* calcd for $C_{16}H_{14}NO_4S$ $[M+H]^+$: 316.0638, found 316.0638.

((1*R,8b*S**)-3,3-dioxido-1,8b-dihydroazirino[1,2-*c*]benzo[*e*][1,2,3]oxathiazin-1-yl)(4-methoxyphenyl)methanone (3ac):** White solid; mp 146-148 °C; yield = 75% (49.6 mg); R_f = 0.20 (EtOAc/Hexane = 15:85); ^{1}H NMR (500 MHz, $CDCl_3$) δ 8.10 (d, *J* = 8.7 Hz, 2H), 7.52 (d, *J* = 7.4 Hz, 1H), 7.44 (t, *J* = 7.6 Hz, 1H), 7.33 (t, *J* = 7.5 Hz, 1H), 7.16 (d, *J* = 8.1 Hz, 1H), 7.00 (d, *J* = 8.7 Hz, 2H), 4.66 (d, *J* = 3.5 Hz, 1H), 4.29 (d, *J* = 3.4 Hz, 1H), 3.90 (s, 3H) ppm; ^{13}C NMR (125 MHz, $CDCl_3$) δ 187.2, 164.9, 149.8, 131.5, 130.6, 129.6, 128.1, 126.9, 119.5, 118.3, 114.4, 55.6, 47.6, 45.1 ppm; HRMS (ESI-TOF) *m/z* calcd for $C_{16}H_{13}NNaO_5S$ $[M+Na]^+$: 354.0407, found 354.0409.

((1*R,8b*S**)-(4-(*tert*-Butyl)phenyl)-3,3-dioxido-1,8b-dihydroazirino[1,2-*c*]benzo[*e*][1,2,3]oxathiazin-1-yl)methanone (3ad):** Colorless solid; mp 130-132 °C; yield = 68% (48.6 mg); dr = 99:1; R_f = 0.40 (EtOAc/Hexane = 15:85); ^{1}H NMR (500 MHz, $CDCl_3$) δ 8.05 (d, *J* = 8.5 Hz, 2H), 7.56 (d, *J* = 8.5 Hz, 2H), 7.52 (dd, *J* = 5.8, 1.5 Hz, 1H), 7.45-7.42 (m, 1H), 7.34-7.31 (m, 1H), 7.17 (d, *J* = 8.1 Hz, 1H), 4.69 (d, *J* = 3.6 Hz, 1H), 4.28 (d, *J* = 3.6 Hz, 1H), 1.35 (s, 9H) ppm; ^{13}C NMR (125 MHz, $CDCl_3$) δ 188.6, 158.9, 149.8, 132.5, 130.6, 129.5, 129.0, 127.0, 126.1, 119.5, 118.2, 47.6, 45.2, 35.4, 30.9 ppm; HRMS (ESI-TOF) *m/z* calcd for $C_{19}H_{19}NNaO_4S$ $[M+Na]^+$: 380.0927, found 380.0927.

((1*R,8b*S**)[1,1'-Biphenyl]-4-yl-3,3-Dioxido-1,8b-dihydroazirino[1,2-*c*]benzo[*e*][1,2,3]oxathiazin-1-yl)methanone (3ae):** Colorless solid; mp 148-150 °C; yield = 66% (49.8 mg); dr = 99:1; R_f = 0.33 (EtOAc/Hexane = 15:85); ^{1}H NMR (500 MHz, $CDCl_3$) δ 8.19 (d, *J* = 8.1 Hz, 2H), 7.77 (d, *J* = 8.1 Hz, 1H), 7.69-7.59 (m, 3H), 7.55-7.43 (m, 5H), 7.35 (t, *J* = 7.4 Hz, 1H), 7.19 (d, *J* = 8.1 Hz, 1H), 4.74 (d, *J* = 3.3 Hz, 1H), 4.32 (d, *J* = 3.2 Hz, 1H) ppm; ^{13}C NMR (125 MHz, $CDCl_3$) δ 188.6, 149.9, 147.5, 139.3, 133.7, 132.2, 130.7, 129.6, 129.0, 128.8, 127.7, 127.3, 127.0, 119.5, 118.1, 47.7, 45.2 ppm; HRMS (ESI-TOF) *m/z* calcd for $C_{21}H_{15}NNaO_4S$ $[M+Na]^+$: 400.0614, found 400.0615.

((1*R,8b*S**)-3,3-Dioxido-1,8b-dihydroazirino[1,2-*c*]benzo[*e*][1,2,3]oxathiazin-1-yl)(4- fluorophenyl)methanone (3af):** Colorless solid; mp 140-142 °C; yield = 65% (41.5 mg); dr = 99:1; R_f = 0.31 (EtOAc/Hexane = 15:85); ^{1}H NMR (500 MHz, $CDCl_3$) δ 8.14-8.02 (m, 2H), 7.45 (dd, *J* = 7.6, 1.2 Hz, 1H), 7.38-7.35 (m, 1H), 7.26 (q, *J* = 7.1 Hz, 1H), 7.18-7.11 (m, 2H), 7.08 (d, *J* = 8.2 Hz, 1H), 4.58 (d, *J* = 3.6 Hz, 1H), 4.21 (d, *J* = 3.6 Hz, 1H) ppm; ^{13}C NMR (125 MHz, $CDCl_3$) δ 186.6, 166.6 (d, J_{C-F} = 256.6 Hz), 148.7, 130.8 (d, J_{C-F} = 9.5 Hz), 130.4 (d, J_{C-F} = 2.8 Hz), 129.7, 128.6, 126.0, 118.5, 116.9, 115.4 (d, J_{C-F} = 21.9 Hz), 46.6, 44.1 ppm; ^{19}F NMR (470 MHz, $CDCl_3$) δ -101.39 ppm; HRMS (ESI-TOF) *m/z* calcd for $C_{15}H_{11}FNO_4S$ $[M+H]^+$: 320.0387, found 320.0358.

((1*R,8b*S**)-(4-Chlorophenyl)-3,3-dioxido-1,8b-dihydroazirino[1,2-*c*]benzo[*e*][1,2,3]oxathiazin-1- yl)methanone (3ag):** White solid; mp 130-132 °C; yield = 67% (44.8 mg); dr = 99:1; R_f = 0.31 (EtOAc/Hexane = 15:85); ^{1}H NMR (500 MHz, $CDCl_3$) δ 8.06 (d, *J* = 8.5 Hz, 2H), 7.55-7.51 (m, 3H), 7.46 (t, *J* = 7.9 Hz, 1H), 7.34 (t, *J* = 7.5 Hz, 1H), 7.18 (d, *J* = 8.2 Hz, 1H), 4.64 (d, *J* = 3.6 Hz, 1H), 4.29 (d, *J* = 3.5 Hz, 1H) ppm; ^{13}C NMR (125 MHz, $CDCl_3$) δ 188.1, 149.8, 141.5, 133.3, 130.8, 130.4, 129.6, 129.5, 127.1, 119.5, 117.9, 47.6, 45.1 ppm; HRMS (ESI-TOF) *m/z* calcd for $C_{15}H_{10}ClNNaO_4S$ $[M+Na]^+$: 357.9911, found 357.9912.

((1*R,8b*S**)-(4-Bromophenyl)-3,3-dioxido-1,8b-dihydroazirino[1,2-*c*]benzo[*e*][1,2,3]oxathiazin-1-yl)methanone (3ah):** White solid; mp 162-164 °C; yield = 64% (48.5 mg); dr = 99:1; R_f = 0.31 (EtOAc/Hexane = 15:85); ^{1}H NMR (500 MHz, $CDCl_3$) δ 7.96 (d, *J* = 8.4 Hz, 2H), 7.68 (d, *J* = 8.4 Hz, 2H), 7.53 (d, *J* = 7.3 Hz, 1H), 7.45 (t, *J* = 7.7 Hz, 1H), 7.34 (t, *J* = 7.5 Hz, 1H), 7.16 (d, *J* = 8.2 Hz, 1H), 4.64 (d, *J* = 3.4 Hz, 1H), 4.27 (d, *J* = 3.2 Hz, 1H) ppm; ^{13}C NMR (125 MHz, $CDCl_3$) δ 188.4, 149.8, 133.7, 132.5, 130.8, 130.4, 130.3, 129.6, 127.1, 119.5, 117.8, 47.7, 45.0 ppm; HRMS (ESI-TOF) *m/z* calcd for $C_{15}H_{10}{}^{79}BrNNaO_4S$ $[M+Na]^+$: 401.9406, found 401.9388; HRMS (ESI-TOF) *m/z* calcd for $C_{15}H_{10}{}^{81}BrNNaO_4S$ $[M+Na]^+$: 403.9386, found 403.9382.

((1*R,8b*S**)-3,3-Dioxido-1,8b-dihydroazirino[1,2-*c*]benzo[*e*][1,2,3]oxathiazin-1-yl)(4-(trifluoromethyl)phenyl)methanone**

(3ai): White solid; mp 162-164 °C; yield = 62% (45.7 mg); dr = 99:1; R_f = 0.27 (EtOAc/Hexane = 15:85); ^{1}H NMR (500 MHz, $CDCl_3$) δ 8.23 (d, *J* = 8.1 Hz, 2H), 7.81 (d, *J* = 8.2 Hz, 2H), 7.54 (d, *J* = 7.3 Hz, 1H), 7.46 (t, *J* = 7.8 Hz, 1H), 7.35 (t, *J* = 7.5 Hz, 1H), 7.18 (d, *J* = 8.2 Hz, 1H), 4.68 (d, *J* = 3.5 Hz, 1H), 4.30 (d, *J* = 3.5 Hz, 1H) ppm; ^{13}C NMR (125 MHz, $CDCl_3$) δ 188.6, 149.8, 137.5, 136.2, 135.9, 135.7, 135.4, 130.9, 129.6, 129.4, 127.1, 126.5, 126.22 (q, J_{C-F} = 3.4 Hz), 124.4, 122.2, 120.0, 119.6, 117.7, 47.7, 45.2 ppm; ^{19}F NMR (470 MHz, $CDCl_3$) δ -63.34 ppm; HRMS (ESI-TOF) *m/z* calcd for $C_{16}H_{10}F_3NNaO_4S$ $[M+Na]^+$: 392.0175, found 392.0175.

((1*R,8b*S**)-(2,4-Dimethylphenyl)-3,3-dioxido-1,8b-dihydroazirino[1,2-*c*]benzo[*e*][1,2,3]oxathiazin-1-yl)methanone (3aj):** White solid; mp 178-180 °C; yield= 68% (44.7 mg); R_f = 0.35 (EtOAc/Hexane = 15:85); ^{1}H NMR (500 MHz, $CDCl_3$) δ 8.07 (s, 1H), 7.53 (dd, *J* = 7.6, 1.4 Hz, 1H), 7.46-7.43 (m, 1H), 7.35- 7.32 (m, 1H), 7.26 (s, 1H), 7.20-7.15 (m, 2H), 4.53 (d, *J* = 3.5 Hz, 1H), 4.23 (d, *J* = 3.5 Hz, 1H), 2.49 (s, 3H), 2.43 (s, 3H) ppm; ^{13}C NMR (125 MHz, $CDCl_3$) δ 190.0, 149.8, 143.9, 139.1, 134.7, 133.8, 133.7, 130.7, 129.5, 127.0, 121.9, 119.6, 117.9, 47.9, 46.4, 23.0, 20.9 ppm; HRMS (ESI-TOF) *m/z* calcd for $C_{17}H_{15}NNaO_4S$ $[M+Na]^+$: 352.0614, found 352.0587.

((1*R,8b*S**)-(2-Chlorophenyl)-3,3-dioxido-1,8b-dihydroazirino[1,2-*c*]benzo[*e*][1,2,3]oxathiazin-1-yl)methanone (3ak):** White solid; mp 136-138 °C; yield = 59% (39.6 mg); R_f = 0.31 (EtOAc/Hexane = 15:85); ^{1}H NMR (500 MHz, $CDCl_3$) δ 7.72 (d, *J* = 7.5 Hz, 1H), 7.51 (d, *J* = 6.9 Hz, 2H), 7.46-7.41 (m, 3H), 7.33 (t, *J* = 7.4 Hz, 1H), 7.15 (d, *J* = 8.1 Hz, 1H), 4.66 (d, *J* = 2.6 Hz, 1H), 4.18 (d, *J* = 2.6 Hz, 1H) ppm; ^{13}C NMR (125 MHz, $CDCl_3$) δ 191.7, 149.8, 136.2, 133.8, 132.2, 131.0, 130.7, 130.6, 129.5, 127.5, 127.0, 119.5, 117.9, 49.2, 47.7 ppm; HRMS (ESI-TOF) *m/z* calcd for $C_{15}H_{10}ClNNaO_4S$ $[M+Na]^+$: 357.9911, found 357.9919.

((1*R,8b*S**)-(2-Bromophenyl)-3,3-dioxido-1,8b-dihydroazirino[1,2-*c*]benzo[*e*][1,2,3]oxathiazin-1-yl)methanone (3al):** White solid; mp 174-176 °C; yield = 57% (43.3 mg); R_f = 0.31 (EtOAc/Hexane = 15:85); ^{1}H NMR (500 MHz, $CDCl_3$) δ 7.66 (t, *J* = 6.2 Hz, 1H), 7.52-7.40 (m, 5H), 7.33 (t, *J* = 7.5 Hz, 1H), 7.15 (d, *J* = 8.2 Hz, 1H), 4.63 (d, *J* = 3.3 Hz, 1H), 4.19 (d, *J* = 3.2 Hz, 1H)

ppm; ^{13}C NMR (125 MHz, $CDCl_3$) δ 192.5, 149.8, 138.2, 133.9, 133.6, 130.8, 130.6, 129.6, 127.9, 127.0, 119.9, 119.5, 117.8, 49.3, 47.3 ppm; HRMS (ESI-TOF) *m/z* calcd for $C_{15}H_{10}{}^{79}BrNNaO_4S$ $[M+Na]^+$: 401.9406, found 401.9404; HRMS (ESI-TOF) *m/z* calcd for $C_{15}H_{10}{}^{81}BrNNaO_4S$ $[M+Na]^+$: 403.9386, found 403.9385.

((1*R,8b*S**)-3,3-Dioxido-1,8b-dihydroazirino[1,2-*c*]benzo[*e*][1,2,3]oxathiazin-1-yl)(3-methylphenyl)methanone (3am):** White solid; mp 170-172 °C; yield = 73% (46.0 mg); R_f = 0.33 (EtOAc/Hexane = 15:85); ^{1}H NMR (500 MHz, $CDCl_3$) δ 7.89 (d, *J* = 6.4 Hz, 2H), 7.55-7.39 (m, 4H), 7.33 (t, *J* = 7.5 Hz, 1H), 7.16 (d, *J* = 8.2 Hz, 1H), 4.70 (d, *J* = 3.5 Hz, 1H), 4.27 (d, *J* = 3.5 Hz, 1H), 2.44 (s, 3H) ppm; ^{13}C NMR (125 MHz, $CDCl_3$) δ 189.3, 149.8, 139.1, 135.6, 135.1, 130.7, 129.6, 129.4, 129.0, 127.0, 126.2, 119.5, 118.1, 47.8, 45.1, 21.3 ppm; HRMS (ESI-TOF) *m/z* calcd for $C_{16}H_{13}NNaO_4S$ $[M+Na]^+$: 338.0457, found 338.0423.

((1*R,8b*S**)-(3-Fluorophenyl)-3,3-Dioxido-1,8b-dihydroazirino[1,2-*c*]benzo[*e*][1,2,3]oxathiazin-1-yl)methanone (3an):** White solid; mp 146-148 °C; yield = 67% (42.7 mg); R_f = 0.31 (EtOAc/Hexane = 15:85); ^{1}H NMR (500 MHz, $CDCl_3$) δ 7.92 S10 (d, *J* = 7.8 Hz, 1H), 7.78-7.74 (m, 1H), 7.56-7.52 (m, 2H), 7.47-7.43 (m, 1H), 7.40-7.33 (m, 2H), 7.17 (d, *J* = 8.2 Hz, 1H), 4.66 (d, *J* = 3.6 Hz, 1H), 4.29 (d, *J* = 3.6 Hz, 1H) ppm; ^{13}C NMR (125 MHz, $CDCl_3$) δ 188.2 (d, J_{C-F} = 1.9 Hz), 162.9 (d, J_{C-F} = 248.6 Hz), 149.8, 136.9 (d, J_{C-F} = 6.5 Hz), 131.2 – 130.7 (m), 129.6, 127.1, 124.94 (d, J_{C-F} = 2.9 Hz), 121.9 (d, J_{C-F} = 21.2 Hz), 119.5, 117.8, 115.6 (d, J_{C-F} = 22.7 Hz), 47.8, 45.1 ppm; ^{19}F NMR (470 MHz, $CDCl_3$) δ -110.30 (m) ppm; HRMS (ESI-TOF) *m/z* calcd for $C_{15}H_{11}FNO_4S$ $[M+H]^+$: 320.0387, found 320.0360.

((1*R,8b*S**)-(3-Bromophenyl)-3,3-dioxido-1,8b-dihydroazirino[1,2-*c*]benzo[*e*][1,2,3]oxathiazin-1-yl)methanone (3ao):** White solid; mp 166-168 °C; yield = 66% (50.1 mg); R_f = 0.31 (EtOAc/Hexane = 15:85); ^{1}H NMR (500 MHz, $CDCl_3$) δ 8.22 (s, 1H), 8.08 (d, *J* = 7.7 Hz, 1H), 7.82 (d, *J* = 7.7 Hz, 1H), 7.56 (d, *J* = 7.4 Hz, 1H), 7.49-7.44 (m, 2H), 7.37 (t, *J* = 7.5 Hz, 1H), 7.20 (d, *J* = 8.2 Hz, 1H), 4.67 (d, *J* = 3.3 Hz, 1H), 4.30 (d, *J* = 3.3 Hz, 1H) ppm; ^{13}C NMR (125 MHz, $CDCl_3$) δ 188.1, 149.8, 137.6, 136.6, 131.7, 130.9, 130.7, 129.6,

127.6, 127.1, 123.5, 119.6, 117.8, 47.8, 45.0 ppm; HRMS (ESI-TOF) *m/z* calcd for $C_{15}H_{10}{}^{79}BrNNaO_4S$ $[M+Na]^+$: 401.9406, found 401.9400; HRMS (ESI-TOF) *m/z* calcd for $C_{15}H_{10}{}^{81}BrNNaO_4S$ $[M+Na]^+$: 403.9386, found 403.9371.

((1*R,8b*S**)-3,3-Dioxido-1,8b-dihydroazirino[1,2-*c*]benzo[*e*][1,2,3]oxathiazin-1-yl)(naphthalen-2-yl)methanone (3ap):** White solid; mp 160-162 °C; yield = 72% (50.5 mg); R_f = 0.28 (EtOAc/Hexane = 15:85); ^1H NMR (500 MHz, $CDCl_3$) δ 8.72 (s, 1H), 8.12-8.07 (m, 1H), 8.06-8.02 (m, 1H), 7.96 (d, *J* = 8.4 Hz, 1H), 7.91 (d, *J* = 8.0 Hz, 1H), 7.69-7.65 (m, 1H), 7.62-7.59 (m, 1H), 7.56 (d, *J* = 6.3 Hz, 1H), 7.47 (dd, *J* = 10.4, 4.8 Hz, 1H), 7.37-7.34 (m, 1H), 7.21 (d, *J* = 8.0 Hz, 1H), 4.86 (d, *J* = 3.3 Hz, 1H), 4.36 (d, *J* = 3.3 Hz, 1H) ppm; ^{13}C NMR (125 MHz, $CDCl_3$) δ 189.0, 149.9, 136.2, 132.4, 131.8, 130.6, 130.5, 130.0, 129.6, 129.5, 129.1, 127.9, 127.3, 127.0, 123.6, 119.5, 118.2, 47.8, 45.2 ppm; HRMS (ESI-TOF) *m/z* calcd for $C_{19}H_{13}NNaO_4S$ $[M+Na]^+$: 374.0457, found 374.0475.

((1*R,8b*S**)-5-Methoxy-3,3-dioxido-1,8b-dihydroazirino[1,2-*c*]benzo[*e*][1,2,3]oxathiazin-1-yl)(phenyl)methanone (3ca):** White solid; mp 178-180 °C; yield = 69% (45.7 mg); R_f = 0.20 (EtOAc/Hexane = 15:85); ^1H NMR (500 MHz, $CDCl_3$) δ 8.10 (d, *J* = 7.7 Hz, 2H), 7.67 (t, *J* = 7.4 Hz, 1H), 7.54 (t, *J* = 7.7 Hz, 2H), 7.26 (t, *J* = 3.9 Hz, 1H), 7.08-7.02 (m, 2H), 4.73 (d, *J* = 3.5 Hz, 1H), 4.26 (d, *J* = 3.5 Hz, 1H), 3.92 (s, 3H) ppm; ^{13}C NMR (125 MHz, $CDCl_3$) δ 189.2, 149.4, 138.8, 135.1, 134.7, 129.1, 128.9, 127.1, 120.6, 119.1, 113.9, 56.4, 47.8, 44.9 ppm; HRMS (ESI-TOF) *m/z* calcd for $C_{16}H_{13}NNaO_5S$ $[M+Na]^+$: 354.0407, found 354.0412.

((1*R,8b*S**)-5-Ethoxy-3,3-dioxido-1,8b-dihydroazirino[1,2-*c*]benzo[*e*][1,2,3]oxathiazin-1-yl)(phenyl)methanone (3da):** White solid; mp 182-184 °C; yield = 67% (46.1 mg); R_f = 0.20 (EtOAc/Hexane = 15:85); ^1H NMR (500 MHz, $CDCl_3$) δ 8.12 (d, *J* = 7.3 Hz, 2H), 7.69 (t, *J* = 6.8 Hz, 1H), 7.56 (t, *J* = 7.1 Hz, 2H), 7.25 (t, *J* = 7.8 Hz, 1H), 7.08 (d, *J* = 7.3 Hz, 1H), 7.04 (d, *J* = 8.1 Hz, 1H), 4.75 (s, 1H), 4.27 (s, 1H), 4.21 – 4.09 (m, 2H), 1.49 (t, *J* = 6.6 Hz, 3H) ppm; ^{13}C NMR (125 MHz, $CDCl_3$) δ 189.2, 148.8, 139.0, 135.1, 134.7, 129.1, 128.9, 127.0, 120.5, 119.1, 115.1, 65.2, 47.8, 44.9, 14.6 ppm;

HRMS (ESI-TOF) *m/z* calcd for $C_{17}H_{16}NO_5S$ $[M+H]^+$: 346.0744, found 346.0748.

((1*R,8b*S**)-5-Methyl-3,3-dioxido-1,8b-dihydroazirino[1,2-*c*]benzo[*e*][1,2,3]oxathiazin-1-yl)(phenyl)methanone (3ba):** White solid; mp 176-178 °C; yield =71% (44.6 mg); R_f = 0.26 (EtOAc/Hexane = 15:85); ^{1}H NMR (500 MHz, $CDCl_3$) δ 8.10 (d, *J* = 7.5 Hz, 2H), 7.67 (t, *J* = 7.1 Hz, 1H), 7.54 (t, *J* = 7.4 Hz, 2H), 7.34-7.19 (m, 3H), 4.70 (d, *J* = 3.0 Hz, 1H), 4.25 (d, *J* = 3.0 Hz, 1H), 2.33 (s, 3H) ppm; ^{13}C NMR (125 MHz, $CDCl_3$) δ 189.3, 148.2, 135.1, 134.7, 132.3, 129.2, 129.1, 128.9, 127.1, 126.4, 117.7, 48.0, 45.0, 14.8 ppm; HRMS (ESI-TOF) *m/z* calcd for $C_{16}H_{14}NO_4S$ $[M+H]^+$: 316.0638, found 316.0608.

((1*R,8b*S**)-5-Methyl-3,3-dioxido-1,8b-dihydroazirino[1,2-*c*]benzo[*e*][1,2,3]oxathiazin-1-yl)(4- methylphenyl)methanone (3bb):** White solid; mp 188-190 °C; yield = 69% (45.4 mg); R_f = 0.31 (EtOAc/Hexane = 15:85); ^{1}H NMR (500 MHz, $CDCl_3$) δ 8.00 (d, *J* = 8.0 Hz, 2H), 7.33 (d, *J* = 7.7 Hz, 3H), 7.28 (t, *J* = 8.1 Hz, 1H), 7.21 (t, *J* = 7.6 Hz, 1H), 4.68 (d, *J* = 3.5 Hz, 1H), 4.24 (d, *J* = 3.5 Hz, 1H), 2.44 (s, 3H), 2.33 (s, 3H) ppm; ^{13}C NMR (125 MHz, $CDCl_3$) δ 188.7, 148.2, 146.0, 132.7, 132.2, 129.8, 129.1, 129.0, 127.1, 126.4, 117.8, 47.9, 45.0, 21.8, 14.8 ppm; HRMS (ESI-TOF) *m/z* calcd for $C_{17}H_{15}NNaO_4S$ $[M+Na]^+$: 352.0614, found 352.0614.

((1*R,8b*S**)-4-Flurophenyl-5-methyl-3,3-dioxido-1,8b-dihydroazirino[1,2-*c*]benzo[*e*][1,2,3]oxathiazin-1-yl)methanone (3bf):** White solid; mp 182-184 °C; yield = 63% (41.9 mg); R_f = 0.35 (EtOAc/Hexane = 15:85); ^{1}H NMR (400 MHz, $CDCl_3$) δ 8.17-8.13 (m, 2H), 7.34 (d, *J* = 7.2 Hz, 1H), 7.29 (d, *J* = 7.3 Hz, 1H), 7.26-7.18 (m, 3H), 4.64 (d, *J* = 3.4 Hz, 1H), 4.25 (d, *J* = 3.4 Hz, 1H), 2.33 (s, 3H) ppm; ^{13}C NMR (100 MHz, $CDCl_3$) δ 187.8, 166.7 (d, J_{C-F} = 256.5 Hz), 148.2, 132.4, 131.8 (d, J_{C-F} = 9.7 Hz), 131.56 (d, J_{C-F} = 2.9 Hz), 129.2, 127.1, 126.5, 117.6, 116.4 (d, J_{C-F} = 21.9 Hz), 47.8, 45.0, 14.8 ppm; ^{19}F NMR (470 MHz, $CDCl_3$) δ -101.50 (m) ppm; HRMS (ESI-TOF) *m/z* calcd for $C_{16}H_{12}FNNaO_4S$ $[M+Na]^+$: 356.0363, found 356.0363.

((1*R,8b*S**)-5-Methyl-3,3-dioxido-1,8b-dihydroazirino[1,2-*c*]benzo[*e*][1,2,3]oxathiazin-1-yl)(4-(trifluoromethyl)phenyl)methanone**

(3bi): White solid; mp 190-192 °C; yield = 60% (46.0 mg); R_f = 0.33 (EtOAc/Hexane = 15:85); ^{1}H NMR (500 MHz, $CDCl_3$) δ 8.22 (d, *J* = 8.2 Hz, 2H), 7.81 (d, *J* = 8.2 Hz, 2H), 7.35 (d, *J* = 7.3 Hz, 1H), 7.30 (d, *J* = 7.4 Hz, 1H), 7.22 (t, *J* = 7.6 Hz, 1H), 4.67 (d, *J* = 3.6 Hz, 1H), 4.26 (d, *J* = 3.6 Hz, 1H), 2.33 (s, 3H) ppm; ^{13}C NMR (125 MHz, $CDCl_3$) δ 188.8, 148.2, 137.5, 136.1, 135.9, 135.6, 135.3, 132.5, 129.35 (d, J_{C-F} = 6.2 Hz), 128.8, 128.47 (d, J_{C-F} = 2.2 Hz), 127.2, 126.5, 126.18 (q, J_{C-F} = 3.3 Hz), 124.4, 122.2, 120.0, 117.3, 47.9, 45.1, 14.8 ppm; ^{19}F NMR (470 MHz, $CDCl_3$) δ -63.32 (s) ppm; HRMS (ESI-TOF) *m/z* calcd for $C_{17}H_{12}F_3NNaO_4S$ $[M+Na]^+$: 406.0331, found 406.0321.

((1*R,8b*S**)-(2-Chlorophenyl)-5-methoxy-3,3-dioxido-1,8b-dihydroazirino[1,2-*c*]benzo[*e*][1,2,3]oxathiazin-1-yl)methanone (3ck):** White solid; mp 190-192 °C; yield = 65% (47.5 mg); R_f = 0.20 (EtOAc/Hexane = 15:85); ^{1}H NMR (500 MHz, $CDCl_3$) δ 7.71 (d, *J* = 7.3 Hz, 1H), 7.53-7.48 (m, 1H), 7.48-7.39 (m, 2H), 7.26 (d, *J* = 6.3 Hz, 1H), 7.06-7.01 (m, 2H), 4.68 (d, *J* = 2.7 Hz, 1H), 4.15 (d, *J* = 2.6 Hz, 1H), 3.90 (s, 3H) ppm; ^{13}C NMR (125 MHz, $CDCl_3$) δ 191.7, 149.3, 138.8, 136.2, 133.8, 132.2, 130.7, 130.6, 127.4, 127.0, 120.5, 118.9, 114.0, 56.3, 49.3, 47.6 ppm; HRMS (ESI-TOF) *m/z* calcd for $C_{16}H_{12}ClNNaO_5S$ $[M+Na]^+$: 388.0017, found 388.0012.

((1*R,8b*S**)-5-Methoxy-3,3-dioxido-1,8b-dihydroazirino[1,2-*c*]benzo[*e*][1,2,3]oxathiazin-1-yl)(4- methylphenyl)methanone (3cb):** White solid; mp 190- 192 °C; yield =70% (48.3 mg); R_f = 0.21 (EtOAc/Hexane = 15:85); ^{1}H NMR (500 MHz, $CDCl_3$) δ 7.99 (d, *J* = 7.4 Hz, 2H), 7.33 (d, *J* = 7.1 Hz, 2H), 7.28-7.22 (m, 1H), 7.07-7.01 (m, 2H), 4.71 (s, 1H), 4.24 (s, 1H), 3.91 (s, 3H), 2.44 (s, 3H) ppm; ^{13}C NMR (125 MHz, $CDCl_3$) δ 188.6, 149.4, 146.0, 138.8, 132.6, 129.8, 129.1, 127.0, 120.6, 119.2, 113.8, 56.4, 47.8, 44.9, 21.8 ppm; HRMS (ESI-TOF) *m/z* calcd for $C_{17}H_{16}NO_5S$ $[M+H]^+$: 346.0744, found 346.0738.

((1*R,8b*S**)-(3-Bromophenyl)-5-methoxy-3,3-dioxido-1,8b-dihydroazirino[1,2-*c*]benzo[*e*][1,2,3]oxathiazin-1-yl)methanone (3co):** White solid; mp 194-196 °C; yield = 63% (51.7 mg); R_f = 0.20 (EtOAc/Hexane = 15:85); ^{1}H NMR (500 MHz, $CDCl_3$) δ 8.20 (s, 1H), 8.05 (d, *J* = 7.3 Hz, 1H), 7.79 (d, *J* = 7.4 Hz, 1H), 7.43 (t, *J* = 7.5 Hz, 1H), 7.27 (d, *J* = 6.6 Hz, 1H), 7.08-

7.03 (m, 2H), 4.66 (s, 1H), 4.24 (d, *J* = 1.2 Hz, 1H), 3.91 (s, 3H) ppm; ^{13}C NMR (125 MHz, $CDCl_3$) δ 188.2, 149.4, 138.7, 137.6, 136.6, 131.7, 130.7, 127.6, 127.2, 123.5, 120.6, 118.8, 114.0, 56.4, 47.9, 44.8 ppm; HRMS (ESI-TOF) *m/z* calcd for $C_{16}H_{12}{}^{79}BrNNaO_5S$ $[M+Na]^+$: 435.9512, found 435.9510; HRMS (ESI-TOF) *m/z* calcd for $C_{16}H_{12}{}^{81}BrNNaO_5S$ $[M+Na]^+$: 433.9491, found 433.9487.

((1*R,8b*S**)-5-Chloro-3,3-dioxido-1,8b-dihydroazirino[1,2-*c*]benzo[*e*][1,2,3]oxathiazin-1-yl)(phenyl)methanone (3ea):** White solid; mp 90-92 °C; yield = 72% (48.3 mg); R_f = 0.51 (EtOAc/Hexane = 15:85); ^{1}H NMR (500 MHz, $CDCl_3$) δ 8.11 (d, *J* = 7.2 Hz, 2H), 7.69 (t, *J* = 6.4 Hz, 1H), 7.59-7.49 (m, 3H), 7.44 (d, *J* = 7.0 Hz, 1H), 7.28 (d, *J* = 7.9 Hz, 1H), 4.74 (d, *J* = 2.3 Hz, 1H), 4.32 (d, *J* = 1.9 Hz, 1H) ppm; ^{13}C NMR (125 MHz, $CDCl_3$) δ 188.7, 145.7, 134.9, 131.4, 129.2, 129.1, 128.9, 127.8, 127.2, 124.9, 120.0, 47.4, 44.7 ppm; HRMS (ESI-TOF) *m/z* calcd for $C_{15}H_{11}ClNO_4S$ $[M+H]^+$: 336.0092, found 336.0065.

((1*R,8b*S**)-6-Methyl-3,3-dioxido-1,8b-dihydroazirino[1,2-*c*]benzo[*e*][1,2,3]oxathiazin-1-yl)(phenyl)methanone (3fa):** White solid; mp 172-174 °C; yield = 71% (44.7 mg); R_f = 0.28 (EtOAc/Hexane = 15:85); ^{1}H NMR (500 MHz, $CDCl_3$) δ 8.10- 8.08 (m, 2H), 7.67 (t, *J* = 7.4 Hz, 1H), 7.54 (t, *J* = 7.8 Hz, 2H), 7.39 (d, *J* = 7.7 Hz, 1H), 7.13 (d, *J* = 7.7 Hz, 1H), 6.98 (s, 1H), 4.67 (d, *J* = 3.6 Hz, 1H), 4.25 (d, *J* = 3.6 Hz, 1H), 2.40 (s, 3H) ppm; ^{13}C NMR (125 MHz, $CDCl_3$) δ 189.3, 149.7, 141.7, 135.1, 134.7, 129.2, 129.1, 128.9, 127.7, 119.9, 114.8, 47.8, 45.2, 21.3 ppm; HRMS (ESI-TOF) *m/z* calcd for $C_{16}H_{14}NO_4S$ $[M+H]^+$: 316.0638, found 316.0611.

((1*R,8b*S**)-6-Methyl-3,3-dioxido-1,8b-dihydroazirino[1,2-*c*]benzo[*e*][1,2,3]oxathiazin-1-yl)(4-methylphenyl)methanone (3fb):** White solid; mp 190-192 °C; yield = 69% (45.4 mg); R_f = 0.32 (EtOAc/Hexane = 15:85); ^{1}H NMR (500 MHz, $CDCl_3$) δ 7.99 (d, *J* = 7.4 Hz, 2H), 7.38 (d, *J* = 7.5 Hz, 1H), 7.33 (d, *J* = 7.4 Hz, 2H), 7.12 (d, *J* = 7.3 Hz, 1H), 6.98 (s, 1H), 4.65 (s, 1H), 4.24 (s, 1H), 2.45 (s, 3H), 2.40 (s, 3H) ppm; ^{13}C NMR (125 MHz, $CDCl_3$) δ 188.7, 149.7, 146.0, 141.6, 132.7, 129.8, 129.2, 129.1, 127.6, 119.9,

114.9, 47.8, 45.2, 21.8, 21.3 ppm; HRMS (ESI-TOF) *m/z* calcd for $C_{17}H_{16}NO_4S$ $[M+H]^+$: 330.0795, found 330.0797.

((1*R,8b*S**)-(3-Bromophenyl)-6-methyl-3,3-dioxido-1,8b-dihydroazirino[1,2-*c*]benzo[*e*][1,2,3]oxathiazin-1-yl)methanone (3fo):** White solid; mp 176-178 °C; yield = 63% (49.6 mg); R_f = 0.35 (EtOAc/Hexane = 15:85); ^{1}H NMR (500 MHz, $CDCl_3$) δ 8.19 (s, 1H), 8.04 (d, *J* = 7.7 Hz, 1H), 7.79 (d, *J* = 7.7 Hz, 1H), 7.47-7.35 (m, 2H), 7.14 (d, *J* = 7.6 Hz, 1H), 6.98 (s, 1H), 4.60 (d, *J* = 3.5 Hz, 1H), 4.23 (d, *J* = 3.4 Hz, 1H), 2.40 (s, 3H) ppm; ^{13}C NMR (125 MHz, $CDCl_3$) δ 188.3, 149.7, 141.9, 137.5, 136.7, 131.7, 130.7, 129.3, 127.8, 127.5, 123.5, 120.0, 114.5, 47.9, 45.1, 21.3 ppm; HRMS (ESI-TOF) *m/z* calcd for $C_{16}H_{12}{}^{79}BrNNaO_4S$ $[M+Na]^+$: 415.9563, found 415.9553; HRMS (ESI-TOF) *m/z* calcd for $C_{16}H_{12}{}^{81}BrNNaO_4S$ $[M+Na]^+$: 417.9542, found 417.9526.

((1*R,8b*S**)-(4-Bromophenyl)-6-methyl-3,3-dioxido-1,8b-dihydroazirino[1,2-*c*]benzo[*e*][1,2,3]oxathiazin-1-yl)methanone (3fh):** White solid; mp 184-186 °C; yield = 66% (52.0 mg); R_f = 0.32 (EtOAc/Hexane = 15:85); ^{1}H NMR (400 MHz, $CDCl_3$) δ 8.02-7.94 (m, 2H), 7.69 (d, *J* = 8.0 Hz, 2H), 7.39 (d, *J* = 7.6 Hz, 1H), 7.13 (d, *J* = 7.4 Hz, 1H), 6.98 (s, 1H), 4.59 (d, *J* = 3.0 Hz, 1H), 4.24 (d, *J* = 2.8 Hz, 1H), 2.40 (s, 3H) ppm; ^{13}C NMR (100 MHz, $CDCl_3$) δ 188.5, 149.7, 141.8, 133.7, 132.5, 130.3, 129.2, 128.4, 127.7, 120.0, 114.6, 47.7, 45.2, 21.3 ppm; HRMS (ESI-TOF) *m/z* calcd for $C_{16}H_{12}{}^{79}BrNNaO_4S$ $[M+Na]^+$: 415.9563, found 415.9563; HRMS (ESI-TOF) *m/z* calcd for $C_{16}H_{12}{}^{81}BrNNaO_4S$ $[M+Na]^+$: 417.9542, found 417.9540.

((1*R,8b*S**)-6-Chloro-3,3-dioxido-1,8b-dihydroazirino[1,2-*c*]benzo[*e*][1,2,3]oxathiazin-1-yl)(phenyl)methanone (3ga):** White solid; mp 86-88 °C; yield = 75% (50.3 mg); R_f = 0.51 (EtOAc/Hexane = 15:85); ^{1}H NMR (500 MHz, $CDCl_3$) δ 8.10 (d, *J* = 7.6 Hz, 2H), 7.69 (t, *J* = 7.4 Hz, 1H), 7.56 (t, *J* = 7.7 Hz, 2H), 7.47 (d, *J* = 8.2 Hz, 1H), 7.33 (dd, *J* = 8.2, 1.6 Hz, 1H), 7.20 (d, *J* = 1.4 Hz, 1H), 4.70 (d, *J* = 3.5 Hz, 1H), 4.29 (d, *J* = 3.5 Hz, 1H) ppm; ^{13}C NMR (125 MHz, $CDCl_3$) δ 188.7, 150.1, 136.4, 134.9, 130.4, 129.3, 129.0, 128.9, 127.3, 120.2, 116.6, 47.2, 45.0 ppm; HRMS (ESI-TOF) *m/z* calcd for $C_{15}H_{10}ClNNaO_4S$ $[M+Na]^+$: 357.9911, found 357.9916.

((1*R,8b*S**)-7-Methyl-3,3-dioxido-1,8b-dihydroazirino[1,2-*c*]benzo[*e*][1,2,3]oxathiazin-1-yl)(phenyl)methanone (3ha):** Colorless solid; mp 116-118 °C; yield = 69% (43.5 mg); R_f = 0.28 (EtOAc/Hexane = 15:85); ^{1}H NMR (500 MHz, $CDCl_3$) δ 8.10 (d, *J* = 7.5 Hz, 2H), 7.67 (t, *J* = 7.4 Hz, 1H), 7.55 (t, *J* = 7.7 Hz, 2H), 7.32 (s, 1H), 7.22 (d, *J* = 8.1 Hz, 1H), 7.05 (d, *J* = 8.3 Hz, 1H), 4.67 (d, *J* = 3.5 Hz, 1H), 4.23 (d, *J* = 3.5 Hz, S16 1H), 2.38 (s, 3H) ppm; ^{13}C NMR (125 MHz, $CDCl_3$) δ 189.2, 147.7, 137.1, 135.1, 134.7, 131.1, 129.9, 129.1, 128.9, 119.2, 117.6, 47.8, 45.2, 20.8 ppm; HRMS (ESI-TOF) *m/z* calcd for $C_{16}H_{14}NO_4S$ $[M+H]^+$: 316.0638, found 316.0610.

((1*R,8b*S**)-7-Methoxy-3,3-dioxido-1,8b-dihydroazirino[1,2-*c*]benzo[*e*][1,2,3]oxathiazin-1-yl)(phenyl)methanone (3ia):** White solid; mp 140-142 °C; yield = 67% (44.3 mg); R_f = 0.20 (EtOAc/Hexane = 15:85); ^{1}H NMR (500 MHz, $CDCl_3$) δ 8.11 (d, *J* = 7.6 Hz, 2H), 7.68 (t, *J* = 7.4 Hz, 1H), 7.55 (t, *J* = 7.7 Hz, 2H), 7.10 (d, *J* = 9.0 Hz, 1H), 7.02 (d, *J* = 2.8 Hz, 1H), 6.92 (dd, *J* = 9.0, 2.8 Hz, 1H), 4.68 (d, *J* = 3.6 Hz, 1H), 4.23 (d, *J* = 3.5 Hz, 1H), 3.83 (s, 3H) ppm; ^{13}C NMR (125 MHz, $CDCl_3$) δ 189.2, 157.9, 143.2, 135.0, 134.7, 129.1, 128.9, 120.5, 118.8, 115.5, 114.6, 55.8, 47.7, 45.2 ppm; HRMS (ESI-TOF) *m/z* calcd for $C_{16}H_{13}NNaO_5S$ $[M+Na]^+$: 354.0407, found 354.0407.

((1*R,8b*S**)-7-Fluoro-3,3-dioxido-1,8b-dihydroazirino[1,2-*c*]benzo[*e*][1,2,3]oxathiazin-1-yl)(phenyl)methanone (3ja):** White solid; mp 98-100 °C; yield = 74% (47.2 mg); R_f = 0.60 (EtOAc/Hexane = 15:85); ^{1}H NMR (500 MHz, $CDCl_3$) δ 8.10 (d, *J* = 2.8 Hz, 2H), 7.69 (s, 1H), 7.56 (s, 2H), 7.26 (s, 1H), 7.16 (s, 2H), 4.71 (s, 1H), 4.26 (s, 1H) ppm; ^{13}C NMR (125 MHz, $CDCl_3$) δ 188.7, 160.3 (d, J_{C-F} = 247.1 Hz), 145.72 (d, J_{C-F} = 2.3 Hz), 134.9, 129.2, 129.1, 121.2 (d, J_{C-F} = 8.6 Hz), 119.8 (d, J_{C-F} = 8.6 Hz), 117.5 (d, J_{C-F} = 23.6 Hz), 116.7 (d, J_{C-F} = 25.5 Hz), 47.1, 44.9. ppm; ^{19}F NMR (470 MHz, $CDCl_3$) δ -112.93 ppm; HRMS (ESI-TOF) *m/z* calcd for $C_{15}H_{10}FNNaO_4S$ $[M+Na]^+$: 342.0207, found 342.0207.

((1*R,8b*S**)-7-Chloro-3,3-dioxido-1,8b-dihydroazirino[1,2-*c*]benzo[*e*][1,2,3]oxathiazin-1-yl)(phenyl)methanone (3ka):** White solid; mp 74-76 °C; yield = 75% (50.3 mg); R_f = 0.60 (EtOAc/Hexane = 15:85); ^{1}H NMR (500 MHz, $CDCl_3$) δ 8.24-8.01 (m, 2H), 7.74-7.65 (m, 1H), 7.57-7.54 (m, 3H),

7.42 (d, *J* = 7.1 Hz, 1H), 7.18-7.08 (m, 1H), 4.70 (s, 1H), 4.26 (s, 1H) ppm; ^{13}C NMR (125 MHz, $CDCl_3$) δ 188.6, 148.2, 134.9, 134.8, 132.5, 130.7, 129.5, 129.2, 129.0, 120.9, 119.8, 47.0, 44.9 ppm; HRMS (ESI-TOF) *m/z* calcd for $C_{15}H_{10}ClNNaO_4S$ $[M+Na]^+$: 357.9911, found 357.9881.

((1*R,8b*S**)-7-Bromo-3,3-dioxido-1,8b-dihydroazirino[1,2-*c*]benzo[*e*][1,2,3]oxathiazin-1-yl)(phenyl)methanone (3la):** White solid; mp 88-90 °C; yield = 73% (55.5 mg); R_f = 0.60 (EtOAc/Hexane = 15:85); ^{1}H NMR (500 MHz, $CDCl_3$) δ 8.10 (d, *J* = 7.1 Hz, 2H), 7.69 (s, 2H), 7.57 (t, *J* = 7.0 Hz, 3H), 7.07 (d, *J* = 8.4 Hz, 1H), 4.69 (d, *J* = 1.9 Hz, 1H), 4.25 (d, *J* = 1.2 Hz, 1H) ppm; ^{13}C NMR (125 MHz, $CDCl_3$) δ 188.6, 148.8, 134.9, 134.8, 133.7, 132.4, 129.2, 129.0, 121.2, 120.1, 119.9, 46.8, 44.9 ppm; HRMS (ESI-TOF) *m/z* calcd for $C_{15}H_{11}{}^{79}BrNO_4S$ $[M+H]^+$: 379.9587, found 379.9580; HRMS (ESI-TOF) *m/z* calcd for $C_{15}H_{11}{}^{81}BrNO_4S$ $[M+H]^+$: 381.9566, found 381.9565.

((1*R,8b*S**)-7-Fluoro-3,3-dioxido-1,8b-dihydroazirino[1,2-*c*]benzo[*e*][1,2,3]oxathiazin-1-yl)(3-methylphenyl)methanone (3jm):** White solid; mp 170-172 °C; yield = 73% (48.5 mg); R_f = 0.50 (EtOAc/Hexane = 15:85); ^{1}H NMR (500 MHz, $CDCl_3$) δ 7.90 (s, 2H), 7.48-7.43 (m, 2H), 7.32-7.08 (m, 3H), 4.69 (d, *J* = 0.3 Hz, 1H), 4.25 (d, *J* = 0.7 Hz, 1H), 2.45 (s, 3H) ppm; ^{13}C NMR (125 MHz, $CDCl_3$) δ 188.8, 160.2 (d, J_{C-F} = 246.8 Hz), 145.7, 139.2, 135.7, 134.9, 129.4, 129.0, 126.2, 121.25 (d, J_{C-F} = 8.7 Hz), 119.96 (d, J_{C-F} = 8.7 Hz), 117.5, 117.3, 116.70 (d, J_{C-F} = 25.7 Hz), 47.1, 45.0, 21.3 ppm; ^{19}F NMR (470 MHz, $CDCl_3$) δ -112.99 ppm; HRMS (ESI) *m/z* calcd for $C_{16}H_{12}FNNaO_4S$ $[M+Na]^+$: 356.0363, found 356.0353.

((1*R,8b*S**)-(2,4-Dimethylphenyl)-7-fluoro-3,3-dioxido-1,8b-dihydroazirino[1,2-*c*]benzo[*e*][1,2,3]oxathiazin-1-yl)methanone (3jj):** White solid; mp 194-196 °C; yield = 70% (48.6 mg); R_f = 0.50 (EtOAc/Hexane = 15:85); ^{1}H NMR (500 MHz, $CDCl_3$) δ 8.08 (s, 1H), 7.28-7.25 (m, 2H), 7.20 (s, 1H), 7.16-7.15 (m, 1H), 7.15-7.11 (m, 1H), 4.53 (d, *J* = 3.5 Hz, 1H), 4.20 (d, *J* = 3.5 Hz, 1H), 2.49 (s, 3H), 2.43 (s, 3H) ppm; ^{13}C NMR (125 MHz, $CDCl_3$) δ 189.5, 160.2 (d, J_{C-F} = 246.5 Hz), 145.6, 144.1, 139.2, 134.8, 133.7 (d, J_{C-F} = 17.3 Hz), 128.1, 127.8, 121.9, 121.31 (d, J_{C-F} = 8.5 Hz), 119.75 (d, J_{C-F} = 8.4 Hz), 117.6, 117.4, 116.7, 116.5, 47.3, 46.1, 23.1, 21.0 ppm; ^{19}F NMR (470

MHz,) δ -112.96 ppm; HRMS (ESI-TOF) *m/z* calcd for $C_{17}H_{14}FNNaO_4S$ $[M+Na]^+$: 370.0520, found 370.0527.

((1*R,8b*S**)-7-Chloro-3,3-dioxido-1,8b-dihydroazirino[1,2-*c*]benzo[*e*][1,2,3]oxathiazin-1-yl)(2,4-dimethylphenyl)methanone (3kj):** White solid; mp 184-186 °C; yield = 69% (50.2 mg); R_f = 0.51 (EtOAc/Hexane = 15:85); ^{1}H NMR (500 MHz, $CDCl_3$) δ 8.07 (s, 1H), 7.53 (d, *J* = 2.2 Hz, 1H), 7.41 (dd, *J* = 8.7, 2.3 Hz, 1H), 7.26 (s, 1H), 7.20 (s, 1H), 7.12 (d, *J* = 8.7 Hz, 1H), 4.52 (d, *J* = 3.5 Hz, 1H), 4.20 (d, *J* = 3.4 Hz, 1H), 2.49 (s, 3H), 2.43 (s, 3H) ppm; ^{13}C NMR (125 MHz, $CDCl_3$) δ 189.4, 148.2, 144.2, 139.2, 134.8, 133.8, 133.6, 132.5, 130.7, 129.5, 121.9, 120.9, 119.6, 47.2, 46.1, 23.1, 21.0 ppm; HRMS (ESI-TOF) *m/z* calcd for $C_{17}H_{15}ClNO_4S$ $[M+H]^+$: 364.0405, found 364.0413.

((1*R,8b*S**)-7-Chloro-3,3-dioxido-1,8b-dihydroazirino[1,2-*c*]benzo[*e*][1,2,3]oxathiazin-1-yl)(3-methylphenyl)methanone (3km):** White solid; mp 184-186 °C; yield = 74% (51.7 mg); R_f = 0.52 (EtOAc/Hexane = 15:85); ^{1}H NMR (500 MHz, $CDCl_3$) δ 7.90 (s, 2H), 7.53 (s, 1H), 7.49 (d, *J* = 7.2 Hz, 1H), 7.44-7.40 (m, 2H), 7.12 (d, *J* = 8.7 Hz, 1H), 4.68 (d, *J* = 3.0 Hz, 1H), 4.24 (d, *J* = 2.8 Hz, 1H), 2.45 (s, 3H) ppm; ^{13}C NMR (125 MHz, $CDCl_3$) δ 188.8, 148.2, 139.2, 135.7, 134.9, 132.5, 130.6, 129.5, 129.4, 129.0, 126.2, 120.9, 119.8, 47.0, 44.9, 21.3 ppm; HRMS (ESI-TOF) *m/z* calcd for $C_{16}H_{12}ClNNaO_4S$ $[M+Na]^+$: 372.0068, found 372.0070.

((1*R,8b*S**)-7-Chloro-3,3-dioxido-1,8b-dihydroazirino[1,2-*c*]benzo[*e*][1,2,3]oxathiazin-1-yl)(4-methylphenyl)methanone (3kb):** White solid; mp 180-182 °C; yield =72% (50.3 mg); R_f = 0.52 (EtOAc/Hexane = 15:85); ^{1}H NMR (500 MHz, $CDCl_3$) δ 7.99 (d, *J* = 8.1 Hz, 2H), 7.52 (d, *J* = 2.3 Hz, 1H), 7.40 (dd, *J* = 8.7, 2.3 Hz, 1H), 7.34 (d, *J* = 8.0 Hz, 2H), 7.12 (d, *J* = 8.7 Hz, 1H), 4.67 (d, *J* = 3.6 Hz, 1H), 4.24 (d, *J* = 3.5 Hz, 1H), 2.45 (s, 3H) ppm; ^{13}C NMR (125 MHz, $CDCl_3$) δ 188.1, 148.2, 146.2, 132.5, 132.4, 130.6, 129.9, 129.5, 129.1, 120.9, 119.9, 46.9, 44.9, 21.9 ppm; HRMS (ESI-TOF) *m/z* calcd for $C_{16}H_{13}ClNO_4S$ $[M+H]^+$: 350.0248, found 350.0242.

((1*R,10c*S**)-3,3-Dioxido-1,10c-dihydroazirino[1,2-*c*]naphtho[1,2-*e*][1,2,3]oxathiazin-1- yl)(phenyl)methanone (3ma):** White solid; mp 120-

122 °C; yield = 70% (49.1 mg); R_f = 0.28 (EtOAc/Hexane = 15:85); ^{1}H NMR (500 MHz, $CDCl_3$) δ 8.14 (d, *J* = 7.4 Hz, 2H), 8.08 (d, *J* = 8.2 Hz, 1H), 7.97-7.91 (m, 2H), 7.68 (t, *J* = 7.0 Hz, 2H), 7.61-7.53 (m, 3H), 7.29 (d, *J* = 8.9 Hz, 1H), 4.99 (d, *J* = 2.7 Hz, 1H), 4.81 (d, *J* = 2.8 Hz, 1H) ppm; ^{13}C NMR (125 MHz, $CDCl_3$) δ 189.4, 148.3, 135.0, 134.8, 131.7, 131.6, 131.1, 129.3, 129.2, 129.0, 128.6, 126.8, 121.9, 118.0, 112.1, 45.8, 44.9 ppm; HRMS (ESI-TOF) *m/z* calcd for $C_{19}H_{14}NO_4S$ $[M+H]^+$: 352.0638, found 352.0611.

((1*R,8b*S**)-(5-Methoxy-1-methyl-3,3-dioxido-1,8b-dihydroazirino[1,2-*c*]benzo[*e*][1,2,3]oxathiazin-1-yl)(4-methoxyphenyl)methanone (3cq):** White solid; mp 156-158 °C; yield = 33% (24.7 mg); R_f = 0.20 (EtOAc/Hexane = 15:85); ^{1}H NMR (500 MHz, $CDCl_3$) δ 8.21 (d, *J* = 8.6 Hz, 2H), 7.28 (d, *J* = 7.9 Hz, 1H), 7.13 (d, *J* = 7.6 Hz, 1H), 7.03 (t, *J* = 9.8 Hz, 3H), 4.22 (s, 1H), 3.91 (d, *J* = 7.8 Hz, 6H), 1.85 (s, 3H) ppm; ^{13}C NMR (125 MHz, $CDCl_3$) δ 191.5, 164.5, 149.3, 138.9, 132.5, 126.6, 125.3, 121.1, 117.4, 114.2, 113.5, 56.3, 55.6, 55.1, 50.4, 12.1 ppm; HRMS (ESI-TOF) *m/z* calcd for $C_{18}H_{17}ClNNaO_6S$ $[M+Na]^+$: 398.0669, found 398.0691.

((1*R,7b*S**)-6-Methyl-3,3-dioxido-1,7b-dihydroazirino[1,2-*b*]benzo[*d*]isothiazol-1-yl)(phenyl)methanone (3na):** White solid; mp 174-176 °C; yield = 78% (62.2 mg); R_f = 0.21 (EtOAc/Hexane = 15:85); ^{1}H NMR (500 MHz, $CDCl_3$) δ 8.11 (d, *J* = 7.4 Hz, 2H), 7.66-7.63 (m, 2H), 7.53 (t, *J* = 7.7 Hz, 2H), 7.44 (s, 1H), 7.41 (d, *J* = 8.0 Hz, 1H), 4.57 (d, *J* = 3.0 Hz, 1H), 3.89 (d, *J* = 3.2 Hz, 1H), 2.49 (s, 3H) ppm; ^{13}C NMR (125 MHz, $CDCl_3$) δ 189.2, 145.1, 135.5, 135.0, 134.6, 131.6, 130.8, 129.2, 129.0, 126.1, 123.2, 54.9, 46.2, 21.7 ppm; HRMS (ESI-TOF) *m/z* calcd for $C_{16}H_{14}NO_3S$ $[M+H]^+$: 300.0689, found 300.0709.

Ethyl (1*R,8b*S**)-1-benzoylazirino[1,2-*c*]benzo[*e*][1,2,3]oxathiazine-8b(1*H*)-carboxylate 3,3-dioxide (3oa):** Gummy liquid; yield = 36% (26.8 mg); R_f = 0.19 (EtOAc/Hexane = 15:85); ^{1}H NMR (500 MHz, $CDCl_3$) δ 7.99 (d, *J* = 7.5 Hz, 2H), 7.74 (d, *J* = 7.7 Hz, 1H), 7.67-7.63 (m, 1H), 7.53-7.48 (m, 3H), 7.38 (d, *J* = 7.5 Hz, 1H), 7.23 (d, *J* = 8.0 Hz, 1H), 4.73 (s, 1H), 4.30 (q, *J* = 6.9 Hz, 2H), 1.25 (t, *J* = 6.7 Hz, 3H) ppm; ^{13}C NMR (125 MHz, $CDCl_3$) δ 187.74, 162.4, 149.5, 135.2, 134.5, 131.5, 128.9, 128.8, 128.6, 127.2, 120.1, 116.3, 63.4,

55.5, 50.6, 13.77 ppm; HRMS (ESI-TOF) *m/z* calcd for $C_{18}H_{16}NO_6S$ $[M+H]^+$: 374.0693, found 374.0706.

(3a*R,10b*S**)-3-Phenyl-3a,10b-dihydro-4*H*-benzo[*f*]isoxazolo[4,5-*d*][1,2,3]oxathiazepine 5,5-dioxide (4aa):** White solid; yield = 73% (23.0 mg); R_f = 0.40 (EtOAc/Hexane = 15:85); ^{1}H NMR (500 MHz, $CDCl_3$) δ 7.81 (d, *J* = 7.2 Hz, 2H), 7.66 (dd, *J* = 6.5, 1.9 Hz, 1H), 7.52-7.39 (m, 5H), 7.30 (dd, *J* = 7.5, 1.6 Hz, 1H), 5.81 (d, *J* = 13.4 Hz, 1H), 5.56 (d, *J* = 11.9 Hz, 1H), 5.39 (dd, *J* = 13.1, 12.2 Hz, 1H) ppm; ^{13}C NMR (125 MHz, $CDCl_3$) δ 156.5, 149.1, 131.5, 129.9, 129.3, 129.0, 127.9, 127.2, 126.2, 125.0, 122.6, 85.2, 66.3 ppm; HRMS (ESI-TOF) *m/z* calcd for $C_{15}H_{12}N_2NaO_4S$ $[M+Na]^+$: 339.0410, found 339.0439.

(3a*R,10b*S**)-3-(4-*tert*-Butylphenyl)-3a,10b-dihydro-4*H*-benzo[*f*]isoxazolo[4,5-*d*][1,2,3]oxathiazepine 5,5-dioxide (4ad):** White solid; yield = 66% (24.5 mg); R_f = 0.48 (EtOAc/Hexane = 15:85); ^{1}H NMR (500 MHz, $CDCl_3$) δ 7.74 (d, *J* = 8.4 Hz, 2H), 7.68-7.63 (m, 1H), 7.47 (d, *J* = 8.4 Hz, 2H), 7.42-7.37 (m, 2H), 7.30 (dd, *J* = 7.4, 1.6 Hz, 1H), 5.77 (d, *J* = 13.2 Hz, 1H), 5.49 (d, *J* = 11.9 Hz, 1H), 5.39-5.29 (m, 1H), 1.33 (s, 9H) ppm; ^{13}C NMR (125 MHz, $CDCl_3$) δ 156.5, 155.1, 149.1, 129.8, 129.4, 127.9, 127.1, 126.0, 125.0, 123.2, 122.6, 85.1, 66.3, 35.0, 31.0 ppm; HRMS (ESI-TOF) *m/z* calcd for $C_{19}H_{21}N_2O_4S$ $[M+H]^+$: 373.1217, found 373.1215.

(3a*R,10b*S**)-8-Methyl-3-phenyl-3a,10b-dihydro-4*H*-benzo[*f*]isoxazolo[4,5-*d*][1,2,3]oxathiazepine 5,5-dioxide (4fa):** White solid; yield = 73% (24.0 mg); R_f = 0.44 (EtOAc/Hexane = 15:85); ^{1}H NMR (500 MHz, $CDCl_3$) δ 7.81 (d, *J* = 7.2 Hz, 2H), 7.52-7.43 (m, 4H), 7.19 (d, *J* = 7.8 Hz, 1H), 7.12 (s, 1H), 5.75 (d, *J* = 12.8 Hz, 1H), 5.44-5.32 (m, 2H), 2.41 (s, 3H) ppm; ^{13}C NMR (125 MHz, $CDCl_3$) δ 156.5, 148.9, 140.5, 131.4, 129.0, 128.5, 127.2, 126.2, 126.1, 124.6, 123.1, 85.2, 66.4, 21.1 ppm; HRMS (ESI-TOF) *m/z* calcd for $C_{16}H_{15}N_2O_4S$ $[M+H]^+$: 331.0747, found 331.0747.

(3a*R,10b*S**)-7-Methoxy-3-phenyl-3a,10b-dihydro-4*H*-benzo[*f*]isoxazolo[4,5-*d*][1,2,3]oxathiazepine 5,5-dioxide(4ca):** White solid; yield = 70% (24.2 mg); R_f = 0.40 (EtOAc/Hexane = 15:85); ^{1}H NMR (500 MHz, $CDCl_3$+DMSO-d_6) δ 8.62 (d, *J* = 11.3 Hz, 1H), 7.89-7.82 (m, 2H), 7.49-7.41 (m, 3H), 7.29 (d, *J* = 7.5 Hz, 1H), 7.18 (d, *J* = 7.7 Hz, 1H), 6.98 (d, *J* = 8.2 Hz,

1H), 5.91 (d, *J* = 13.4 Hz, 1H), 5.35 – 5.29 (m, 1H), 3.92 (s, 3H) ppm; ^{13}C NMR (125 MHz, $CDCl_3$+DMSO-d_6) δ 156.9, 152.0, 138.3, 131.6, 130.9, 128.7, 128.0, 127.2, 127.1, 115.7, 112.9, 84.5, 66.3, 56.3 ppm; HRMS (ESI-TOF) *m/z* calcd for $C_{16}H_{14}N_2NaO_5S$ $[M+Na]^+$: 369.0516, found 369.0508.

(3a*R,10b*S**)-3-(4-Chlorophenyl)-3a,10b-dihydro-4*H*-benzo[*f*]isoxazolo[4,5-*d*][1,2,3]oxathiazepine 5,5-dioxide (4ag):** White solid; yield = 75% (26.3 mg); R_f = 0.42 (EtOAc/Hexane = 15:85); ^{1}H NMR (500 MHz, $CDCl_3$) δ 7.77 (d, *J* = 8.4 Hz, 2H), 7.68-7.63 (m, 1H), 7.48-7.37 (m, 4H), 7.31 (d, *J* = 7.7 Hz, 1H), 5.82 (d, *J* = 13.3 Hz, 1H), 5.56 (d, *J* = 12.1 Hz, 1H), 5.38 (t, *J* = 12.7 Hz, 1H) ppm; ^{13}C NMR (125 MHz, $CDCl_3$) δ 155.6, 149.1, 137.7, 130.0, 129.6, 129.4, 128.4, 127.9, S24 125.1, 124.9, 122.7, 85.3, 66.2 ppm; HRMS (ESI-TOF) *m/z* calcd for $C_{15}H_{12}ClN_2O_4S$ $[M+H]^+$: 351.0201, found 351.0213.

(3a*R,10b*S**)-3-(4-Fluorophenyl)-7-methyl-3a,10b-dihydro-4*H*-benzo[*f*]isoxazolo[4,5- *d*][1,2,3]oxathiazepine 5,5-dioxide (4bf):** White solid; yield = 78% (27.1 mg); R_f = 0.40 (EtOAc/Hexane = 15:85); ^{1}H NMR (500 MHz, $CDCl_3$) δ 7.84-7.81 (m, 2H), 7.46-7.44 (m, 1H), 7.28 (d, *J* = 7.8 Hz, 2H), 7.15 (t, *J* = 8.6 Hz, 2H), 5.80 (d, *J* = 13.3 Hz, 1H), 5.48 (d, *J* = 12.1 Hz, 1H), 5.34 (t, *J* = 12.7 Hz, 1H), 2.38 (s, 3H) ppm; ^{13}C NMR (125 MHz, $CDCl_3$) δ 164.0 (d, J_{C-F} = 252.0 Hz), 155.4, 147.9, 132.0, 131.5, 129.4 (d, J_{C-F} = 8.4 Hz), 127.6, 122.5 (d, J_{C-F} = 3.2 Hz), 122.3, 116.4, 116.2, 85.4, 66.3, 15.8 ppm; ^{19}F NMR (470 MHz, $CDCl_3$) δ -107.04 ppm; HRMS (ESI-TOF) *m/z* calcd for $C_{16}H_{14}FN_2O_4S$ $[M+H]^+$: 349.0653, found 349.0637.

(3a*R,10b*S**)-3-(3-Bromophenyl)-8-methyl-3a,10b-dihydro-4*H*-benzo[*f*]isoxazolo[4,5- *d*][1,2,3]oxathiazepine 5,5-dioxide (4fo):** White solid; yield = 71% (29.0 mg); R_f = 0.46 (EtOAc/Hexane = 15:85); ^{1}H NMR (500 MHz, $CDCl_3$+DMSO-d_6) δ 9.46 (dd, *J* = 10.7, 4.2 Hz, 1H), 8.05 (s, 1H), 7.89 (d, *J* = 6.3 Hz, 1H), 7.74 (d, *J* = 6.1 Hz, 1H), 7.55 (dd, *J* = 7.4, 3.2 Hz, 1H), 7.51-7.47 (m, 1H), 7.29 (d, *J* = 6.4 Hz, 1H), 7.18 (d, *J* = 2.0 Hz, 1H), 5.97-5.88 (m, 1H), 5.39-5.29 (m, 1H), 2.68 (s, 3H) ppm; ^{13}C NMR (125 MHz, $CDCl_3$+DMSO-d_6) δ 160.8, 153.7, 144.7, 138.5, 135.4, 134.4, 134.2, 132.8, 131.4, 130.6, 129.1, 127.8, 127.3, 89.3, 70.8, 25.8 ppm; HRMS (ESI-TOF) *m/z*

calcd for $C_{16}H_{14}{}^{79}BrN_2O_4S$ $[M+H]^+$: 408.9852, found 408.9832; HRMS (ESI-TOF) *m/z* calcd for $C_{16}H_{14}{}^{81}BrN_2O_4S$ $[M+H]^+$: 410.9832, found 410.9810.

(3a*R,10b*S**)-7-Methyl-3-(4-(trifluoromethyl)phenyl)-3a,10b-dihydro-4*H*-benzo[*f*]isoxazolo[4,5-*d*][1,2,3]oxathiazepine 5,5- dioxide (4bi):** White solid; yield = 74% (29.4 mg); R_f = 0.44 (EtOAc/Hexane = 15:85); ^{1}H NMR (500 MHz, $CDCl_3$+DMSO-d_6) δ 9.09 (s, 1H), 8.00 (d, *J* = 8.2 Hz, 2H), 7.71 (d, *J* = 8.3 Hz, 2H), 7.43 (t, *J* = 4.6 Hz, 1H), 7.24 (d, *J* = 4.8 Hz, 2H), 5.95 (d, *J* = 13.5 Hz, 1H), 5.28 (d, *J* = 13.5 Hz, 1H), 2.38 (s, 3H) ppm; ^{13}C NMR (125 MHz, $CDCl_3$+DMSO-d_6) δ 156.0, 148.0, 132.4, 132.1, 131.9, 131.1, 130.8, 129.7, 127.5, 127.1, 125.6 (q), 124.7, 122.5, 122.1, 120.4, 85.0, 66.1, 15.8 ppm; ^{19}F NMR (470 MHz, $CDCl_3$) δ -62.98 ppm; HRMS (ESI-TOF) *m/z* calcd for $C_{17}H_{14}F_3N_2O_4S$ $[M+H]^+$: 399.0621, found 399.0622.

(9-Methyl-2,2-dioxido-3*H*-benzo[*f*][1,2,3]oxathiazepin-4-yl)(phenyl)methanone (5ba): White solid; yield = 83% (26.1 mg); R_f = 0.24 (EtOAc/Hexane = 15:85); ^{1}H NMR (500 MHz, $CDCl_3$) δ 8.21 (s, 1H), 7.74 (d, *J* = 7.4 Hz, 2H), 7.64 (t, *J* = 7.4 Hz, 1H), 7.53 (t, *J* = 7.6 Hz, 2H), 7.32 (d, *J* = 7.3 Hz, 1H), 7.18 (t, *J* = 7.6 Hz, 1H), 7.07 (d, *J* = 7.5 Hz, 1H), 6.70 (s, 1H), 2.40 (s, 3H) ppm; ^{13}C NMR (125 MHz, $CDCl_3$) δ 190.6, 147.7, 135.3, 133.6, 132.7, 131.4, 130.9, 129.7, 129.3, 128.6, 126.9, 125.5, 121.7, 16.2 ppm; HRMS (ESI-TOF) *m/z* calcd for $C_{16}H_{13}NNaO_4S$ $[M+Na]^+$: 338.0457, found 338.0463.

(2,2-Dioxido-3*H*-benzo[*f*][1,2,3]oxathiazepin-4-yl)(phenyl)methanone (5aa): White solid; yield = 79% (23.6 mg); R_f = 0.23 (EtOAc/Hexane = 15:85); ^{1}H NMR (500 MHz, $CDCl_3$) δ 8.20 (s, 1H), 7.74 (d, *J* = 7.3 Hz, 2H), 7.65 (t, *J* = 7.4 Hz, 1H), 7.53 (t, *J* = 7.6 Hz, 2H), 7.45 (t, *J* = 7.2 Hz, 1H), 7.29 (t, *J* = 7.5 Hz, 1H), 7.23 (d, *J* = 6.7 Hz, 2H), 6.69 (s, 1H) ppm; ^{13}C NMR (125 MHz, $CDCl_3$) δ 190.5, 149.1, 135.2, 133.4, 132.8, 131.9, 129.8, 129.3, 128.6, 127.2, 125.3, 122.0, 121.7 ppm; HRMS (ESI-TOF) *m/z* calcd for $C_{15}H_{11}NNaO_4S$[M+Na]$^+$: 324.0301, found 324.0274.

(9-Methyl-2,2-dioxido-3*H*-benzo[*f*][1,2,3]oxathiazepin-4-yl)(4-methylphenyl)methanone (5bb): White solid; yield = 81% (26.6 mg); R_f = 0.23 (EtOAc/Hexane = 15:85); ^{1}H NMR (500 MHz, $CDCl_3$) δ 8.20 (s, 1H), 7.66 (d, *J* = 8.0 Hz, 2H), 7.36-7.28 (m, 3H), 7.18 (t, *J* = 7.6 Hz, 1H), 7.07 (d, *J* = 7.6

Hz, 1H), 6.70 (s, 1H), 2.47 (s, 3H), 2.39 (s, 3H) ppm; ^{13}C NMR (125 MHz, $CDCl_3$) δ 190.3, 147.7, 143.7, 133.4, 132.5, 131.4, 130.8, 129.7, 129.5, 129.3, 126.9, 125.6, 121.2, 21.7, 16.2 ppm; HRMS (ESI-TOF) *m/z* calcd for $C_{17}H_{15}NNaO_4S$ $[M+Na]^+$: 352.0614, found 352.0618.

(9-Methoxy-2,2-dioxido-3H-benzo[f][1,2,3]oxathiazepin-4-yl)(phenyl)methanone (5ca): White solid; yield = 80% (26.5 mg); R_f = 0.20 (EtOAc/Hexane = 15:85); ^{1}H NMR (400 MHz, $CDCl_3$+DMSO-d_6) δ 9.56 (s, 1H), 7.76 (d, *J* = 6.9 Hz, 2H), 7.66-7.60 (m, 1H), 7.51 (t, *J* = 7.2 Hz, 2H), 7.20 (t, *J* = 7.8 Hz, 1H), 7.04 (d, *J* = 7.9 Hz, 1H), 6.79 (d, *J* = 7.4 Hz, 1H), 6.62 (s, 1H), 3.92 (s, 3H) ppm; ^{13}C NMR (100 MHz, $CDCl_3$) δ 190.7, 151.4, 138.0, 135.7, 132.6, 130.8, 129.4, 128.5, 127.7, 127.1, 124.1, 121.2, 114.4, 56.3 ppm; HRMS (ESI-TOF) *m/z* calcd for $C_{16}H_{13}NNaO_5S$ $[M+Na]^+$: 354.0407, found 354.0412.

(8-Methyl-2,2-dioxido-3*H*-benzo[*f*][1,2,3]oxathiazepin-4-yl)(phenyl)methanone (5fa): White solid; yield = 79% (24.8 mg); R_f = 0.23 (EtOAc/Hexane = 15:85); ^{1}H NMR (500 MHz, $CDCl_3$) δ 8.16 (s, 1H), 7.73 (d, *J* = 7.4 Hz, 2H), 7.63 (t, *J* = 7.3 Hz, 1H), 7.52 (t, *J* = 7.5 Hz, 2H), 7.14- 7.02 (m, 3H), 6.67 (s, 1H), 2.40 (s, 3H) ppm; ^{13}C NMR (125 MHz, $CDCl_3$) δ 190.5, 148.9, 143.5, 135.4, 133.3, 132.6, 129.2, 129.1, 128.6, 128.0, 122.5, 122.3, 122.2, 21.2 ppm; HRMS (ESI-TOF) *m/z* calcd for $C_{16}H_{13}NNaO_4S$ $[M+Na]^+$: 338.0457, found 338.0459.

(6-Methyl-1,1-dioxido-2*H*-benzo[*e*][1,2]thiazin-3-yl)(phenyl)methanone (5na): White solid; yield = 34% (10.1 mg); R_f = 0.23 (EtOAc/Hexane = 15:85); ^{1}H NMR (500 MHz, $CDCl_3$) δ 7.93 (d, *J* = 8.1 Hz, 1H), 7.80 (d, *J* = 7.6 Hz, 2H), 7.67 (t, *J* = 7.7 Hz, 1H), 7.55 (t, *J* = 7.7 Hz, 2H), 7.45 (d, *J* = 8.7 Hz, 1H), 7.32 (s, 1H), 6.93 (s, 1H), 2.46 (s, 3H) ppm; ^{13}C NMR (125 MHz, $CDCl_3$) δ 189.4, 143.2, S27 135.2, 134.3, 133.0, 131.6, 131.4, 131.3, 129.5, 129.3, 128.7, 121.9, 117.7, 21.5 ppm; HRMS (ESI-TOF) *m/z* calcd for $C_{16}H_{13}NNaO_3S$ $[M+Na]^+$: 322.0508, found 322.0531.

2-(7-Methyl-2,2-dioxido-3,4-dihydrobenzo[*e*][1,2,3]oxathiazin-4-yl)-1-phenylethan-1-one(6fa): White solid; mp 148-150 °C; yield = 91%; R_f = 0.24 (EtOAc/Hexane = 15:85); ^{1}H NMR (500 MHz, $CDCl_3$) δ 7.96 (d, *J* = 7.6 Hz,

2H), 7.62 (t, *J* = 7.3 Hz, 1H), 7.49 (t, *J* = 7.7 Hz, 2H), 7.02 (d, *J* = 7.9 Hz, 1H), 6.95 (d, *J* = 7.9 Hz, 1H), 6.86 (s, 1H), 5.89 (d, *J* = 8.1 Hz, 1H), 5.37-5.34 (m, 1H), 4.24 (dd, *J* = 18.1, 7.3 Hz, 1H), 3.38 (dd, *J* = 18.1, 3.6 Hz, 1H), 2.32 (s, 3H) ppm; ^{13}C NMR (125 MHz, $CDCl_3$) δ 197.9, 151.0, 140.1, 136.2, 134.1, 128.9, 128.2, 126.3, 125.6, 119.3, 118.4, 53.5, 41.7, 20.9 ppm; HRMS (ESI-TOF) *m/z* calcd for $C_{16}H_{16}NO_4S$ $[M+H]^+$: 318.0795, found 318.0815.

Ethyl 4-(2-oxo-2-phenylethyl)-3,4-dihydrobenzo[*e*][1,2,3]oxathiazine-4-carboxylate 2,2- dioxide (6oa): White solid; mp 104-106 °C; yield = 21%: R_f = 0.20 (EtOAc/Hexane = 15:85); ^{1}H NMR (500 MHz, $CDCl_3$) δ 7.94 (d, *J* = 7.4 Hz, 2H), 7.65 (d, *J* = 7.9 Hz, 1H), 7.60 (t, *J* = 7.4 Hz, 1H), 7.47 (t, *J* = 7.7 Hz, 2H), 7.40 (t, *J* = 7.2 Hz, 1H), 7.26 (t, *J* = 7.1 Hz, 1H), 7.09 (d, *J* = 8.1 Hz, 1H), 6.44 (s, 1H), 4.56 (d, *J* = 17.9 Hz, 1H), 4.37 (q, *J* = 7.1 Hz, 2H), 3.82 (d, *J* = 17.9 Hz, 1H), 1.32 (t, *J* = 7.1 Hz, 3H) ppm; ^{13}C NMR (125 MHz, $CDCl_3$) δ 195.2, 169.4, 150.7, 135.9, 133.8, 130.9, 128.8, 128.2, 127.3, 125.8, 120.0, 119.4, 65.2, 63.9, 47.0, 13.9 ppm; HRMS (ESI-TOF) *m/z* calcd for $C_{18}H_{17}NO_6Na$ $[M+Na]^+$: 398.0669, found 398.0653.

Crystallographic data: Single crystal X-ray structural of compound **3aa** was measured on the SuperNova, Dual, Mo at home/near, Eos- XRD at 150(2) K using graphite monochromated Mo Kα radiation (λα = 0.71073 Å). The strategy for the Data collection was evaluated by using the CrysAlisPro CCD software. The data were collected by the standard 'phi-omega scan techniques,and were scaled and reduced using CrysAlisPro RED software. The structure was solved by direct methods using SHELXS-97, and refined by full matrix least-squares with SHELXL-97, refining on *F*2. The positions of all the atoms were obtained by direct methods. All non-hydrogen atoms were refined anisotropically. The remaining hydrogen atoms were placed in geometrically constrained positions, and refined with isotropic temperature factors, generally 1.2Ueq of their parent atoms. The crystal data are summarized in **Table 4.5.** The **CCDC** number (**2264093**) can be obtained free of charge via www.ccdc.cam.ac.uk (or from the Cambridge Crystallographic Data Centre,12 union Road, Cambridge CB21 EZ, UK; Fax: (+44) 1223-336-033; or deposit@ccdc.cam.ac.uk).

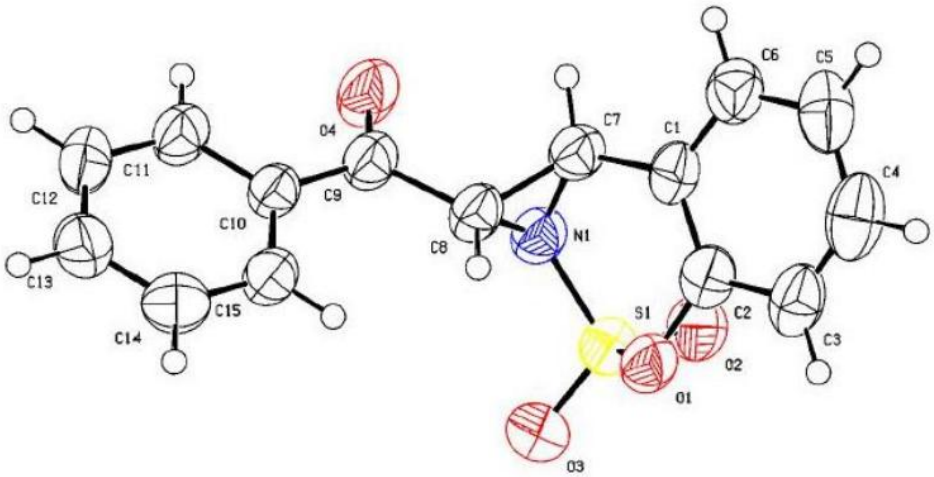

Figure 4.2 ORTEP diagram of compound **3aa** (CCDC **2264093**), thermal ellipsoids drawn at the 50% probability level.

Table 4.5 Crystal data of compound **3aa.**

Compound	**3aa**
Empirical formula	$C_{15}H_{11}NO_4S$
Formula weight	301.31
Temperature	293 K
Wave length (A°)	0.71073 A°
Crystal system,space group	Monoclinic, $P2_1/c$
a (Å) b (Å) c (Å) α (°) β (°) γ (°)	a = 17.2401(12) A° b = 5.9036(3) A° c = 14.1754(10) A° alpha = 90 deg. beta = 109.535(7) deg. gamma = 90 deg.
Volume ($Å^3$)	1359.70(16) A^3
Z, Calculated density (mg/m^3)	4, 1.472 Mg/m^3
Absorption coefficient (mm^{-1})	0.253
F(000)	624.0
Θ range (deg)	3.050 to 24.984 deg.
Limiting indices	-20<=h<=18, -7<=k<=7, -16<=l<=16
Reflections collected / unique	14688 / 2383 [R_{int} = 0.0879]

Completeness to Θ = 24.984	99.9%
Max. and min. transmission	1.000 0.577 and
Absorption correction	none
Data / restrains / parameters	2383/0/191
Goodness-of-fit on F^2	1.067
Finel R indices [I>2sigma(I)]	R_1 = 0.0622, wR_2 = 0.1461
R indices (all data)	R_1 = 0.1097, wR_2 = 0.1840
Extinction coefficient	n/a
Largest diff.peak and hole (e.A^{-3})	0.24 and -0.33 e.A^-3
CCDC	**2264093**

Crystallographic data: Single crystal X-ray structural of compound **4fa** was measured on the SuperNova, Dual, Mo at home/near, Eos- XRD at 150(2) K using graphite monochromated Mo Kα radiation (λα = 0.71073 Å). The strategy for the Data collection was evaluated by using the CrysAlisPro CCD software. The data were collected by the standard 'phi-omega scan techniques,and were scaled and reduced using CrysAlisPro RED software. The structure was solved by direct methods using SHELXS-97, and refined by full matrix least-squares with SHELXL-97, refining on *F*2. The positions of all the atoms were obtained by direct methods. All non-hydrogen atoms were refined anisotropically. The remaining hydrogen atoms were placed in geometrically constrained positions, and refined with isotropic temperature factors, generally 1.2Ueq of their parent atoms. The crystal data are summarized in **Table 4.6** The **CCDC** number **2264094**) can be obtained free of charge via www.ccdc.cam.ac.uk (or from the Cambridge Crystallographic Data Centre,12 S22 union Road, Cambridge CB21 EZ, UK; Fax: (+44) 1223-336-033; or deposit@ccdc.cam.ac.uk).

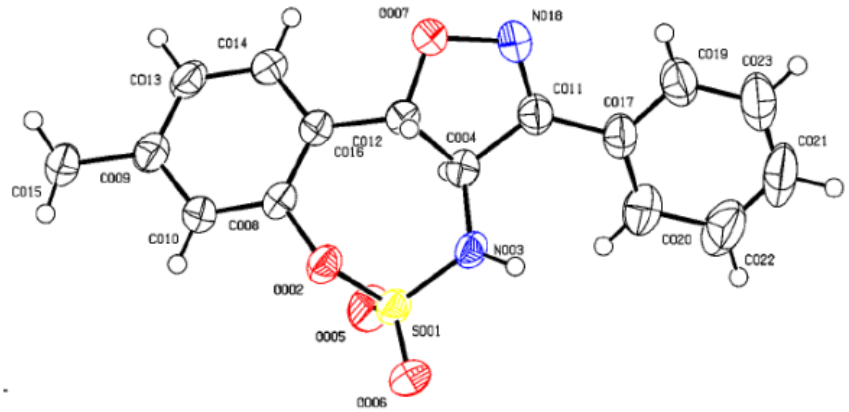

Figure 4.3 ORTEP diagram of compound **4fa** (CCDC **2264094**), thermal ellipsoids drawn at the 50% probability level.

Table 4.6 Crystal data for compound **4fa**.

Compound	**4fa**
Empirical formula	$C_{16}H_{14}N_2O_4S$
Formula weight	330.35
Temperature	293 K
Wave length (Å)	0.71073 Å
Crystal system,space group	Triclinic, P-1
a (Å) b (Å) c (Å) α (°) β (°) γ (°)	a = 5.0953(4) Å b = 12.2774(9) Å c = 12.7804(8) Å alpha = 72.856(6) deg. beta = 85.579(5) deg. gamma = 84.146(6) deg.
Volume ($Å^3$)	759.07(10) A^3
Z, Calculated density (mg/m^3)	2, 1.445 Mg/m^3
Absorption coefficient (mm^{-1})	0.236 mm^-1
F(000)	344.0
Θ range (deg)	6.58 to 49.978
Limiting indices	-6<=h<=6, -14<=k<=14, -15<=l<=15
Reflections collected / unique	6813 / 2653 [R_{int} = 0.0393]

Max. and min. transmission	0.600 and 1.000
Absorption correction	none
Data / restrains / parameters	2653/0/209
Goodness-of-fit on F^2	1.091
Finel R indices [I>2sigma(I)]	R_1 = 0.0479, wR_2 = 0.1351
R indices (all data)	R_1 = 0.0542, wR_2 = 0.1417
Extinction coefficient	n/a
Largest diff.peak and hole (e.A^{-3})	0.50 and -0.51 e.A^-3
CCDC	**2264094**

Radical Trapping Experiments:

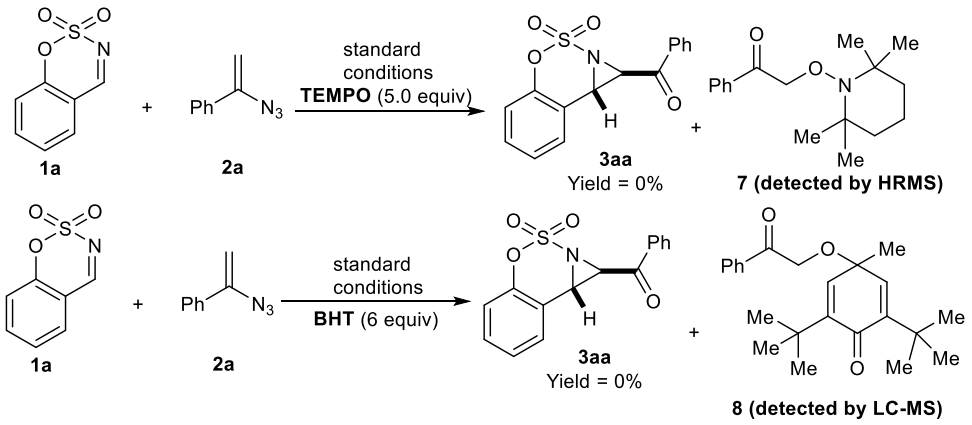

Scheme 4.18 Radical Trapping Experiments

TEMPO or BHT: The compounds **1a** (36.64 mg, 0.2 mmol), **2a** (58.0 mg, 0.4 mmol), 2,2′-bpy (3.12 mg, 10 mol%), CuI (3.81 mg, 10 mol%) and TEMPO (156.2 mg, 1.0 mmol) or BHT (254.2 mg, 6.0 equiv) in MeCN:H_2O (3.0 mL, 5:1) was taken in a screw capped test tube (25 mL), followed by degassing with argon (four times). The mixture was further stirred under blue LEDs (4×5W, 450 nm) light irradiation at room temperature for 16h. Then, the reaction mixtures were analyzed by mass spectrometry. Results showed that the trapping products **7** and **8** were detected by MS. **(Scheme 4.18)**

Radical trap mass data of 7 and 8:

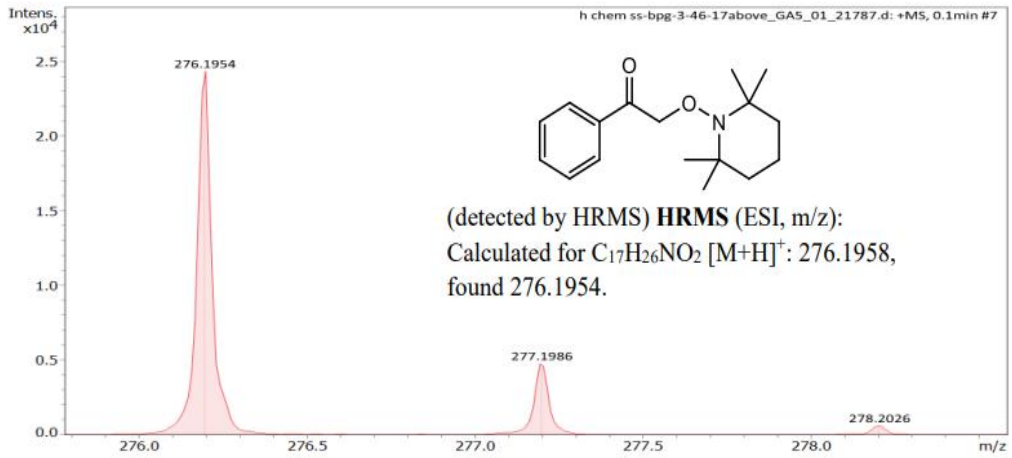

Figure 4.4 TEMPO radical Experiment.

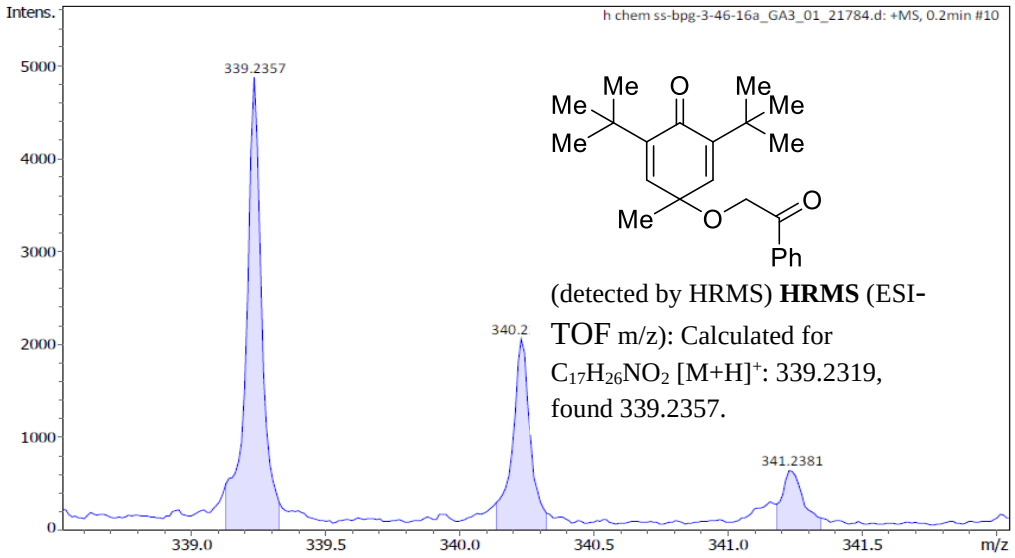

Figure 4.5 BHT radical Experiment.

Coordination reaction between CuI and 2,2´-bipyridine:

a) CuI in MeCN **b) 2,2′-bipyridine in MeCN** **c) CuI and 2,2′-bipyridine in MeCN**

Figure 4.6 The coordination reaction between CuI and 2,2´-bipyridine

As shown in **Figure 4.6**, an equimolecular combination of CuI with 2,2′-bipyridine was turned into red-orange color, indicating that the complexation between CuI and 2,2′-bipyridine obviously occurred.

UV-Visible experiments:

The UV-Vis experiments were monitored in a quartz cuvette (10 × 10 mm^2) using a Varian carry 100 Bio UV−Vis spectrophotometer.

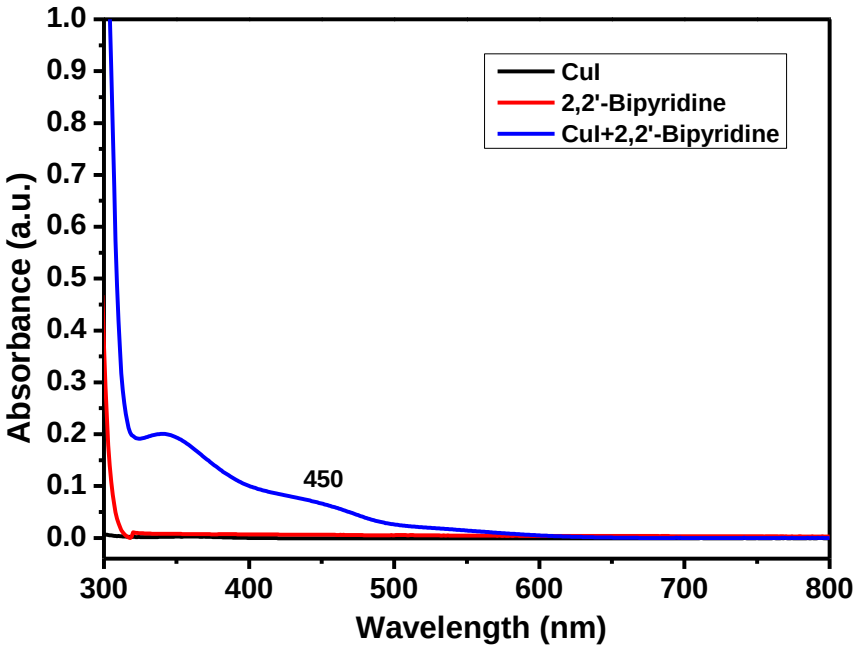

Figure 4.7 UV-Vis spectra of CuI (0.167 ×10^{-3} M in MeCN), 2,2´-bipyridine (0.167 × 10^{-3} M in MeCN) and CuI +2,2´-bipyridine (for each species 0.167 × 10^{-3} M in MeCN).

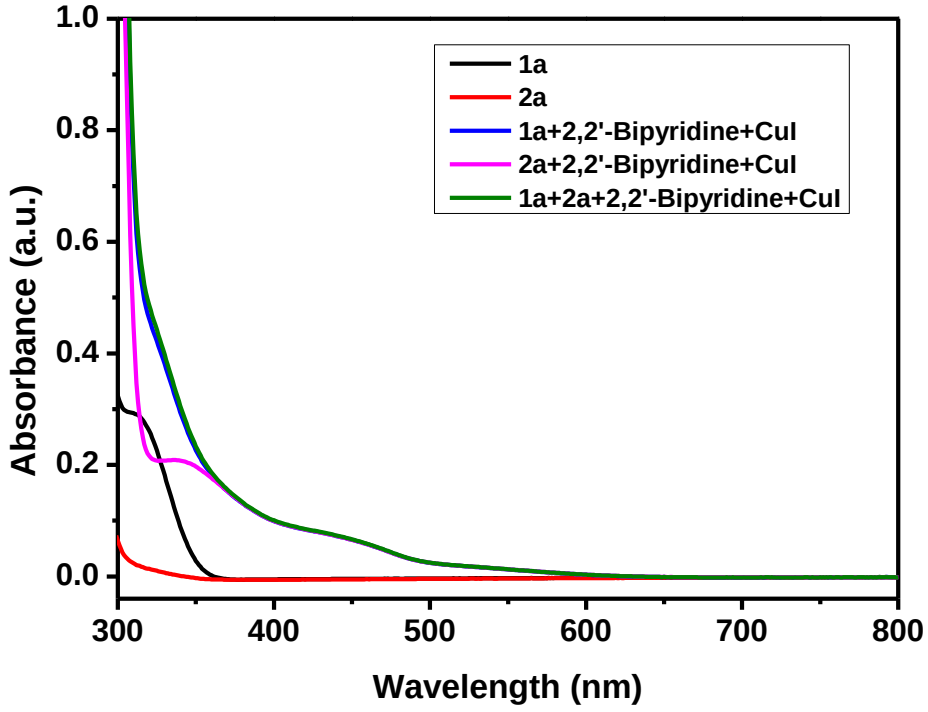

Figure 4.8 UV-Vis spectra of **1a** (0.167×10^{-3} M in MeCN, **black** line), **2a** (0.167×10^{-3} M in MeCN, **red** line), **1a** +2,2′-bipyridine + CuI (for each species 0.167×10^{-3} M in MeCN, **blue** line), **2a** + 2,2´-bipyridine + CuI (for each species 0.167×10^{-3} M, **pink** colour) and **1a** + **2a** + 2,2´-bipyridine + CuI (for each species 0.167×10^{-3} M in MeCN, **green** colour).

Cyclic voltammetry study:

Cyclic voltammetry was measured by using Metrohm Potentiostat/Galvanostat with the three electrode system at room temperature. The working electrode was glassy carbon, with platinum wire as the counter electrode and Ag/AgCl as a reference electrode. The experiments were performed in CH_3CN with tetrabutylammonium hexafluorophosphate (0.1M) at 80 mV/s scan rate. Samples were prepared with 0.1 mmol of the substrate in 20 mL CH_3CN. Cyclic voltammogram plot of **1a** showed an oxidation potential peak at +0.40 V, whereas in the case of **2a** showed both oxidation and reduction potential peaks at +0.92 V and -0.48 V, respectively. However, the combination of CuI and 2,2´-bipyridine(1:1) showed oxidation potential peaks at +0.75, and +1.08, reduction potential peak at -0.90.

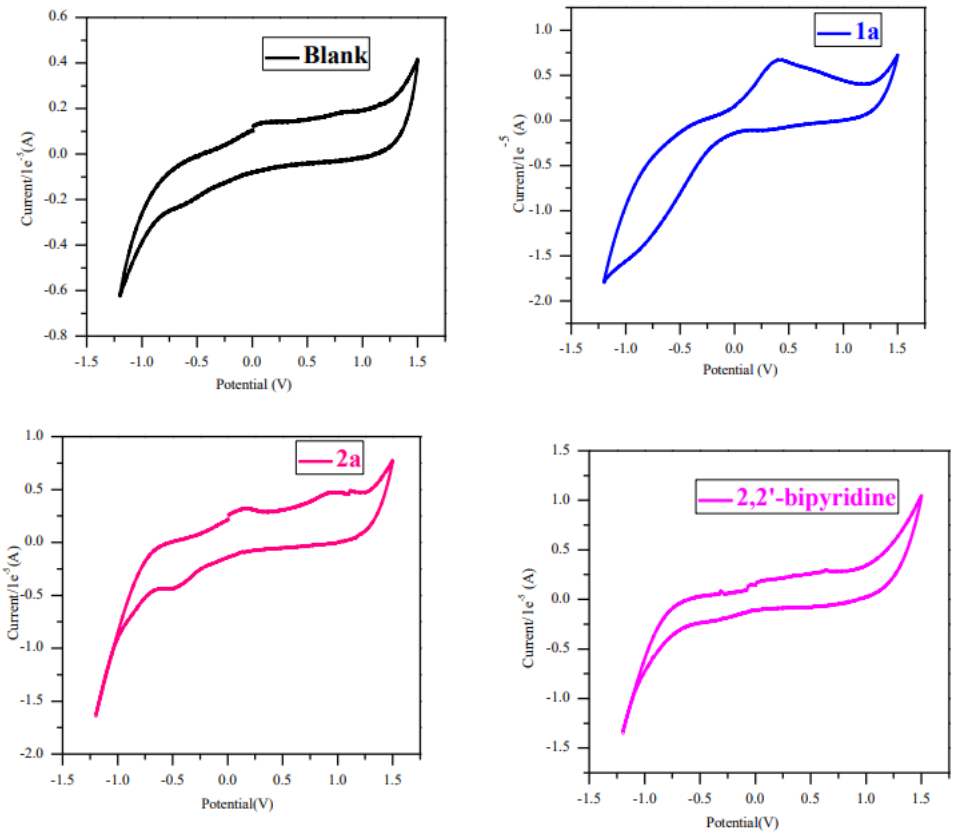

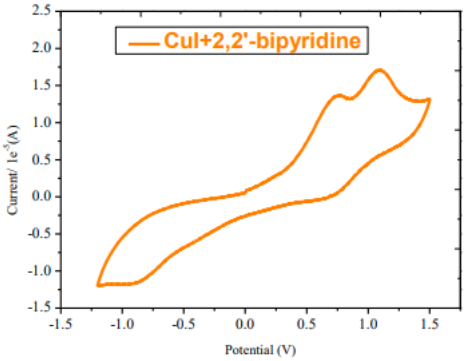

Figure 4.9 Cyclic voltammogram plots of **1a, 2a, 2,2′-bipyridine** and CuI/bpy.

Light ON-OFF Experiments:

A mixture of compound **1a** (54 mg, 0.2 mmol, 1.0 equiv), **2a** (0.4 mmol, 2.0 equiv), CuI (3.81 mg, 0.02 mmol), 2,2´-bipyridine (3.12 mg, 0.02 mmol), MeCN:H_2O (2.0 mL, 50:1) were placed in 25 mL glass tube. The reaction tube was degassed and purged with argon four times. Then, the mixture was irradiated using 5W blue LED lights for 2h. Afterwards, the reaction progress was monitored by measuring the yield based on ^{1}H NMR using mesitylene as an internal standard. Then, the reaction was kept in the dark for 2h (monitored by ^{1}H NMR). The same operations (light and dark) were performed up to 16h. The results are summarized in **Table 4.7.**

Entry	Time (h)	Light source	Yield (%)
1	2	on	12
2	4	off	13
3	6	on	25
4	8	off	27
5	10	on	38
6	12	off	38
7	14	on	53
8	16	off	54

Table 4.7 Light ON-OFF experiment results.

Copies of ^{1}H and ^{13}C NMR spectra of some important compounds described in Chapter 4

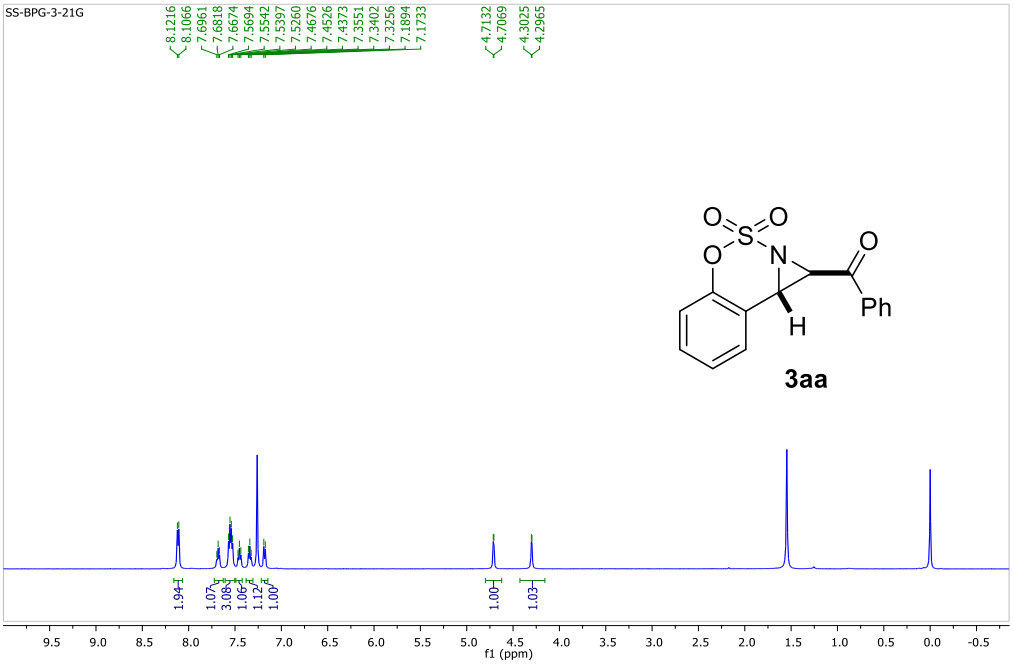

Figure 4.10 500 MHz ^{1}H NMR spectrum of **3aa** in $CDCl_3$.

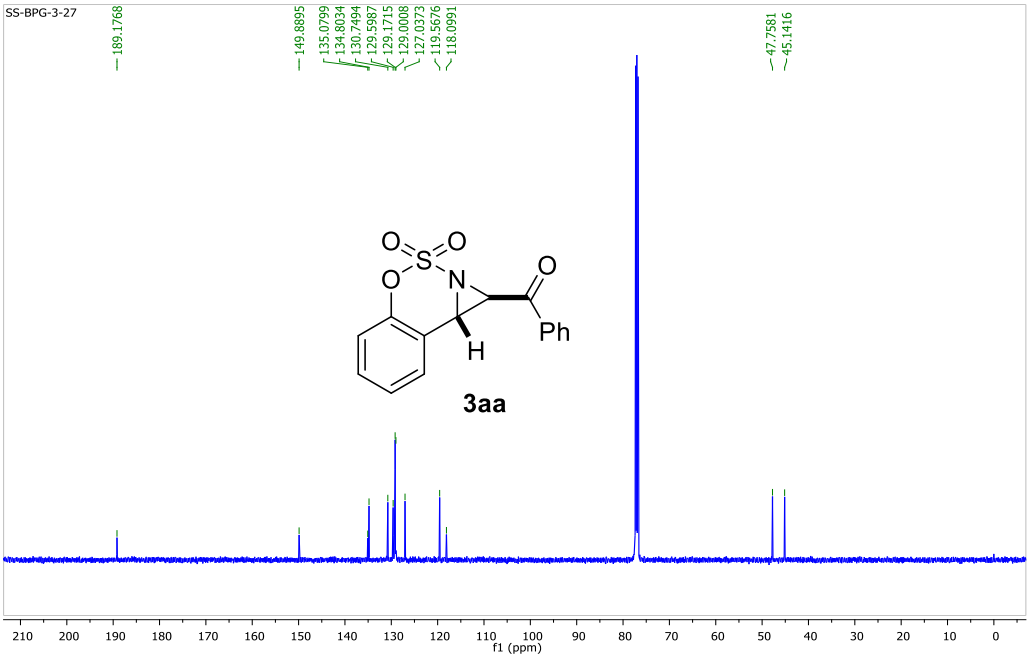

Figure 4.11 125 MHz ^{13}C NMR spectrum of **3aa** in $CDCl_3$.

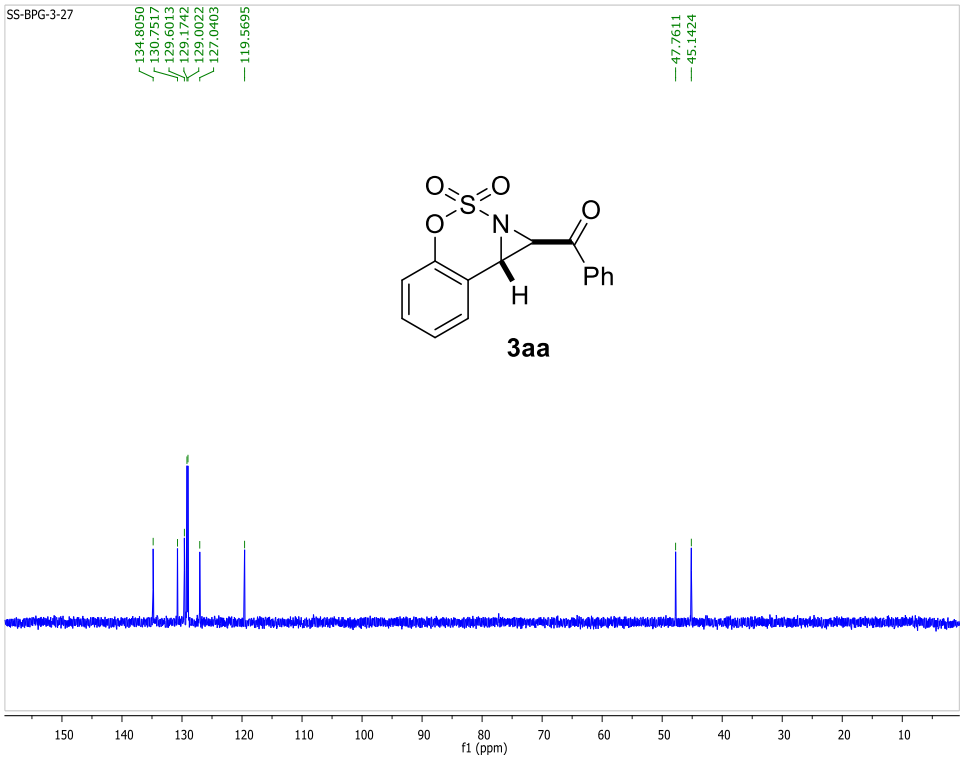

Figure 4.12 125 MHz DEPT-135 NMR spectrum of **3aa** in $CDCl_3$.

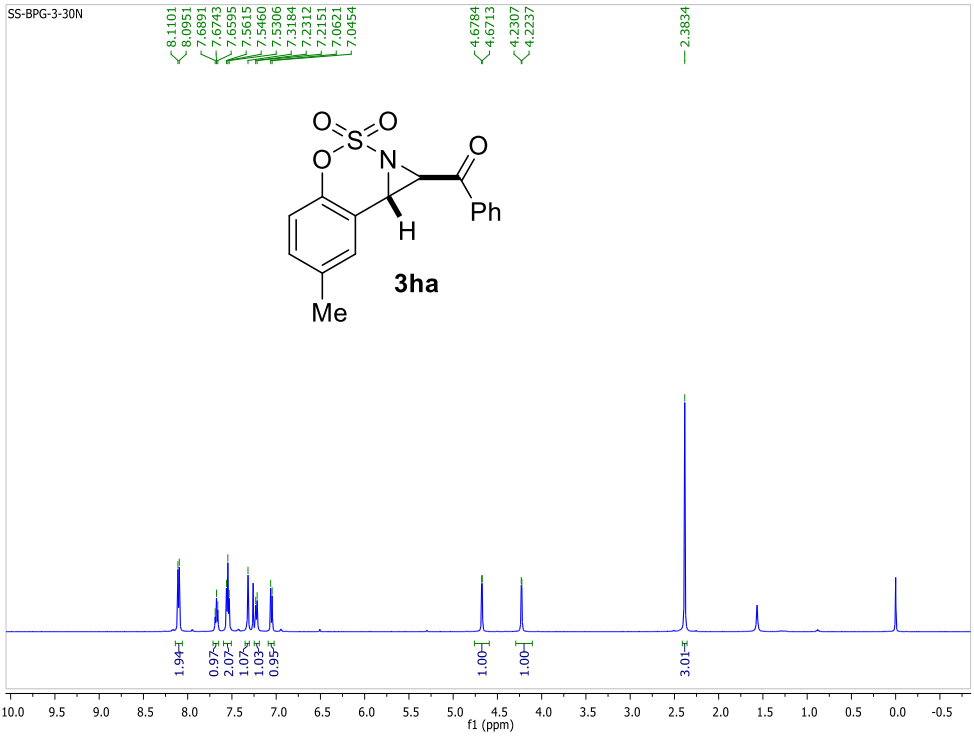

Figure 4.13 500 MHz ^{1}H NMR spectrum of **3ha** in $CDCl_3$.

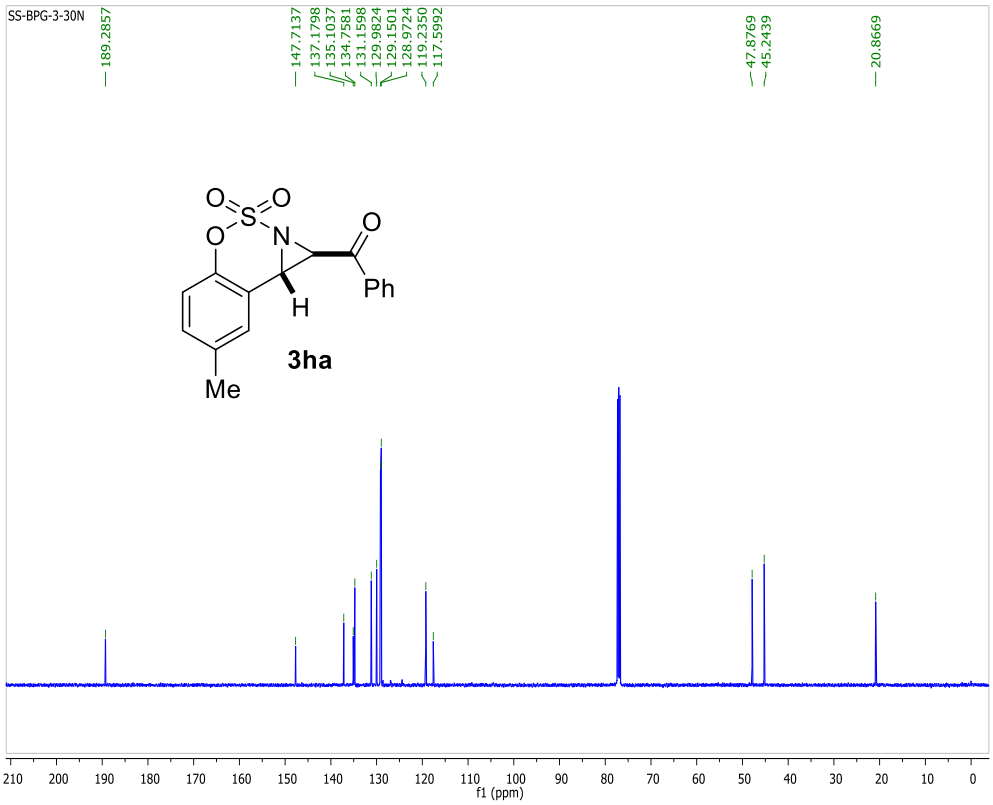

Figure 4.14 125 MHz ^{13}C NMR spectrum of **3ha** in $CDCl_3$.

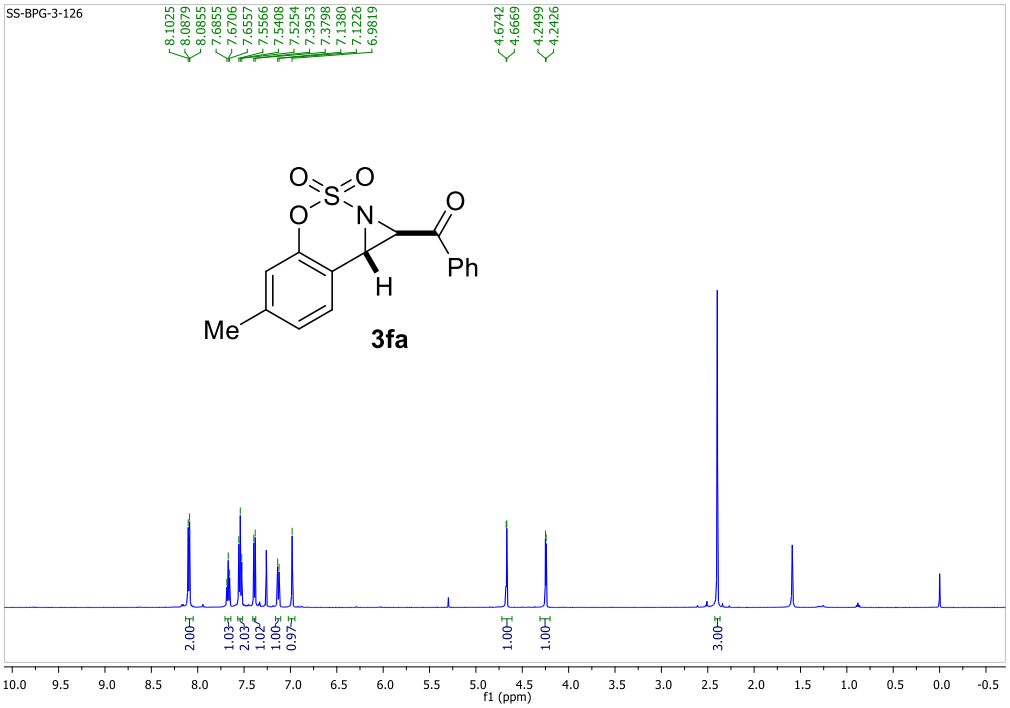

Figure 4.15 500 MHz ^{1}H NMR spectrum of **3fa** in $CDCl_3$.

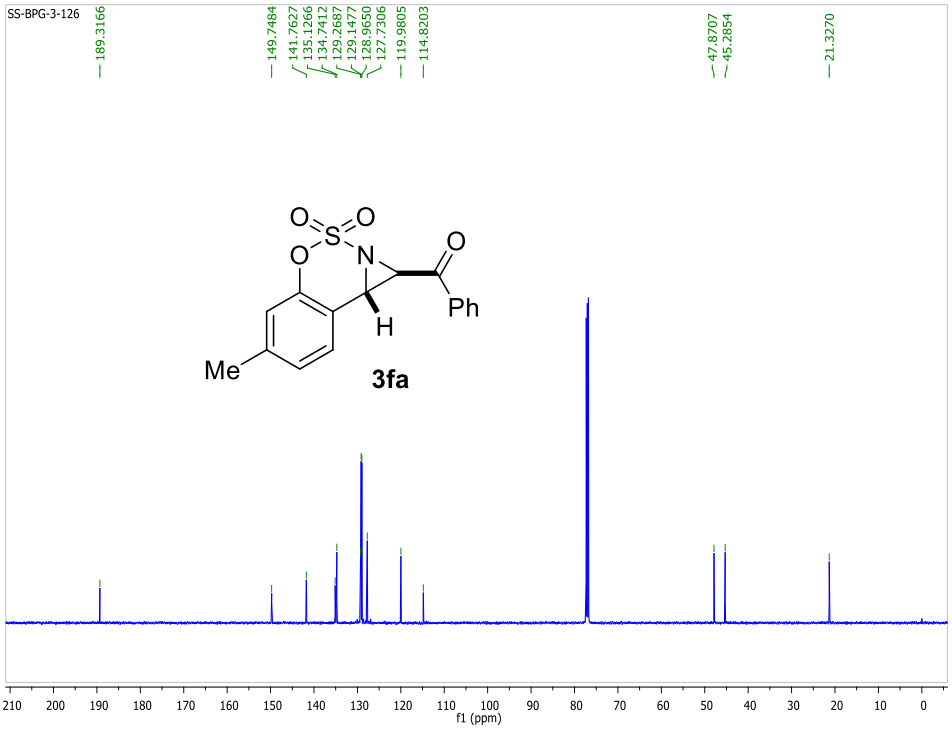

Figure 4.16 125 MHz ^{13}C NMR spectrum of **3fa** in $CDCl_3$.

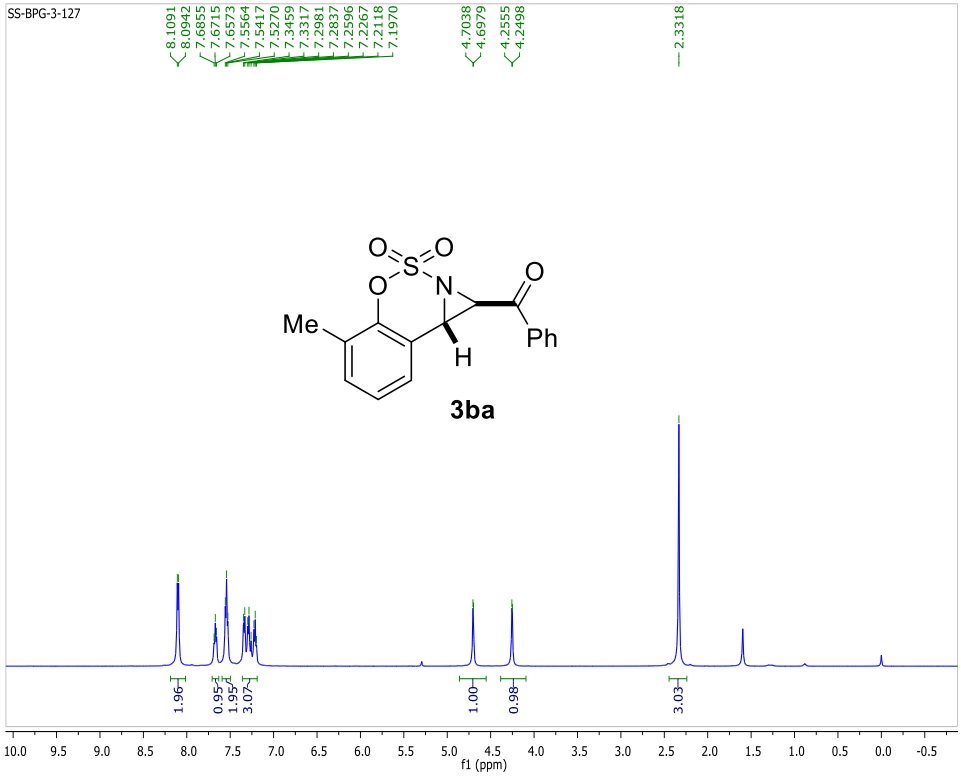

Figure 4.17 500 MHz ^{1}H NMR spectrum of **3ba** in $CDCl_3$.

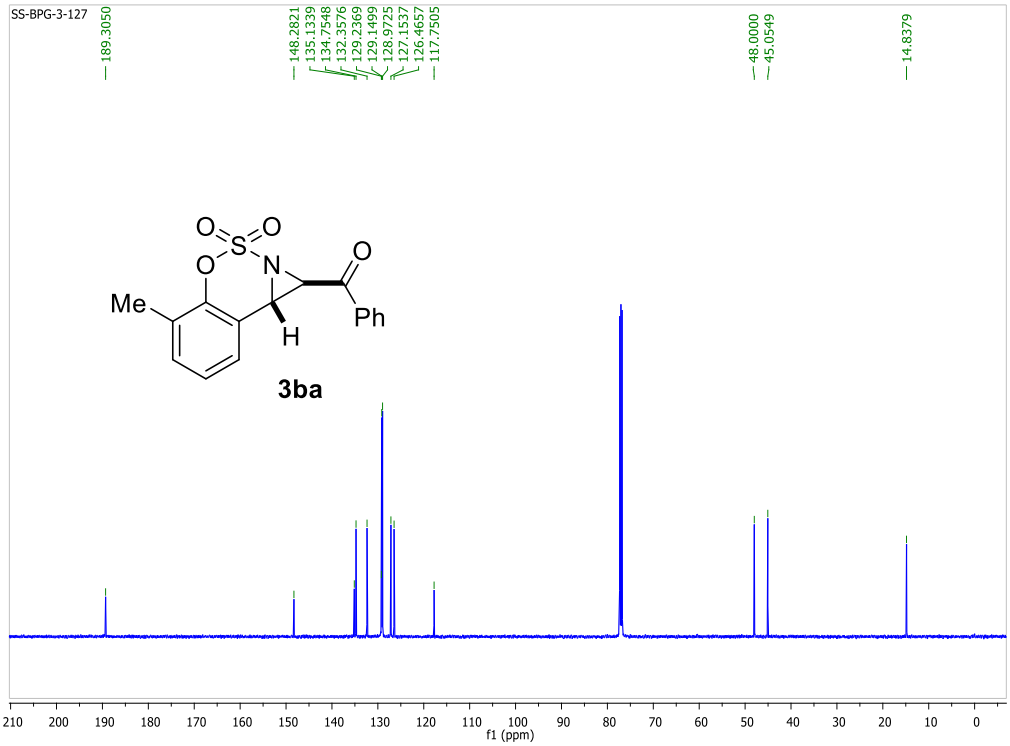

Figure 4.18 125 MHz ^{13}C NMR spectrum of **3ba** in $CDCl_3$.

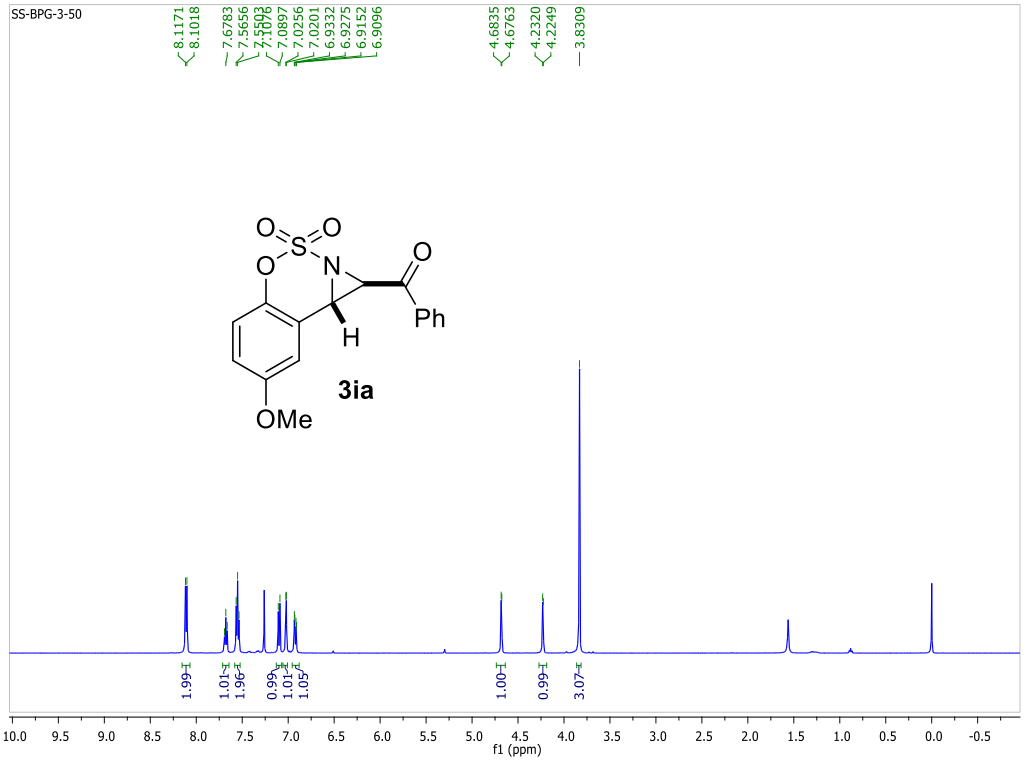

Figure 4.19 500 MHz ^{1}H NMR spectrum of **3ia** in $CDCl_3$.

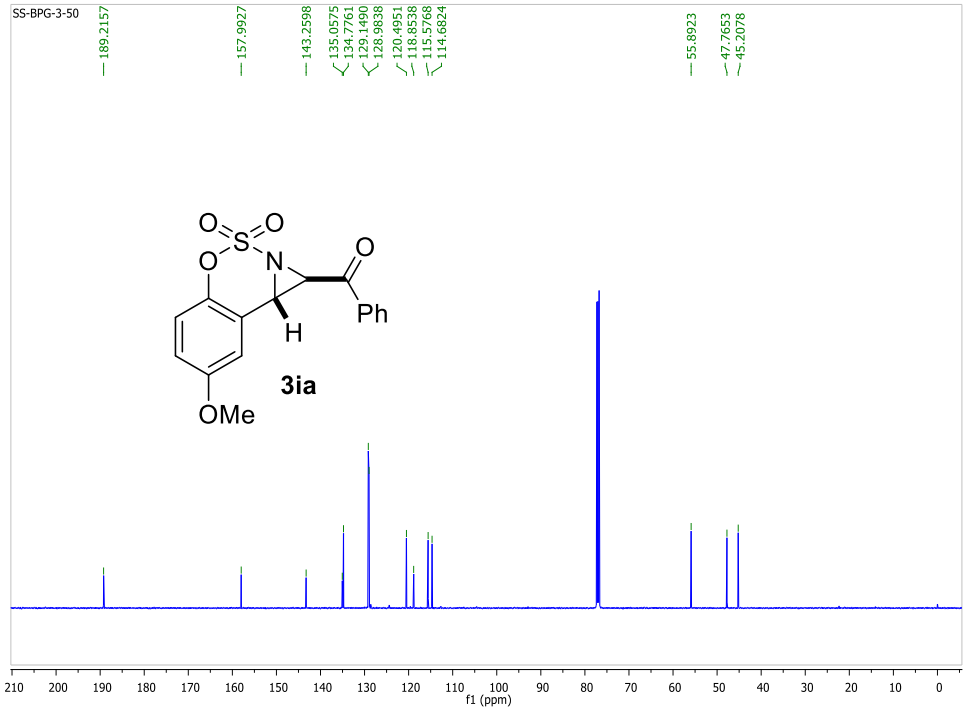

Figure 4.20 125 MHz ^{13}C NMR spectrum of **3ia** in $CDCl_3$.

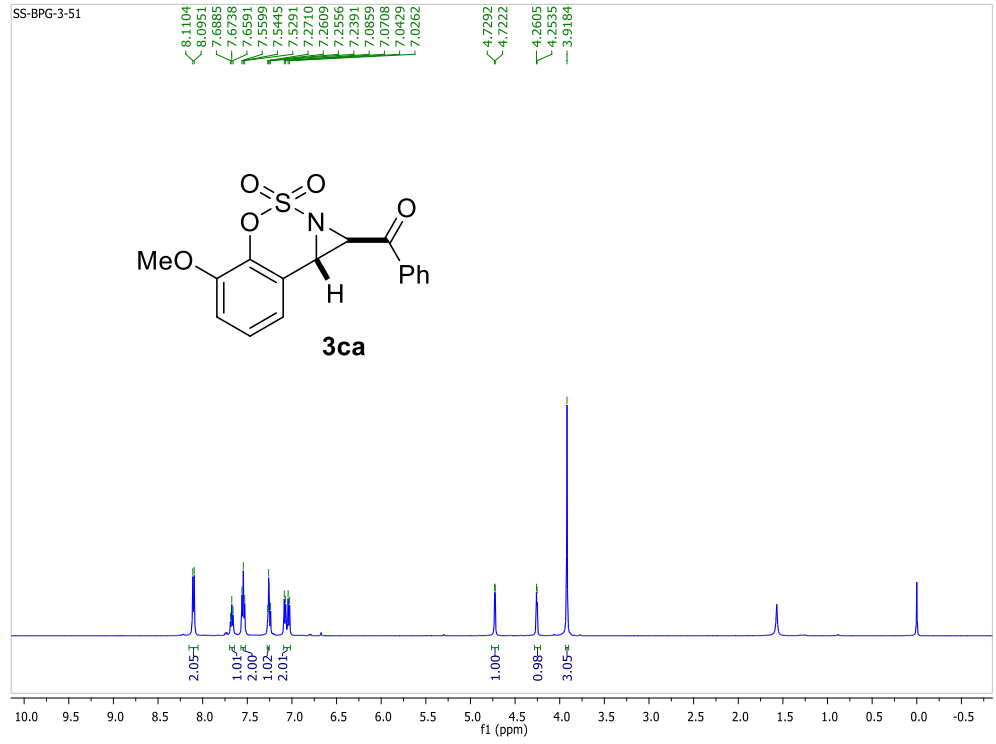

Figure 4.21 500 MHz ^{1}H NMR spectrum of **3ca** in $CDCl_3$.

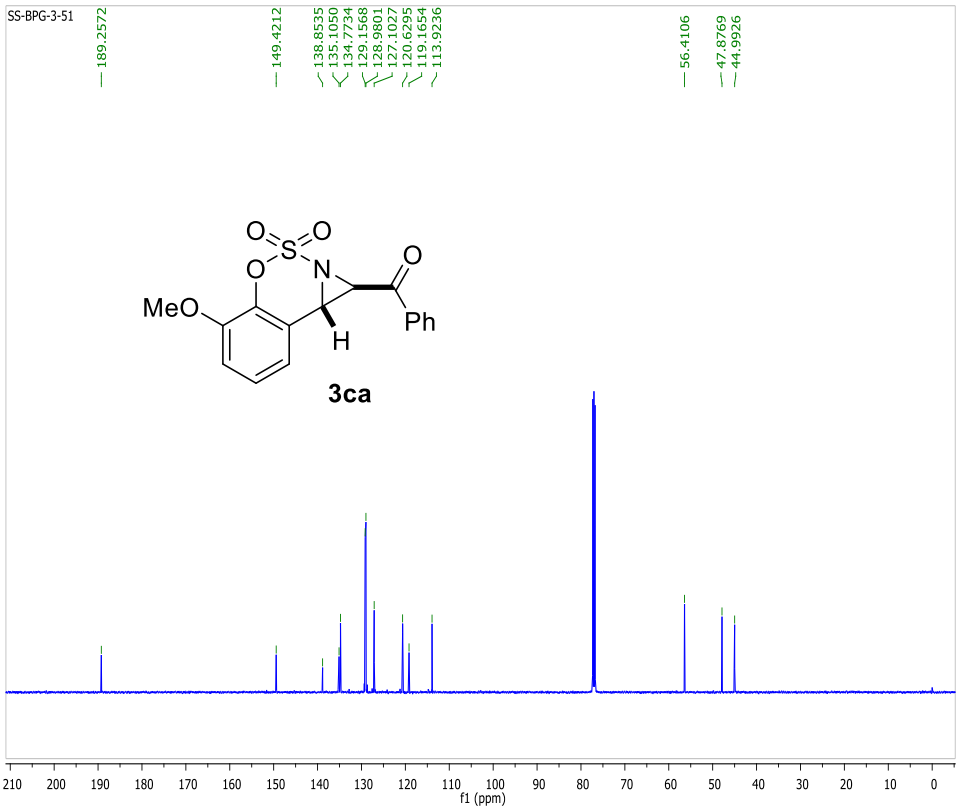

Figure 4.22 125 MHz ^{13}C NMR spectrum of **3ca** in $CDCl_3$.

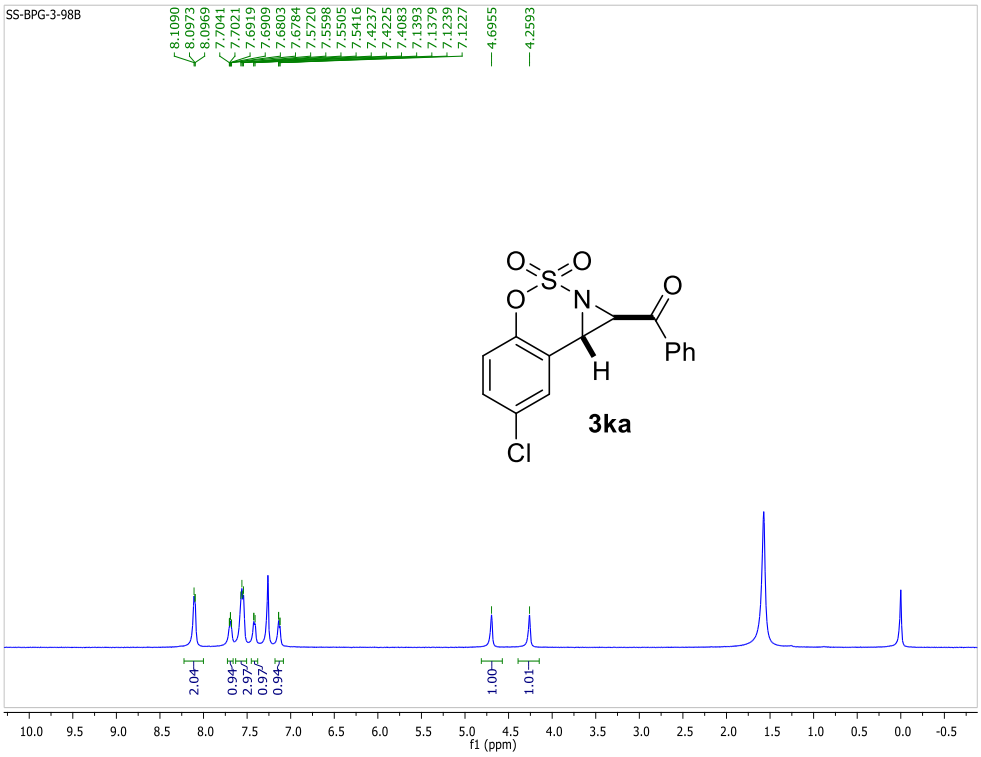

Figure 4.23 500 MHz ^{1}H NMR spectrum of **3ka** in $CDCl_3$.

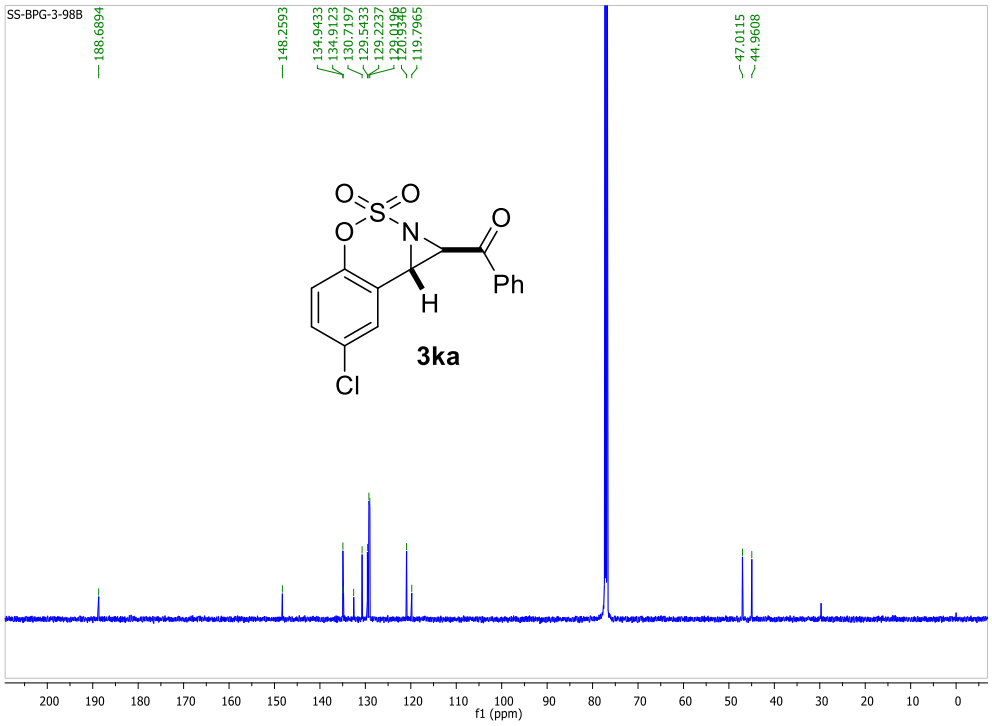

Figure 4.24 125 MHz ^{13}C NMR spectrum of **3ka** in $CDCl_3$.

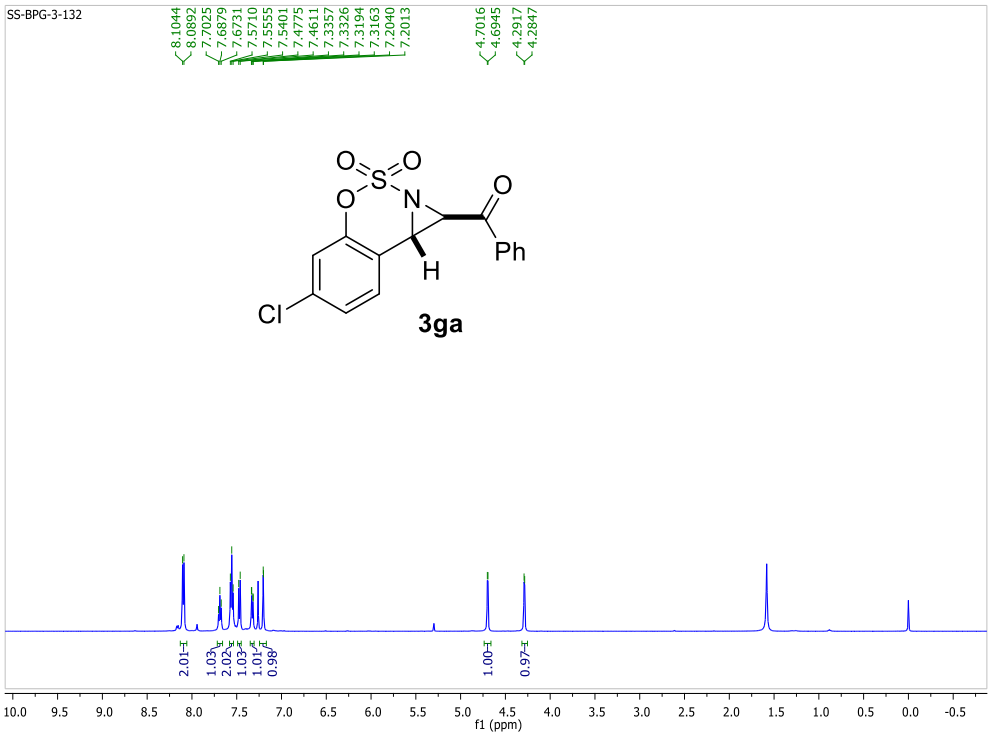

Figure 4.25 500 MHz ^{1}H NMR spectrum of **3ga** in $CDCl_3$.

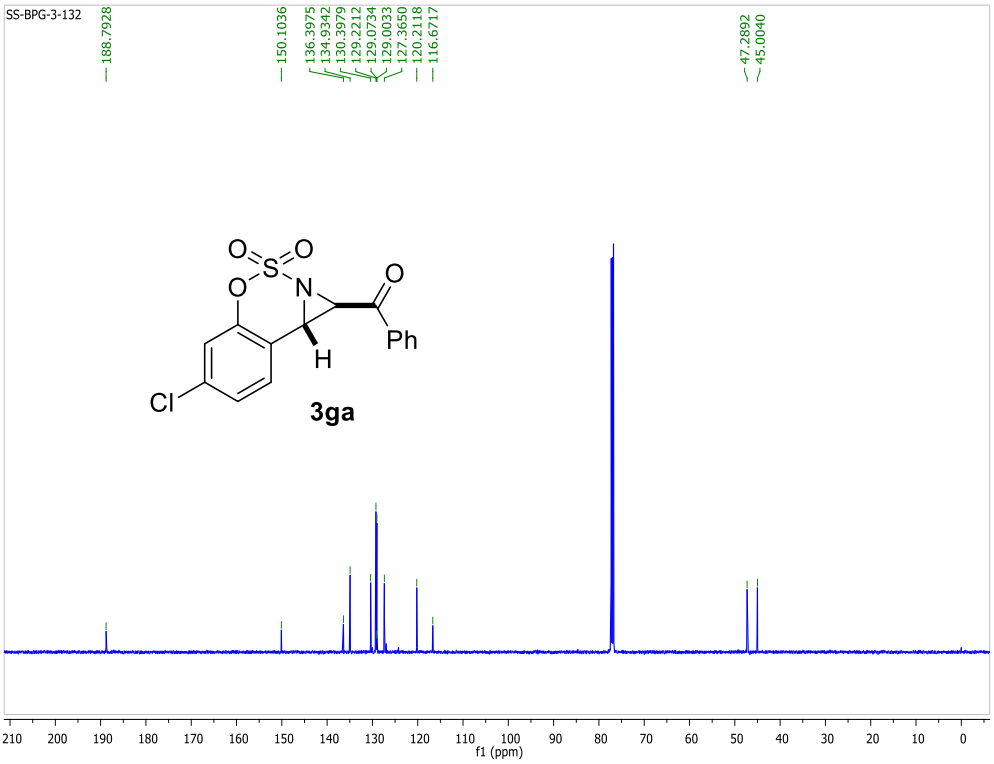

Figure 4.26 125 MHz ^{13}C NMR spectrum of **3ga** in $CDCl_3$.

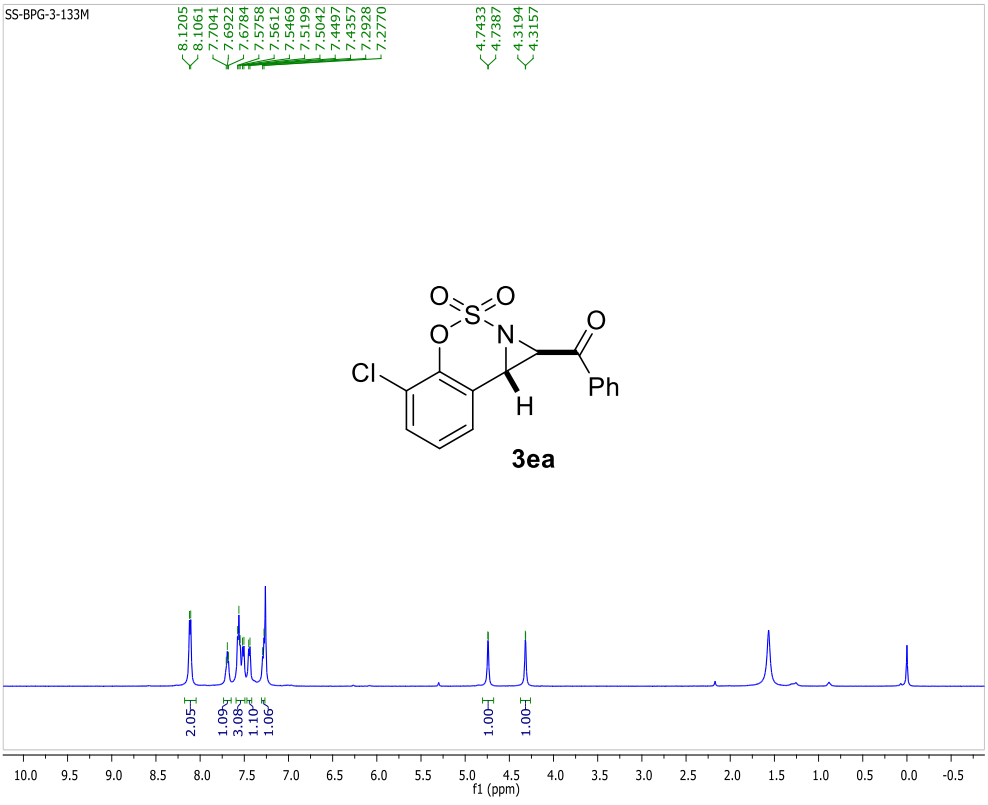

Figure 4.27 500 MHz ^{1}H NMR spectrum of **3ea** in $CDCl_3$.

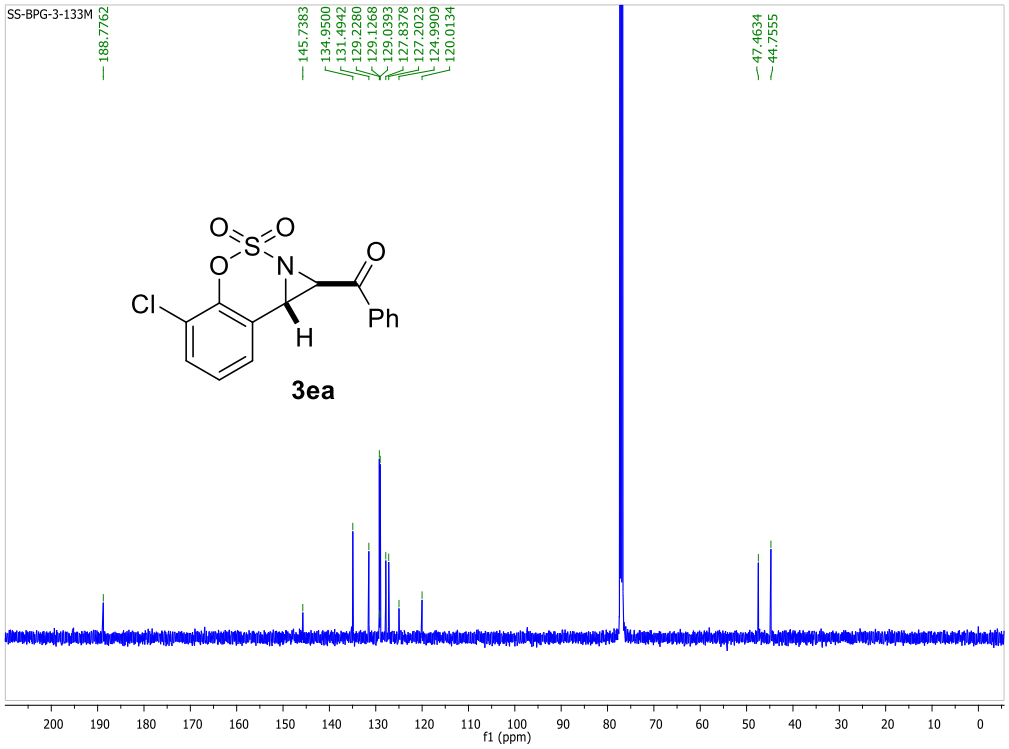

Figure 4.28 125 MHz ^{13}C NMR spectrum of **3ea** in $CDCl_3$.

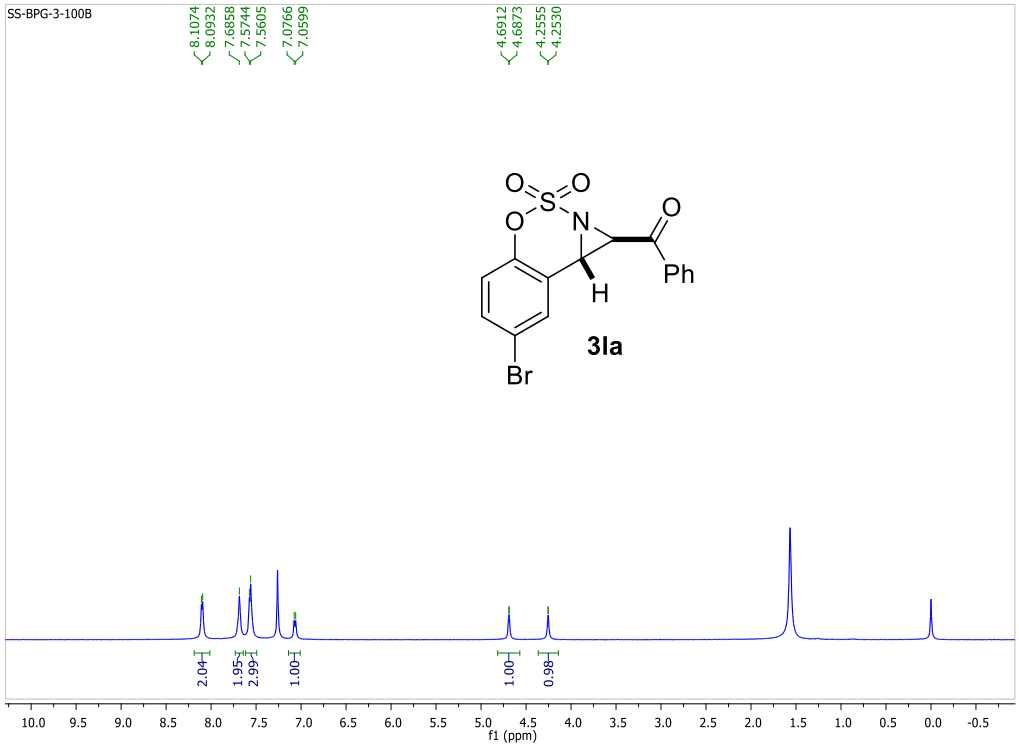

Figure 4.29 500 MHz ^{1}H NMR spectrum of **3la** in $CDCl_3$.

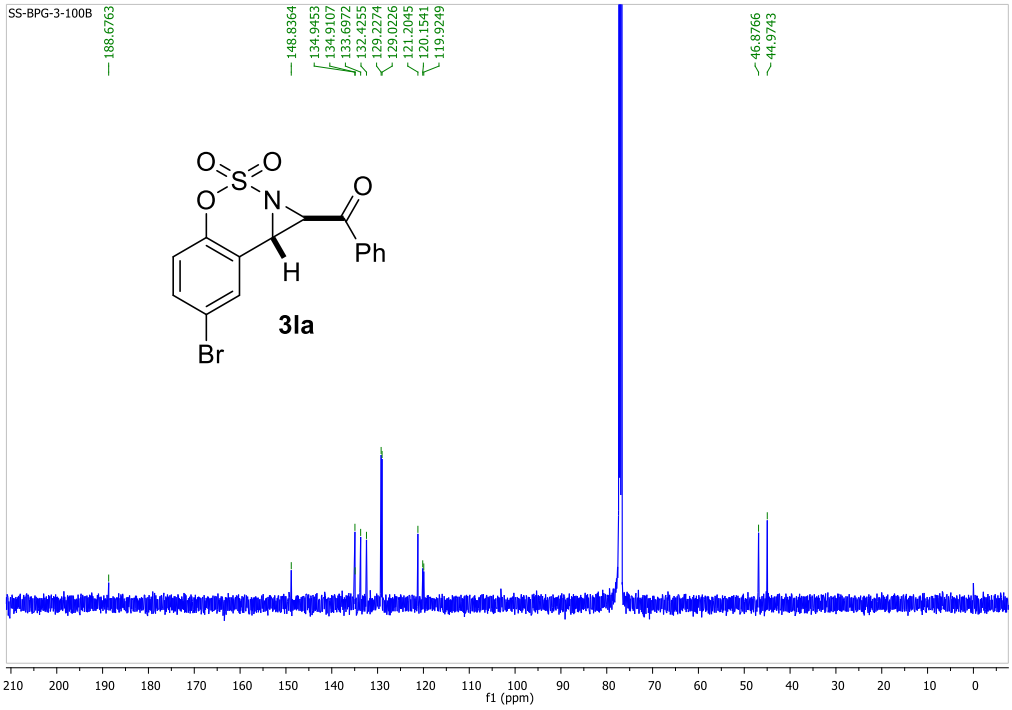

Figure 4.30 125 MHz ^{13}C NMR spectrum of **3la** in $CDCl_3$.

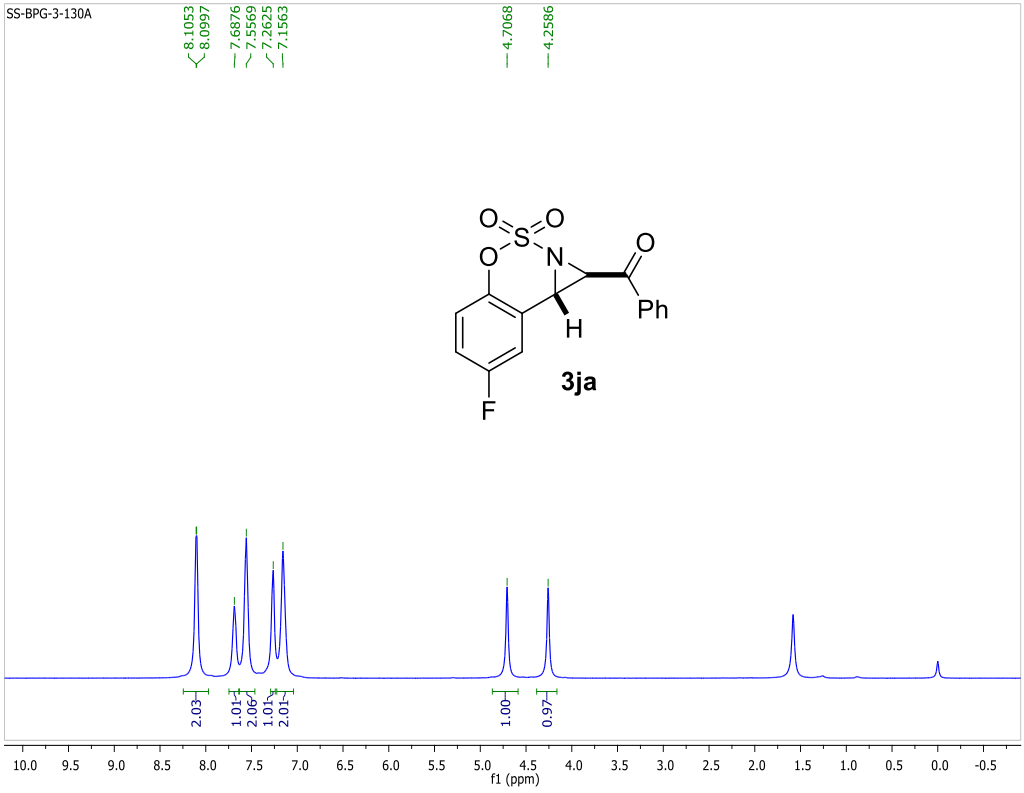

Figure 4.31 500 MHz ^{1}H NMR spectrum of **3ja** in $CDCl_3$.

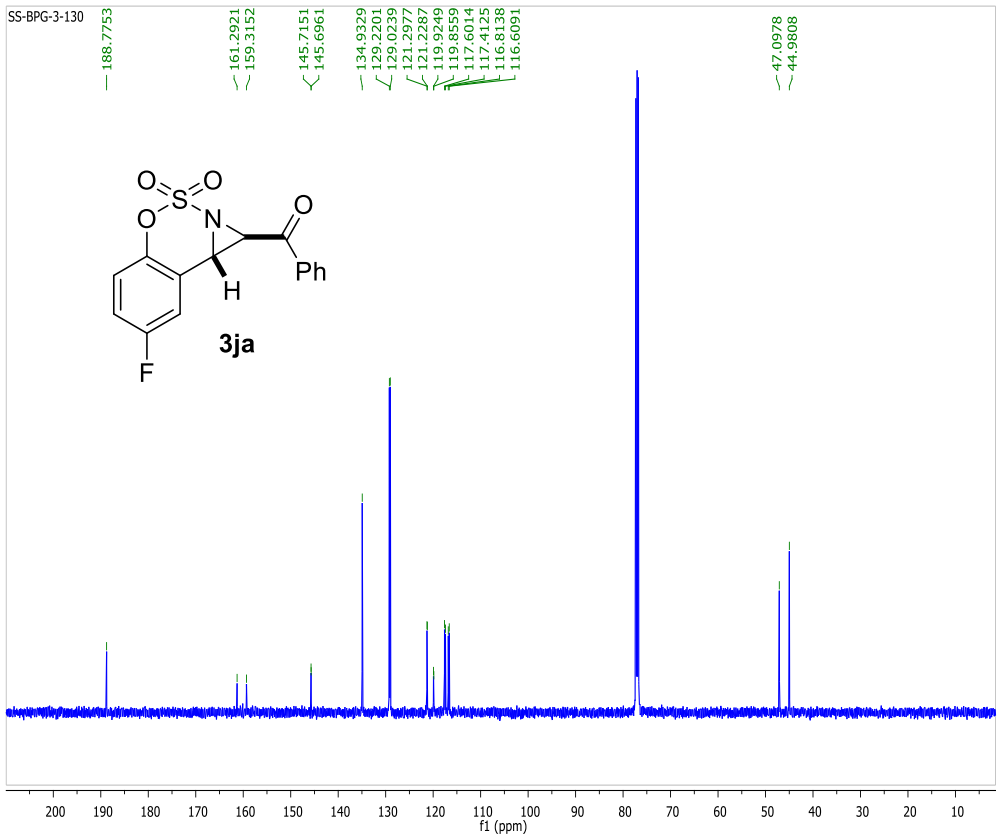

Figure 4.32 125 MHz ^{13}C NMR spectrum of **3ja** in $CDCl_3$.

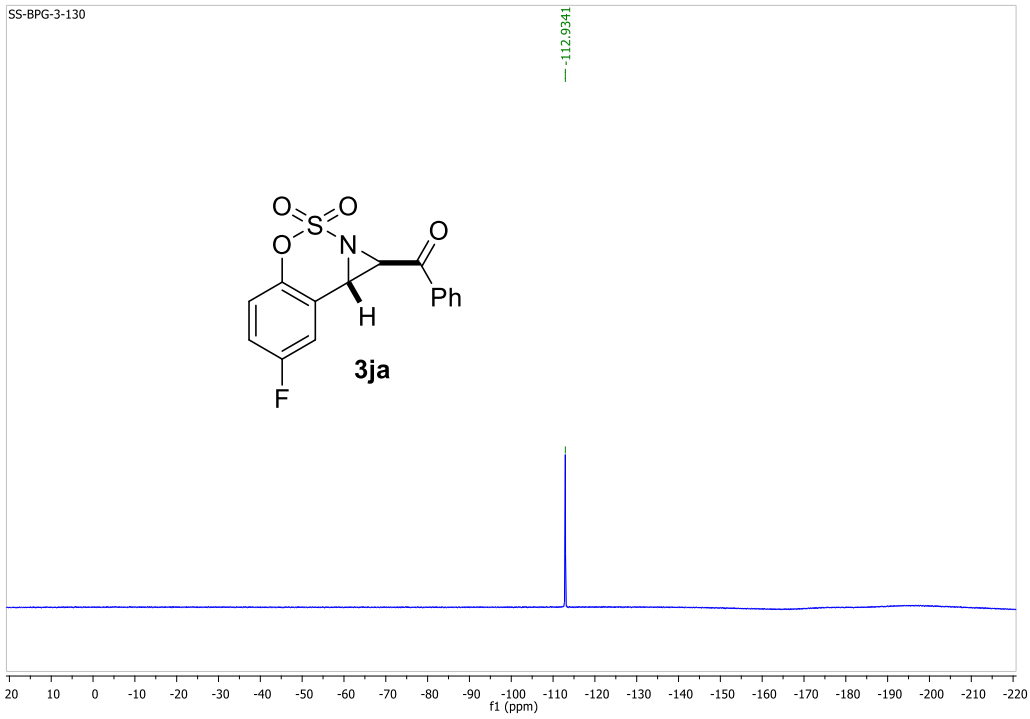

Figure 4.33 470 MHz ^{19}F NMR spectrum of **3ja** in $CDCl_3$.

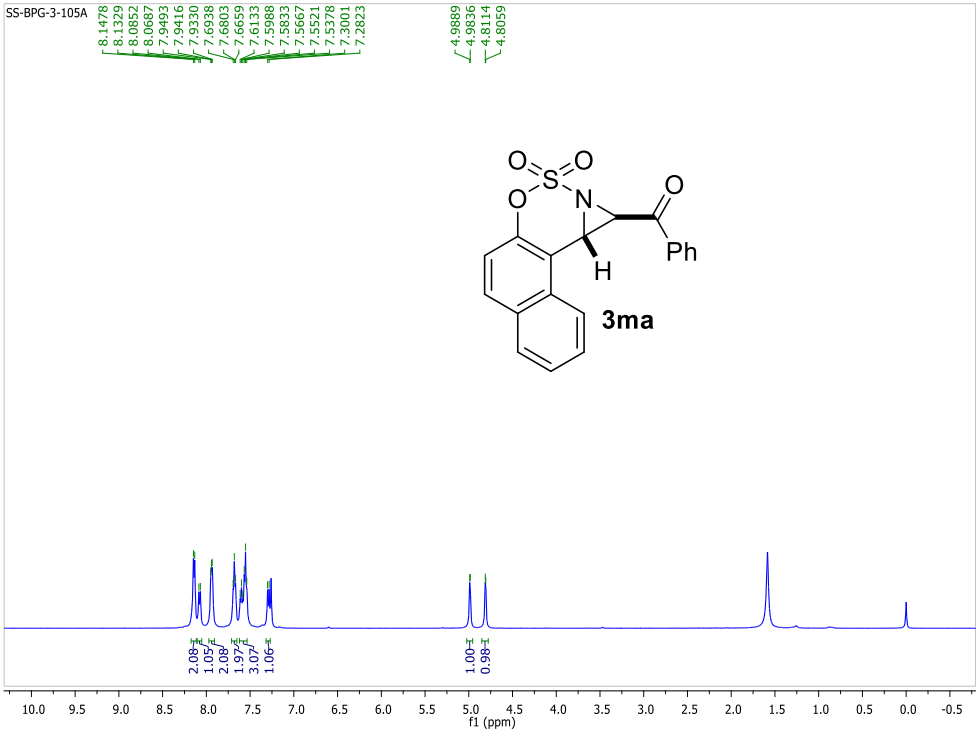

Figure 4.34 500 MHz ^{1}H NMR spectrum of **3ma** in $CDCl_3$.

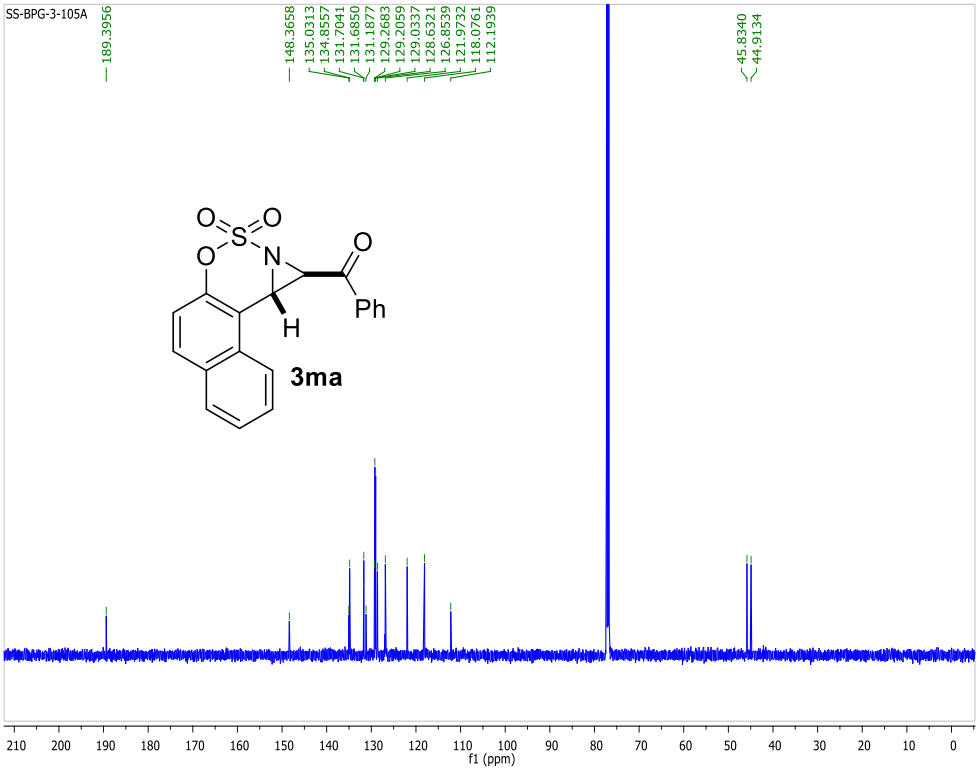

Figure 4.35 125 MHz ^{13}C NMR spectrum of **3ma** in $CDCl_3$.

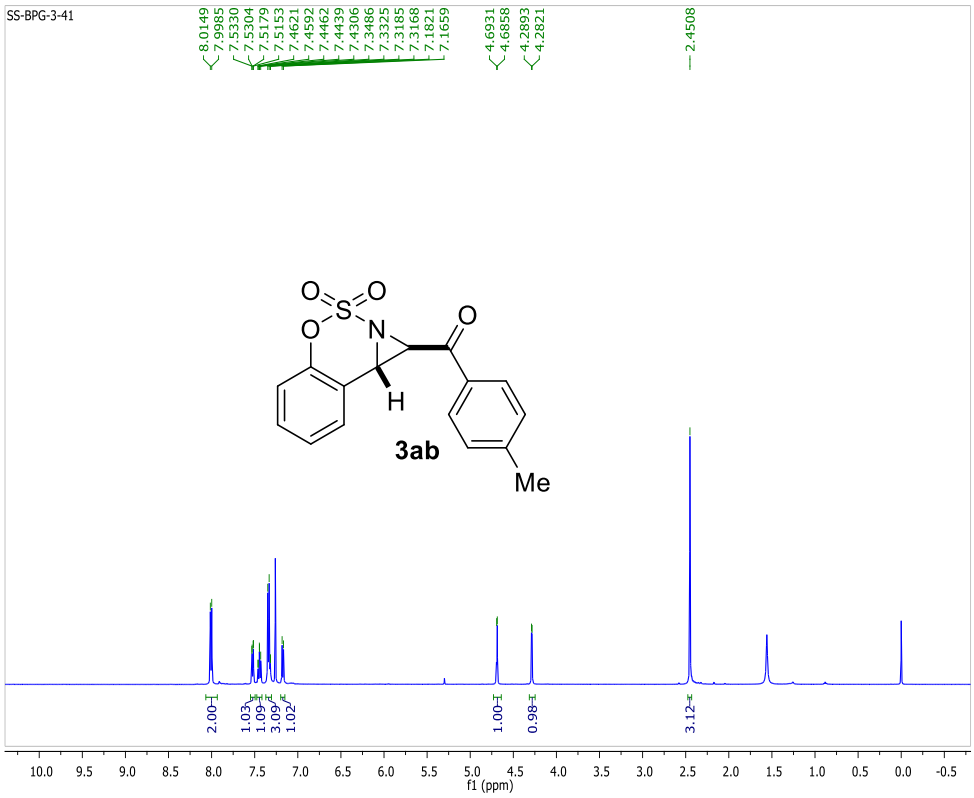

Figure 4.36 500 MHz ^{1}H NMR spectrum of **3ab** in $CDCl_3$.

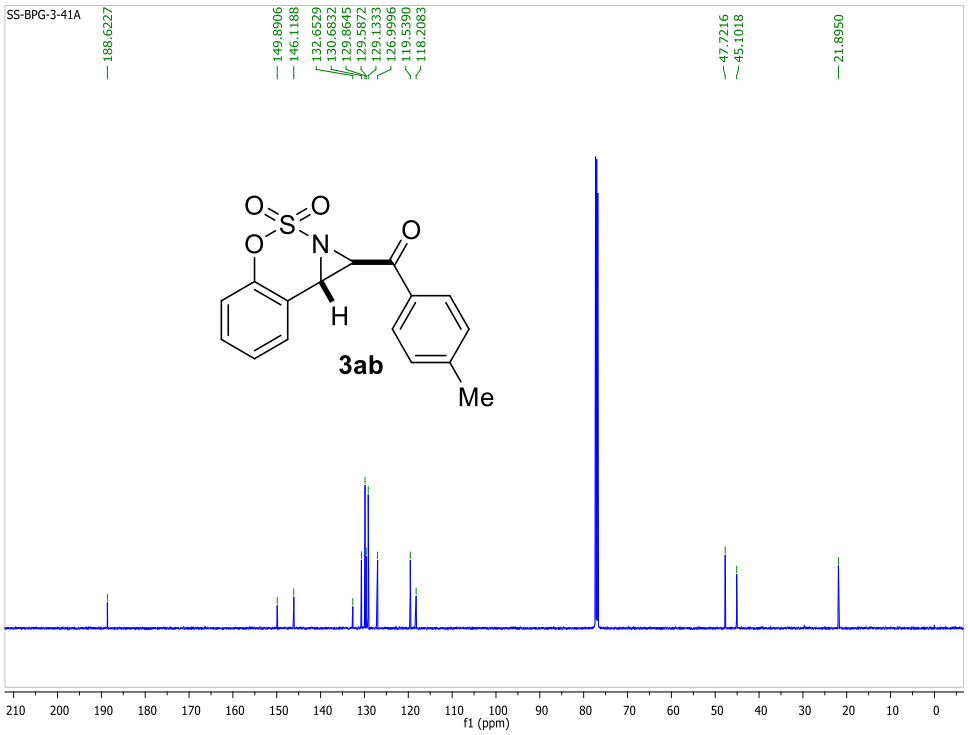

Figure 4.37 125 MHz ^{13}C NMR spectrum of **3ab** in $CDCl_3$.

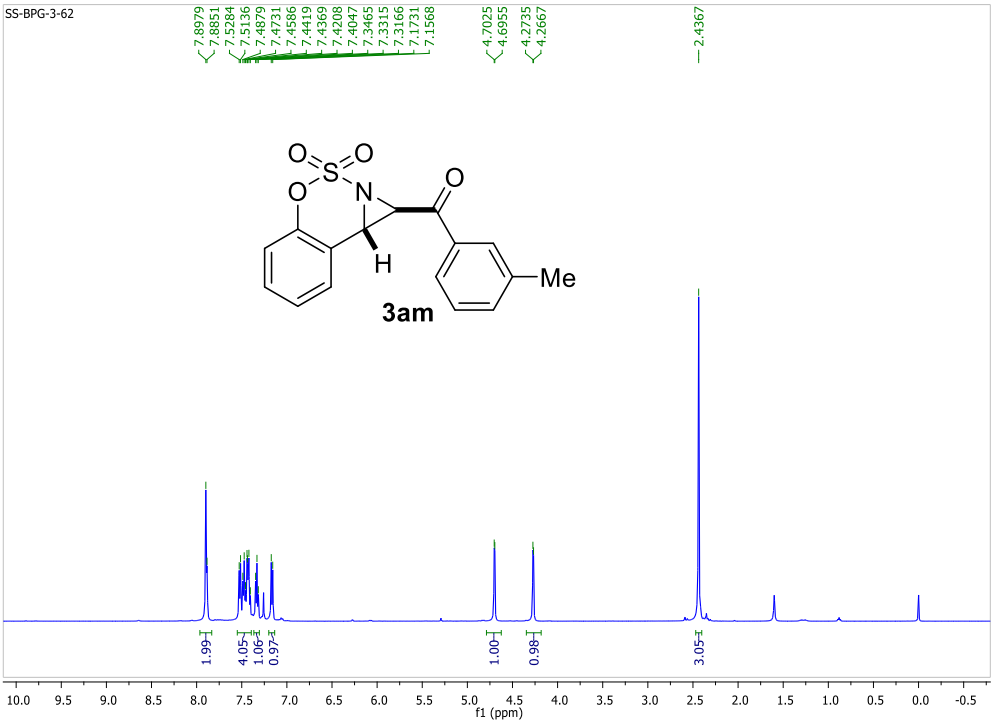

Figure 4.38 500 MHz ^{1}H NMR spectrum of **3am** in $CDCl_3$.

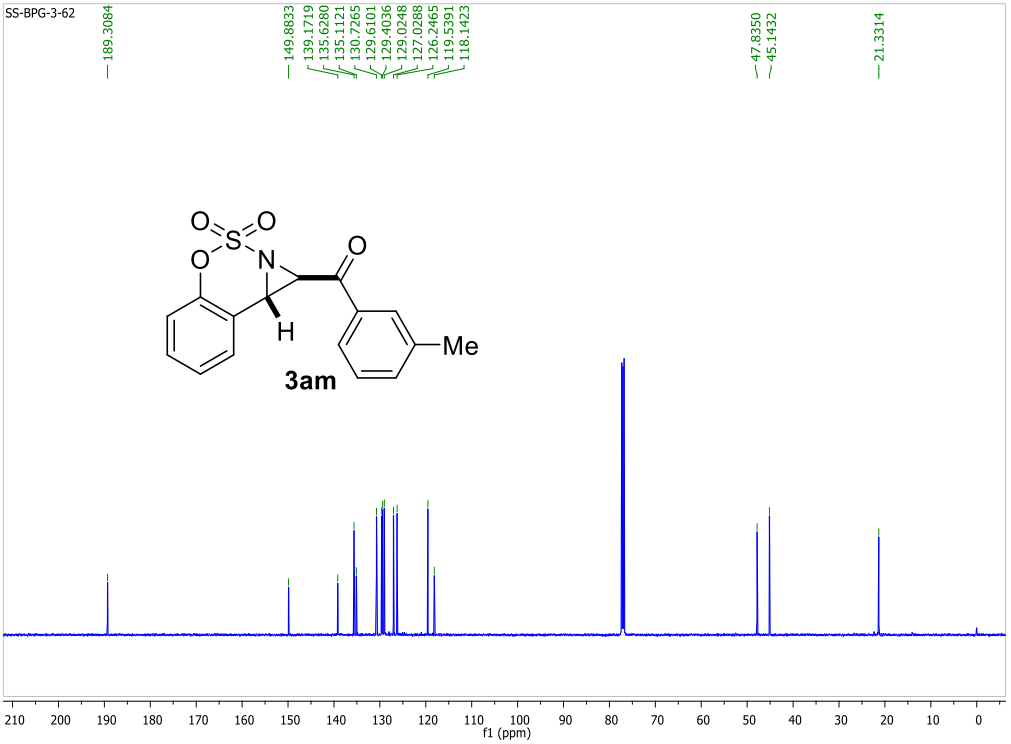

Figure 4.39 125 MHz ^{13}C NMR spectrum of **3am** in $CDCl_3$.

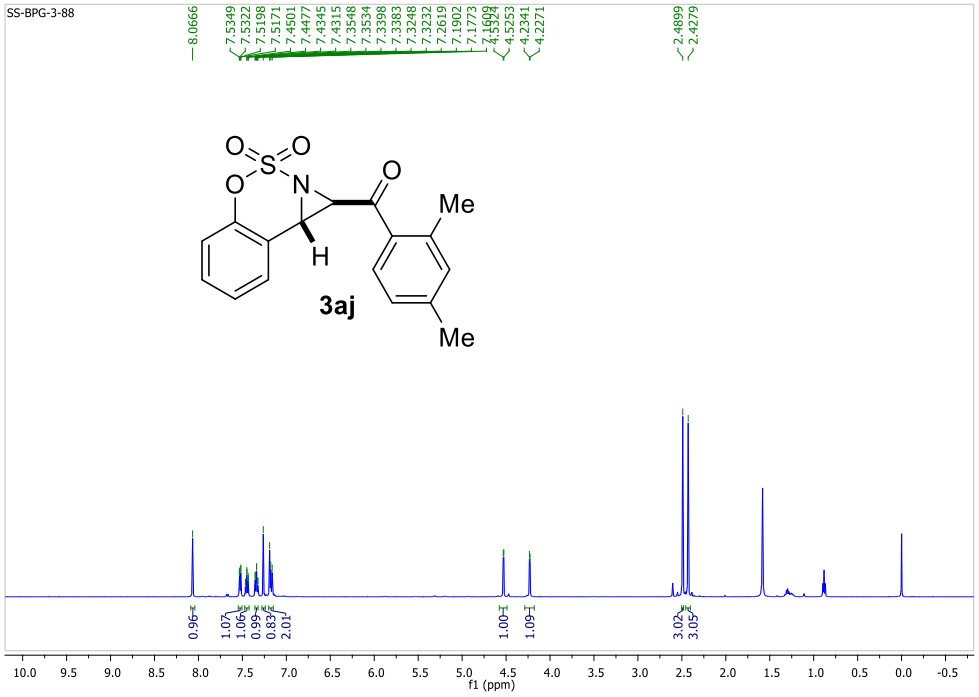

Figure 4.40 500 MHz ^{1}H NMR spectrum of **3aj** in $CDCl_3$.

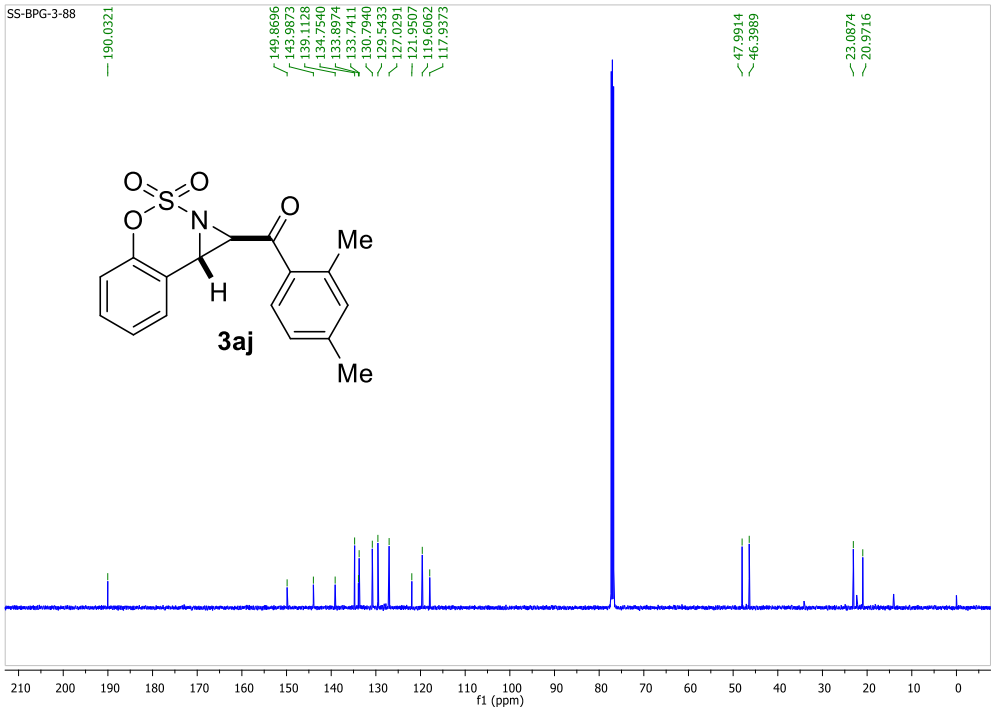

Figure 4.41 125 MHz ^{13}C NMR spectrum of **3aj** in $CDCl_3$.

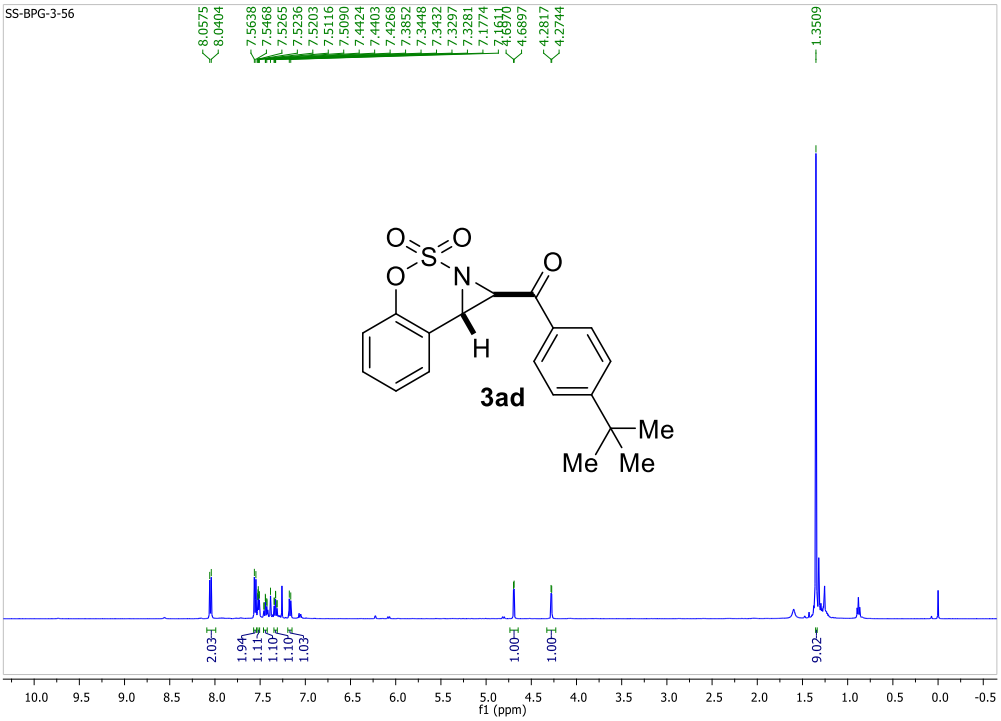

Figure 4.42 500 MHz ^{1}H NMR spectrum of **3ad** in $CDCl_3$.

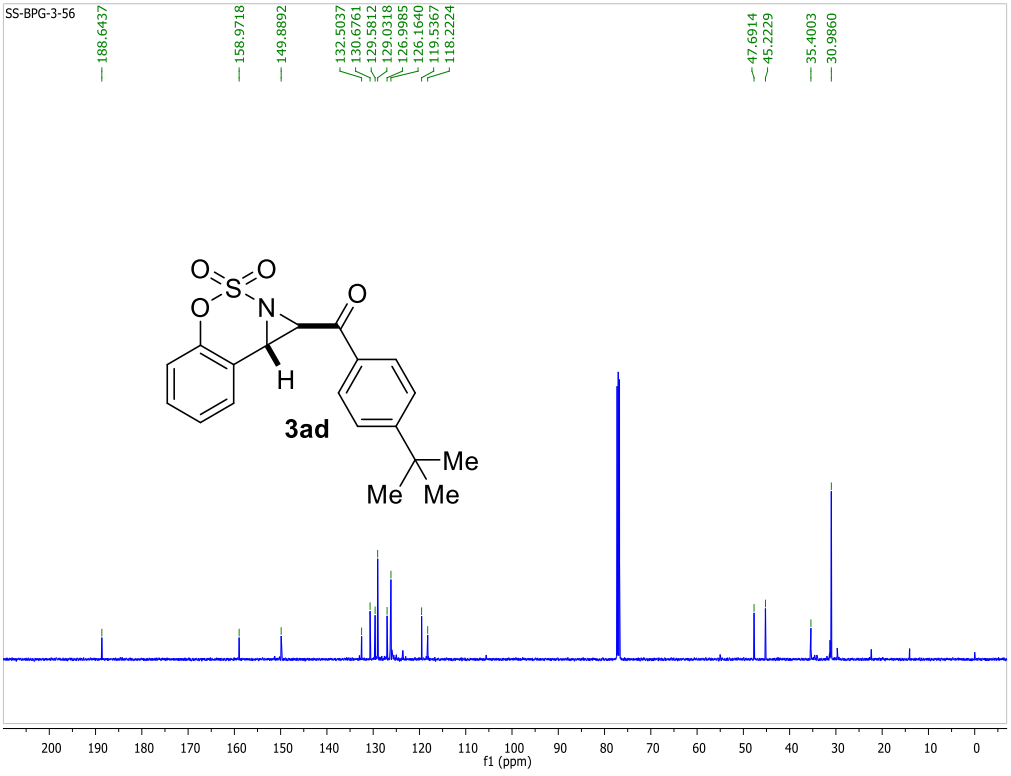

Figure 4.43 125 MHz ^{13}C NMR spectrum of **3ad** in $CDCl_3$.

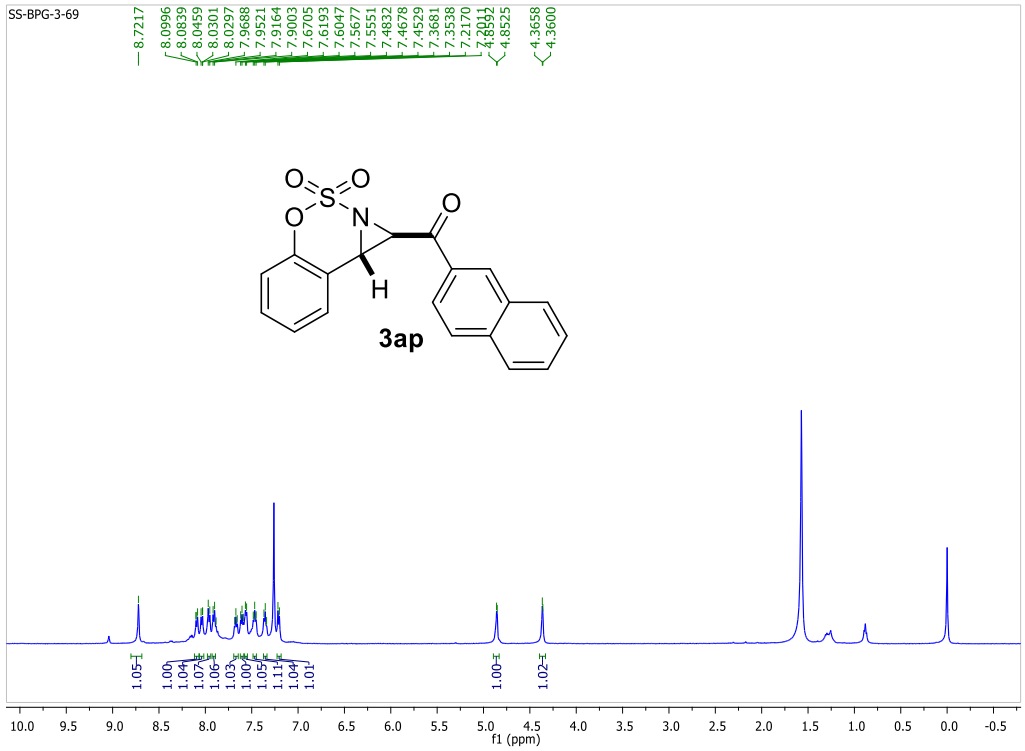

Figure 4.44 500 MHz ^{1}H NMR spectrum of **3ap** in $CDCl_3$.

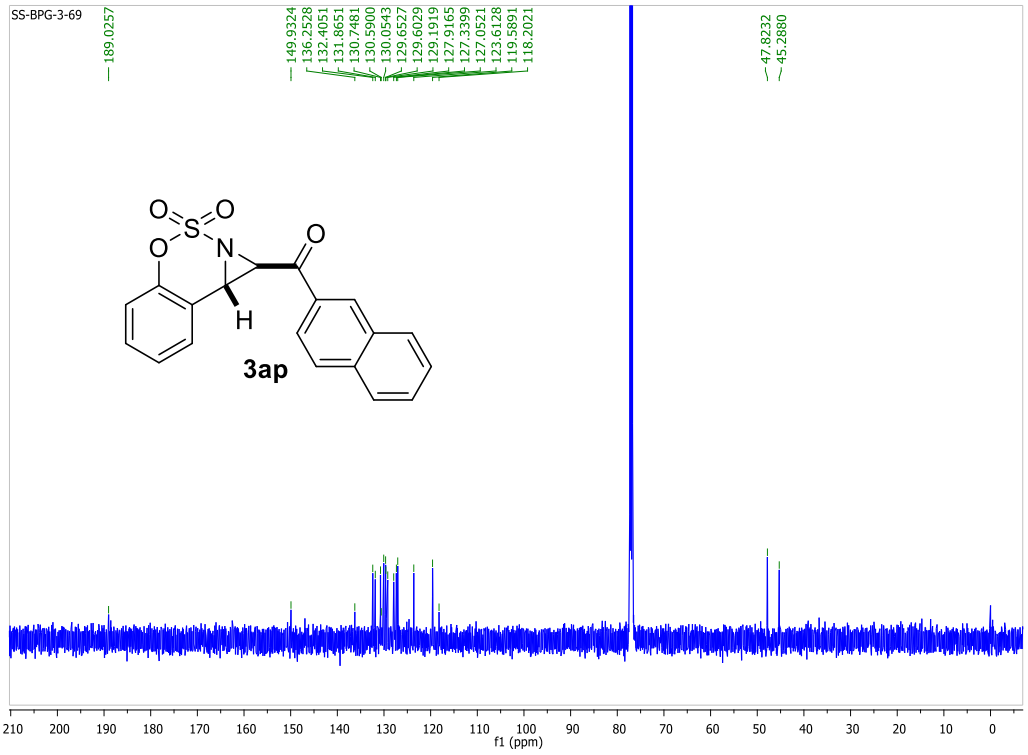

Figure 4.45 125 MHz ^{13}C NMR spectrum of **3ap** in $CDCl_3$.

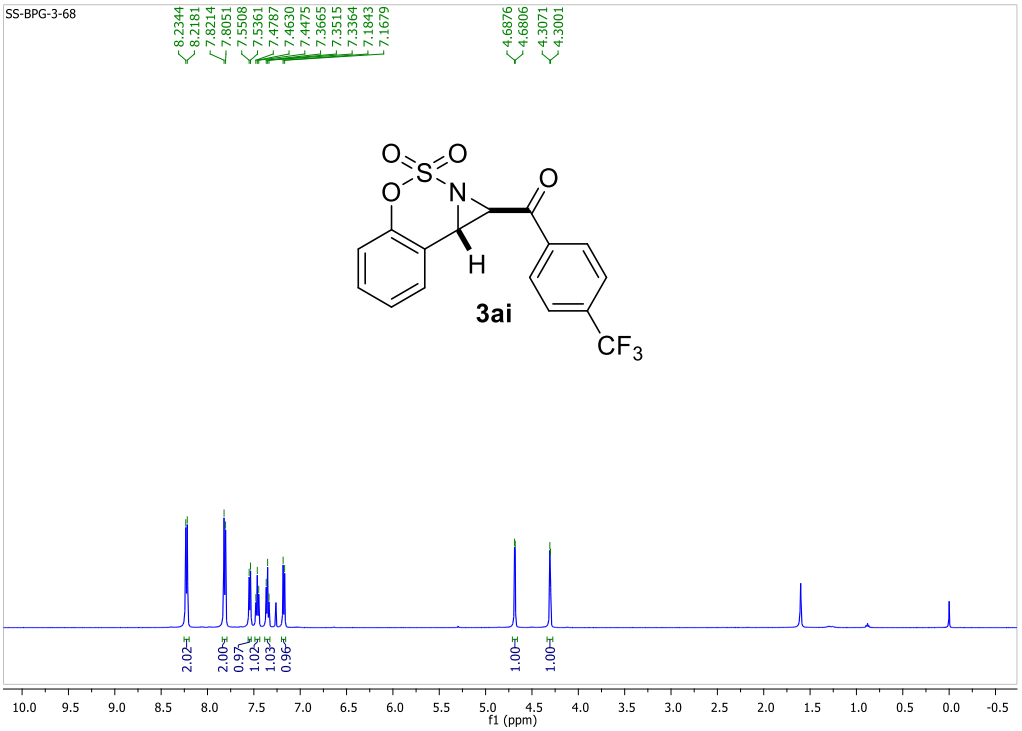

Figure 4.46 500 MHz ^{1}H NMR spectrum of **3ai** in $CDCl_3$.

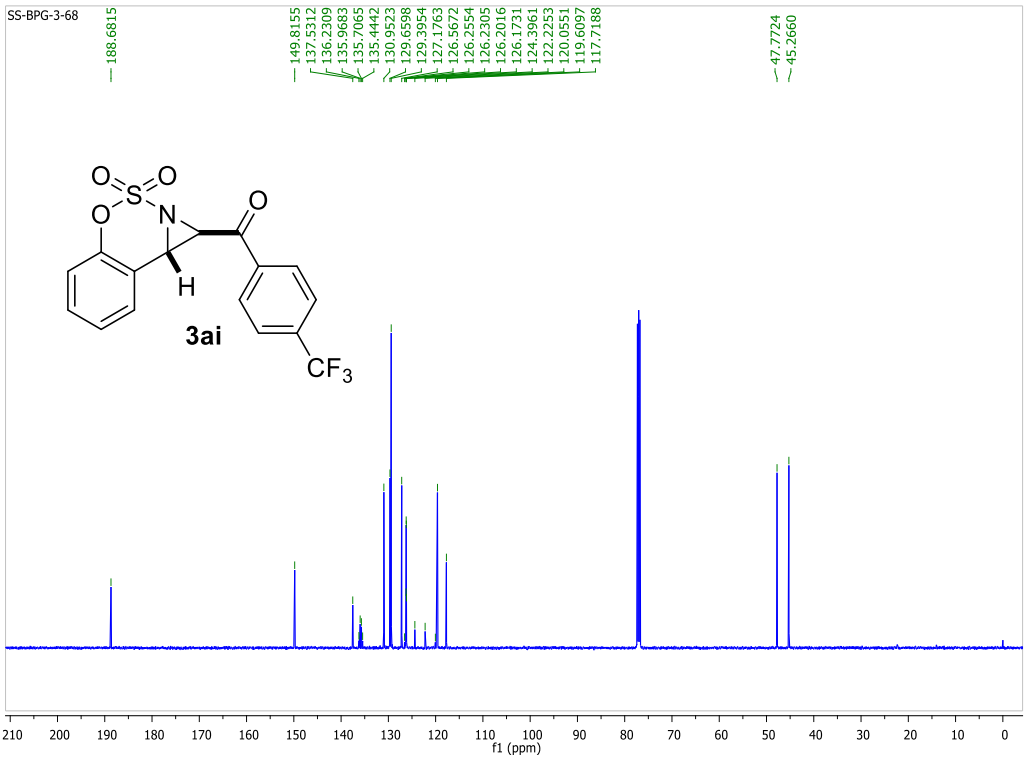

Figure 4.47 125 MHz ^{13}C NMR spectrum of **3ai** in $CDCl_3$.

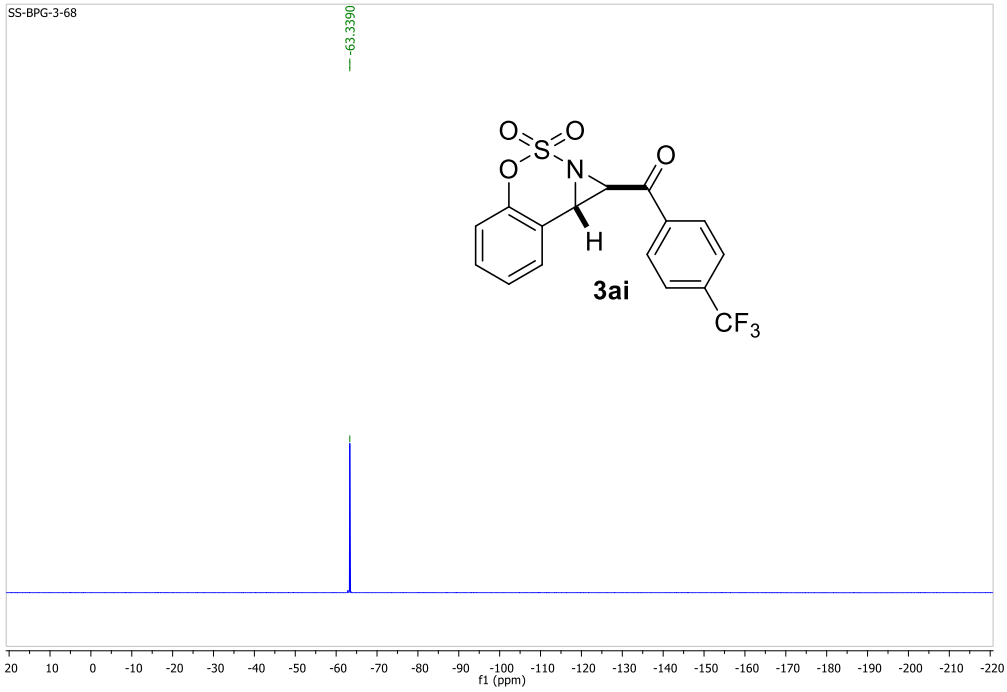

Figure 4.48 470 MHz ^{19}F NMR spectrum of **3ai** in $CDCl_3$.

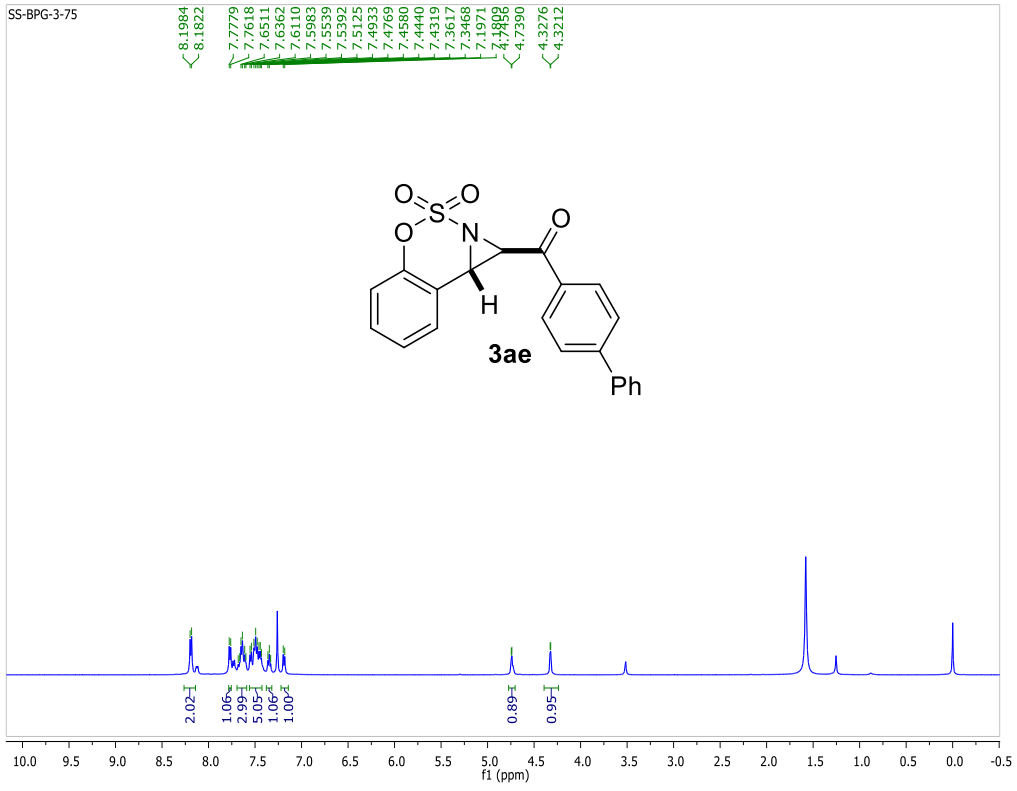

Figure 4.49 500 MHz ^{1}H NMR spectrum of **3ae** in $CDCl_3$.

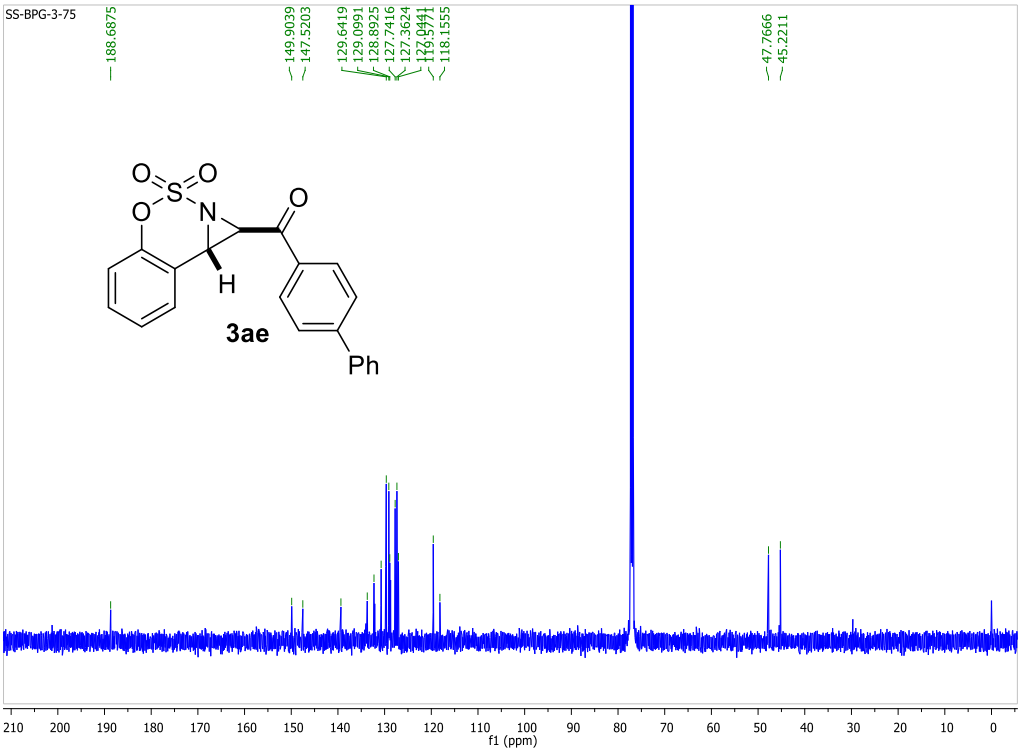

Figure 4.50 125 MHz ^{13}C NMR spectrum of **3ae** in $CDCl_3$.

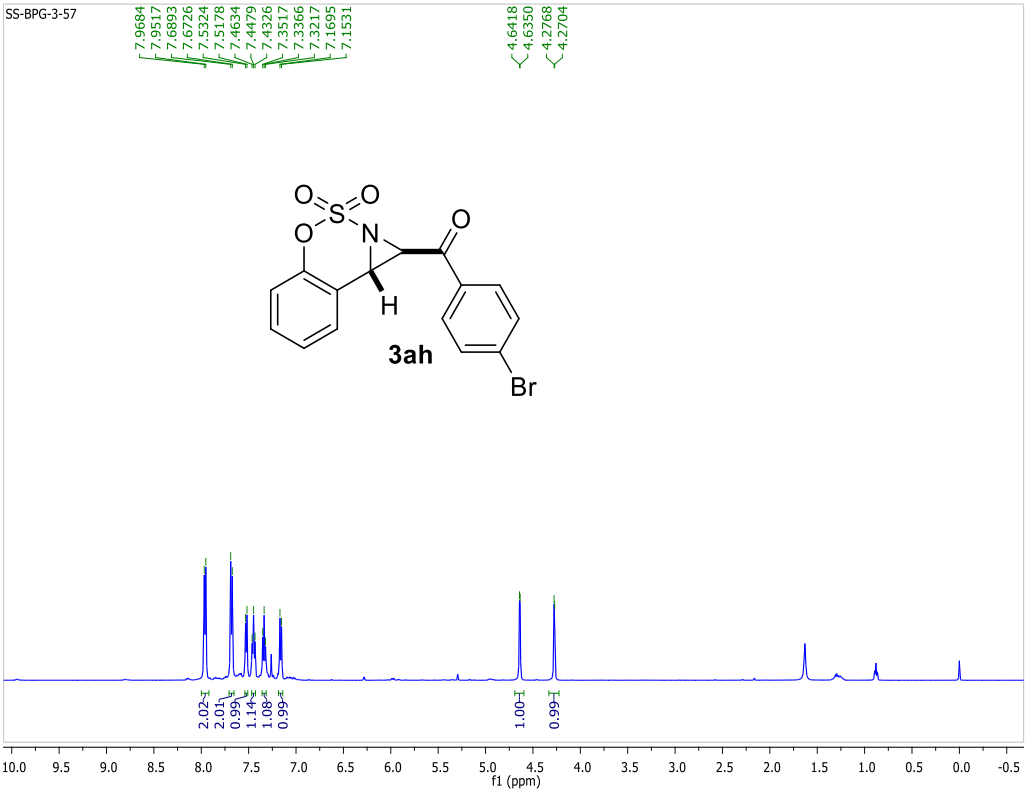

Figure 4.51 500 MHz ^{1}H NMR spectrum of **3ah** in $CDCl_3$.

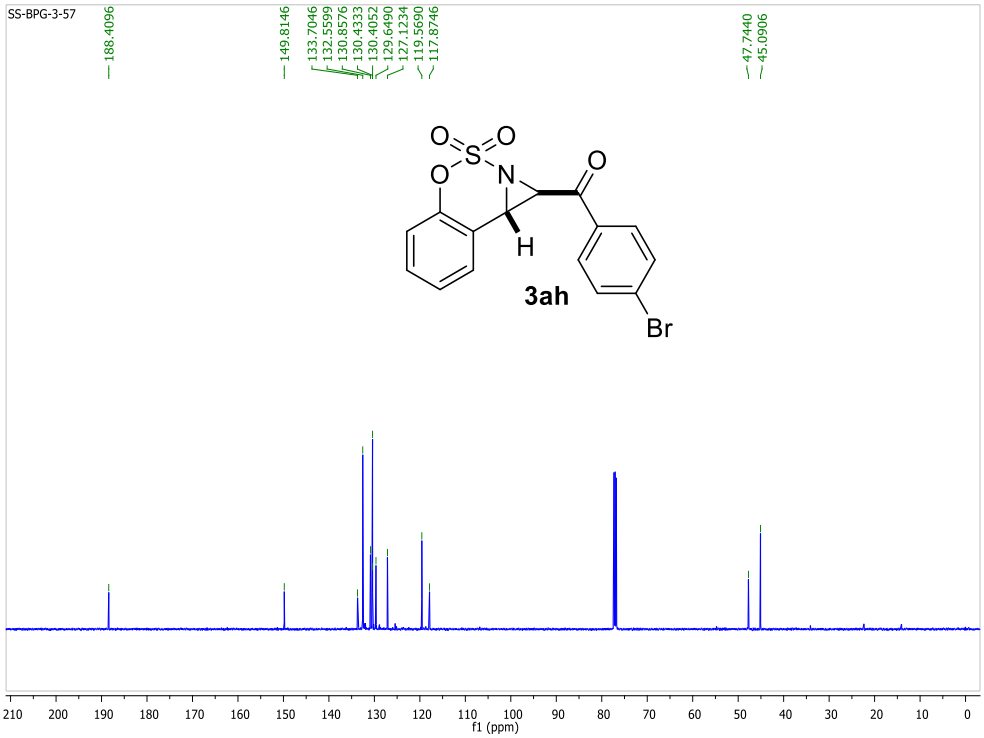

Figure 4.52 125 MHz ^{13}C NMR spectrum of **3ah** in $CDCl_3$.

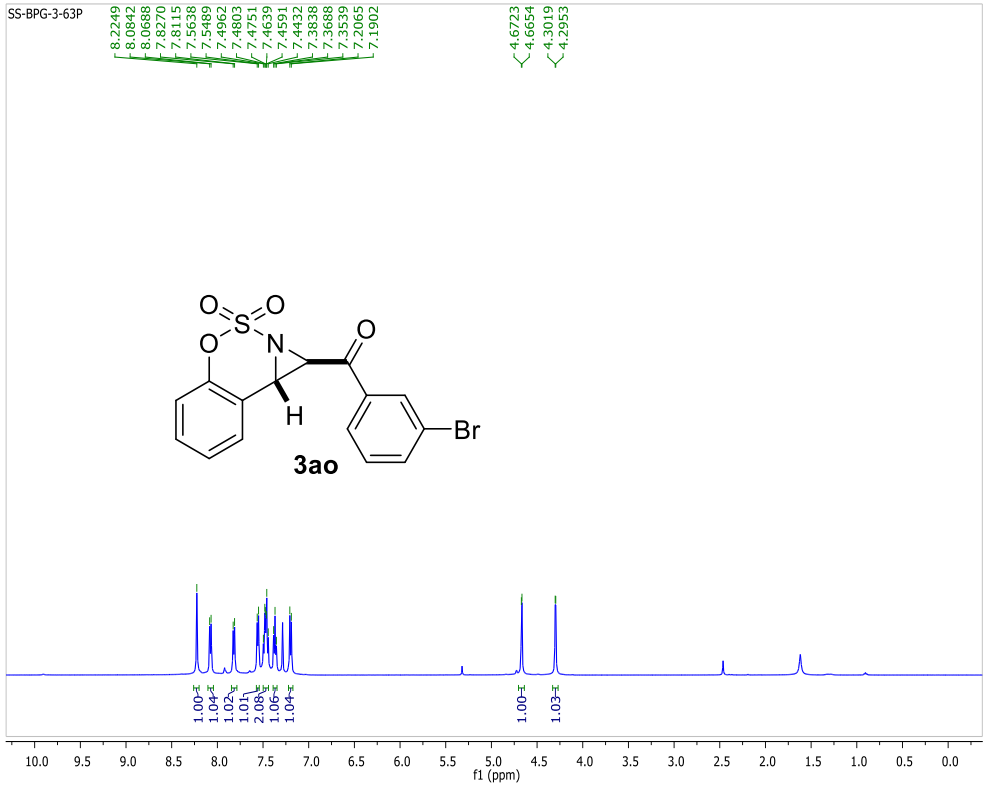

Figure 4.53 500 MHz ^{1}H NMR spectrum of **3ao** in $CDCl_3$.

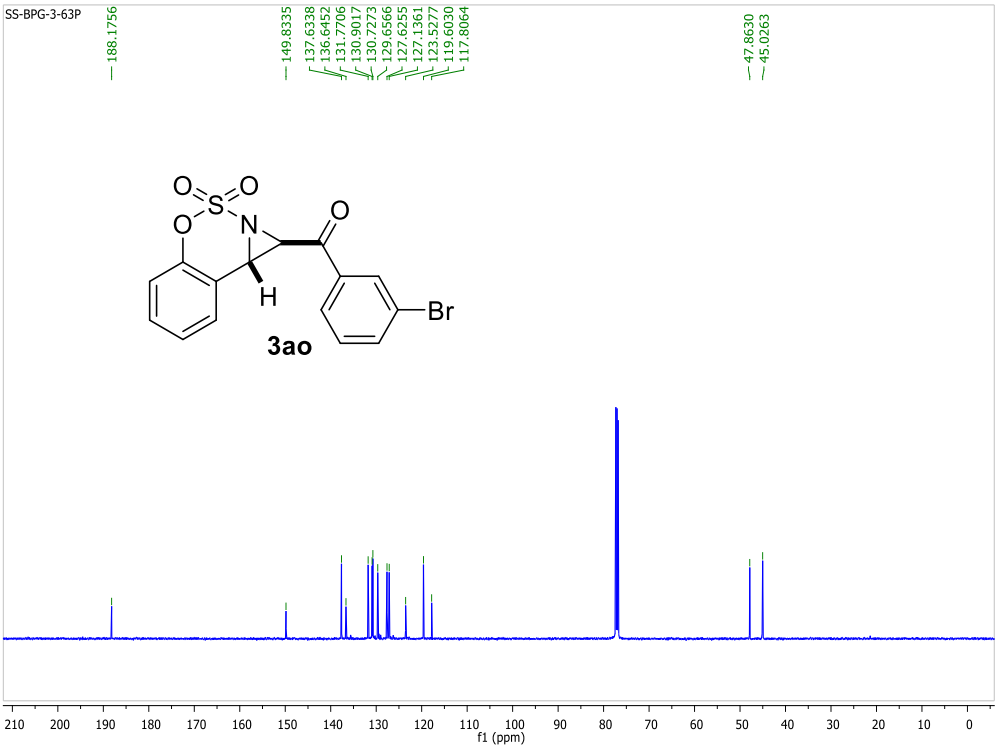

Figure 4.54 125 MHz ^{13}C NMR spectrum of **3ao** in $CDCl_3$.

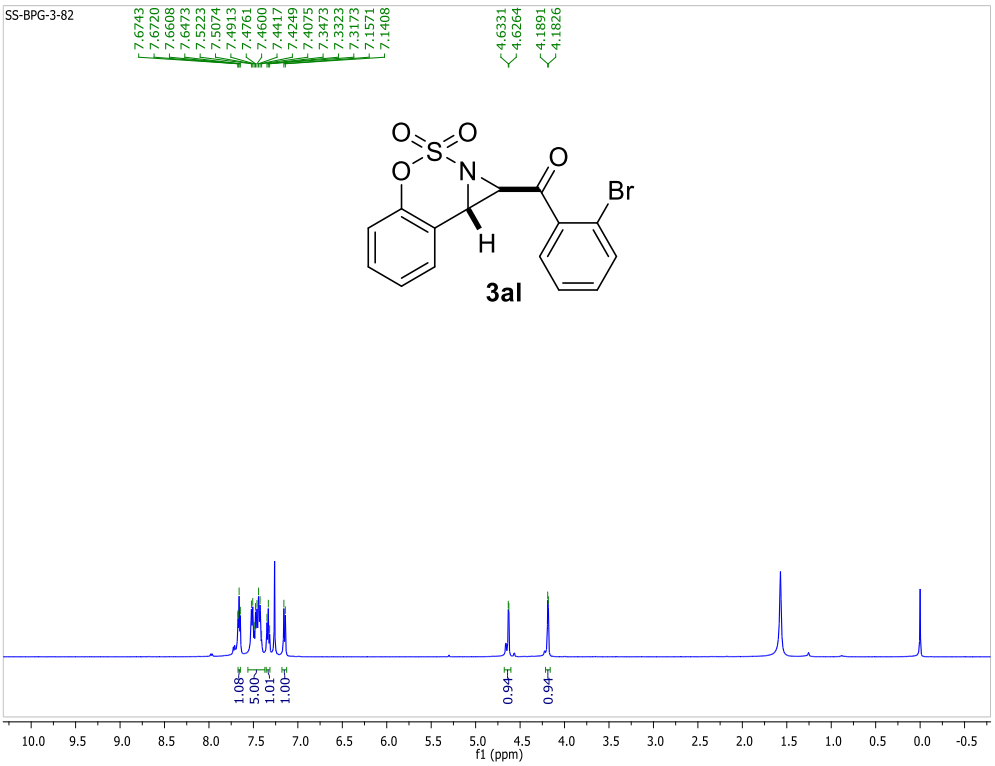

Figure 4.55 500 MHz ^{1}H NMR spectrum of **3al** in $CDCl_3$.

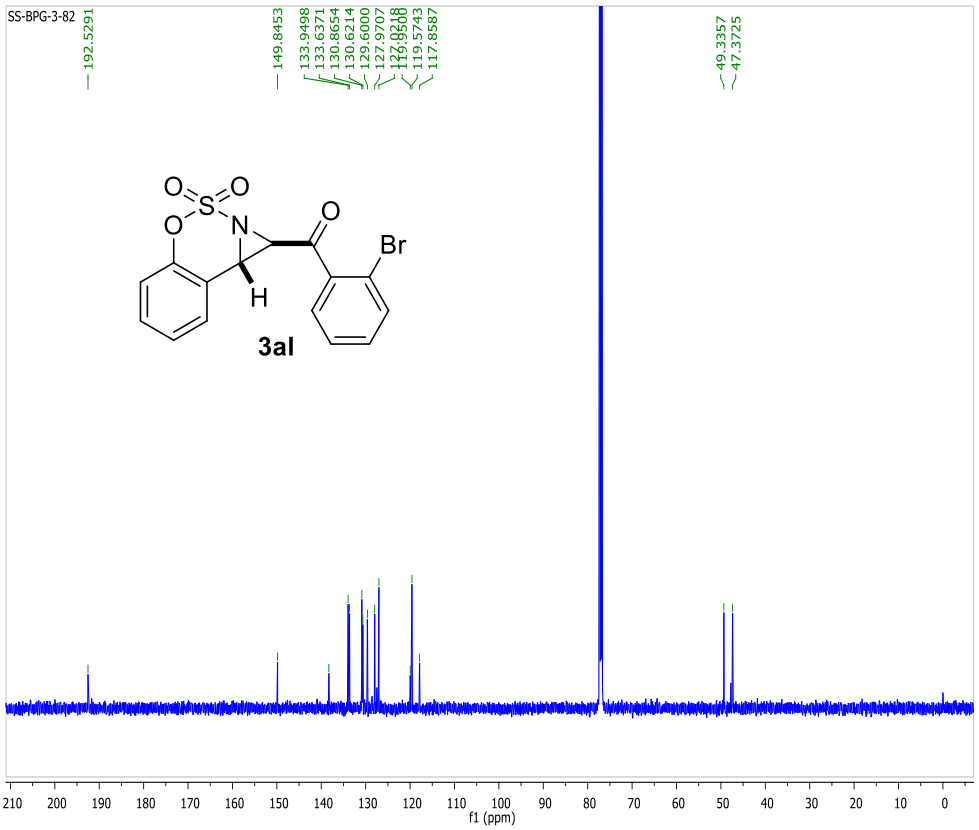

Figure 4.56 125 MHz ^{13}C NMR spectrum of **3al** in $CDCl_3$.

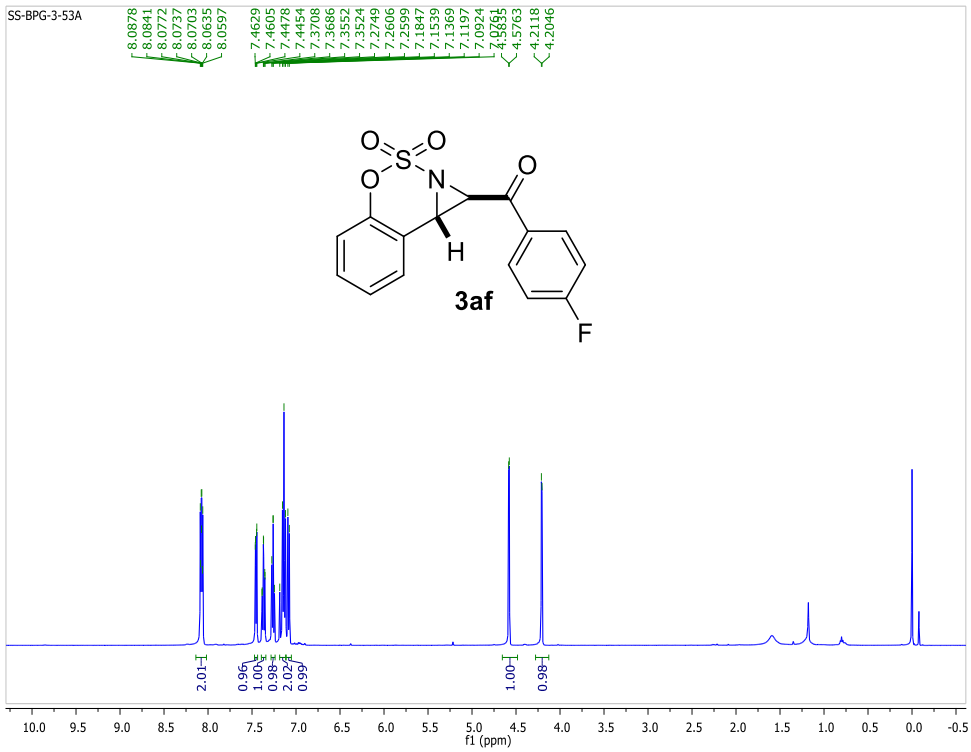

Figure 4.57 500 MHz ^{1}H NMR spectrum of **3af** in $CDCl_3$.

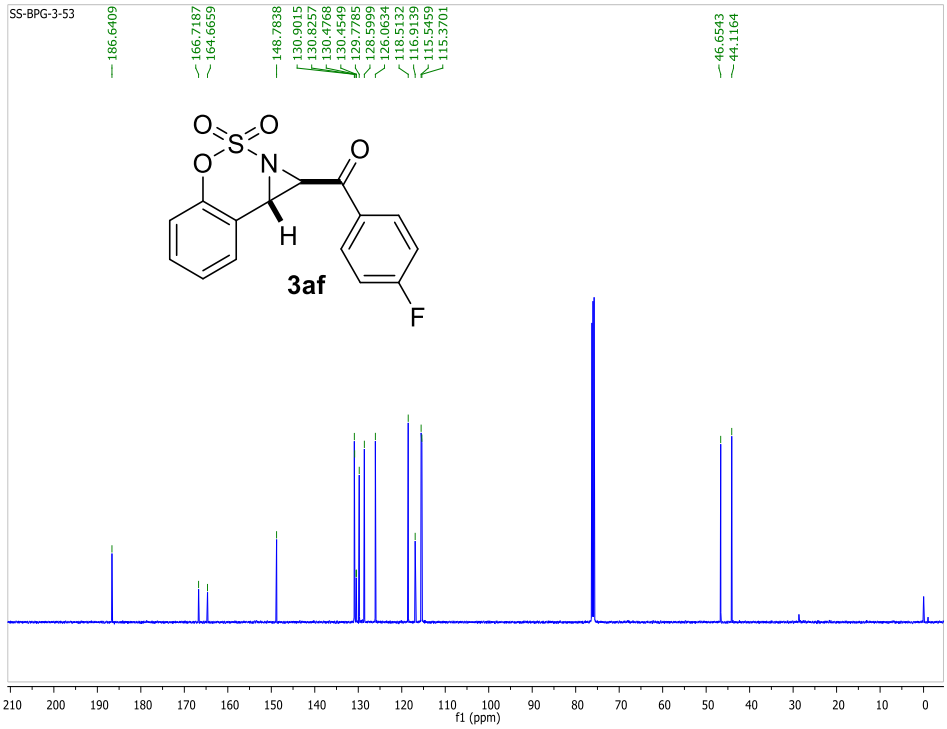

Figure 4.58 125 MHz ^{13}C NMR spectrum of **3af** in $CDCl_3$.

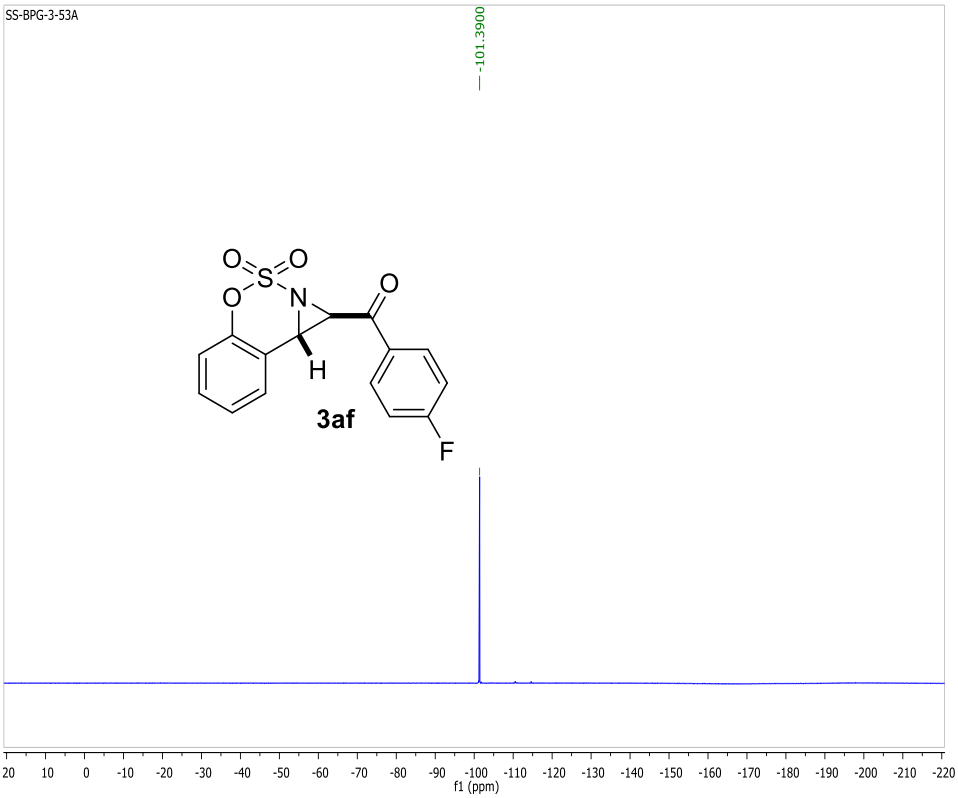

Figure 4.59 470 MHz ^{19}F NMR spectrum of **3af** in $CDCl_3$.

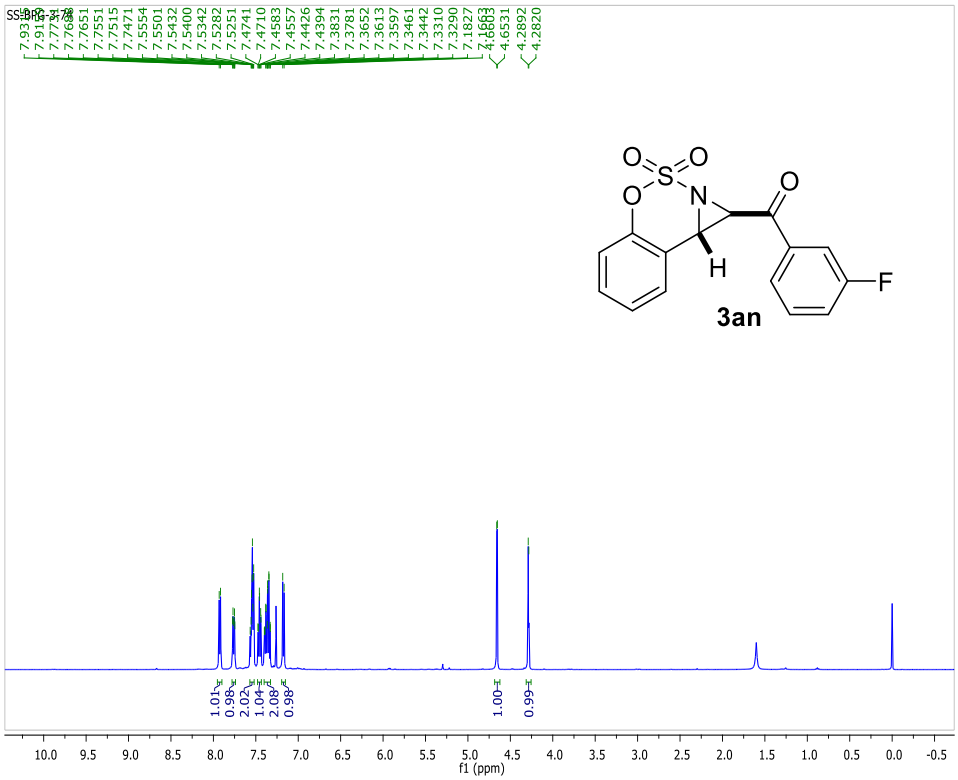

Figure 4.60 500 MHz ^{1}H NMR spectrum of **3an** in $CDCl_3$.

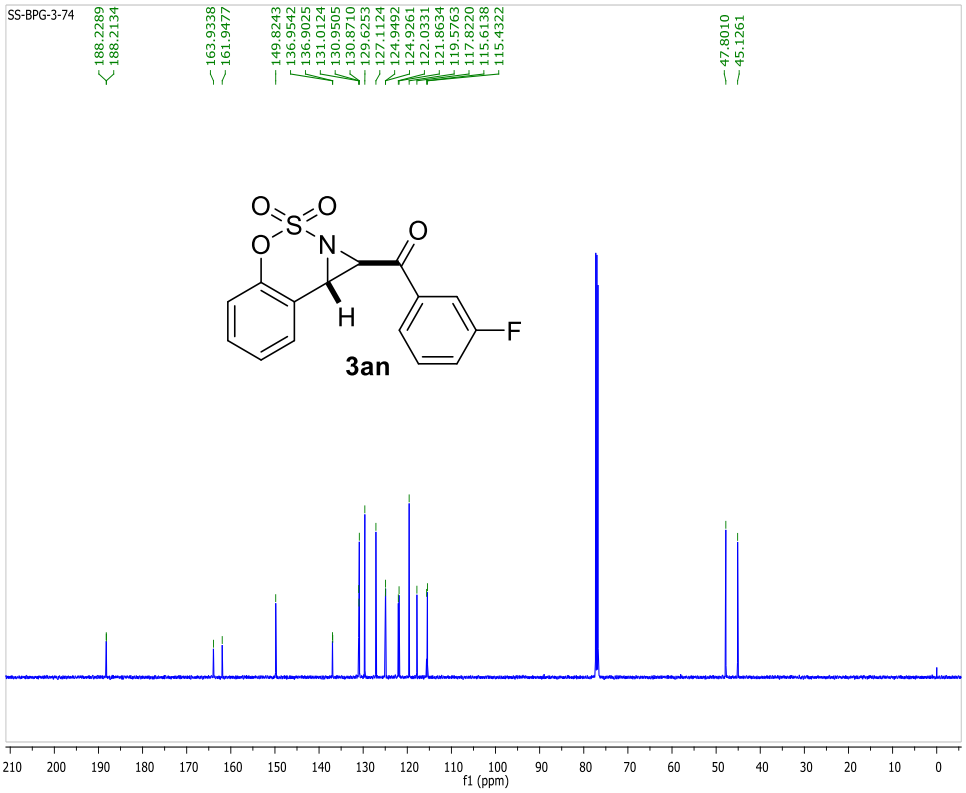

Figure 4.61 125 MHz ^{13}C NMR spectrum of **3an** in $CDCl_3$.

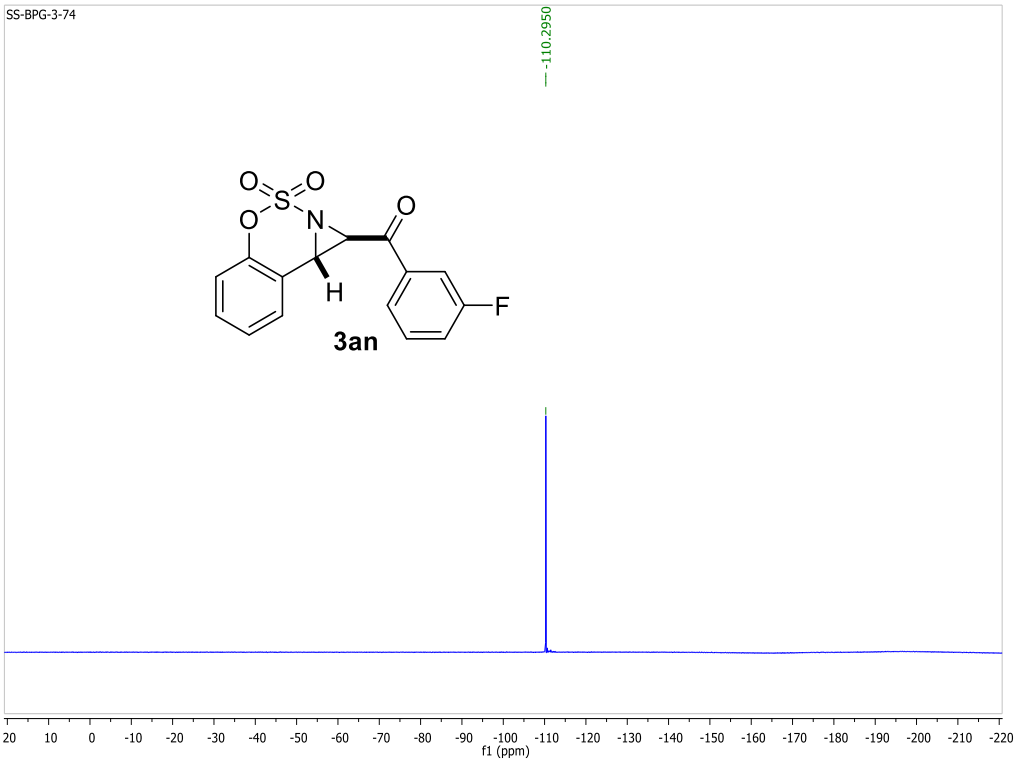

Figure 4.62 470 MHz ^{19}F NMR spectrum of **3an** in $CDCl_3$.

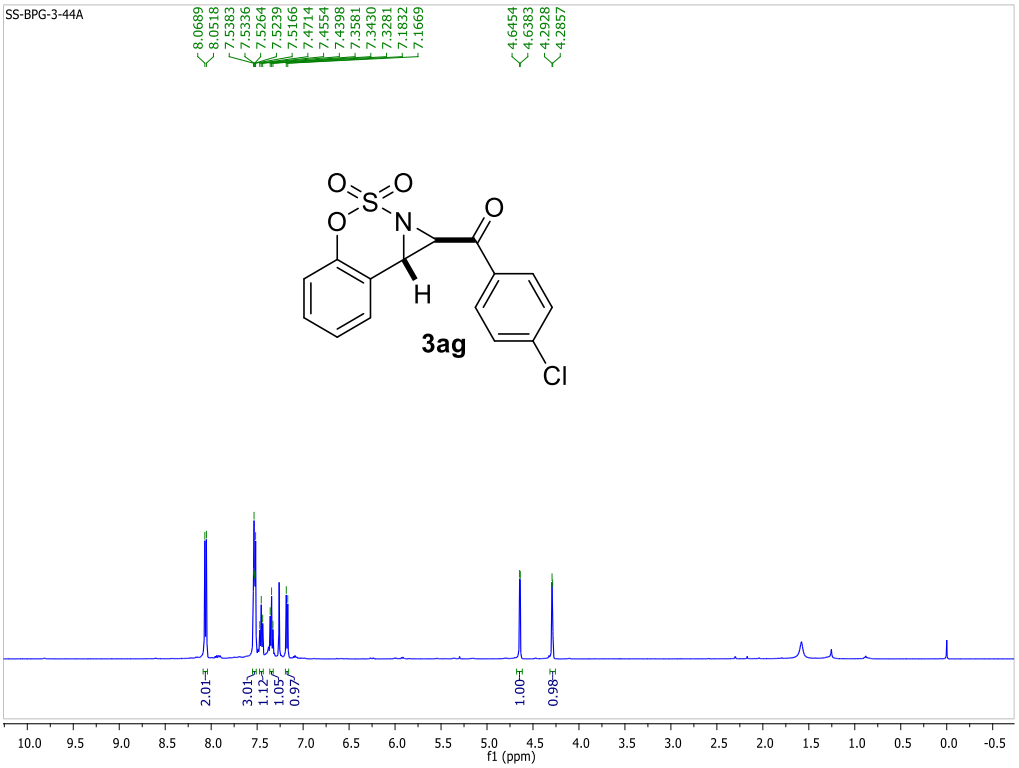

Figure 4.63 500 MHz ^{1}H NMR spectrum of **3ag** in $CDCl_3$.

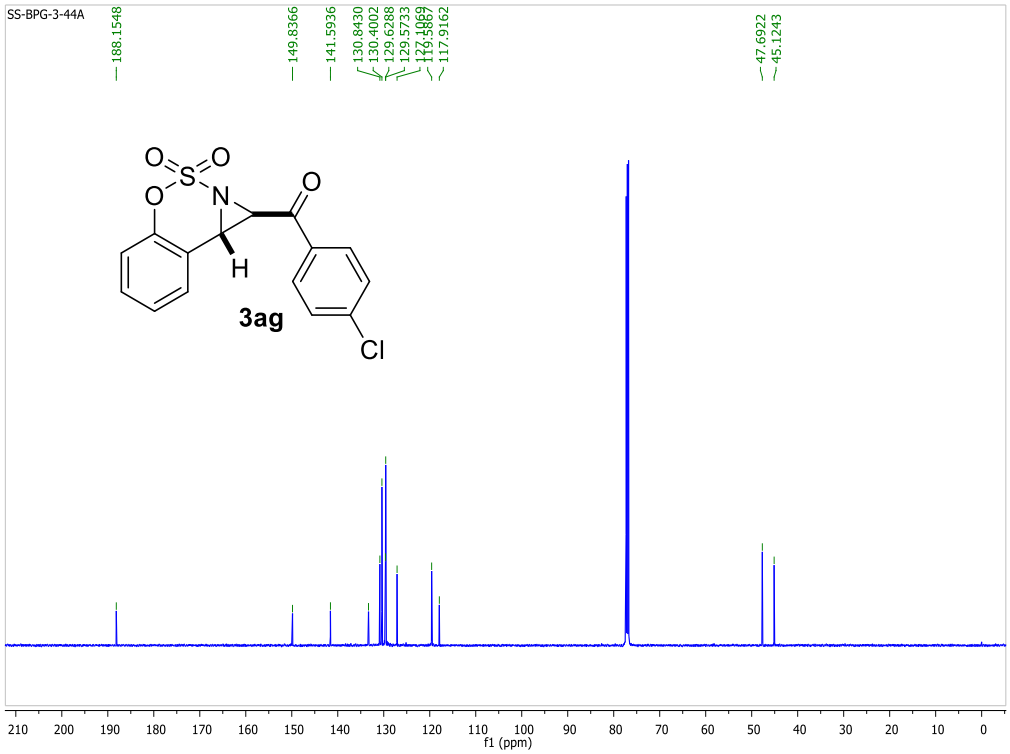

Figure 4.64 125 MHz ^{13}C NMR spectrum of **3ag** in $CDCl_3$.

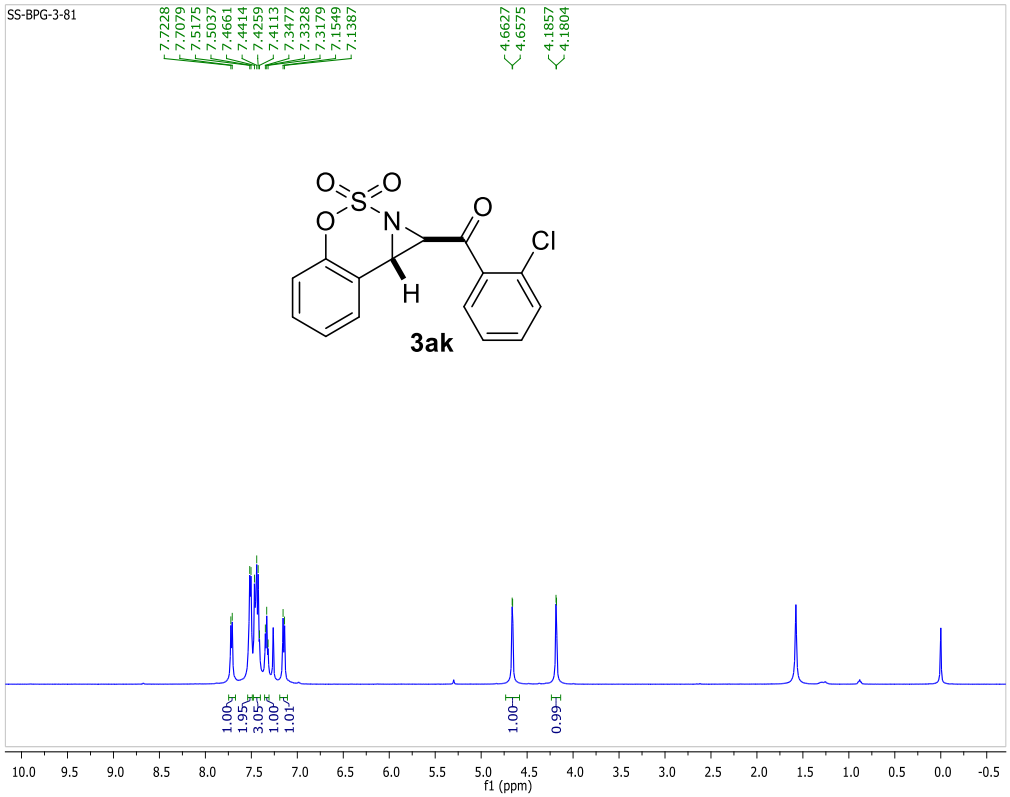

Figure 4.65 500 MHz ^{1}H NMR spectrum of **3ak** in $CDCl_3$.

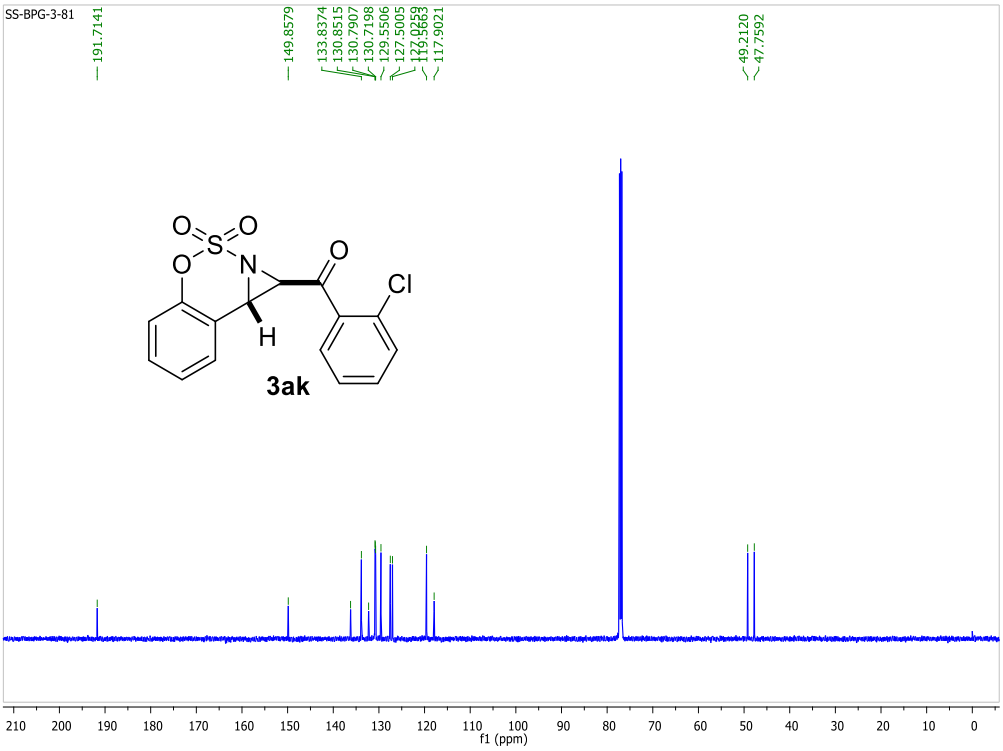

Figure 4.66 125 MHz ^{13}C NMR spectrum of **3ak** in $CDCl_3$.

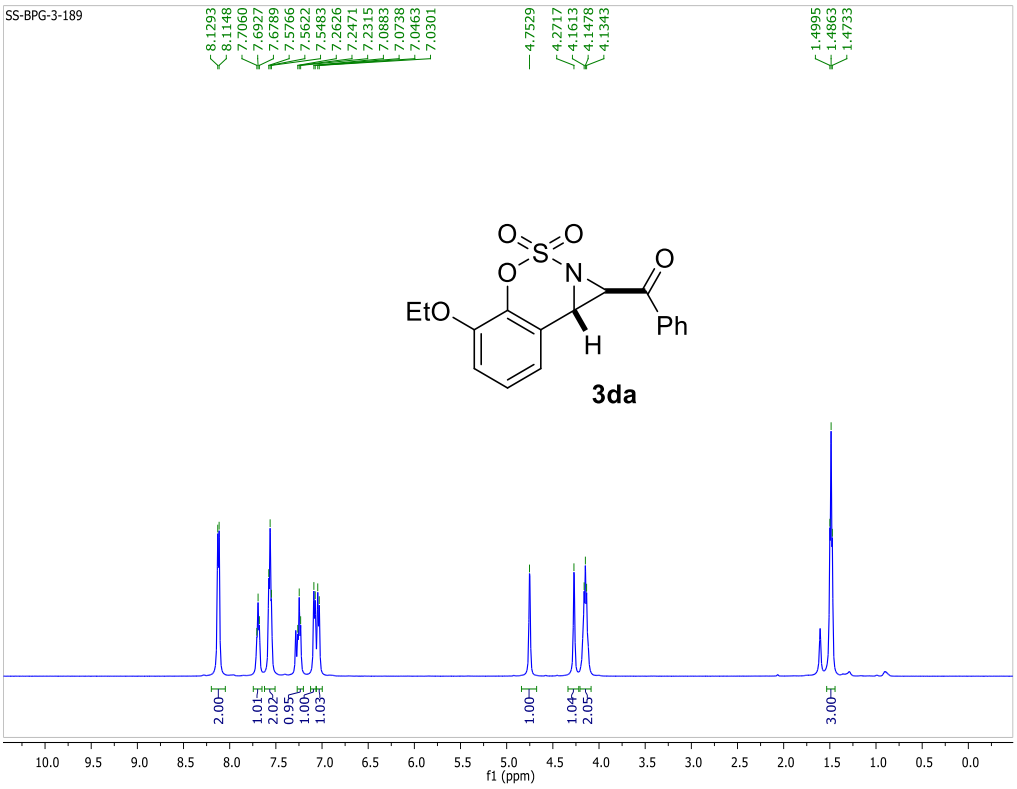

Figure 4.67 500 MHz ^{1}H NMR spectrum of **3da** in $CDCl_3$.

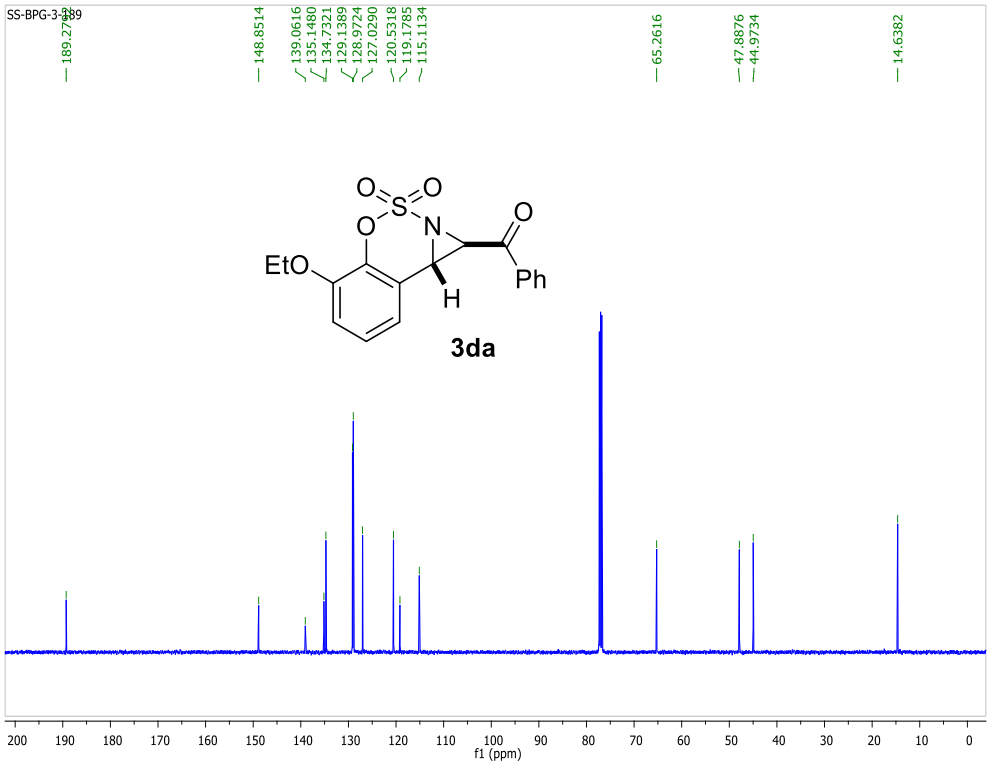

Figure 4.68 125 MHz ^{13}C NMR spectrum of **3da** in $CDCl_3$.

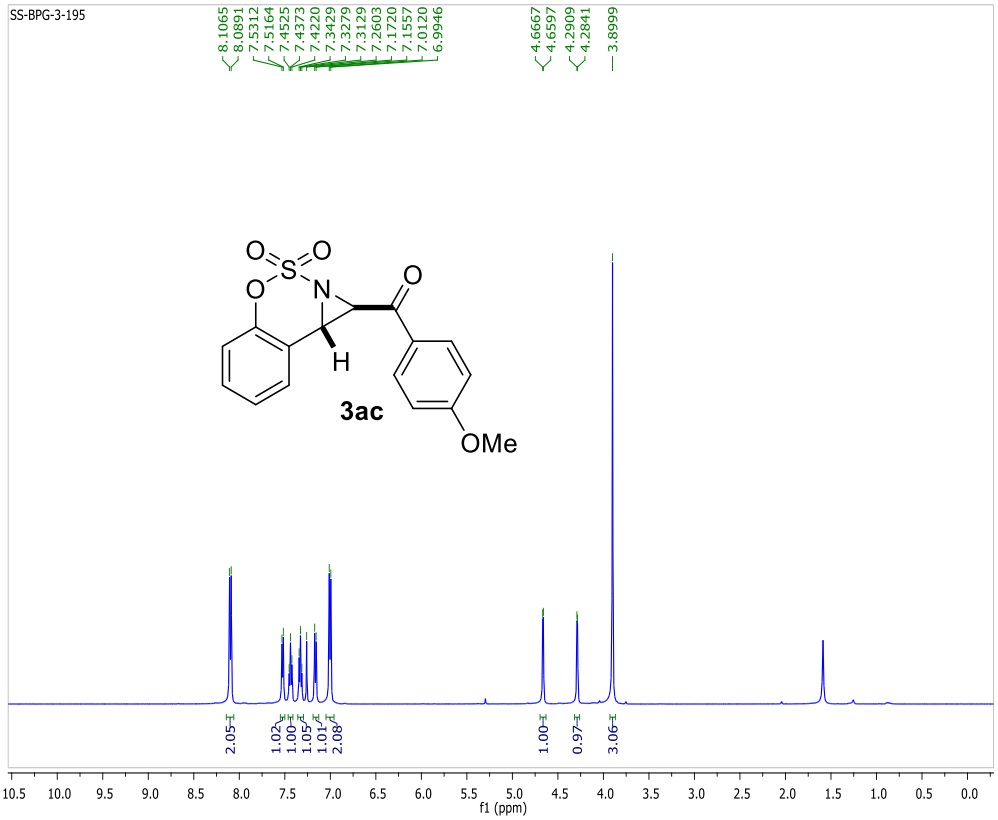

Figure 4.69 500 MHz ^{1}H NMR spectrum of **3ac** in $CDCl_3$.

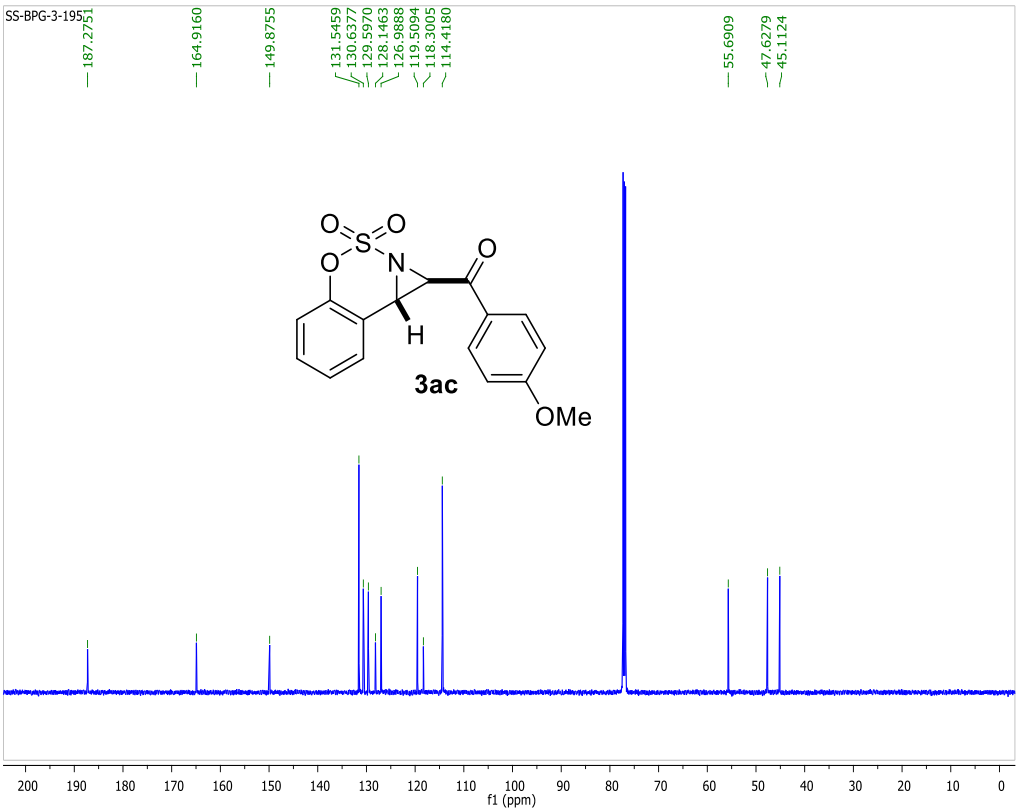

Figure 4.70 125 MHz ^{13}C NMR spectrum of **3ac** in $CDCl_3$.

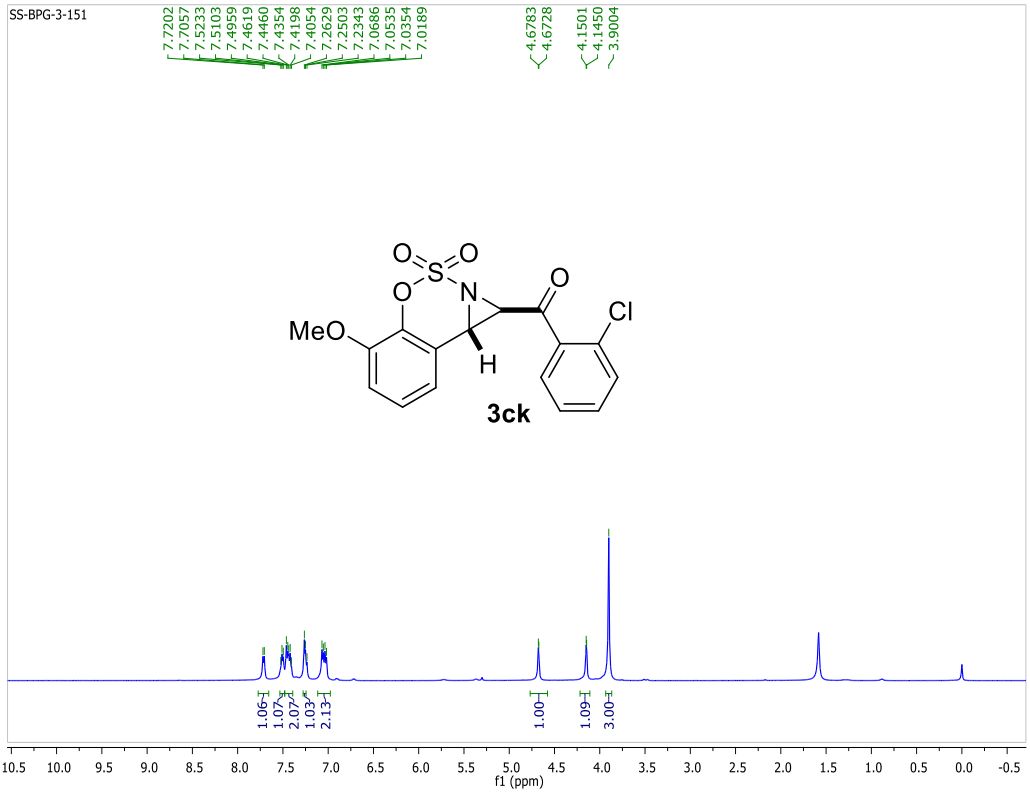

Figure 4.71 500 MHz ^{1}H NMR spectrum of **3ck** in $CDCl_3$.

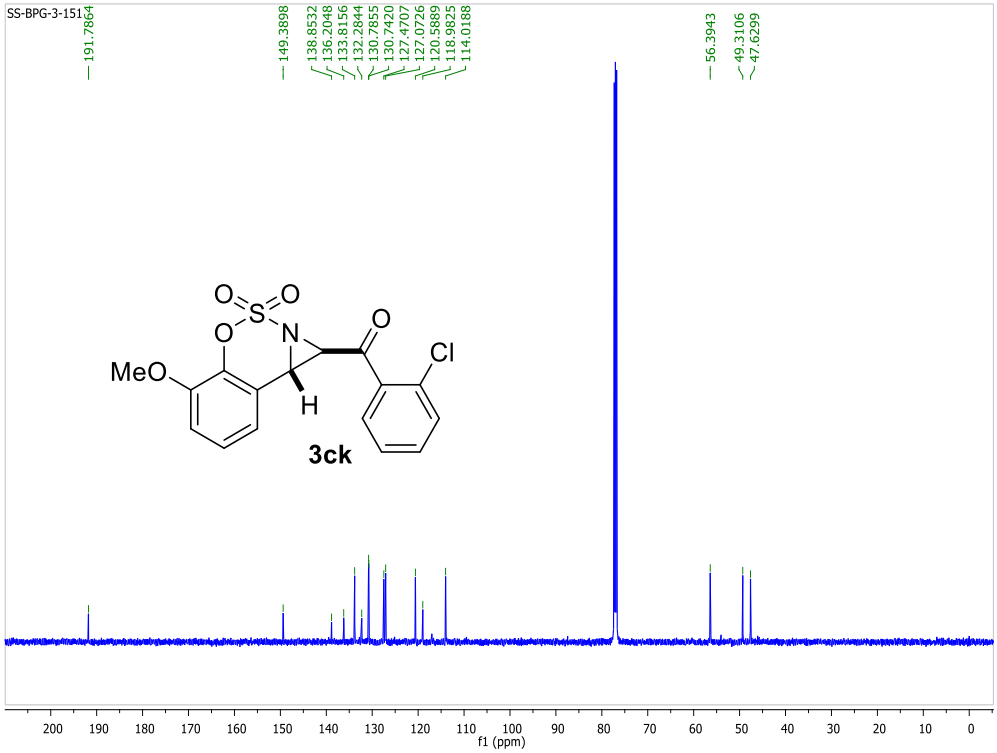

Figure 4.72 125 MHz ^{13}C NMR spectrum of **3ck** in $CDCl_3$.

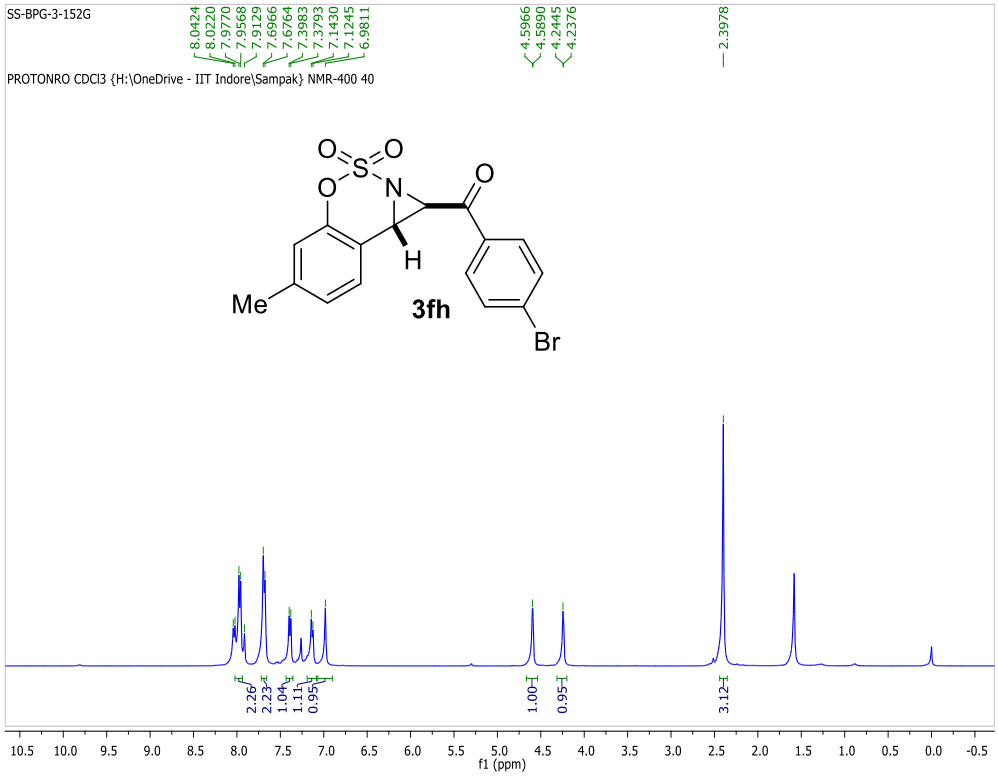

Figure 4.73 400 MHz ^{1}H NMR spectrum of **3fh** in $CDCl_3$.

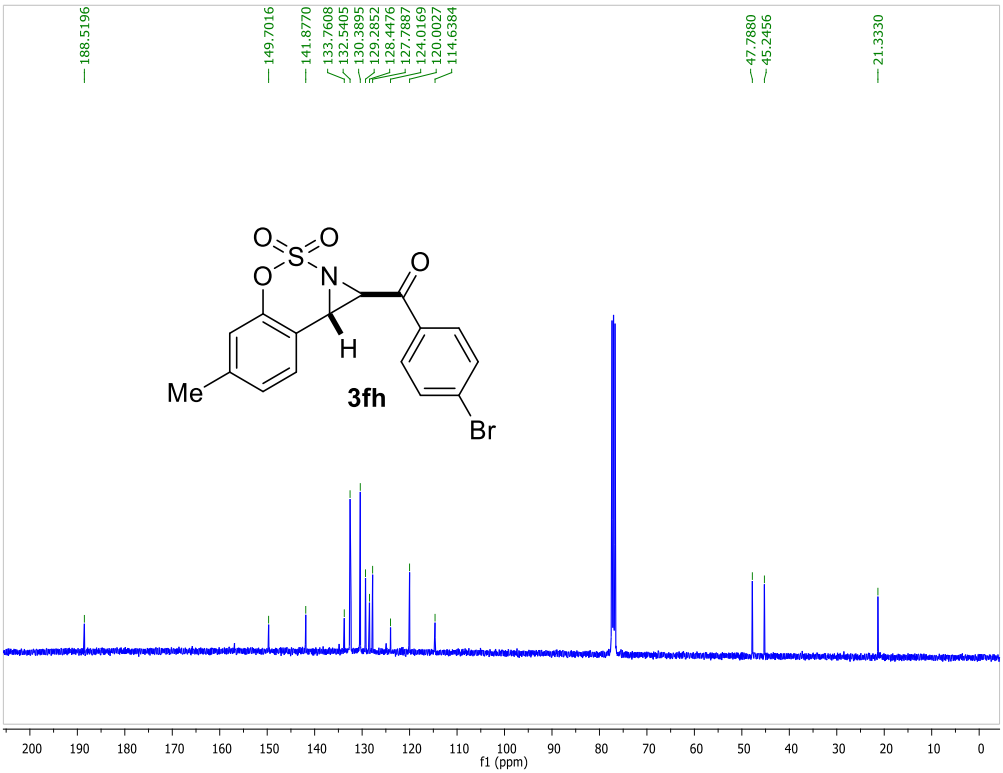

Figure 4.74 100 MHz ^{13}C NMR spectrum of **3fh** in $CDCl_3$.

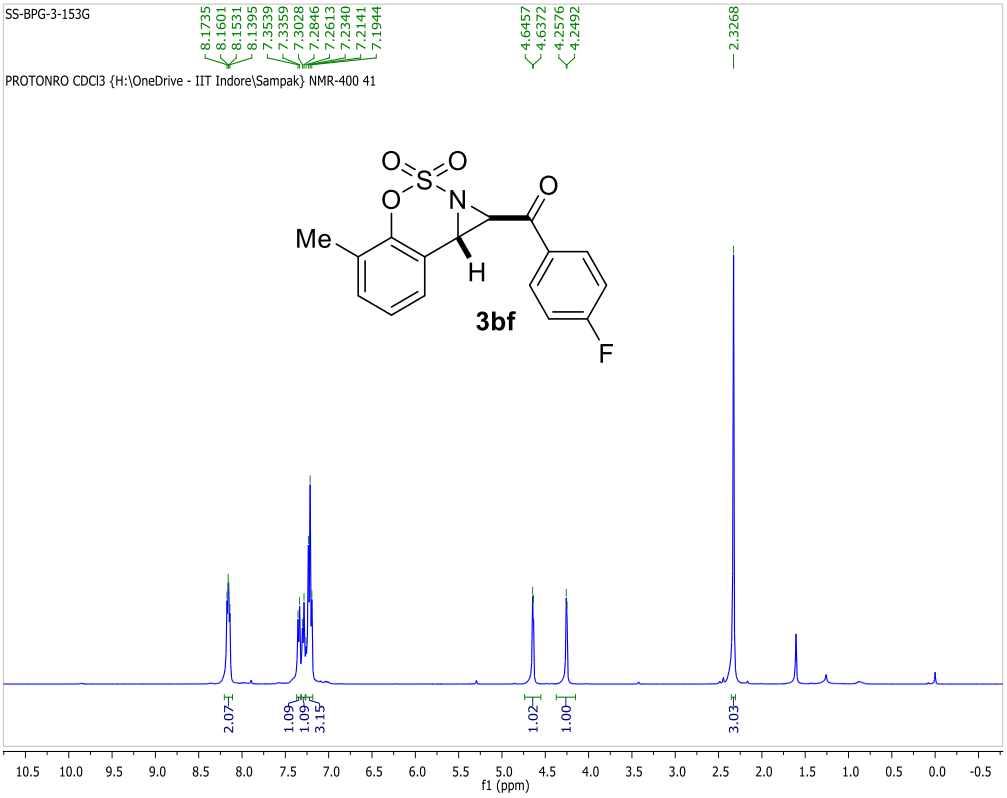

Figure 4.75 500 MHz ^{1}H NMR spectrum of **3bf** in $CDCl_3$.

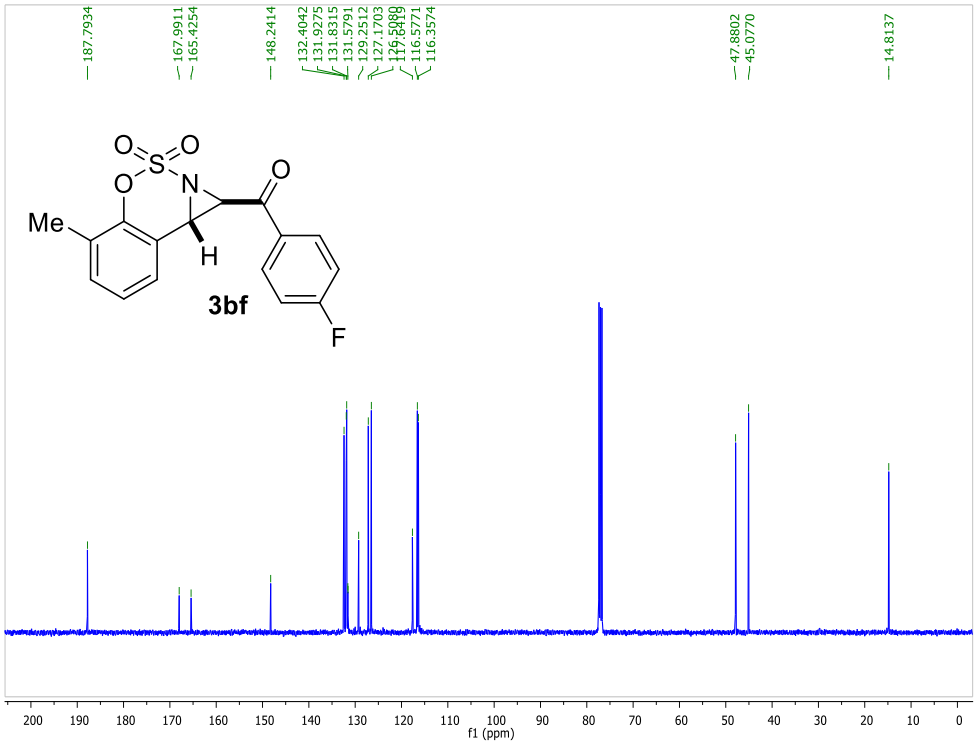

Figure 4.76 100 MHz ^{13}C NMR spectrum of **3bf** in $CDCl_3$.

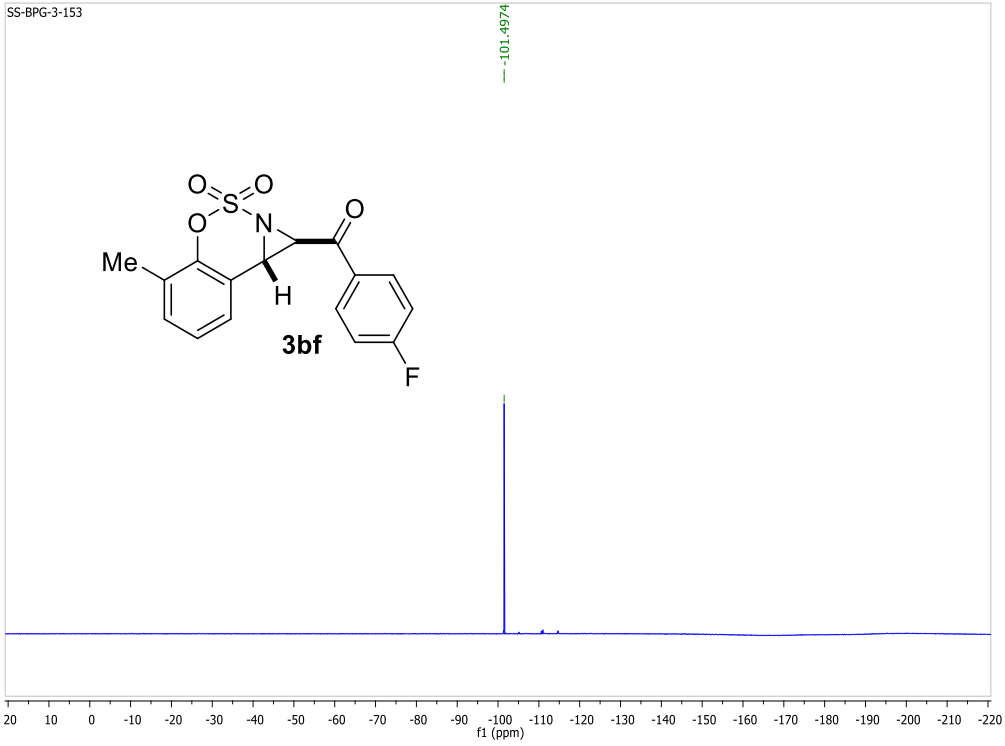

Figure 4.77 470 MHz ^{19}F NMR spectrum of **3bf** in $CDCl_3$.

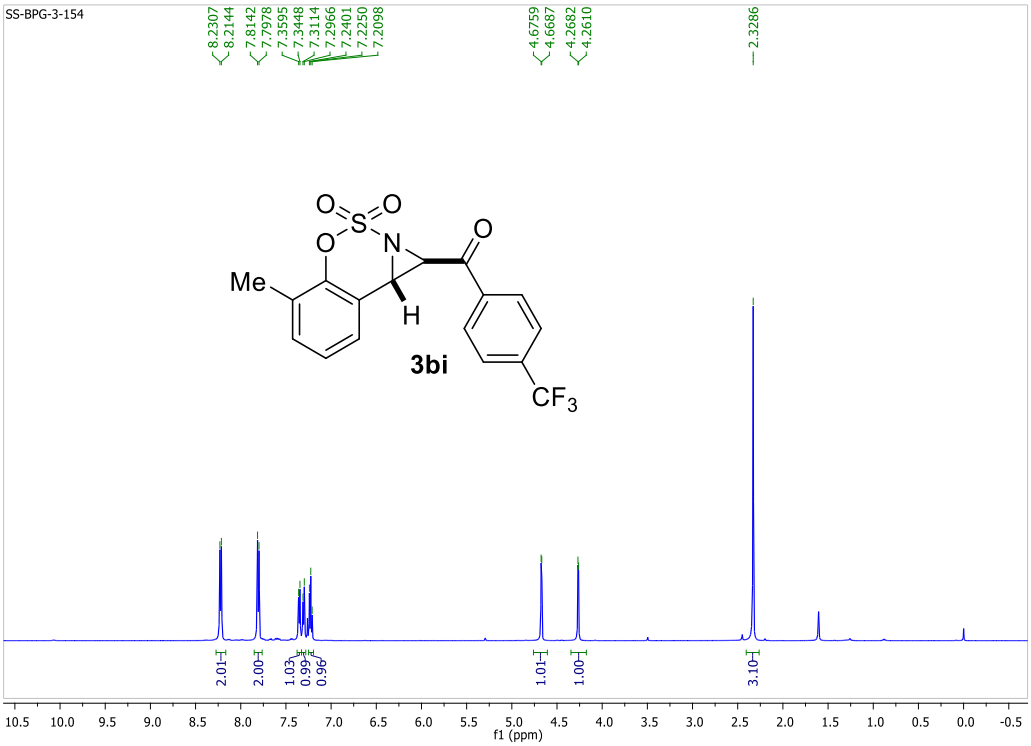

Figure 4.78 500 MHz ^{1}H NMR spectrum of **3bi** in $CDCl_3$.

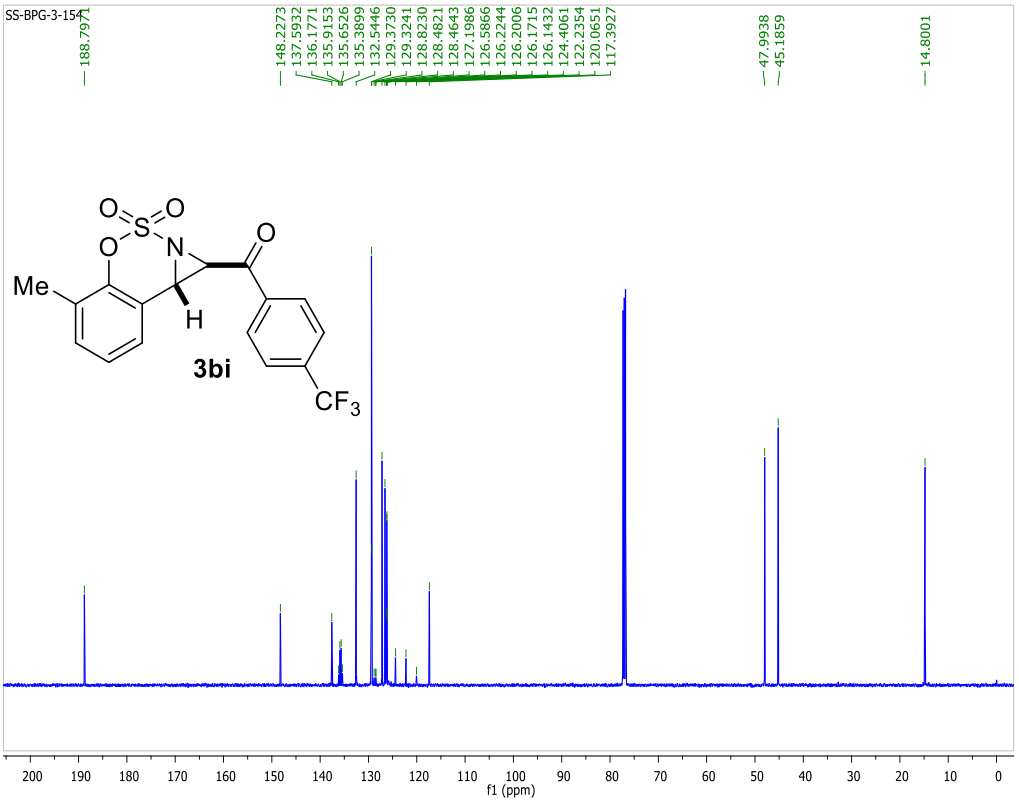

Figure 4.79 125 MHz ^{13}C NMR spectrum of **3bi** in $CDCl_3$.

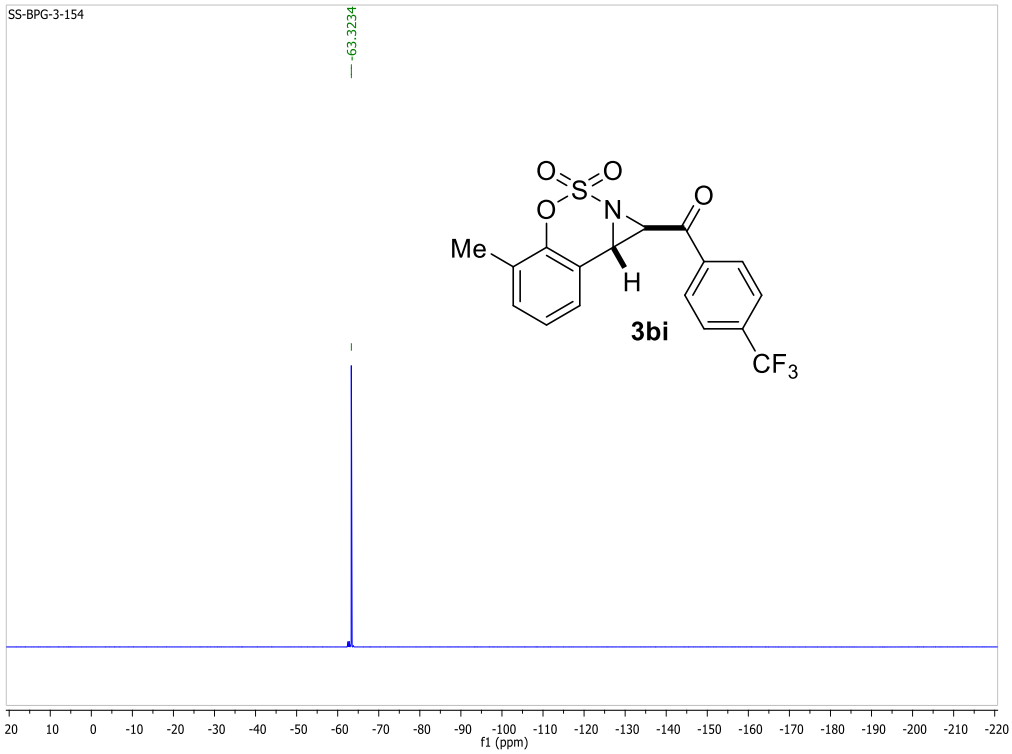

Figure 4.80 470 MHz ^{19}F NMR spectrum of **3bi** in $CDCl_3$.

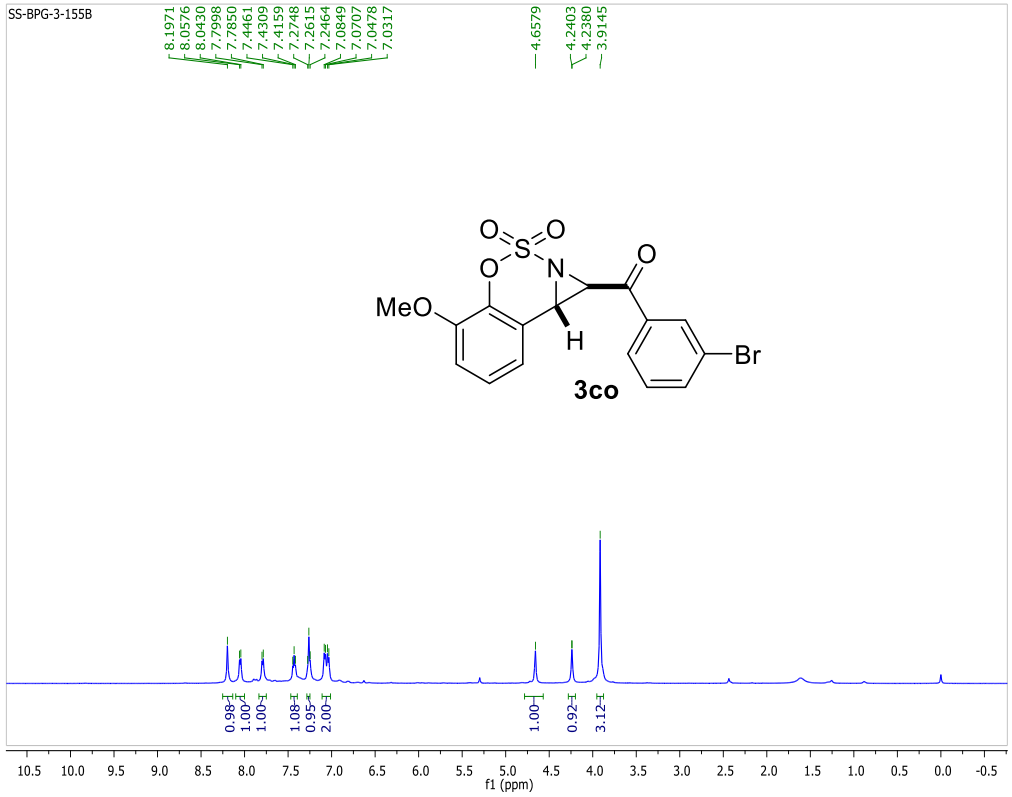

Figure 4.81 500 MHz ^{1}H NMR spectrum of **3co** in $CDCl_3$.

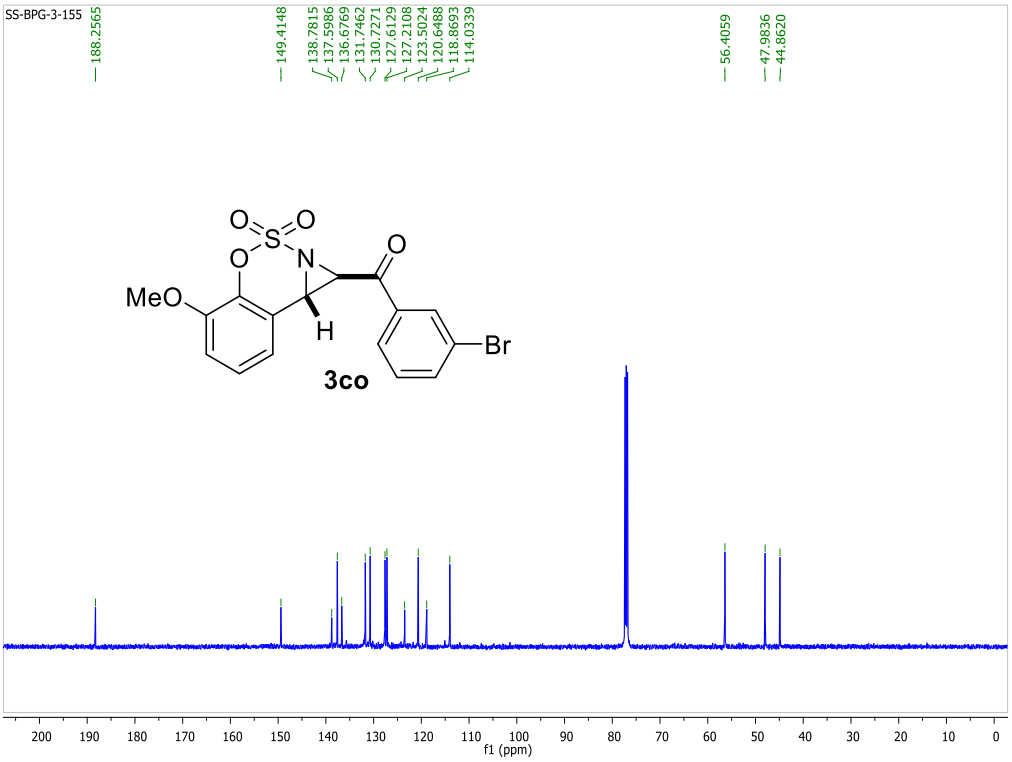

Figure 4.82 125 MHz ^{13}C NMR spectrum of **3co** in $CDCl_3$.

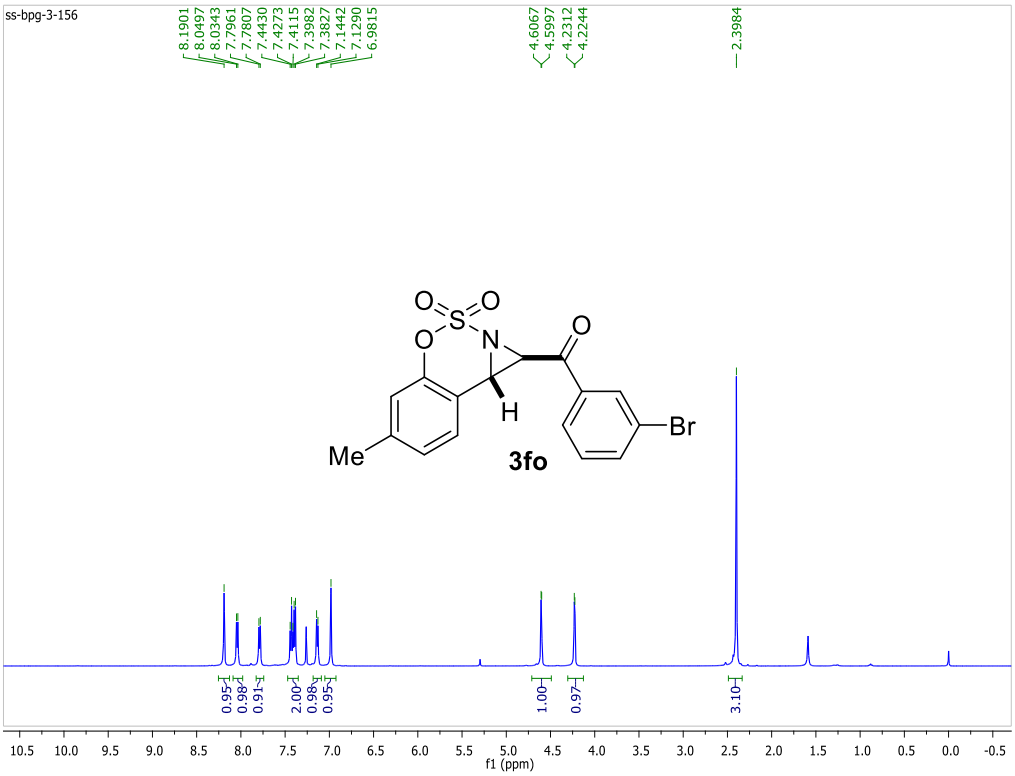

Figure 4.83 500 MHz ^{1}H NMR spectrum of **3fo** in $CDCl_3$.

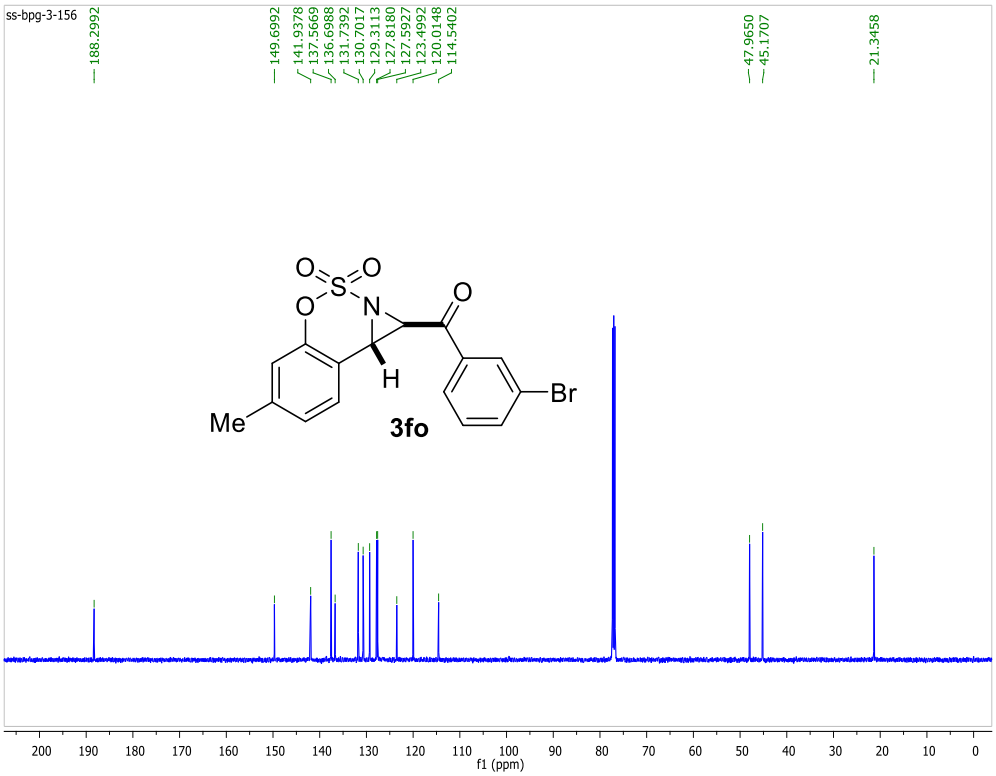

Figure 4.84 125 MHz ^{13}C NMR spectrum of **3fo** in $CDCl_3$.

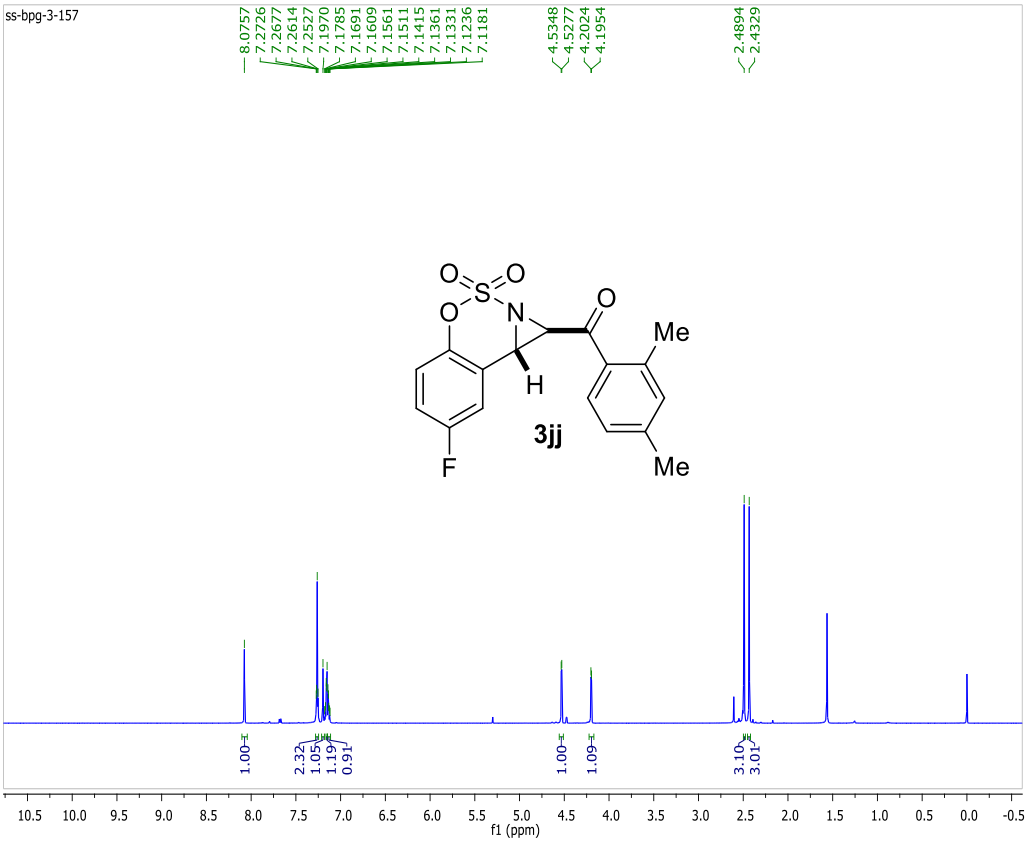

Figure 4.85 500 MHz ^{1}H NMR spectrum of **3jj** in $CDCl_3$.

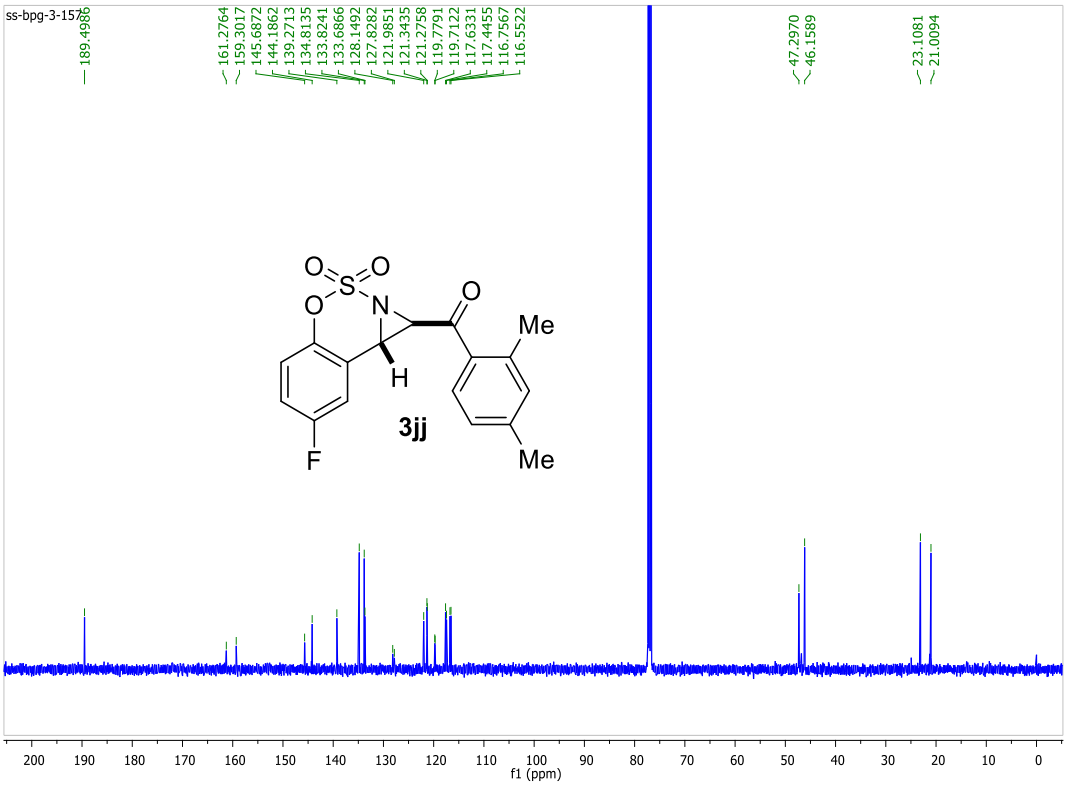

Figure 4.86 125 MHz ^{13}C NMR spectrum of **3jj** in $CDCl_3$.

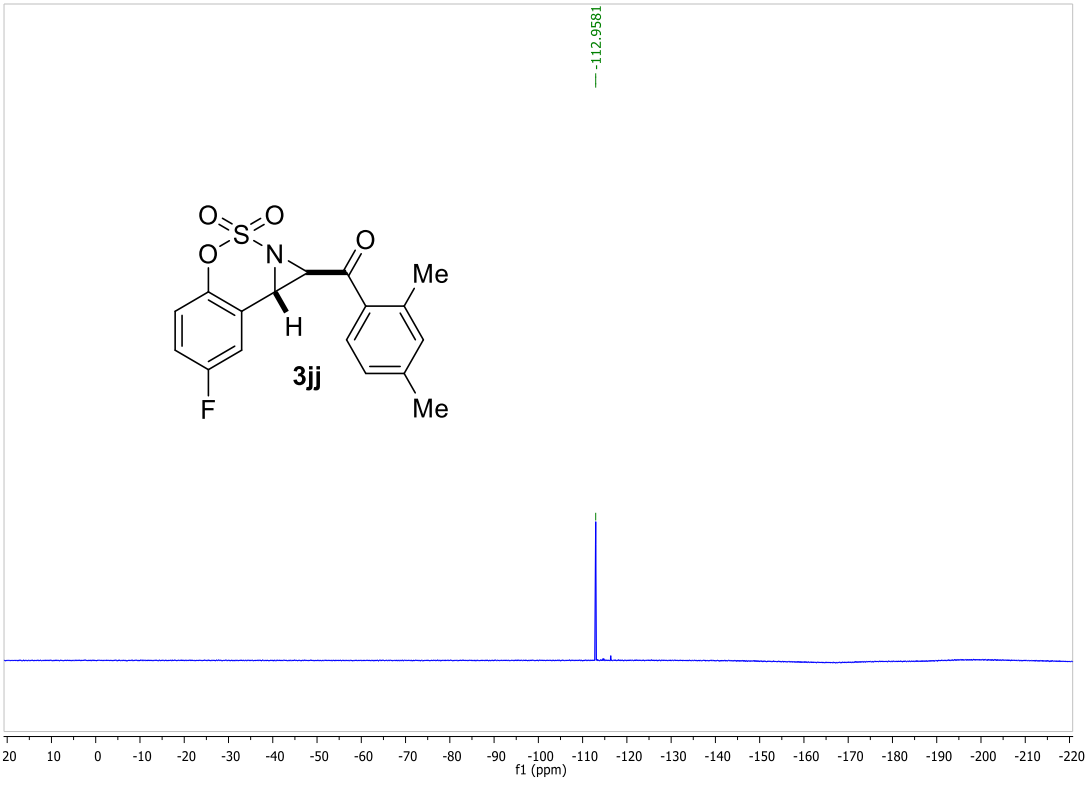

Figure 4.87 470 MHz ^{19}F NMR spectrum of **3jj** in $CDCl_3$.

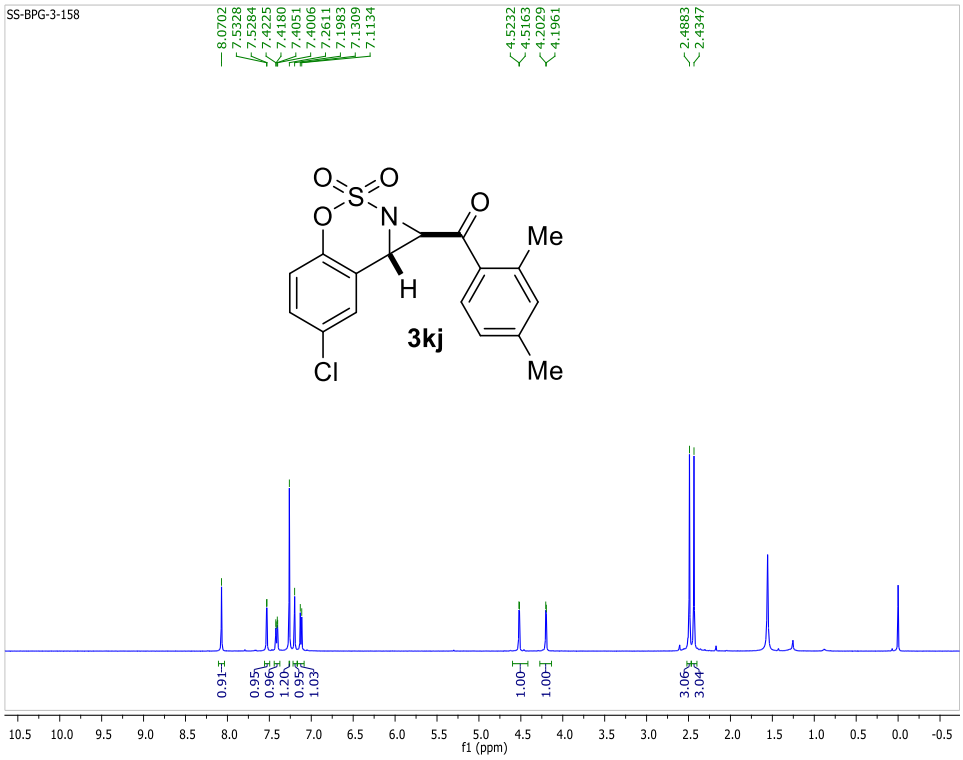

Figure 4.88 500 MHz ^{1}H NMR spectrum of **3kj** in $CDCl_3$.

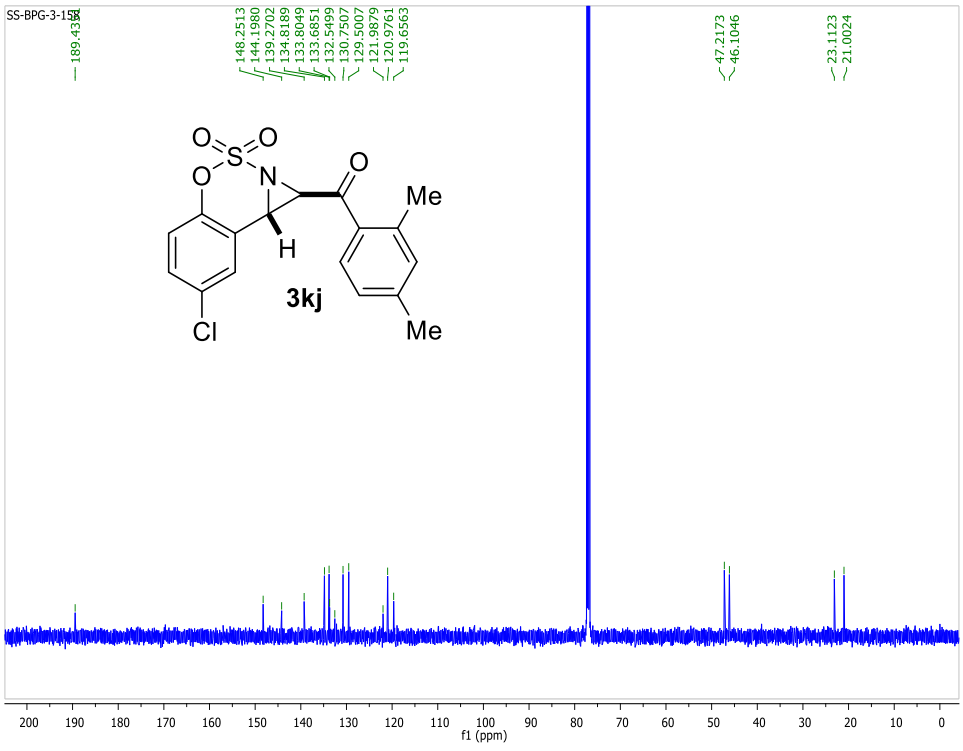

Figure 4.89 125 MHz ^{13}C NMR spectrum of **3kj** in $CDCl_3$.

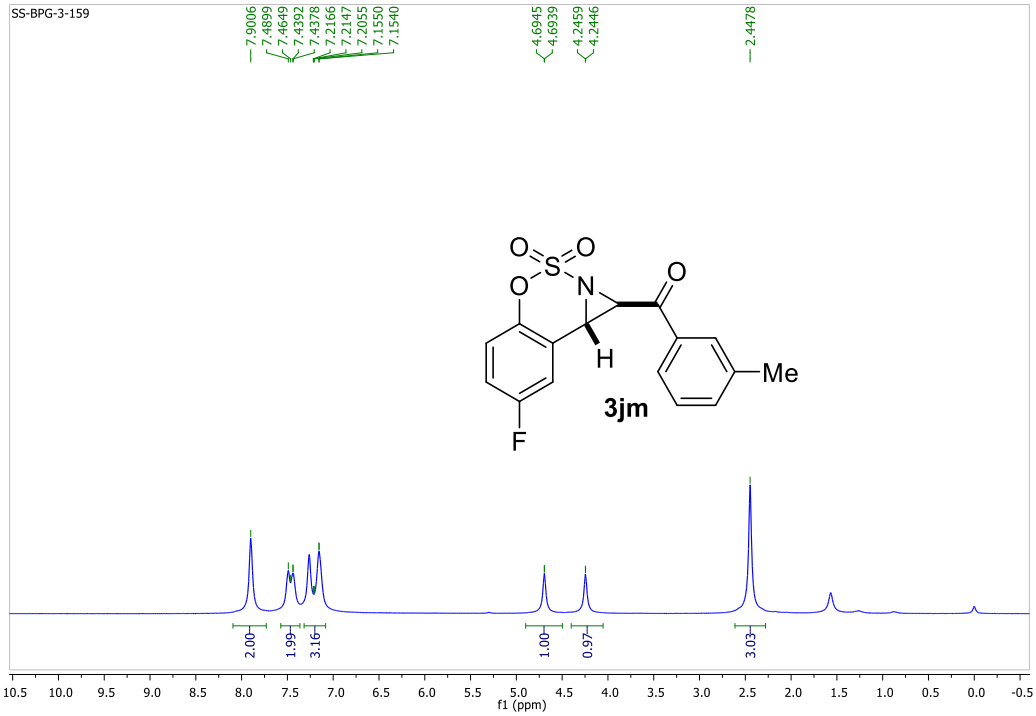

Figure 4.90 500 MHz ^{1}H NMR spectrum of **3jm** in $CDCl_3$.

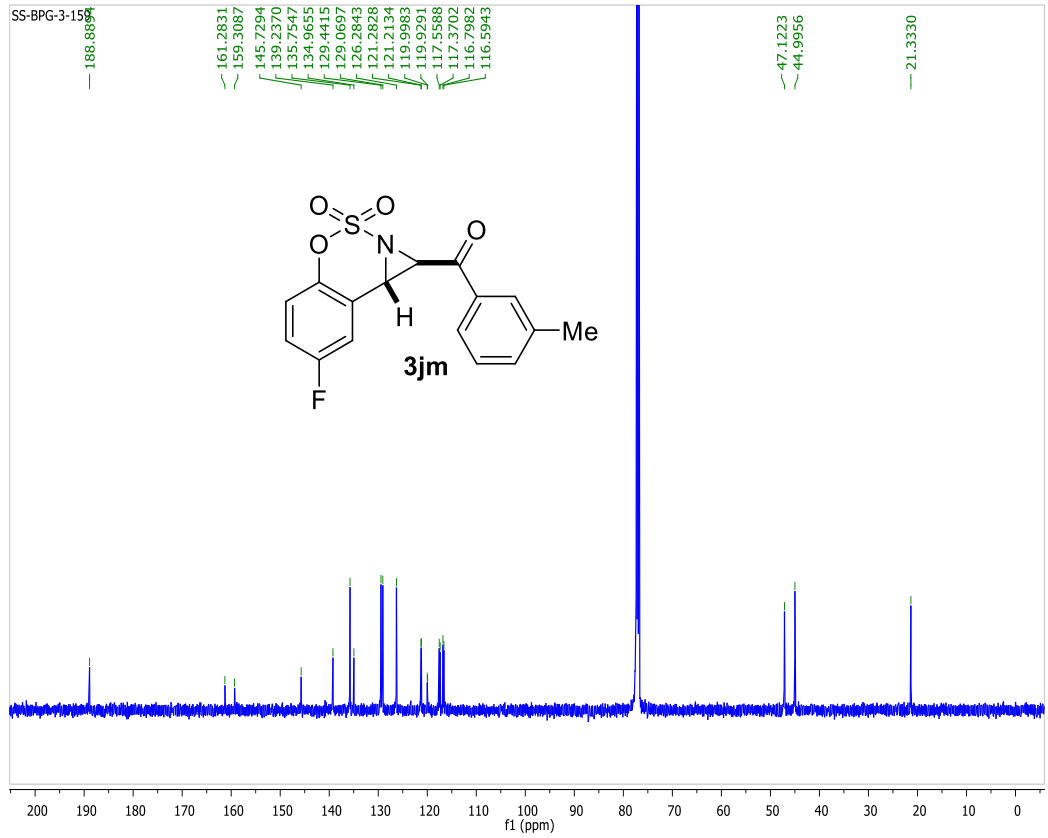

Figure 4.91 125 MHz ^{13}C NMR spectrum of **3jm** in $CDCl_3$.

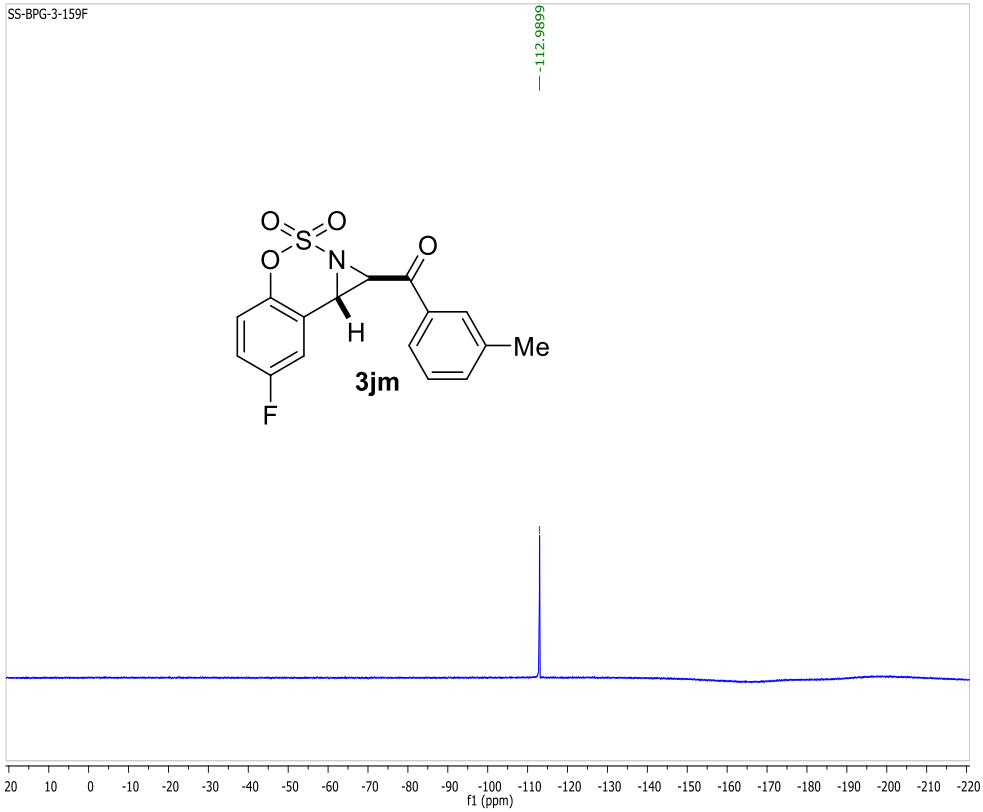

Figure 4.92 470 MHz ^{19}F NMR spectrum of **3jm** in $CDCl_3$.

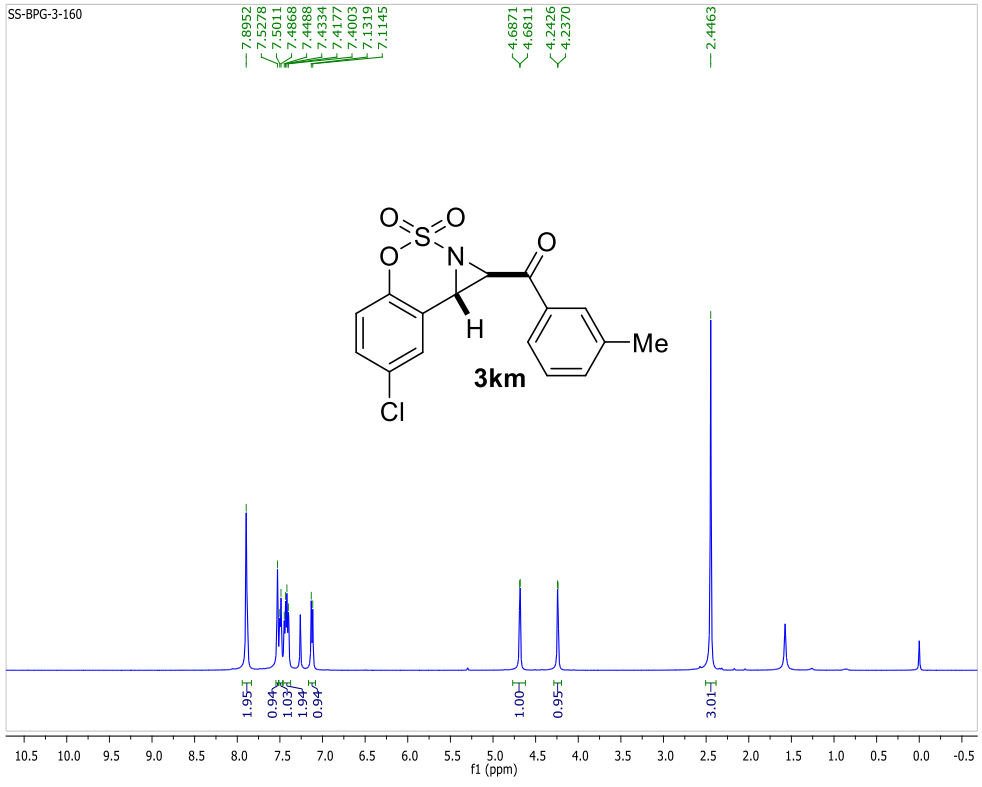

Figure 4.93 500 MHz ^{1}H NMR spectrum of **3km** in $CDCl_3$.

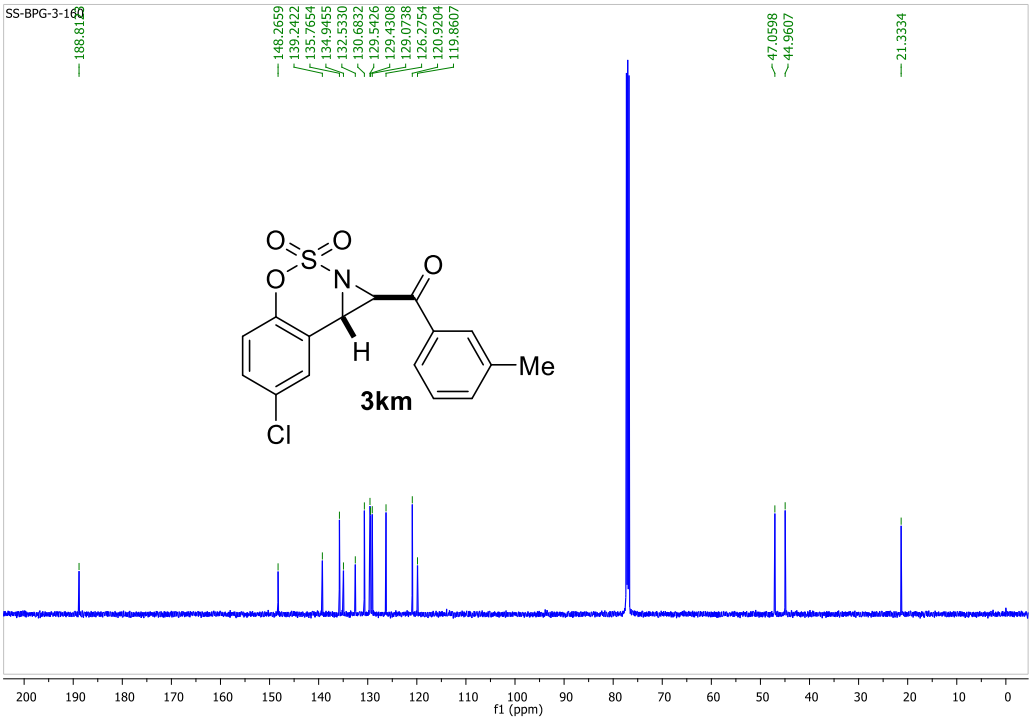

Figure 4.94 125 MHz ^{13}C NMR spectrum of **3km** in $CDCl_3$.

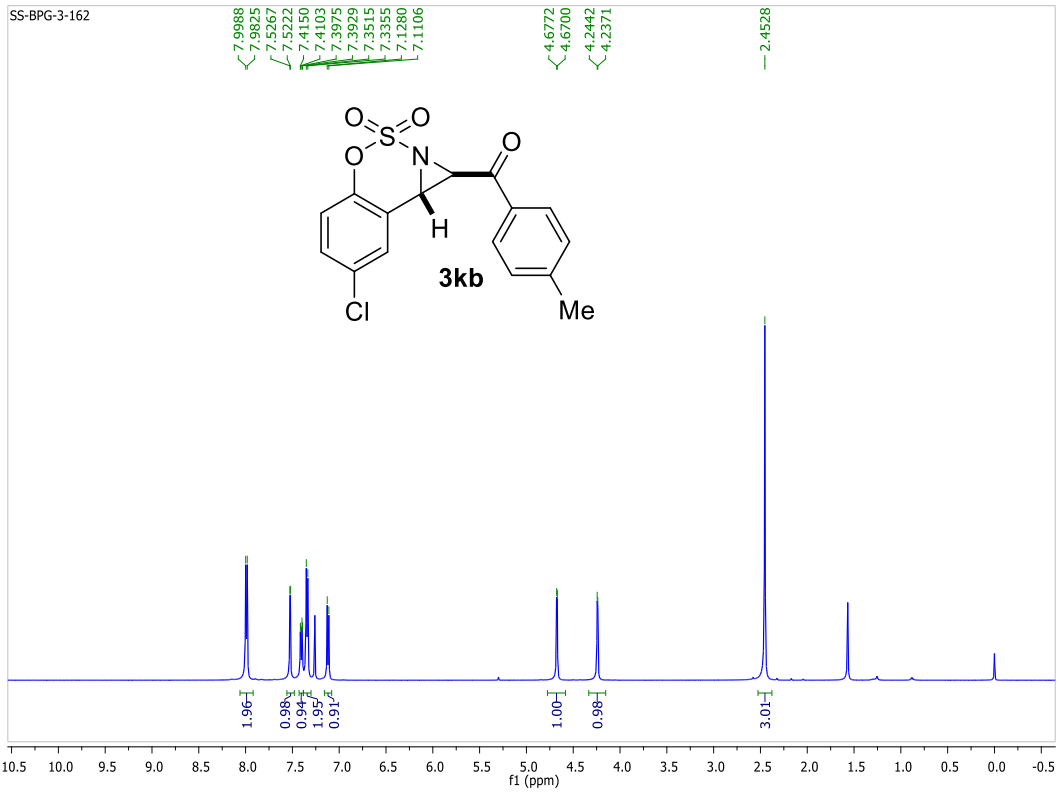

Figure 4.95 500 MHz ^{1}H NMR spectrum of **3kb** in $CDCl_3$.

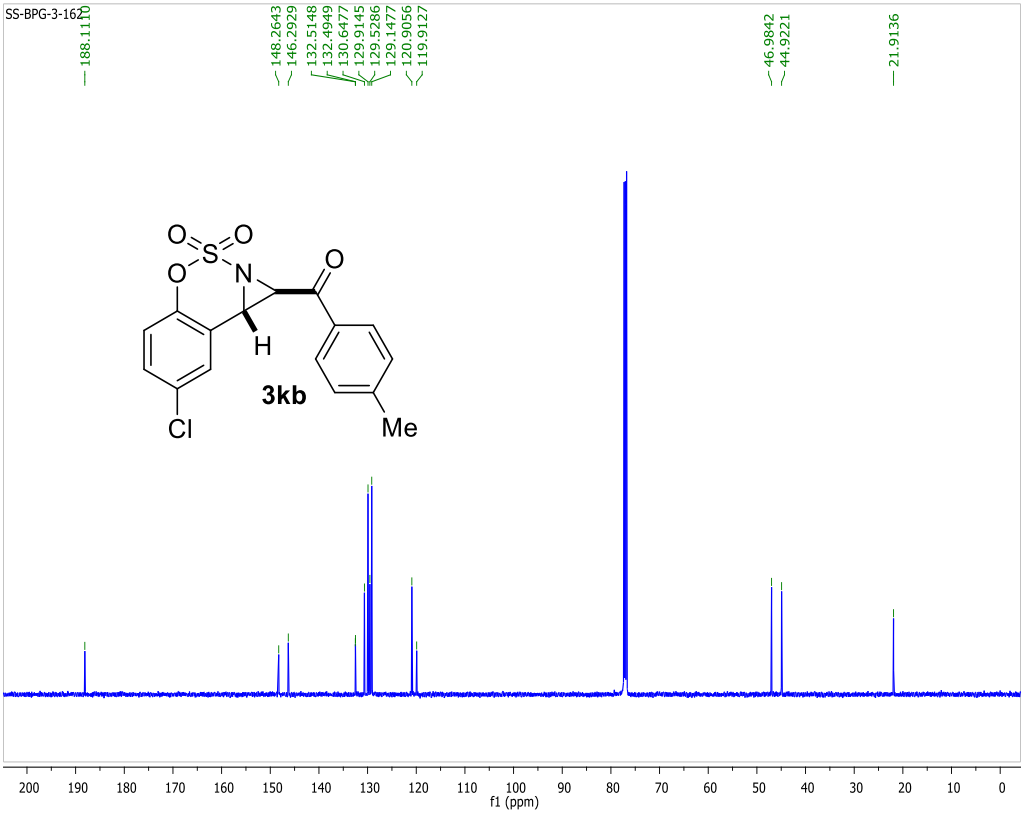

Figure 4.96 125 MHz ^{13}C NMR spectrum of **3kb** in $CDCl_3$.

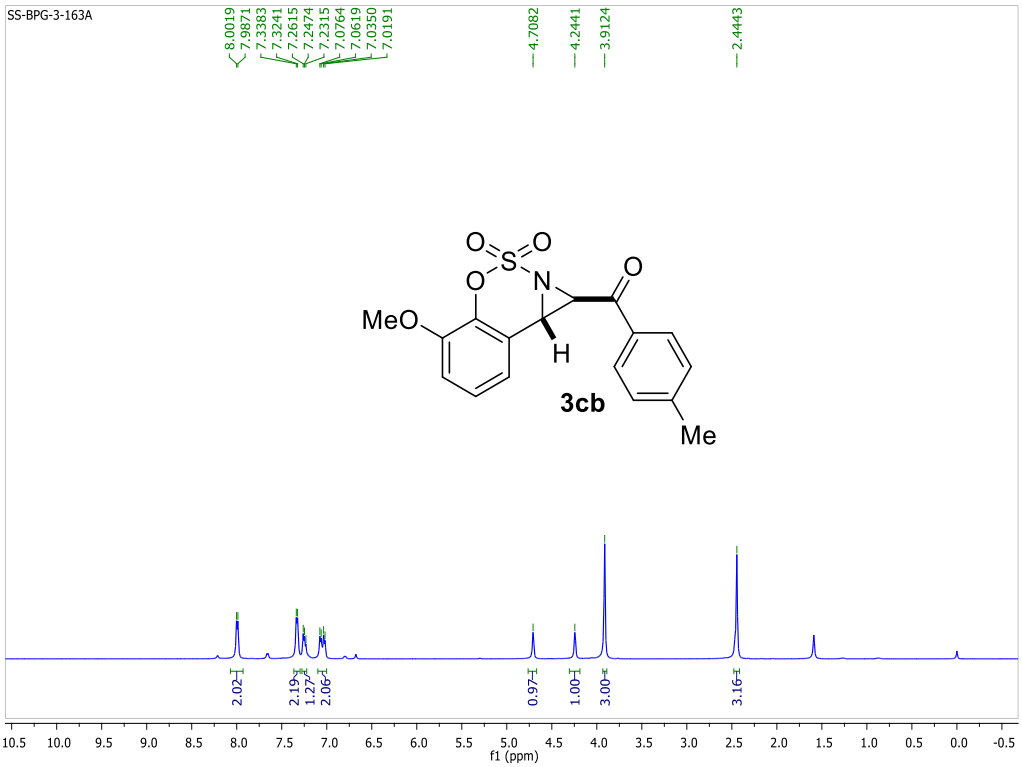

Figure 4.97 500 MHz ^{1}H NMR spectrum of **3cb** in $CDCl_3$.

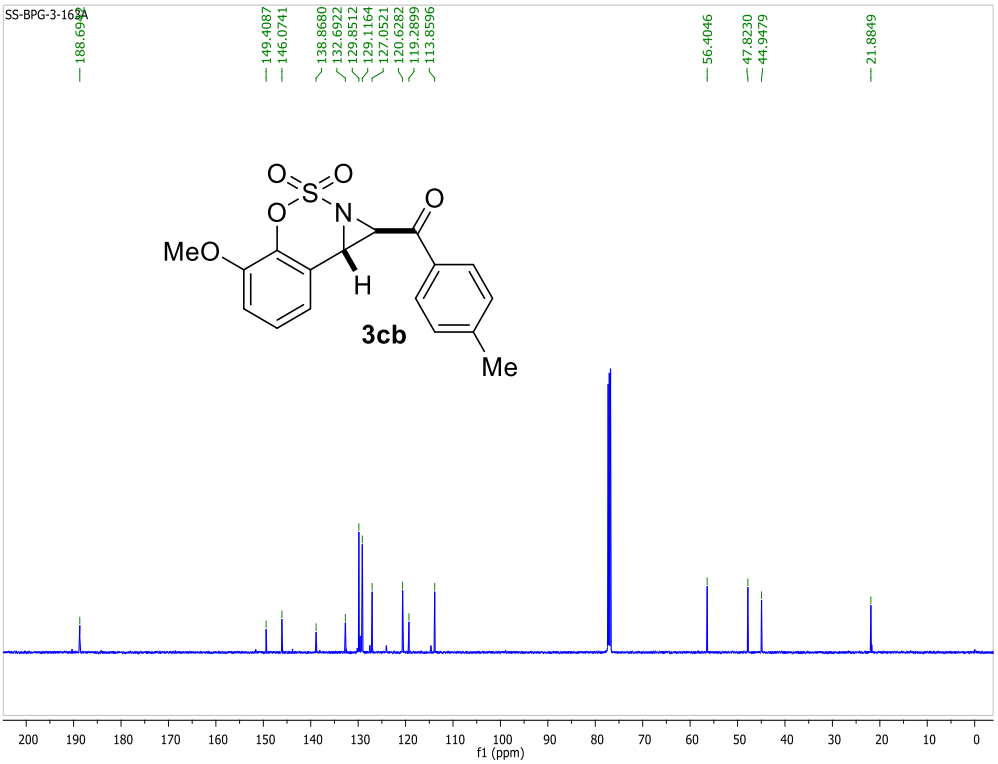

Figure 4.98 125 MHz ^{13}C NMR spectrum of **3cb** in $CDCl_3$.

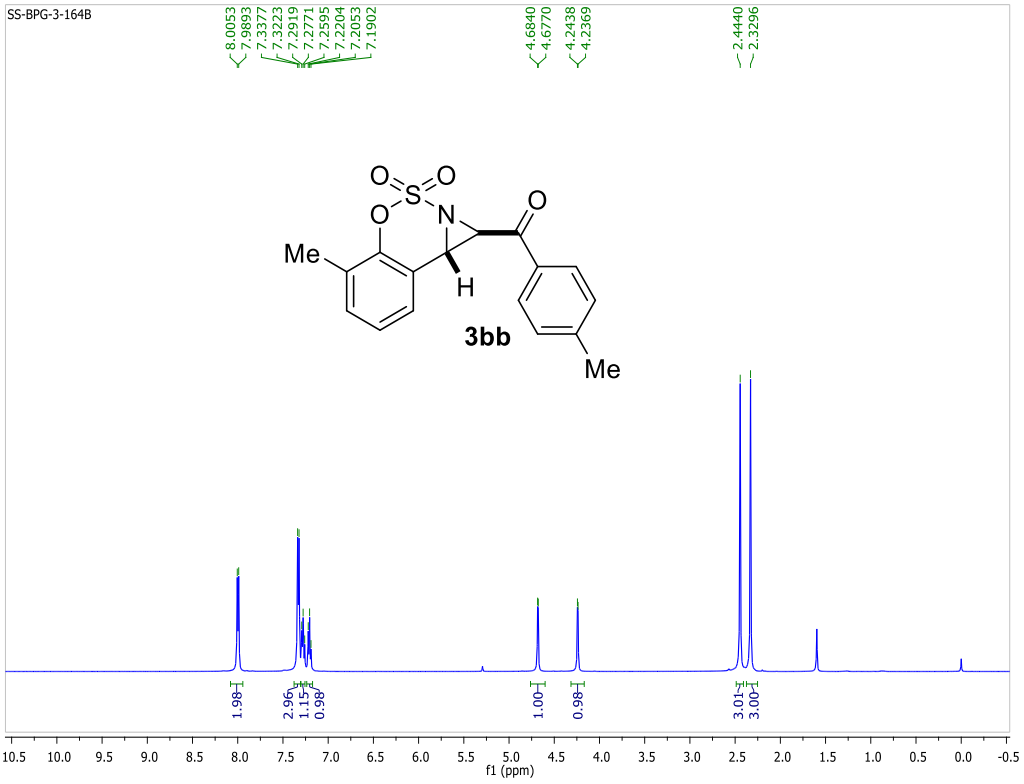

Figure 4.99 500 MHz ^{1}H NMR spectrum of **3bb** in $CDCl_3$.

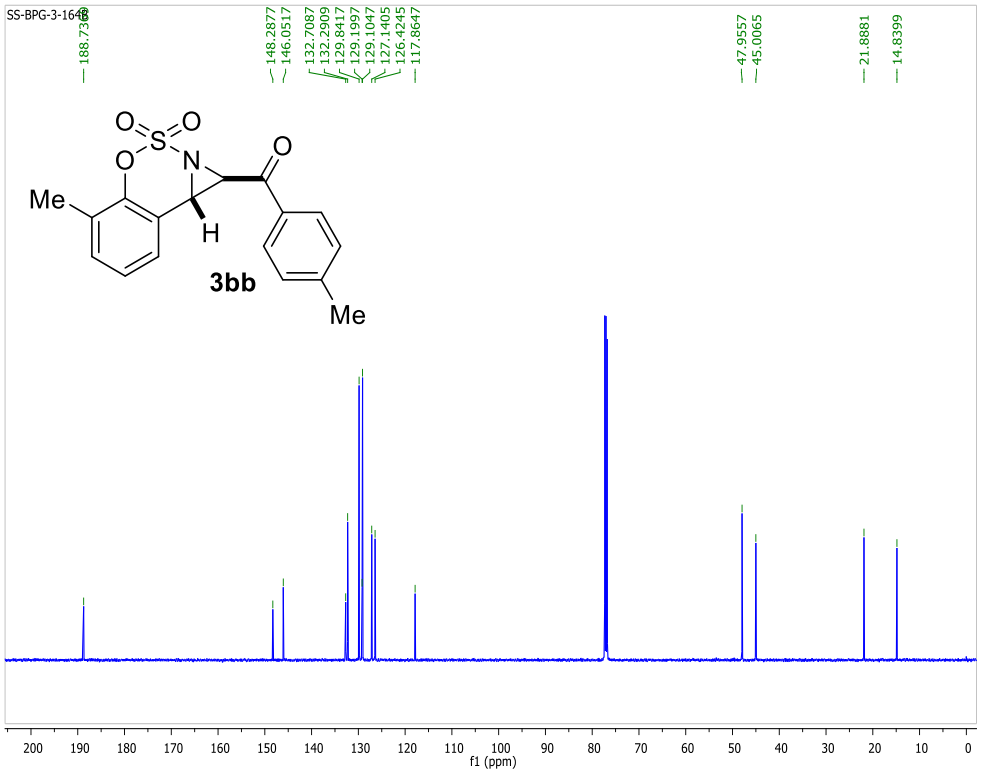

Figure 4.100 125 MHz ^{13}C NMR spectrum of **3bb** in $CDCl_3$.

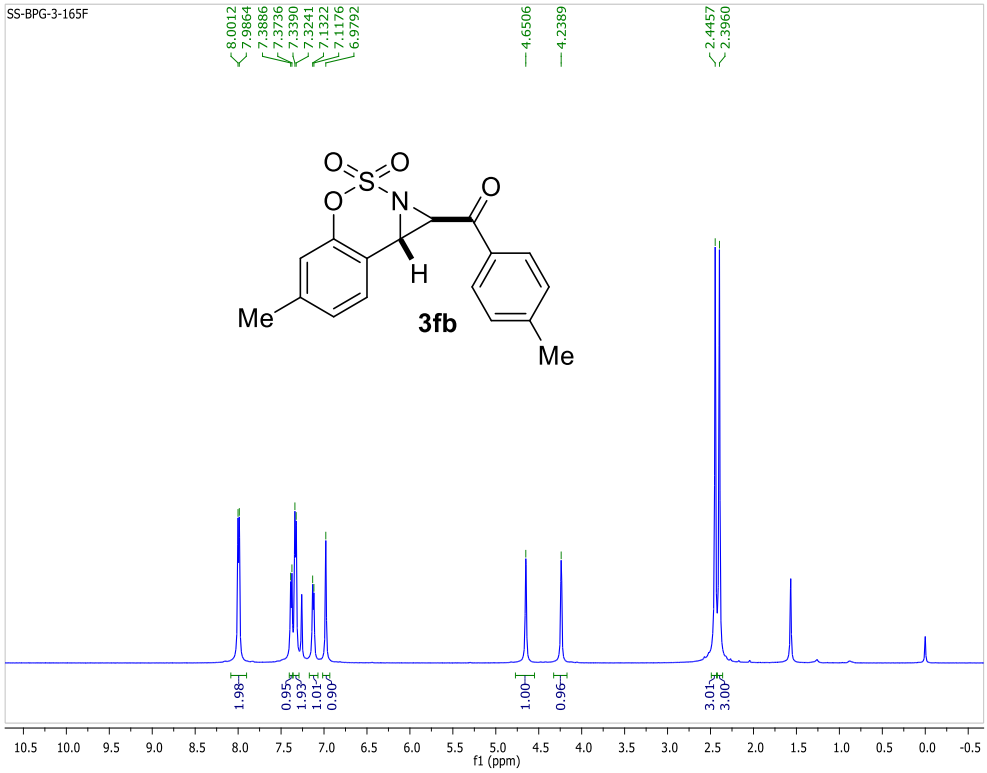

Figure 4.101 500 MHz ^{1}H NMR spectrum of **3fb** in $CDCl_3$.

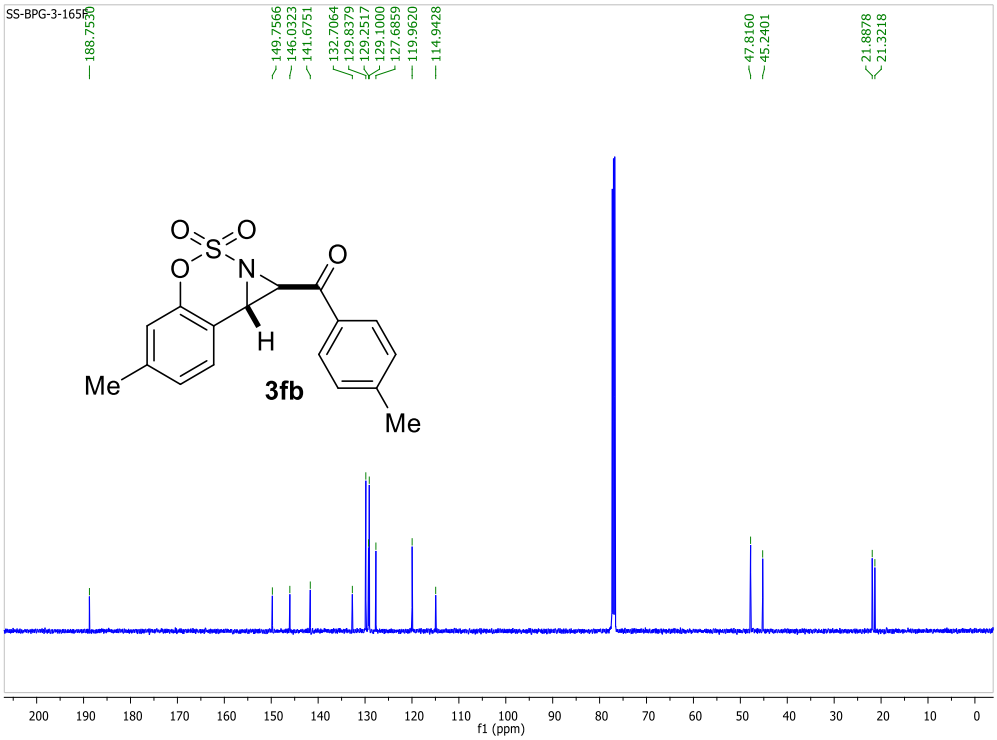

Figure 4.102 125 MHz ^{13}C NMR spectrum of **3fb** in $CDCl_3$.

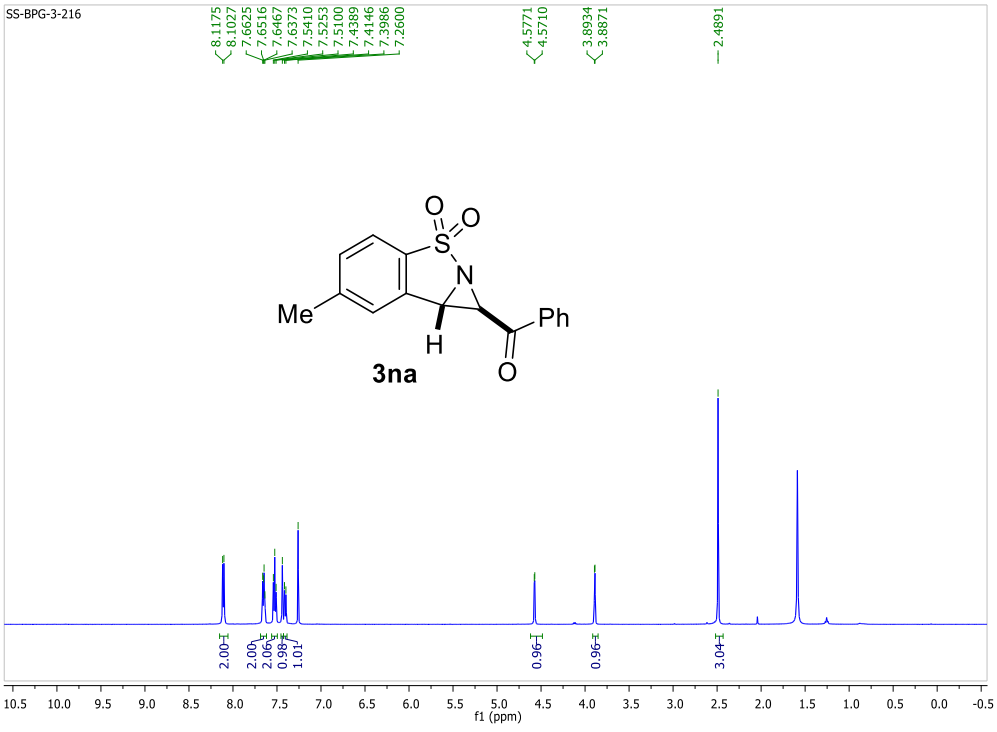

Figure 4.103 500 MHz ^{1}H NMR spectrum of **3na** in $CDCl_3$.

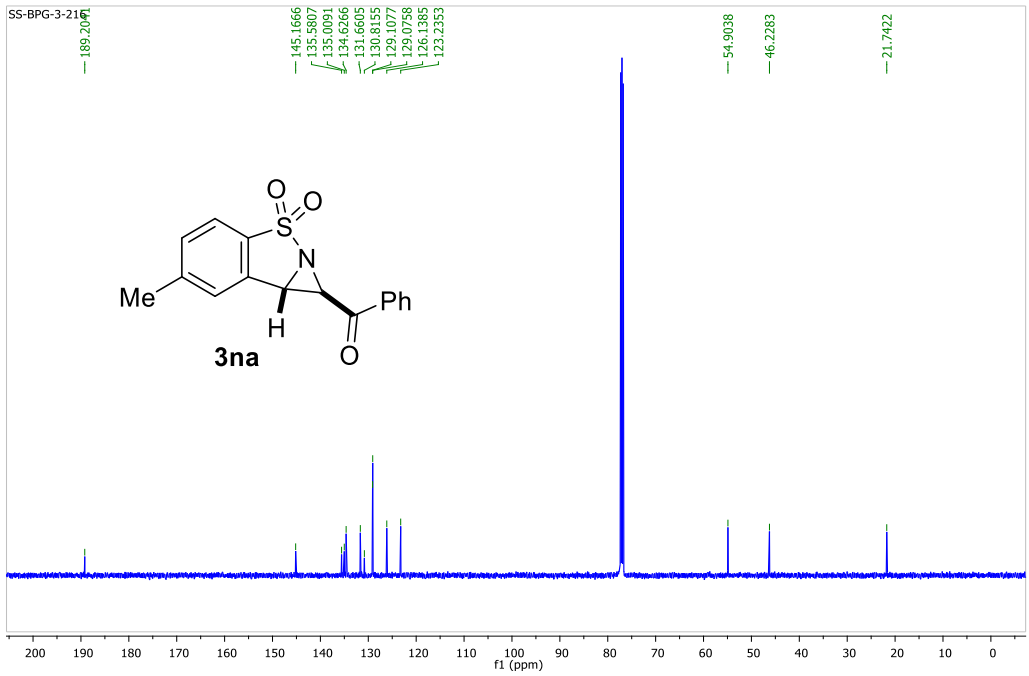

Figure 4.104 125 MHz ^{13}C NMR spectrum of **3na** in $CDCl_3$.

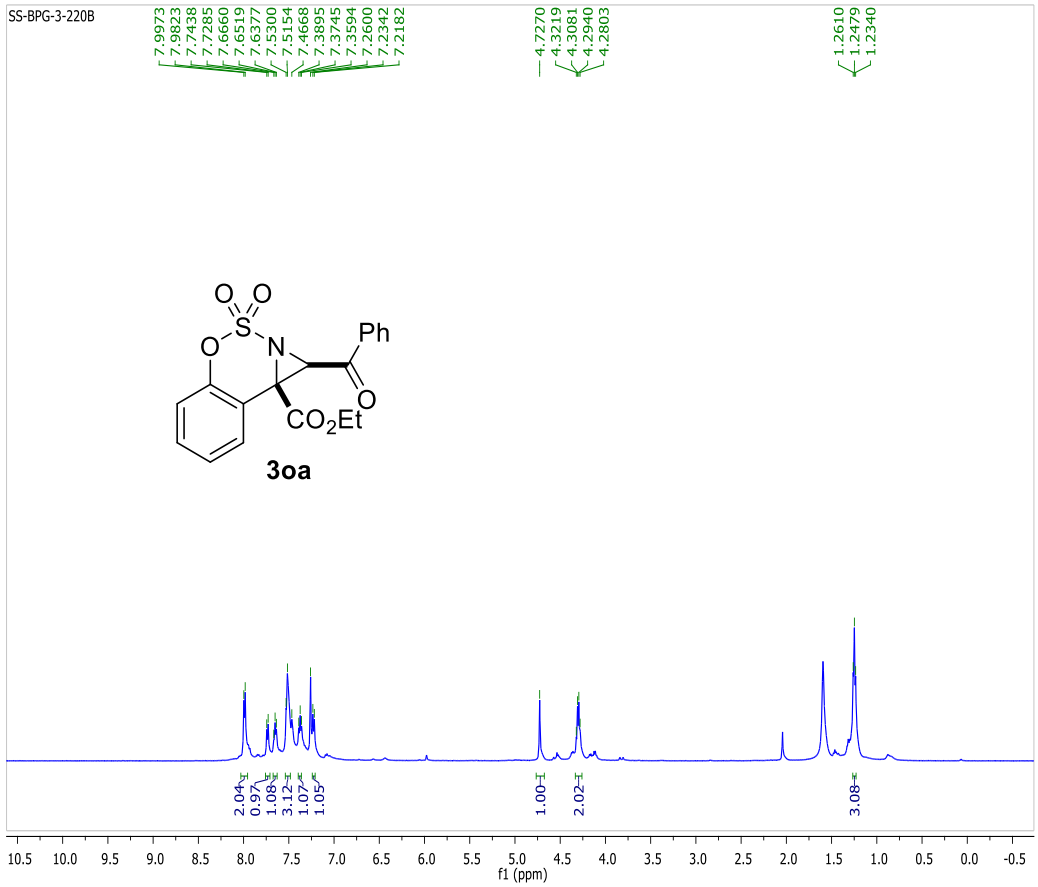

Figure 4.105 500 MHz ^{1}H NMR spectrum of **3oa** in $CDCl_3$.

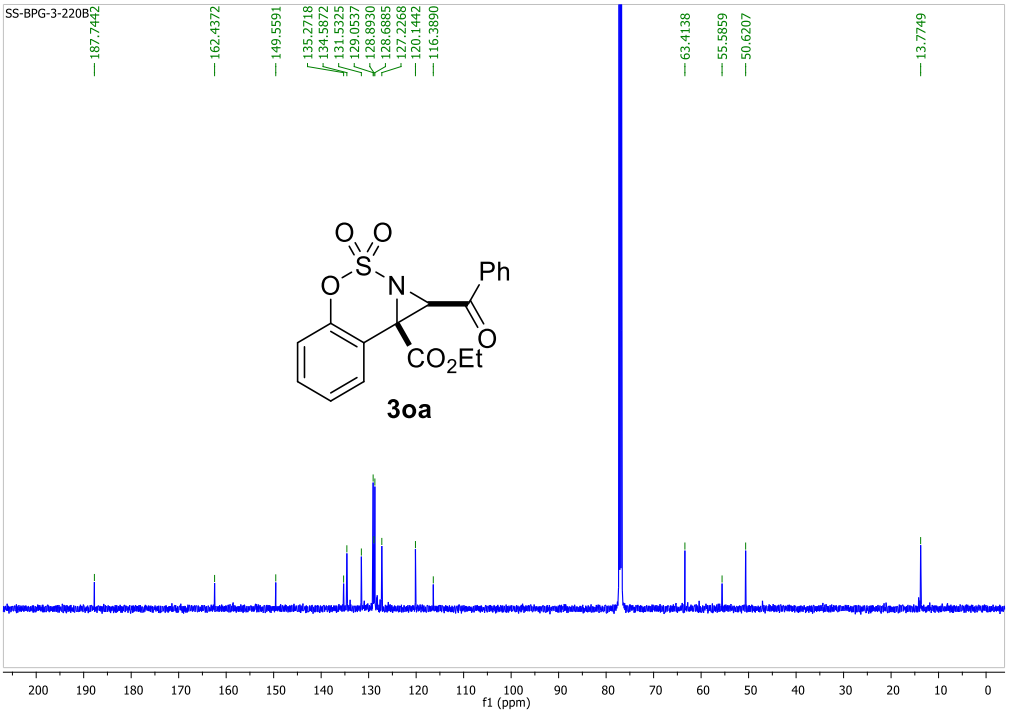

Figure 4.106 125 MHz ^{13}C NMR spectrum of **3oa** in $CDCl_3$.

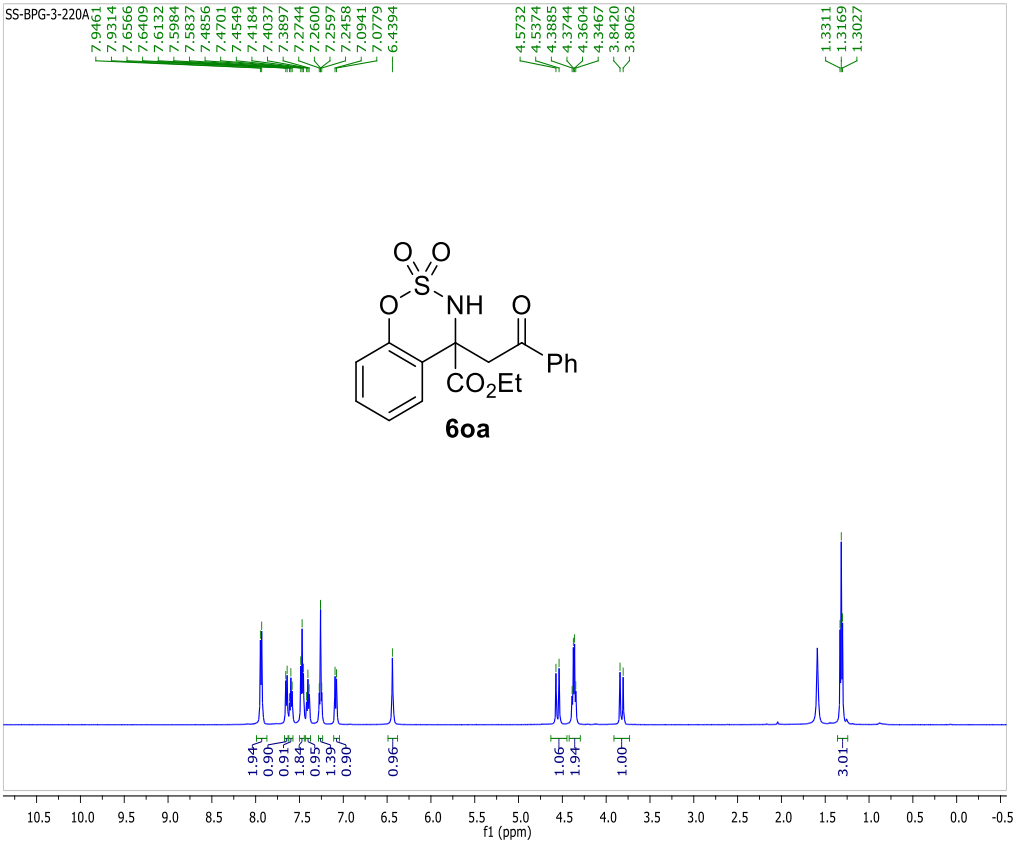

Figure 4.107 500 MHz ^{1}H NMR spectrum of **6oa** in $CDCl_3$.

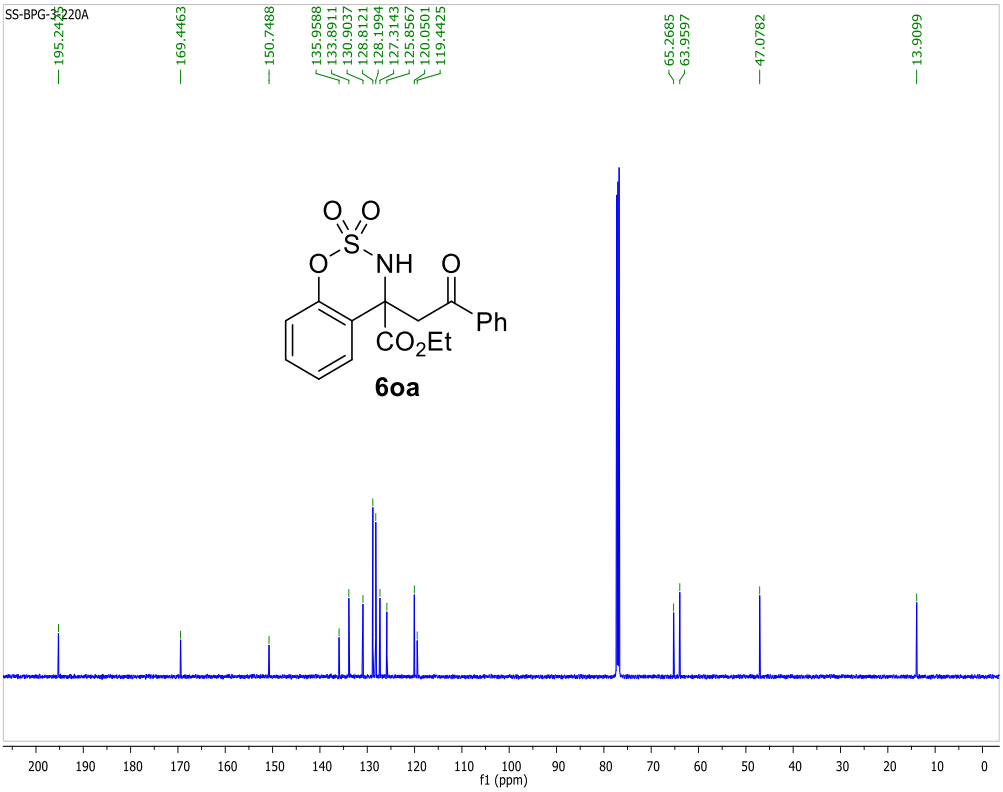

Figure 4.108 125 MHz ^{13}C NMR spectrum of **6oa** in $CDCl_3$.

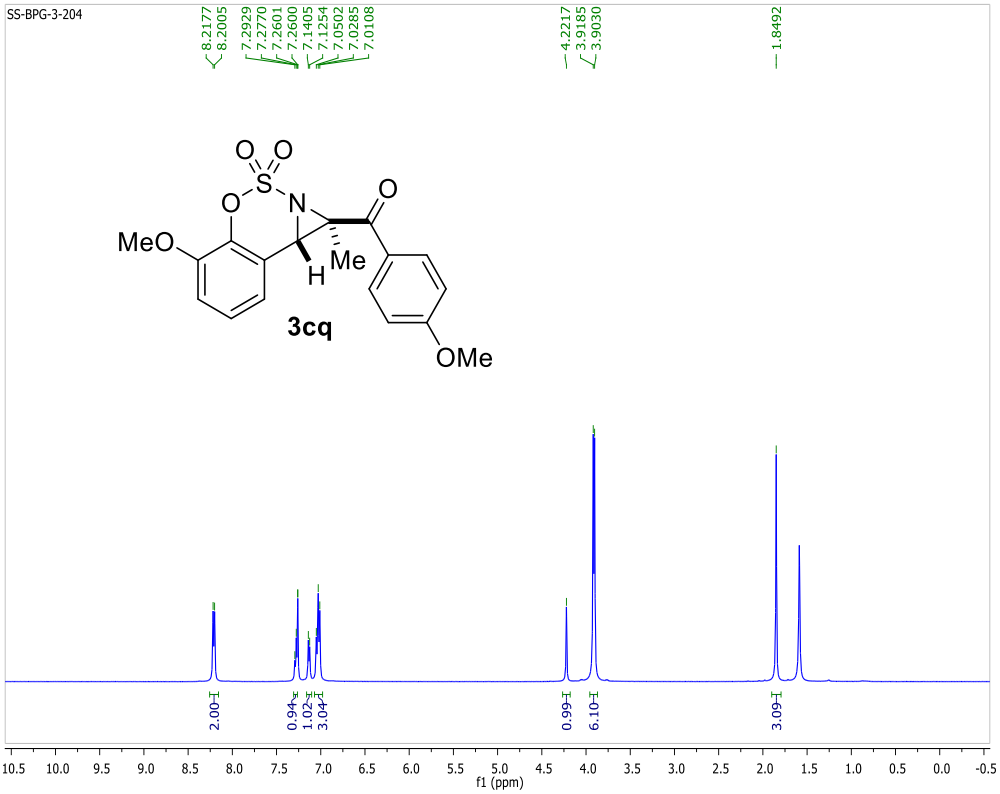

Figure 4.109 500 MHz ^{1}H NMR spectrum of **3cq** in $CDCl_3$.

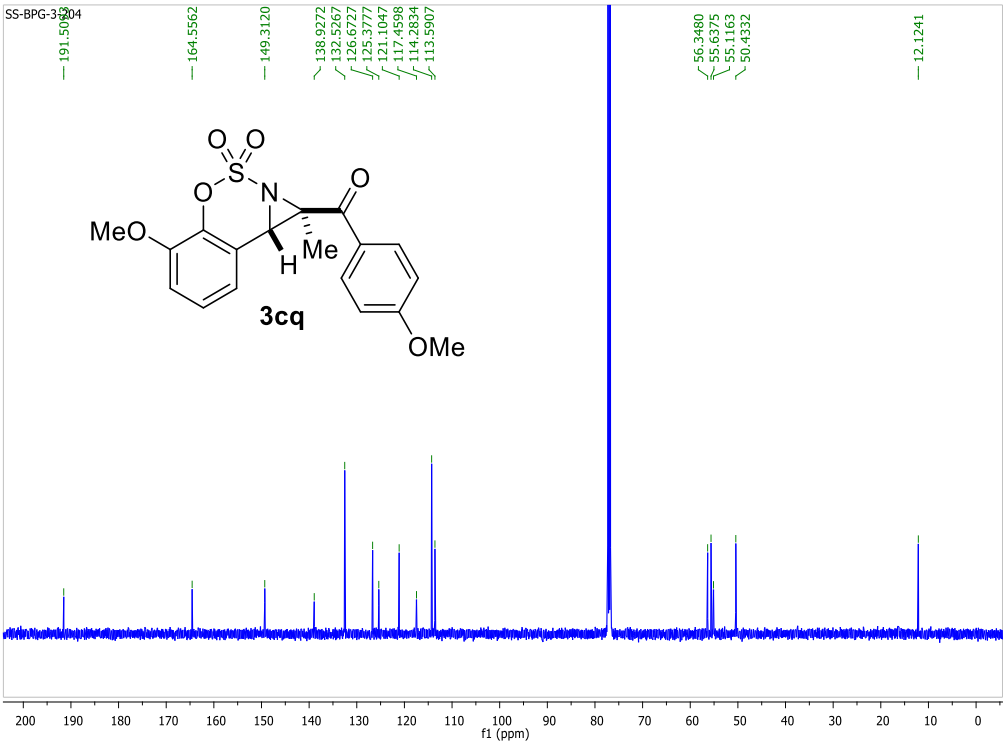

Figure 4.110 125 MHz ^{13}C NMR spectrum of **3cq** in $CDCl_3$.

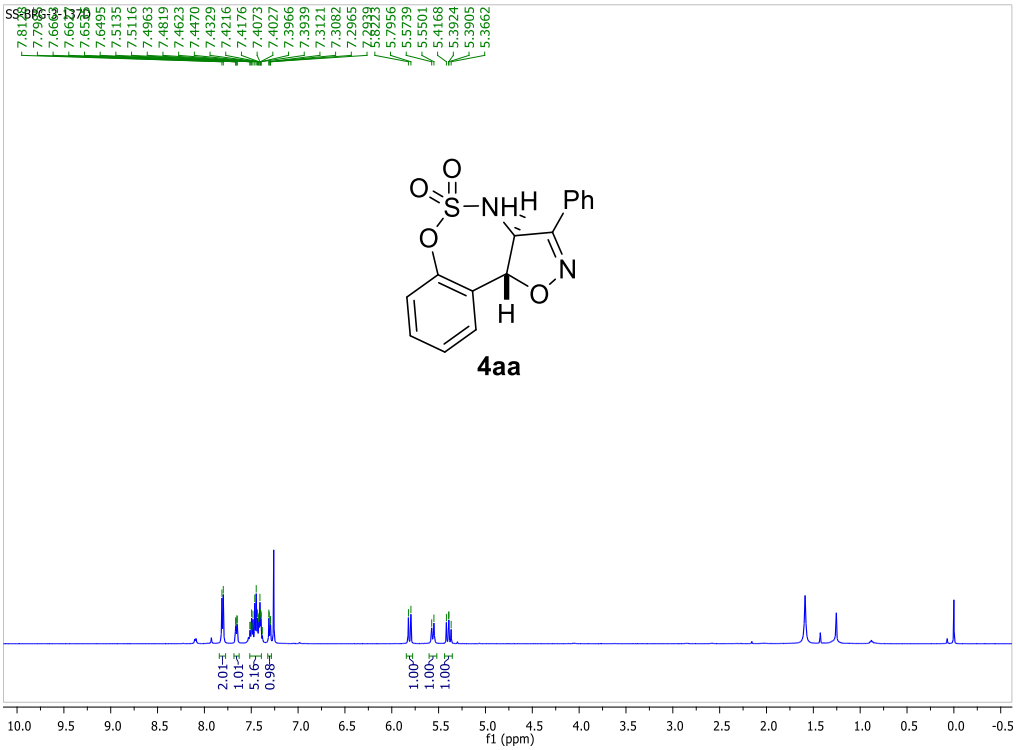

Figure 4.111 500 MHz ^{1}H NMR spectrum of **4aa** in $CDCl_3$.

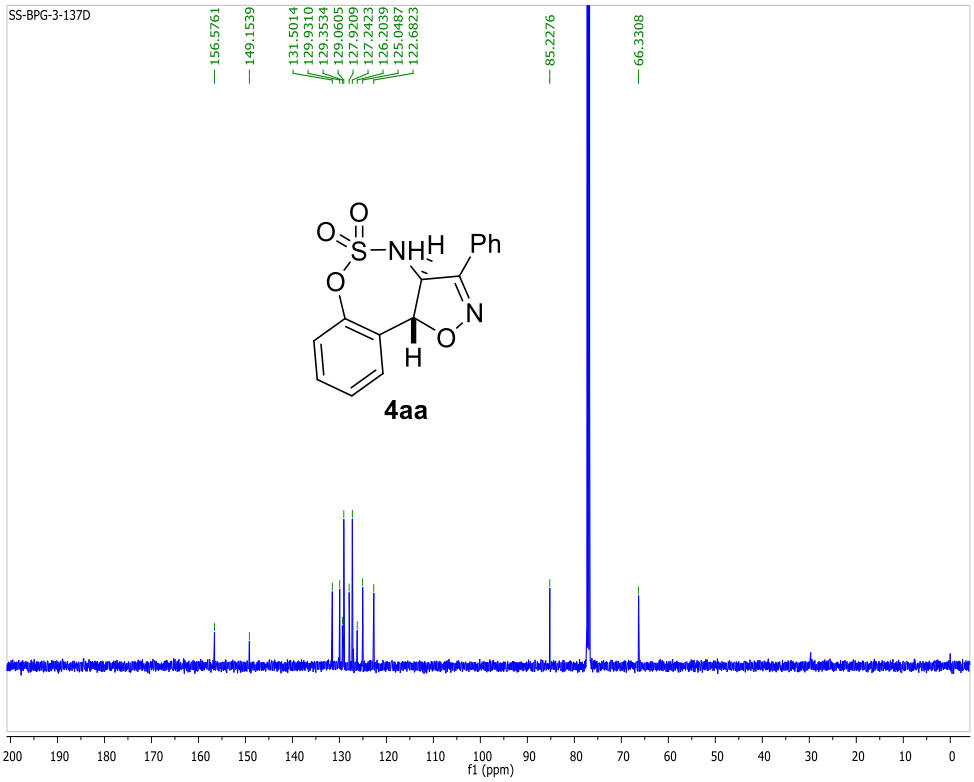

Figure 4.112 125 MHz ^{13}C NMR spectrum of **4aa** in $CDCl_3$.

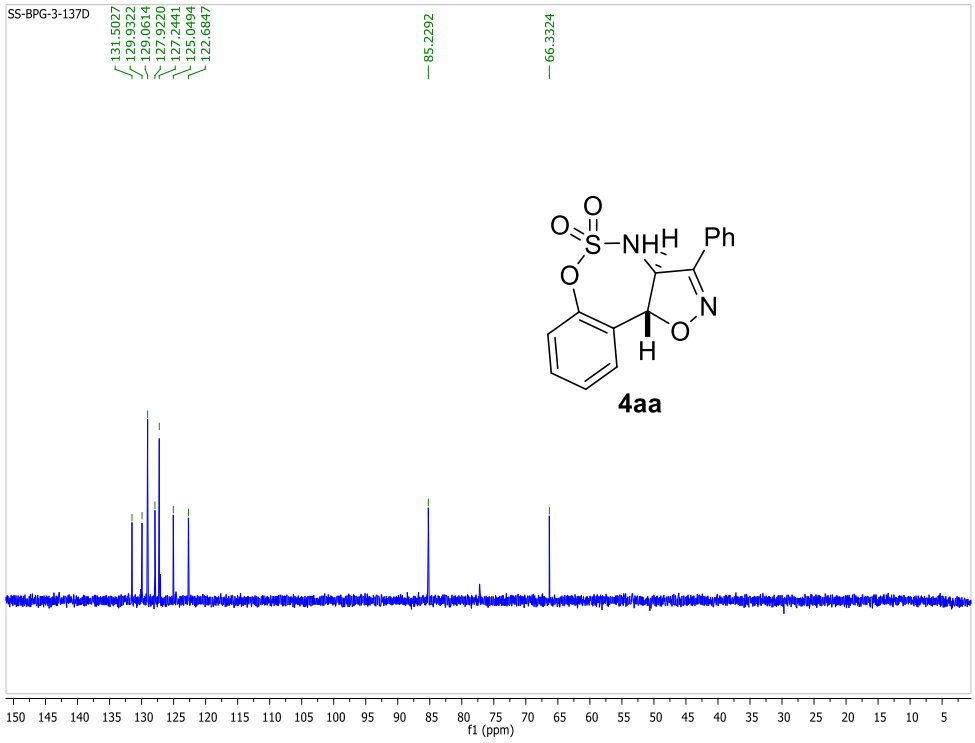

Figure 4.113 125 MHz DEPT-135 NMR spectrum of **4aa** in $CDCl_3$.

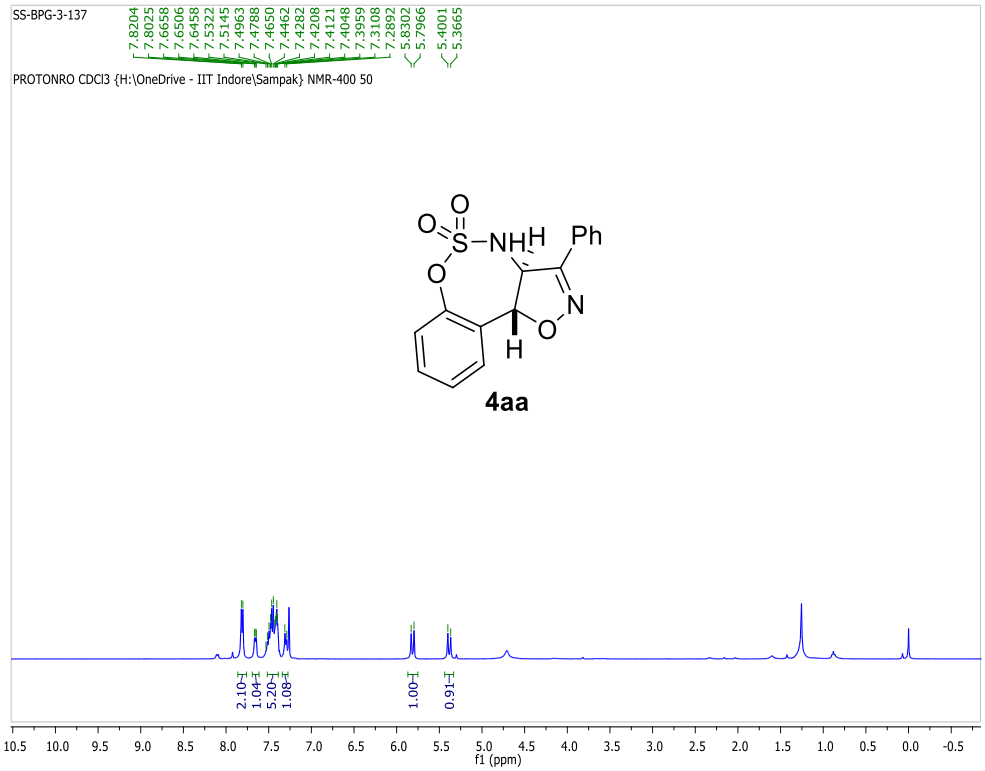

Figure 4.114 400 MHz ^{1}H NMR spectrum of **4aa** in $CDCl_3$+D_2O.

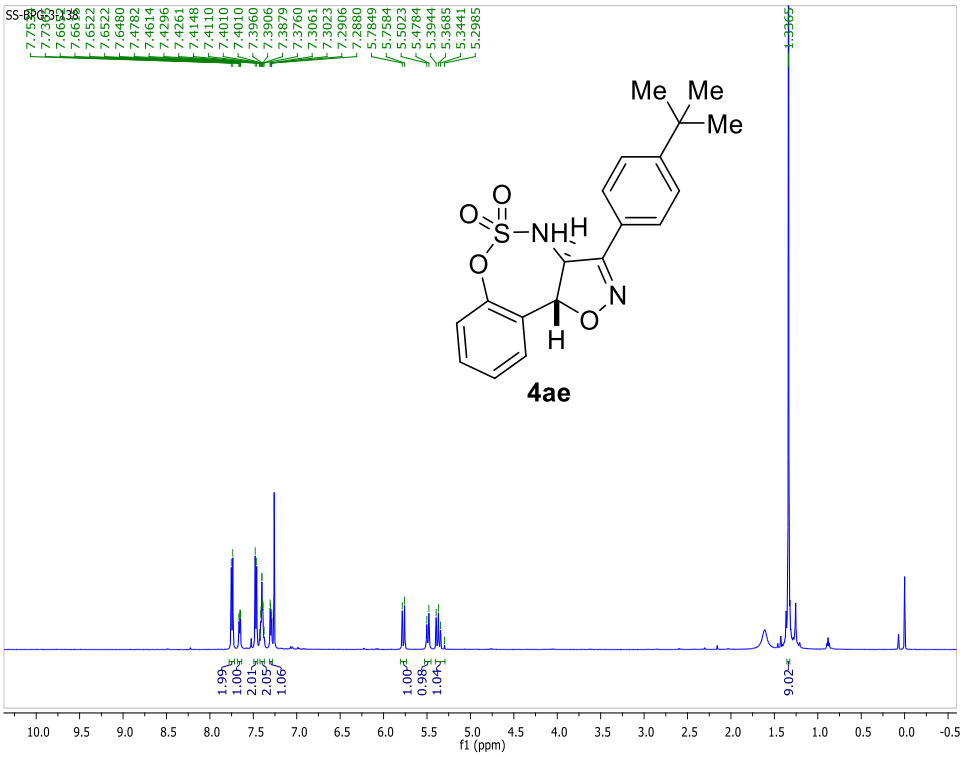

Figure 4.115 500 MHz ^{1}H NMR spectrum of **4ae** in $CDCl_3$.

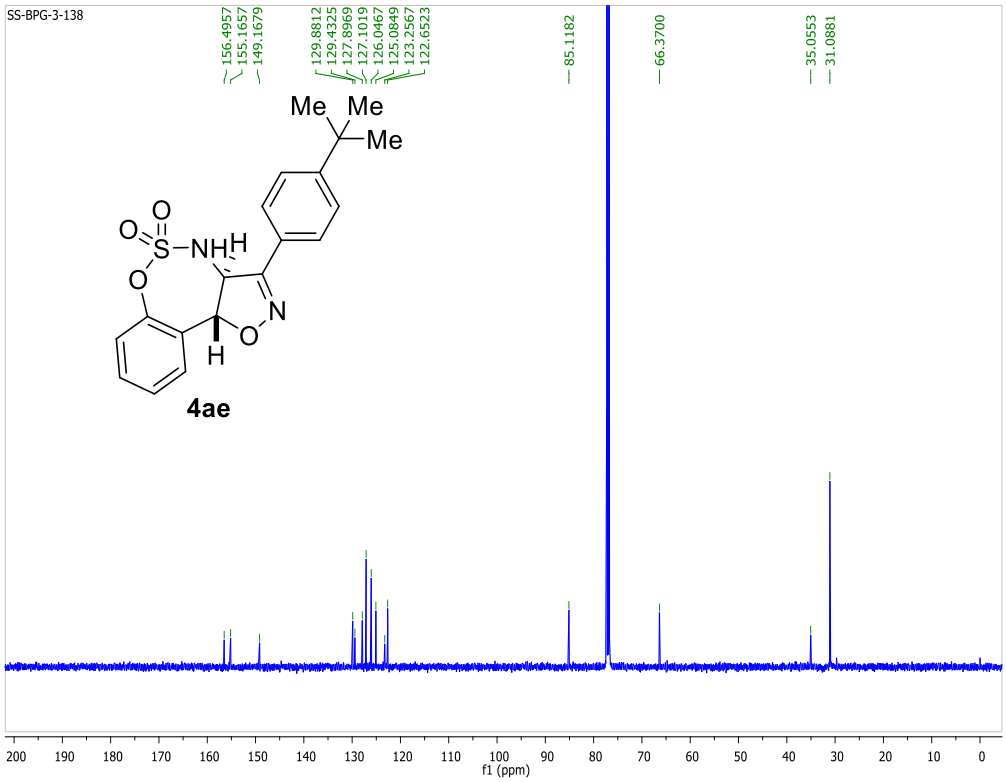

Figure 4.116 125 MHz ^{13}C NMR spectrum of **4ae** in $CDCl_3$.

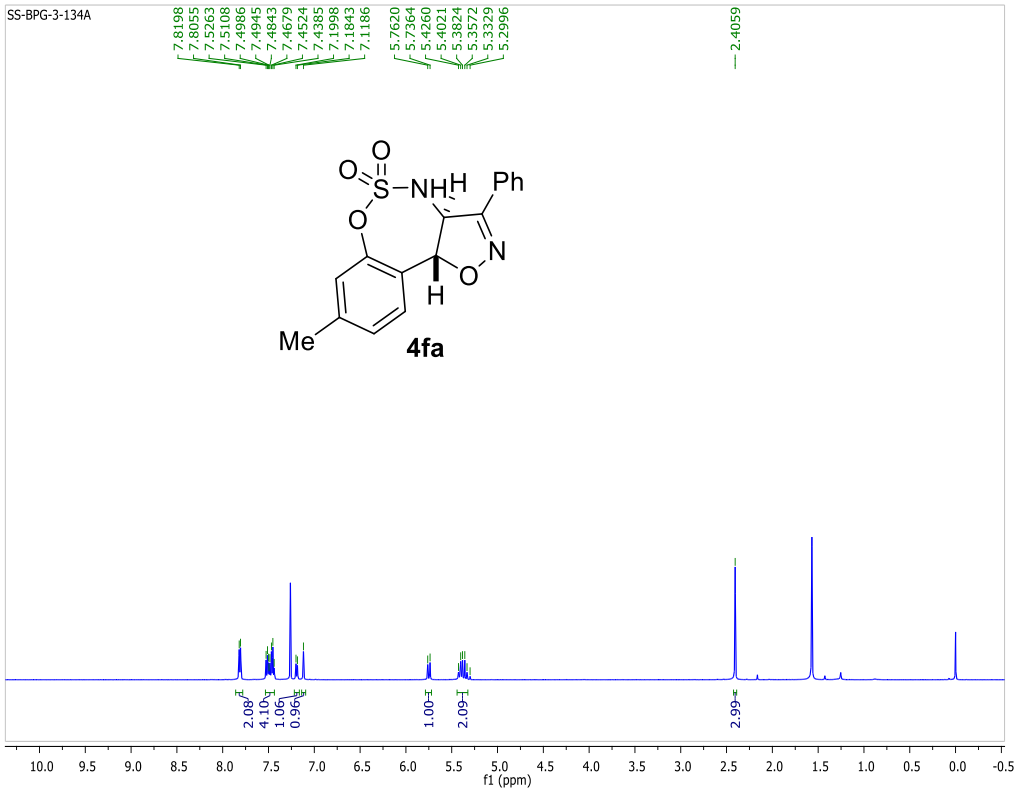

Figure 4.117 500 MHz ^{1}H NMR spectrum of **4fa** in $CDCl_3$.

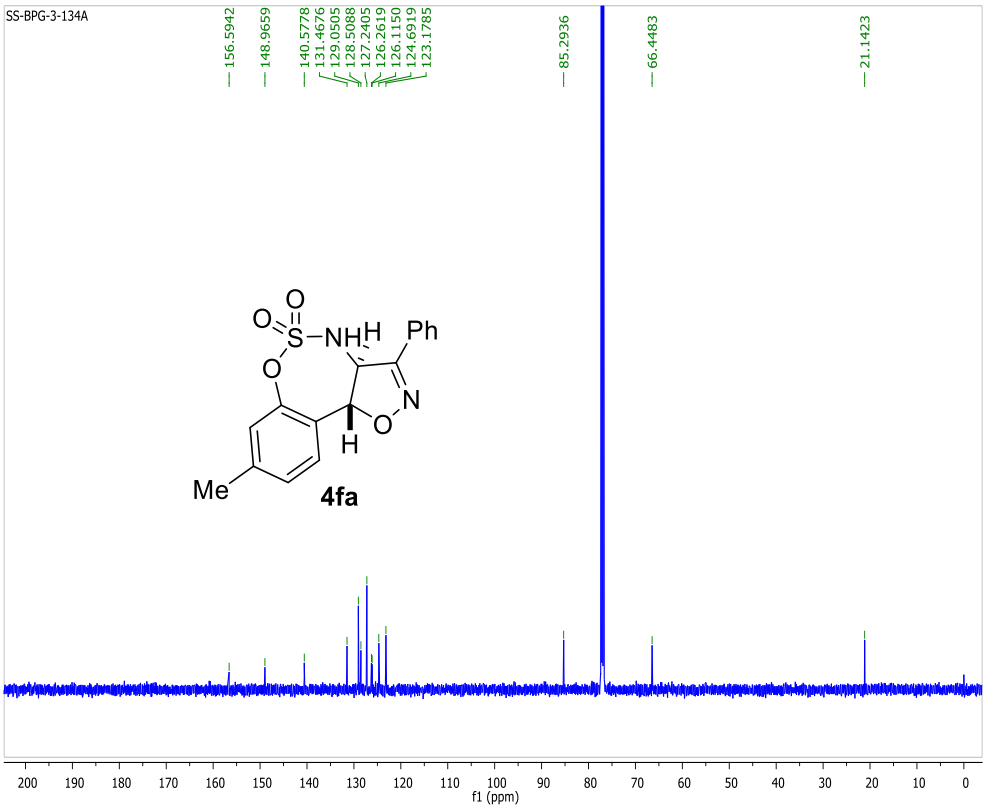

Figure 4.118 125 MHz ^{13}C NMR spectrum of **4fa** in $CDCl_3$.

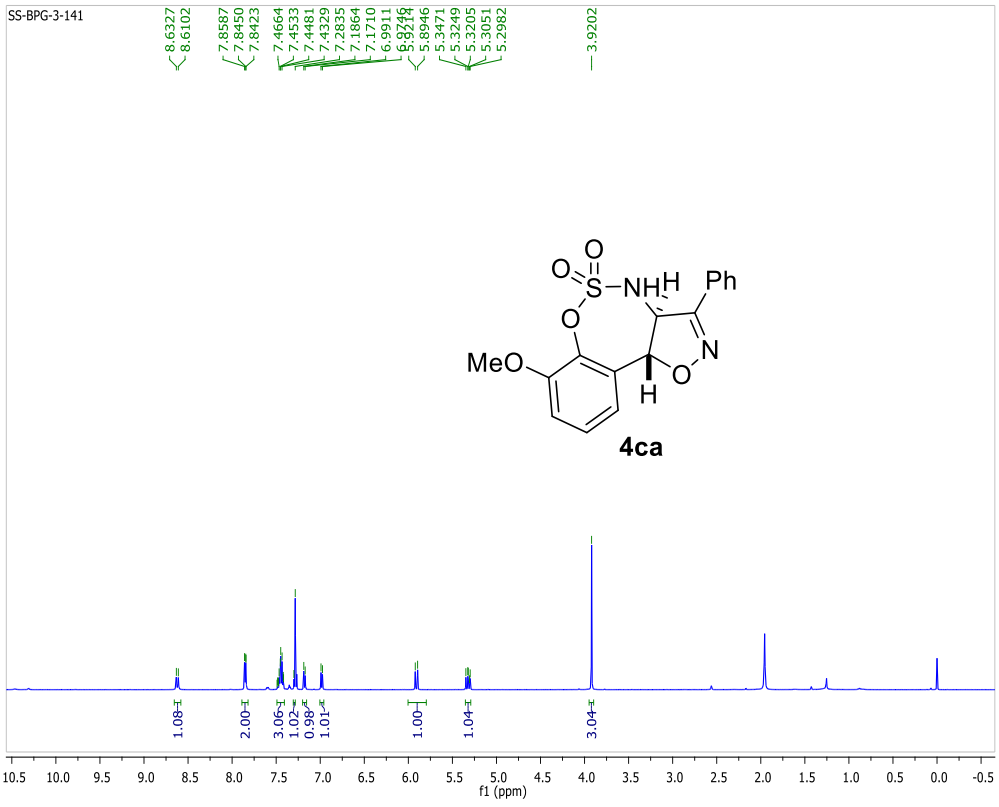

Figure 4.119 500 MHz ^{1}H NMR spectrum of **4ca** in $CDCl_3$+DMSO-d_6.

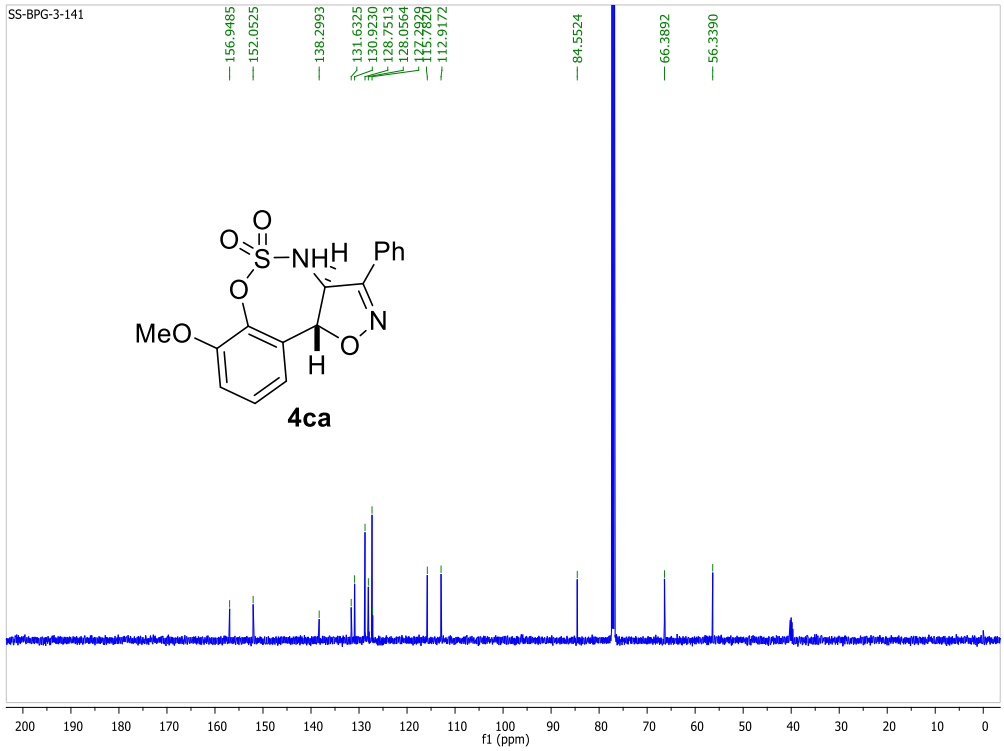

Figure 4.120 125 MHz ^{13}C NMR spectrum of **4ca** in $CDCl_3$+ DMSO-d_6.

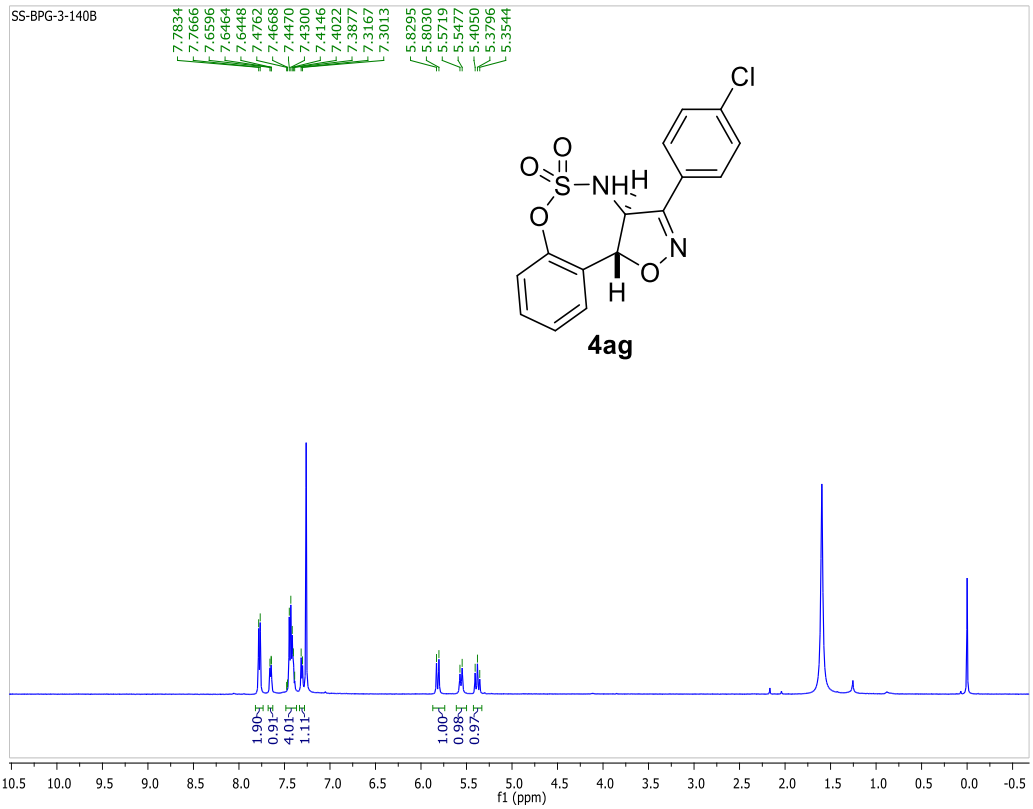

Figure 4.121 500 MHz ^{1}H NMR spectrum of **4ag** in $CDCl_3$.

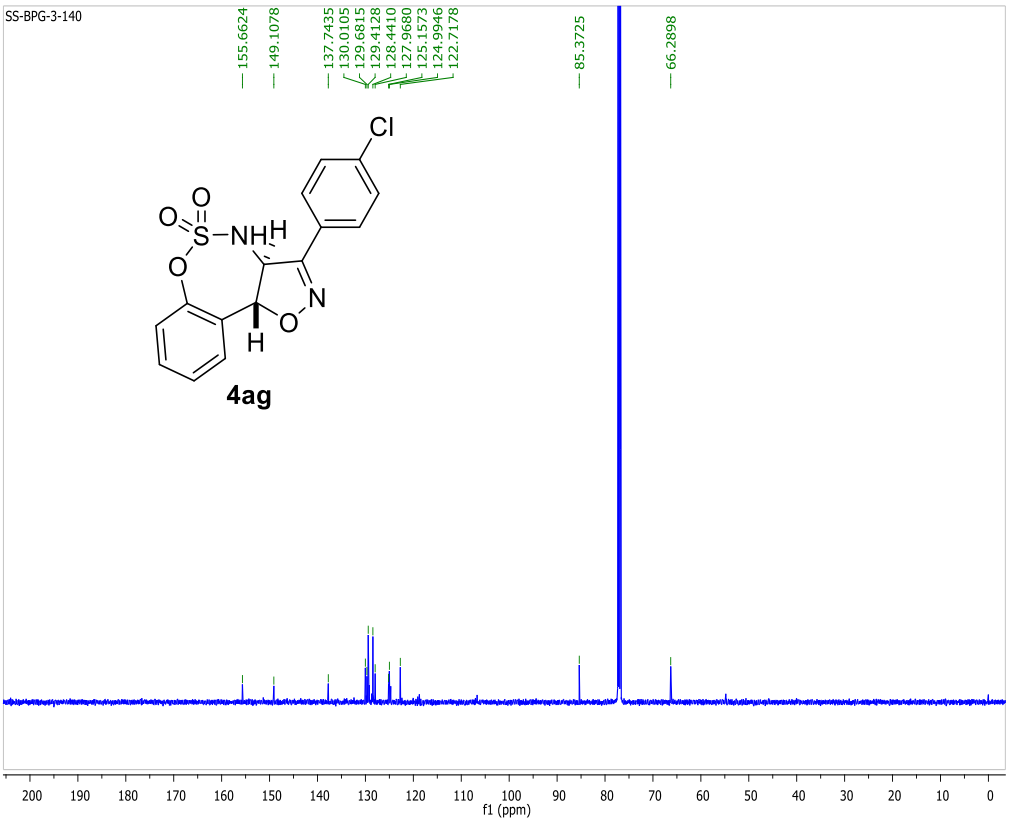

Figure 4.122 125 MHz ^{13}C NMR spectrum of **4ag** in $CDCl_3$.

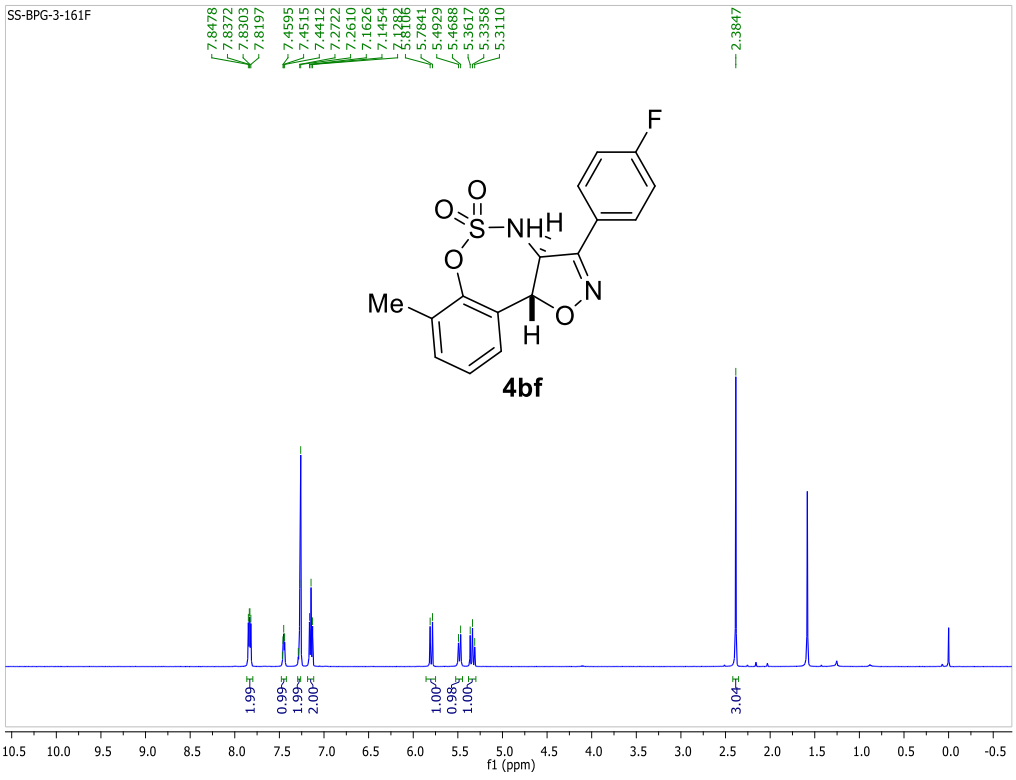

Figure 4.123 500 MHz ^{1}H NMR spectrum of **4bf** in $CDCl_3$.

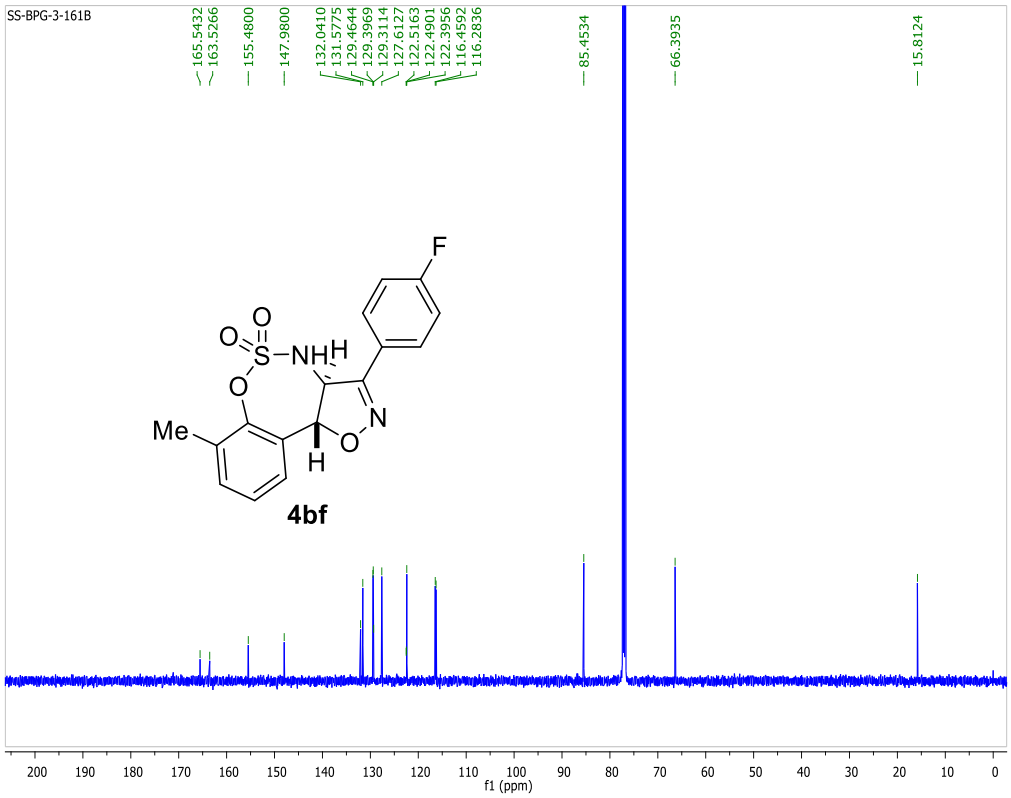

Figure 4.124 125 MHz ^{13}C NMR spectrum of **4bf** in $CDCl_3$.

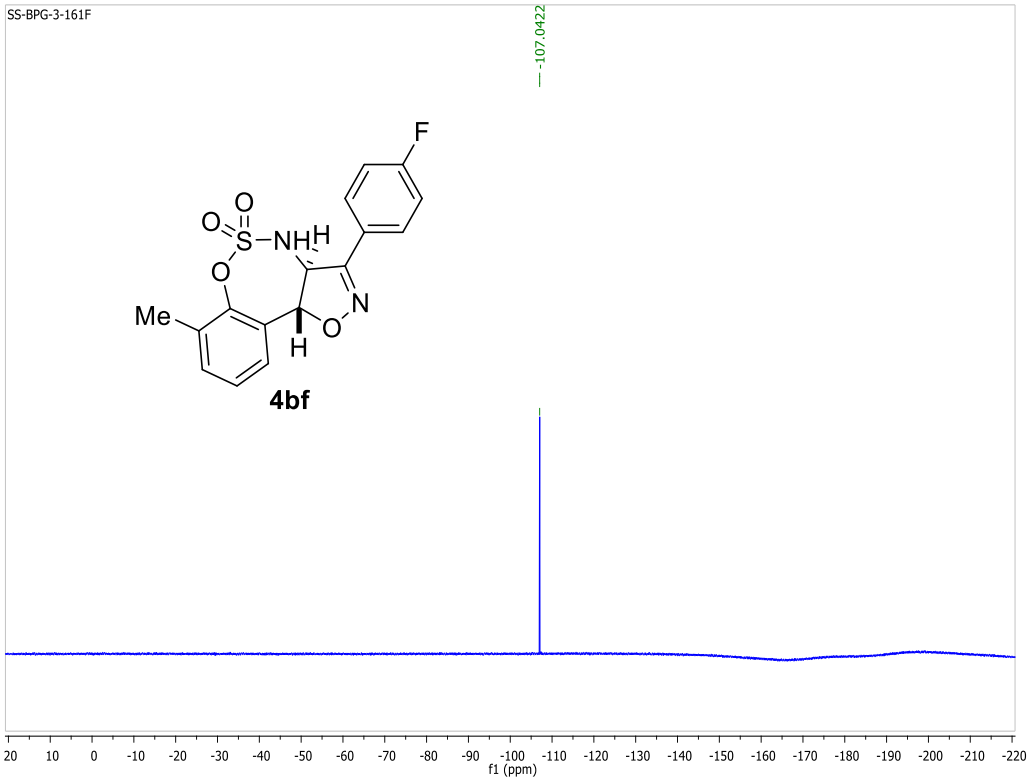

Figure 4.125 470 MHz ^{19}F NMR spectrum of **4bf** in $CDCl_3$.

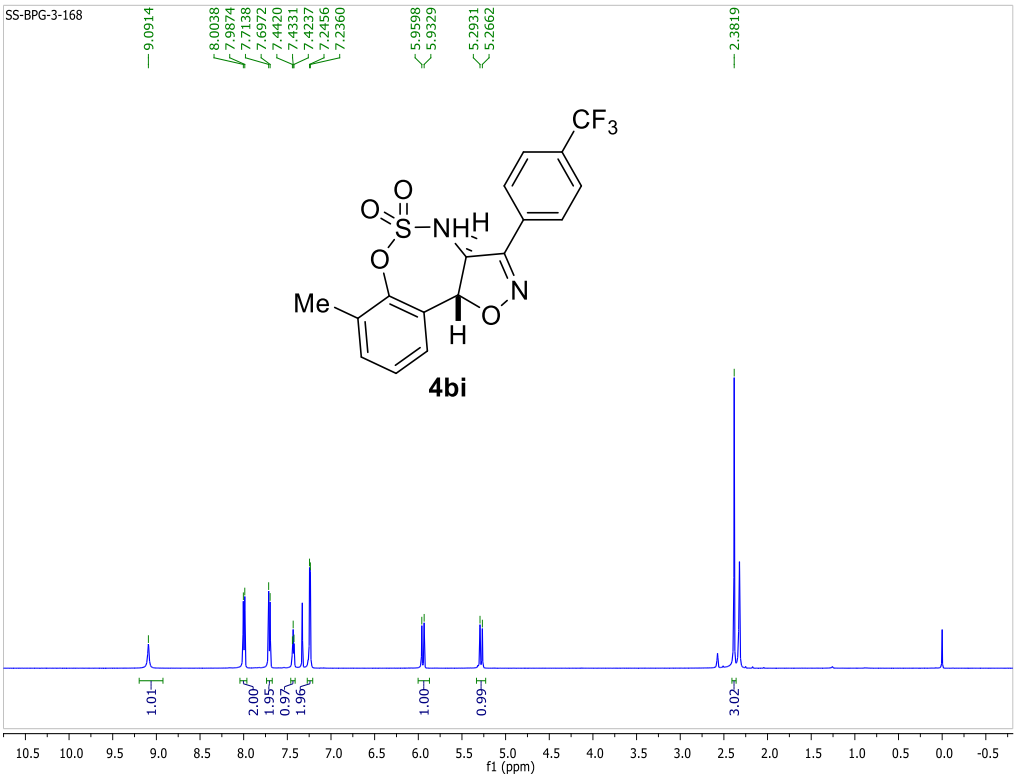

Figure 4.126 500 MHz ^{1}H NMR spectrum of **4bi** in $CDCl_3$+ DMSO-d_6.

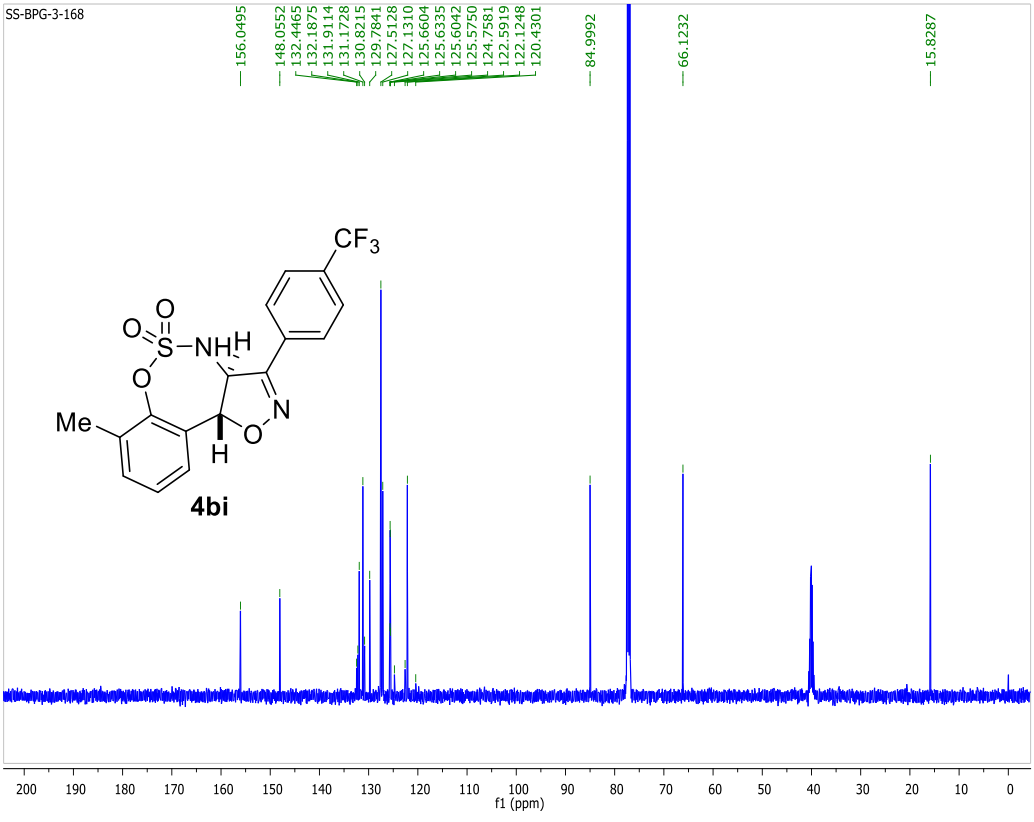

Figure 4.127 125 MHz ^{13}C NMR spectrum of **4bi** in $CDCl_3$+ DMSO-d_6.

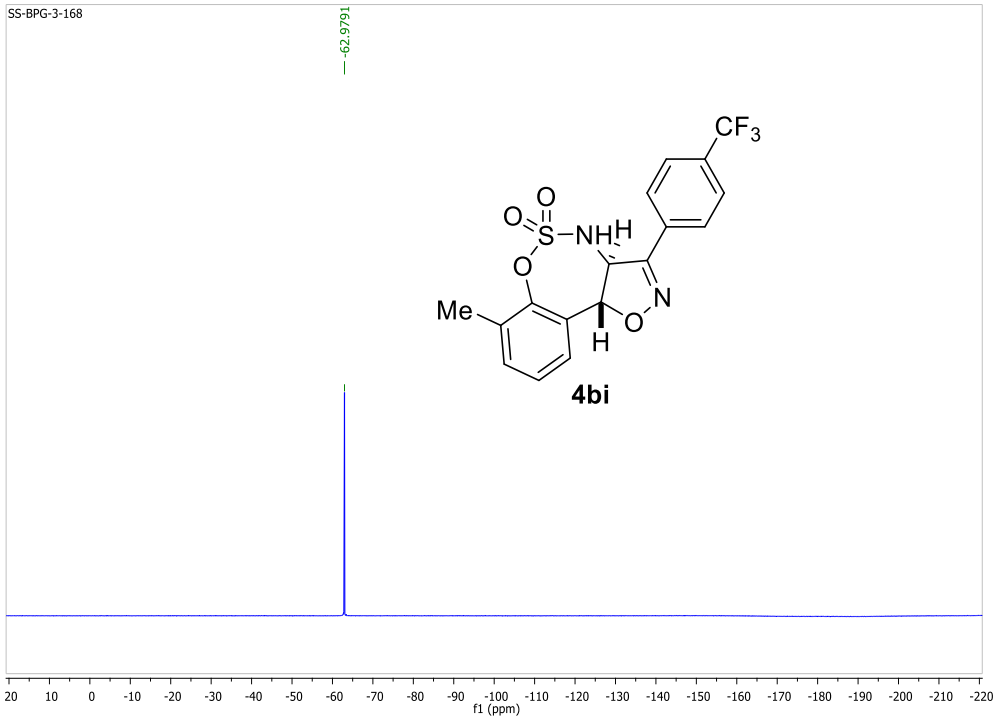

Figure 4.128 470 MHz ^{19}F NMR spectrum of **4bi** in $CDCl_3$+DMSO-d_6.

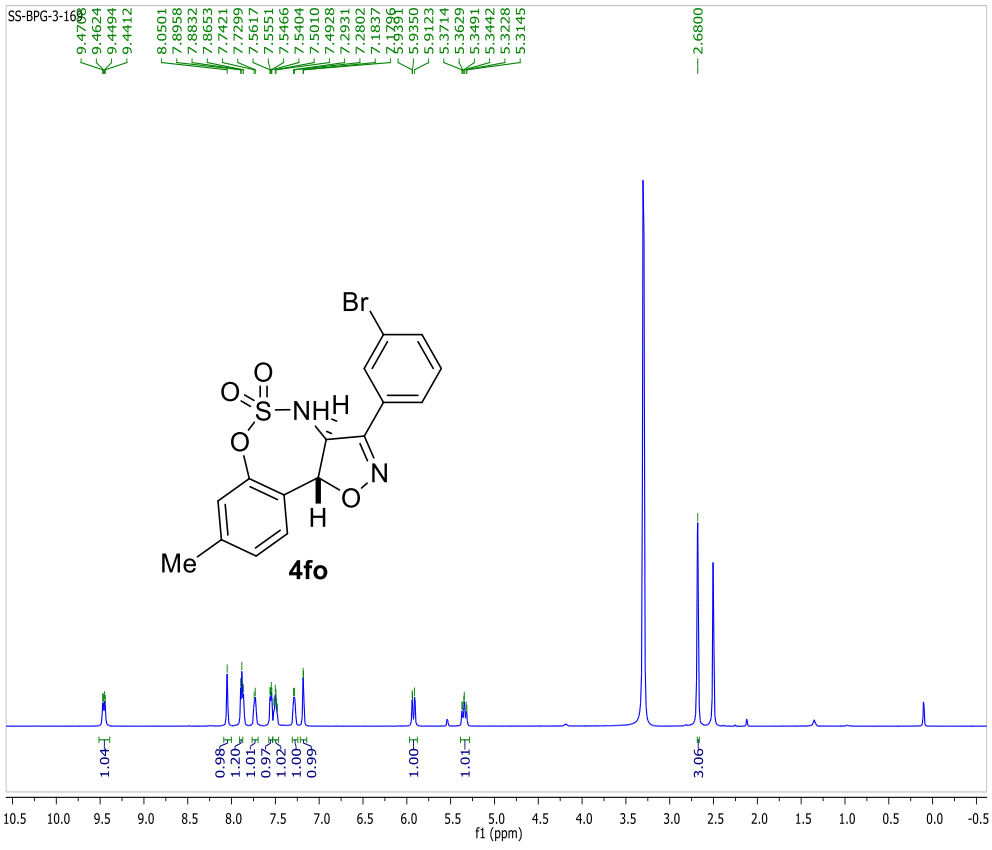

Figure 4.129 500 MHz ^{1}H NMR spectrum of **4fo** in $CDCl_3$+DMSO-d_6.

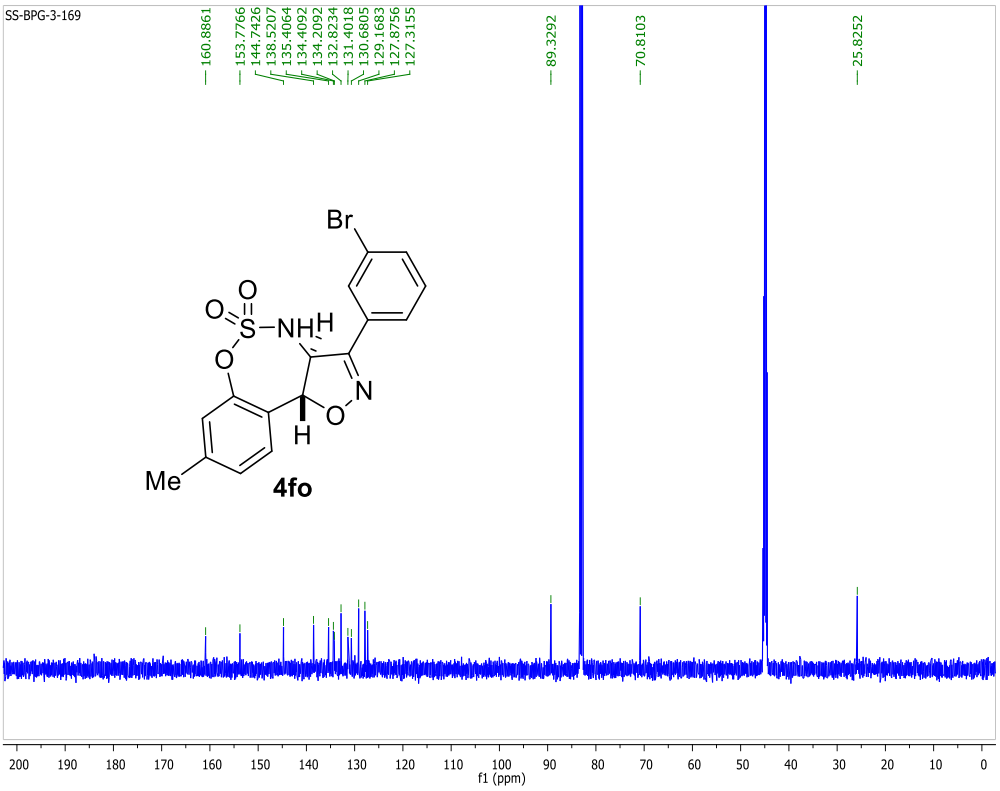

Figure 4.130 125 MHz ^{13}C NMR spectrum of **4fo** in $CDCl_3$+DMSO-d_6.

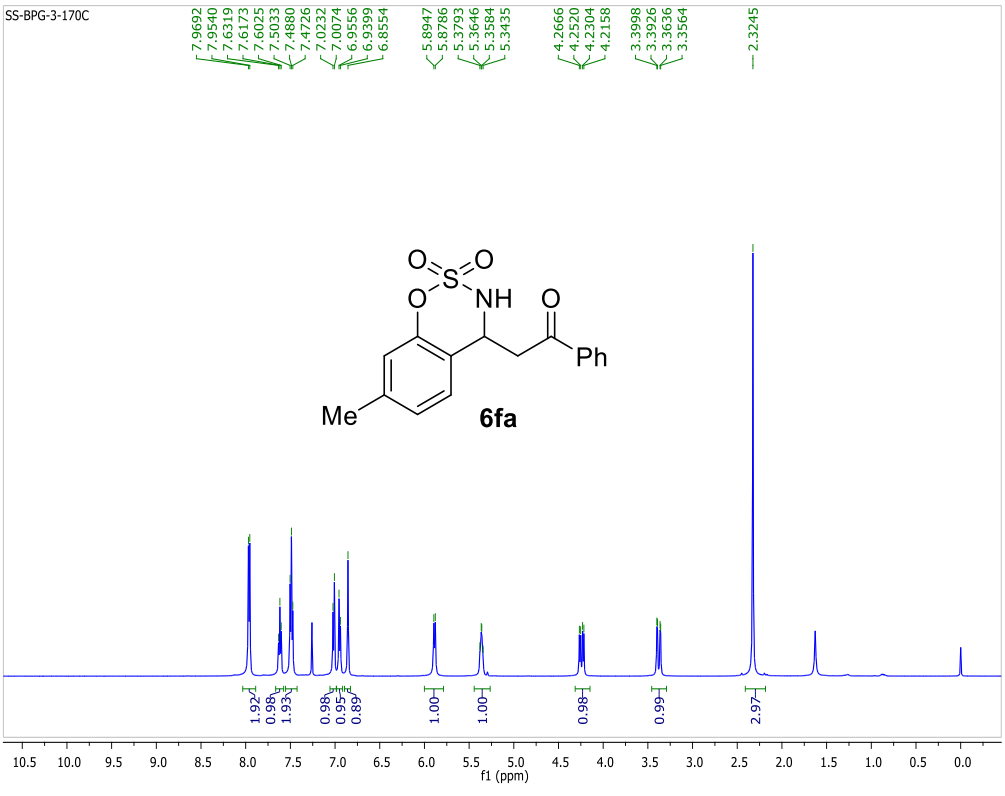

Figure 4.131 500 MHz ^{1}H NMR spectrum of **6fa** in $CDCl_3$.

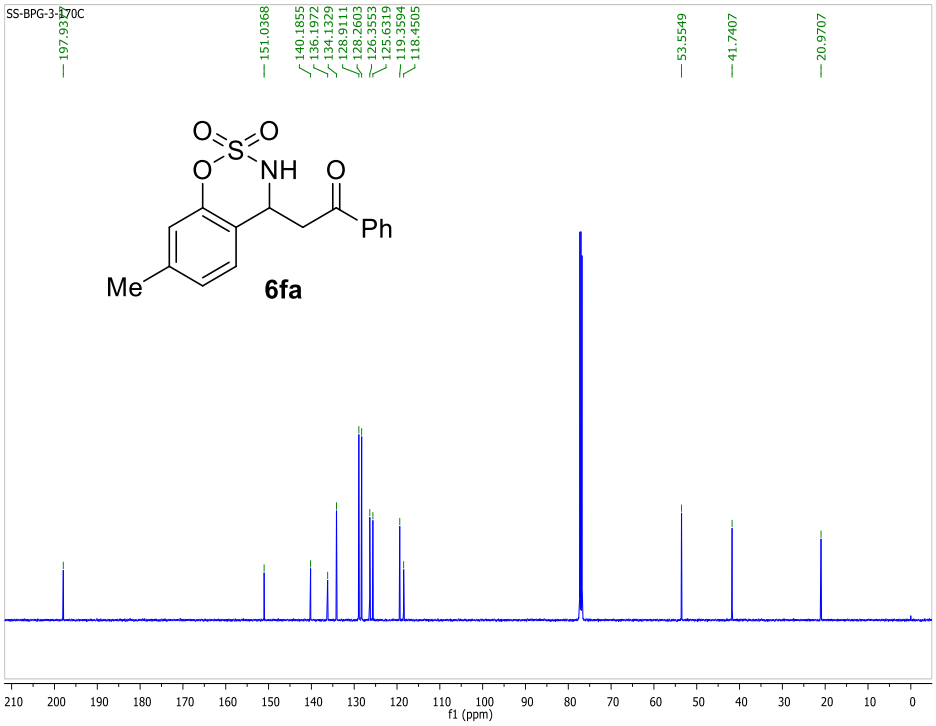

Figure 4.132 125 MHz ^{13}C NMR spectrum of **6fa** in $CDCl_3$.

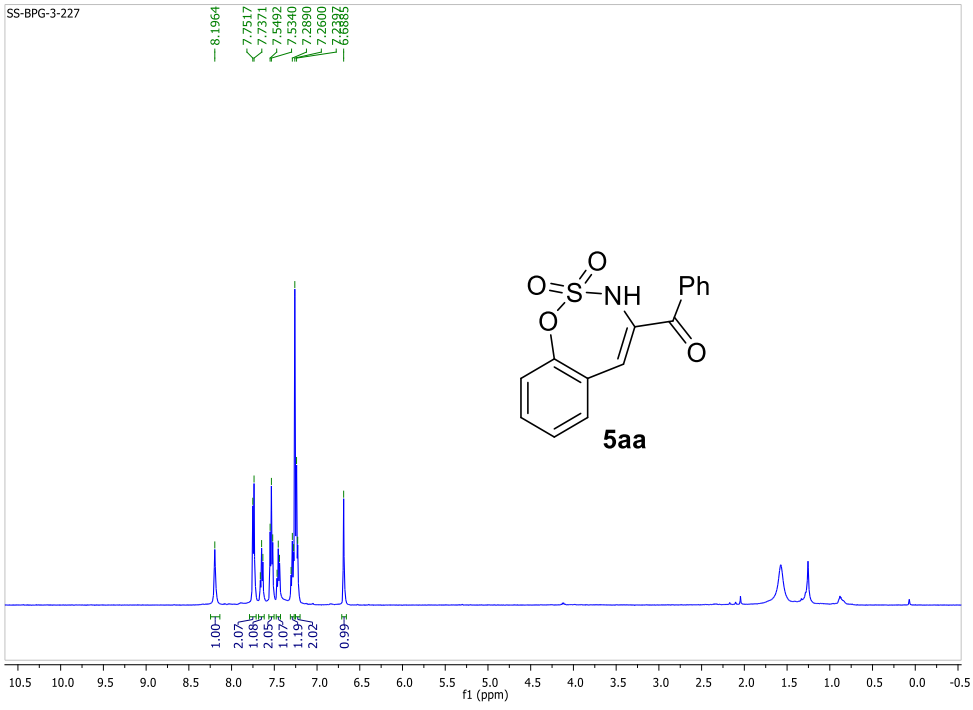

Figure 4.133 500 MHz ^{1}H NMR spectrum of **5aa** in $CDCl_3$.

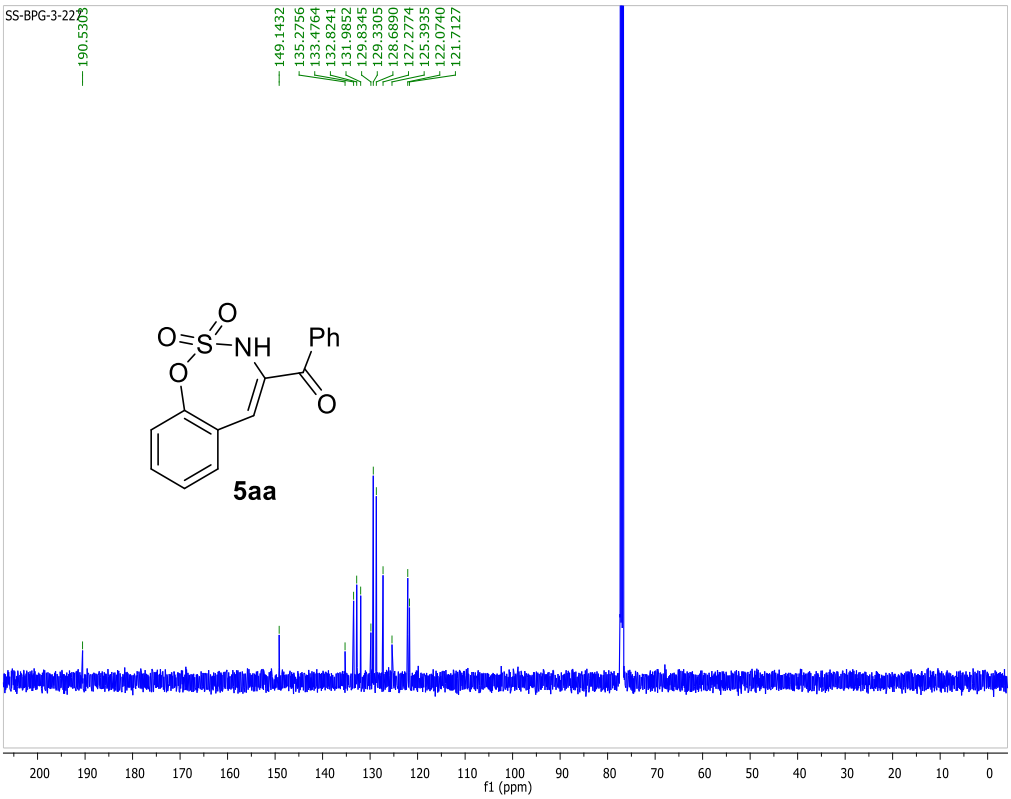

Figure 4.134 125 MHz ^{13}C NMR spectrum of **5aa** in $CDCl_3$.

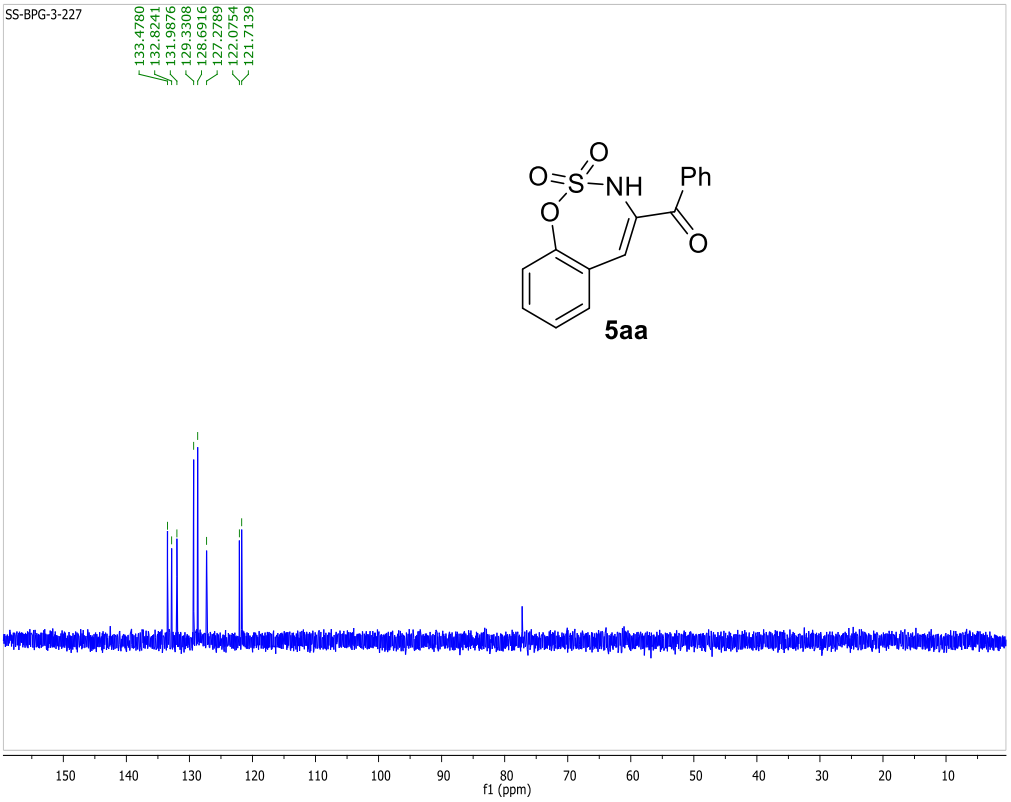

Figure 4.135 100 MHz DEPT-135 NMR spectrum of **5aa** in $CDCl_3$.

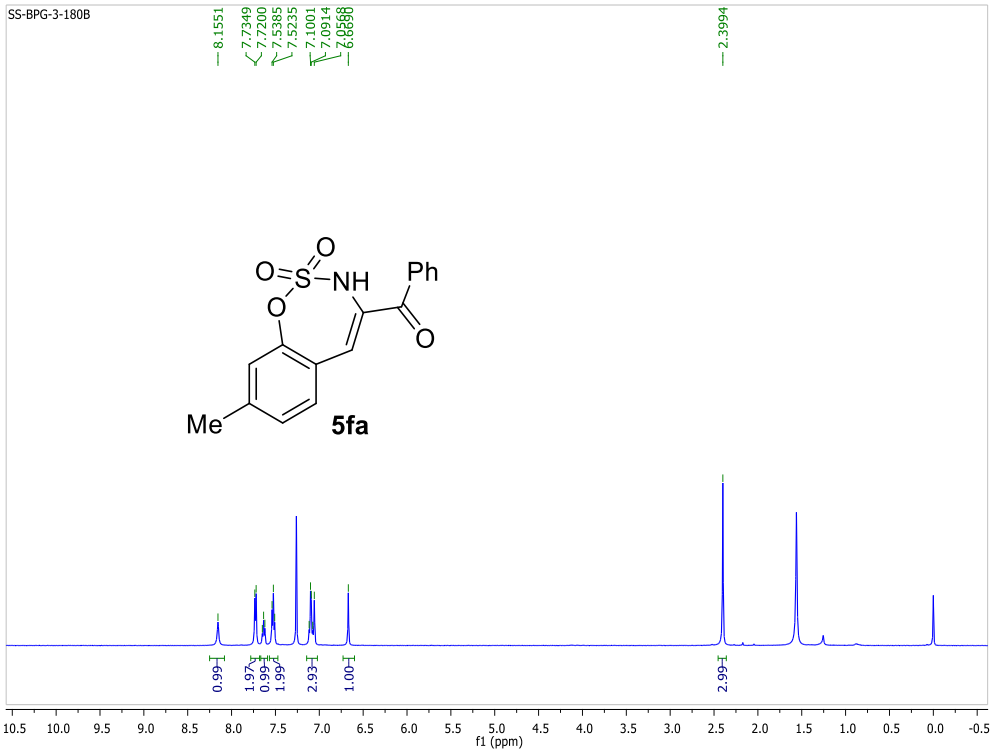

Figure 4.136 500 MHz ^{1}H NMR spectrum of **5fa** in $CDCl_3$.

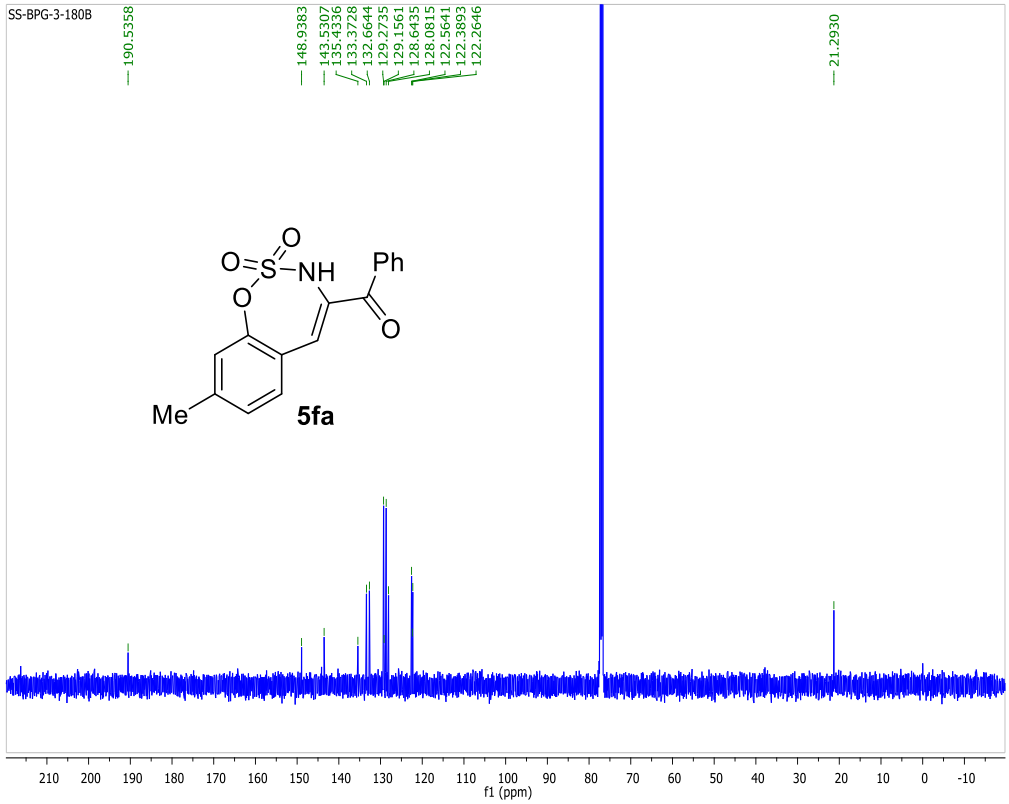

Figure 4.137 125 MHz ^{13}C NMR spectrum of **5fa** in $CDCl_3$.

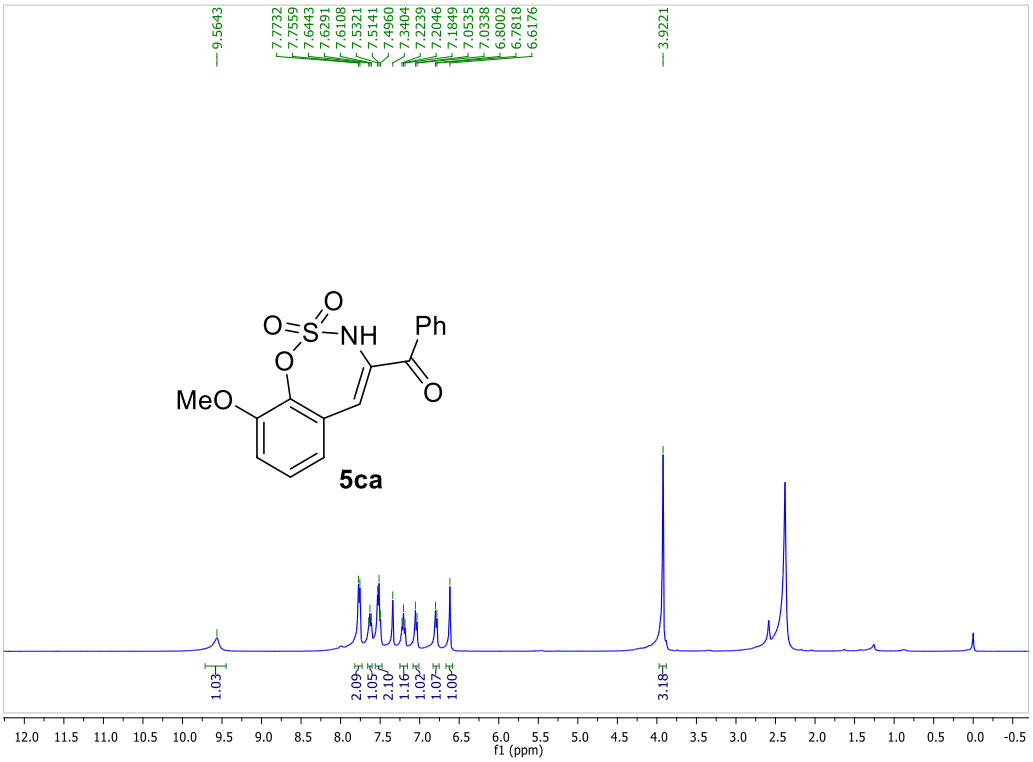

Figure 4.138 400 MHz ^{1}H NMR spectrum of **5ca** in $CDCl_3$+DMSO-d_6.

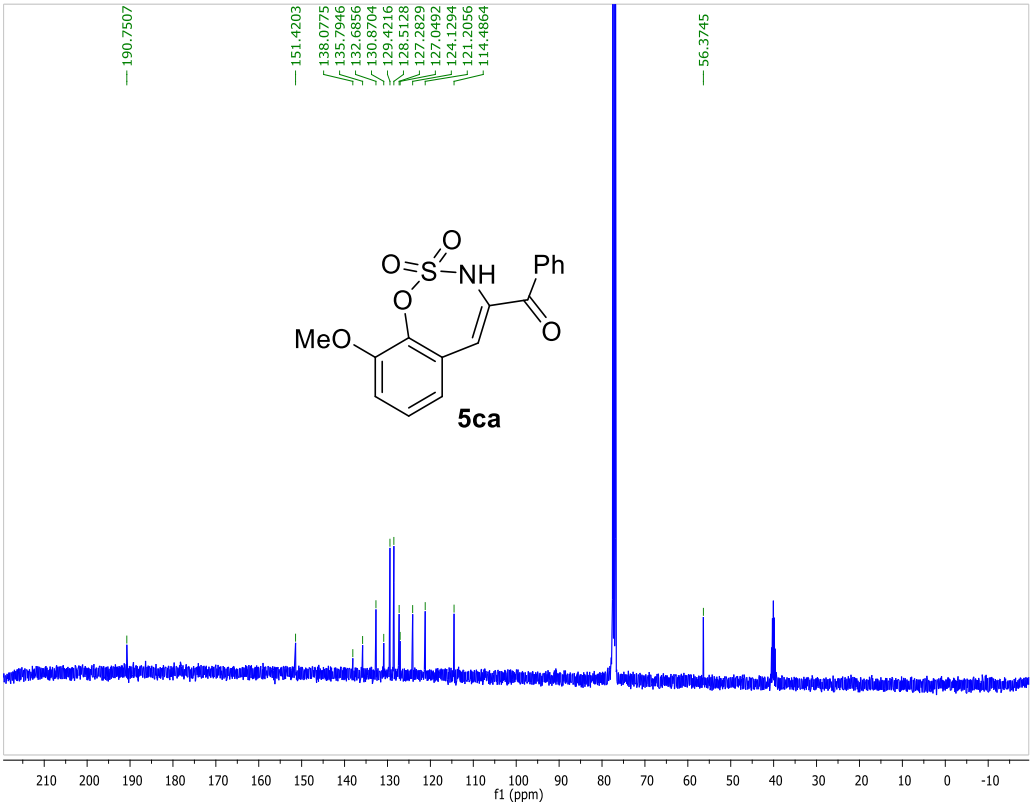

Figure 4.139 100 MHz ^{13}C NMR spectrum of **5ca** in $CDCl_3$+DMSO-d_6.

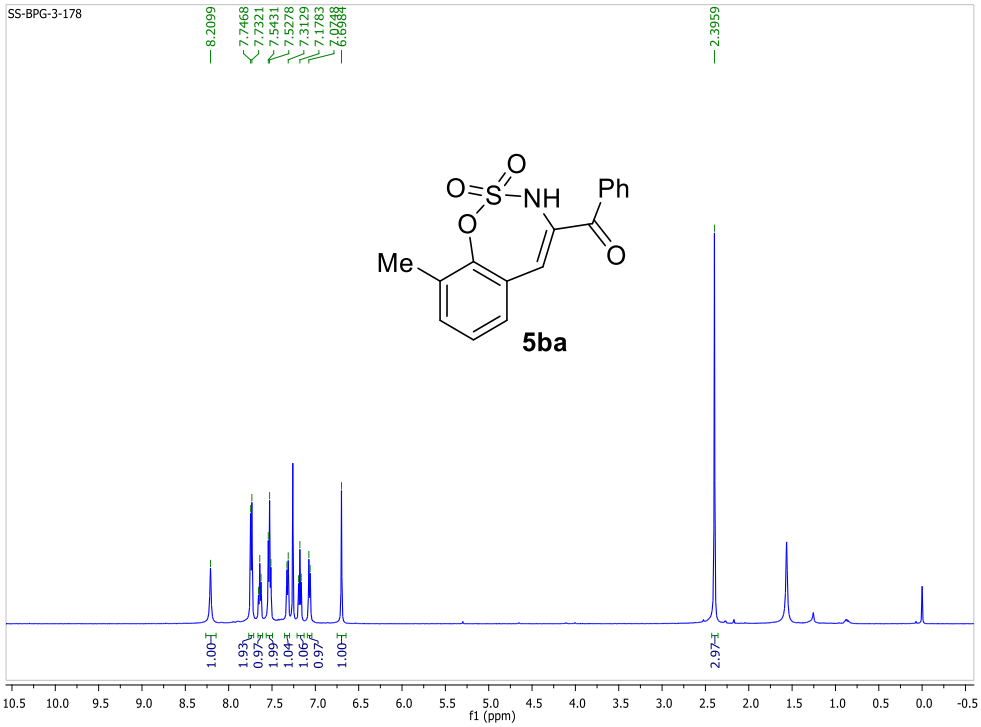

Figure 4.140 500 MHz ^{1}H NMR spectrum of **5ba** in $CDCl_3$.

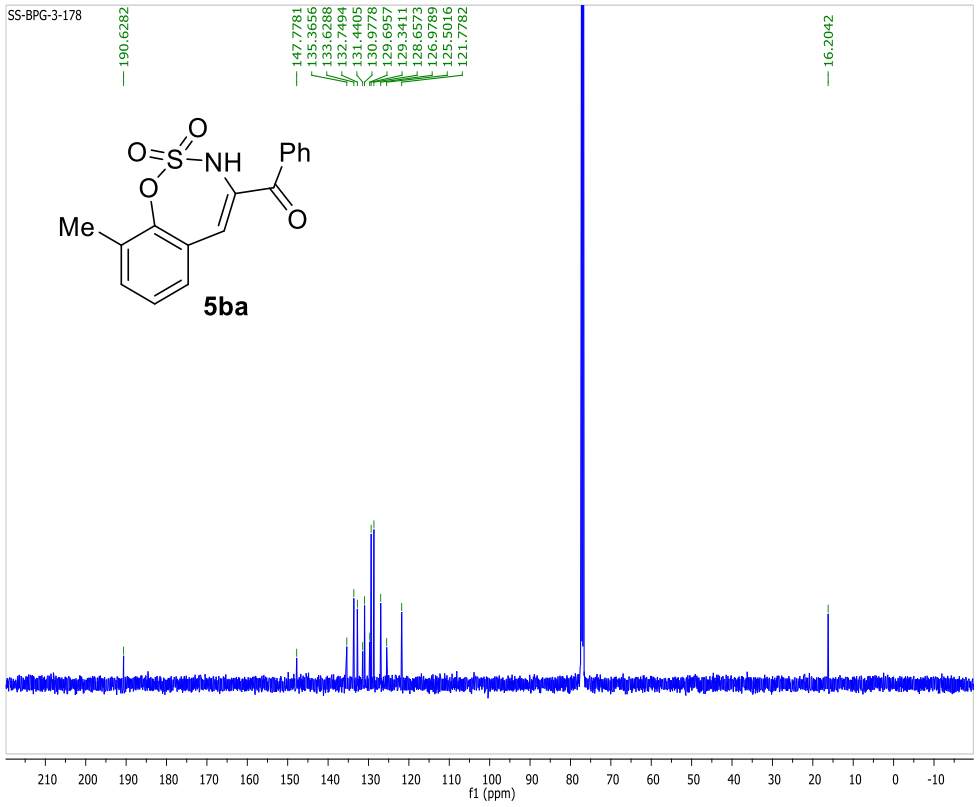

Figure 4.141 125 MHz ^{13}C NMR spectrum of **5ba** in $CDCl_3$.

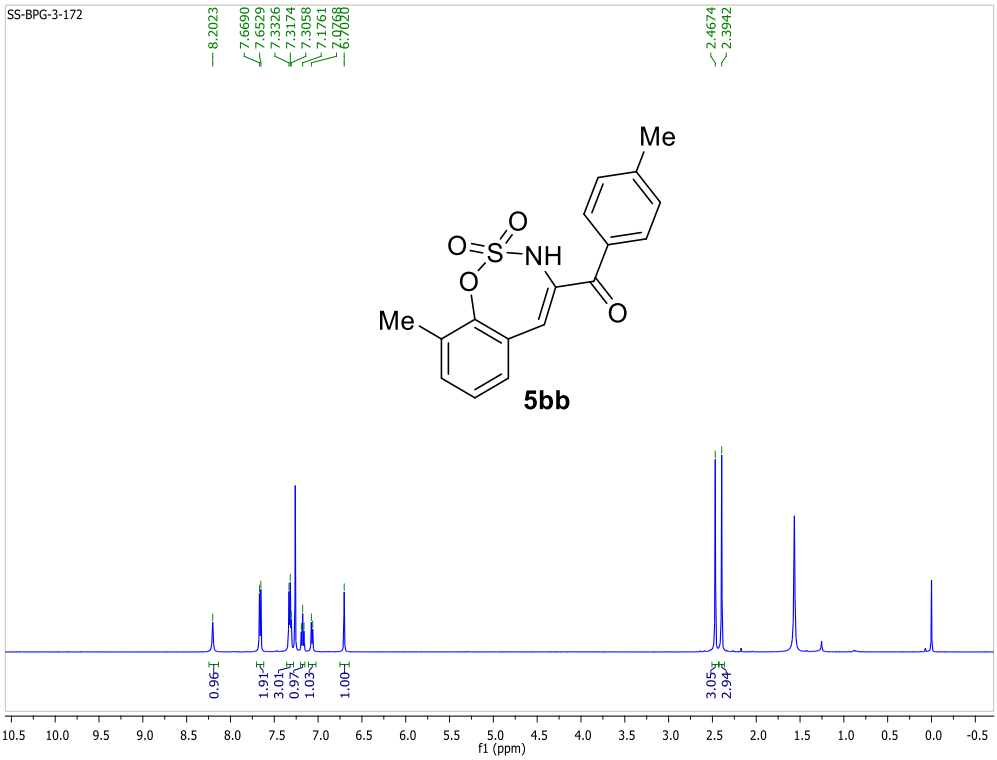

Figure 4.142 500 MHz ^{1}H NMR spectrum of **5bb** in $CDCl_3$.

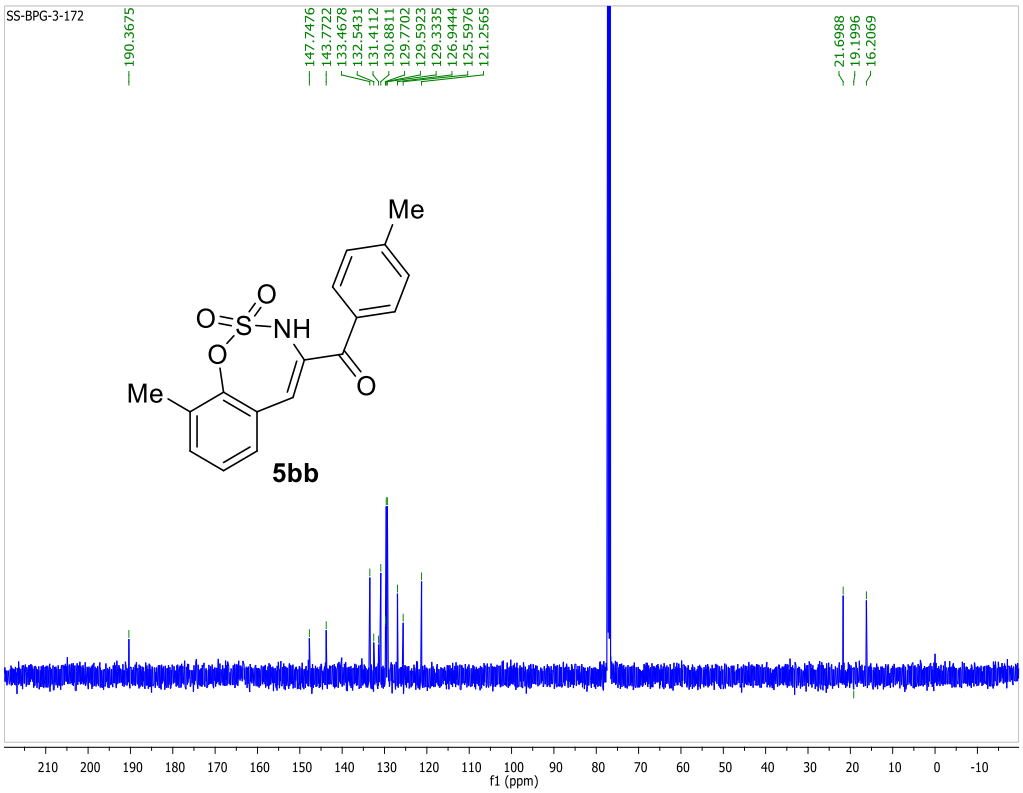

Figure 4.143 125 MHz ^{13}C NMR spectrum of **5bb** in $CDCl_3$.

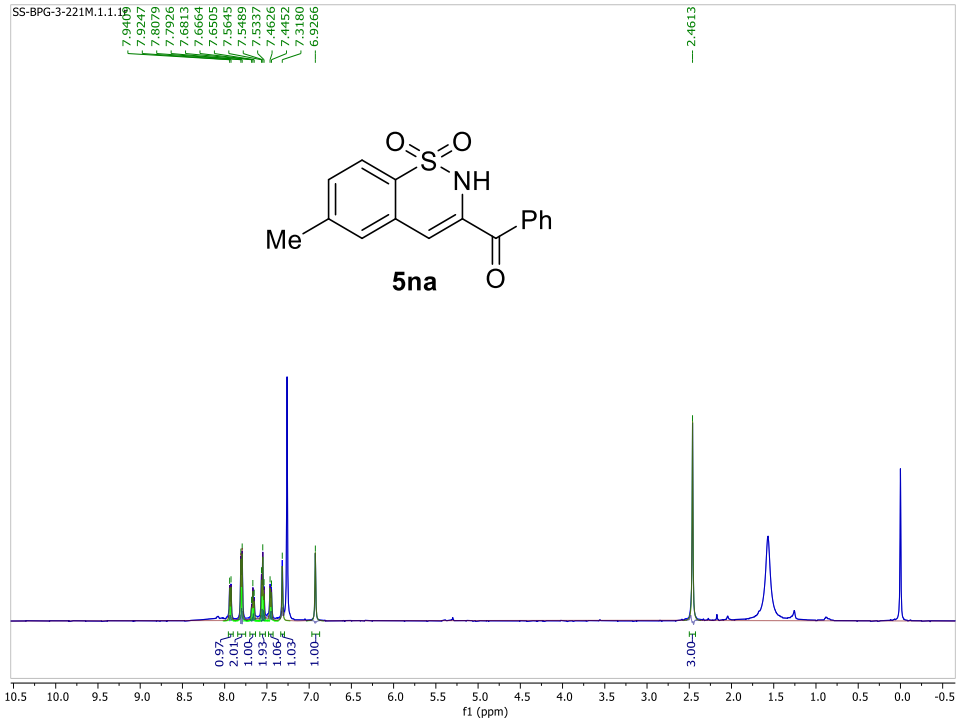

Figure 4.144 500 MHz ^{1}H NMR spectrum of **5na** in $CDCl_3$.

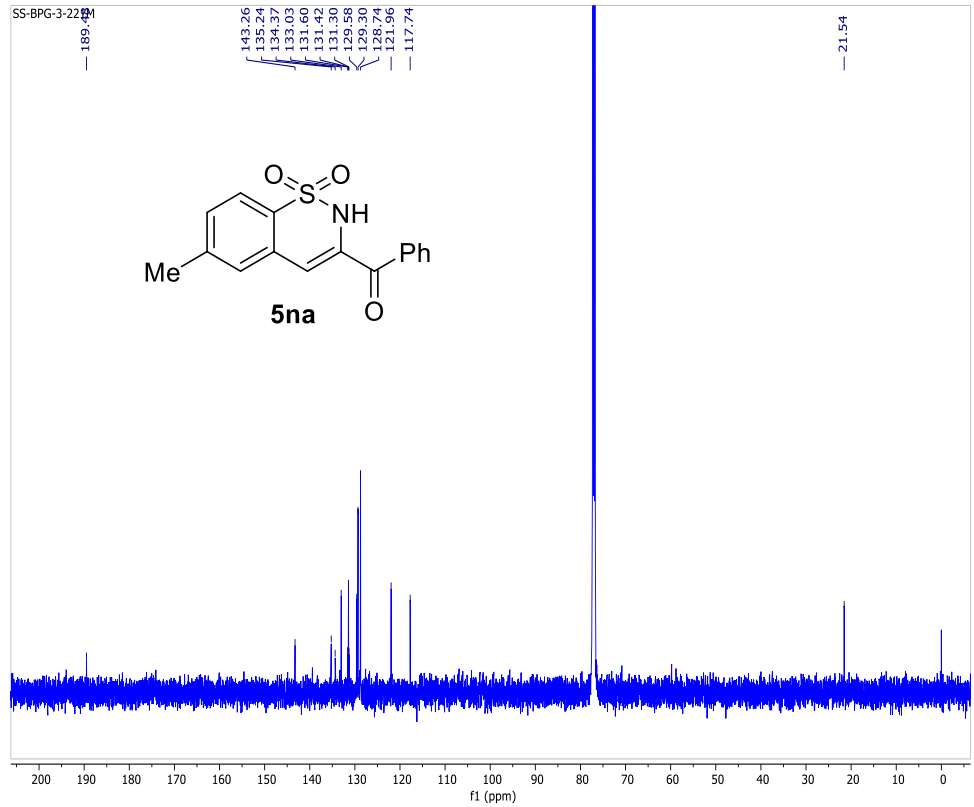

Figure 4.145 125 MHz ^{13}C NMR spectrum of **5na** in $CDCl_3$.

4.8 References

1 Kametani T., Honda T. (1986), Application of aziridines to the synthesis of natural products, *Adv. Heterocycl. Chem.*, 39, 181-236 (DOI: 10.1016/S0065-2725(08)60765-5).

2. Coleman R. S., Kong J.-S., Richardson T. E. (1999), Synthesis of naturally occurring antitumor agents: stereocontrolled synthesis of the azabicyclic ring system of the azinomycins, *J. Am. Chem. Soc.*, 121, 9088-9095 (DOI: 10.1021/ja992274w).

3. Sweeney J. B. (2002), Aziridines: epoxides' ugly cousins?, *Chem. Soc. Rev.*, 31, 247-258 (DOI: 10.1039/B006015L).

4. Ismail F. M. D., Levitsky D. O., Dembitsky V. M. (2009), Aziridine alkaloids as potential therapeutic agents *Eur. J. Med. Chem.*, 44, 3373-3387 (DOI: 10.1016/j.ejmech.2009.05.013).

5. Thibodeaux C. J., Chang W.-F., Liu H.-W. (2012), Enzymatic chemistry of cyclopropane, epoxide, and aziridine biosynthesis, *Chem. Rev.*, 112, 1681-1709 (DOI: 10.1021/cr200073d).

6. Schaschke N. (2004), Miraziridine A: natures blueprint towards protease class-spanning inhibitors, *Bioorg. Med. Chem. Lett.*, 14, 855-857 (DOI: 10.1016/j.bmcl.2003.12.030).

7. Zang H., Gates K. S. (2000), DNA binding and alkylation by the "left half" of azinomycin B *Biochemistry*, 39, 14968-14975 (DOI: 10.1021/bi001998d).

8. Aggarwal V. K., Vasse J.-L. (2003), Asymmetric sulfur ylide mediated aziridination: application in the synthesis of the side chain of taxol, *Org. Lett.*, 5, 3987-3990 (DOI: 10.1021/ol035554w).

9. Yeung Y.-Y., Hong S., Corey E. J. (2006), A short enantioselective pathway for the synthesis of the anti-influenza neuramidase inhibitor oseltamivir from 1,3-butadiene and acrylic acid, *J. Am. Chem. Soc.*, 128, 6310-6311 (DOI: 10.1021/ja0616433).

10. Wang Z., Li F., Zhao L., He Q., Chen F., Zheng C. (2011), An efficient enantioselective synthesis of florfenicol *via* asymmetric aziridination, *Tetrahedron,* 67, 9199-9203 (DOI: 10.1016/j.tet.2011.09.052).

11. Dank C., Ielo L. (2023), Recent advances in the accessibility, synthetic utility, and biological applications of aziridines, *Org. Biomol. Chem.,* 21, 4553-4573 (DOI: 10.1039/D3OB00424D).

12. Callebaut G., Meiresonne T., De Kimpe N., Mangelinckx S. (2014), Synthesis and reactivity of 2-(carboxymethyl)aziridine derivatives, *Chem. Rev.,* 114, 7954-8015 (DOI: 10.1021/cr400582d).

13. Mukherjee A., Ghosal N. C., Zyryanov G. V., Majee A., Santra S. (2019), An updated library on the synthesis of aziridines, *Curr. Green Chem.,* 6, 226-241 (DOI: 10.2174/2213346106666191024123452).

14. Karila D., Dodd R. H. (2011), Recent progress in iminoiodane-mediated aziridination of olefins *Curr. Org. Chem.,* 15, 1507-1538 (DOI: 10.2174/138527211795378128).

15. Liu Y., Dong X., Deng G., Zhou L. (2016), Synthesis of aziridines by visible-light induced decarboxylative cyclization of N-aryl glycines and diazo compounds, *Sci. China Chem.,* 59, 199-202 (DOI: 10.1007/s11426-015-5513-8).

16. Cheng X., Cai B.-G., Mao H., Lu J., Li L., Wang K., Xuan J. (2021), Divergent synthesis of aziridine and imidazolidine frameworks under blue LED irradiation, *Org. Lett.,* 23, 4109-4114 (DOI: 10.1021/acs.orglett.1c00979).

17. Scholz S. O., Farney E. P., Kim S., Bates D. M., Yoon T. P. (2016), Spin-selective generation of triplet nitrenes: olefin aziridination through visible-light photosensitization of azidoformates, *Angew. Chem. Int. Ed.,* 55, 2239-2242 (DOI: 10.1002/anie.201510868).

18. Yu W.-L., Chen J.-Q., Wei Y.-L., Wang Z.-Y., Xu P.-F. (2018), Alkene functionalization for the stereospecific synthesis of substituted aziridines by visible-light photoredox catalysis, *Chem. Commun.,* 54, 1948-1951 (DOI: 10.1039/c7cc09151f).

19. Guo Y., Pei C., Jana S., Koenigs R. M. (2021), Synthesis of trifluoromethylated aziridines via photocatalytic amination reaction, *ACS Catal.*, 11, 337-342 (DOI: 10.1021/acscatal.0c04564).

20. Srivastava O. S., Anand V., Rastogi N. (2023), Visible light photoredox aziridination of chalcones, *Asian J. Org. Chem.*, 12, e202300415 (DOI: 10.1002/ajoc.202300415).

21. Kim E., Choi S., Kim H., Cho E. J. (2013), Generation of CF_3-containing epoxides and aziridines by visible-light-driven trifluoromethylation of allylic alcohols and amines, *Chem. Eur. J.*, 19, 6209-6212 (DOI: 10.1002/chem.201300564).

22. Zhu B.-H., Zheng J.-C., Yu C.-B., Sun X.-L., Zhou Y.-G., Shen Q., Tang Y. (2010), One-pot highly diastereoselective synthesis of *cis*-vinylaziridines *via* the sulfur ylide-mediated aziridination and palladium(0)-catalyzed isomerization, *Org. Lett.*, 12, 504-507 (DOI: 10.1021/ol9027072).

23. Lai B.-N., Qiu J.-F., Zhang H.-X., Nie J., Ma J.-A. (2016), Stereoselective synthesis of fused aziridines via one-pot sequential decarboxylative mannich reaction and oxidative C–H amination of cyclic imines with β-ketoacids, *Org. Lett.*, 18, 520-523 (DOI: 10.1021/acs.orglett.5b03551).

24. Zhang S., Li L., Xin L., Liu W., Xu K. (2017), Asymmetric aziridination of N-sulphonyl ketimines with unfunctionalized ketones: a one-pot approach to multisubstituted fused aziridines, *J. Org. Chem.*, 82, 2399-2406 (DOI: 10.1021/acs.joc.6b02827).

25. Fu J., Zanoni G., Anderson E. A., Bi X. (2017), α-Substituted vinyl azides: an emerging functionalized alkene, *Chem. Soc. Rev.*, 46, 7208-7228 (DOI: 10.1039/C7CS00017K).

26. Gholami F., Yousefnejad F., Larijani B., Mahdavi M. (2023), Vinyl azides in organic synthesis: an overview, *RSC Adv.*, 13, 990-1018 (DOI: 10.1039/D2RA06726A).

27. Goud S., Guin S., Prakash M., Samanta S. (2022), $Cu(OAc)_2$/DABCO-mediated domino reaction of vinyl malononitriles with cyclic sulfamidate

imines: access to 6-hydroxyaryl-2-aminonicotinonitriles, *Org. Biomol. Chem.*, 20, 352-357 (DOI: 10.1039/D1OB02095A).

28. Guin S., Majee D., Samanta S. (2021), Unmasking the reverse reactivity of cyclic N-sulfonyl ketimines: multifaceted applications in organic synthesis, *Chem. Commun.*, 57, 9010-9028 (DOI: 10.1039/D1CC03439A).

29. Pandhurnekar C. P., Pandhurnekar H. C., Mungole A. J., Butoliya S. S., Yadao B. G. (2023), A review of recent synthetic strategies and biological activities of isoxazole, *J. Heterocycl. Chem.*, 60, 537-565 (DOI: 10.1002/jhet.4586).

30. Lopes E. F., Penteado F., Thurow S., Pinz M., Reis A. S., Wilhelm E. A., Luchese C., Barcellos T., Dalberto B., Dalberto B. (2019), Synthesis of isoxazolines by the electrophilic chalcogenation of β,γ-unsaturated oximes: fishing novel anti-inflammatory agents, *J. Org. Chem.*, 84, 12452-12462 (DOI: 10.1021/acs.joc.9b01754).

31. Tollefson M. B., Kolodziej S. A., Fletcher T. R., Vernier W. F., Beaudry J. A., Keller B. T., Reit D. B. (2003), A novel class of apical sodium co-dependent bile acid transporter inhibitors: the 1,2-benzothiazepines, *Bioorg. Med. Chem. Lett.*, 13, 3727-3730 (DOI: 10.1016/j.bmcl.2003.08.004).

32. Ganguly A. K., Alluri S. S., Caroccia D., Biswas D., Wang C.-H., Kang E., Zhang Y., McPhail A. T., Carroll S. S., Burlein C., Munshi V., Orth P., Strickland C. (2011), Design, synthesis, and X-ray crystallographic analysis of a novel class of HIV-1 protease inhibitors, *J. Med. Chem.*, 54, 7176-7183 (DOI: 10.1021/jm200778q).

33. Thornton A. R., Martin V. I., Blakey S. B. (2009), π-Nucleophile traps for metallonitrene/alkyne cascade reactions: a versatile process for the synthesis of α-aminocyclopropanes and β-aminostyrenes, *J. Am. Chem. Soc.*, 131, 2434-2435 (DOI: 10.1021/ja809078d).

34. Xia A.-J., Kang T.-R., He L., Chen L.-M., Li W.-T., Yang J.-L., Liu Q.-Z. (2016), Metal-Free Ring-Expansion reaction of six-membered sulfonylimines

with diazomethanes: an approach toward seven-membered enesulfonamides, *Angew. Chem. Int. Ed.,* 55, 1441-1444 (DOI: 10.1002/anie.201508804).

35. Winum J. Y., Scozzafava A., Montero J.-L., Supuran C.T. (2005), Sulfamates and their therapeutic potential, *Med. Res. Rev.,* 25, 186-228 (DOI: 10.1002/med.20021).

36. Lloyd J., Atwal K. S., Finlay H. J., Huynh M. T., Bhandaru R., Kover A., Schmidt J., Vaccaro W., Conder M. L., Jenkins-West T., Levesque P. (2007), Benzopyran sulfonamides as $K_V1.5$ potassium channel blockers *Bioorg. Med. Chem. Lett.,* 17, 3271-3275 (DOI: 10.1016/j.bmcl.2007.04.020).

37. Reddy M. K., Bhajammanavar V., Baidya M. (2021), Annulation cascade of sulfamate-derived cyclic imines with glycine aldimino esters: synthesis of 1,3-benzoxazepine scaffolds, *Org. Lett.,* 23, 3868-3872 (DOI: 10.1021/acs.orglett.1c01001).

38. Jethava K. P., Fine J., Chen Y., Hossain A., Chopra G. (2020), Accelerated reactivity mechanism and interpretable machine learning model of N-sulfonylimines toward fast multicomponent reactions, *Org. Lett.,* 22, 8480-8486 (DOI: 10.1021/acs.orglett.0c03083).

39. Jia C.-M., Zhang H.-X., Nie J., Ma J.-A. (2016), Catalytic asymmetric decarboxylative mannich reaction of malonic acid half esters with cyclic aldimines: access to chiral β-amino esters and chroman-4-amines, *J. Org. Chem.,* 81, 8561-8569 (DOI: 10.1021/acs.joc.6b01750).

40. Zhenhua L., Peiqiu L., Xihe B. (2014), General silver-catalyzed hydroazidation of terminal alkynes by combining TMS-N_3 and H_2O: synthesis of vinyl azides, *Org. Lett.,* 16, 3668-3671 (DOI: 10.1021/ol501661k).

41. Barry M. T., Chuanle Z. (2020), Zn-prophenol catalyzed enantioselective mannich reaction of 2*H*-azirines with alkynyl ketones, *Org. Lett.,* 22, 9683-9687 (DOI: 10.1021/acs.orglett.0c03737).

42. Donthiri R. R., Pappula V., Reddy N. N. K., Bairagi D., Adimurthy S. (2014), Copper-catalyzed C–H functionalization of pyridines and isoquinolines

with vinyl azides: synthesis of imidazo heterocycles, *J. Org. Chem.*, 79, 11277-11284 (DOI: 10.1021/jo5021618).

Chapter 5

Conclusion and Future Outlook

The invention of one-pot methods for creating a variety of nitrobenzene, pyridine, and aziridine scaffolds from readily available reactants is the subject of the scientific effort presented in this thesis. Under ideal reaction circumstances, the present techniques tolerate a wide variety of synthetically valuable functional groups and provide good to outstanding yields, and promising diastereoselectivities of the compounds mentioned above. Furthermore, our proposed approaches have effectively enabled efficient access to interesting classes of biologically appealing compounds, including scaffolds for 2′-nitro-1,1′:4′,1″-terphenyl, substituted sulfamidate fused aziridines, and 6-hydroxyaryl-2-aminonicotinonitriles.

The developed methods have several benefits, such as avoiding costly and toxic metal salts, no need for powerful acids and additional oxidants, minimizing volatile and hazardous organic solvents, multi-step, etc. As a result, the techniques presented in this thesis will be very valuable in both synthetic and medicinal chemistry as effective strategies for sustaining access to the scaffolds above.

As a future outlook, the synthetic conversions described in this thesis offer several new concepts and their practical applications towards the rapid access to value-added carbo- and azacyclic scaffolds in an atom-economical and eco-friendly manner, underscoring the advancement of research in organic synthesis. Therefore, the versatility and scope of these transformations have a great future where they could be extended to various value-added chemical syntheses to broaden the potential application in pharmacology.

Appendix

General experimental procedure for all the experiments described in chapters 2-4: All the reactions were carried out under an inert atmosphere and monitored by TLC using Merck 60 F_{254} precoated silica-gel plates (0.25 mm thickness), and the products were visualized by UV detection. Flash chromatography was carried out with silica gel (200-300 mesh). ^{1}H and ^{13}C NMR spectra were recorded on 400 and 500 MHz spectrometers. Data for ^{1}H NMR are reported as a chemical shift (δ ppm), multiplicity (s = singlet, d = doublet, t = triplet, q = quartet, m = multiplet), coupling constant *J* (Hz), integration, and assignment, data for ^{13}C are reported as a chemical shift. High resolutions mass spectral analyses (HRMS) were carried out using ESI-QTOF-MS (Microtof Q-II Bruker, condition: capillary voltage = -4500V, temperature = 250 °C, N_2 gas flow = 7 lit/min, nebulizer pressure = 2 bar, instrument is calibrated using ESI tune low calibration mixture before HRMS sample analysis). Single-crystal X-ray diffraction data was measured on the Bruker D8 Quest Single-Crystal XRD instrument at 150(2) K using graphite monochromated Mo Kα radiation (λα = 0.71073 Å). Melting points were recorded on an Electrothermal melting point apparatus and are uncorrected.